National Library of Canada
Acquisitions and Bibliographic Services Branch
395 Wellington Street
Ottawa, Ontario
K1A 0N4

Bibliothèque nationale du Canada
Direction des acquisitions et des services bibliographiques
395, rue Wellington
Ottawa (Ontario)
K1A 0N4

Your file Votre référence

Our file Notre référence

NOTICE

The quality of this microform is heavily dependent upon the quality of the original thesis submitted for microfilming. Every effort has been made to ensure the highest quality of reproduction possible.

If pages are missing, contact the university which granted the degree.

Some pages may have indistinct print especially if the original pages were typed with a poor typewriter ribbon or if the university sent us an inferior photocopy.

Reproduction in full or in part of this microform is governed by the Canadian Copyright Act, R.S.C. 1970, c. C-30, and subsequent amendments.

AVIS

La qualité de cette microforme dépend grandement de la qualité de la thèse soumise au microfilmage. Nous avons tout fait pour assurer une qualité supérieure de reproduction.

S'il manque des pages, veuillez communiquer avec l'université qui a conféré le grade.

La qualité d'impression de certaines pages peut laisser à désirer, surtout si les pages originales ont été dactylographiées à l'aide d'un ruban usé ou si l'université nous a fait parvenir une photocopie de qualité inférieure.

La reproduction, même partielle, de cette microforme est soumise à la Loi canadienne sur le droit d'auteur, SRC 1970, c. C-30, et ses amendements subséquents.

Canada

A MODEL FOR PREDICTING THE PRESSURE GRADIENT ALONG A HEATED CHANNEL DURING FLOW BOILING

by

Laurence Kim-Hung Leung

A dissertation submitted to the School of Graduate Studies and Research of the Ottawa-Carleton Institute for Mechanical and Aeronautical Engineering at the University of Ottawa in partial fulfilment of the requirements for the degree of Doctor of Philosophy in Mechanical Engineering.

Ottawa-Carleton Institute for Mechanical and Aeronautical Engineering
University of Ottawa, Ottawa, Ontario, Canada K1N 6N5

1994 May

ISBN 0-315-95933-9

Canada

UNIVERSITÉ D'OTTAWA
UNIVERSITY OF OTTAWA

For Alice.

Abstract

A model has been derived to predict the frictional pressure gradient along a heated channel. It focuses mainly on flow boiling at high-pressure conditions (10 MPa). Based on a force-momentum balance, the overall pressure gradient is divided into three components: friction, acceleration and gravity. This model analyzes the frictional pressure drop for all heat-transfer modes encountered inside a heated channel: single-phase heat transfer, subcooled boiling, saturated (bulk) boiling, forced convective evaporation and film boiling. The heating effect is introduced through a change in flow structure in two-phase flow (i.e., the phase distribution), particularly the significant differences in entrained liquid fraction between adiabatic and boiling two-phase flow (two separate correlations have been derived in this study). One of the major components in this model is the relation between shear stress and velocity gradient. Based primarily on the theory in single-phase flow, this relation is extended to two-phase flow boiling through the assumption of a homogeneous mixture having the characteristics of a single-phase flow. In the forced-convective evaporation region (mainly wispy-annular flow), a four-layer structure is introduced to analyze the liquid film and two-phase core. A number of assumptions and modifications to the expressions for single-phase flow are introduced to account for the

presence of two phases. Empirical corrections, however, are used for the effects of surface roughness and viscosity difference between near-wall fluid and bulk fluid on two-phase frictional pressure drop.

Experimental data for validating the present model were obtained in a vertical tubular test section, installed in a high-pressure steam-water facility at the Chalk River Laboratories of AECL Research. A strong effect of surface heating on frictional pressure drop was observed. With increasing heat flux, the frictional pressure drop decreases in single-phase flow, increases in nucleate boiling, and decreases in forced convective evaporation. The effect of heat flux in the film-boiling region (post-dryout conditions) appears to be small. However, the frictional pressure gradient is much smaller in the film-boiling region than in the pre-CHF region for the same flow conditions (i.e., pressure, mass flux and quality). For most flow conditions, a maximum in two-phase frictional pressure drop is encountered at a quality lower than the value corresponding to the occurrence of dryout. In addition to heating, other effects on frictional pressure drop (such as pressure, mass flux, etc.) have also been examined.

Comparisons between model predictions and experimental data have shown relatively good agreement for most conditions, with an overall root-mean-square error of 12% and an average error of 8%. The overprediction is mainly observed at conditions corresponding to nucleate boiling and forced convective evaporation at high qualities. Both the forced-convective evaporation data at low qualities and the film-boiling data are predicted with good accuracy.

An assessment of 19 empirical correlations has been carried out to examine their validity for flow boiling. All of them are shown to be valid for pre-dryout conditions only and overpredict the pressure drop significantly at the post-dryout conditions. A multi-correlation approach has been set up to use different empirical correlations for various heat-transfer modes. Good agreement with experimental data has been obtained when either the Reddy et al., Chisholm, or Beattie annular-flow correlation is used for the pre-dryout conditions. Beyond dryout, the Beattie post-dryout correlation predicts the experimental data very well. None of the assessed correlations is capable of (i) capturing the transition between the maximum pressure-drop and the dryout points, and (ii) predicting the decreasing trend of two-phase pressure drop as the heated surface

approaches dryout. When the predictions are examined in detail, a systematic trend of underprediction at both pre-dryout and post-dryout conditions and/or overprediction at conditions between the maximum pressure-drop and the dryout point is noted.

Acknowledgements

The final task of this study is the acknowledgement of a number of people who have either guided or assisted me in the course. All of them have contributed to the success of this work.

I am deeply grateful to Dr. D.C. Groeneveld, my co-supervisor, for his guidance and patience during the study. His expertise on two-phase flow and boiling heat transfer has led me smoothly throughout the course. The acquired knowledge, from Dr. Groeneveld, is definitely a benefit to not only my Ph.D. study, but also my career. His cheerful encouragement and helpful suggestions have always been part of the solution to my many problems. I enjoyed, particularly, the many after-work-hour discussions provided (voluntarily) by Dr. Groeneveld, and will always remember his "KISS" theory - Keep It Short and Simple.

A sincere thank to Dr. S.C. Cheng, my co-supervisor, for his support, encouragement and helpful comments during the course of my study. His administering of my academic progress and records is also appreciated.

I am also thankful to Dr. S.T. Yin for his constructive comments and recommendations for improving my work and thesis.

The experimental work of this study was partly funded by the Candu Owners Group (COG) and performed at Chalk River Laboratories, AECL Research. I would like to take this opportunity to thank the financial support of COG and AECL Research (for allowing me to use the test facility and release the experimental data).

A number of staffs in the Thermalhydraulics Development Branch of Chalk River Laboratories have assisted me in the experiment. I thank Mr. T. Kennedy (retired member), Mr. B. Lutes (retired member) and Mr. J. Schenk for the construction of test section, Mr. B. Cowhey for setting up the electronic instrument, Mr. J. Martin for programming the data-acquisition system, and Mr. K.F. Rudzinski, Mr. K. Moore and Mr. E. Lindeman (retired member) for operating the MR-1 high-pressure loop.

The comments and suggestions provided by the Advisory Committee for my Ph.D. program (consisting of Dr. W.L. Hallett and Dr. R. Milane of University of Ottawa as well as Dr. E.G. Plett of Carleton University) are also appreciated.

Table of Contents

NOMENCLATURE

Symbol	Definition	Unit
A	Flow Area	m^2
B	Chisholm Parameter	-
B_1..... B_5	Chexal-Lellouche Constants	-
Bo	Boiling Number (= $q/(G\ H_{fg})$)	-
C, C_2	Chisholm Parameters	-
C_o	Distribution Parameter	-
C_p	Specific Heat Capacity	$J.kg^{-1}.K^{-1}$
D	Tube Diameter	m
E	Entrained-Liquid Fraction	-
F	Liquid-Film Fraction (or Enhancement Factor, Chisholm Integral Term)	-
Fr	Froude Number ($=G^2/(g\ D\ \rho^2)$)	-
f	Friction Factor	-
G	Mass Flux	$kg.m^{-2}.s^{-1}$

g	Acceleration due to Gravity (= 9.806)	$m.s^{-2}$
h	Heat-Transfer Coefficient	$W.m^{-2}.K^{-1}$
H	Enthalpy	$J.kg^{-1}$
H_{fg}	Latent Heat of Vaporization	$J.kg^{-1}$
j	Superficial Velocity	$m.s^{-1}$
K	Slip Ratio	-
k	Thermal Conductivity	$W.m^{-1}.K^{-1}$
L	Length	m
m	Constant	-
Nu	Nusselt Number (= h D / k)	-
n	Constant	-
P	Pressure	kPa, MPa
Pe	Peclet Number (= G D C_p / k)	-
Pr	Prandtl Number (= μ C_p / k)	-
Q	Volumetric Flow Rate	$m^3.s^{-1}$
q	Surface Heat Flux	$W.m^{-2}$
q_o	Internal Heat Generation	$W.m^{-3}$
R	Tube Radius	m
Re	Reynolds Number (= G D / μ)	-
r	Radial Distance	m
r_2	Martinelli-Nelson Multiplier for Pressure Gradient due to Acceleration	-
S	Tube Perimeter (or Suppression Factor)	m (-)
St	Stanton Number (= q / (G C_p (T_{sat} - T_l)))	-
T	Temperature	^oC, K
u	Axial Velocity	$m.s^{-1}$
u^*	Shear-Stress Velocity	$m.s^{-1}$
u_{gj}	Drift Velocity	$m.s^{-1}$
W	Mass Flow Rate	$kg.s^{-1}$
We	Weber Number (= G^2 D / (ρ σ))	-
X	Martinelli Parameter	-
x	Quality	-

y	Radial Distance from the Tube Wall	m
Z	Chisholm Shear-Force Function	-
z	Axial Distance	m

Greek	Definition	Unit
α	Void Fraction	-
β	Liquid Volume Fraction	-
ΔP	Pressure Drop	kPa, MPa
δ	Liquid-Film Thickness	m
δ_l	Laminar Sublayer Thickness	m
ε	Absolute Roughness Height (or Eddy Viscosity, emissivity)	m (or $m^2.s^{-1}$, -)
Γ	Chisholm Property Index	-
ι	Mixing Length	m
κ	Prandtl Single-Phase Constant (=0.4)	-
μ	Dynamic Viscosity	$kg.m^{-1}.s^{-1}$
ν	Kinematic Viscosity	$m^2.s^{-1}$
ϕ^2	Two-Phase Multiplier	-
ψ	Groeneveld-Delorme Parameter	-
ρ	Density	$kg.m^{-3}$
σ	Surface Tension	$N.m^{-1}$
τ	Shear Stress	Pa
θ	Angle of Tube Orientation from a Horizontal Plane	rad

Subscript	Definition
A	Apparent
a	Acceleration, Actual Vapour Mass
adia.	Adiabatic Flow

b	Bulk Fluid Condition
boil	Boiling Flow
bub	Bubbly Flow
Ber	Berenson Correlation
c	Critical Condition (or Core Condition in Annular Flow)
core	Core Condition in Annular Flow
cp	Constant Fluid Property Value
conv	Convection
D	Due to Drag
dffb	Dispersed Flow Film Boiling
drop	Droplet Flow
e	Equilibrium
f	Friction, Saturated-Liquid Condition
film	Film Condition
g	Gravity, Gas/Vapour, Gas-Only Flow
go	Total Flow as Gas or Vapour
H	Homogeneous Flow
he	Heated Section
heated	Heated Tube
i	Interfacial
iafb	Inverted Annular Film Boiling
in	Inlet
iT	Turbulent Fluctuation of Phase i
iW	Wave Fluctuation of Phase i
Lf	Laminar Film
LT	Laminar-Turbulent Transition
l	Liquid, Liquid-Only Flow
lam	Laminar Sublayer
lo	Total Flow as Liquid
m	Maximum
mix	Mixture

NS	No-Slip Conditions
NVG	At Onset of Net-Vapour Generation Point
nb	Nucleate Boiling
pool	Pool Boiling
rad	Radiation
sat	At Saturation
sp	Single-Phase
sub	Subcooled
Tc	Turbulent Core
Tf	Turbulent Film
th	Thermodynamic
tp	Two-Phase
tt	Turbulent-Liquid/Turbulent-Gas Mixture
unheated	Unheated Tube
v	Vapour
va	Actual Vapour
ve	Equilibrium Vapour
vf	Vapour Film
vv	Viscous-Liquid/Viscous-Gas
w	Near-Wall Condition

Superscript	Definition
+	Non-Dimensional Parameter
'	Fluctuating Component in Turbulent Flow

Abbreviation	Definition
CHF	Critical Heat Flux

DNB	Departure from Nucleate Boiling
DP	Differential Pressure
NVG	Onset of Net-Vapour Generation
ONB	Onset of Nucleate Boiling
OSV	Onset of Significant Void
PDO	Post-Dryout
rms	Root-Mean-Square
SNB	Suppression of Nucleate Boiling

LIST OF TABLES

LIST OF FIGURES

1. INTRODUCTION

A pumped system is often employed for circulating and transporting flow mediums (solid, liquid, and vapour, either by themselves or in combination with others) through various components from one location to another. The most common examples of this system are municipal water and natural-gas pipelines. All piping components (including the straight pipes) installed in the flow system have a common characteristic of reducing the system pressure. This is mainly caused by friction between flow medium and channel wall, a change in static head due to a variation in channel elevation, and an additional turbulent effect introduced by local obstructions (such as valves) and a change in flow direction (such as an elbow). Ideally, this reduction in pressure can be minimized by increasing the pipe size, maximizing the number of long straight pipes in a horizontal orientation and minimizing the number of valves and elbows in any flow system. However, it is not always feasible, due to the restriction of the geographical layout and the control of flow circulation. To ensure a smooth operation and maintain a desired flow rate, the pump capacity has to be matched properly with the system requirements.

Economically, the cost is much higher for pumps with large than small capacity. This is especially true for those pumps designed for special applications (e.g., coolant circulation through a nuclear-reactor core, or crude-oil and/or natural-gas transportation through pipelines). There are many causes for this escalation in cost: e.g., design complexity, material and labour requirement, small specific market demand, and energy consumption during operation. It is, therefore, essential to match properly the pump and system requirements for both design and analysis purposes, so that the pump capacity (and therefore the cost) can be minimized.

Pressure drop has been widely investigated for single-phase flow, as demonstrated in the chapters on laminar and turbulent flows in many text books. This information, however, is usually limited to adiabatic flow. Some studies have examined the effect of heating (or large temperature difference between channel wall and bulk fluid) on pressure drop in a single-phase flow. This effect appears to be small at low heat-flux (or small temperature difference) conditions, but becomes significant at high heat-flux (or large temperature difference) conditions. Various methods have been introduced to account for this effect, but the deviation among their predictions is large.

For the past two decades, many studies have focused on pressure drop in two-phase flow. This is mainly in response to the need of information for analyzing problems related to the oil-gas transportation and nuclear-reactor operation. In most studies, two-phase pressure drop was measured with adiabatic two-phase flow. The results have often been employed in analyses of flow inside heated channels as well, primarily based on the assumption that the effect of heating on two-phase pressure drop is negligible. Although this assumption may be valid for low heat-flux conditions, other studies have shown a strong effect of heating on two-phase pressure drop at high heat fluxes. While several empirical correlations were developed to account for this effect, no specific prediction method or model is applicable to high-pressure and high-flow conditions encountered in a nuclear-reactor operation.

As described above, an accurate prediction of pressure drop is essential for hydraulic analysis of a flow system. To improve this accuracy, it is important to properly account for the heat-flux

effect on pressure drop. This study focuses on the two-phase pressure drop in a heated channel, in particular to one with a high surface heat flux that leads to a large temperature difference between channel wall and bulk fluid. It is the objective of this study to derive a generalised model for predicting the pressure drop along a heated channel during flow boiling at high-pressure and high-flow conditions. This model will be used for applications related to the nuclear-reactor, boiler, process, chemical, and electronic industry.

The discussion begins in Chapter 2, where the fluid-flow phenomena related to single-phase pressure drop are presented. Both the single-phase flow structure and the velocity distribution are described. The present study focuses mainly on the frictional pressure gradient, but the equations for the pressure gradients due to acceleration and gravity are also discussed for both unheated (adiabatic flow) and heated channels. Most textbooks on fluid flow and heat transfer may be used as a reference for additional information (e.g., Streeter and Wylie [1975] and Özişik [1985]). In view of the general nature of these books, a detailed discussion is presented here of the effect of temperature gradient between the channel wall and the bulk fluid on the frictional pressure drop. Some recent investigations of this effect in single-phase flow are also described.

Chapter 3 presents a general description of two-phase flow, including the flow-pattern (or phase-distribution) determination, vapour mass quality and void fraction. A review of two-phase pressure-drop prediction methods is given, which includes the differences between single-phase and two-phase flow, and calculation methods for the pressure gradients due to acceleration and gravity.

A description of heat-transfer modes and transition points encountered during flow boiling inside a heated tube is presented in Chapter 4. The relation of heat flux and wall temperature (or wall superheat) is shown with the boiling curve. It is followed by a presentation of corresponding prediction methods for heat-transfer rates.

A literature review of previous studies on two-phase frictional pressure gradient is presented in Chapters 5 and 6. It examines the empirical prediction methods (Chapter 5) and modelling

studies (Chapter 6) for flow inside unheated and heated channels. Chapter 5 provides a description of various definitions in expressing the two-phase pressure drop, and a discussion of both the graphical prediction methods and correlations. Experimental studies are presented for both adiabatic flow and flow boiling that indicates either a negligible or strong effect of surface heating on pressure drop. Chapter 6 examines the analytical models commonly used in predicting the two-phase frictional pressure gradient. These models are separated into five categories based on the underlying assumptions and methodology.

The derivation of a generalised model for predicting pressure drop in a heated channel is presented in Chapter 7. It is based on the force-momentum balance approach, with the frictional pressure drop expressed in terms of the wall shear stress. The mixing-length approach, as in single-phase flow, is used to determine the shear-stress and velocity distributions. Iteration of the volumetric flow rate, based on the integration of velocity gradient, is employed to provide the solution. Due to the complexity of the flow phenomenon, several simplifying assumptions have been introduced. It is the goal of this study to provide a simple but relatively accurate model for a wide range of conditions.

Experimental data have been obtained with steam-water flow in a vertical tube to validate the model. Chapter 8 provides the experimental set up and the procedure for these tests. A description of the high-pressure steam-water test loop and the test section is also presented. This experiment covers a wide range of flow conditions (pressures of 5, 7 and 9.6 MPa, mass fluxes of 1 to 10 $Mg.m^{-2}.s^{-1}$, and inlet qualities of -25% to -1%). A number of observations made during the experiment are described.

Chapter 9 analyzes the experimental results. The data are shown as functions of various parameters and are closely examined for specific trends. Wherever available, the results are shown for different ranges of flow conditions, to indicate either similarity or differences. Besides the measured parameters, the effects of calculated parameters such as vapour-mass quality and void fraction on pressure drop are also discussed.

Comparisons between model predictions and experimental data are shown in Chapter 10. The overall prediction accuracy of the model is presented in a general comparison. Specific parametric trends are discussed. An in-depth examination of the predictions for one independent variable (with other parameters constant) is also carried out. This provides the range of conditions that are valid for the present model.

An assessment of 19 different correlations for two-phase frictional pressure drop is presented in Chapter 11. Comparisons between correlation predictions and experimental data are made, to examine the validity of the correlations for flow boiling (both pre- and post-dryout conditions). A multi-correlation method is also introduced, to extend the application of these correlations. These comparisons focus on both the general and specific prediction accuracy of the correlations. A close examination of the comparison is performed for the best available correlation.

The study is concluded in Chapter 12, where highlights of the model and experimental results are discussed. Specific contributions to the improvement of various prediction methods are emphasized. The limitations of the present model and some recommendations for future work are also described.

2. SINGLE-PHASE FLOW

The single-phase pressure drop is affected by a number of parameters (e.g., pressure, flow rate and fluid temperature). Two of the most important parameters are the flow structure and the velocity distribution, and both of them have a strong impact on the pressure-drop calculation. They are described in Sections 2.1 and 2.2, respectively. Single-phase pressure drop is discussed in Section 2.3.

2.1 SINGLE-PHASE FLOW STRUCTURE

Single-phase flow is generally categorised by its structure: laminar or turbulent. These structures represent different degrees of randomness within the flow streams. Laminar flow occurs when each stream flows orderly and in parallel with its neighbours. Even with a non-uniform velocity distribution, there is no mixing or crossing over. Turbulent flow, on the other hand, represents a completely random flow structure. Interaction between various flow streams is frequent and

continuous, and a strong mixing between the high- and low-velocity fluids significantly affects the velocity distribution. In a flow system, a criteria based on the Reynolds number is generally accepted as a means of identifying the flow structure. The Reynolds number is defined as

$$Re = \frac{G\,D}{\mu} \tag{2.1}$$

where G is the mass flux in $kg.m^{-2}.s^{-1}$, D is the tube diameter in m and μ is the dynamic viscosity of fluid in $kg.m^{-1}.s^{-1}$. Laminar flow is often assumed when the Reynolds number is less than 2300 (values from 2000 to 4000 have been suggested in various studies). Otherwise, the flow is considered to be turbulent. While a variation in fluid temperature does not affect strongly the mass flux and diameter, it has a large impact on the dynamic viscosity of liquid. Figure 2.1

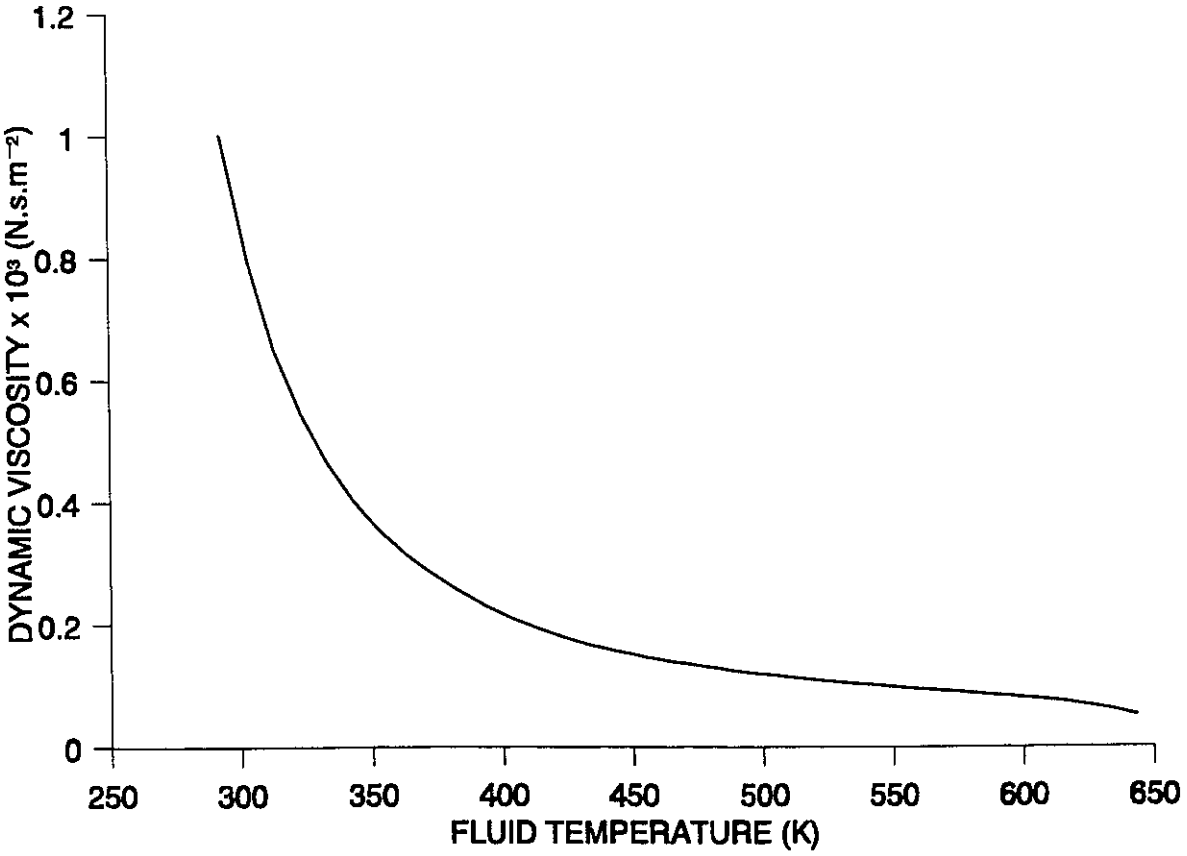

Figure 2.1: Relation Between Dynamic Viscosity and Temperature for Water.

shows the relation between dynamic viscosity of water and temperature. The dynamic viscosity of water changes from 133.9 x 10^{-6} to 90.7 x 10^{-6} $kg.m^{-1}.s^{-1}$ (a reduction of over 30%) when the temperature varies from 200 to 300°C (473.15 to 573.15 K). This difference is even larger at low-temperature conditions (less than 100°C). With the reduction in dynamic viscosity, the Reynolds number is increased accordingly. Therefore, the effect of heating, which primarily raises the temperature of the fluid, has a strong impact on the turbulence level.

2.2 VELOCITY DISTRIBUTION

For flow inside a tube, the fluid can be hypothetically divided into cylindrical layers travelling concentrically with the channel wall as the boundary. Since the channel wall is stationary, the fluid layer at the wall is also assumed to be stationary under the no-slip condition. Away from the wall, the velocity increases and approaches a maximum at the centre-line axis, as shown in Figure 2.2. This velocity distribution also results in a shear-stress distribution between the fluid layers, since shear stress, τ, is proportional to the variation in velocity, u, with respect to a change in radial distance from the wall, y; i.e.,

$$\tau \propto \frac{du}{dy} \tag{2.2}$$

where u is the radial velocity in $m.s^{-1}$ and y is the radial distance from the channel wall in m. Contrary to the velocity distribution, the maximum shear stress occurs in the near-wall region where the steepest variation in velocity is encountered. On the other hand, there is no shear stress in the fluid at the centre-line axis, since the velocity gradient is zero. These represent the two boundary conditions employed in a channel flow.

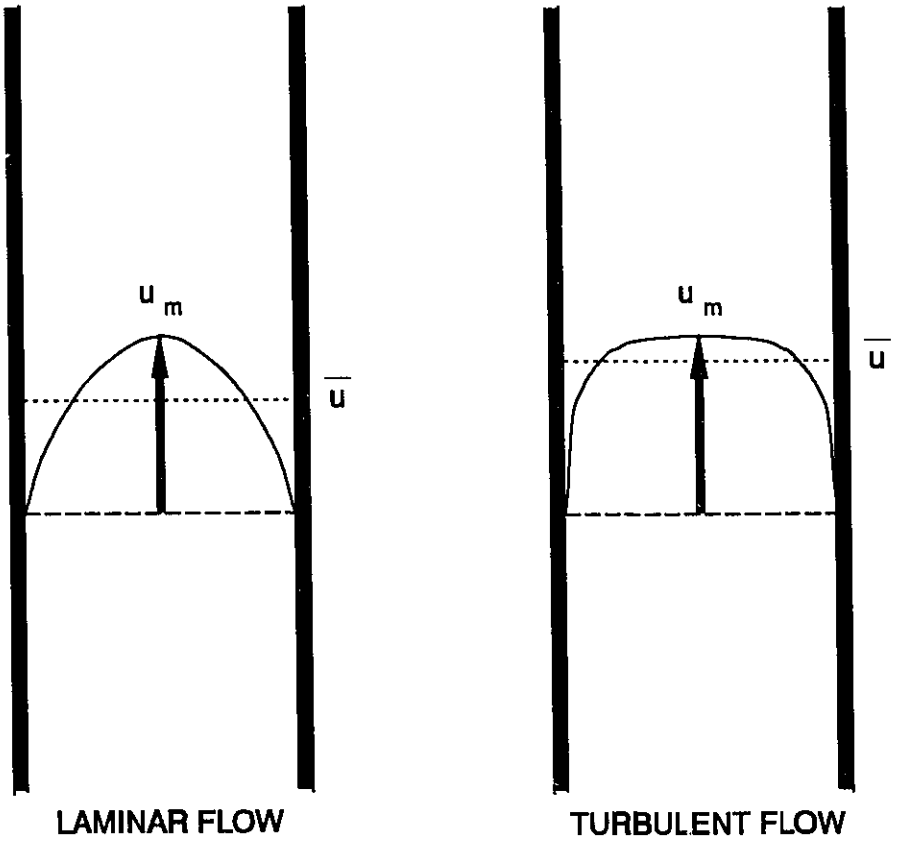

Figure 2.2: Velocity Distributions Inside Tubes.

2.2.1 Laminar Flow

The fluid layers flow in an orderly fashion beside each other and the retardation effect of the wall on flow velocity diminishes slowly in laminar flow. Therefore, a gradual change is exhibited in the radial-velocity distribution. The shear stress is expressed as

$$\tau = \mu \frac{du}{dy} \tag{2.3}$$

where μ is the dynamic viscosity of the fluid, and the velocity gradient becomes

$$\frac{du}{dy} = \frac{\tau}{\mu} \tag{2.4}$$

Expressing the radial shear-stress distribution in terms of the pressure gradient (see Section 2.3), the velocity distribution is obtained from

$$u = \int_0^y \frac{\tau}{\mu}\, dy = \frac{-1}{2\mu}\left(\frac{dP}{dz} + G\frac{du}{dz} + \rho g\right)\int_0^y (R - y)\, dy \tag{2.5}$$

where P is the pressure in Pa, z is the axial distance in m, ρ is the fluid density in $kg.m^{-3}$, g is the acceleration due to gravity in $m.s^{-2}$ and R is the tube radius in m. Integrating Equation (2.5) gives the velocity distribution as

$$u = \frac{-1}{2\mu}\left(\frac{dP}{dz} + G\frac{du}{dz} + \rho g\right)\left(R y - \frac{y^2}{2}\right) \tag{2.6}$$

At the tube centre axis, the local velocity is

$$u = \frac{-1}{2\mu}\left(\frac{dP}{dz} + G\frac{du}{dz} + \rho g\right)\frac{R^2}{2} \tag{2.7}$$

which represents the maximum point of the velocity profile. If the axial velocity gradient is small (e.g., in incompressible flow), the velocity distribution can be further simplified into

$$u = \frac{-1}{2\mu}\left(\frac{dP}{dz} + \rho g\right)\left(R y - \frac{y^2}{2}\right) \tag{2.8}$$

The velocity ratio with respect to the maximum velocity at the centre axis, u_{max}, depends only on the radial location, and is written as

$$\frac{u}{u_m} = \frac{2y}{R} - \left(\frac{y}{R}\right)^2 = 1 - \left(\frac{r}{R}\right)^2 \tag{2.9}$$

2.2.2 Turbulent Flow

The randomness within turbulent flow enhances the mixing of high- and low-velocity fluids, and equalizes the velocity distribution within the central region. In the near-wall region, however, the velocity gradient increases drastically, due to the surface effect that brings the local flow velocity to zero at the wall (no-slip condition). This is illustrated in Figure 2.2. Despite the reduction in velocity gradient in the turbulent core, the shear stress remains significant, since the turbulent effect hampers any free movement of the flow.

In most analyses, turbulent flow in tubes is assumed to consist of three sublayers: laminar, buffer and turbulent. The boundary between sublayers has been determined empirically from Nikuradse's experimental data and is presented with respect to a non-dimensional distance from the wall

$$y^+ = \frac{y\,u^*}{\nu} \tag{2.10}$$

where ν is the kinematic viscosity of the fluid in $m^2.s^{-1}$ and u* is the shear-stress velocity in $m.s^{-1}$

$$u^* = \sqrt{\frac{\tau_w}{\rho}} \tag{2.11}$$

where τ_w is the wall shear stress in $N.m^{-2}$. The laminar sublayer is assumed for y^+ less than 5, turbulent core is considered for y^+ larger than 30, and the buffer zone covers y^+ from 5 to 30.

In a number of recent studies, the buffer zone was not considered (i.e., only two sublayers) to simplify the analysis (e.g., Matthew [1986] in single-phase flow and Abolfadl and Wallis [1985, 1986] in two-phase annular flow). Although this approach is less accurate at the laminar/turbulent flow transition region, the differences in velocity and shear-stress calculations are small. The transition point between the laminar sublayer and the turbulent core is assumed at $y^+ = 11.6$, which is obtained by solving the velocity profiles at both the laminar sublayer and the turbulent core.

In the laminar sublayer, the shear stress is caused by the viscous effect only. The velocity distribution is expressed as the same form of Equation (2.6) covering the thickness of the laminar sublayer, δ_l.

In the buffer zone, the shear stress is affected by both the viscous and turbulent effects. It is expressed as

$$\tau = (\mu + \rho\ \varepsilon)\ \frac{du}{dy} \tag{2.12}$$

A relationship of eddy viscosity, ε, was derived by Deissler [1952] for the buffer layer. It is expressed as

$$\varepsilon = n^2 u y (1 - e^{-\rho n^2 u y/\mu}) \tag{2.13}$$

with a constant n of 0.1.

In the turbulent core, the viscous effect diminishes and the shear-stress distribution in Equation (2.12) can be simplified to

$$\tau = \rho \, \varepsilon \, \frac{du}{dy} \tag{2.14}$$

Several mathematical formulations of eddy viscosity in turbulent flow have been introduced. Von Karman defined the eddy viscosity, ε, as

$$\varepsilon = \kappa^2 \, \frac{(du/dy)^3}{(d^2u/dy^2)^2} \tag{2.15}$$

where κ is the single-phase coefficient having a value of 0.4. Other definitions consist of empirical constants that have to be determined with experimental data. Among them, the Prandtl mixing-length theory is the most widely used, and has been described in detail by Schlichting [1960]. In this theory, the eddy viscosity is expressed as

$$\epsilon = l^2 \left| \frac{du}{dy} \right| \tag{2.16}$$

The mixing length, ι, is stated by Schlichting [1960] as

> *"... distance in the transverse direction which must be covered by an agglomeration of fluid particles travelling with its original mean velocity in order to make the difference between its velocity and the velocity in the new lamina equal to the mean transverse fluctuation in turbulent flow."*

It is a proportionality factor that cannot be measured experimentally, but a number of correlations have been derived from experimental data of wall shear stress and velocity profile.

Ignoring the viscous effect, the shear-stress distribution is expressed as

$$\tau = \rho\, l^2 \left| \frac{du}{dy} \right| \frac{du}{dy} \tag{2.17}$$

and the velocity gradient becomes

$$\frac{du}{dy} = \sqrt{\frac{\tau}{\rho\, l^2}} \tag{2.18}$$

Expressing the radial shear-stress distribution in terms of the pressure gradient, the velocity distribution is

$$u = \int_{\delta_l}^{y} \sqrt{\frac{\tau}{\rho\, l^2}}\, dy = \sqrt{\frac{-1}{2\rho}\left(\frac{dP}{dz} + G\frac{du}{dz} + \rho g\right)} \int_{\delta_l}^{y} \sqrt{\frac{R-y}{l^2}}\, dy \tag{2.19}$$

Empirical representation of the velocity distribution is often used to simplify the analysis. Similar to the velocity profile in laminar flow, the velocity distribution in turbulent flow is also a function of radial location and can be represented with a power-law relationship

$$\frac{u}{u_m} = \left(\frac{y}{R} \right)^m \tag{2.20}$$

Nikuradse indicated that the exponent, m, varies from 1/6 to 1/10, depending on the Reynolds number. Figure 2.3 shows the variation of velocity profile inside smooth tubes [Bhatti and Shah, 1987]. This relationship is a convenient way to present the velocity distribution and provides a continuous function with respect to the distance away from the wall. However, strictly speaking, it is only valid for the core region, where turbulent flow is fully established. Close to the surface, a laminar sublayer exists and the velocity distribution corresponds closely to laminar

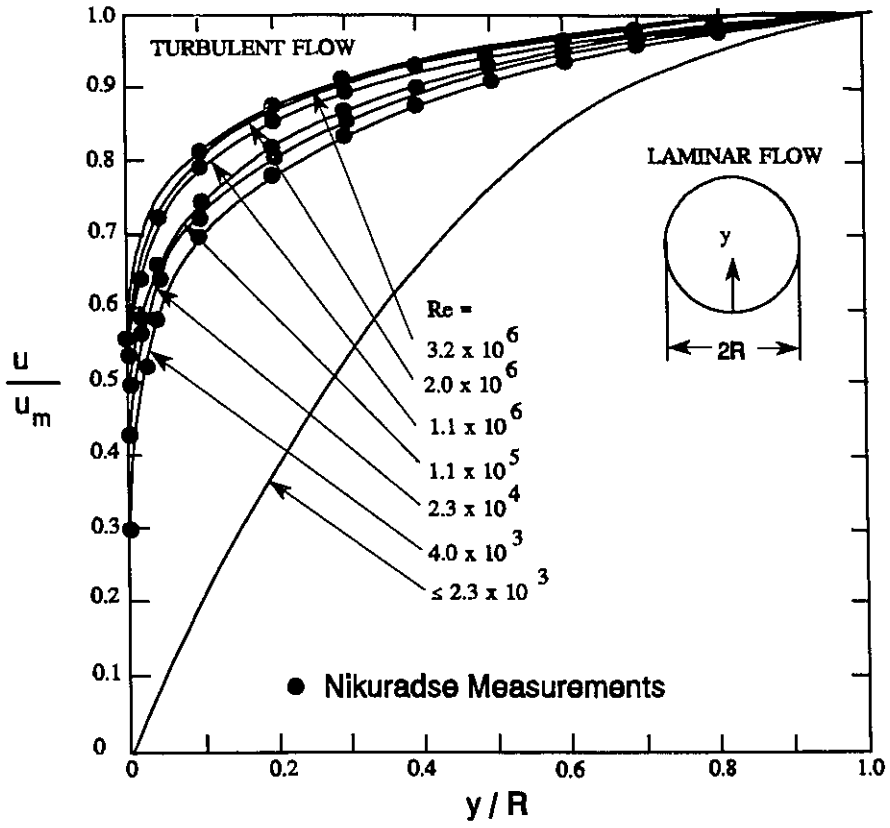

Figure 2.3: Velocity Profiles inside Smooth Tubes for Various Reynolds Numbers [Bhatti and Shah, 1987].

flow. Since the turbulent intensity in the flow becomes strong and the laminar flow cannot be sustained, this sublayer exists only a very short distance from the wall. Between the turbulent core and laminar sublayer, there is a small transition zone, referred to as the buffer zone. Over this zone, a quasi-laminar (or quasi-turbulent) flow is observed and the velocity distribution becomes difficult to identify. Often, an assumed profile (usually linear) is used to relate the laminar and turbulent distributions.

2.2.3 Definitions of Mixing Length for Smooth Pipes

Prandtl introduced the simplest definition of mixing length by assuming a linear proportionality with distance away from the wall; i.e.,

$$l = \kappa\, y \tag{2.21}$$

A value of 0.4 is assumed for the single-phase coefficient, κ. This definition was shown to have limited validity at the near-wall region only. Based on the Von Karman definition (Equation (2.15)), the mixing length is expressed in terms of velocity gradient; i.e.,

$$l = \kappa \left| \frac{du/dy}{d^2u/dy^2} \right| \tag{2.22}$$

This equation predicts a zero mixing length at the centre axis of pipes (where the velocity gradient becomes zero), which has not been observed in experimental results. Furthermore, both definitions are invalid within the laminar sub-layer region, where zero mixing length is anticipated.

An empirical function was introduced by Schlichting [1960] and represents closely the mixing length calculated from experimental data. It is written as

$$\frac{l}{R} = 0.14 - 0.08\left(1 - \frac{y}{R}\right)^2 - 0.06\left(1 - \frac{y}{R}\right)^4 \tag{2.23}$$

At the near-wall region (where y is small), this equation can be simplified to a similar form as the Prandtl definition (i.e., Equation (2.21)), but it is also invalid at the laminar sublayer.

Many other definitions have been proposed, but none of them seems to be valid for all regions. Recently, a composite mixing-length definition was introduced by Matthew [1986], who employed a two-layer (rather than three-layer) analysis by ignoring the buffer region (i.e., direct transition from the laminar sublayer to the turbulent core). In terms of dimensionless parameters (defined as in Equation (2.10) with respective parameter), the mixing length is expressed as

$$l^+ = 0 \tag{2.24}$$

for y^+ less than the laminar sublayer thickness, δ_l^+, and

$$l^+ = \kappa \, (y^+ - \delta_l^+) \left(1 - \frac{y^+ - \delta_l^+}{2 \, (R^+ - \delta_l^+)} \right) \tag{2.25}$$

for y^+ greater than δ_l^+. The constants κ and δ_l^+ were optimized with experimental data and are 0.41 and 6.99, respectively.

2.2.4 Universal Velocity Profile for Smooth Pipes

Based on the Prandtl definition of mixing length (Equation (2.21)), the velocity distribution in turbulent flow can be obtained by integrating the shear-stress expression. It is written as

$$\frac{u}{u^*} = \frac{1}{\kappa} \ln y^+ + constant \tag{2.26}$$

This distribution can also be presented with respect to the maximum velocity, u_m, at the centre axis (where y = R) to eliminate the constant term. It is expressed as

$$\frac{u_m - u}{u^*} = \frac{1}{\kappa} \ln \frac{R^+}{y^+} \tag{2.27}$$

which is often referred to as the velocity-deficiency equation.

Based on the experimental data of turbulent flow inside a smooth tube, the velocity distribution can be expressed as

$$u^+ = \frac{u}{u^*} = \frac{u^* y}{\nu} = y^+ \tag{2.28}$$

in the laminar sublayer (i.e., $y^+ \leq 5$),

$$u^+ = 5 \ln y^+ - 3.05 \tag{2.29}$$

in the buffer zone (i.e., $5 < y^+ < 30$), and

$$u^+ = 2.5 \ln y^+ + 5.5 \tag{2.30}$$

in the turbulent core (i.e., $y^+ \geq 30$). The composite velocity distribution of Equations (2.28) to (2.30) is referred to as the universal-velocity profile.

If the buffer zone is ignored (a two-region flow), the thickness of the laminar sublayer can be derived by solving Equations (2.28) and (2.30). It is expressed as

$$\delta_l = \frac{11.6\ \nu}{u^*} \tag{2.31}$$

This is different from the empirical value presented by Matthew [1986], who suggests a constant of 6.99 rather than 11.6. The universal velocity distribution law for smooth tubes is illustrated in Figure 2.4.

2.2.5 Velocity Profiles for Rough Pipes

The velocity profile for flow inside a rough pipe depends on the height of the roughness projections. For projections that do not extend beyond the laminar sublayer thickness, there is no effect on the velocity profile, and the pipe is considered to be smooth. Once the projections protrude into the buffer or turbulent zone, the laminar sublayer cannot be established due to the additional turbulence effect caused by the surface roughness. Therefore, the turbulent velocity

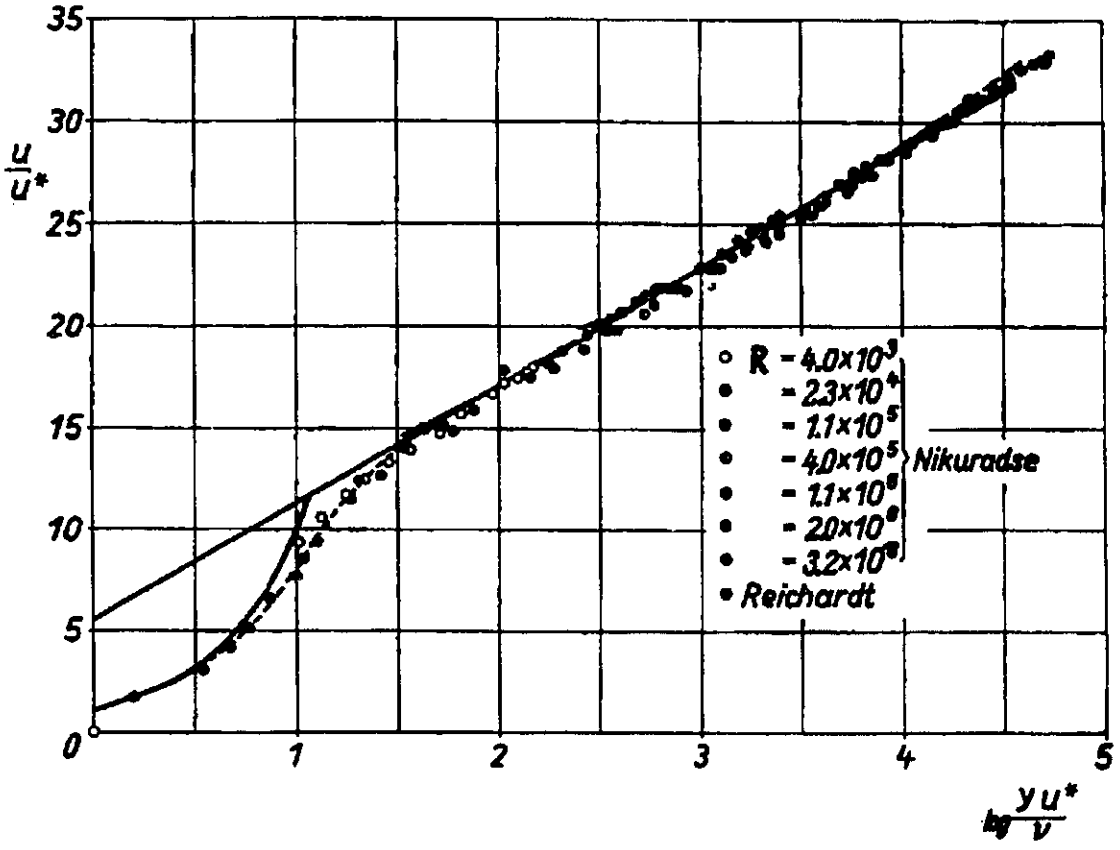

Figure 2.4: Universal Velocity Profiles for Various Reynolds Numbers [Schlichting, 1960].

distribution is extended from the characteristic height of the roughness element to the centre axis of the flow. An equation similar to the one for a smooth surface is used to calculate the velocity distribution. However, the characteristic height of the roughness is used as the boundary-layer thickness; i.e.,

$$\frac{u}{u^*} = 2.5\ ln\left(\frac{y}{\varepsilon}\right) + 8.5 \tag{2.32}$$

where ε is the roughness height in m. This equation is referred to as the Karman-Prandtl equation. The constant value of 8.5 was determined empirically with Nikuradse's experimental data. Figure 2.5 shows the data of Nikuradse for pipes with various relative-roughness values. The velocity-deficiency law (Equation (2.27)) is valid for both smooth and rough pipes.

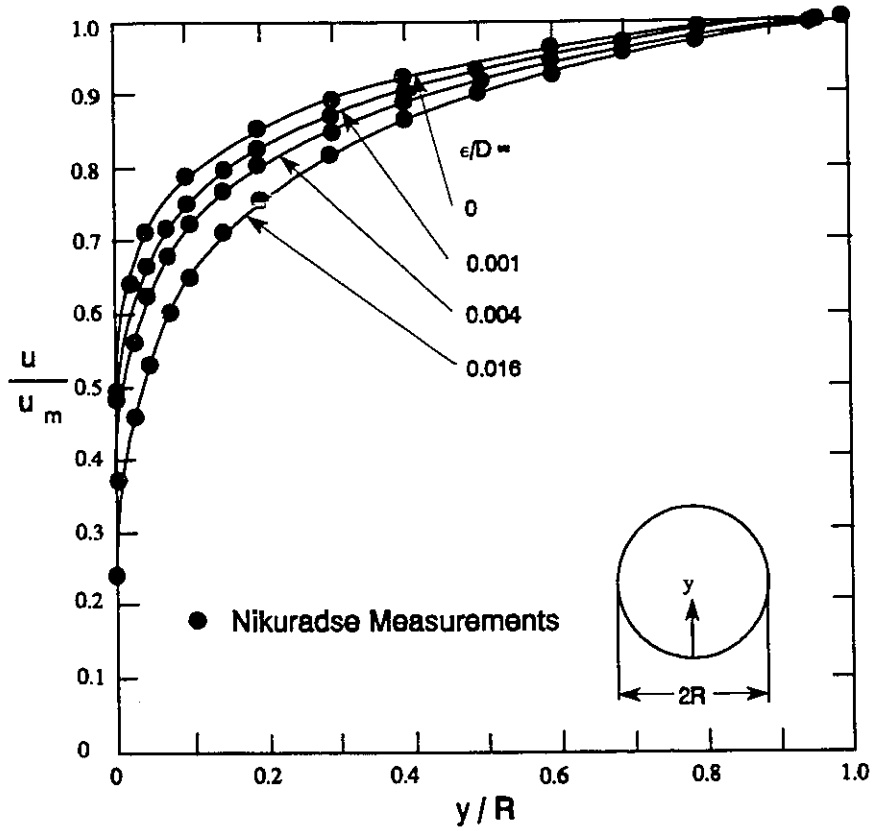

Figure 2.5: Fully Developed Turbulent Velocity Distributions in a Rough Tube.

In addition to the empirical approach, a number of studies have attempted to model the effect of surface roughness on velocity distribution (e.g., Han [1991]) by modifying the mixing-length expressions. This appears to contradict the experimental results shown in Figure 2.6 [Schlichting, 1960], where the same radial mixing-length distribution is valid for several pipe-roughness values.

2.2.6 Effect of Heating on Velocity Distribution

A temperature gradient between the heated surface and the bulk fluid changes the velocity distributions in both laminar and turbulent flow [Rohsenow and Hartnett, 1973, Kakac, 1987 and Buhr et al., 1972]. It tends to steepen the velocity gradient for a liquid flow at the near-wall

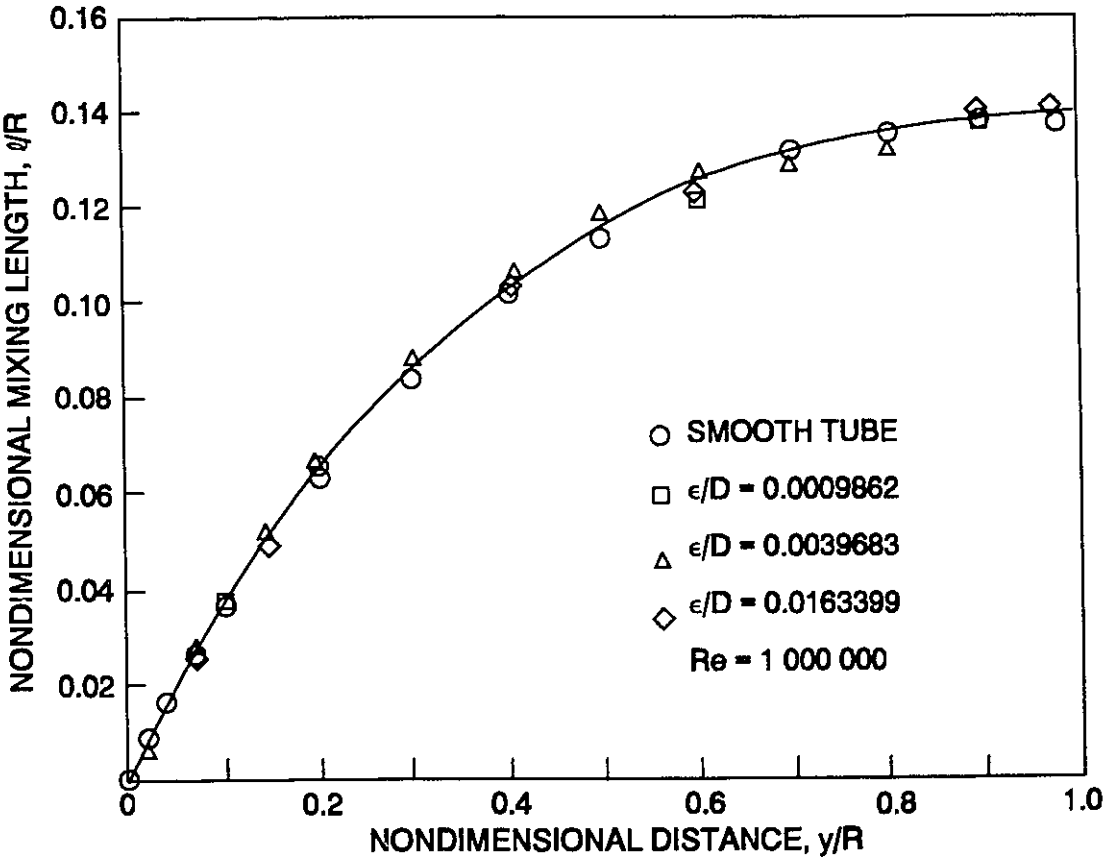

Figure 2.6: Mixing-Length Variation in Rough Pipes [Schlichting, 1960].

region of a heated surface (Figure 2.7) (caused by a reduction in fluid viscosity). Due to the rather uniform velocity distribution at regions beyond the laminar sublayer, the effect of temperature gradient is less severe in turbulent flow, compared to laminar flow.

For a fluid of a low Reynolds number, a localized effect may be encountered. This was shown by Buhr et al. [1972], who observed a change in radial velocity distribution from a power-law (Equation (2.19)) to a saddle shape in a turbulent flow of mercury with increasing surface heat flux. For a gas flow, however, the viscosity increases with increasing temperature. Therefore, the velocity gradient is reduced near the heated surface, but increased in the core.

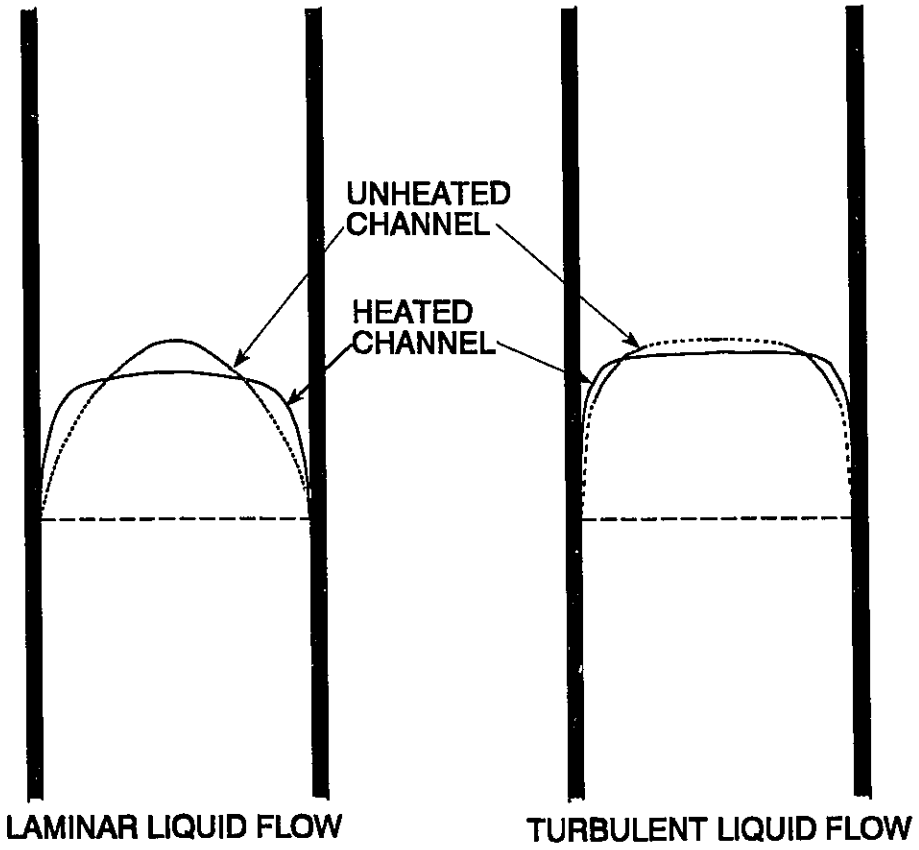

Figure 2.7: Velocity Gradient of Flow Inside a Heated Tube.

2.3 SINGLE-PHASE PRESSURE DROP

Pressure drop is a measure of the change in forces applied by the flow on the flow boundary. Considering the control volume in a uniform tube as shown in Figure 2.8, a force-momentum balance results in

$$\int_A \left[P - \left(P + \frac{dP}{dz} \delta z \right) \right] dA = \int_S \tau_w \delta z \, dS + \int_A \frac{d}{dz}(Gu)\, \delta z \, dA + \int_A \rho \, g \sin\theta \, \delta z \, dA \tag{2.33}$$

where A is the cross-sectional flow area in m^2, S is the tube perimeter in m and θ is the angle of tube orientation from a horizontal plane. For a constant flow velocity, mass flux, wall shear stress and fluid density (i.e., adiabatic flow inside an unheated tube), this equation is reduced to

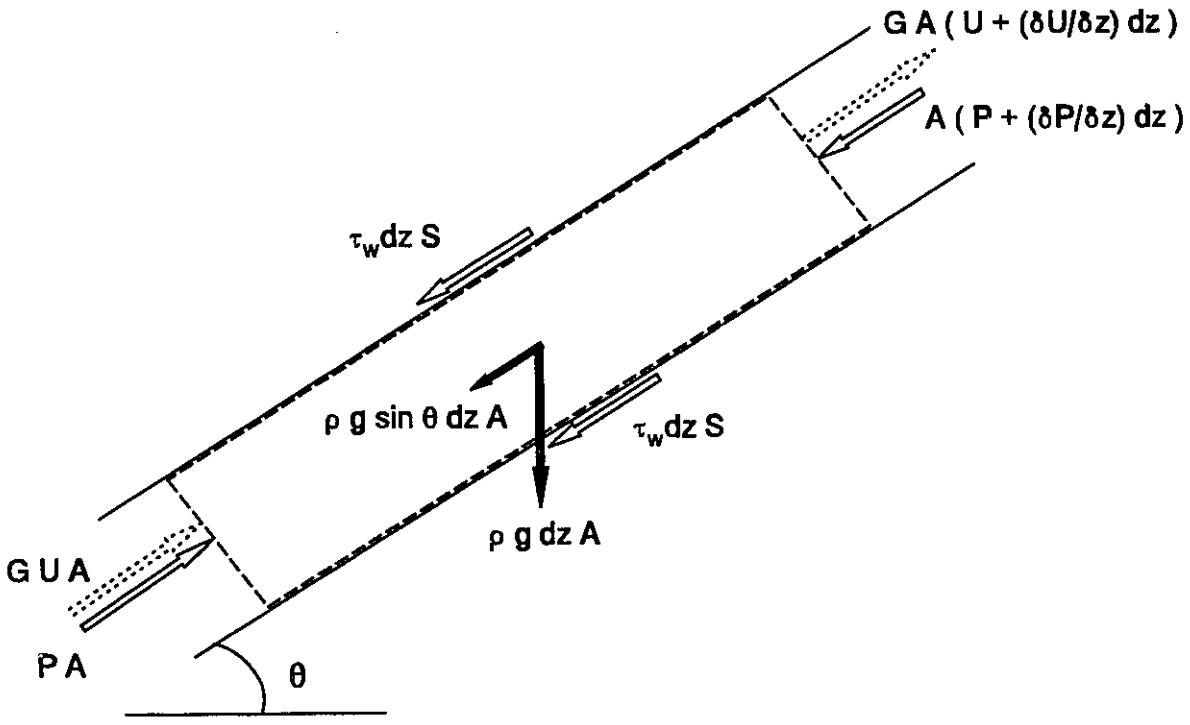

Figure 2.8 : A Force-Momentum Balance on a Control Volume of Flow inside a Tube.

$$-\frac{dP}{dz} = \frac{S}{A}\tau_w + G\frac{du}{dz} + \rho g \sin\theta \tag{2.34}$$

The overall pressure gradient consists of three components: friction, acceleration and gravity.

Assuming a constant pressure gradient over the cross-sectional area, the radial shear-stress distribution can also be calculated using Equation (2.34); i.e.,

$$\tau = -\frac{r}{2}\left(\frac{dP}{dz} + G\frac{du}{dz} + \rho g \sin\theta\right) \tag{2.35}$$

2.3.1 Pressure Gradient due to Friction

The frictional pressure gradient is mainly caused by the skin friction between the fluid and the channel surface. As indicated above, it is expressed in terms of the wall shear stress based on the force-momentum balance; i.e.,

$$-\left(\frac{dP}{dz}\right)_f = \frac{S}{A}\tau_w = \frac{4\tau_w}{D} \tag{2.36}$$

The wall shear stress can be evaluated analytically for laminar flow with the velocity profile. However, an empirical approach is used for turbulent flow as the velocity distribution remains uncertain. The frictional pressure gradient is assumed to be proportional to the kinetic energy of the flow, and is expressed as

$$-\left(\frac{dP}{dz}\right)_f = \frac{f}{D}\frac{\rho u^2}{2} \tag{2.37}$$

where f is the friction factor that is obtained empirically. This is often referred to as the D'Arcy-Weisbach equation. Comparing Equations (2.36) and (2.37), the relation between wall shear stress and friction factor is

$$\sqrt{\frac{\tau_w}{\rho}} = \sqrt{\frac{f}{8}}\, u \tag{2.38}$$

2.3.1.1 Flow Inside an Unheated Channel (Adiabatic Flow)

For laminar flow, the friction factor is expressed as

$$f = \frac{64}{Re} \tag{2.39}$$

This equation was derived analytically (e.g., see Streeter and Wylie [1975]) and is referred to as the Hagen-Poiseuille law. It indicates a linear relationship between the friction factor and the Reynolds number, and is independent of the surface roughness.

For turbulent flow, however, no analytical solution is available and the friction factor is obtained empirically. Based on Nikuradse's experimental data, the friction factor for smooth pipes is implicitly presented as

$$\frac{1}{\sqrt{f}} = 0.86 \ln (Re \sqrt{f}) - 0.8 \tag{2.40}$$

and for rough pipes in the fully developed turbulent-flow region

$$\frac{1}{\sqrt{f}} = 1.14 - 0.86 \ln \frac{\varepsilon}{D} \tag{2.41}$$

where ε/D is the relative roughness of the pipe surface. A number of simplified equations, which express friction factor explicitly in term of Reynolds number only, have been presented for smooth pipes (e.g., Guislain [1980] and Kakac [1987]). These equations, however, have a limited range of validity. For example, the Blasius equation for the friction factor of a smooth pipe is written as

$$f = 0.316\ Re^{-0.25} \tag{2.42}$$

and is valid for Reynolds numbers up to about 100 000.

In the transition region between laminar and fully developed turbulent flow, the friction factor is affected by both relative roughness and the Reynolds number. Based on the data of commercial pipes, Colebrook [1939] presented the friction factor as

$$\frac{1}{\sqrt{f}} = -0.86 \ln \left(\frac{\varepsilon / D}{3.7} + \frac{2.51}{Re\sqrt{f}} \right) \tag{2.43}$$

which has been used as the reference equation for pipe-flow calculation. Since the friction factor is implicitly presented, its evaluation is rather difficult. To simplify the evaluation procedure, Moody [1944] devised a graph that shows the friction factor as a function of Reynolds number and relative roughness based on the Colebrook equation. Moody's graph is shown in Figure 2.9 and is particularly useful for hand calculations. A number of explicit equations have since been presented for the friction factor over the transition and the fully developed turbulent-flow regions [Kakac, 1987]. Gregory and Fogarasi [1985] compared the friction factors evaluated with 12 different equations and found that the Chen equation [1979] agrees the closest with the Colebrook equation. The Chen equation is expressed as

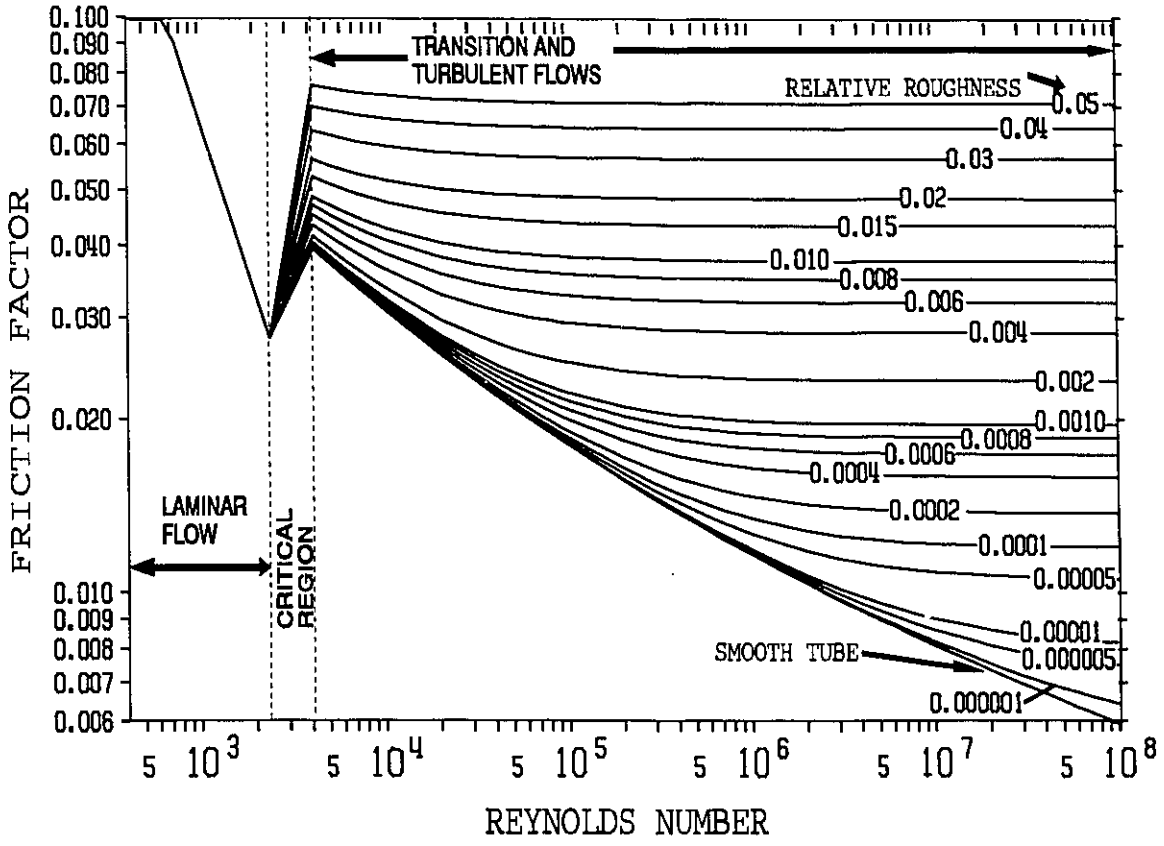

Figure 2.9: Moody's Graph for Friction Factor in Pipes.

$$\frac{1}{\sqrt{f}} = -2\log\left(\frac{\varepsilon/D}{3.7065} - \frac{5.0452}{Re}\log\left(\frac{(\varepsilon/D)^{1.1098}}{2.8257} + \frac{5.8506}{Re^{0.8981}}\right)\right) \tag{2.44}$$

2.3.1.2 Flow Inside A Heated Channel

A temperature gradient between a heated surface and bulk fluid can significantly affect the pressure drop. This is mainly caused by changes in the near-wall viscosity and velocity distribution. These changes, however, have a compensating effect on each other, since a rise in temperature gradient reduces the near-wall viscosity but increases the near-wall velocity gradient (see Figure 2.7). In view of the moderate effect on velocity gradient, but strong effect on viscosity, a reduction in pressure gradient is anticipated in turbulent flow of liquid.

Due to the coupling effect between the conservation equations of momentum and energy, an analytical solution of the effect of heating on pressure gradient is difficult to achieve. Most analyses were performed on a purely empirical or semi-analytical basis.

Colburn [1933] examined a large number of data of various fluids. He observed that the heating effect can be accounted for by simply employing the fluid properties based on the film temperature, rather than the bulk-fluid temperature, in the friction factor for adiabatic flow (e.g., Equations (2.39) to (2.44)). The film temperature was expressed as

$$T_{film} = \frac{T_b + T_w}{2} \tag{2.45}$$

The subscripts "b" and "w" correspond to parameters evaluated at the bulk and near-wall fluid conditions, respectively.

Sieder and Tate [1936] found that the use of film-temperature properties does not apply for all conditions. They recommended a correction to the adiabatic friction factor based on the viscosity ratio between near-wall and bulk fluids. Their correction factor is expressed as

$$\frac{f_{heated}}{f_{unheated}} = \left(\frac{\mu_b}{\mu_w} \right)^m \tag{2.46}$$

Based on their data, the optimized values for the exponent, m, were -0.25 for laminar flow and -0.14 for turbulent flow. These values also agreed with the experimental data of Davis [1943] and Jens and Lottes [1951]. The result of Deissler's numerical analysis of laminar liquid flow, however, indicated a value of -0.58 as the exponent [Deissler, 1951]. The difference may be caused by the inclusion of the pressure drop due to acceleration in the Sieder and Tate analysis.

Rohsenow and Clark [1951] showed that the value of -0.14 agreed rather well with their overall pressure-drop data of high-pressure water flow inside a horizontal tube (pressure drop due to gravity is not present). When only the pressure drop due to friction was considered (i.e., subtract the pressure drop due to acceleration from the total pressure drop), an exponent of -0.6 was more appropriate than -0.14. Owens and Schrock [1960], however, found that their frictional pressure-drop data were best correlated with a value of -0.4.

Maurer and LeTourneau [1963] measured the pressure drop of water flow for a wide range of conditions inside a rectangular channel. They noted a relatively good agreement between their data and the correction factor of Equation (2.46) with an exponent of -0.25. Furthermore, a flow-rate effect on the exponent and a density effect on the friction factor were also observed from their data. A modification to the correction factor was introduced

$$\frac{f_{heated}}{f_{unheated}} = \left(\frac{\mu_b}{\mu_w} \right)^m \left(\frac{\rho_b}{\rho_w} \right)^n \tag{2.47}$$

where n was -0.5 and m was expressed as

$$m = -10\, f_{unheated}$$

The flow-rate dependency for the exponent was not observed by Dormer and Bergles [1964], who indicated that a value of -0.35 was suitable for their low-pressure data. Recently, Petukhov [1970] compared a relatively large number of experimental data obtained with various types of oil flow. A different correction factor was introduced for the heating effect

$$\frac{f_{heated}}{f_{unheated}} = \frac{1}{6} \left(7 - \frac{\mu_b}{\mu_w} \right) \tag{2.48}$$

This correction factor was suggested for the ranges of bulk-fluid Reynolds number from 10^4 to 23×10^4, bulk-fluid Prandtl number from 1.3 to 10, and viscosity ratio (μ_w/μ_b) from 0.35 to 1. Since the result becomes invalid for a viscosity ratio, μ_w/μ_b, less than 0.143 (negative friction factor), this equation should only be used within these ranges. Furthermore, the calculated values of this equation are similar to those obtained from Equation (2.46) with an exponent of -0.11 over these ranges. This would mean that the pressure gradient due to acceleration was probably included in Petukhov's analysis. Recently, Hoffman and Wong [1992] also noted the invalid trend of the Petukhov equation, and used Equation (2.46) with an exponent of -0.3 in their analysis. However, no justification was provided for selecting this value.

Until now, no clear recommendation has been available for the correction of the heating effect on single-phase frictional pressure drop (or gradient). This has been mainly due to the difficulty in measuring accurately the small pressure drops with various types of cooling fluid. However, this correction can have an impact on the prediction of two-phase frictional pressure drop which is often based on the single-phase value.

2.3.2 Pressure Gradient due to Acceleration

The pressure gradient due to acceleration is a measure of the momentum change within the flow along the channel, and is expressed as

$$-\left(\frac{dP}{dz} \right)_a = G \frac{du}{dz} \tag{2.49}$$

In single-phase flow, it is an important component for flow inside a diverging or converging channel where the momentum changes with varying flow area. For an adiabatic liquid flow inside a straight tube, however, this component is not present, since both the mass flux and the flow velocity remain constant. When the channel is heated, the fluid density is no longer

constant axially and hence the fluid momentum changes as well. This is particularly severe in a gas flow, where the pressure gradient due to acceleration can be a significant component.

2.3.3 Pressure Gradient due to Gravity

The pressure gradient due to gravity represents the head loss due to the weight of fluid. It is expressed as

$$-\left(\frac{dP}{dz} \right)_g = \rho \; g \; \sin\theta \tag{2.50}$$

For a vertical channel (where θ is 90°), this gradient is equivalent to the weight of fluid between two points (it is not present in a horizontal channel where θ is 0°). For a varying density condition (such as a heated channel), a mean fluid density is used.

3. TWO-PHASE FLOW

Two-phase flow consists of a simultaneous flow of two different states of matter (i.e., vapour and liquid, liquid and solid, as well as vapour and solid). It is much more difficult to analyze than single-phase flow, since the interaction between the two phases is still uncertain. Similar to single-phase flow, the primary factor influencing two-phase flow is the randomness of flow structure (i.e., laminar or turbulent). A variety of combinations of flow structures can be encountered between the two phases (e.g., laminar-liquid/laminar-vapour flow, laminar-liquid/turbulent-vapour flow, etc.).

In a heated channel, two-phase flow is encountered after boiling (or flashing) has been initiated. One significant difference in two-phase flow between heated and unheated channels is the continuous variation of quality (or fluid enthalpy) for the former, as opposed to a constant quality for the latter, along the axial distance. For the same local conditions, the basic structure of two-phase flow is similar in a heated channel to an unheated channel, except in the near-wall region, where a large temperature gradient exists between the heated surface and bulk fluid.

The first three sections of this chapter describe some of the major parameters affecting two-phase pressure drop: flow patterns (Section 3.1), vapour mass quality (Section 3.2) and void fraction (Section 3.3). Since this study focuses mainly on two-phase pressure drop, only an overview of these parameters is presented with the recommended prediction methods. The general discussion on two-phase pressure drop (due to friction, acceleration and gravity) is introduced later in Section 3.4.

3.1 FLOW PATTERNS

The distribution of phases inside a channel depends on the flow conditions and temperature gradient within the fluid. It is often referred to as the flow pattern or the flow regime, and has a significant influence on both the hydrodynamic and heat-transfer aspects of two-phase flow. For example: the heat-transfer rate at the heated wall is higher for a liquid-to-wall than vapour-to-wall contact, due to a higher thermal conductivity for liquid; the same is true for pressure drop, since viscosity is also higher for liquid. Overall, there are five different patterns identified in vertical channels, and six in horizontal channels for adiabatic flow [Hewitt, 1977]. The main difference between vertical and horizontal flow patterns arises from the effect of gravity on the horizontal flow. This effect tends to bring the liquid flow towards the bottom of the channel at low mass-flux values.

3.1.1 Flow-Pattern Description

Detailed descriptions of various flow patterns have been presented by Collier [1981] and Hewitt and Hall-Taylor [1970]. They have been summarised for horizontal flow in a previous study [Leung, 1983]. A brief description of flow patterns in vertical flow (Figure 3.1) is presented in this study. Although various terminologies have been used to describe the flow patterns, they can be roughly categorised as bubbly, slug, churn, annular, and wispy-annular in adiabatic flow.

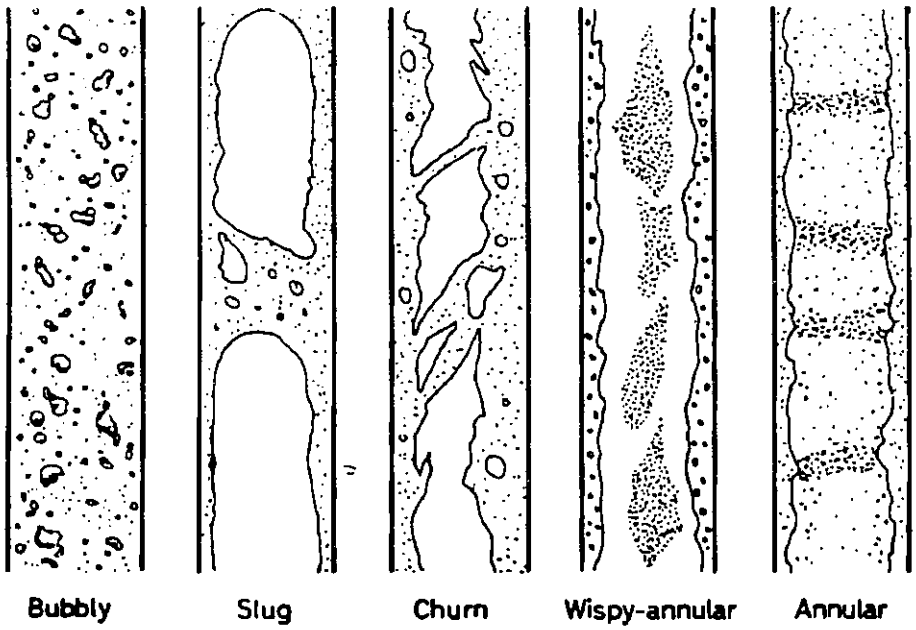

Figure 3.1: Flow Regimes in Vertical Co-Current Flow [Collier, 1981].

In a heated channel, the flow regime varies continuously, due to a change in local conditions along the channel. Figure 3.2 presents the flow-pattern variations for high- and low-quality flows. While the flow patterns of adiabatic flows are also observed inside a heated channel, two additional regimes (inverted-annular and dispersed-droplet flows) can be encountered at conditions beyond the critical heat flux (CHF).

3.1.1.1 Bubbly Flow

Flow inside an Unheated Channel

Bubbly (or bubble) flow comprises a dispersion of bubbles travelling within the liquid. The size and distribution of these bubbles depend mainly on the flow conditions, fluid properties, and the method used to introduce the phases in adiabatic flow.

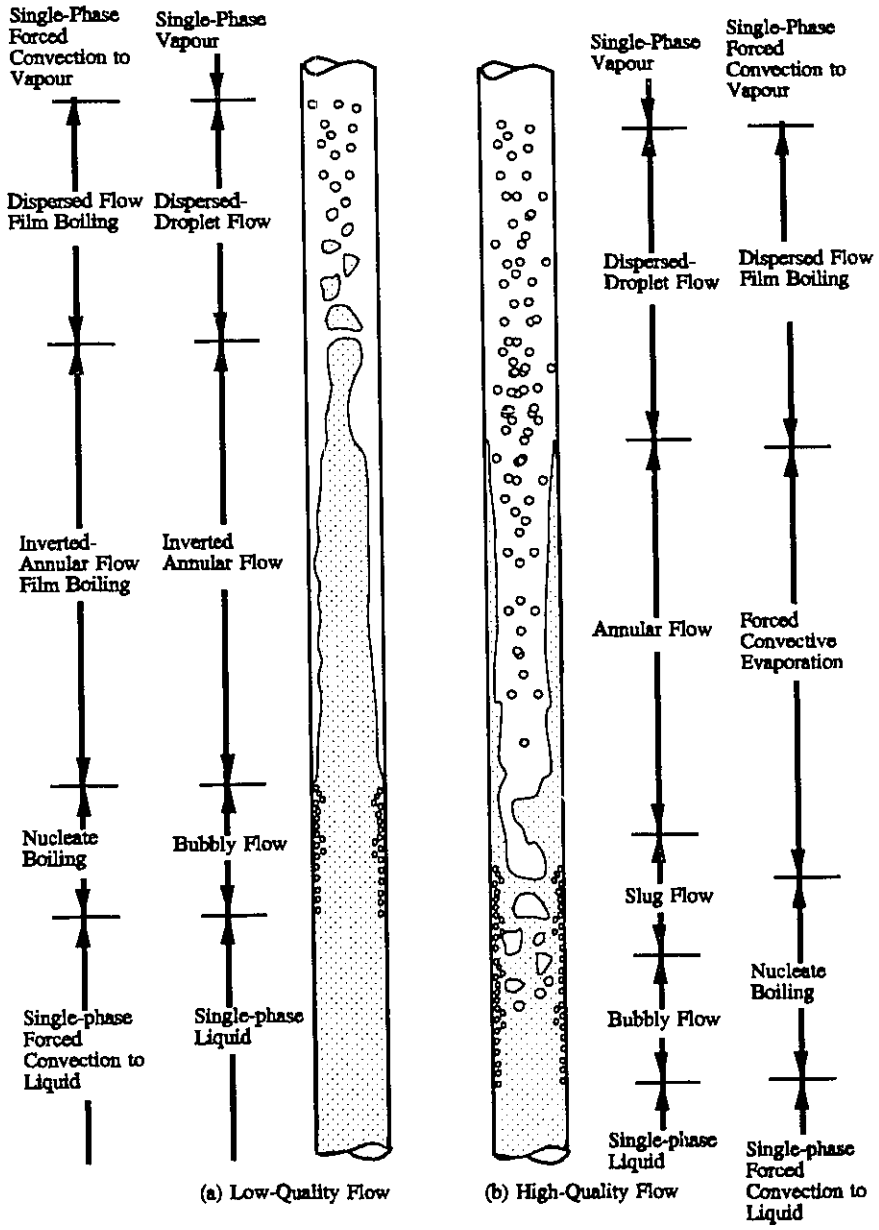

Figure 3.2: Flow-Pattern Variations in Heated Channels.

For a low-quality flow, the bubbles are generally small. The high shear force of liquid breaks up the large bubble and prohibits coalescence among small bubbles. On the other hand, the concentration of bubbles is usually high in the vicinity of the surface in both adiabatic and boiling flow. A saddle-shaped profile of vapour volumetric fraction is often encountered (Figure 3.3).

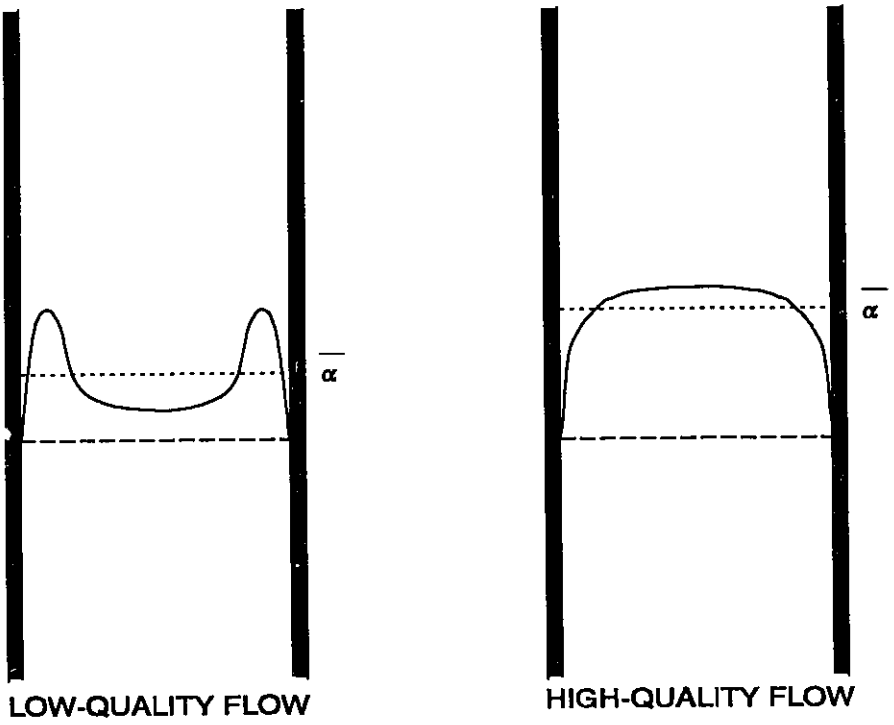

Figure 3.3: Void-Fraction Distributions in Bubbly Flow.

For a high-quality flow, the bubble size tends to be large and the distribution of bubbles is more uniform across the flow area than the low-quality flow (Figure 3.3). Bankoff [1960] suggested the use of a power-law relation for vapour volumetric fraction. The transition between these two cases is still uncertain, but is known to be affected by the primary flow parameters, such as pressure and flow velocity.

At very high flow velocity, the bubble concentration becomes high and a well-mixed bubbly mixture is formed inside the channel. This is often referred to as the froth flow.

Flow inside a Heated Channel

In a heated channel, bubbles can be formed through bulk or surface nucleation. The distribution of these bubbles in the channel is not only affected by the same dominant factors as in adiabatic flow, but also by the temperature gradient within the fluid.

Bulk nucleation occurs within the liquid core and is mainly caused by a change in pressure where the bulk fluid exceeds the saturation temperature (i.e., flashing). Bubbles are preferentially created on any impurity inside the fluid. They are often large and grow rapidly. This type of nucleation is more significant at low-pressure than high-pressure conditions, since pressure drop over the channel is much higher at low pressure.

Surface nucleation is the main source of bubble generation. It occurs in cavities of a surface that reach a certain liquid superheat. At low liquid-superheat conditions, bubbles form and collapse frequently. None of them is able to attain a fully developed shape, since the fluid enthalpy is still below saturation. With an increase in liquid superheat, bubbles sustain from collapse and remain in the vicinity of the heated surface. With increasing bubble population, a saddle-shaped distribution is formed (see Figure 3.3). The density of bubbles in the core region increases with increasing fluid enthalpy; the bubble distribution changes from a saddle to a power-law profile.

3.1.1.2 Slug Flow

With an increase in bubble population, bubble coalescence becomes more prevalent. This increases the bubble size and the buoyancy force on the bubble, hence the bubble velocity. For a low liquid velocity, where the shear force is weak, bubble coalescence occurs rapidly, forming a large vapour slug. The bullet-shaped slug travels at a much higher velocity than the liquid. As the liquid upstream of the slug moves downstream through the liquid film between the slug and the surface of the channel, a stagnant liquid flow, or even flow reversal, can be encountered in the near-wall region. Due to the high turbulence level in the wake of the slug, a stream of trailing bubbles is often encountered.

In a heated channel, the liquid film between the surface and the vapour slug is at saturation and only limited amount of superheat is permitted. Due to the low flow velocity, bubbles may still be generated in the liquid film, since the heat-transfer rate is significantly reduced. For high

heat-flux conditions, the liquid film could break down, leading to a burnout situation (this will be discussed in a later section).

3.1.1.3 Churn Flow

Churn flow has a similar structure as the slug flow, but it occurs mainly at high liquid velocity. A transition from slug to churn flow is also encountered as the vapour velocity increases. Due to the high turbulence level, an irregular-shaped pocket of vapour with liquid bridging across the flow area is formed, rather than a bullet-shaped slug. It occupies a much smaller cross-sectional flow area than the slug, and has a wavy liquid-vapour interface. While this pocket also travels at a higher velocity than the liquid, unlike the slug flow, no stagnant flow or flow reversal is encountered in the near-wall region. The displacement of liquid upstream of the vapour pocket results in a liquid film with high velocity. This increases the heat-transfer rate in a heated channel and hence suppresses the bubble formation at the surface. Due to the wavy liquid-vapour interface, the interfacial shear stress is also high.

3.1.1.4 Annular Flow

At high vapour velocities, the liquid bridges (which are characteristic of churn flow) collapse and the vapour phase in the core becomes continuous and is surrounded by a liquid film. This is referred to as annular flow. For most conditions, part of the liquid from the collapsed bridge is entrained inside the vapour core. Therefore, while only liquid is observed in the film, a mixture of liquid droplets and vapour flows in the core. The structure of the liquid/vapour interface depends strongly on the flow conditions. It is smooth at low flow but becomes wavy as the flow increases. With an increase in wave amplitude, the high-velocity vapour can shear off the crest of the wave. This leads to an increase in droplet population in the core, and a reduction in the liquid-film thickness with increasing vapour velocity. With an increase in entrained liquid

fraction (droplet concentration), droplet deposition back to the film becomes important as well. An equilibrium entrained liquid fraction exists for each set of flow conditions (Figure 3.4).

A phenomenon similar to that in single-phase liquid flow occurs in a heated channel. That is, the velocity gradient is increased and the liquid viscosity is reduced at the near-wall region. However, the change in velocity gradient also reduces the local velocity of the liquid phase at the region close to the interface. This increases the interfacial shear stress, and in turn, the entrainment rate.

3.1.1.5 Wispy-Annular Flow

Wispy-annular flow can be encountered at high velocity (both liquid and vapour) conditions. Its structure is similar to annular flow, but it has a very high concentration of entrained droplets in

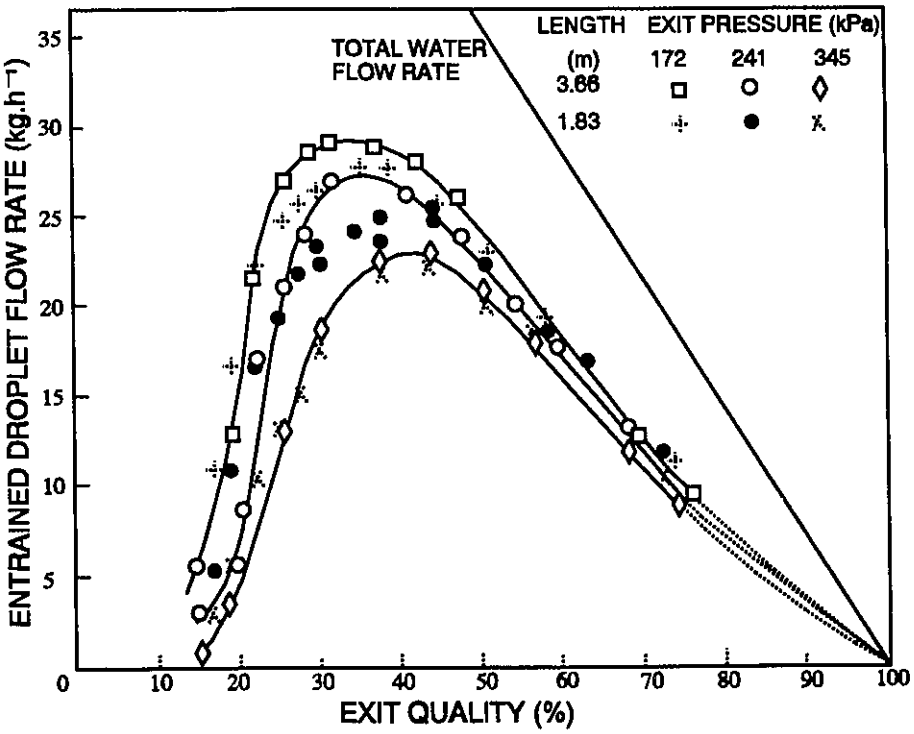

Figure 3.4: Entrainment Flow Rate in Steam-Water Flow [Hewitt and Hall-Taylor, 1970].

the vapour core. In some cases, the entrained droplets coalesce together, forming filaments of liquid in the core. The liquid film may contain entrained vapour bubbles. An unstable liquid/vapour interface has also been observed, and results in an increased entrainment rate.

The effect of heating on the liquid-film flow is similar to that encountered in annular flow. However, the entrainment rate becomes high and the deposition rate may be considerably reduced (due to droplet coalescence), resulting in a rapid depletion of the liquid film. In the vapour core, a suppression of turbulence is anticipated due to the high concentration of entrained droplets and liquid filaments.

3.1.1.6 Dispersed-Droplet and Inverted-Annular Flows

Dispersed-droplet and inverted-annular flow are primarily encountered in a heated channel where the surface is so hot that continuous liquid contact cannot be sustained (see Figure 3.2). For adiabatic flow at high quality and high void fraction, the liquid film can be undercut by the high shear force of vapour, and dispersed-droplet flow may also be observed. This is referred to as the hydrodynamic dryout [Beattie, 1975].

Dispersed-droplet flow corresponds mainly to high void fraction where liquid content is low. It has the reverse structure of bubbly flow, with a continuous vapour flow (instead of a continuous liquid flow) and entrained liquid droplets (instead of bubbles). The size of droplets depends on the flow conditions and fluid properties.

Inverted-annular flow is observed in low void fractions. It has the reverse structure of high void-fraction annular flow, with a continuous liquid core surrounded by a thin vapour film. Liquid entrainment in the vapour film and vapour entrainment in the liquid core are possible. In most cases, the liquid/vapour interface is agitated.

3.1.2 Flow-Pattern Transition

The transition between various flow patterns depends very much on flow conditions (such as pressure, mass flow rate or flow velocity, and quality), flow geometry (such as diameter and length), and surface temperature (in a heated channel). Different techniques (such as high-speed photography and X-ray photography) have been employed to identify the flow patterns and their transition boundaries. The data have been compiled into flow-pattern maps presenting the approximate boundaries of various flow patterns with respect to different flow parameters. Mandhane et al. [1974] provided the most comprehensive flow-pattern maps for horizontal flow based on a large amount of low-pressure data of various types of fluid mixtures. A generalised flow-pattern map was introduced by Hewitt and Roberts [1969] for vertical flow (Figure 3.5). It was based on both the low-pressure (atmospheric) air-water and high-pressure (3.5 and 7 MPa) steam-water data. Taitel et al. [1980] introduced several criteria for flow-pattern transition based on a force balance of the phases. Mishima and Ishii [1984], on the other hand, derived the transition based on a mechanistic model.

For heated channels, the flow-pattern maps were often presented in terms of equilibrium quality and mass velocity [Bennett et al., 1965; Bergles et al., 1968]. Figure 3.6 presents the flow-pattern map of Bennett et al. [1965]. Hewitt and Roberts [1969] indicated that the effect of heating on flow-pattern transition is insignificant in a tube flow. This is also reflected in the flow-pattern observations of Ng et al. [1987] in horizontal Freon-113 flow. Ying and Weisman [1989] noted a slight shift in the boundary between bubbly and intermittent flow towards higher qualities in a heated channel cooled with

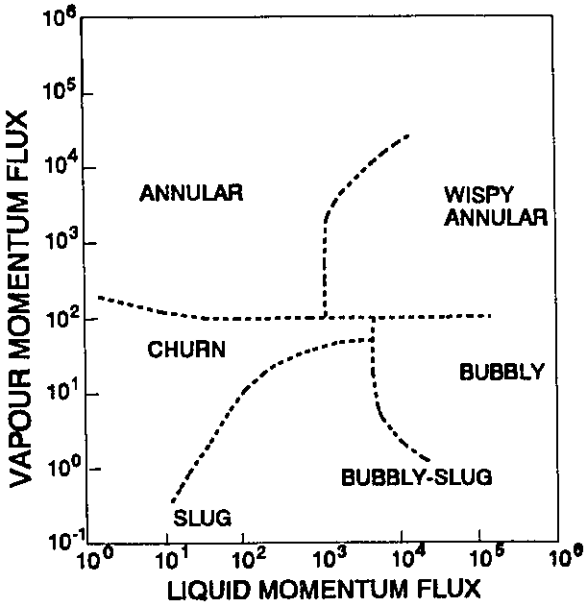

Figure 3.5: Flow-Regime Map for Vertical, Co-Current, Upward Flow [Hewitt and Roberts, 1969].

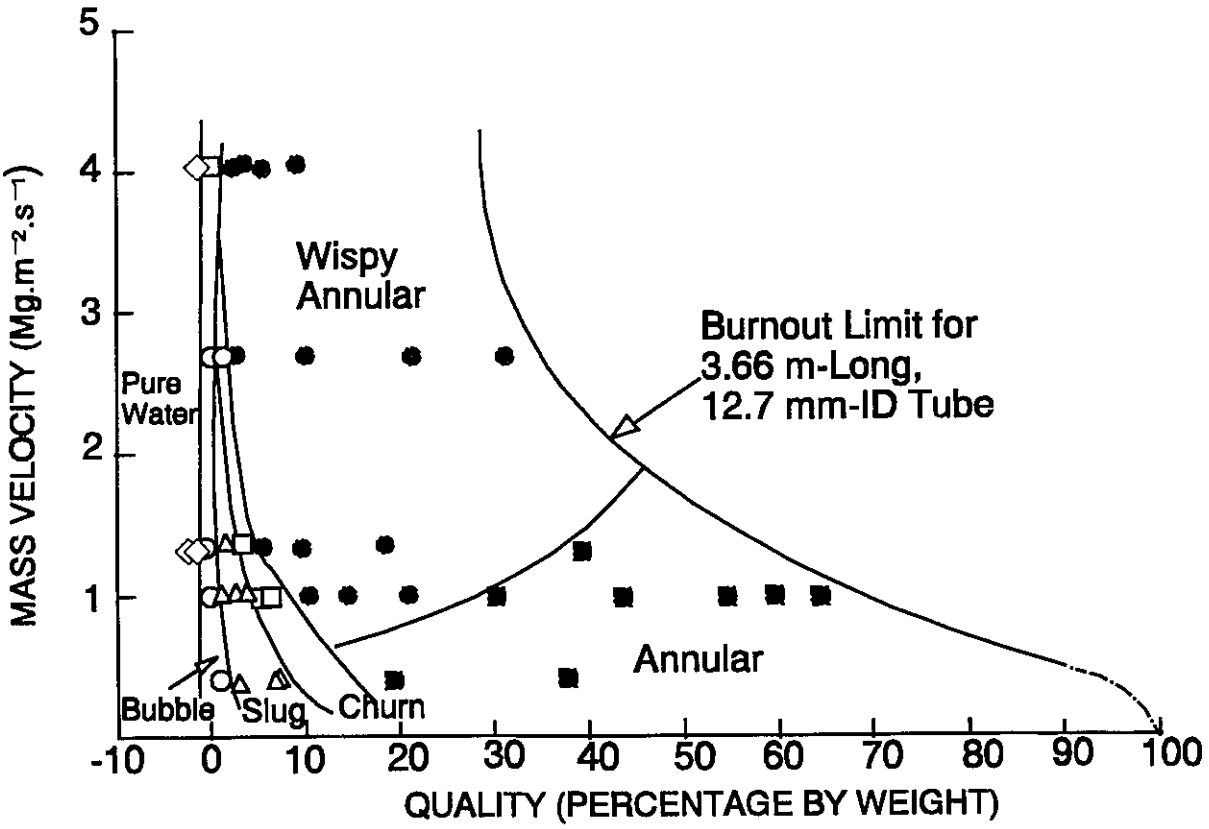

Figure 3.6: Flow-Regime Map for Steam-Water Flow at a Pressure of 6.89 MPa Inside a Heated Channel [Bennett et al., 1965].

Freon-113, compared to an unheated channel.

3.2 VAPOUR-MASS QUALITY

Vapour-mass quality of a two-phase mixture is one of the most important parameters in two-phase flow analysis. It is defined as the mass flow-rate ratio between vapour and total flow; i.e.,

$$x_a = \frac{W_g}{W_g + W_l} \tag{3.1}$$

where W is the mass flow rate in $kg.s^{-1}$ and the subscripts "g" and "l" refer to the vapour and liquid phases, respectively. For an adiabatic flow where the phases are introduced separately into the system, this quality can be determined by measuring individual mass-flow rates. It is constant throughout the flow channel when mass transfer and heat transfer are not present.

For a heated channel, however, the vapour-mass quality varies along the flow direction and is difficult to measure or calculate. Hence, the thermodynamic quality is often used and is calculated based on an energy balance

$$x_{th} = \frac{H_l - H_f}{H_{fg}} \tag{3.2}$$

where H_l, H_f and H_{fg} are fluid enthalpy, saturated-liquid enthalpy and latent heat of vaporization, respectively, in $J.kg^{-1}$. The thermodynamic quality can vary from negative values (at subcooled conditions) to values greater than 1 (at superheated conditions). A qualifying condition is often introduced to limit the range of calculated thermodynamic quality between 0 and 1. This limiting quality is referred to as the equilibrium quality.

Equilibrium conditions can never be completely achieved in a heated channel, due to the superheating of near-wall liquid along the surface and the subcooling of bulk fluid in the core. Figure 3.7 illustrates schematically the differences between thermodynamic and vapour-mass qualities for a flow inside a heated channel. Among various heat-transfer modes, only the forced-convective evaporation approaches thermodynamic-equilibrium conditions. For others, equations must be introduced to calculate the vapour-mass quality.

Mechanistically, the mass quality begins to rise from 0 at the point where vapour is first generated. Therefore, it is essential to locate the initiation point of bubble formation, referred to as the point of onset of nucleate boiling. Strictly speaking, two-phase flow should be considered at conditions beyond this point. However, the bubbles formed at conditions close to this point are generally small, attach only to the wall, and collapse either during growth or once

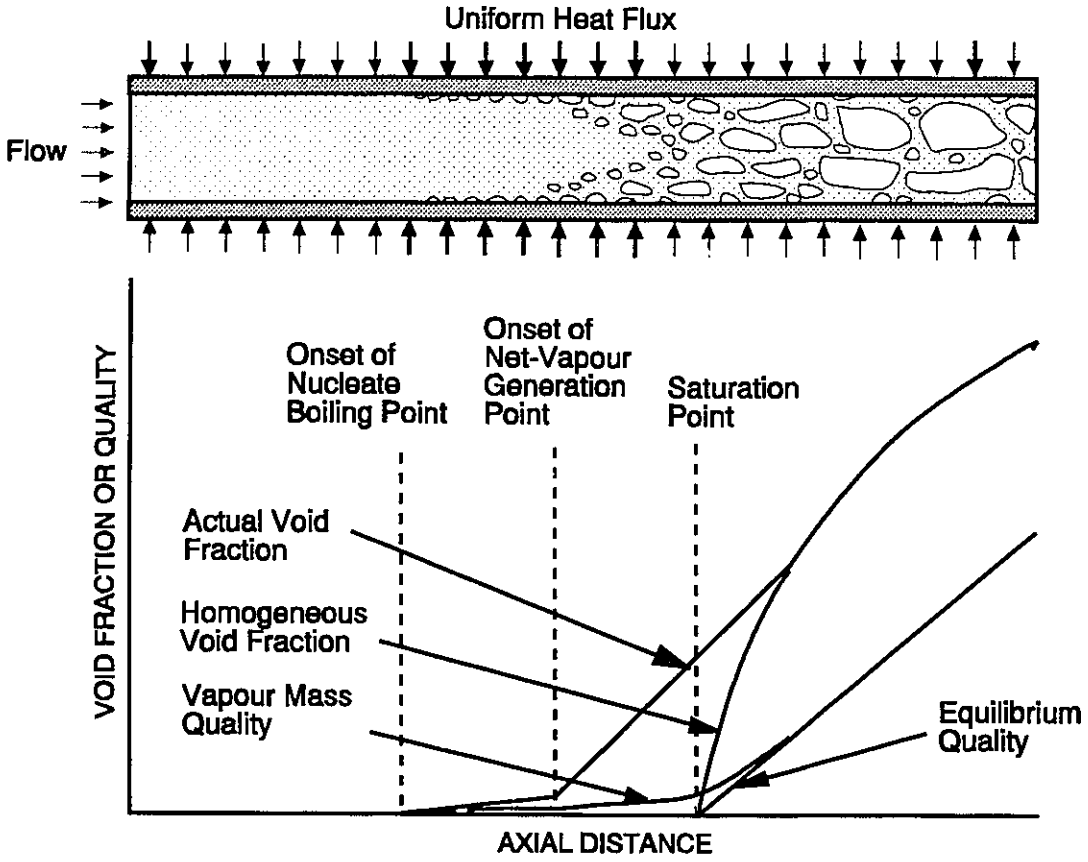

Figure 3.7: Axial Distributions of Void Fraction and Quality Inside a Heated Channel.

they are detached from the surface. There is no net-vapour flow in the core and the vapour-mass quality remains very close to 0. The effect of this bubble formation on hydrodynamics may not be significant, but can be significant on heat transfer. As the fluid enthalpy increases, the departed bubbles sustain from condensation and remain in the flow. This is called the point of onset of net vapour generation (NVG). Further discussions on the points of onset of nucleate boiling and onset of net vapour generation are provided in Chapter 4.

Vapour-mass quality is calculated primarily with empirical equations for conditions beyond the point of onset of net vapour generation. Most studies used a profile-fit function, which describes the relation between the thermodynamic quality, x_{th}, and vapour-mass quality, x_a, based on the measurements of void fraction. This function accounts for the deviation of local equilibrium

quality to that at the point of onset of net vapour generation, x_{NVG}. Levy [1967] has suggested the following function:

$$x_a = x_{th} - x_{NVG}\ exp\left(\frac{x_{th}}{x_{NVG}} - 1\right) \tag{3.3}$$

This equation provides the correct asymptotic trend of (i) zero vapour-mass quality when the local thermodynamic quality equals that at the point of net vapour generation, and (ii) vapour-mass quality approaching thermodynamic quality when the thermodynamic quality is very much larger than that at the point of net vapour generation. However, the calculated vapour-mass quality approaches rapidly to 1 as the thermodynamic quality at the point of net vapour generation becomes small. A modification was introduced by Kroeger and Zuber [1968] with

$$x_a = \frac{x_{th} - x_{NVG}\ exp\left(\frac{x_{th}}{x_{NVG}} - 1\right)}{1 - x_{NVG}\ exp\left(\frac{x_{th}}{x_{NVG}} - 1\right)} \tag{3.4}$$

Both Equations (3.3) and (3.4) are invalid for film boiling or superheat conditions (i.e., $x_{th}>1$). The vapour-mass quality is calculated from a model or a thermal non-equilibrium equation (see, for example, Groeneveld and Delorme [1976]).

Several models have been developed to predict mechanistically the vapour-mass quality in subcooled-boiling flows [Lahey and Moody, 1975, Sami and Duong, 1987]. They account separately for the heat transferred from the surface to the fluid through convection, evaporation, condensation and liquid agitation, and require empirical interfacial relationships. The vapour-mass quality is calculated by integrating the vapour generated from the point of net vapour generation to the point of interest. These complex mechanistic models are particularly useful for

(i) transient analysis where the empirical approach is usually invalid, and (ii) steady-state applications outside the data base, as the models tend to provide more realistic parametric trends than empirical equations for vapour-mass quality.

3.3 VOID FRACTION

Void fraction is defined as the cross-sectional area ratio of vapour and total flow; i.e.,

$$\alpha = \frac{A_g}{A_F} = \frac{A_g}{A_g + A_f} \tag{3.5}$$

where A is the flow area in m^3 and subscripts "F", "g" and "f" correspond to total flow, gas/vapour flow and liquid flow, respectively. It is a key parameter in the evaluation of two-phase pressure drop (to be described in the next section), but is very difficult to obtain for high-pressure steam-water flow in a heated channel. Most void-fraction measurements were carried out at low-pressure adiabatic conditions. This introduces the question of the validity of extrapolating equations based on low-pressure data to high-pressure conditions.

The simplest void-fraction prediction method is the homogeneous-flow model, which assumes both liquid and vapour travelling as a mixture at the same velocity. It is expressed as

$$\alpha_H = \frac{x_a \rho_l}{x_a \rho_l + (1 - x_a) \rho_g} \tag{3.6}$$

The separated-flow model assumes the two phases travelling individually at different velocities, and uses the slip ratio, K, which is a velocity ratio (u_g/u_l) between the two phases:

$$\alpha = \frac{x_a \rho_l}{x_a \rho_l + K (1 - x_a) \rho_g} \tag{3.7}$$

The slip ratio was often determined empirically and was expressed in terms of cross-sectional average parameters or fluid properties [Zivi, 1964 and Thom, 1964]. For example, Zivi [1964] expressed the slip ratio as

$$K = \left(\frac{\rho_l}{\rho_g} \right)^{1/3} \tag{3.8}$$

Based on the assumptions, the homogeneous-flow model seems to be more appropriate for bubbly flow and the separated-flow model for annular flow. However, both models have only limited ranges of validity, since a combination of flow regimes is often observed.

An improved separated-flow model, based on the relative velocity between each phase and the homogeneous velocity (referred to as the drift velocity, u_{gj}), was introduced by Zuber and Findlay [1965]. The void fraction is calculated with

$$\alpha = \frac{x_a \rho_l G}{G C_o (x_a \rho_l + (1 - x_a) \rho_g) + \rho_l \rho_g u_{gj}} \tag{3.9}$$

where C_o is the distribution parameter. Like the slip ratio, the distribution parameter and the drift velocity are functions of flow patterns, geometries and flow conditions [Collier, 1981, Hewitt, 1982]. Zuber and Findlay [1965] suggested a value of 1.13 as the distribution parameter for a tube flow and the following definition as the drift velocity for churn-turbulent bubbly flow

$$u_{gj} = 1.41 \left(\frac{\sigma g (\rho_f - \rho_g)}{\rho_f^2} \right)^{1/4} \tag{3.10}$$

where σ is the surface tension in $N.m^{-1}$. Levy [1967], however, recommended a coefficient of 1.18 rather than 1.41 for the drift velocity to calculate void fraction in subcooled boiling.

While a constant distribution parameter represents most void-fraction data, Rouhani [1969] observed also a dependency of flow rate and velocity distribution. He used the Levy modification to the drift velocity, but expressed the distribution parameter as

$$C_o = 1 + 0.2 \frac{(1 - x_a)(9.806\ D)^{1/4}}{(G/\rho_l)^{1/2}} \tag{3.11}$$

Different expressions have been introduced for both the distribution parameter and drift velocity. An assessment of 18 different correlations for void fraction showed that the Rouhani correlation agreed closely with over 9000 experimental data in adiabatic flow [Friedel, 1980]. Similar to the evaluation of vapour-mass quality, the void fraction can also be calculated with a mechanistic model [Lahey and Moody, 1975, Sami and Duong, 1987].

Recently, an extensive study was carried out by Chexal et al. [1991] to derive values for the distribution parameter and the drift velocity for various flow conditions (e.g., upward flow and downward flow), geometries (e.g., tubes, annuli and rectangular channels) and fluids (e.g., air-water, steam-water and Freon flow). For a vertical upward flow of steam-water mixtures, the distribution parameter is expressed as

$$C_o = \frac{B_1}{B_2 + (1 - B_2)\,\alpha^{B_3}} \tag{3.12}$$

where the Chexal-Lellouche fluid parameter, B_1, is defined as

$$B_1 = \frac{1 - \exp(-B_4\ \alpha)}{1 - \exp(-B_4)} \tag{3.13}$$

with

$$B_4 = \frac{4\ P_c^2}{P\ (P_c - P)} \tag{3.14}$$

where P and P_c are the system and critical pressure, respectively, in Pa. The flow parameter, B_2, is defined as

$$B_2 = B_5 + (1 - B_5)\ (\rho_g / \rho_l)^{1/4} \tag{3.15}$$

$$B_3 = \frac{1.0 + 1.57\ \rho_g / \rho_l}{1 - B_5} \tag{3.16}$$

where

$$B_5 = \min(0.8, (1 + \exp(-Re / 60\,000))^{-1}) \tag{3.17}$$

$$Re = Re_g = \frac{x_a\ G\ D}{\mu_g} \qquad (\ if\ Re_g > Re_f\ ) \tag{3.18}$$

$$Re = Re_f = \frac{(1 - x_a)\ G\ D}{\mu_l} \qquad (\ if\ Re_g \le Re_f\ ) \tag{3.19}$$

Predictions from the Chexal et al. correlation agree closely with the experimental data of Bartolomei et al. [1982], obtained at high-pressure steam-water conditions in a vertical tube [Chexal et al., 1991].

The effect of surface heating on void fraction appears to be small, as indicated in the analysis of Yamazaki and Yamaguchi [1976] for the same local conditions. Abramyan and Bartolomei [1985], however, observed an increase in void fraction with increasing heat flux at subcooled-liquid and low-quality regions. This increasing trend diminished at high qualities. Ying and Weisman [1989] indicated a small effect of heating on void fraction in Freon-113 flow. The difference in void fraction between a heated and an unheated channel is large at low-flow conditions, but becomes small as the flow rate increases. Using the same distribution parameter and drift-velocity calculation, predictions evaluated from the Chexal et al. correlation agree relatively well with the experimental data of both adiabatic and heated steam-water flow [Chexal et al., 1991].

3.4 TWO-PHASE PRESSURE DROP

Two-phase pressure drop is more complicated than single-phase pressure drop, primarily due to the complex nature of phase distribution that affects the velocity and shear-stress distributions within the cross-section of a channel. Nevertheless, the basic one-dimensional analysis can still be applied.

For a channel where no fluid is extracted from the wall, the variation in phasic mass flow is primarily due to a change in phase; i.e.,

$$dW_g = -dW_l \tag{3.20}$$

where

$$W_g = A_g \rho_g u_g = W x_a \tag{3.21}$$

$$W_l = A_l \rho_l u_l = W (1 - x_a) \tag{3.22}$$

As described in Section 3.2, the vapour-mass quality, x_a, can be measured in adiabatic flow, but must be calculated from an energy balance, correlations or semi-analytical models for flow-boiling conditions.

In general, the force-momentum balance within the control volume, as illustrated in Figure 2.8, is also valid for two-phase flow. Equation (2.33), however, has to be modified to account for the presence of two phases. It is expressed as

$$\int_A \left[P - \left(P + \frac{dP}{dz} \delta z \right) \right] dA = \int_S \tau_w \delta z \, dS + \int_A \frac{d}{dz} (G_l u_l + G_g u_g) \, \delta z \, dA + \int_A \rho_{tp} g \sin\theta \, \delta z \, dA \tag{3.23}$$

A number of definitions have been introduced for two-phase density, ρ_{tp}, and the one based on volumetric fraction is often used

$$\rho_{tp} = \alpha \rho_g + (1 - \alpha) \rho_l \tag{3.24}$$

The calculation of void fraction, α, has been discussed in Section 3.3. Integrating Equation 3.23, the pressure gradient becomes

$$-\frac{dP}{dz} = \frac{S}{A} \tau_w + \frac{d}{dz} (\alpha G_g u_g + (1 - \alpha) G_l u_l) + (\alpha \rho_g + (1 - \alpha) \rho_l) g \sin\theta \tag{3.25}$$

and, similar to single-phase flow, consists of three components: friction, acceleration and gravity. Equation (3.25) can be further expanded to

$$-\frac{dP}{dz}=\frac{S}{A}\tau_w+G^2\frac{d}{dz}\left(\frac{x_a^2}{\alpha\rho_g}+\frac{(1-x_a)^2}{(1-\alpha)\rho_l}\right)+(\alpha\rho_g+(1-\alpha)\rho_l)g\sin\theta \tag{3.26}$$

by introducing the following definitions

$$G_l = \frac{W\ (1\ -\ x_a)}{A\ (1\ -\ \alpha)} = \frac{G\ (1\ -\ x_a)}{1\ -\ \alpha} \tag{3.27}$$

$$G_g = \frac{W\ x_a}{A\ \alpha} = \frac{G\ x_a}{\alpha} \tag{3.28}$$

$$u_l = \frac{G_l}{\rho_l} \tag{3.29}$$

$$u_g = \frac{G_g}{\rho_g} \tag{3.30}$$

A slightly different equation for pressure gradient can be derived from the conservation equation of energy. It is due to the different distribution of the unrecoverable pressure loss (see Collier [1981] or Hewitt [1982]).

3.4.1 Two-Phase Pressure Gradient due to Friction

In general, the two-phase pressure drop is higher than single-phase pressure drop, especially at low-pressure conditions. This is primarily caused by the increase in flow velocity (or velocity gradient and hence shear stress at the wall) as a result of an increase in vapour volume, and the subsequent increase in liquid velocity due to the reduction in liquid flow area.

In a heated channel, the difference in pressure gradient between single- and two-phase flow is not consistent. Previous experiments have indicated that frictional pressure drop can be larger or smaller in two-phase flow than in single-phase flow, depending on the flow pattern encountered inside the channel for the same local conditions.

As shown in Equation (3.26), the general definition for two-phase pressure gradient due to friction is the same as single-phase flow; i.e.,

$$-\left(\frac{dP}{dz}\right)_{f,tp} = \frac{S}{A}\,\tau_w \tag{3.31}$$

However, the prediction of this pressure gradient has been proven to be more complex than in single-phase flow. A number of prediction methods, including graphical methods, empirical correlations and semi-analytical models, were derived. While some methods predict the two-phase frictional pressure drop directly, others provide an estimation of the wall shear stress instead. A literature review on two-phase pressure drop due to friction will be presented in Chapters 5 and 6.

3.4.2 Two-Phase Pressure Gradient due to Acceleration

Two-phase pressure gradient due to acceleration is the result of a change in momentum flux. It is a significant factor in two-phase flow with phase change [Martinelli and Nelson, 1948, Thom, 1964], but may be neglected in adiabatic flow when little or no vapour generation takes place [Delhaye et al., 1981] and the density gradients are small.

In Equation (3.26), the two-phase pressure gradient due to acceleration is expressed as

$$-\left(\frac{dP}{dz}\right)_{a,tp} = G^2 \frac{d}{dz}\left(\frac{x_a^2}{\alpha \rho_g} + \frac{(1-x_a)^2}{(1-\alpha)\rho_l}\right) \tag{3.32}$$

and is derived for a separated flow (i.e., the phases flow separately from each other). For a well-mixed (homogeneous) flow, the same analysis as in single-phase flow can be applied, and the two-phase pressure gradient due to acceleration is written as

$$-\left(\frac{dP}{dz}\right)_{a,tp} = G^2 \frac{d}{dz}\left(\frac{1}{\rho_H}\right) \tag{3.33}$$

where the density for homogeneous flow is defined as

$$\frac{1}{\rho_H} = \frac{x_a}{\rho_g} + \frac{(1-x_a)}{\rho_l} \tag{3.34}$$

Equation (3.32) is widely used in analyses because the separate-flow assumption is more typical of a real-flow situation. However, the homogeneous-flow equation (i.e., Equation (3.33)) appears to agree closely with the experimental results in steam-water [Andeen and Griffith, 1968] and air-water flow [Baumeister et al., 1972]. This is probably due to the uncertainty within the experimental data.

For forced-convective flow boiling, Martinelli and Nelson [1948] derived a multiplier, r_2, for the homogeneous-flow equation as

$$r_2 = \frac{x_a^2}{\alpha}\frac{\rho_l}{\rho_g} + \frac{(1-x_a)^2}{(1-\alpha)} - 1 \tag{3.35}$$

This multiplier was presented graphically as functions of pressure and quality in Figure 3.8, and was used by Thom [1964] and Andeen and Griffith [1968].

For annular flow with a significant amount of entrained droplets in the vapour core, Hewitt and Hall-Taylor [1970] suggested a modification to the separate-flow equation. This modification accounts for the momentum change of the droplets in the high-velocity vapour flow. They expressed the two-phase pressure gradient due to acceleration as

$$-\left(\frac{dP}{dz}\right)_{a,tp} = G^2 \frac{d}{dz}\left(\frac{x_a^2}{\alpha \rho_g} + \frac{(1-E)^2(1-x_a)^2}{\beta \rho_l} + \frac{E^2(1-x_a)^2}{(1-\beta-\alpha)\rho_l}\right) \tag{3.36}$$

where E is the fraction of liquid phase entrained in the vapour core and β is the volume fraction occupied by the liquid film. The difficulty in applying this equation lies in the estimation of the entrained fraction, E, and the volume fraction of the liquid film, β. Simplifying assumptions were therefore introduced to eliminate the dependence on the volume fraction of the liquid film, β, in this equation [Hewitt and Hall-Taylor, 1970]. Measurements of liquid-film thickness were obtained in low-pressure adiabatic flow by Steen and Wallis [1964], Cousin and Hewitt [1968] and others, but their results did not agree, due to differences in the techniques used in the experiment, and in the interpretation of the experimental results. Furthermore, a considerable difference in

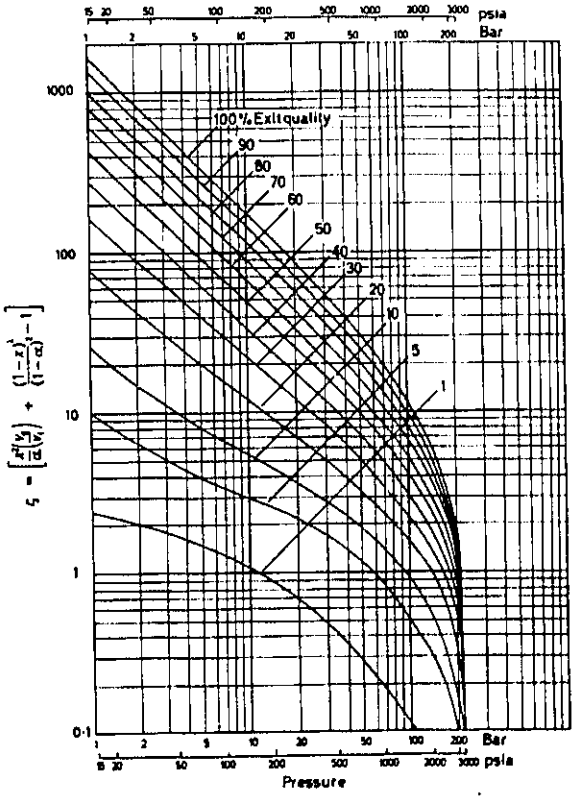

Figure 3.8: Multiplier, r_2, to Two-Phase Pressure Gradient due to Acceleration of Homogeneous Flow [Martinelli and Nelson, 1948].

liquid-film thickness between a heated and an unheated channel is anticipated, thus increasing the uncertainty in using this equation. Hence, the use of a simplified equation (Equation (3.32), without considering the momentum of the entrained droplets) may be preferable.

3.4.3 Two-Phase Pressure Gradient due to Gravity

Two-phase gravitational pressure drop is synonymous with the hydrostatic-head difference between two locations, and is expressed as

$$-\left(\frac{dP}{dz}\right)_{g,tp} = \rho_H \, g \, \sin\theta \tag{3.37}$$

for homogeneous flow, and

$$-\left(\frac{dP}{dz}\right)_{g,tp} = \rho_{tp} \, g \, \sin\theta \tag{3.38}$$

for separate flow. The homogeneous-flow density, ρ_H, and two-phase density, ρ_{tp}, are defined in Equations (3.24) and (3.34), respectively. In vertical flow, the angle θ is 90° and hence sin θ becomes 1. Except for the cases of low flow and natural circulation, this component is generally the smallest among the three components, and can be neglected at high flow and high void-fraction conditions.

4. FLOW BOILING

Pressure drop in a heated channel is affected by the radial (or transverse) temperature gradient within the flow. Depending on the heat-transfer mode (which has a strong effect on flow distribution), it can be higher or lower than that in adiabatic flow. Therefore, to properly account for the heating effect on pressure drop, it is essential to predict accurately the heat-transfer rates (and hence the surface temperature) for various heat-transfer modes, including the transition points between them.

Section 4.1 describes the heat-transfer modes and transition points encountered inside a heated tube. The boiling curve, which shows the relation between heat flux and surface temperature (or superheat) for specific conditions, is presented in Section 4.2. The prediction methods of heat-transfer coefficient for various heat-transfer modes and transition points are discussed in Section 4.3.

4.1 HEAT-TRANSFER MODES AND TRANSITION POINTS

A number of heat-transfer modes can be encountered in flow boiling, depending on the flow conditions. The present discussion focuses on those inside a heated tube where heat flux is the controlling parameter. This includes the single-phase forced convection to liquid, nucleate boiling, forced-convective evaporation, film boiling and single-phase forced-convection to vapour (see Figure 3.2). Information on cases where surface temperature is the controlling parameter can be obtained from, for example, Groeneveld et al. [1989].

4.1.1 Single-Phase Forced Convection to Liquid

The surface temperature increases when heat is supplied to a tube that is cooled with a forced flow of fluid. For single-phase flow, it is generally maintained at a stable level slightly above the bulk-fluid temperature. Boiling on the surface is suppressed if the heat-transfer coefficient is high. When heat transfer through single-phase forced convection is unable to remove all supplied heat from the surface, the excess heat vaporizes the near-wall fluid to form bubbles. The initiation point of bubble formation is referred to as the point of onset of nucleate boiling (ONB), which serves as a transition point from single-phase forced convection to liquid to nucleate boiling.

4.1.2 Nucleate Boiling

As more heat is supplied or the bulk-fluid enthalpy is increased, both the size and population of bubbles will increase. Once the combined drag and buoyancy force overcomes the surface-tension force, the bubbles depart from the surface, but will be condensed immediately in the relatively cold bulk fluid. Therefore, the bubble concentration is high in the near-wall region, but non-existent in the core (see Figures 3.2 and 3.7). A further increase in heat flux or bulk-

fluid enthalpy allows the bubbles to sustain from condensation in the flow. The initial point of sustainable bubbles in the flow is referred to as the point of net vapour generation (NVG). The heat-transfer mode corresponding to this bubbly-flow regime is classified as nucleate boiling. Since the liquid temperature at and before the NVG point are usually below saturation, it is identified as the subcooled nucleate-boiling region.

For a highly subcooled flow in tubes of a high surface heat flux, the bubble population in the near-wall region becomes so dense that liquid contact can be disrupted. Within a localized area, the surface is cooled by a slow-moving vapour film (film boiling). This leads to a sharp drop in heat-transfer rate, but a rapid increase in surface temperature, causing possible destruction to the heating surface (burnout phenomenon). Figure 3.2a illustrates the direct transition from nucleate boiling to film boiling. The surface heat flux corresponding to burnout is called the critical heat flux, which is the transition point between, in this case, nucleate boiling and film boiling. Hence, this phenomenon is also referred to as the "departure from nucleate boiling" (DNB).

Bulk boiling begins at (or slightly before) the saturation point, where bubbles can travel across the cross-section of the channel (saturated nucleate boiling).

4.1.3 Forced Convective Evaporation

The transition from bubbly flow to either slug or annular flow takes place as the vapour content increases inside the channel. In general, bubbly-to-slug flow transition is associated with low flow-rate conditions, whereas bubbly-to-annular flow is observed at high flow rate. The corresponding heat-transfer mode for annular flow is the forced-convective evaporation, and the transition between saturated nucleate boiling and forced-convective evaporation is called the point of suppression of nucleate boiling (SNB).

4.1.3.1 Low Flow-Rate Conditions

At low flow and increasing quality (and thus bubble population), the bubbles coalesce together to form large bubbles. With a further increase in bulk fluid enthalpy or quality, these bubbles group into a large pocket of vapour (or a slug), having a similar cross-sectional size to the diameter of the tube. Due to the velocity gradient in the flow, the slug travels with a bullet-shaped leading edge. The thin liquid film between the slug and the heated surface is often maintained at a low velocity (close to or at laminar-flow level), and a flow reversal (where the liquid at the film flows down and the bulk fluid flows in an upward direction) can occur periodically. With a high surface heat flux, the liquid film can be vaporized, exposing the surface to the low-velocity vapour, which has a much lower thermal conductivity and capacity than the liquid. This reduces the heat-transfer rate and can lead to a sharp increase in surface temperature, which may cause destruction of the heated surface.

The tail of the slug has a high turbulence level. Therefore, the trailing edge is often irregular and followed with a dense cloud of small bubbles. With a further increase in heat flux (but still below the critical level) or bulk fluid enthalpy, the liquid bridge between two adjacent slugs is reduced to a point where it can no longer be maintained. A transition from slug to annular flow then occurs. Since the quality and void fraction is high, the liquid film will be evaporated shortly thereafter. This is called the dryout phenomenon, which is less destructive than DNB or burnout. Nevertheless, it can also endanger the integrity of the heated surface.

4.1.3.2 High Flow-Rate Conditions

At high flow, the size of bubbles is usually small, due to the high turbulence level that deters bubble coalescence. As the bubble population grows, the mixture core displays a foam-type structure, where bubbles closely interlock with each other through a thin liquid interface. With increasing heat flux or fluid enthalpy, these interfaces at the channel core will eventually burst, ejecting a stream of liquid droplets into a continuous vapour core. This is the transition from a

bubbly into a wispy-annular flow. Because of the high liquid velocity, the liquid film is quickly established between the vapour and the heated surface.

Unlike annular flow, the wispy-annular flow consists of a large amount of entrained droplets in the vapour core and a high-velocity liquid film, which maintains the high heat-transfer rate. Very often, nucleation is suppressed on the surface. For a high vapour flow in the core, the velocity difference between vapour and liquid film becomes large and roll waves begin to form at the liquid/vapour interface. As the magnitude of waves increases, the high velocity vapour flow can shear off the crests of these waves, bringing more entrainment into the vapour core. Both the entrainment and the evaporation processes deplete the liquid film rapidly. When the liquid film becomes very thin, the entrainment process terminates but the liquid film is continuously depleted by evaporation. Dryout occurs when the liquid film is completely evaporated and a sharp rise in surface temperature results.

In general, the surface heat flux, corresponding to either dryout or burnout phenomena, is referred to as the critical heat flux. It serves as the transition point between forced-convective evaporation and film boiling (see Figure 3.2b).

4.1.4 Film Boiling

In film boiling, the heated surface is primarily cooled by a vapour film. Heat transfer from the surface to liquid is by means of conduction, convection and radiation through the vapour. Due to the poor heat-transfer rate, the surface temperature is high in film boiling and results in a large gradient in fluid temperature between the near-wall and core regions. The phase distribution in film boiling depends strongly on the flow quality and is described in the following two sections.

4.1.4.1 Inverted Annular-Flow Film Boiling

Inverted annular-flow film boiling consists of a liquid core and is usually preceded by a bubble-crowding type of CHF phenomenon (see Section 4.1.2) with low void fraction. Due to the highly unstable conditions, a wavy liquid-vapour interface is exhibited. Liquid entrainments in the vapour film may be encountered as the vapour velocity increases. The crests of the liquid-core waves and entrained droplets are a contributing source of heat removal as they impinge on the heated surface. The size of the liquid core decreases due to vaporization and liquid entrainment. At high void fraction, the liquid core breaks up into droplets, and the heat-transfer mode becomes dispersed-flow film boiling (see Figure 3.2a).

4.1.4.2 Dispersed-Flow Film Boiling

The dispersed-flow film boiling consists of a mixture of droplets inside a vapour core. Other than developed through a gradual change from the inverted annular-flow film boiling, it can also be preceded by forced-convective evaporation (see Section 4.1.3) and a subsequent film dryout. The main difference between these two development processes is the associated heat flux and surface temperature, which are much higher for the transition from inverted annular-flow film boiling than from forced convective evaporation in a tube of a uniform axial heat-flux distribution. Other differences, such as the size and distribution of droplets, also affect the heat transfer and hydrodynamic characteristics.

4.1.5 Single-Phase Forced Convection to Vapour

The cooling of the heated surface relies only on forced convection to vapour and on radiation after all the liquid has been vaporized (i.e., $x_{th} > 1$). Although forced convection to vapour has the same basic characteristics as the forced convection to liquid, the heat-transfer rate is drastically reduced, due to the poor heat transport capability of vapour.

4.2 BOILING CURVE

The efficiency of heat-removal capability in each heat-transfer mode can be illustrated with a plot of heat flux against temperature difference, between heated surface and bulk fluid, for a constant pressure, mass flux and thermodynamic quality. This type of plot is usually referred to as the flow-boiling curve (Figure 4.1). The heat-transfer coefficient (or heat-transfer rate) is defined as

$$h = \frac{q}{T_w - T_b} \tag{4.1}$$

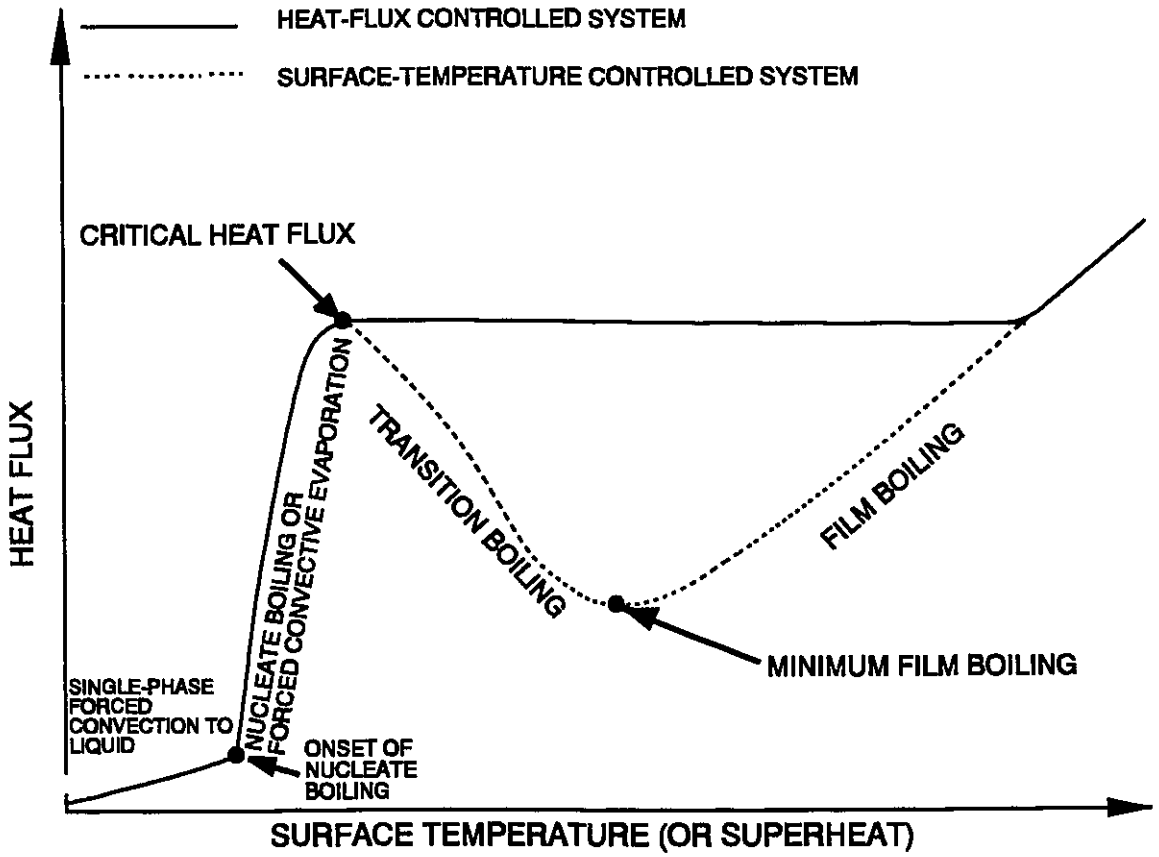

Figure 4.1: Boiling Curve.

where q is the surface heat flux in $W.m^{-2}$, T_w and T_b are the surface and bulk-fluid temperature, respectively, in K. Figure 4.2 shows the variation in boiling curve for various thermodynamic qualities.

For single-phase forced convection to a liquid, the heat-transfer rate is relatively efficient. A change in slope, indicating that the heat-transfer coefficient (gradient) becomes more efficient than that of single-phase flow, is shown at the point of onset of nucleate boiling. This change continues until the point of net vapour generation is reached. A steep rise in heat flux is associated with a small increase in temperature difference. This signifies the fully developed nucleate-boiling region, where the heat-transfer rate is the highest. The region between single-phase heat transfer and fully developed nucleate boiling is categorised as the partial-boiling mode (mainly at subcooled conditions). At positive flow qualities, nucleate boiling is primarily encountered under low-flow conditions, while forced-convective evaporation is observed at high flow.

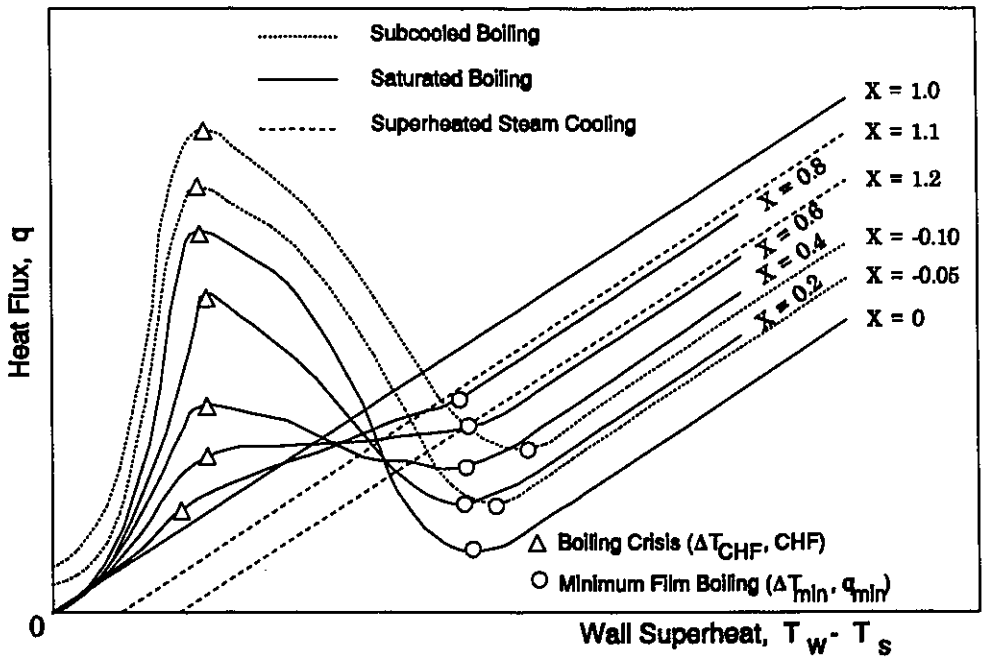

Figure 4.2: Effect of a Change in Thermodynamic Quality on the Flow-Boiling Curve.

Nucleate boiling or forced-convective evaporation terminates at the critical heat flux (CHF). The heat-transfer mode beyond CHF is governed by the method of heating at the surface (see Section 4.1). For a heat-flux controlled surface, a sharp rise in surface temperature is usually observed once the local heat flux exceeds CHF (the solid line in Figure 4.1), and film boiling is encountered inside the channel. At a very high flow rate, however, the rise in surface temperature is gradual beyond CHF. It is due to (i) high vapour velocity that maintains a relatively efficient heat-transfer rate, and (ii) a high content of liquid droplets, which act as a heat sink in the vapour core. This is often referred to as the developing film-boiling region. With increasing heat flux, the fully developed film boiling is approached.

The transition from film boiling to forced convection to vapour depends on the flow enthalpy, and is usually very gradual.

4.3 PREDICTION OF HEAT-TRANSFER RATE AND TRANSITION POINTS

The heat-transfer rates for various heat-transfer modes and the transition points can be predicted with correlations or models. Frequently, there are a large number of prediction methods available, making it difficult to select an appropriate one for the application. Most of these prediction methods are valid only for a limited range of conditions. A review of prediction methods used in heat-transfer analysis was presented by Groeneveld and Snoek [1986].

4.3.1 Single-Phase Forced Convection to Liquid

A large number of heat-transfer correlations have been presented for single-phase flow. They are expressed in terms of the Nusselt number, Nu, as

$$Nu = \frac{h\,D}{k} \tag{4.2}$$

where h is the heat-transfer coefficient in $W.m^{-2}.K^{-1}$, D is the tube diameter in m, and k is the thermal conductivity of the bulk fluid in $W.m^{-1}.K^{-1}$. In laminar flow, the Nusselt number is independent of the pressure and mass flux, but is affected by the method of heating. It is expressed [Bhatti and Shah, 1987], for a constant-temperature surface, as

$$Nu = 3.6568 \tag{4.3}$$

and for a constant heat-flux surface as

$$Nu = 4.3636 \tag{4.4}$$

In turbulent flow, most correlations are expressed as functions of Reynolds and Prandtl numbers. One of the most well-known correlations is the Dittus-Boelter correlation [1930], where the Nusselt number is expressed as

$$Nu = 0.024\ Re^{0.8}\ Pr^{0.4} \tag{4.5}$$

with the Prandtl number defined as

$$Pr = \frac{\mu\ C_p}{k} \tag{4.6}$$

where C_p is the specific heat capacity in $J.kg^{-1}.K^{-1}$. All fluid properties are evaluated with the bulk-fluid temperature. The Dittus-Boelter correlation is one of the simplified correlations that is valid for a smooth tube. For a rough tube, the Nusselt number is also expressed in terms of a friction factor, to account for the effect of tube roughness on heat transfer. Bhatti and Shah

[1987] listed a large number of available correlations for single-phase heat transfer, both with and without the friction-factor term. They recommended the Gnielinski correlation [1976], which is a modification of the Petukhov correlation [1970], for the general applications. The Gnielinski correlation is expressed as

$$Nu = \frac{(f/8)\,(Re - 1000)\,Pr}{1 + 12.7\,(f/8)^{1/2}\,(Pr^{2/3} - 1)} \tag{4.7}$$

for a range of Reynolds numbers from 2300 to $5x10^6$, and Prandtl numbers from 0.5 to 2000. This equation was also expressed in a simplified form as

$$Nu = 0.0214\,(Re^{0.8} - 100)\,Pr^{0.4} \tag{4.8}$$

for Prandtl numbers less than 1.5 and, otherwise,

$$Nu = 0.012\,(Re^{0.87} - 280)\,Pr^{0.4} \tag{4.9}$$

All correlations are derived with the assumption that the temperature difference between near-wall and bulk fluid is small. For a large temperature difference, the variation in fluid properties and its effect on the heat-transfer coefficient must be considered. Colburn [1933] indicated that this effect can be accounted for by simply using the properties based on the film, rather than the bulk-fluid temperature in his equation,

$$Nu = 0.023\,Re_{film}^{0.8}\,Pr_{film}^{1/3} \tag{4.10}$$

where the fluid properties are evaluated based on the film temperature defined as

$$T_{film} = \frac{T_w + T_b}{2} \tag{4.11}$$

Sieder and Tate [1936] recommended a correction to the Nusselt Number based on the bulk-fluid properties. The same correction factor for pressure drop is suggested; i.e.,

$$\frac{Nu}{Nu_{cp}} = \left(\frac{\mu_b}{\mu_w} \right)^m \tag{4.12}$$

with m being -0.14. The subscript "cp" refers to constant fluid-property values. Petukhov [1970], however, suggested a value of -0.11 as the exponent for a heating flow. Similar to the correction for pressure drop, different values of exponent have been recommended in various studies [Bhatti and Shah, 1987].

The correction for varying fluid properties on heat transfer is generally small. Therefore, a simple heat-transfer correlation with modified coefficients may be valid for compensating the effect. Rohsenow and Clark [1951] presented the Nusselt number as

$$Nu = 0.019\ Re^{0.8}\ Pr^{1/3} \tag{4.13}$$

for their high-pressure heat-transfer data of steam-water flow. Dormer and Bergles [1964], on the other hand, showed that their low-pressure data of steam-water flow was well-represented with

$$Nu = 0.0157\ Re^{0.85}\ Pr^{0.4} \tag{4.14}$$

With a large scatter among various data bases, it is difficult to identify the effect of varying properties. Whenever possible, ad hoc experimental heat-transfer data should be used to calculate the surface temperature. Otherwise, the effect of varying fluid properties on heat-transfer coefficients can be ignored for small viscosity ratios (less than 1.2) between the near-wall and

bulk fluid. For large viscosity ratios, however, the Petukhov correction for the Nusselt number is recommended.

4.3.2 Point of Onset of Nucleate Boiling

The point of onset of nucleate boiling (ONB) is the initial point of bubble formation on the surface. Several correlations (e.g., Bergles and Rohsenow [1963] and Jens and Lottes [1951]) were suggested to predict the point of ONB. They are only valid for conditions within their respective data bases. An analytical equation was derived by Davis and Anderson [1966]. It is expressed as

$$(\Delta T_{sat})_{ONB} = (T_w - T_{sat})_{ONB} = \left(\frac{8\ \sigma\ q_{ONB}\ T_{sat}}{H_{fg}\ k_l\ \rho_g} \right)^{0.5} \tag{4.15}$$

where σ is the surface tension in $N.m^{-1}$, T_w and T_{sat} are the wall and surface temperature in K, respectively, k_l is the thermal conductivity of liquid in $W.m^{-1}.K^{-1}$ and ρ_g is the vapour density in $kg.m^{-3}$. This equation was validated with a number of experimental data at both low- and high-pressure conditions.

4.3.3 Partial Boiling (or Developing Nucleate Boiling) Region

Partial boiling represents the transition region between single-phase flow and nucleate boiling. A complex evaluation procedure for heat-transfer coefficients in this region has been introduced by Bergles and Rohsenow [1963]. It requires the evaluation of wall superheats and surface heat fluxes at both single-phase flow and nucleate boiling. The wall superheat at partial boiling is determined by interpolation. Groeneveld et al. [1989] introduced a simplified approach to by-pass this region, forcing a direct transition from single-phase heat transfer to fully developed

nucleate boiling. The heat-transfer rate is based on the maximum value between heat-transfer coefficients of single-phase forced convection to liquid and of nucleate boiling for the same conditions. A similar approach was used by Zyatnina et al. [1989]. Although the transition based on this approach is abrupt, the difference in heat-transfer calculation is generally small between this simplified approach and the complex procedure of Bergles and Rohsenow.

4.3.4 Point of Net Vapour Generation (Onset of Significant Void or Bubble Departure)

The point of net vapour generation (onset of significant void or bubble departure) is the location where the departed bubbles from the heated surface do not immediately collapse due to condensation, but travel a relatively far distance from the surface. A number of studies have been performed to derive prediction methods for the point of net vapour generation [Levy, 1967; Staub, 1967; Ahmad, 1969]. These prediction methods, however, are valid for specific conditions only. In particular, the inlet subcooling has been shown to be a dominant factor affecting the accuracy of these methods.

Saha and Zuber [1974] considered the point of net vapour generation to be either a thermally or hydrodynamically controlled phenomenon, depending on the flow conditions. They compiled a set of data obtained in tubes, annuli and rectangular channels with water, Freon-114 and Freon-22 as coolants. When these data were presented in terms of Stanton number, St, and Peclet number, Pe, a systematic trend was noted despite a large data scatter. The Stanton number decreases with increasing Peclet number and becomes constant for Peclet numbers larger than 70 000. Based on this trend, a correlation was presented by Saha and Zuber for predicting the point of net vapour generation. It is expressed as

$$St = \frac{455}{Pe} \tag{4.16}$$

for Peclet numbers less than 70 000, and

$$St = 0.0065 \tag{4.17}$$

for Peclet numbers larger than 70 000. The Stanton and Peclet numbers are defined as

$$St = \frac{q}{G\ C_{pl}\ (T_{sat} - T_{b,z})} \tag{4.18}$$

and

$$Pe = \frac{G\ D\ C_{pl}}{k_l} \tag{4.19}$$

The value of 0.0065 corresponds to a relative apparent roughness (ε_a/D) of 0.02 for the bubble layer attached on the heated surface. In terms of thermodynamic quality at the point of net vapour generation, the Saha and Zuber correlations can also be expressed as

$$x_{NVG} = -0.0022\ \frac{q\ D\ Cp_l}{H_{fg}\ k_l} \tag{4.20}$$

for Peclet numbers less than 70 000, and

$$x_{NVG} = -154\ \frac{q}{G\ H_{fg}} \tag{4.21}$$

for Peclet numbers larger than 70 000. In view of the small number of data used to establish the constant value of 0.0065 (for Peclet number values between 70 000 and 400 000), this correlation may not be valid for large Peclet numbers (such as those beyond 400 000).

A subsequent analytical study by Avdeev [1988] resulted in the same set of equations. The constants, however, are slightly different. A value of 400 (instead of 455) is used in the equation for Peclet numbers less than 57 000 (70 000 in the Saha and Zuber correlation), and 0.007 (rather than 0.0065) for the other. The data used to validate Avdeev's analysis consisted mainly of high-pressure water data and covered Peclet numbers up to 800 000.

The predictions of the Saha and Zuber and the Avdeev correlations followed the general trend exhibited in their data bases. The uncertainty of these predictions is quite high (±25% in Saha and Zuber analysis and ±100% in Avdeev analysis), and may be due to an inlet-subcooling effect which is not accounted for in both correlations.

4.3.5 Nucleate Boiling

Many prediction methods for nucleate boiling have been developed, either in the form of correlations or graphs. They were usually derived for specific flow conditions: subcooled or saturated boiling. For subcooled boiling, most correlations were empirically based, resulting in a very limited range of application (e.g., Jens and Lottes [1951] and Thom et al. [1965]). Unless used for similar flow conditions, they are not recommended and have been superseded by new prediction methods.

For saturated boiling, a wide variety of prediction methods are available. Shah [1982] presented a graphical method for evaluating the heat-transfer ratio between nucleate boiling and single-phase liquid-only flow. This graphical method was later transformed into correlations. Chen [1963] divided the heat transfer during forced-convective nucleate boiling into two components: forced convection and pool nucleate boiling. The contribution of each component was determined from two empirically derived factors: enhancement and suppression. This correlation is still the most widely used and has been recommended by Collier [1981], Hsu [1982] and Hewitt [1982].

Several new prediction methods have since been derived using the same approach as used by Chen (e.g., Gungor and Winterton [1987], Kandlikar [1987] and Kenning and Cooper [1989]). Based on larger data bases (in terms of ranges of conditions and fluid types) than those used for deriving the Chen correlation, improvements were introduced for the heat-transfer prediction of pool nucleate boiling and for the empirical factors. Due to the large data scatter within each data base and the differences between various data bases, the uncertainty among the predictions of these new methods is also higher than the Chen correlation. Cooper [1989] recommended that the Chen correlation should be used, since there is no significant advantage in using other prediction methods in nucleate boiling.

The Chen correlation is expressed as

$$h_{nb} = F\ h_{conv} + S\ h_{pool} \tag{4.22}$$

where

$$h_{conv} = 0.023\ \frac{k_l}{D}\ Re_l^{0.8}\ Pr_l^{0.4} \tag{4.23}$$

$$h_{pool} = 0.00122 \left(\frac{k_l^{0.79}\ C_{pl}^{0.45}\ \rho_l^{0.49}}{\sigma^{0.5}\ \mu_l^{0.29}\ H_{fg}^{0.24}\ \rho_g^{0.24}} \right) \Delta T_{sat}^{0.24}\ \Delta P_{sat}^{0.75} \tag{4.24}$$

The enhancement factor, F, and suppression factor, S, were presented graphically by Chen [1963]. They were later optimized into two sets of equations [Bjornard and Griffith, 1977]. The enhancement factor was expressed as a function of the Martinelli parameter, X_{tt}, with

$$F = 1 \tag{4.25}$$

for $X_{tt}^{-1} \leq 0.1$, and

$$F = 2.35\ (X_{tt}^{-1} + 0.213)^{0.736} \tag{4.26}$$

for $X_{tt}^{-1} > 0.1$. The Martinelli parameter, X_{tt}, is defined as

$$X_{tt} = \left(\frac{1 - x_a}{x_a}\right)^{0.9} \left(\frac{\rho_g}{\rho_l}\right)^{0.5} \left(\frac{\mu_l}{\mu_g}\right)^{0.1} \tag{4.27}$$

The suppression factor is expressed as a function of the two-phase Reynolds number, Re_{tp}, with

$$S = \frac{1}{1 + 0.12\ Re_{tp}^{1.14}} \tag{4.28}$$

for $Re_{tp} < 32.5$, and

$$S = \frac{1}{1 + 0.42\ Re_{tp}^{0.78}} \tag{4.29}$$

for $32.5 \leq Re_{tp} \geq 70.0$, and

$$S = 0.1 \tag{4.30}$$

for $Re_{tp} > 70.0$. The two-phase Reynolds number is defined as

$$Re_{tp} = \frac{F^{1.25}\ G\ (1 - x_a)}{10000\ \mu_l} \tag{4.31}$$

4.3.6 Point of Suppression of Nucleate Boiling

The transition from saturated nucleate boiling to forced-convective evaporation occurs smoothly. In general, a combined phenomena of the two heat-transfer modes can be encountered at the transition region; i.e., a high bubble population at the liquid film and large amounts of droplets at the vapour core. A correlation was presented by Collier [1981] to predict the heat flux corresponding to this point. It is expressed as

$$\phi_{SNB} = \frac{98\ h_{fo}^2\ \sigma\ T_{sat}\ (\rho_l - \rho_g)}{h_{fg}\ k_l\ X_{tt}\ \rho_l\ \rho_g} \tag{4.32}$$

where h_{fo} is the single-phase heat-transfer coefficient for the total flow as liquid.

4.3.7 Forced-Convective Evaporation

Most heat-transfer prediction methods for nucleate boiling, derived from the mechanistic approach (such as the Chen correlation), are also applicable for forced-convective evaporation. Therefore, a separate prediction method is usually not needed.

4.3.8 Critical Heat Flux

The critical heat flux (CHF) point is the transition between forced convective evaporation and film boiling at high-quality flow (or between nucleate boiling and film boiling at low-quality flow). Many prediction methods for CHF exist in the literature (over 400, as indicated by Groeneveld et al. [1986]). The majority were derived for water-cooled tubes and have relatively narrow ranges of validity. Extrapolation is usually not recommended, but has become common practice. This can result in unrealistic CHF predictions (e.g., negative CHF) for those

correlations having incorrect parametric and asymptotic trends. Recent efforts have focused on deriving prediction methods that are applicable for a wide range of conditions.

The CHF for a tubular geometry is primarily a function of pressure, mass flux, quality and diameter, provided that the heated-length/diameter ratio is large. Various minimum heated-length/diameter ratios, ranging from 10 to 100 [Tong, 1972], depending on the flow conditions, were introduced as criteria. Collier [1981] indicated that a ratio of 80 is generally sufficient for dryout occurrence to be independent on the heated length, based on a constant dryout-quality condition (or local condition approach). The tube diameter, on the other hand, was shown to have a strong effect on CHF; the CHF increases with a decrease in tube diameter for dryout qualities greater than 0. Hence, most prediction methods use the tube diameter to characterize the geometry effect on CHF.

Among various prediction methods, the CHF look-up table has been widely used for general applications. This technique was initiated by Doroshchuk et al. [1975] and showed a significant improvement over the CHF correlation approach. Their table, however, did not cover all conditions of interest for a safety analysis of nuclear reactors. Groeneveld et al. [1986] expanded the CHF look-up table to a wider range of conditions. The predictions of their CHF table agreed closely with the experimental data in both their own and other independent assessments (e.g., Smith [1986]). Although the CHF table of Groeneveld et al. was derived from data for steam-water flow, it has also been found valid for other fluids as well, based on valid fluid-to-fluid modelling parameters [Groeneveld et al., 1992]. Recently, both CHF tables of Doroshchuk et al. and Groeneveld et al. have been updated and improved with a larger data base and wider ranges of application than their respective previous versions [Kirillov et al., 1991, Groeneveld et al., 1993]. An assessment of these tables with a large data base (over 22 000 data) indicated that the new CHF table of Groeneveld et al. [1993] is better than other available prediction methods [Leung and Groeneveld, 1993].

The CHF look-up table provides CHF values for discrete values of pressure, mass flux and quality covering the ranges of 0.1 to 20.0 MPa, 0 to 8 $Mg.m^{-2}.s^{-1}$, and -0.5 (subcooled conditions)

to 1.0, respectively. Linear interpolation between tabulated values is used for in-between conditions. Extrapolation is generally not needed, as the table covers a wide enough range of conditions for practical engineering applications (except perhaps for the fusion-reactor analysis, where mass flux is much higher than available). Part of the 1993 CHF table, which corresponds to the conditions of interest in this study, is shown in Appendix I.

All CHF tables were derived for vertical upward flow inside uniformly heated 8-mm tubes. Groeneveld et al. [1986] introduced a number of correction factors to be applied with the CHF look-up table for other geometries and flow conditions. For the diameter effect on CHF, Groeneveld et al. [1993] recommended the following correction factor

$$CHF_D = CHF_{D=8mm} \left(\frac{D}{8} \right)^{-0.5} \tag{4.33}$$

where $CHF_{D=8mm}$ is the CHF value for an 8-mm tube and can be obtained from the look-up table, and D is the diameter in mm.

4.3.9 Film Boiling

Precise prediction of film-boiling heat transfer over wide ranges of conditions is a nearly impossible task, since the dominant heat-transfer mechanisms vary with a change in flow conditions. The heated surface is cooled by:

a) forced convection to the vapour,
b) conduction to liquid (either in droplet or continuous form) through vapour,
c) liquid impingement on the heated surface, and
d) radiation to the liquid.

Accurate evaluation of these heat-transfer components requires knowledge of parameters such as droplet size and void fraction. Because of the high sheath temperature, measurement of these parameters is nearly impossible. Simplifying assumptions are routinely made to ease the evaluation procedures; this naturally results in less accurate predictions of film-boiling temperature. It is for this reason that the mechanistic models are less successful in predicting the film-boiling heat transfer over a wide range of conditions.

The prediction of film-boiling heat transfer is further complicated by different post-dryout flow regimes: dispersed flow and inverted annular flow. For dispersed-flow film boiling (also known as the liquid deficient regime), the vapour phase flows continuously with the droplets travelling at a similar velocity to the vapour. It occurs usually at high mass flux and high-quality conditions. For low-quality inverted-annular-flow film boiling, the liquid phase flows continuously in the core surrounded by the vapour phase. With increasing vapour velocity, waves are formed at the liquid-vapour interface. If the velocity is high, the wave crests could be sheared off and entrained into the vapour stream as droplets. Some of these droplets may be able to impinge and cool down the surface. The transition region between the two patterns is characterised by the entrained droplets and elongated slugs of liquid in the core, surrounded by the vapour phase.

Generally, three types of film-boiling heat transfer correlations can be encountered in the literature: empirical correlations, thermal equilibrium correlations and phenomenological correlations. The empirical correlations are simply based on the fitting of experimental results to various flow parameters. Most of them express heat flux as a function of wall superheat with a number of empirical factors (e.g., Collier [1962] and Lee [1970]). They are usually more accurate than other types of correlations within the ranges of their data base. However, their prediction accuracy deteriorates rapidly when extrapolated outside the data base. This is because the empirical correlation often exhibits incorrect asymptotic trends when extended beyond the valid range.

The thermal equilibrium correlations (e.g., Dougall & Rohsenow [1963]) assume that (i) heat transfer is due to forced convection between the wall and the vapour, and (ii) the liquid and the vapour are in thermal equilibrium; i.e., the liquid and vapour temperatures are equal to the saturation temperature. This assumption is reasonable for medium to high qualities and high mass flows, where the interfacial heat transfer is efficient. For high heat flux and low flows, however, the interfacial heat transfer is insufficient and large vapour superheats can occur. This has been confirmed in experimental studies (Groeneveld [1972]; Forslund & Rohsenow [1966]). Thermal equilibrium correlations are generally valid for the dispersed-flow film-boiling regime only. In inverted-annular flow film boiling, the vapour travels at lower velocity and can become highly superheated.

Phenomenological correlations are an improvement over the above two types, because they are based on physically correct assumptions. Hence, they tend to have the correct asymptotic trends. These correlations generally assume that the phases are in non-equilibrium (i.e., saturated-liquid and superheated-steam), and predict the vapour superheat as a function of flow, quality, heat flux, geometry and fluid properties. Examples of non-equilibrium correlations include the Tong-Young correlation [1974], Groeneveld-Delorme correlation [1976], and Chen et al. correlation [1979]. Their predictions, in general, provide closer agreement with the experimental results than those based on the thermal equilibrium assumption. However, these correlations are complex and usually require many iterations.

In inverted-annular flow film boiling, the heat transfer becomes more conduction controlled and, hence, depends strongly on the vapour film thickness. For high subcoolings, the vapour film becomes very thin, resulting in an increase in conduction heat transfer when compared to saturated inverted-annular film boiling. Thin vapour films usually correspond to low vapour velocity, due to the surface friction. Pool film-boiling equations presented by Bromley [1950] and Berenson [1961], with modifications to account for subcooling, vapour velocity or void fraction have been suggested for this regime [Groeneveld & Rousseau, 1983]. Due to the much lower convective heat-transfer rates in inverted-annular flow film boiling, high sheath-temperature

values are often encountered. As a result, heat transfer through radiation from the heated surface to the liquid core becomes significant.

Despite the advantage over other types of correlations, phenomenological correlations are usually valid for a single flow regime. Since they tend to have the correct asymptotic trends, extrapolation outside the data base range is often carried out. However, the prediction accuracy becomes poor when the correlation is being used in a different flow regime. To avoid this loss of accuracy, phenomenological correlations for different flow regimes have been combined into a hybrid type of correlation, which has a much wider range of validity.

Usually a hybrid correlation involves two different correlations, which cover both the dispersed flow and inverted-annular flow regimes. (In some cases, the natural convection equation is also included.) To select the correlation, the heat transfer coefficients for both correlations are first evaluated. The maximum value of heat transfer coefficient is chosen and used to calculate either the surface heat flux or the surface temperature. Groeneveld et al. [1989] recommended a combination of the Groeneveld-Delorme correlation and a modified Berenson equation. The modifications in the Berenson equation were introduced to account for the effect of subcooling (which improves the heat transfer) and void fraction (which decreases the heat transfer). The Groeneveld-Delorme correlation is expressed as

$$h_{dffb} = 0.008348 \frac{k_{vf}}{D} \left(Re_{vf} \left(x_a + (1 - x_a) \frac{\rho_v}{\rho_l} \right) \right)^{0.8774} Pr^{0.6112} \tag{4.34}$$

where ρ_v is the vapour density at the actual vapour temperature, T_{va}. The vapour-film properties are evaluated with the vapour-film temperature

$$T_{vf} = \frac{T_{va} + T_w}{2} \tag{4.35}$$

The actual vapour temperature is obtained from the actual vapour enthalpy, which is calculated from

$$H_{va} = H_{ve} + H_{fg} \exp(-\tan \psi) \tag{4.36}$$

where

$$\psi = 0.13864\ Pr_g^{0.2031} \left(Re_g \left(x_e + (1 - x_e) \frac{\rho_g}{\rho_l} \right) \right)^{0.20006} \left(\frac{q\ D\ C_{pg}}{k_g\ H_{fg}} \right)^{-0.09232} \cdot (1.3072 - 1.0833\ x_e + 0.84955\ x_e^2) \tag{4.37}$$

with $\psi = 0$ for $\psi < 0$, $\psi = \psi$ for $0 < \psi < \pi/2$, and $\psi = \pi/2$ for $\psi > \pi/2$.

The modified Berenson equation is expressed as

$$h_{Ber} = 0.425 \left(\frac{k_{vf}^3\ g^{1.5}\ \rho_{vf}\ (\rho_l - \rho_{vf})^{1.5}\ (H_{vf} - H_f)}{\mu_{vf}\ \Delta T_{sat}\ \sigma^{0.5}} \right)^{0.25} \tag{4.38}$$

$$h_{iafb} = h_{Ber} \left(1 + 25.5 \frac{\Delta T_{sub}}{T_b^*} \right) \left(1 - \alpha_H \right)^{0.5} \tag{4.39}$$

where T_b^* is the bulk-fluid temperature in K, and α_H is the void fraction based on the homogeneous-flow model

$$\alpha_H = \frac{\rho_l\ x_a}{\rho_l\ x_a + (1 - x_a)\ \rho_g} \tag{4.40}$$

At high sheath temperatures, radiation heat transfer becomes significant. Several methods can be used to evaluate the radiation heat transfer. The simplest one is the two grey-planes method, which assumes a continuous cylindrical liquid core and grey surface for both the wall and the liquid. The vapour phase is treated as an optically thin medium. Other methods are usually more complicated, and require the knowledge of parameters such as absorptivity, and transmissivity of vapour. These parameters are not well known for high pressure steam. Hence, the two grey-planes method is used

$$q_{rad} = 5.67\,x\,10^{-8}\frac{T_w^{*4} - T_{sat}^{*4}}{1/\varepsilon_w + 1/\varepsilon_l - 1} \tag{4.41}$$

4.3.10 Single-Phase Forced Convection to Vapour

Several of the phenomenological film-boiling correlations for tubes are based on the superheated-vapour equation of Hadaller and Banerjee [1969]. They are valid for both film boiling and superheated vapour, and provide a smooth transition. Thus, an additional equation for the heat transfer by forced convection to vapour is not necessary.

5. LITERATURE REVIEW OF EXPERIMENTAL AND EMPIRICAL STUDIES ON TWO-PHASE PRESSURE DROP DUE TO FRICTION

Numerous studies have focused on two-phase pressure drop due to friction. Most of them were performed under adiabatic conditions, with the majority in air-water flow. This has resulted in a number of correlations and semi-analytical models. Due to the large discrepancies among various data bases, a considerable difference in predictions can be noted from different correlations. Furthermore, the application of pressure-drop correlations for adiabatic flow to a heated channel, where a temperature gradient is present, introduces additional uncertainty.

A large amount of experimental work was performed to study two-phase frictional pressure drop for various flow conditions, geometries, channel orientations and fluids. In adiabatic flow, most studies were carried out with air-water flow at low-pressure conditions in horizontal channels to simulate oil-gas flow. For flow with heat addition, experiments were mainly performed with

steam-water flow. Due to the high operating cost, various types of refrigerant have recently been used as the modelling fluid for steam-water flow. The present discussion focuses primarily on steam-water or refrigerant flow in vertical heated tubes. It is divided into two groups, based on observations of the effect of heating on two-phase pressure drop. Other relevant experiments, such as those with adiabatic steam-water flow, are also described.

In general, there are two groups of empirical prediction methods for two-phase frictional pressure drop: graphs and correlations. Both of them are developed with experimental data, and each has its advantages and disadvantages as compared against the other.

Various terminologies, often used to represent two-phase frictional pressure drop, are described in Section 5.1. They are mainly the non-dimensional parameters with reference to single-phase frictional pressure drop. Section 5.2 describes the empirical studies that lead to various graphical prediction methods. Some adiabatic-flow studies are presented in Section 5.3. Since the present study focuses mainly on flow boiling, only a representation of correlations is described. The flow-boiling studies are presented in Sections 5.4 and 5.5. They are separated into two groups: no heating effect (Section 5.4) and strong heating effect (Section 5.5).

5.1 DEFINITIONS OF TWO-PHASE MULTIPLIER

The most widely used parameter used to present two-phase pressure drop due to friction is referred to as the two-phase multiplier, which expresses the ratio of frictional pressure drop between two-phase and single-phase flows. Different definitions of frictional pressure drop in single-phase flow, however, have been used.

The two-phase multiplier for liquid-only single-phase flow, which considers only the liquid portion of two-phase flow travelling in the same channel (based on $G_l = (1 - x_a)\, G$), is defined as

$$\phi_l^2 = \frac{(\Delta P / \Delta z)_{tp}}{(\Delta P / \Delta z)_l} \tag{5.1}$$

Similarly, the two-phase multiplier can be presented for only the vapour portion of two-phase flow travelling in the same channel as single-phase flow (based on $G_g = x_a G$), i.e.,

$$\phi_g^2 = \frac{(\Delta P / \Delta z)_{tp}}{(\Delta P / \Delta z)_g} \tag{5.2}$$

Equations (5.1) and (5.2) are often used in adiabatic flow, where no phase change takes place and the mass flow rate for each phase is known.

For flow with heat addition, the total mass-flow rate of both phases is often considered as liquid in single-phase flow (based on G), and the two-phase multiplier with total flow as single liquid phase is expressed as

$$\phi_{lo}^2 = \frac{(\Delta P / \Delta z)_{tp}}{(\Delta P / \Delta z)_{lo}} \tag{5.3}$$

or, with total flow as single vapour phase,

$$\phi_{go}^2 = \frac{(\Delta P / \Delta z)_{tp}}{(\Delta P / \Delta z)_{go}} \tag{5.4}$$

The relation between Equations (5.1) and (5.3) can be derived with the D'Arcy-Weisbach equation for pressure drop (Equation (2.37)) and the Blasius equation for friction factor (Equation (2.42)). The two-phase multiplier for total flow as liquid becomes

$$\phi_{lo}^2 = \phi_l^2 \, (1 - x_a)^{2-n} \tag{5.5}$$

where n is the geometry-dependent exponent in the Blasius equation. Similarly, between Equations (5.2) and (5.4), the two-phase multiplier for total flow as vapour is expressed as

$$\phi_{go}^2 = \phi_g^2 \, x_a^{2-n} \tag{5.6}$$

In addition to the two-phase multiplier, another non-dimensional two-phase pressure-drop function is often used in Russian publications. It is expressed as

$$\Delta P_{tp}^* = \frac{\Delta P_{tp} - \Delta P_{lo}}{\Delta P_{go} - \Delta P_{lo}} \tag{5.7}$$

In terms of the two-phase multiplier, Equation (5.7) can be written as

$$\Delta P_{tp}^* = \frac{\phi_{lo}^2 - 1}{\Delta P_{go} / \Delta P_{lo} - 1} \tag{5.8}$$

5.2 STUDIES LEADING TO GRAPHICAL METHOD

The graphical method presents plots of two-phase multiplier versus various parameters. It is an ideal tool for simple calculation, but is difficult to use in computer applications. In most cases, smoothing techniques and interpolation are required to maintain a systematic trend. This introduces additional uncertainties in the predictions.

5.2.1 The Lockhart and Martinelli Method

Lockhart and Martinelli [1949] presented the first graphical presentation of two-phase multipliers for adiabatic air-water flow inside horizontal channels. The two-phase multipliers are evaluated for both the liquid-only (i.e., ϕ_l^2) and vapour-only (i.e., ϕ_g^2) single-phase flows. They are shown in Figure 5.1 against the Martinelli parameter, X^2,

$$X^2 = \frac{(\Delta P / \Delta z)_l}{(\Delta P / \Delta z)_g} \tag{5.9}$$

which is the pressure-drop ratio between liquid-only and vapour-only flow. Different Martinelli parameters can be derived for various flow structures: viscous-liquid/viscous-vapour, viscous-liquid/turbulent-vapour, turbulent-liquid/viscous-vapour, turbulent-liquid/turbulent-vapour. Based on the D'Arcy-Weisbach equation for pressure drop and the Blasius equation for friction factor,

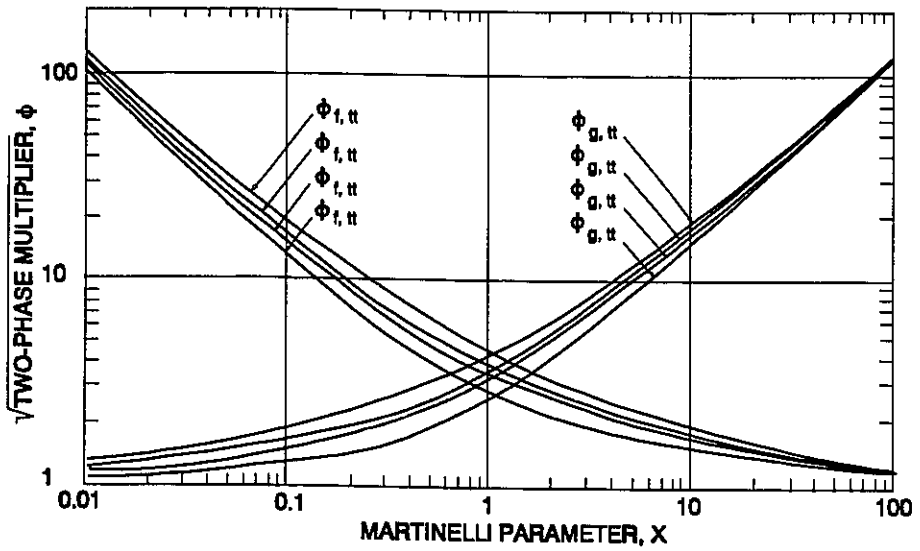

Figure 5.1: The Lockhart-Martinelli Graph of Two-Phase Multipliers for Air-Water Flow Inside Horizontal Channels.

the Martinelli parameter for turbulent-liquid/turbulent-vapour flow is expressed as a function of quality and fluid properties, i.e.,

$$X_{tt}^2 = \left(\frac{1 - x_a}{x_a} \right)^{2-n} \left(\frac{\rho_g}{\rho_l} \right) \left(\frac{\mu_l}{\mu_g} \right)^n \tag{5.10}$$

A systematic trend of decreasing ϕ_l with increasing X is shown in the Lockhart-Martinelli graph. Since this graph was developed with only the low-pressure air-water data, it is not recommended for other fluid mixtures. Furthermore, experimental data of two-phase frictional pressure drop indicated a strong effect of mass flux, which was not included in the Lockhart-Martinelli graphical method [Isbin et al., 1959, Muscettola, 1963].

5.2.2 The Martinelli and Nelson Method

Martinelli and Nelson [1948] extended the graphical approach used by Lockhart and Martinelli [1949] to steam-water flow inside a horizontal-heated channel. The two-phase multiplier, however, was based on single-phase flow evaluated with total flow as liquid (i.e., ϕ_{lo}^2), and was shown against the flow quality for various pressures. Figure 5.2 shows the Martinelli and Nelson graph, which is valid for the turbulent-liquid/turbulent-vapour flow only. Since the actual data base of Martinelli and Nelson was limited (primarily at conditions close to atmospheric and critical pressures), the curves for other pressures were obtained from interpolation.

The two-phase multiplier increases with decreasing pressure and increasing quality (except beyond ~90%, where a decreasing trend is shown). This increase is sharp at small quality (less than 10%) and low pressures. The maximum two-phase multiplier is about 700 at a quality of 90% and atmospheric pressure.

Due to the variations of local conditions along the axial flow direction, a non-linear pressure drop is exhibited in a heated channel. An average two-phase multiplier over the channel is calculated by integrating the local two-phase multiplier with respect to quality. It is expressed as

$$\overline{\phi_{lo}^2} = \frac{1}{x_a} \int_0^{x_a} \phi_{lo}^2 \, dx_a \qquad (5.11)$$

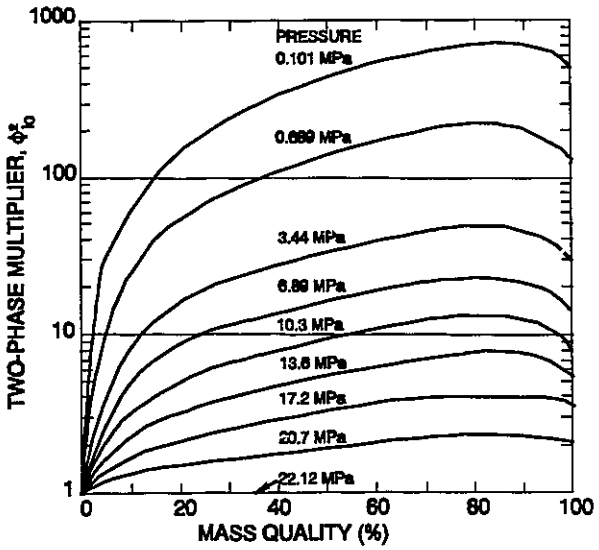

Figure 5.2: The Martinelli and Nelson Graphs for a Steam-Water Flow.

To simplify the evaluation, Martinelli and Nelson also presented graphically the average two-phase multiplier over the heated channel for flow of $x_{th} = 0$ (i.e., at saturation) at the inlet. Figure 5.3 shows the average two-phase multiplier as functions of exit qualities and pressures. The trends of the two-phase multiplier are similar to those presented in Figure 5.2 with respect to pressure and quality.

The Martinelli-Nelson graphs were developed with different fluid mixtures and flow conditions from the Lockhart-Martinelli graphs. However, Cravarolo et al. [1963] observed similarities between these graphs, and introduced a correction factor to transform the Lockhart-Martinelli to Martinelli-Nelson graphs. This correction factor is expressed as

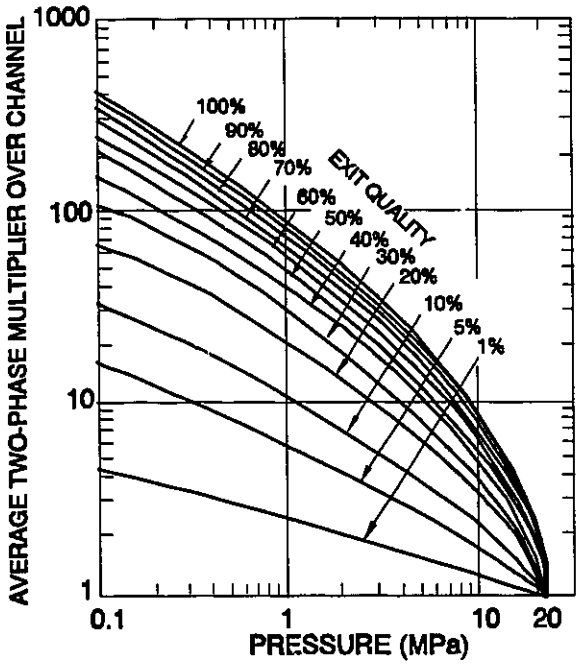

Figure 5.3: Average Two-Phase Multipliers for Steam-Water Flow inside a Horizontal-Heated Channel.

$$\frac{\phi^2_{l,M-N}}{\phi^2_{l,L-M}} = \left(\frac{\sigma}{45} \right)^{0.5} \tag{5.12}$$

5.2.3 The Thom Method

Thom [1964] extended the graphical method of Martinelli and Nelson [1948] to vertical steam-water flow boiling. The local two-phase multipliers (Figure 5.4) and the average two-phase multipliers over the heated channel (Figure 5.5) were presented with experimental data covering a much wider range of conditions than those used by Martinelli and Nelson.

Both sets of graphs exhibit similar trends, but the Thom method predicts generally smaller two-phase multipliers than the Martinelli-Nelson method. Furthermore, the Thom graphs cover a smaller range of pressures (from 1 to 22 MPa) than the Martinelli-Nelson graph (from 0.1 to 22 MPa). Thom showed a better agreement between predictions and steam-water data of Muscettola [1963] for his graph than the Martinelli-Nelson [1948] graph. However, both graphs did not account for the effect of mass flux (which is significant) on two-phase frictional pressure drop.

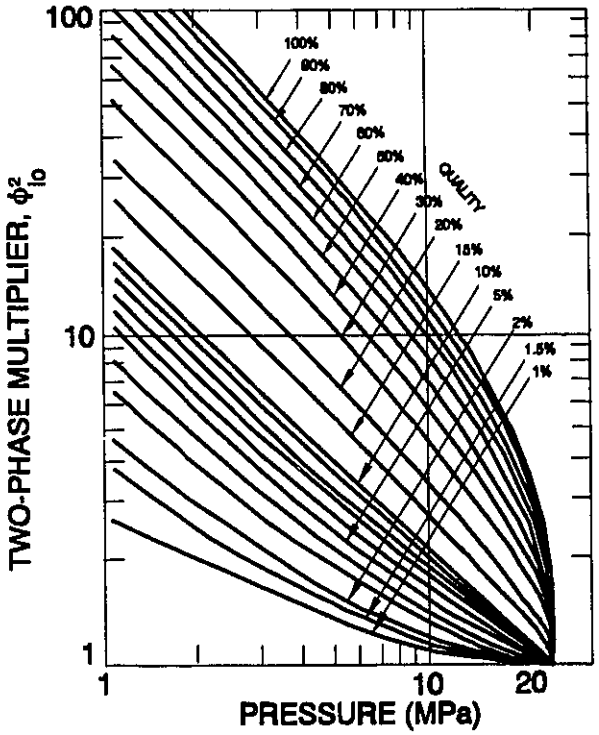

Figure 5.4: The Thom Graph of Local Two-Phase Multiplier for Steam-Water Flow in a Vertical Heated Channel.

5.2.4 The Baroczy Method

Baroczy [1965] developed a generalised graph that is valid for many types of fluids (including steam-water, air-water, Freon-22

flows). The two-phase multiplier is also calculated with the single-phase flow evaluated for total liquid flow rate. Figure 5.6 presents the Baroczy graph for a constant mass flux of 1356.3 $kg.m^{-2}.s^{-1}$. To extend the method to multi-fluid applications, the two-phase multiplier is shown against a property index defined as

$$\frac{(\mu_l/\mu_g)^{0.2}}{(\rho_l/\rho_g)} \qquad (5.13)$$

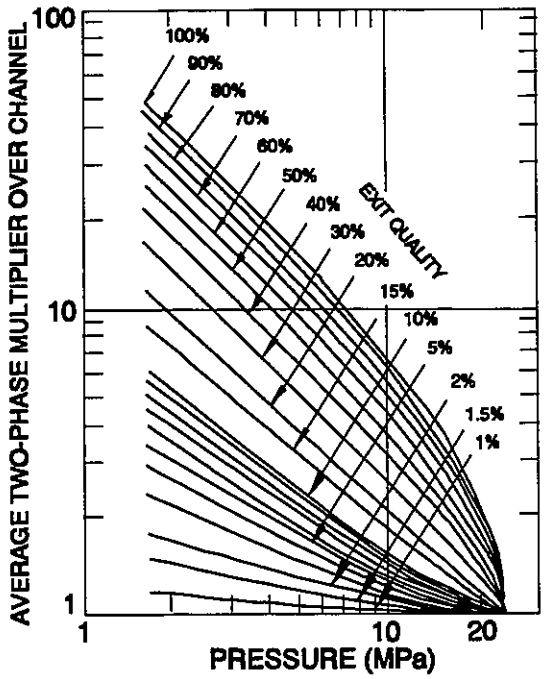

Figure 5.5: The Thom Graph of Average Two-Phase Multiplier for Steam-Water Flow Over a Vertical Heated Channel.

Overall, the two-phase multiplier decreases with increasing property index. The variation is larger at high than low qualities. In view

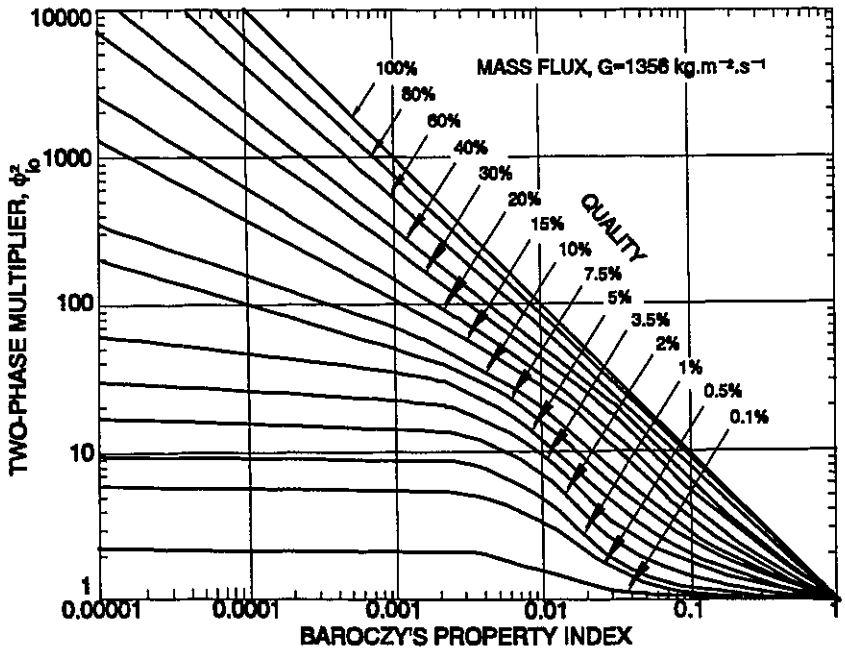

Figure 5.6: The Baroczy Generalised Graph of Two-Phase Multipliers.

of the strong mass-flux effect on the two-phase multiplier, Baroczy introduced four different graphs of correction factor to the two-phase multiplier obtained from Figure 5.6 (which is valid for a mass flux of 1356.3 $kg.m^{-2}.s^{-1}$). These correction factors are shown in Figure 5.7 and cover the mass-flux values of 339.1, 678.15, 2712.6 and 4068.9 $kg.m^{-2}.s^{-1}$. There is no systematic trend for these correction factors with respect to quality or property index.

A good agreement was shown by Baroczy between predictions and experimental data that were used in the development. However, a large deviation was observed for other experimental data

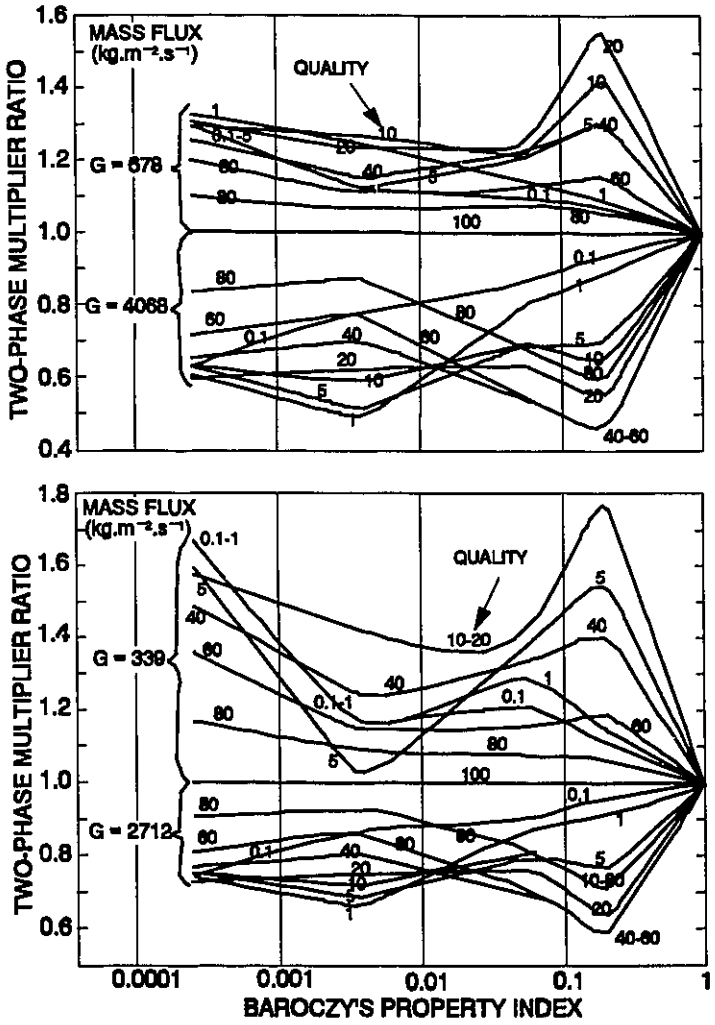

Figure 5.7: Baroczy's Correction Factors of Two-Phase Multiplier for Mass Fluxes Other Than 1356.3 $kg.m^{-2}.s^{-1}$.

[Baroczy, 1965], especially at high qualities. This method is better than the Martinelli-Nelson graph, mainly because of its inclusion of the mass-flux correction.

5.2.5 The Kirillov et al. Method

Kirillov et al. [1982] presented a graphical method for predicting the two-phase frictional pressure drop in vertical steam-water flow. The frictional pressure drop was presented in terms of the two-phase multiplier based on total liquid as single-phase flow. Figure 5.8 shows the two-phase multiplier for various qualities (from 0 to 1), pressures (from 6.86 to 22.1 MPa), and mass fluxes (from 0.5 to 3 $Mg.m^{-2}.s^{-1}$).

The two-phase multiplier depends strongly on the flow conditions. An increasing trend of two-phase multiplier is generally exhibited with increasing quality, decreasing mass flux and decreasing pressure. With increasing qualities at low flow, a local maximum pressure-drop ratio is shown. Kirillov et al. [1982] indicated that five pressure-drop regions (corresponding to different flow patterns) have been introduced, but the flow-pattern transitions were not presented. Hence, the relation between these local maximum two-phase multipliers and flow-pattern transitions cannot be substantiated. The corresponding quality to this maximum point shifts from high to low values with increasing pressure. At mass-flux values higher than 1 $Mg.m^{-2}.s^{-1}$, the local maximum point becomes a point of inflection only and the two-phase multiplier consistently increases with increasing quality.

The two-phase multiplier presented in Figure 5.8 is valid only for tubes of diameter larger than 17 mm. For a tube of diameter less than 17 mm, a correction factor was introduced by Kirillov et al., and is expressed as

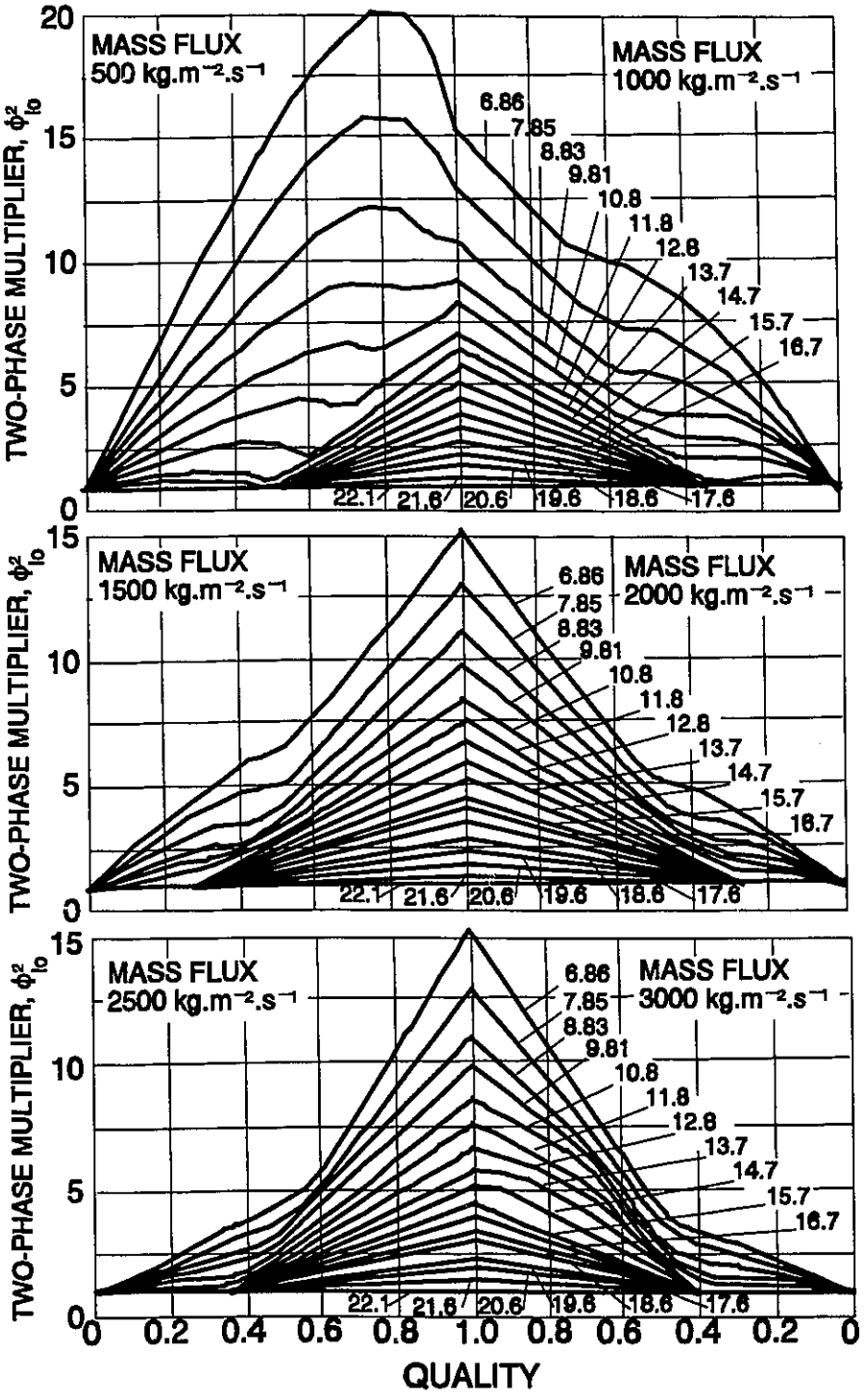

Figure 5.8: The Kirillov et al. Graph of Two-Phase Multiplier for Vertical Steam-Water Flow. (Each curve is labelled with the pressure in MPa.)

$$\frac{\phi_{lo}^{2'}}{\phi_{lo}^{2}} = -4\,(2.1 - 124D)\,x_a^2 + 4\,(2.1 - 124D)\,x_a + 1 \qquad (5.14)$$

where $\phi_{lo}^{2'}$ and ϕ_{lo}^{2} are the two-phase multipliers for tubes of D < 0.017 m and D ≥ 0.017 m (evaluated from Figure 5.8), respectively. The diameter effect diminishes at pressure greater than 17 MPa, and the correction factor becomes 1.

Kirillov et al. noted that the effect of surface heating on two-phase pressure drop is small. They recommended the Tarasova et al. [1965, 1966] correction factor to the two-phase multiplier obtained from Figure 5.8. This correction factor will be further discussed in a later section. It is expressed as

$$\frac{\phi_{lo,\,heated}^{2}}{\phi_{lo,\,adia.}^{2}} = 1 + 0.0044\left(\frac{q}{G}\right)^{0.7} \qquad (5.15)$$

5.3 ADIABATIC-FLOW STUDIES

Most studies with adiabatic flow were performed with air-water flow, which falls outside the scope of this review. However, several correlations derived from the works have been validated with experimental data of flow boiling. They will be described briefly in this section.

5.3.1 The Chisholm Correlation

Chisholm carried out a number of analytical and experimental studies on two-phase frictional pressure drop. He showed that the two-phase multipliers of the Lockhart-Martinelli graph can be represented by [Chisholm, 1967]

$$\phi_l^2 = 1 + \frac{C}{X} + \frac{1}{X^2} \tag{5.16}$$

$$\phi_g^2 = 1 + C\,X + X^2 \tag{5.17}$$

where X is the Martinelli parameter defined in Equation (5.10). The constants, C, for various flow structures are shown in Table 5.1. The agreement between predictions of these equations and the curves is better for the turbulent-liquid/turbulent-vapour than for the other conditions.

Table 5.1: Constant, C, in Equations (5.16) and (5.17) for Various Flow Structures.

Liquid	Vapour	Constant, C
viscous	viscous	5
viscous	turbulent	12
turbulent	viscous	10
turbulent	turbulent	20

Chisholm and Sutherland [1969] extended the applications of Equations (5.16) and (5.17) by introducing a varying parameter, C, for various flow geometries (e.g., elbows, valves and rough pipes). The parameter, C, is expressed as

$$C = \left(1+(C_2-1)\left(\frac{\rho_l-\rho_g}{\rho_l}\right)^{0.5}\right)\left(\left(\frac{\rho_l}{\rho_g}\right)^{0.5}+\left(\frac{\rho_g}{\rho_l}\right)^{0.5}\right) \tag{5.18}$$

The recommended values of C_2 are presented in Table 5.2. Using appropriate values for C_2, Chisholm and Sutherland showed that the combination of Equations (5.16) (or (5.17)) and (5.18) can generate curves closely agree with those of Lockhart and Martinelli [1949] and Baroczy [1965].

Equations (5.16) and (5.17) are valid only for adiabatic flow. Chisholm [1970] attempted to extend these equations to flow boiling, and noted that numerical integration is required. To simplify the applications, he derived a correlation that fits well with curves of various graphical methods. This correlation is expressed as

$$\phi_{lo}^2 = 1 + (\Gamma^2 - 1)(B x_a (1 - x_a) + x_a^2) \quad (5.19)$$

where Γ is the property index defined as

$$\Gamma = \left(\frac{\rho_l}{\rho_g} \right)^{0.5} \left(\frac{\mu_g}{\mu_l} \right)^{n/2} \quad (5.20)$$

This is similar to the one defined by Baroczy [1965] (Equation (5.13)) who used a value of 0.2 instead of 0.25 for the exponent. The coefficient, B, is defined as

$$B = \frac{C\,\Gamma - 2}{\Gamma^2 - 1} = \frac{C_2\,(\Gamma^2 + 1) - 2}{\Gamma^2 - 1} \quad (5.21)$$

Table 5.2: Recommended Values of C_2 in the Chisholm and Sutherland Correlation [1969].

	C_2
Reduction in pipe diameter	1
Thick plate (thickness > 10 mm)	1.5
Enlargement in pipe diameter	0.5
Thin plate (thickness ≤ 10 mm)	0.5
90° bends	1+35D/L
Tees	1.75
Gate valve	1.5
Globe valve	2.3
Friction in rough tubes:	
$G>1.5$ Mg.m^{-2}.s^{-1} or $30>(\rho_l / \rho_g)^{0.5}>9$	1
$G < 1.5$ Mg.m^{-2}.s^{-1} and $(\rho_l / \rho_g)^{0.5} < 9$	1.5/G
Friction in smooth tubes:	
$G>2$ Mg.m^{-2}.s^{-1} or $30 > (\rho_l / \rho_g)^{0.5} >9$	1
$G < 2$ Mg.m^{-2}.s^{-1} and $(\rho_l / \rho_g)^{0.5} < 9$	2/G

where C is the coefficient used in Equations (5.16) and (5.17), and C_2 is the coefficient used in Equation (5.18) and is presented in Table 5.2. This correlation could be integrated analytically for flow-boiling conditions, but is valid only for a rough pipe (n = 0).

In a later study, Chisholm [1973] extended Equation (5.19) to both smooth and rough pipes. The generalised correlation is expressed as

$$\phi_{lo}^2 = 1 + (\Gamma^2 - 1)\,(B\,x_a^{(2-n)/2}\,(1 - x_a)^{(2-n)/2} + x_a^{2-n}) \quad (5.22)$$

where the coefficient, B, is defined as

$$B = \frac{C\,\Gamma - 2^{2-n} + 2}{\Gamma^2 - 1} \tag{5.23}$$

Chisholm showed a good agreement between the Baroczy [1965] curves and Equation (5.22) using the optimized coefficient, B, in Table 5.3. The optimized values of 2.365 for the coefficient, B, and 0.25 for the Blasius exponent, n, provide also good agreement between Equation (5.22) and the Martinelli-Nelson curves. The coefficient, B, for general applications in smooth tubes is shown in Table 5.4.

Table 5.3: Coefficient, B, Used in the Chisholm Correlation to Fit Baroczy's Curves.

Property Index, Γ	Coefficient, B
$\Gamma \leq 9.5$	$55 / G^{0.5}$
$9.5 < \Gamma < 28$	$520 / (\Gamma\, G^{0.5})$
$\Gamma \geq 28$	$15\,000 / (\Gamma^2\, G^{0.5})$

For flow boiling, Chisholm [1973] did not indicate any effect of heat flux on the frictional pressure drop. The average two-phase multiplier for a uniformly heated channel is calculated by integrating Equation (5.22) from the saturation point to the outlet of the test section. It is expressed as

$$\overline{\phi_{lo}^2} = \frac{1}{z_o}\int_0^{z_o} \phi_{lo}^2\, dz = 1 + (\Gamma^2 - 1)\left(B\,F + \frac{x_{a,o}^{2-n}}{3-n}\right) \tag{5.24}$$

Table 5.4 : Values of Coefficient, B, Used in the Chisholm Correlation.

Property Index, Γ	Mass Flux ($kg.m^{-2}.s^{-1}$)	Coefficient, B
≤ 9.5	≤ 500	4.8
	$500 < G < 1900$	$2400 / G$
	≥ 1900	$55 / G^{0.5}$
$9.5 < \Gamma < 28$	≤ 600	$520 / (\Gamma\, G^{0.5})$
	> 600	$21 / \Gamma$
≥ 28		$15\,000 / (\Gamma^2\, G^{0.5})$

where

$$F = \frac{1}{x_{a,o}} \int_0^{x_{a,o}} x_a^{(2-n)/2} (1 - x_a)^{(2-n)/2} \, dx_a \tag{5.25}$$

$x_{a,o}$ is the vapour mass quality at the outlet of the test section and z_o is the axial distance from the point of saturation to the outlet. A tabulation of the integral term, F, was presented by Chisholm for various vapour mass qualities and Blasius exponents, and is shown in Table 5.5.

Table 5.5: Values of F in Equation (5.21).

Outlet Vapour Mass Quality	Exponent, n		
	0.25	0.20	0.10
0.01	0.00943	0.00829	0.00642
0.02	0.01720	0.01538	0.01232
0.03	0.02438	0.02202	0.01799
0.04	0.03117	0.02836	0.02349
0.05	0.03767	0.03446	0.02885
0.06	0.04393	0.04036	0.03408
0.07	0.04997	0.04608	0.03919
0.08	0.05582	0.05164	0.04421
0.09	0.06151	0.05706	0.04912
0.1	0.06704	0.06234	0.05392
0.2	0.11540	0.10895	0.09714
0.3	0.15366	0.14621	0.13242
0.4	0.18348	0.17540	0.16036
0.5	0.20562	0.19711	0.18122
0.6	0.22037	0.21159	0.19513
0.7	0.22788	0.21893	0.20213
0.8	0.22817	0.21915	0.20223
0.9	0.22101	0.21209	0.19536
1.0	0.20562	0.19711	0.18122

The Chisholm correlation was also validated with the flow-boiling data of Becker et al. [1962a]. However, a systematic overprediction was indicated and could be caused by the effect of heating on two-phase multiplier.

5.3.2 The Friedel Correlation

Friedel [1980] assessed 14 correlations for two-phase frictional pressure drop using 12 868 experimental data, and found that none of them was applicable for a wide range of conditions. Based on an expanded data base (with over 25 000 points), he subsequently derived a generalised correlation that is independent of flow pattern [Friedel, 1979]. The Friedel correlation is expressed as

$$\phi_{lo}^2 = (1 - x_a)^2 + x_a^2 \frac{\rho_f f_{go}}{\rho_g f_{lo}} + \frac{3.24\, x_a^{0.78} (1 - x_a)^{0.24} (\rho_f / \rho_g)^{0.91} (\mu_g / \mu_f)^{0.19} (1 - \mu_g / \mu_f)^{0.7}}{Fr^{0.045}\, We^{0.035}} \tag{5.26}$$

where

$$Fr = \frac{G^2}{g\, D\, \rho_{TP}^2} \tag{5.27}$$

$$We = \frac{G^2\, D}{\rho_{TP}\, \sigma} \tag{5.28}$$

and

$$\rho_{TP} = \left(\frac{x_a}{\rho_g} + \frac{1 - x_a}{\rho_f} \right)^{-1} \tag{5.29}$$

This correlation provides generally satisfactory predictions over a wide range of conditions. However, the uncertainty of its predictions remains high: the standard deviation is 26%, 32% and 25% for upward, horizontal and downward flow of a single-component mixture, respectively, and close to 52%, 43% and 54%, respectively, for two-component flow. This high uncertainty is primarily due to the large scatter among the data.

The Friedel correlation was also validated against the data of Freon-113 flow in horizontal tube [Ng et al., 1987]. Snoek and Leung [1986] assessed 11 different correlations using data of steam-water flow in horizontal 37-element bundles having various axial heat-flux distributions. The Friedel correlation provides the best agreement with their experimental data. Kohler and Kastner [1987] showed also a good agreement between the Friedel correlation with their flow-boiling data in tubes.

5.3.3 The Storek and Brauer Correlation

Storek and Brauer [1980] derived an extremely complex correlation for two-phase frictional pressure in adiabatic flow by examining the parametric trend of their data. Their correlation is based on the homogeneous-flow model, but includes a correction for the turbulent effect. It is expressed as

$$\left(\frac{dP}{dz} \right)_f = \phi_h \, \phi_k \, \frac{G^2}{2 \, \rho_h \, D} \tag{5.30}$$

where

$$\phi_h = \left(\left(\frac{64}{Re_h} \right)^2 + \left(\frac{0.3164}{Re_h^{0.25}} \right)^2 + \left(\frac{0.036}{Re_h^{0.1}} \right)^2 \right)^{0.5} \tag{5.31}$$

$$\phi_k = h_1 \, h_2^{-0.25} \tag{5.32}$$

$$h_1 = \left(1 + 51 \, (\varepsilon / D)^{0.8} \right)^{0.5} \tag{5.33}$$

$$h_2 = \left[\left(1 + C_1 \left(\frac{1-x}{x} \right)^{0.4} \right)^{-1} + \left(C_2 \left(\frac{1-x}{x} \right)^{-0.8} + C_3 \left(\frac{1-x}{x} \right) \right)^{-2} + \left(1 + 16 \left(\frac{1-x}{x} \right)^{-0.4} \right)^{-1} \right]^{-1/4} \tag{5.34}$$

The parameters, C_1, C_2, and C_3 were correlated for vertical upward flow as

$$C_1 = 50 \, Fr_h^{-0.37} \left(\frac{\rho_g}{\rho_l} \right)^{0.2} \frac{\mu_l}{\mu_g} \tag{5.35}$$

$$C_2 = 4.1 \left(\frac{\rho_g}{\rho_l} \right)^{0.55} \frac{\mu_l}{\mu_g} \tag{5.36}$$

$$C_3 = 0.01 \; Fr_h^{0.2} \; We_h^{0.05} \tag{5.37}$$

and for horizontal flow as

$$C_1 = 0.6 \; Fr_h^{0.08} \; \frac{\mu_l}{\mu_g} \tag{5.38}$$

$$C_2 = 1.6 \; Fr_h^{0.4} \left(\frac{\rho_g}{\rho_l} \right)^{0.6} \left(\frac{\mu_l}{\mu_g} \right)^{0.3} \tag{5.39}$$

$$C_3 = 0.02 \; Fr_h^{0.2} \; We_h^{0.17} \left(\frac{\rho_g}{\rho_l} \right)^{0.47} \tag{5.40}$$

The two-phase density is defined as

$$\rho_h = \frac{\rho_g \; \rho_l}{x \; (\rho_l - \rho_g) + \rho_g} \tag{5.41}$$

the two-phase Froude number is

$$Fr_h = \frac{G^2}{g \; D \; \rho_h^2} \tag{5.42}$$

the two-phase Weber number is

$$We_h = \frac{G^2 D}{\rho_h \sigma} \tag{5.43}$$

the two-phase Reynolds number is

$$Re_h = \frac{G D}{\mu_h} \tag{5.44}$$

and the two-phase viscosity is

$$\mu_h = \frac{\mu_g \mu_l}{x (\mu_l - \mu_g) + \mu_g} \tag{5.45}$$

This correlation provides a better agreement with the experimental data than the Bandel [1973], Chawla [1969], Lockhart and Martinelli [1949] and Bankoff [1960] correlations. It also predicts closely the two-phase frictional pressure drops in heated channels with argon and nitrogen flow, but the much simpler Cicchitti and Lombardi correlation [1960] gives equally good predictions for the same data base [Müller and Steiner, 1983].

5.3.4 The Reddy et al. Correlation

Reddy et al. [1982] examined 2397 pressure-drop data obtained by Bertoletti et al. [1963] and Gaspari et al. [1968] with adiabatic and boiling steam-water flows in vertical tubes. A correlation was derived with a modification to the homogeneous model. It is expressed as

$$\phi_{lo}^2 = 1 + x_a \left(\frac{\rho_f}{\rho_g} - 1 \right) C \tag{5.46}$$

where

$$C = 0.0397\ x_a^{-0.175}\ G^{-0.45} \tag{5.47}$$

for a pressure higher than 4136 kPa, and

$$C = 0.0139\ \left(1 + \frac{P}{P_{cr}}\right)\ x_a^{-0.175}\ G^{-0.45} \tag{5.48}$$

for a pressure between 2068 and 4136 kPa.

Using the homogeneous void model and the Blasius friction factor in the comparison against the adiabatic-flow data, this correlation provides better predictions than the homogeneous model, the Dukler et al. [1964] and Chisholm correlations [1973], as well as the Martinelli and Nelson [1948], Thom [1964], and Baroczy graphical methods [1965]. However, the difference in accuracy between this correlation and the Chisholm correlation was small.

This correlation can be integrated analytically (as compared to numerical integration, required by most correlations) for calculating the average two-phase multiplier over a heated channel. Based on the average two-phase multiplier, it was shown to be better than the other correlations when compared to flow-boiling pressure-drop data. However, this might not be a fair comparison, since the test data were used in optimizing the coefficients of this correlation. Furthermore, the assessment did not include cases with subcooled flow, since all of their data were obtained with a two-phase inlet condition, which could have a strong impact on the flow distribution and hence the pressure drop.

5.4 FLOW-BOILING STUDIES AND CORRELATIONS (NO HEATING EFFECT)

Most flow-boiling studies did not consider the effect of heating on two-phase frictional pressure drop. The same prediction methods for adiabatic flow are often used to evaluate the local two-phase multiplier based on the local conditions in a heated channel. Several studies with this approach have been described in Sections 5.2 and 5.3. Since the flow conditions (and hence flow patterns) vary along the heated channel, a combination of specific correlations (which are valid for individual flow pattern) has been recommended for predicting the overall pressure drop (e.g., the Jia and Schrock [1986] model for subcooled-boiling conditions).

5.4.1 The Becker Correlation

Becker et al. [1961, 1962a, 1962b, 1962c, 1962d] initiated an extensive program to study the pressure gradient of water flow inside a heated vertical tube. Their experiments covered a wide range of flow conditions and several tube-diameter values. Overall, the pressure drop was affected by pressure and quality, but not by the mass flux, inlet subcooling, surface heat flux and diameter. An empirical correlation was optimized with their data base and is expressed as

$$\phi_{lo}^2 = 1 + 2500 \left(\frac{x}{P} \right)^{0.96} \tag{5.49}$$

where P is the pressure in $kg.cm^{-2}$. Compared against the predictions of other correlations, limited success was indicated with the Lockhart-Martinelli graph at some conditions, but the Martinelli-Nelson graph significantly underpredicted the data. This is surprising, since the latter was derived with steam-water data and the former with air-water data.

5.4.2 The CISE Studies

Lombardi and Pedrocchi [1972] compiled close to 1400 two-phase pressure-drop data obtained in vertical tubes, annuli and rod bundles, with the majority obtained in both heated and unheated steam-water flows. Unlike others, the pressure drop over the channel was derived with an energy, rather than a momentum, balance (see Section 3.4). For simplicity, the two-phase pressure drops due to acceleration and gravity were calculated using the homogeneous-flow model. Based on the observed parametric trends, the frictional pressure drop was correlated as

$$dP_f = K\ G^n\ \frac{\sigma^{0.4}}{\rho_{tp}^{0.86}\ D^{1.2}}\ dz \tag{5.50}$$

where

$$\frac{1}{\rho_{tp}} = \frac{x_a}{\rho_g} + \frac{1 - x_a}{\rho_f} \tag{5.51}$$

The constants K and n are geometry-dependent values which are 0.83 and 1.4, respectively, for round tubes, and 0.213 and 1.6, respectively, for annuli and rod bundles. An assessment based on the total pressure drop (i.e., summation of all three components) indicated a close agreement between the predictions and the experimental data. The effect of heating cannot be examined, since the constants in this correlation were optimized with data of both adiabatic flow and flow boiling.

With the D'Arcy-Weisbach equation for single-phase liquid flow in round tubes, this correlation can be presented in terms of a two-phase multiplier

$$\phi_{lo}^2 = \frac{1.66\ \sigma^{0.4}\ \rho_l}{f\ \rho_{tp}^{0.86}\ G^{0.6}\ D^{0.2}} \tag{5.52}$$

This correlation, together with the Chisholm-Baroczy correlation, was found to provide the least root-mean-square errors (which were between 27% and 65%, depending on the fluid mixture) in an assessment of 14 correlations for two-phase frictional pressure drop based on a large data bank of adiabatic flow [Friedel, 1980].

Lombardi and Ceresa [1978] modified the Lombardi and Pedrocchi correlation to improve the parametric trend of two-phase frictional pressure drop at low-quality and high-quality regions. They expressed the frictional pressure drop as

$$dP_f = \frac{2\,G^2}{\rho_{tp}\,D}\,(f_g\,p_g + f_l\,p_l + f_{tp}\,p_{tp})\,dz \tag{5.53}$$

For a smooth tube, the friction factors for the gas/vapour phase, f_g, and the liquid phase, f_l, were calculated for turbulent flow with

$$f_g = 0.046\,Re_g^{-0.2} \tag{5.54}$$

$$f_l = 0.046\,Re_l^{-0.2} \tag{5.55}$$

and for laminar flow (i.e., Re less than 2400) with

$$f_g = 16\,Re_g^{-1} \tag{5.56}$$

$$f_l = 16\,Re_l^{-1} \tag{5.57}$$

where

$$Re_g = \frac{G\,D}{\mu_g} \tag{5.58}$$

$$Re_l = \frac{G\ D}{\mu_l} \tag{5.59}$$

The two-phase friction factor was correlated in terms of a dimensionless parameter

$$Lo = \frac{G^2\ D}{\rho_{tp}\ \sigma}\left(\frac{\mu_g}{\mu_l}\right)^{0.5} \tag{5.60}$$

and a transition point

$$Lo_t = a_1\ \frac{D^2}{\sigma^{0.5}}\ \frac{\mu_g}{\mu_l} \tag{5.61}$$

It is expressed as, for Lo greater than or equal to Lo_t,

$$f_{tp} = K_1\ (Lo)^n \tag{5.62}$$

or otherwise

$$f_{tp} = K_2\ (Lo)^{a_2} \tag{5.63}$$

where

$$K_2 = K_1\ (Lo_t)^{n - a_2} \tag{5.64}$$

The weighting functions, p_g, p_l and p_{tp} were correlated as

$$p_g = x^{a_3} \tag{5.65}$$

$$p_l = (1 - x)^{a_4} \tag{5.66}$$

$$p_{tp} = 1 - p_g - p_l \tag{5.67}$$

The recommended values for constants a_1, a_2, a_3, a_4, K_1 and n are 1.65×10^6, -1, 40, 100, 0.046 and -0.25, respectively. However, Lombardi and Ceresa suggested re-optimizing these constants using a specific set of experimental data to further improve the accuracy. While the parametric trend of this correlation is improved, the prediction accuracy becomes worse than the Lombardi and Pedrocchi correlation. The overall rms error for steam-water flow is about 13% in both adiabatic-flow and flow-boiling conditions.

Bonfanti et al. [1979] re-optimized the constants in the Lombardi and Ceresa correlation to improve the prediction at the low flow-rate region. Based on the same values for K_1, n and a_4, a flow-dependent value was introduced for a_3 which is 20 for a mass flux less than 100 $kg.m^{-2}.s^{-1}$, and 7 otherwise. The values a_1 and a_2, on the other hand, become geometry dependent. They are 1.25×10^6 and -1.25, respectively, for round tubes, and 1.65×10^6 and -1, respectively, for rod bundles.

5.4.3 The Bandel and Schlűnder Correlation

Bandel and Schlűnder [1974b] observed similar characteristics between frictional pressure drop and mass flux in a log-log plot for both the stratified-flow and annular-flow regimes in horizontal flow. By modifying the single-phase pressure-drop equation to include the interface momentum exchange, they derived a correlation for these flow regimes based on the following assumptions:

i) pressure drop is equal for both phases,

ii) friction factor at the wall for either phase is obtained with the Blasius equation (i.e., $f_{g,w} = 0.3164\ Re_g^{-0.25}$ and $f_{l,w} = 0.3164\ Re_l^{-0.25}$), and

iii) interfacial friction factor is also proportional to $Re^{-0.25}$.

The pressure drops for the vapour and the liquid phases were expressed as

$$\left(\frac{\Delta P}{\Delta z} \right)_{g,tp} = (f_{g,w} + f_{g,i}) \frac{\rho_g j_g^2}{2 D_{h,g}} \tag{5.68}$$

$$\left(\frac{\Delta P}{\Delta z} \right)_{l,tp} = (f_{l,w} + f_{l,i}) \frac{\rho_l j_l^2}{2 D_{h,l}} \tag{5.69}$$

where f is the friction factor, ρ is the density in $kg.m^{-3}$, j is the superficial phasic velocity in $m.s^{-1}$ and D_h is the hydraulic equivalent diameter in m. The subscripts 'g', 'l', 'i' and 'w' represent corresponding values of vapour phase, liquid phase, interface, and wall regions. From assumption (i), the two-phase pressure gradient can be expressed as either

$$\left(\frac{\Delta P}{\Delta z}\right)_{tp} = \left(\frac{\Delta P}{\Delta z}\right)_{g,tp} = \left(\frac{\Delta P}{\Delta z}\right)_{g,sp}\left(1+\frac{F_g}{0.3164}\right)\left(\frac{D}{D_{h,g}}\right)^{1.25}\left(\frac{A_F}{A_{F,g}}\right)^{1.75} \tag{5.70}$$

or

$$\left(\frac{\Delta P}{\Delta z}\right)_{tp} = \left(\frac{\Delta P}{\Delta z}\right)_{l,tp} = \left(\frac{\Delta P}{\Delta z}\right)_{l,sp}\left(1+\frac{F_l}{0.3164}\right)\left(\frac{D}{D_{h,l}}\right)^{1.25}\left(\frac{A_F}{A_{F,l}}\right)^{1.75} \tag{5.71}$$

where A_F is the flow area in m^2. The functions, F_g and F_l for the interfacial friction factor were correlated with their Refrigerant-22 data obtained inside a horizontal heated tube [Bandel and Schlűnder, 1974a] and the Dukler data. For stratified flow, both F_g and F_l are zero. For annular flow, the function, F_g, is expressed as

$$F_g = 0.15 \left(\frac{1 - x_a}{x_a} \right)^{0.5} \left(\frac{\mu_l}{\mu_g} \right)^{0.3} \tag{5.72}$$

for $x_a \leq 0.5$, and

$$F_g = 0.16\ (1 - x_a)^{0.1} \left(\frac{\mu_l}{\mu_g}\right)^{0.3} \tag{5.73}$$

for $x_a > 0.5$, and the function,F_l, is calculated with

$$F_l = -0.31\ x_a \tag{5.74}$$

where x_a is the flow quality and μ is the viscosity in $kg.m.s^{-1}$. Two criteria were derived from the balance of gravitational and frictional forces for the flow-pattern transitions to which this correlation is limited. The functions for stratified flow are valid when

$$Fr.Eu = \frac{\Delta P\ /\ \Delta z}{\rho_l\ g} \leq \frac{x_a}{15} \left(\frac{\mu_g}{\mu_l}\right)^{0.2} \tag{5.75}$$

and for annular flow when

$$Fr.Eu = \frac{\Delta P\ /\ \Delta z}{\rho_l\ g} \geq \frac{1}{10\ x_a^{0.3}} \tag{5.76}$$

For the intermittent-flow regime, the pressure drop is evaluated by a logarithmic interpolation between the transition criterion from stratified to intermittent flow and from intermittent to annular flow. Compared against the experimental data of air-water, air-oil, steam-water, and refrigerant flow, this combination of correlations shows a better agreement than the Lockhart-Martinelli and the Chawla correlations. For steam-water flow, however, the prediction error is large.

5.4.4 The Muller-Steinhagen and Heck Study

Muller-Steinhagen and Heck [1986] derived a simple correlation for predicting the two-phase frictional pressure drop for various fluids. The correlation is based on a linear interpolation between single-phase pressure drop of liquid and of gas with respect to quality over the range of 0 to 0.7. It is superimposed in the single-phase pressure drop of gas to cover the range from 0.7 to 1. The Muller-Steinhagen and Heck correlation is expressed as

$$\left(\frac{dP}{dz}\right)_{fric.,tp} = \left[\left(\frac{dP}{dz}\right)_{fric.,lo} + 2\,x_a\left(\left(\frac{dP}{dz}\right)_{fric.,go} - \left(\frac{dP}{dz}\right)_{fric.,lo}\right)\right](1-x_a)^{1/3} + x_a^3\left(\frac{dP}{dz}\right)_{fric.,go} \tag{5.77}$$

where

$$\left(\frac{dP}{dz}\right)_{fric.,lo} = f_{lo}\,\frac{G^2}{2\,\rho_l\,D} \tag{5.78}$$

$$\left(\frac{dP}{dz}\right)_{fric.,go} = f_{go}\,\frac{G^2}{2\,\rho_g\,D} \tag{5.79}$$

with

$$f_{lo} = \frac{64}{Re_{lo}} \qquad f_{go} = \frac{64}{Re_{go}} \qquad for\ Re_{lo},\ Re_{go} \le 1187 \tag{5.80}$$

$$f_{lo} = \frac{0.3164}{Re_{lo}^{1/4}} \qquad f_{go} = \frac{0.3164}{Re_{go}^{1/4}} \qquad for\ Re_{lo},\ Re_{go} > 1187 \tag{5.81}$$

and

$$Re_{lo} = \frac{G\,D}{\mu_l} \qquad Re_{go} = \frac{G\,D}{\mu_g} \tag{5.82}$$

Muller-Steinhagen and Heck recommended that the application of their correlation should be limited to flow conditions where Re_{lo} is greater than 100, and to fluids with larger single-phase pressure drop of gas than of liquid. For flow boiling, this correlation can be integrated analytically to obtain the frictional pressure drop over the channel. The pressure drop due to acceleration, however, must be calculated separately.

A comparison of predictions from this and 14 other correlations against their data bank of 9313 data indicates only relative success with this correlation. Among various correlations, the predictions of the Bandel and Schlünder correlation [1974a] have the lowest root-mean-square (rms) error (32.6%) and the most data within the ±30% error range (60%). The Muller-Steinhagen and Heck correlation yields a rms error of 42%, with 50% of the data within the ±30% error range. It is better than the performance of the Friedel correlation [1979] and many others.

Paliwoda [1989] modified the correlation of Muller-Steinhagen and Heck and presented a dimensionless form of the correlation. By integrating the dimensionless correlation, he derived an equation to calculate the ratio of average two-phase pressure drop over a section of a horizontal heated channel to the single-phase pressure drop corresponding to total flow as vapour.

5.4.5 The Kohler and Kastner, and Brand et al. Experiments

Kohler and Kastner [1987] and Brand et al. [1987] presented their measurements of two-phase pressure drop in a vertical boiler tube. These data cover heat-transfer modes from single-phase to post-dryout flows. However, the range of conditions are not extensive enough to provide detailed information of the heating effect. For pre-dryout conditions, Kohler and Kastner indicated that the frictional pressure drops are similar in adiabatic flow to those of flow boiling.

A steep drop in two-phase multiplier has been observed at dryout. Beyond dryout, the two-phase multiplier is significantly smaller than that of adiabatic flow.

A comparison was made between their experimental data in the pre-dryout region, and the predictions of the homogeneous-flow model as presented by Owen [1961], and the Lombardi and Pedrocchi [1972], the Friedel [1979], and the Storek and Brauer [1980] correlations. The Friedel correlation is the best for the pre-dryout data, and the Beattie correlation [1973] (the only correlation available) agrees closely with the post-dryout data. A modification to the Friedel correlation was also introduced by Kohler and Kastner [1987], to account for the effect of surface roughness on two-phase frictional pressure drop.

5.5 FLOW-BOILING STUDIES AND CORRELATIONS (STRONG HEATING EFFECT)

Prediction methods examined in Section 5.4 have not considered any direct effect of heating on frictional pressure drop in flow boiling, although this effect is indirectly included through the calculation of flow quality based on heat balance. These methods have the advantage of being applicable to both adiabatic flow and flow with heat addition. However, further studies have shown a particularly strong effect of surface heat flux on two-phase frictional pressure drop.

In early studies of flow boiling, the total pressure drop was often examined and presented for a constant inlet condition (e.g., Owen and Schrock [1960]). Since the pressure drop due to acceleration can be significant, especially at low-pressure conditions, the results are not always useful for analyzing the frictional pressure drop only. Furthermore, the correlations derived from these studies were often expressed in terms of boiling length. They become geometry dependent and cannot be used for a local-conditions type of analysis.

5.5.1 The Dormer and Bergles Experiment

Dormer and Bergles [1964] obtained pressure-drop measurements for subcooled boiling at low-pressure (0.2 to 0.55 MPa) but high mass-flux (up to 15 $Mg.m^{-2}.s^{-1}$) conditions along several horizontal test sections. Their tests cover several tube-diameter and heated-length values, but the overall heated-length to diameter (L/D) ratios are small. Most data were obtained with L/D ratios less than 100, where the flow may still be in the hydrodynamic-developing region.

A strong effect of heating on total pressure drops (due to friction and acceleration) over the channel was shown in the data of Dormer and Bergles, who indicated 3 regions of pressure drop at various heat-flux values. The first region represents the non-boiling region (i.e., single-phase flow) where total pressure drop decreases with increasing heat flux. These results have been mentioned in Section 2.3.1.2, where a correction factor to the adiabatic pressure drop was presented. The second region is the highly subcooled flow-boiling region, where a gradual increase in total pressure drop is observed with increasing heat flux. Dormer and Bergles stated that this increase is caused by the bubble agitation due to surface boiling. The rate of increase, however, is reduced due to the reduction in near-wall viscosity. A sharp increase in total pressure drop is shown for the third region, where low-subcooled flow boiling takes place.

After combining all data and smoothing out the trend, a graphical correlation was presented to predict the two-phase pressure drop inside the heated tube. It is shown in Figure 5.9, which presents the total pressure-drop ratio between boiling and adiabatic flow with respect to a ratio between local heat flux and heat flux required to bring the fluid to saturation. In addition, the heated-length to diameter ratio was included as a controlling parameter. This correlation is not valid for conditions outside the experimental range.

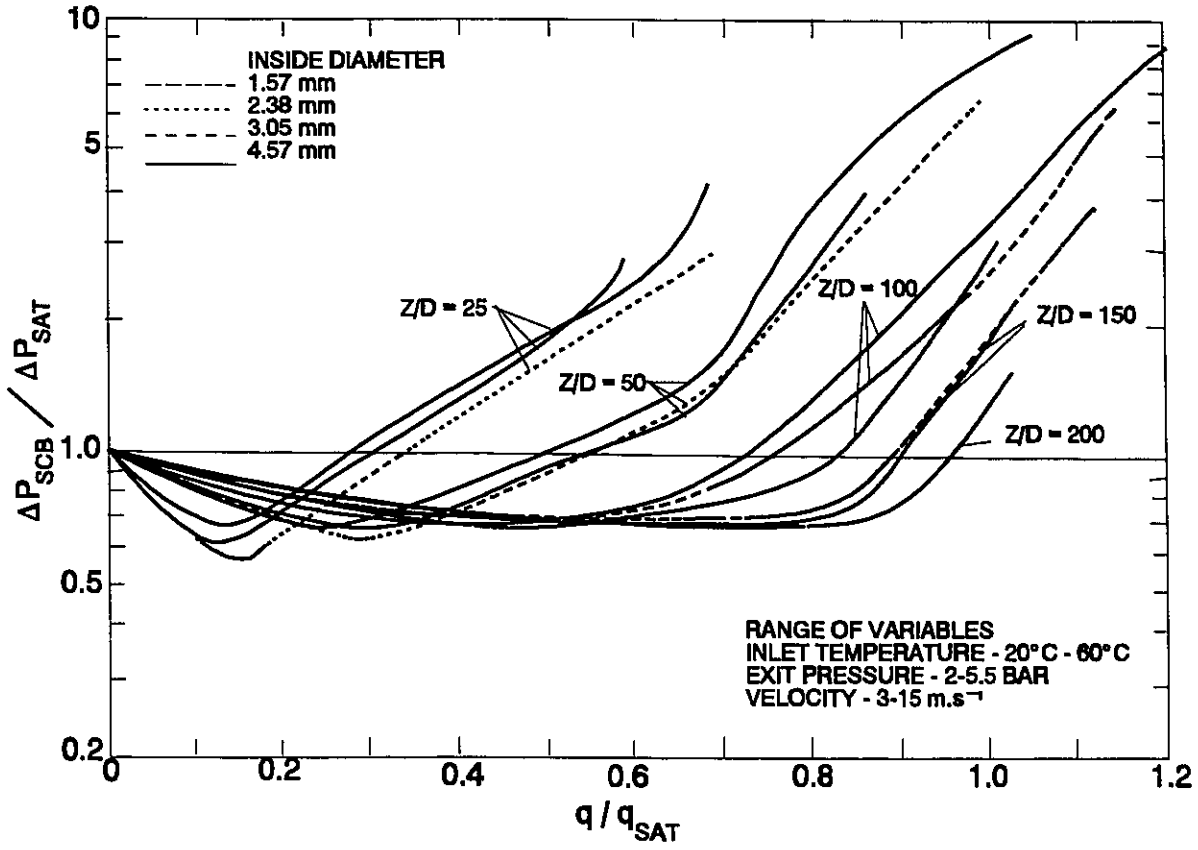

Figure 5.9: The Dormer and Bergles Correlation for Pressure Drop in Subcooled Boiling.

5.5.2 The Tarasova et al. Experiment

Tarasova et al. [1966] observed a heating effect at the same local conditions for high-pressure steam-water flow inside tubes and annuli. The pressure gradient increases for subcooled and saturated boiling (the bubbly-flow regime), but it decreases for forced-convective evaporation (the annular or wispy-annular flow regime) in a heated channel. For the transition region, a local maximum pressure drop followed by a local minimum is exhibited in the heated channel. For adiabatic flow, however, only a point of inflection in pressure drop was noted over the same region. At high system pressures, the two-phase frictional pressure drop decreases and the region bounded between the local maxima and minima becomes wide. Figure 5.10 illustrates the effect of heating on the two-phase frictional multiplier in an annulus.

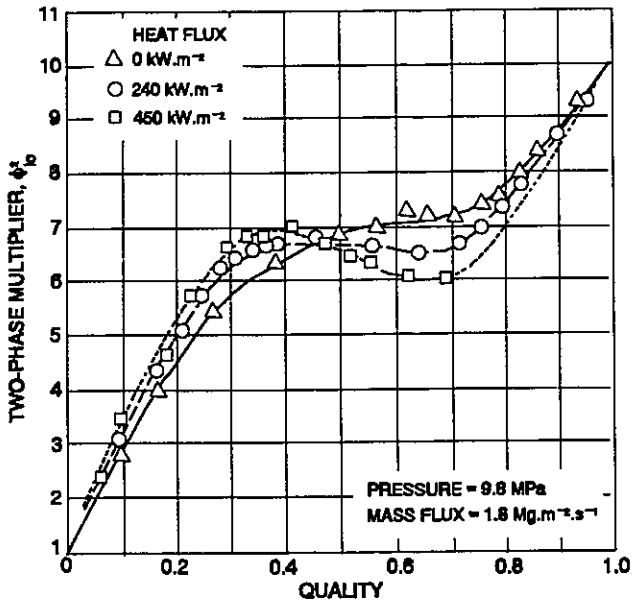

Figure 5.10: Effect of Heating on Two-Phase Multipliers in Annulus [Tarasova et al., 1966].

Tarasova et al. presented correction factors for the heating effect on frictional pressure drop in subcooled-boiling and in saturated-boiling regions. The correction factor for subcooled boiling is expressed as

$$\frac{(\Delta P / \Delta z)_{tp,\,heated}}{(\Delta P / \Delta z)_{tp,\,unheated}} = 1 + \frac{20\ Z}{1.315 - Z} \left(\frac{q}{H_{fg}\ G} \right)^{0.7} \left(\frac{\rho_f}{\rho_g} \right)^{0.08} \tag{5.83}$$

where

$$Z = \frac{H - H_{ONB}}{H_{NVG} - H_{ONB}} = \frac{z - z_{ONB}}{z_{NVG} - z_{ONB}} \tag{5.84}$$

For saturated boiling, the correction factor is expressed as

$$\frac{\Delta P_{tp,\,heated}}{\Delta P_{tp,\,unheated}} = 1 + 0.0044 \left(\frac{q}{G} \right)^{0.7} \tag{5.85}$$

It is limited to the bubbly-flow region, where the pressure drop increased with increasing heat flux. Correction factor was not provided for a regime where a decrease in pressure drop was observed with increasing heat flux.

5.5.3 The Izumi et al. Experiment

Izumi et al. [1975] measured the pressure drop over a heated, horizontal, copper pipe cooled with R-12 flow. The heated length of the pipe was 1.34 m and the pressure taps were installed outside the heated length and were 1.59 m apart. For a constant two-phase inlet condition, the total pressure drop was found to increase with increasing heat flux and mass flux, but with decreasing system pressure. For adiabatic two-phase flow, Izumi et al. correlated their results as

$$\frac{\Delta P_{tp}}{\Delta P_z} = 1.515\ (1 - \alpha)^{-1.57} \tag{5.86}$$

with an accuracy of ±10% error. The void fraction was evaluated with the Zivi equation

$$\alpha = \left[1 + \left(\frac{1 - x_a}{x_a} \right) \left(\frac{\rho_g}{\rho_f} \right)^{2/3} \right]^{-1} \tag{5.87}$$

For a heated channel, the two-phase total pressure drop was corrected with an empirical factor, which is expressed as

$$\frac{\Delta P_{heated}}{\Delta P_{unheated}} = 1 + 493.63 \left(\frac{q}{G\ H_{fg}} \right)^{0.91} \tag{5.88}$$

By integrating the empirical equation of two-phase total pressure drop over the entire heated length, the experimental data for the heated channel were predicted within ±15% error.

5.5.4 The Steiner and Schlűnder Experiment

Steiner and Schlűnder [1976a, 1976b] measured the wall temperature and pressure drop of a horizontal, heated copper tube with nitrogen flow. The heating effect was assumed to influence only the pressure drop, due to acceleration, but not the friction. Their data showed an increase in total pressure drop (i.e., sum of the components due to friction and acceleration) with increasing mass flux and increasing heat flux, but with decreasing system pressure.

Comparing the predictions of eight different correlations against their experimental data obtained at low heat-flux values (less than 500 $W.m^{-2}$), the best agreement was shown for the Bandel correlation. However, a large scattering was also observed and the data was consistently underpredicted by about 30%. Steiner and Schlűnder suspected a high uncertainty in their data, due to pressure oscillations during the experiments, and the neglect of the entrainment effect in the Bandel correlation.

5.5.5 The Boom et al. Experiment

Boom et al. [1978] measured total pressure drops inside an unheated and a heated channel with helium-I flow. Over the range of qualities between 0 and 1, the two-phase frictional multiplier increases consistently with increasing quality. The increase, however, is much larger at low-quality and high-quality regions, but becomes small at medium qualities. Boom et al. noted that this variation is related to the flow-pattern transition where the flow is bubbly at low qualities, annular at medium qualities and mist at high qualities. In a heated channel, the frictional pressure drop is significantly reduced. An increase in frictional pressure drop was observed with decreasing system pressure and mass flux for both heated and unheated channels. The effect of

tube diameter, however, appears to be small on adiabatic pressure drop. A comparison of the predictions of the homogeneous model against their experimental data showed a reasonable agreement for the adiabatic data, but not for the flow-boiling data.

5.5.6 The Bartolomei et al. Experiment

Bartolomei et al. [1979] measured pressure drops over a heated tube with subcooled-boiling flow over a wide range of pressures. For single-phase conditions (i.e., no boiling was encountered inside the channel), they observed a decrease in frictional pressure drop. However, the magnitude of this decrease was not presented.

Once boiling is encountered inside the channel (Bartolomei et al. [1979] assumed boiling initiated at the point where the surface temperature reached saturation), the two-phase frictional multiplier increases with increasing heat flux, decreasing mass flux and decreasing pressure when other flow conditions are constant. Bartolomei et al. noted that the predictions of the Tarasova et al. correlation [1966] for a heated channel were much larger than their experimental data. They suspected that the large error was probably caused by the neglect of void-fraction effect in pressure drop in the Tarasova et al. correlation.

5.5.7 The Petukhov et al. Experiment

Petukhov et al. [1980] studied critical heat flux and two-phase pressure drop for both heated and unheated channels with helium flow. The frictional pressure-drop data were presented in terms of a non-dimensional parameter (Equation (5.7))

$$\Delta P_{tp}^{*} = \frac{\Delta P_{tp} - \Delta P_{lo}}{\Delta P_{go} - \Delta P_{lo}} \tag{5.89}$$

where ΔP_{tp} is the two-phase frictional pressure drop, and ΔP_{lo} and ΔP_{go} are the single-phase frictional pressure drop for total flow as liquid and vapour, respectively.

The non-dimensional pressure drop increases with increasing quality until reaching a localized maximum point (referred to as the pressure-drop crisis). Beyond the maximum point, it decreases with increasing quality. After reaching a minimum point, it increases with increasing quality again. Similar trends have been observed in both the heated and unheated channels (Figure 5.11). However, this non-dimensional pressure drop is larger inside the unheated than the heated channel over the complete range of qualities at the same local conditions. Furthermore, the pressure-drop crisis shifted to a lower quality for the heated channel.

A shift of the pressure-drop crisis to a lower quality was also observed for increasing mass flux in both the unheated and heated channel. When compared against the predictions from the homogeneous model, the pressure drops were generally underpredicted before the maximum point, but overpredicted after the minimum point.

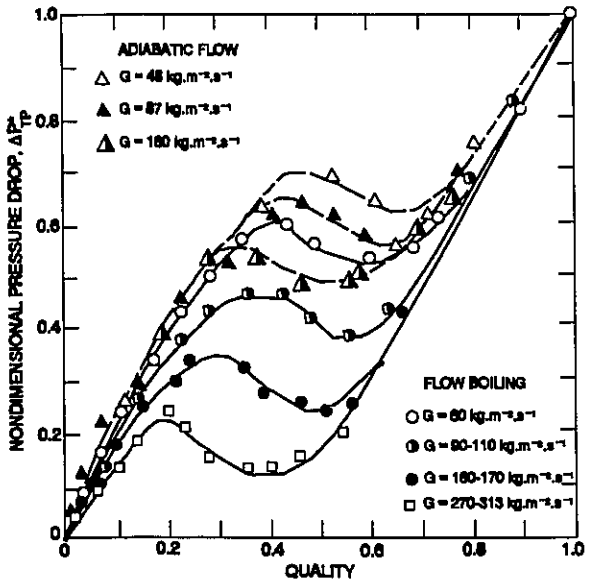

Figure 5.11: Effect of Heating on Non-Dimensional Pressure Drop in Helium Flow (Not all Data shown) [Petukhov et al., 1980].

5.5.8 The Shoukri Experiment

Shoukri [1980] and Shoukri et al. [1981] studied the effect of heating on pressure drop for low-pressure conditions (from atmospheric up to 1 MPa) in a horizontal tube. They observed a difference in two-phase frictional pressure drops between adiabatic and heated flows. However, this difference is not affected by the magnitude of heat flux.

Shoukri et al. [1981] expressed the difference as a ratio of two-phase frictional pressure drops between heated and adiabatic flows, which is 1 at zero quality. With increasing quality at constant pressure, mass flux and heat flux, the pressure-drop ratio increases from 1 and reaches a maximum point, which is generally encountered at a ratio of 1.5. Beyond the maximum point, it decreases and approaches back to 1. Shoukri et al. [1981] noted that the quality corresponding to the maximum point is affected by pressure and mass flux. This trend has also been observed by Hosler [1963] in his study of flow-pattern transition in a heated flow.

Compared with the flow-pattern map of Mandhane et al. [1974], Shoukri et al. [1981] found a close relation between these maximum points and the slug-to-annular flow transition. At high-flow and low-quality conditions (corresponding to the bubbly-flow region), Shoukri [1980] observed a much larger increase in pressure-drop ratio (2.5 times the adiabatic frictional pressure drop). He indicated that this large difference is the result of a nucleate-boiling effect that increases the apparent roughness of the wall. Therefore, the effect of heating on pressure drop is significant over the low-quality region (both the bubbly-flow and the slug-flow regions), where an increase in pressure drop is shown for a heated channel. The rise in pressure drop terminates at the transition from slug to annular flow. In the developing region of annular flow, the pressure-drop gradient with respect to quality actually decreases, even though the magnitude of pressure drop remains higher in the heated than the adiabatic flow. When annular flow is fully developed, the difference in two-phase frictional pressure drops between heated and unheated channels diminishes.

5.5.9 The Nicholson et al. Experiment (A Simulated Heated Channel)

Nicholson et al. [1982] observed flow-pattern variation and pressure drop of air-water mixture inside an annulus with a porous inner tube. Air was injected from the inner tube to the flow to simulate the bubble formation on a heated surface. While the boundaries of most flow patterns are not affected by the injection technique, the intermittent regime has not been observed in the flow simulating a heated surface. For increasing quality and constant mass flux, the ratio of two-phase multipliers between a simulated-heated and adiabatic flow increases at low quality, reaches a maximum point, decreases exponentially, and approaches a constant value at high quality. This is similar to the trend observed by Shoukri et al. [1981].

The mass flux of injected air has a strong influence on the ratio of two-phase multiplier. For low air mass-flux conditions, a large ratio of two-phase multiplier is obtained (indicating that the two-phase pressure drop for the simulated-heated flow is higher than that of adiabatic flow) and the quality corresponding to the maximum point becomes high (flow-transition point). At high mass flux of air and high quality, the ratio decreases below 1 (indicating that the two-phase pressure drop for the simulated-heated flow is lower than that of adiabatic flow). As noted by Nicholson et al. [1982], the two-phase multiplier in flow boiling has different characteristics from adiabatic flow. Hence, the traditional prediction methods are inappropriate.

5.5.10 The Arkhipov et al. Experiment

Arkhipov et al. [1983] measured two-phase pressure drops in a heated channel with helium flow. In terms of the dimensionless parameter, ΔP_{tp}^*, they observed the same trend as Petukhov et al. [1980]. With increasing quality, they noted an increase in ΔP_{tp}^* until a local maximum point is reached. Beyond the maximum point, the dimensionless parameter decreases at low mass-flux conditions, but displays only an inflection at high flow. The quality corresponding to the maximum point, $x_{\Delta P}$, is affected by both pressure and mass flux. Arkhipov et al. correlated this quality in terms of a modified Froude number

$$Fr^* = \frac{G}{\rho_l}\left(\frac{\rho_l - \rho_g}{g\,\sigma}\right)^{0.25} \tag{5.90}$$

and the expression for the quality at maximum point is

$$x_{\Delta P} = 0.38 + \frac{2 + (\rho_f/\rho_g - 7.65)^{0.5}}{10 + 0.25\left(\dfrac{Fr^*}{2 + (\rho_f/\rho_g - 7.65)^{0.5}}\right)^3} \tag{5.91}$$

An empirical correlation for two-phase frictional pressure drop was correlated based on their data base. It is expected to be valid only for helium flow within the conditions of their data.

5.5.11 The Zeigarnik et al. Experiment

Zeigarnik et al. [1983] observed a different trend of two-phase pressure drop from Petukhov et al. [1980] and Arkhipov et al. [1983] at low pressure and high mass-flux (up to 18.8 $Mg.m^{-2}.s^{-1}$) conditions. At constant inlet conditions and with an increasing heat flux, the pressure drop decreases at low heat fluxes (where single-phase forced convection was anticipated by Zeigarnik et al.). It is followed with a relatively constant pressure-drop region at surface boiling. As bulk boiling becomes intense, the pressure drop increases sharply. While no detailed measurements were presented with increasing heat flux up to critical heat flux, a pressure-drop distribution along the channel was shown at each measuring point with respect to the pressure at the inlet end.

As compared to adiabatic single-phase flow, the pressure drop increases sharply at low heat flux, but changes gradually at high heat flux. However, a decreasing trend was observed as the section approaches the dryout conditions (critical heat flux). This, as Zeigarnik et al. explained, indicates a decrease in momentum transfer between vapour core and liquid film.

5.5.12 The Inasaka et al. Experiment

Inasaka et al. [1989] measured pressure drop with subcooled boiling flow at low-pressure, high mass-flux and high heat-flux conditions. They employed two tubes of 1 and 3 mm in diameter, and the heated length varied from 1 to 10 cm. In view of the small heated-length/diameter ratio, a developing flow may be present inside the tubes. Their results indicated different trends in pressure drop between the 3-mm and 1-mm tubes. They were similar to those of other published data for the 3-mm tube, but were quite unique for the 1-mm tube.

Based on the constant inlet fluid temperature, the total pressure drop decreases with increasing heat flux for the 3-mm tube at low heat-flux conditions. As the heat flux is increased, the pressure drop reaches a minimum, which appears to agree with the prediction of the onset of nucleate-boiling point with the Bergles and Rohsenow correlation. Beyond this minimum point, the pressure drop increases gradually with increasing heat flux. Inasaka et al. also observed another transition point where the rate of pressure drop increases sharply. This second transition point corresponds closely to the bubble-detachment point, as predicted using the Saha-Zuber correlation.

Comparison between the predictions of the Bergles-Dormer correlation and the experimental results showed only minor success, because the mass-flux effect on pressure drop is not included in the correlation. On the other hand, these results are overpredicted considerably with the Lockhart and Martinelli correlation. The trend of these results, however, is similar to that of the correlation.

The decreasing trend of pressure drop with heat flux is not shown for the 1-mm tube. For most conditions, the difference in pressure drop is small between a heated and an unheated channel. Both the Bergles-Dormer and the Lockhart-Martinelli correlations are not valid for these results. Except for a few data at low-flow and low-quality conditions, the Lockhart-Martinelli correlation overpredicts the results significantly.

5.6 DISCUSSION

5.6.1 Experimental Studies

The review of experimental studies showed that the effect of surface heating on two-phase pressure drop is insignificant for some conditions, but can be a dominant factor at others. This is caused primarily by (i) the test conditions and, sometimes, (ii) the pressure-drop measurements.

A number of experiments were carried out with high flows of high inlet subcooling (i.e., low inlet temperature). The conditions at the test-section outlet corresponded mainly to bubbly flow. For those studies that focused mainly on the low-quality bubbly-flow regions, the effect of surface heating tended to be small on two-phase pressure drops. Once the high-quality annular-flow data were included, this effect became significant. For example: the effect of surface heating on two-phase pressure drop can easily be ignored for the low-quality data (e.g., less than 0.2) presented in Figure 5.10 by Tarasova et al. [1966]. The variation can be considered simply as the uncertainties in the data base. However, once the low-quality and high-quality data are combined, the trend becomes obvious.

In most experiments, the pressure drop was measured over a long heated length that covered mainly single-phase liquid flow and bubbly flow (where the effect of surface heating on two-phase pressure drop is insignificant). Even though annular flow (where the surface-heating effect becomes dominant) could be encountered at the downstream end of the test section, the surface-heating effect might not be noticeable.

The present review of experimental studies concludes that the two-phase pressure drop is affected by surface heating. However, this effect is not strong at low-quality bubbly flows but significant at high-quality annular flows at the present conditions of interest. Furthermore, the parametric trend of two-phase pressure drop with respect to heat flux depends also strongly on the flow conditions (as shown in the studies of Tarasova et al. [1966], Petukhov et al. [1980], etc.).

5.6.2 Empirical Correlations

The review of empirical studies showed that a wide variety of prediction methods were proposed for predicting two-phase pressure drop. Among them, the graphical method is the simplest to use but the uncertainties of its predictions are high.

The adiabatic correlations examined in this review are generally valid for a wide range of conditions and have been tested against flow-boiling data. Among them, the generalised Friedel correlation [1979] was derived with the largest data base and has been shown to be valid for various conditions and geometries. However, the data scatter is also large. The Chisholm correlation [1973], on the other hand, was analytically based but relies very much on the empirical coefficient (see Section 5.3.1). This correlation was also validated with data of wide ranges of flow conditions and fluids. It tends to overpredict the flow-boiling data obtained at pressures less than 4.13 MPa. The Reddy et al. [1982] equation was derived with both adiabatic-flow and flow-boiling data obtained at conditions that are close to those of interest in this study. It was shown to be valid within its own data base and has a better prediction accuracy than other correlations. The difference between the Reddy et al. [1982] and the Chisholm [1973] correlations, however, is small. Since the flow-boiling data were primarily obtained with a two-phase inlet conditions at test section of relatively short heated length, the applications of the Reddy et al. correlation may be limited to conditions within its data base. None of these correlations includes the effect of surface heating on two-phase pressure drop. The two-phase pressure drop in flow boiling is calculated by integrating the pressure-drop correlation with respect to flow quality over the channel.

Several correction factors to adiabatic pressure drop were recommended to account for the effect of surface heating on two-phase pressure drop. They are limited to the bubbly-flow region where an increase in pressure drop was shown with increasing heat flux. No specific method was suggested for other flow patterns that exhibit a decreasing trend of pressure drop with increasing heat flux.

6. LITERATURE REVIEW OF MODELLING STUDIES ON TWO-PHASE PRESSURE DROP DUE TO FRICTION

Empirical correlations are usually the most accurate prediction methods for two-phase pressure drop within their data base. However, the uncertainty of their prediction becomes high once extrapolated beyond their range of validity. This is mainly due to the incorrect parametric trends exhibited by most correlations. Phenomenological models, on the other hand, provide generally correct parametric trends, but their predictions are less accurate than those of empirical correlations over specific conditions. This is primarily due to the simplified assumptions introduced in the calculation.

A number of models have been developed for predicting two-phase pressure drop. They are generally flow-pattern dependent and can be categorised into two major types: homogeneous flow, which assumes a well-mixed fluid with the same characteristic in both phases, and

separated flow, which treats the phases individually. These two models represent mainly the two extreme cases of two-phase flow; the real flow is somewhere in-between. More realistic assumptions have been introduced to improve the prediction capability of various models.

Section 6.1 describes the homogeneous-flow model with various definitions of two-phase viscosity. A number of separated-flow models have been proposed and are presented in Section 6.2. Section 6.3 introduces the modified homogeneous-flow model, which is based on the homogeneous-flow equation and an empirical correction, to account for the difference in flow structure. The mixing-length theory of single-phase flow is extended to two-phase flow. It is primarily used in the vapour core of an annular flow, where a two-phase mixture is encountered. Various mixing-length models are described in Section 6.4. The most complex modelling of two-phase flow is the use of multi-fluid model, which requires a complete set of conservation equations for both the liquid and gas/vapour phases. Several multi-fluid models are described in Section 6.5.

6.1 HOMOGENEOUS-FLOW MODEL

In homogeneous flow, the two phases are assumed to travel at the same velocity and have similar flow characteristics (e.g., velocity profile) as the single-phase flow. Therefore, this model employs the equations derived for single-phase flow with modified fluid properties to account for the presence of two phases. The application of the homogeneous-flow model is limited to the fully developed bubbly and dispersed-droplet (post-dryout region) flows, where the two phases travel at approximately the same velocity. Husain et al. [1978] observed that the transition from homogeneous (froth and mist flow) to non-homogeneous flow (bubbly, plug, slug, annular, stratified and wavy flow) occurs at a constant mass flux of 2716 $kg.m^{-2}.s^{-1}$ ($2x10^6$ $lb.ft^{-2}.h^{-1}$) in both low-pressure air-water and high-pressure steam-water horizontal flow.

The frictional pressure gradient for a single-phase flow is expressed as

$$-\left(\frac{dP}{dz}\right)_f = \frac{f}{D}\frac{\rho u^2}{2} = \frac{f}{D}\frac{G^2}{2\rho} \tag{6.1}$$

Assuming the same equation is valid, the frictional pressure gradient for two-phase flow is expressed as

$$-\left(\frac{dP}{dz}\right)_{tp,f} = \frac{f_{tp}}{D}\frac{G^2}{2\rho_{tp}} \tag{6.2}$$

and the two-phase multiplier becomes

$$\phi_{lo}^2 = \frac{(dP/dz)_{tp}}{(dP/dz)_{lo}} = \frac{f_{tp}}{f_l}\frac{\rho_l}{\rho_{tp}} = \frac{f_{tp}}{f_l}\left(1 + x_a\left(\frac{\rho_l}{\rho_g} - 1\right)\right) \tag{6.3}$$

where the two-phase density, ρ_{tp}, is defined as

$$\frac{1}{\rho_{tp}} = \frac{x_a}{\rho_g} + \frac{(1 - x_a)}{\rho_l} \tag{6.4}$$

The only unknown parameter in evaluating the homogeneous two-phase multiplier (Equation (6.3)) in adiabatic flow is the two-phase friction factor, f_{tp}.

A number of definitions have been introduced for f_{tp}. The simplest one assumes the same friction factor for both single- and two-phase flow (i.e., $f_{tp} = f_{lo}$) [Owens, 1961]. This results in the following form of two-phase multiplier

$$\phi_{lo}^2 = 1 + x_a \left(\frac{\rho_l}{\rho_g} - 1 \right) \tag{6.5}$$

Another approach assumes that the two-phase friction factor can be calculated with the single-phase equation (e.g., Blasius equation), but with the Reynolds number evaluated with a two-phase mixture viscosity, instead of the single-phase liquid viscosity. It is expressed as

$$f_{tp} = a\ Re_{tp}^{b} \tag{6.6}$$

where a and b are empirical constants, which are channel dependent, and the two-phase Reynolds number, Re_{tp}, is defined as

$$Re_{tp} = \frac{G\ D}{\mu_{tp}} \tag{6.7}$$

For a smooth tube, the Blasius equation is assumed valid and the constants, a and b, become 0.316 and -0.25, respectively. Several definitions of two-phase mixture viscosity have been introduced. McAdam et al. [1942] assumed the same form as two-phase density and the two-phase mixture viscosity was expressed as

$$\frac{1}{\mu_{tp}} = \frac{x_a}{\mu_g} + \frac{(1 - x_a)}{\mu_l} \tag{6.8}$$

Cicchitti et al. [1960], on the other hand, suggested the weighted average value of two-phase mixture viscosity, i.e.,

$$\mu_{tp} = x_a\ \mu_g + (1 - x_a)\ \mu_l \tag{6.9}$$

Dukler et al. [1964] derived a more complex form of equation than the above. The two-phase mixture viscosity is expressed as

$$\mu_{tp} = \rho_{tp} \left(\frac{x_a \mu_g}{\rho_g} + \frac{(1 - x_a) \mu_l}{\rho_l} \right) \tag{6.10}$$

It was used by Ansari and Sylvester [1988] in a bubbly-flow model that was shown to predict closely the two-phase pressure drop of oil-gas flow.

Since a large uncertainty remains in various definitions of two-phase mixture viscosity, the simple one suggested by McAdam et al. [1942] is often adopted in calculations. Based on this equation and the Blasius friction factor, the two-phase multiplier for a homogeneous flow is expressed as

$$\phi_{lo}^2 = \left(1 + x_a \left(\frac{\rho_l}{\rho_g} - 1 \right) \right) \left(1 + x_a \left(\frac{\mu_l}{\mu_g} - 1 \right) \right)^{-0.25} \tag{6.11}$$

6.2 SEPARATED-FLOW MODEL

The separated-flow model assumes that the two phases travel separately with different velocities. Empirically, the equation for homogeneous flow can be used by including a parameter called the slip factor to account for the difference in phase velocities. Analytically, two sets of equations are introduced to describe separately the velocities of liquid and vapour. This model is often used to describe annular flow in either vertical or horizontal channels and stratified flow in horizontal channels. The present discussion focuses mainly on the annular-flow pattern.

6.2.1 The Levy Momentum Model

Levy [1952] derived equations of two-phase pressure drop and heat transfer analytically for two-phase and two-component annular flows in horizontal pipes (no gravity effect). He assumed that the phases travel separately with vapour in the core and liquid between the vapour and channel wall. The momentum equation of laminar flow was used for viscous flow, and the one-seventh power profile was employed for turbulent flow. No liquid entrainment in the vapour or vapour bubbles in the liquid film was modelled. At the liquid-vapour interface, the two phases were assumed to have the same velocity (i.e., no slip condition). The equations covered the viscous-liquid/viscous-gas, the viscous-liquid/turbulent-gas, and the turbulent-liquid/turbulent-gas conditions.

The two-phase pressure drop was presented in terms of the two-phase multiplier for liquid-only flow, ϕ_l^2, which was expressed, for viscous-liquid/viscous-gas flow, as

$$\phi_l^2 = \left(\frac{Y}{Y - 1} \right)^2 \tag{6.12}$$

where

$$Y = 1 + X_{vv} \frac{\mu_g}{\mu_l} + X_{vv} \sqrt{1 + \left(X_{vv} \frac{\mu_g}{\mu_l} \right)^2} \tag{6.13}$$

$$X_{vv} = \left(\frac{1 - x_a}{x_a} \frac{\rho_g}{\rho_l} \frac{\mu_l}{\mu_g} \right)^{1/2} \tag{6.14}$$

for viscous-liquid/turbulent-gas flow, as

$$\phi_l^2 = \frac{1}{(1 - \alpha)^2} \tag{6.15}$$

and, for the turbulent-liquid/turbulent-gas flow, as

$$\phi_l^2 = \left(\frac{7}{120}\right)^{7/4} \frac{1}{(1 - \alpha^{1/2})\left(0.125 - \frac{1}{15}(1 - \alpha^{1/2})\right)^{7/4}} \tag{6.16}$$

Complex equations of void fraction, α, were derived for the above two cases. They will not be shown here, since simpler and more accurate equations are available for estimating void fraction (see Section 3.3). The Levy model follows the same trend as the Lockhart-Martinelli curves, but predicts generally a larger two-phase multiplier. This was caused by the discrepancies to the idealized assumption of the annular pattern, the effect of the flow-pattern transition, and the assumption of steady-state and constant-property conditions.

6.2.2 The Calvert and Williams Annular-Flow Model

Calvert and Williams [1955] analyzed the two-phase annular flow in a vertical channel. Similar to the Levy model, the phases were assumed to travel separately with no entrainment. The analyses of both liquid-film thickness and two-phase pressure drop were provided.

The liquid film was assumed to consist of laminar and turbulent layers with single-phase velocity profiles. In the turbulent layer, the Prandtl mixing-length theory was employed. The liquid film thickness was determined by integrating the velocity profile from the channel wall to a location where the calculated and input mass flow rate become the same (within tolerance).

Based on the assumption of equal pressure gradient in both the liquid film and vapour core, only the two-phase pressure gradient in the vapour core was analyzed. It consisted of two components: (i) the frictional pressure gradient of total flow with gas-phase properties in the same channel, and (ii) the profile drag at the interface (i.e., interfacial pressure gradient). While

the first component was evaluated using the single-phase friction-factor equation, the second component was calculated using (in British units)

$$\Delta P_D = \left(\frac{2\ G}{D}\right)^{3/2} \left(\frac{\rho_g}{(60\ \pi)^2\ 2\ g}\right)\left(C_D\ A_D\ \frac{2\ \sqrt{G}}{D}\right)\left(\frac{4\ z}{D}\right) \tag{6.17}$$

where C_D is the drag coefficient, and A_D is the projected area for drag. Based on their experimental data of air-water flow, Calvert and Williams presented graphically the relationship between the drag-force term (third term at the right-hand side of this equation) and the liquid-film thickness.

Compared against their experimental data of two-phase pressure gradient in air-water flow, this model agrees with data of low water flow rate (less than 25 $kg.m^{-2}.s^{-1}$) only, but underpredicts data of high water flow rate. Calvert and Williams indicated that the deviation was probably caused by the neglect of wave entrainment in the analysis.

6.2.3 The Ueda Model

Ueda [1967a] derived an expression for wall shear stress in vertical upward flow. In his model, a laminar liquid sublayer is assumed at the wall, and has the same velocity gradient as in single-phase flow. The wall-shear stress is presented as a function of velocity at the transition point between laminar sublayer and turbulent flow, u_δ, and is expressed as

$$\tau_w = \frac{\frac{\rho_l\ u_\delta^2}{50} - \frac{50\ \nu_l}{2\ u_\delta}\rho_l\ g\ \alpha}{1 - \frac{50\ \nu_l}{u_\delta\ D}} \tag{6.18}$$

In annular flow, a much steeper gradient in the turbulent sublayer was proposed for two-phase flow, compared to single-phase flow, for the same flow conditions. Based on the difference in mean velocity of the liquid phase between single-phase and two-phase flow, the velocity, u_δ, was derived, in part, empirically using Ueda's data of vertical air-water annular and slug flows [Ueda, 1967b]. It is expressed as

$$u_\delta = \frac{1.10}{Re_{mean}^{1/8}} u^*_{mean} \tag{6.19}$$

where

$$Re_{mean} = \frac{u^*_{mean} D}{\nu_l} \tag{6.20}$$

$$u^*_{mean} = u_l + 1.20\, Re_s^{-1/4} u_s - 12\, Fr_{ed} u_{ed} + 16\, Fr_s^{5/4} u_s \tag{6.21}$$

$$u_l = \frac{j_l}{1 - \alpha} \tag{6.22}$$

$$u_s = u_g - u_l \tag{6.23}$$

$$u_g = \frac{j_g}{\alpha} \tag{6.24}$$

$$Re_s = \frac{u_s D (1 - \sqrt{\alpha})}{\nu_l} \tag{6.25}$$

$$u_{ed} = j_g + j_l \tag{6.27}$$

$$Fr_s = \frac{g\ \alpha\ D\ (1 - \sqrt{\alpha})}{u_s^2} \tag{6.26}$$

$$Fr_{ed} = \frac{g\ \alpha\ D\ (1 - \sqrt{\alpha})}{u_{ed}^2} \tag{6.28}$$

This model has been extended to bubbly flow by considering the increase in mean liquid velocity in the presence of gas bubbles. A different equation for u_δ was optimized using the bubbly-flow data of Aoki and Inoue, and is expressed as

$$u_\delta = \frac{1.39}{Re_{mean}^{1/8}}\ u_{mean}^* \tag{6.29}$$

where

$$u_{mean}^* = u_l + 5.0\ Fr_s^{4/5}\ u_s \tag{6.30}$$

Due to the large data scattering, the agreement between this model and the bubbly flow data is relatively poor. In general, the two-phase multiplier decreases with increasing quality as the flow pattern changes from bubbly to either slug or annular. This decrease is more distinct for low than high liquid velocity.

6.2.4 The Chisholm Momentum Model

Chisholm [1967] analyzed the horizontal flow based on the momentum equation in addition to the empirical approach described in Section 5.3.1. A set of general equations were introduced for stratified flow where both liquid and gas phase contact the channel wall and each other. Homogeneous and annular flows were considered as special cases of the general equations. A

shear force was included between the two phases in his analysis. The two-phase multiplier based on the liquid-only single-phase flow is presented as

$$\phi_l^2 = \frac{1}{(D_l/D)^{1+n}} \left(1 + \frac{A_g}{A_l} \right)^{1-n} \left(\frac{A_g}{A_l Z^2} + 1 \right) \tag{6.31}$$

where D_l is the hydraulic diameter of liquid phase in two-phase flow (which is four times the ratio of cross-sectional area to wetted perimeter occupied by the liquid phase, i.e., $4A_l/p_l$), A_g and A_l are the cross-sectional area occupied by the gas and liquid phase, respectively, and Z is the shear-force function. A value of 14 for the shear-force function in the equation provides satisfactory agreement with the two-phase multiplier of Lockhart and Martinelli.

In annular flow, the shear-force function becomes infinite and the two-phase multiplier is expressed as

$$\phi_l^2 = \left(1 + \frac{A_g}{A_l} \right)^2 \tag{6.32}$$

for a rough tube (where n = 0). On the other hand, the shear-force function for a no-slip flow (i.e., homogeneous flow) is

$$Z = \left(\frac{\rho_l}{\rho_g} \right)^{0.5} \tag{6.33}$$

and the two-phase multiplier for a rough tube becomes

$$\phi_l^2 = \left(\frac{1}{1 - x_a}\right)^2 \left((1 - x_a) + x_a \frac{\rho_l}{\rho_g} \right) \tag{6.34}$$

No comparison with other data, except those used in deriving the Lockhart and Martinelli graphical method, has been shown. Due to the complexity of this equation and no apparent improvement in prediction, Chisholm recommended his empirical equation (Equation (5.16)) instead of this analytical model.

Chisholm and Sutherland [1969] related the coefficient C to the phasic velocity ratio (or slip ratio), K. The coefficient, C, is expressed as

$$C = \frac{1}{K}\sqrt{\frac{\rho_l}{\rho_g}} + K\sqrt{\frac{\rho_g}{\rho_l}} \tag{6.35}$$

Chisholm and Sutherland noted that the derivation of slip ratio, K, is complex for various flow conditions. Instead, they suggested an empirical correlation of the coefficient, C, for general engineering applications. The coefficient, C, is expressed as

$$C = \left(1 + (C_2 - 1)\left(\frac{\rho_l - \rho_g}{\rho_l}\right)^{0.5}\right)\left(\left(\frac{\rho_l}{\rho_g}\right)^{0.5} + \left(\frac{\rho_g}{\rho_l}\right)^{0.5}\right) \tag{6.36}$$

where C_2 is an empirical function optimized for various channel fixtures (see Table 5.2).

Kubie and Oates [1978] introduced an approximation to the Chisholm equation by relaxing the restriction in the second term of Equation (6.31). This approximation results in the same form as Chisholm's simplified correlation (Equation (5.16)). Since the coefficient, C, also has to be obtained empirically, this approximation does not provide any advantage over the Chisholm correlation.

6.2.5 The Wallis Simplified Annular-Flow Model

Wallis [1969a] introduced a simple annular-flow model where the interfacial friction factor is based on a force balance of the vapour core and the assumption of negligible shear-stress variation in the liquid film. The interfacial friction factor is expressed as

$$f_i = \frac{-dp/dz \; D \; \alpha^{5/2}}{2 \; \rho_g \; j_g^2} \tag{6.37}$$

where j_g is the mean volumetric gas flux and is defined as

$$j_g = \frac{4 \; Q_g}{\pi \; D^2} \tag{6.38}$$

and Q_g is the volumetric gas flow rate. With the available data base, the interfacial friction factor has been correlated by

$$f_i = 0.005 \; (1 + 300 \; \frac{\delta}{D}) \tag{6.39}$$

The pressure gradient is presented in terms of a dimensionless pressure-drop function, which is expressed as

$$\Delta P^* = \frac{-(dp/dz + \rho_g \; g)}{g \; (\rho_l - \rho_g)} \tag{6.40}$$

and from the force-balance equation of the vapour core

$$\Delta P^* = 10^{-2} \; j_g^{*2} \; \frac{1 + 75 \; (1 - \alpha)}{\alpha^{5/2}} \tag{6.41}$$

Based on the analysis of liquid film, the pressure gradient is also presented, for a turbulent film, as

$$\Delta P^* = (1 - \alpha) + 10^{-2} \frac{j_f^* |j_f^*|}{(1 - \alpha)^2} \tag{6.42}$$

and, for a laminar film, as

$$\Delta P^* = 0.684 (1 - \alpha) + \frac{j_f^{1*}}{(1 - \alpha)^2} \tag{6.43}$$

where

$$j_g^* = \frac{j_g \rho_g^{1/2}}{(g D (\rho_l - \rho_g))^{1/2}} \tag{6.44}$$

$$j_f^* = \frac{j_f \rho_f^{1/2}}{(g D (\rho_l - \rho_g))^{1/2}} \tag{6.45}$$

$$j_f^{1*} = \frac{32 j_f \mu_f}{g D^2 (\rho_l - \rho_g)} \tag{6.46}$$

Both the pressure drop and void fraction can be obtained by solving these equations.

Pressure drops predicted with this model were compared against low gas-flow rate data. Good agreement was observed; in particular this model appeared to capture the transition from a laminar to turbulent film accurately despite its simplicity.

At high gas-flow rate, however, the model overpredicted the pressure-drop measurements. This could be caused by neglect of the entrainment process that led to overpredictions of film

thickness and pressure drop. Wallis [1969b] discussed other effects that may have a strong impact on the prediction of two-phase pressure drop in annular flow. Compared against the predictions of a more complex model of Levy [1966], this model was less accurate but provided reasonable predictions.

6.2.6 The Yelin Turbulence Model

Yelin [1985] considered the effect of both turbulent-velocity fluctuation and large-scale fluctuations, induced by wave motion at the liquid-gas interface, on the shear stress, i.e.,

$$\tau = -\alpha_i \rho_i \left(\overline{u_{iT}' v_{iT}'} + \overline{u_{iW}' v_{iW}'} \right) \tag{6.47}$$

where subscript i corresponds to the parameter for each phase (i is l for liquid and g for gas). Similar to the turbulent term, the large-scale fluctuation was also expressed in terms of a large-scale mixing length and the velocity gradient. By assuming that both the wave and gas phase travel at the same velocity, the large-scale fluctuation was affected only by the liquid velocity gradient. The two-phase pressure drop was presented in terms of a mixture friction factor

$$\frac{1}{\sqrt{f_{mix}}} = \frac{0.354}{\sqrt{A}} \left(ln\left(Re\sqrt{f_{mix}}\right) + ln\left(\frac{1-x_a}{1-\alpha}\right) + ln\left(B\sqrt{M}\right) + 5.6\, B \left(\frac{1-x_a}{1-\alpha}\right)\sqrt{A} - 1.08 \right) \tag{6.48}$$

where

$$A = \kappa_T^2 \left(1 + \frac{\rho_g}{\rho_l} \frac{x_a^2 (1-\alpha)}{(1-x_a)^2 \alpha} \right) + \kappa_W^2 \tag{6.49}$$

$$B = \left(1 + \frac{\rho_g}{\rho_l} \frac{\alpha}{1-\alpha} \right)^{-1/2} \tag{6.50}$$

$$Re = \frac{<\bar{u}_{mix}>D}{\nu_l} \tag{6.51}$$

and $<u_{mix}>$ is the cross-sectional mixture velocity, κ_T is the von Karman constant for single-phase flow. The expression, κ_W, for the large-scale wave fluctuation was empirically derived as

$$\kappa_w = 1.5\ \alpha \tag{6.52}$$

This model was validated only with the air-water data obtained at high-quality flow (x > 95%) inside a glass tube.

6.2.7 The Kadambi Model

Kadambi [1985] employed a polynomial function for velocity distributions in both the liquid film and vapour core of annular flow. The polynomial distribution provides wider applications than the parabolic profile (which is valid for laminar flow only) and a continuous gradient at the wall and centre-axis (as compared to the power law and mixing-length theory for turbulent flow). It introduces smooth transitions between various sublayers (i.e., laminar, buffer and turbulent) in turbulent flow, and maintains a continuous slope over any cross-sectional area. Expressed as a function of Reynolds number, this distribution also provides a smooth transition from laminar to turbulent flow.

The non-dimensional velocity distribution for the liquid film is expressed as

$$\frac{u_l}{u_{ml}} = \left(1 + \frac{(s_l - n)\,\eta^2}{n - 1} + \frac{(1 - s_l)\,\eta^{2n}}{n - 1} \right) \tag{6.53}$$

where u_{ml} is the non-dimensional maximum liquid velocity that would exist at the centre of the tube if the liquid fills the tube and flows with the same velocity distribution as in the two-phase flow situation, s_l is the ratio of actual wall shear stress to the shear stress that would exist if the liquid flows through the tube with the same maximum velocity, but under laminar conditions, n is the polynomial exponent and η is the non-dimensional radius (i.e., r/R). Both the shear stress ratio, s_l, and polynomial exponent, n, are expressed in terms of Reynolds number

$$\begin{aligned} s_l &= 1 && (Re_l \le 2040) \\ s_l &= 2.4172\,x\,10^{-12}\,Re_l^{3.51} && (2040 < Re_l < 2800) \\ s_l &= 0.585 + 0.003172\,Re_l^{0.833} && (Re_l \ge 2800) \end{aligned} \tag{6.54}$$

$$n = -0.617 + 0.008211\,Re_l^{0.786} \tag{6.55}$$

Note that the nearest integer value of Equation (6.55) should be chosen as n. Similarly, the non-dimensional velocity distribution for the vapour core is expressed as

$$\frac{u_g - u_i}{u_{mg} - u_i} = \left(1 + \frac{s_g - m}{m - 1} \left(\frac{\eta}{\eta_i} \right)^2 + \frac{1 - s_g}{m - 1} \left(\frac{\eta}{\eta_i} \right)^{2m} \right) \tag{6.56}$$

where the subscript "i" represents condition at the interface. The same definitions in Equations (6.54) and (6.55) are used for s_g and m, but with the vapour Reynolds number instead.

Based on these velocity distributions, the momentum equations, in dimensionless form, for liquid film and vapour core are solved with the assumption of no slip at the liquid-gas interface (i.e.,

$u_g=u_l$), the Wallis correlation [1969a] for the interfacial shear stress, and the Hutchinson and Whalley correlation [1973] for the equilibrium concentration of entrained droplets in the vapour. The agreement is generally good between predictions of this model and some experimental data of adiabatic horizontal and vertical upward flow.

6.2.8 The Lu and Jia Two-Region Model for Subcooled Boiling

Lu and Jia [1988] developed an analytical model based on a two-region approach to predict pressure drop in subcooled boiling flow. Their model solved the momentum equation and the Navier-Stokes equations for the flow having a hypothetical semi-reversal annular-flow pattern (i.e., a liquid core surrounded by a bubbly mixture along the heated surface). A number of empirical parameters were used, but no justification was provided. The heat-flux effect was not accounted for in these equations, but it was assumed to have an influence on the distribution of bubbles in the channel.

A comparison of the predictions of this model, and the Jia and Schrock method [1986], against limited sets of experimental data from Reynolds [1954], Owen and Schrock [1960], and Dormer and Bergles [1964] indicates a better agreement for this model. The difference, however, is not significant. When compared against their own experimental data, the difference between this model and the Jia and Schrock method is further reduced.

6.2.9 The Yao and Sylvester Model

Yao and Sylvester [1987] derived a simple model for predicting two-phase pressure drop in an annular-mist flow. Their calculation focused mainly on the gas-core region and did not include the pressure drop due to friction between the liquid film and the channel wall (thin-film assumption). The relative roughness of the gas-liquid interface is calculated using the Henstock and Hanratty [1976] equation, which is expressed as

$$\frac{\varepsilon}{D} = \frac{6.59\ F}{(1 + 1400\ F)^{1/2}} = \frac{\delta}{D} \tag{6.57}$$

where

$$F = \frac{((0.707\ Re_l^{0.5})^{2.5} + (0.0379\ Re_g^{0.9})^{2.5})^{0.4}}{Re_g^{0.9}\ (\mu_g/\mu_l)\ (\rho_l/\rho_g)^{0.5}} \tag{6.58}$$

$$Re_l = \frac{4\ W_{lf}}{\mu_l\ \pi\ D} \tag{6.59}$$

$$Re_g = \frac{\rho_g\ D\ j_{sg}}{\mu_g} \tag{6.60}$$

with j_{sg} being the vapour superficial velocity. The mass flow rate of liquid film, W_{lf}, is calculated by subtracting the mass flow rate of entrained liquid from the total mass flow rate. For the entrained-liquid fraction, the Wallis correlation [1969a] is used and is defined as

$$E = 1 - exp(-0.125\ (\beta - 1.5)) \tag{6.61}$$

where

$$\beta = \frac{3048\ j_{sg}\ \mu_g}{\sigma} \left(\frac{\rho_g}{\rho_l} \right)^{1/2} \tag{6.62}$$

A homogeneous mixture is assumed in the gas core. The interfacial friction factor is calculated with the modified Zigrang-Sylvester explicit equation based on the above relative effective

roughness of the liquid film. This model was compared against a limited number of water-gas and oil-gas data. Although the average error is relatively small, a large scatter was present.

6.2.10 The Manzano-Ruiz Model

Manzano-Ruiz [1988] developed a semi-empirical model for predicting pressure drop in horizontal annular flow. The effect of stratification is modelled with a thick liquid film at the bottom of the channel and a thin, uniform, liquid film for the rest of the channel circumference. A number of correlations were used as closure equations: the Ishii-Mishima correlation [1982] for liquid entrainment, the Chen-Spedding correlation for void fraction in horizontal annular flow, the Luninski et al. correlation for thickness of the thin liquid film, and the Wallis correlation for interfacial friction factor (see Manzano-Ruiz [1988] for references).

Compared against the experimental data, this model shows only limited success and generally overpredicts the two-phase pressure drop, particularly in air-water flow. Manzano-Ruiz indicated that the differences are caused by the inaccuracy of the Ishii-Mishima correlation for liquid entrainment.

6.2.11 The Skouloudis and Wurtz Power-Law Model

Skouloudis and Wurtz [1991] introduced two power-law functions for the liquid-film and core-flow regions of annular flow. The entrained phases were assumed to flow homogeneously with the continuous phases in both regions. While the tube radius, R, was used as the reference for liquid film, an hypothetical radius, r_h, was assumed for core flow. The velocity distributions were expressed, for the liquid film, as

$$\frac{u_l}{u_{l,m}} = \left(1 - \frac{r}{R}\right)^{1/m} \tag{6.63}$$

and, for the gas core, as

$$\frac{u_g}{u_{g,m}} = \left(1 - \frac{r}{r_h}\right)^{1/n} \tag{6.64}$$

At the liquid-film/gas-core interface, both velocity and shear stress were assumed to be continuous. The latter was determined with the mixing-length approach using the single-phase expression for mixing length.

From a force-momentum balance of steady and adiabatic flow inside a tube, the axial pressure gradient was presented as

$$-\frac{dp}{dz} = \frac{4\,\tau_w}{D} + (\alpha\,\rho_g + (1 - \alpha)\,\rho_l)\,g\,\sin\theta \tag{6.65}$$

The pressure gradient due to acceleration was neglected. Based on a thin liquid-film assumption, a linear shear stress distribution was assumed in the liquid film. The shear stress for the hypothetical radius, r_h, was calculated with

$$\tau_h = \tau_w \frac{r_h}{R} \tag{6.66}$$

or

$$\tau_h = 4\,\rho_c\,\overline{u}_{cT}^2 \left(2\,c_2\,\frac{\overline{u}_{cT}}{u_{c,\max}}\right)^{\frac{2n}{n+1}} \left(\frac{\rho_c\,\overline{u}_{cT}\,2r_h}{\mu_c}\right)^{\frac{2}{n+1}} \tag{6.67}$$

where c_2 is a numerical factor that depends on the power-law exponent (i.e., n). For the liquid-film region, the single-phase power-law exponent varies with respect to the liquid-film Reynolds

number. In the gas-core flow, an empirical expression was used to account for increasing roughness due to wave formation at the interface. It was expressed as

$$\frac{\lambda}{n} = 2 \log_{10}\left(\frac{G\,D}{\mu_g}\left(1 - \frac{r_s}{r_o}\right)\right) - 5 \tag{6.68}$$

for conditions with $\lambda/n \geq 1$, where λ is the single-phase power-law exponent corresponding to the gas-core Reynolds number. The numerical factor, c_2, was correlated as

$$c_2 = 1.24\ (n - 1.9) \tag{6.69}$$

for $n \geq 2$. Skouloudis and Wurtz showed that this factor is smaller than its counterpart in single-phase flow, indicating a less steep velocity profile for a rough wall. The entrainment fractions in both liquid film and core flow were required to solve the equations. Whenever available, the experimental liquid-entrainment fraction was used in the vapour core. Otherwise, the liquid-entrainment fraction was calculated with the Ishii and Mishima correlation [1982]. No correlation was available for predicting the bubble-entrainment fraction in the liquid film. Several values of bubble-entrainment fraction were tested against the experimental data. A value of 0.5% was shown to be reasonable with the air-water data at 0.28 MPa and the low-quality data of steam-water flow at 7 MPa.

6.3 MODIFIED HOMOGENEOUS-FLOW MODEL

The deficiency of the homogeneous-flow model lies mainly in the assumption of uniform phase distribution and velocity, which seldom occur in real two-phase flow. Even for bubbly flow, which exhibits similar flow characteristics as a homogeneous flow, the concentration of gas (or vapour) phase is often high at a localized region (either in the core region for a well-developed

flow or close to the wall for a developing flow). Furthermore, the velocity of the gas phase is higher than that of the liquid phase, due to a lower density and viscosity. This difference in velocity is often referred to as the "slip" velocity.

6.3.1 The Levy Steam-Slip Model

Levy [1959] derived a steam-slip equation from the momentum equations by assuming different pressure gradients for the two phases in a heated channel. The general form of this equation is expressed as

$$\frac{d}{dx_a}\left(\frac{(1-x_a)^2}{1-\alpha}+\frac{x_a^2}{\alpha}\frac{\rho_l}{\rho_g}-\frac{1}{2}\frac{(1-x_a)^2}{(1-\alpha)^2}\right) = -\frac{\alpha\, G\, H_{fg}\, f_o}{2\, D\, Q}\left(\frac{\left(\frac{dP}{dz}\right)_{gtp}-\left(\frac{dP}{dz}\right)_{ltp}+(\rho_l-\rho_g)\sin\theta}{\left(\frac{dP}{dz}\right)_{lo}}\right) \tag{6.70}$$

It shows that steam slip is affected by the heat generation, Q, and latent heat of vaporization, H_{fg}, in addition to common parameters for pressure-drop calculations such as void fraction and quality. Since the pressure gradient for each phase cannot be obtained from experimental data (which present usually the total pressure gradient), Levy derived a momentum-exchange model to calculate the steam slip. The slip ratio, K, between vapour and liquid velocity is expressed as

$$K = \frac{u_g}{u_l} = \sqrt{\frac{\rho_l}{\rho_g}}\sqrt{2\,\alpha} \tag{6.71}$$

The two-phase multiplier, on the other hand, is calculated from

$$\phi_l^2 = \frac{1}{(1 - \alpha)^2} \tag{6.72}$$

This momentum-exchange model is valid for adiabatic conditions and heated flow with low heat-generation rates. Its predictions deviate from the experimental results as the heat-generation rate increases. Levy mentioned that this model is expected to be valid for high heat-generation rates as well. However, this was not validated in any comparison against the experimental data.

6.3.2 The Bankoff Power-Law Model

Bankoff [1960] imposed a power-law distribution for both the local velocity and the local void fraction, i.e.,

$$\frac{u}{u_m} = \left(\frac{y}{R} \right)^{1/m} \tag{6.73}$$

$$\frac{\alpha}{\alpha_m} = \left(\frac{y}{R} \right)^{1/n} \tag{6.74}$$

where u_m and α_m are the maximum velocity and void fraction, respectively, at the centre axis, y is the distance from the wall and R is the tube radius. By integrating these equations to obtain the mass flow rate, the mass quality is presented as

$$\frac{1}{x_a} = 1 - \frac{\rho_l}{\rho_g} \left(1 - \frac{K}{\bar{\alpha}} \right) \tag{6.75}$$

where the average void fraction, $\bar{\alpha}$, is expressed as

$$\frac{\overline{\alpha}}{\alpha_m} = \frac{2\,n^2}{(n+1)(2\,n+1)} \tag{6.76}$$

and the flow parameter, K, as

$$K = \frac{2\,(m+n+m\,n)(m+n+2\,m\,n)}{(n+1)(2\,n+1)(m+1)(2\,m+1)} \tag{6.77}$$

By assuming that both the single- and two-phase flows have similar characteristics, Bankoff suggested a value of 7 for both exponents m and n. Based on a two-phase viscosity defined by the Einstein expression for the apparent viscosity of a suspension of solid spheres in a liquid, the two-phase multiplier is expressed as

$$\phi_{lo}^2 = \left(1 - \overline{\alpha}\left(1 - \frac{\rho_g}{\rho_l}\right)\right)^{3/4}\left(1 - x_a\left(1 - \frac{\rho_l}{\rho_g}\right)\right)^{7/4} \tag{6.78}$$

Compared against the experimental data of void fraction, this model is valid for most conditions and is better than the Levy momentum-exchange model. However, it underpredicts the two-phase pressure drop over a limited comparison. A different value of exponent (i.e., instead of 7) for the velocity distribution may improve the predictions. In addition, the comparison also indicated that the flow parameter, K, appears to be pressure dependent and is given as

$$K = 0.71 + 0.0001\,P \tag{6.79}$$

where P is the pressure in psia.

6.3.3 The Similarity Analyses Between Single- and Two-Phase Flow

Dukler et al. [1964] derived a set of equations based on a similarity analysis. They proposed that the same flow characteristics between two systems are exhibited in both single- and two-phase flow, provided that the systems are dynamically similar (i.e., having the same Reynolds and Euler numbers). For the case of no slip and homogeneous flow, the friction factor (which is one-half of the Euler number) is expressed as

$$f_{NS} = \frac{\delta P}{\delta z} \frac{\rho_{NS} D}{2 G^2} \tag{6.80}$$

where the two-phase density for a no-slip flow is defined as

$$\rho_{NS} = \rho_l (1 - \alpha) + \rho_g \alpha \tag{6.81}$$

For the case of slip flow, Dukler et al. presented the two-phase multiplier as

$$\phi_{lo}^2 = \frac{\rho_l}{\rho_{NS}} \alpha(\lambda) \beta \tag{6.82}$$

where

$$\alpha(\lambda) = 1 + \frac{-ln\,\lambda}{1.281 - 0.478(-ln\,\lambda) + 0.444(-ln\,\lambda)^2 - 0.094(-ln\,\lambda)^3 + 0.00843(-ln\,\lambda)^4} \tag{6.83}$$

$$\beta = \frac{\rho_l}{\rho_{NS}} \frac{\lambda^2}{1 - \alpha} + \frac{\rho_g}{\rho_{NS}} \frac{(1 - \lambda)^2}{\alpha} \tag{6.84}$$

$$\lambda = \frac{Q_l}{Q_l + Q_g} = \frac{\rho_g (1 - x)}{x \rho_l + \rho_g (1 - x)} \tag{6.85}$$

When compared against the experimental data, the equation for a slip flow is better than that for a no-slip flow. However, the agreement with the data is poor, especially for steam-water flow.

Obot et al. [1991] also employed the similarity approach to indicate the same characteristic in frictional pressure drop between single- and two-phase flow. With experimental data of air-water flow, a transition is exhibited between two regions and the two-phase pressure gradient decreases with increasing quality. This is similar to the laminar-to-turbulent flow transition in single-phase flow. Obot et al. introduced an empirical similarity parameter for single-phase flow and two parameters for two-phase flow. Comparison between predictions and experimental data are limited to the data used to derive the parameters only.

6.3.4 The Maroti Model

Maroti [1975] modified the homogeneous-flow model by introducing two additional friction terms that were caused by: (i) the momentum difference between two phases, and (ii) the relative motion of the dispersed phase (i.e., bubbles in bubbly flow and droplets in dispersed flow) due to buoyancy. Both terms resemble the slip factor used in the separated-flow model. An empirical constant was optimized with experimental data in the second term. Comparison of predictions against experimental data indicated generally an underprediction of data at low flows, and showed a strong quality effect at high flows with overprediction for data at high qualities. Agreement is better at low-pressures.

6.4 MIXING-LENGTH MODELS

The mixing-length models described in this section focus primarily on the extension of the single-phase theory to the two-phase region. It does not include any studies that use the same theory on the single-phase liquid-film analysis (such as the Calvert and Williams model [1955]).

6.4.1 The Levy Annular-Flow Models

Levy [1962] extended the single-phase mixing-length theory to the analysis of two-phase flow. Based on the momentum equation and neglecting the gravity and viscous effects, the shear stress is expressed as

$$\tau = \overline{\rho}\ \overline{u'\ v'} + \overline{u}\ \overline{\rho'\ v'} \tag{6.86}$$

From the mixing-length theory, the fluctuating components are presented as

$$u' = v' = l_u \frac{d\overline{u}}{dy} \tag{6.87}$$

$$\rho' = l_\rho \frac{d\overline{\rho}}{dy} \tag{6.88}$$

By assuming the turbulent exchange of momentum and density are equal, i.e.,

$$l_u = l_\rho = l \tag{6.89}$$

the shear stress is expressed as

$$\tau = l^2 \frac{d\overline{u}}{dy} \frac{d(\overline{\rho}\,\overline{u})}{dy} \tag{6.90}$$

Based on the same modification, introduced by Van Driest, as for single-phase flow, i.e.,

$$\begin{aligned} \tau &= \tau_w \\ l &= K\, y\, (1 - \exp(-y/F)) \end{aligned} \tag{6.91}$$

and including also the viscous effect, the wall shear stress is presented as

$$\tau_w = K^2\, y^2 \frac{d\overline{u}}{dy} \frac{d(\overline{\rho}\,\overline{u})}{dy} (1 - \exp(-y/F))^2 + \mu \frac{d\overline{u}}{dy} \tag{6.92}$$

The density distribution, on the other hand, is expressed as

$$\frac{\overline{\rho}}{\rho_l} = \frac{\rho_m\, u_m}{\rho_l\, \overline{u} + \rho_m\, (u_m - \overline{u})} \tag{6.93}$$

based on the boundary conditions that

$$\begin{aligned} \overline{\rho} &= \rho_l \qquad & \overline{u} &= 0 \\ \overline{\rho} &= \rho_m \qquad & \overline{u} &= u_m \end{aligned} \tag{6.94}$$

By introducing the density distribution into the equation for wall shear stress, a complex equation was derived. It involves the mixing-length constant, κ, the non-dimensional wall damping constant and the two-phase viscosity. Levy recommended the use of values of single-phase flow for the constants, but suggested the two-phase viscosity, based on the comparison with experimental data of laminar flow, to be calculated with

$$\mu = \mu_l \left(1 + 2.5 \frac{\rho_l - \rho_g}{\rho_l} \alpha \right) \tag{6.95}$$

The model shows only limited success when compared against the experimental data, although the trend of predictions is similar to those exhibited by the data. This is mainly caused by the mixed-flow assumption, which is not valid for a separated-flow pattern such as annular or slug flow.

Levy [1966] included the interfacial shear and liquid entrainment in his annular-flow model for predicting the wall shear stress (hence, pressure gradient) and liquid film thickness. Mixing-length theory was used in both the liquid film (with only single-phase liquid) and the core flow (with a mixture of vapour and droplets). A film-thickness function, F', was correlated based on the experimental data and was presented graphically. It is expressed as

$$\sqrt{\frac{(-dP/dz)\ (b/2)}{\rho_l}} \frac{\rho_g}{G_g} K \left(\frac{g\ \rho_l}{-dP/dz} \right)^{-n} = F' \tag{6.96}$$

where n = 0 for $(-dP/dz) \geq g\rho_l$ and n = ⅓ for $(-dP/dz) < g\rho_l$. The slip ratio, K, was also presented graphically, but was approximated with $(\rho_l/\rho_g)^{1/3}$ for ρ_l/ρ_g between 1 and 200. Iteration is required to evaluate the pressure drop and liquid-film thickness from the shear-stress formulation and liquid-film flow rate. A good comparison has been shown with data used to derive the function. Only a limited comparison was made with other data of vertical upward and downward flow as well as horizontal flow.

Levy and Healzer [1981] introduced a different approach to the analysis of a wavy liquid film, rather than relying on an empirical correlation of interfacial friction in annular flow. Based on the assumption of a homogeneous mixture of a continuous gas phase and liquid droplets in the core, their approach divides the liquid film into a continuous liquid sublayer and a wavy liquid

sublayer. The single-phase mixing-length analysis is applied to both the core and the continuous liquid sublayer, resulting in similar equations to those presented in Levy [1973]. In the wavy-liquid sublayer (transition region), an exponential decrease of density was used from liquid density at the edge of the continuous liquid sublayer to core density at the edge of the gas core. An empirical parameter was derived to calculate the density variation within the wavy-liquid sublayer.

A procedure for solving the liquid-film flow rate and pressure gradient was provided; however, no estimation of interfacial friction factor was presented. A comparison of predictions against experimental data of air-water and steam-water flows indicated that this model provides a trend similar to that exhibited by the experimental data. While large discrepancies were noted between data sets, this model agreed best with the data of Gill and Hewitt [1962], which were used to derive the empirical parameter. In other comparisons, relatively good agreements were obtained for the high gas-mass-flux data, where the empirical parameter approaches 1. The entrained-liquid fraction was considerably overpredicted at high qualities in steam-water flow.

6.4.2 The Beattie Models

Beattie [1971] compared the experimental data of two-phase pressure drops from various studies and observed different unique characteristics among the data. He found the Colebrook equation, which was derived for a single-phase friction factor, to be applicable for two-phase flow as well, provided that both the friction factor and Reynolds number are properly defined.

The turbulent level of the two-phase mixture in the core was analyzed using the mixing-length theory. Two basic structures were assumed: bubble and droplet flows. The turbulence was assumed to exist in the continuous phase only, and the local void fraction was assumed to be linearly proportional to the local velocity of the continuous phase. Based on the shear-stress distribution and the local void fraction, Beattie [1972] presented two equations for bubbly and

droplet flows. These equations were referred to as the voidage-deficiency equation and were expressed, for bubbly flow, as

$$(1 - \alpha)^{3/2} = (1 - \alpha_c)^{3/2} - \frac{u_l^* a}{2 \kappa / 3} ln \frac{y}{R} \tag{6.97}$$

and for droplet flow as

$$\alpha^{3/2} = \alpha_c^{3/2} + \frac{u_g^* c}{2 \kappa / 3} ln \frac{y}{R} \tag{6.98}$$

where u_l^* and u_g^* are the dimensionless liquid and gas velocity defined as $(\tau_w/\rho_l)^{0.5}$ and $(\tau_w/\rho_g)^{0.5}$, respectively, τ_w is the shear stress at channel wall, α and α_c are the local void fraction at position y and at channel centre axis, respectively, y is the distance from the channel wall, κ is the mixing length constant (which is 0.4 for single-phase flow), and R is the channel radius. The coefficients, a and c, are empirical constants derived for the local void profiles, which are expressed, for bubble flow, as

$$\alpha = a\, u_l + b \tag{6.99}$$

and, for droplet flow, as

$$\alpha = c\, u_g + d \tag{6.100}$$

Although the constants b and d are not used in Equations (6.96) and (6.97), they can also be derived empirically. Comparison against experimental data showed that the above relation adequately represented the void-fraction profiles of bubble flow and core mixture in annular flow. A non-linear void-fraction profile in the liquid-film region for annular flow was shown with respect to relative distance from the wall or velocity. Beattie also presented the experimental

results of radial void distribution obtained by Adorni et al. [1964] in a heated channel with flow conditions up to dryout. While the radial void profile is non-uniform, the distribution remains the same for increasing heat flux, with increasing average void. At dryout, however, the void distribution flattened (i.e., becomes more uniform), signifying a sudden surge of vapour in the near-wall region.

Beattie [1973] noted that the two-phase pressure drop is primarily affected by flow structure close to the wall, and depends strongly on flow pattern. The Colebrook equation for the single-phase friction factor

$$\frac{1}{\sqrt{f}} = 3.48 - 4 \log \left(\frac{2\,\varepsilon}{D} + \frac{9.35}{Re\,\sqrt{f}} \right) \tag{6.101}$$

was also shown to be valid for two-phase pressure drop, provided that the friction factor and the Reynolds number are properly defined with two-phase properties. Beattie employed the Fanning friction factor, which is four times the Blasius friction factor.

Based on the mixing-length theory and the near-wall flow structure, he derived different two-phase friction factors, two-phase Reynolds numbers and two-phase multipliers for various flow conditions: bubble, wavy gas/liquid interface, very small bubbles, flow with attached wall bubbles, and dry wall. However, these equations (presented in Table 6.1) are limited to those flows with similar characteristics to single-phase flow, where the friction factor, f, is proportional to $Re^{-0.2}$ (Blasius type). Modifications to the exponent values must be introduced for other friction-factor functions. In his calculation, the pressure drop due to gravity was evaluated based on the separated-flow approach, but the pressure drop due to acceleration was based on the homogeneous model. The comparison of the predicted values from these equations against a limited data base showed relatively good agreement. For a complex geometry such as a rod bundle, the hydraulic-diameter concept was suggested by Beattie.

Table 6.1: The Beattie Correlations for Various Flow Patterns [Beattie, 1973]

Sublayer Structure	Example	Friction factor	Reynolds number	ϕ_{lo}^2
Bubble	Bubble flow	$\frac{\rho_l D\, dP/dz}{2G^2\left(1+x_a\left(\frac{\rho_l}{\rho_g}-1\right)\right)}$	$\frac{DG}{\mu_l}\frac{1+x_a\left(\frac{\rho_l}{\rho_g}-1\right)}{1+x_a\left(\frac{(3.5\mu_g+2\mu_l)\rho_l}{(\mu_g+\mu_l)\rho_g}-1\right)}$	$\left(1+x_a\left(\frac{\rho_l}{\rho_g}-1\right)\right)^{0.8}\left(1+x_a\left(\frac{(3.5\mu_g+2\mu_l)\rho_l}{(\mu_g+\mu_l)\rho_g}-1\right)\right)^{0.2}$
Wavy gas/liquid interface	Annular flow with no entrainment	as above	$\frac{DG}{\mu_l}\frac{1+x_a\left(\frac{\rho_l}{\rho_g}-1\right)}{1+x_a\left(\frac{\rho_l\mu_g}{\rho_g\mu_l}-1\right)}$	$\left(1+x_a\left(\frac{\rho_l}{\rho_g}-1\right)\right)^{0.8}\left(1+x_a\left(\frac{\rho_l\mu_g}{\rho_g\mu_l}-1\right)\right)^{0.2}$
Very small bubbles	Flow following obstruction (bubble or annular flow)	as above	$\frac{DG}{\mu_l}\frac{1+x_a\left(\frac{\rho_l}{\rho_g}-1\right)}{1+x_a\left(3.5\frac{\rho_l}{\rho_g}-1\right)}$	$\left(1+x_a\left(\frac{\rho_l}{\rho_g}-1\right)\right)^{0.8}\left(1+x_a\left(3.5\frac{\rho_l}{\rho_g}-1\right)\right)^{0.2}$
Dry wall	Post 'burnout' flow	$\frac{\rho_l^2 D\, dP/dz}{2\rho_g G^2\left(1+x_a\left(\frac{\rho_l}{\rho_g}-1\right)\right)^2}$	$\frac{DG}{\mu_g}\frac{\rho_g}{\rho_l}\left(1+x_a\left(\frac{\rho_l}{\rho_g}-1\right)\right)$	$\left(\frac{\mu_g}{\mu_l}\right)^{0.2}\left(\frac{\rho_g}{\rho_l}\right)^{0.8}\left(1+x_a\left(\frac{\rho_l}{\rho_g}-1\right)\right)^{1.8}$
Flow with attached wall bubbles	Boiling flow	$\frac{2\rho_l D\, dP/dz}{G^2\left(1+x_a\left(\frac{\rho_l}{\rho_g}-1\right)\right)}$	$2.4\left(\frac{G^2 D\left(1+x_a\left(\frac{\rho_l}{\rho_g}-1\right)\right)}{\rho_l\sigma}\right)^{1/2}$	complex

While functions provided in Table 6.1 were found to be valid for a number of flow conditions, they are not applicable for others, which have flow characteristics that differ significantly from single-phase flow. Beattie [1974] found that, unlike most flow characteristics where three sublayers are encountered over the flow area, only two sublayers (laminar and buffer) are exhibited in these data. By extending the buffer sublayer to the core axis, the friction factor becomes

$$\frac{1}{\sqrt{f}} = 8.15 \log\left(Re\sqrt{f}\right) - 11.11 \qquad (6.102)$$

This equation is also valid for flows affected by the entrance effect or near the hydrodynamic dryout phenomenon. At hydrodynamic dryout conditions, the liquid film is stripped away from the surface due to high mass flux and quality. This is different from the thermodynamic dryout phenomenon where the liquid film is evaporated away.

Based on the friction factor, the Beattie attached wall-void equation significantly overpredicted the pressure-drop data of Gaspari et al. [1964]. No clarification was provided by Beattie. However, this may have been caused by the differences in near-wall flow structure, where a thin-film annular flow was present, rather than the anticipated attached wall-void phenomenon.

Beattie [1975] extended the analysis of sublayer flow structure to high-pressure steam-water flow. He categorised the flow structures into five groups, each having a unique dimensionless parameter:

(i) Dry wall sublayer:

$$Re = \frac{D\ \rho_g\ \langle j \rangle}{\mu_g} \tag{6.103}$$

(ii) Sublayer containing bubbles with rigid surface:

$$Re = \frac{D\ \rho_{tp}\ \langle j \rangle}{\mu_l\ (1 + 2.5\ \beta)} \tag{6.104}$$

(iii) Sublayer containing bubbles with non-rigid surface:

$$Re = \frac{D\ \rho_{tp}\ \langle j \rangle}{\mu_l \left(1 + \frac{2.5\ \mu_g + \mu_l}{\mu_g + \mu_l}\ \beta \right)} \tag{6.105}$$

(iv) Sublayer with a wavy gas-liquid interface extending to within the laminar sublayer:

$$Re = \frac{D\ \rho_{tp}\ \langle j \rangle}{\mu_l\ (1 - \beta) + \mu_g\ \beta} \tag{6.106}$$

(v) Sublayer containing attached wall voids:

$$We = \frac{D\ \rho_{tp}\ \langle j \rangle^2}{\sigma} \tag{6.107}$$

The average volumetric flow rate is evaluated from

$$\langle j \rangle = \frac{G}{\rho_{tp}} \tag{6.108}$$

where the two-phase density is expressed as

$$\rho_{tp} = \left(\frac{x_a}{\rho_g} + \frac{1 - x_a}{\rho_l} \right)^{-1} \tag{6.109}$$

The gas volumetric flow ratio is defined as

$$\beta = \frac{x_a\ \rho_l}{x_a\ \rho_l + (1 - x_a)\ \rho_g} \tag{6.110}$$

The two-phase pressure gradient was presented in terms of the friction factor as

$$\frac{dP}{dz} = \frac{2 f \rho_{tp} \langle j \rangle^2}{D} \tag{6.111}$$

except for the dry-wall case, where the two-phase pressure gradient was written as

$$\frac{dP}{dz} = \frac{2 f \rho_{g} \langle j \rangle^2}{D} \tag{6.112}$$

Note that the Fanning friction factor is used in all of Beattie's equations, and is 1/4 of the Blasius friction factor. Based on the mixing-length theory and empirical velocity profile, Beattie presented seven different equations for the Fanning friction factor under various flow conditions. These equations are listed as follows:

$$1/\sqrt{f} = 3.48 - 4 \log (2\varepsilon/D + 9.35/(Re \sqrt{f})) \tag{6.113}$$

$$1/\sqrt{f} = 8.15 \log (Re \sqrt{f}) - 11.1 \tag{6.114}$$

$$1/\sqrt{f} = 16 \log (Re \sqrt{f}) - 43 \tag{6.115}$$

$$1/\sqrt{f} = 16 \log (Re \sqrt{f}) - 56.7 \tag{6.116}$$

$$1/\sqrt{f} = 16 \log (Re \sqrt{f}) - 72.4 \tag{6.117}$$

$$1/\sqrt{f} = 5.66 \log (We f) + 1.7 \tag{6.118}$$

$$1/\sqrt{f} = 14 \log(We\, f) - 10.4 \tag{6.119}$$

The two-phase pressure gradient is determined by using the appropriate friction-factor definition and non-dimensional parameter (i.e., Re or We) based on the sublayer structure. No definite boundary of applications for these equations (i.e., Equations (6.113) to (6.119)) were given by Beattie. For heated tubes, Beattie recommended the use of Equation (6.113) with Equation (6.104) for low-quality bubbly flow, Equation (6.119) with Equation (6.107) for high-quality flow, and Equation (6.113) with Equation (6.103) for post-dryout flow. Figure 6.1 shows the comparison between the Beattie combined flow-regime correlation and the experimental data of Gaspari et al. [1964]. The two-phase friction factor was calculated from Equation (6.111) for pre-dryout flow and Equation (6.112) for post-dryout flow. The combined flow-regime correlation seems to predict the experimental data quite well, except at conditions where only part of the tube is beyond dryout. These experimental data, however, were mostly obtained with two-phase inlet conditions in a tube of short heated length. Beattie [1977] grouped the above

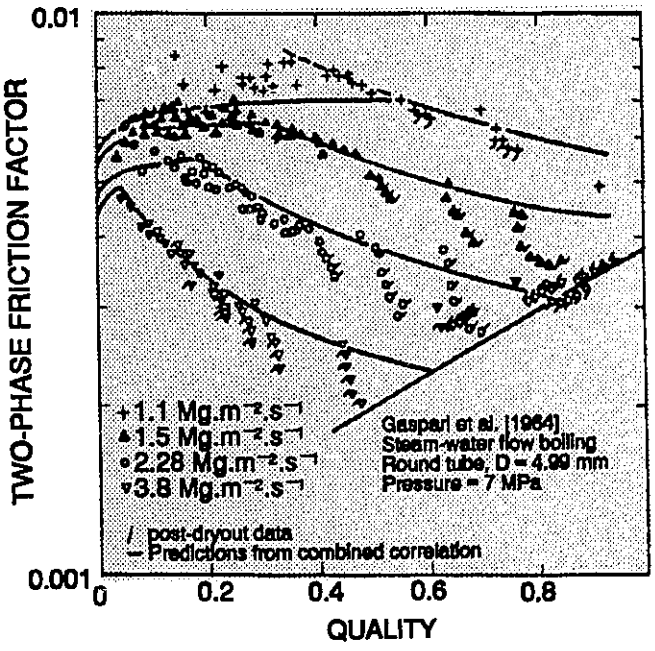

Figure 6.1: Predictions of Beattie's Combined Flow-Regime Correlation and Data [Beattie, 1975].

equations into a generalised equation with the empirical coefficients expressed in terms of two parameters.

In view of the assumed phenomenon associated with the Beattie derivation, the attached wall-void expression (Equations (6.119) and (6.107)) used for the high-quality flow may not be appropriate. Under those conditions, an annular flow is encountered and bubble nucleation is probably suppressed. Therefore, the surface-tension effect (incorporated in the Weber number) may be less significant than the dynamic effect.

The difficulty in using the Beattie equation arises from the need to know the near-wall flow structure, which has to be determined experimentally. Beattie and Whalley [1982] introduced a simplification by modifying the calculation of two-phase viscosity for bubbly and annular flows. This simplification is possible since the same definitions for two-phase friction factor and two-phase Reynolds number are applicable for these flow patterns. The only difference is the definition of two-phase viscosity in the calculation of the two-phase Reynolds number. The two-phase friction factor is defined as

$$f_{tp} = \frac{\rho_{tp}\, D\, (dP/dz)_f}{2\, G^2} \tag{6.120}$$

and the two-phase Reynolds number is

$$Re_{tp} = \frac{D\, G}{\mu_{tp}} \tag{6.121}$$

where the re-defined two-phase viscosity is expressed as

$$\mu_{tp} = \mu_l\, (1 - \beta)\, (1 + 2.5\, \beta) + \mu_g\, \beta \tag{6.122}$$

This modification is anticipated to be less accurate than the equation derived for a specific flow pattern. However, a comparison of its predictions against a large data bank of adiabatic experimental data indicated very good agreement, particularly for vertical steam-water flow. This correlation is better than 11 others (excluding the correlation of Heat Transfer and Fluid-flow Service (HTFS), which was derived from the same data base), including those recommended by Baroczy [1965], Friedel [1979] and Chisholm [1978].

6.4.3 The Dobran Annular-Flow Model

Dobran [1983] separated the annular-flow liquid film into two regions: a continuous layer and a wavy layer of liquid. While the momentum diffusivity (ε_m) in the continuous layer is assumed to be the same as in single-phase liquid flow and is related to the distance from the surface, the one in the wavy layer is a function of the wave height (i.e., the difference in thickness between the wave crest and continuous layer). As for single-phase flow, the velocity profile is presented for the continuous layer based on the assumption of a thin liquid film. The shear-stress distribution, on the other hand, is obtained by ignoring the inertia forces in the momentum equation of this wavy layer

$$\frac{\tau}{\tau_w} = 1 - \left(1 - \frac{\tau_i}{\tau_w}\right)\frac{y^+}{\delta^+} \tag{6.123}$$

where y^+ is the dimensionless distance from the wall

$$y^+ = \frac{\rho_l\, u^*\, y}{\mu_l} \tag{6.124}$$

u* is the friction velocity

$$u^* = \left(\frac{\tau_w}{\rho_l} \right)^{1/2} \tag{6.125}$$

δ^+ is the dimensionless film thickness

$$\delta^+ = \frac{\rho_l \, u^* \, \delta}{\mu_l} \tag{6.126}$$

and τ_i and τ_w are the interfacial and wall shear stress, respectively. The velocity profile in the wavy layer is obtained by assuming that the thin liquid-film approach is also valid in this layer and integrating from $y^+ = \delta_t^+$ to $y^+ > \delta_t^+$. In the vapour core, Dobran indicated that a homogeneous flow should be assumed, but he used 100% core void fraction (i.e., no entrainment) in his analysis.

Two empirical expressions were derived based on other experimental data of upward and downward air-water flows: the thickness of continuous liquid layer and the momentum diffusivity of the wavy layer. The Wallis [1969a] correlation for interfacial friction factor was used to calculate the interfacial shear stress. Using these empirical expressions and velocity profiles, Dobran derived the equation for calculating the dimensionless liquid-film mass-flow rate. The dimensionless liquid film thickness and flow rate were calculated with this model, but they were compared only against the data used to derive the empirical expressions. Even so, only limited success was achieved in the comparison.

Dobran [1985] also included droplet entrainment in the core flow, which was estimated with the Ishii and Mishima correlation [1982]. The inclusion of droplet entrainment improved the prediction accuracy of Dobran's model.

6.4.4 The Abolfadl and Wallis Multi-layer Models

Abolfadl and Wallis [1985] assumed different sublayers in the liquid film and vapour core of annular flow. Similar to other analytical models, the cross-sectional flow includes a liquid film and dispersed flow core with liquid entrainment. The liquid film is divided into two sublayers, viscous and turbulent, and the core flow is assumed to be homogeneous. In the viscous sublayer, the velocity is presented as

$$u_{Lf}^{*} = \frac{N_l}{2}\left(\frac{(\Delta P^{*} - 1)(1 - r^{*2})}{2} - \alpha_c \, r_{core}^{*2} \ln r^{*} \right) \sqrt{\frac{\rho_g}{\rho_l}} \tag{6.127}$$

where u_{Lf}^{*} is the dimensionless laminar-film velocity, defined as

$$u_{Lf}^{*} = \frac{u_{Lf} \, \rho_g^{1/2}}{(g \, D \, (\rho_l - \rho_g))^{1/2}} \tag{6.128}$$

ΔP^{*} is the dimensionless pressure gradient, defined as

$$\Delta P^{*} = \frac{-(dP/dz + \rho_g \, g \cos\theta)}{g \, (\rho_l - \rho_g)} \tag{6.129}$$

r^{*} is the dimensionless radius, defined as

$$r^{*} = \frac{2 \, r}{D} \tag{6.130}$$

N_l is a dimensionless parameter, expressed as

$$N_l = \frac{D\,(\rho_l\, g\, D\,(\rho_l - \rho_g))^{1/2}}{\mu_l} \tag{6.131}$$

α_c is the core void fraction and r^*_{core} is the dimensionless average-core radius (i.e., 2 r_{core}/D). The velocity at the turbulent-film sublayer is expressed as

$$u^*_{Tf} = u^*_{LT} + \left(\frac{\rho_g}{\rho_l}\right)^{1/2} \int_{r^*}^{r^*_t} H \frac{\left(\left| r^*(\Delta P^* - 1) + \frac{\alpha_c r^{*2}_{core}}{r^*} \right|\right)^{1/2}}{2l^*} dr^* \tag{6.132}$$

where u_{LT}^* is the dimensionless velocity at the laminar-turbulent flow transition calculated with the laminar-film equation, H is a toggle function which is 1 for upward flow (i.e., du/dy > 0) and -1 for downward flow (i.e., du/dy < 0), r_t^* is the dimensionless radius at the laminar-turbulent flow transition (which is 1 - δ_{Lf}^*), and l^* is the dimensionless mixing length defined as

$$l^* = \frac{2\,l}{D} \tag{6.133}$$

The dimensionless thickness of the laminar sublayer is calculated using

$$Re_f = \frac{N_l}{2}\sqrt{\frac{\rho_l}{\rho_g}} \int_0^{\delta^*_{Lf}} |u^*_{Lf}| dy^* = 67 \tag{6.134}$$

rather than based on the same definition as in single-phase flow, which is the most common approach used in annular-flow analysis. In the core flow, only turbulent flow was assumed, and the velocity was expressed similarly to the above equation, i.e.,

$$u_{Tc}^{*} = u_i^{*} + \left(\frac{\rho_g}{\rho_c}\right)^{1/2} \int_{r^{*}}^{r_{core}^{*}} H \frac{\left(|r^{*}(\Delta P^{*}-1)+\alpha_c|\right)^{1/2}}{2l^{*}} dr^{*} \tag{6.135}$$

where u_i^* is the dimensionless interfacial velocity and ρ_c is the core density, which is calculated using

$$\rho_c = \alpha_c \rho_g + (1 - \alpha_c) \rho_l \tag{6.136}$$

The dimensionless liquid film volumetric flux was expressed as

$$J_f^{*} = \left(\frac{\rho_l}{\rho_g}\right)^{1/2} \int_{r_i^{*}}^{1} u_{Lf}^{*} 2r^{*} dr^{*} + \left(\frac{\rho_l}{\rho_g}\right)^{1/2} \int_{r_{core}^{*}}^{r_i^{*}} u_{Tf}^{*} 2r^{*} dr^{*} \tag{6.137}$$

the dimensionless gas volumetric flux was

$$J_g^{*} = \int_{0}^{r_{core}^{*}} \alpha_c u_{Tc}^{*} 2r^{*} dr^{*} \tag{6.138}$$

and the dimensionless entrained liquid volumetric flux was

$$J_e^{*} = \left(\frac{\rho_l}{\rho_g}\right)^{1/2} \int_{0}^{r_{core}^{*}} (1 - \alpha_c) V_{Tc}^{*} 2r^{*} dr^{*} \tag{6.139}$$

The total dimensionless liquid volumetric flux was

$$J_l^{*} = J_f^{*} + J_e^{*} \tag{6.140}$$

An empirical function was introduced for the mixing length, which was assumed to cover both the turbulent liquid-film sublayer and the turbulent core flow. It was expressed as

$$l^* = C(\alpha_c)\ F(r^*) \tag{6.141}$$

where

$$F(r^*) = 1 - r^{*2} \tag{6.142}$$

and, for $\alpha_c \geq 0.999$,

$$C(\alpha_c) = 0.12 \tag{6.143}$$

otherwise,

$$C(\alpha_c) = 0.065 - 0.008\ ln(1 - \alpha_c) \tag{6.144}$$

A comparison of predicted gas volumetric fluxes against experimental data indicated a much closer agreement with this empirical two-phase mixing-length definition than the one defined for single-phase flow. The interfacial friction factor, instead of being obtained from an empirical correlation, was derived and calculated with the mixing length (Equation (6.141)). It was expressed as

$$f_i = B\,(1-\delta^*)^5 \left(\frac{1}{4}\, ln \frac{1+(1-\delta^*)^{1/2}}{1-(1-\delta^*)^{1/2}} - \frac{1}{3}(1-\delta^*)^{3/2} - \frac{1}{2}\tan^{-1}(1-\delta^*)^{1/2} \right)^{-2} \tag{6.145}$$

with B defined as, for $\alpha_c \geq 0.999$,

$$B = 0.0072 \tag{6.146}$$

and, for $\alpha_c < 0.999$,

$$B = \frac{(0.0065 - 0.008\, ln(1-\alpha_c))^2}{2} \tag{6.147}$$

These equations were solved simultaneously to obtain pressure drop and film thickness for a given set of gas, liquid and entrained-liquid flow rates. Comparisons with adiabatic data of air-water, air-alcohol, and steam-water flows have indicated generally close agreement. However, it appears that the low pressure-drop data were underpredicted while the high pressure-drop data were overpredicted by this model in steam-water flow.

Abolfadl and Wallis [1986] modified the empirical mixing-length equation, which approaches the value in single-phase flow as the entrained-liquid fraction approaches zero. While the mixing-length expression and its $F(r^*)$ function remained the same, the $C(\alpha_c)$ function became, for $-\ln(1-\alpha_c) \geq 9$,

$$C(\alpha_c) = 0.14 \tag{6.148}$$

otherwise,

$$C(\alpha_c) = 0.0275 - 0.0125\, ln(1 - \alpha_c) \tag{6.149}$$

In turn, the interfacial friction factor had to be modified as well. In addition to the change in mixing-length definition, a laminar sublayer was also introduced to the vapour core. Its thickness was calculated with

$$Re_c = \frac{N_g}{2}\sqrt{\frac{\rho_c}{\rho_g}}\int_{r_{ci}^*}^{r_{core}^*}|u_{Lc}^*|dy^* = 6 \tag{6.150}$$

The criteria (i.e., 6) was obtained based on a small number of Gill and Hewitt [1962] data. The velocity distribution in this sublayer was expressed as

$$u_{Lc}^* = u_i^* + \frac{N_g}{16}(\Delta P^* - 1 + \alpha_c)(1 - r^{*2}) \tag{6.151}$$

Comparison against the same data sets used in their previous analysis indicated slight improvements for some data (e.g., steam-water upward flow), but also a reduction in accuracy for others (e.g., air-water upward flow). This modification provides a correct parametric trend to the model and hence should be used. The model was also extended to horizontal flow, with new definitions for the mixing length and various velocity distributions. These definitions will not be presented here, since horizontal flow is beyond the scope of the present study.

6.5 MULTI-FLUID MODELS

A multi-fluid model utilizes the complete set of conservative equations (i.e., mass, momentum and energy) for the phases. The inter-relationships of these equations are often predicted with closure relationships that rely on other analytical models or experimental results. In general, this model provides a correct parametric trend (depending on the closure equations) and hence it is a prime candidate for extrapolation. However, its complexity often deters potential applications, since a high-speed computer is essential to solve all equations simultaneously. Furthermore, the accuracy of the model depends also on the employed closure equations. Most often, this type of model is set up for predicting dryout in a heated channel, and pressure drop is obtained as a by-product in the solution.

6.5.1 The Saito et al. Formulation

Saito et al. [1978] presented a multi-fluid formulation that can be used for two- to four-fluid analysis. The predictions of their model have been compared against experimental data of adiabatic air-water flow in a tube, and steam-water flows at dryout conditions inside a tube and an annulus. Descriptions of closure equations were provided for various flow conditions.

The comparisons indicated only general agreement with the data, but the parametric trend of data agreed with the predictions. As anticipated, the accuracy of this model was less than that of empirical correlations. For flow inside a heated tube at dryout conditions, the model predicts a decrease in pressure drop as the surface approaches dryout. A sensitivity study showed that the predictions of pressure drop and dryout power are affected strongly by the entrained-liquid fraction at transition to annular-dispersed flow.

6.5.2 The Fujita and Hughes, Two-Fluid, Two-Velocity Model

Fujita and Hughes [1979] developed a two-fluid, two-velocity model that considers only the continuous phases (i.e., liquid and gas/vapour) in the channel. The discrete phase was assumed to blend homogeneously inside the continuous phase. The predictions of their model were compared against the experimental results of Schrock and Grossman [1959].

While good agreement was indicated for both pressure and temperature distributions along the heated channel, the predicted void fraction and slip factor were shown to be rather different from the calculated results based on experimental data. This could be caused by the compensating effect from other parameters, resulting in yet reasonable predictions of pressure drop and wall temperature.

6.5.3 The Adeniji-Fashola et al. Model

Adeniji-Fashola et al. [1986] introduced separate models for different flow patterns. A drift-flux formulation was used for bubble and churn-turbulent flows, and a two-fluid model for annular flow. The transition point between these flow patterns was predicted using the Taitel et al. [1980] criterion. A number of empirical parameters (e.g., interfacial shear stress predicted using the Wallis correlation [1969a]) were introduced. Similar to the findings of Saito et al. [1977], the entrained-liquid fraction at the transition point was shown to be most crucial to the overall pressure-drop prediction.

Predictions obtained from this model were compared against only one set of experimental data of Refrigerant-11 flow [Adelmessih and Yin, 1973]. The parametric trends of pressure drop with respect to mass flux agreed with those observed from the experimental data. A set of inter-related empirical parameters were optimized using this set of data.

6.6 DISCUSSION

A wide variety of analytical or semi-analytical models were presented; strictly speaking, they are valid only for specific flow patterns. Although they can be used for flow boiling, only the Levy steam-slip model [1959] includes the effect of surface heating on two-phase pressure drop (via the calculations of vapour-mass quality and void fraction). In this section, the strength and weaknesses of some analytical models are discussed.

The homogeneous-flow model (expressed in equations as shown in Section 6.1) is the simplest model to use and can provide reasonably good predictions for some flow patterns (low-quality bubbly flow or high quality droplet flow). Its accuracy, however, depends strongly on the definitions of (i) two-phase viscosity and (ii) two-phase friction factor. The use of the Blasius equation as two-phase friction factor is not valid for high two-phase Reynolds numbers. On the

other hand, the Colebrook equation may be more appropriate, as indicated by Beattie [1973, 1974, 1977].

The modified homogeneous-flow model extends the applications of the homogeneous-flow model to a slightly wider range of conditions. It remains primarily valid for bubbly and droplet flow. However, due to the empirical nature of the modification (such as slip ratio or void and velocity profiles), this model should be restricted to the range of its data base.

The separated-flow model has only a limited range of application and is valid mainly for idealized annular flow (with no entrainment) and horizontal stratified flow. Similar to the homogeneous-flow model, its application is relatively simple but it does not result in good prediction accuracy. This is caused by the limitations in predicting the interfacial parameters (such as shear stress and velocity) based on empirical expressions. For annular flow, most models were based on the thin liquid-film assumption (e.g., Calvert and Williams [1955], Ueda [1967a] and Wallis [1969a]). This has limited the applications of this model further to only high-quality flow. The effects of other parameters on this model were presented by Wallis [1969b] for the applications in annular flow.

The mixing-length model is mainly used for analyzing annular flow. Although a relatively good agreement between predictions and experimental data of pressure drop was shown in various studies, its main limitation is the uncertainty in predicting flow parameters such as velocity profile, interfacial shear stress, etc. This is due to the limited data base (available mainly at low-pressure conditions) and large data scatter. In view of the complex nature of annular flow, the mixing-length model is a relatively simple, and yet successful, approach (as compared to the analysis based on two-phase eddy viscosity).

7. MODELLING OF PRESSURE GRADIENT IN A HEATED CHANNEL

The literature survey presented in Chapters 5 and 6 has shown that no specific prediction method is available to account for the surface-heating effect on two-phase pressure drop, despite ample experimental data in support of this strong effect. A number of prediction methods for adiabatic conditions have been extended to flow boiling. However, they were primarily tested with a limited data base, making their application to other conditions questionable. For high-pressure and high-flow conditions, the studies of Becker et al. [1961, 1962a, 1962b, 1962c, 1962d] and Reddy et al. [1982] have shown no heating effect on two-phase pressure drop. Their correlations do not show any variations with respect to heat flux as displayed in the experimental data of Tarasova et al. [1966] and Bartolomei et al. [1979]. Beattie [1975, 1977] showed that reasonable predictions of flow-boiling pressure drop can be achieved if appropriate two-phase parameters are defined.

Although the analytical models were set up in general form, none of them were developed specifically for steam-water flow boiling, since they use the closure relations derived from low-pressure air-water data. The only exception is the Lu and Jia two-region model [1988], which is valid only for subcooled flow boiling. Skouloudis and Wurtz [1991] performed only limited validations of their power-law model for annular flow with adiabatic steam-water data. They introduced empirical modifications, such as vapour entrainment in the liquid film, to improve the agreement between predictions and experimental data. Furthermore, these models are often based on empirical parameters that have inappropriate asymptotic trends (e.g., two-phase mixing length with values different from the single-phase flow at close to 0% or 100% in void fraction). This results in questionable extrapolation to conditions outside the data base.

Limited modelling studies on the effect of surface heating have been provided, but only for a specific flow pattern (e.g., the Weisman and Du [1992] model for bubbly flow). No inter-relation has been introduced to link various flow-pattern specific models; as a result, large discontinuities at the boundaries of flow-pattern transitions may occur.

In view of the lack of validated prediction methods, an analytical model is developed in this study for predicting flow-boiling pressure drop at high-pressure and high-flow conditions. A number of options have been examined for modelling flow boiling (e.g., mixed-flow, two-fluid and drift-flux models). The mechanistic approach is selected, rather than the full set of two-fluid or drift-flux formulations. It can provide a reasonable simulation and yet is simple enough for most applications. For this type of complex analysis, avoiding empirical constants completely is not yet feasible, because the fluid-flow phenomena in both single- and two-phase flows, and flow transitions, are still not fully understood. In the present model, these constants are used as the closure relationship to flow phenomena, and can be easily updated once more information becomes available. An empirical correlation, on the other hand, requires the re-derivation of equations to accommodate any changes.

The general equations for momentum and energy balance are presented in Section 7.1, together with the basic assumptions used in the present model. Section 7.2 presents the modelling

methodology, which describes the area where simplifications are introduced into the model. The modelling of single-phase liquid flow is shown in Section 7.3, which provides the equations for calculating the shear stress and velocity. A solution scheme is also presented. Section 7.4 describes the approach for modelling flow boiling and the equations used in various heat-transfer regimes. Closure relations are also presented with justification. In this study, two correlations have been derived for predicting the entrained-liquid fraction in adiabatic flow and flow boiling for the present conditions of interest. They are described in this section, together with a comparison against the experimental data. The solution scheme for applying the model to predict the pressure gradient due to friction is presented in Section 7.5.

7.1 GENERAL

The pressure gradient in a vertical channel is separated into three components: friction, acceleration and gravity. Based on the force-momentum balance on a control volume with steady-state flow (Figure 7.1), it is expressed as

$$-\frac{dP}{dz}\delta z\, A_F = \tau_w \delta z\, S + \frac{d}{dz}(Gu)\,\delta z\, A_F + \rho\, g\, \delta z\, A_F \tag{7.1}$$

where P is the pressure in Pa, z is the axial distance in m, A_F is the flow area in m^2, S is the channel wetted perimeter in m, τ_w is the wall shear stress in $N.m^{-2}$, G is the mass flux in $kg.m^{-2}.s^{-1}$, u is the flow velocity in $m.s^{-1}$, ρ is the fluid density in $kg.m^{-3}$ and g is the acceleration constant due to gravity (=9.806) in $m.s^{-2}$. Equation (7.1) is valid for both single-phase and two-phase homogeneous (with liquid/surface contact) flow, but has to be modified for two-phase separated flow (i.e., separate equations are needed for liquid and vapour phases). The pressure gradients due to acceleration and gravity are generally small at high-pressure and high-flow conditions. Equations for these pressure gradients are presented in Chapters 2 and 3. Detailed modelling of these two components is not expected to result in significant improvements in

prediction accuracy. Therefore, a simplified approach, as presented in Chapters 2 and 3, is used in the calculation.

The present model focuses on the prediction of frictional pressure gradient in a heated channel. To simplify the calculation, the momentum and energy equations are de-coupled and are solved separately. Assuming that frictional heating is negligible, an energy balance is illustrated in Figure 7.2 over a control volume for steady-state flow. It is expressed as

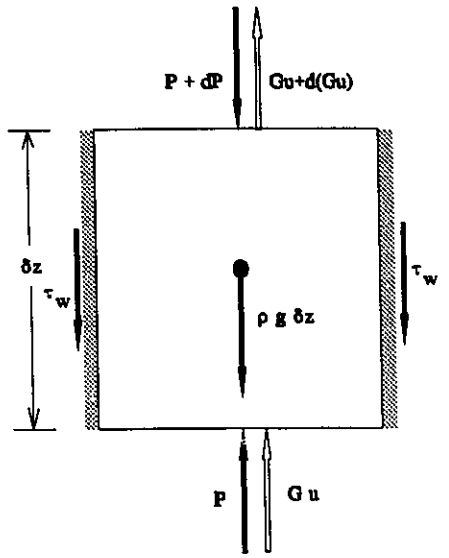

Figure 7.1: Force-Momentum Balance over a Control Volume.

$$\frac{d(WH)}{dz}\delta z + \frac{d(Wu^2)}{dz}\delta z + W g \delta z = q S_{he}\delta z + q_o \delta z A - w \qquad (7.2)$$

where H is the enthalpy in $J.kg^{-1}$, q is the surface heat flux in $W.m^{-2}$, S_{he} is the heated perimeter in m, q_o is the internal heat generation in $W.m^{-3}$, and w is the work done by the fluid. Again, this equation is valid for single-phase and two-phase homogeneous (with liquid/surface contact) flow, and has to be modified for separated two-phase flow. Assuming further that (i) the changes in fluid properties are negligible, (ii) the kinetic and potential-energy terms are much smaller than heat input and enthalpy, and hence are also negligible, (iii) there is no internal heat generation within the fluid, and (iv) there is no work done, the energy equation can be simplified for a channel of constant flow area, and is written as

$$\frac{d(WH)}{dz} = q\, S_{he} \qquad (7.3)$$

The fluid enthalpy can be expressed as

$$H = H_f + x H_{fg} \tag{7.4}$$

where H_f is the saturated-liquid enthalpy in $J.kg^{-1}$, H_{fg} is the latent heat of vaporisation in $J.kg^{-1}$ and x is the flow quality. Based on the continuity equation (i.e., conservation of mass) and assuming that the variations of saturated-liquid enthalpy and latent heat of vaporisation are negligible (i.e., $dH_f/dz \sim 0$ and $dH_{fg}/dz \sim 0$, no flashing), Equation (7.3) is re-written as

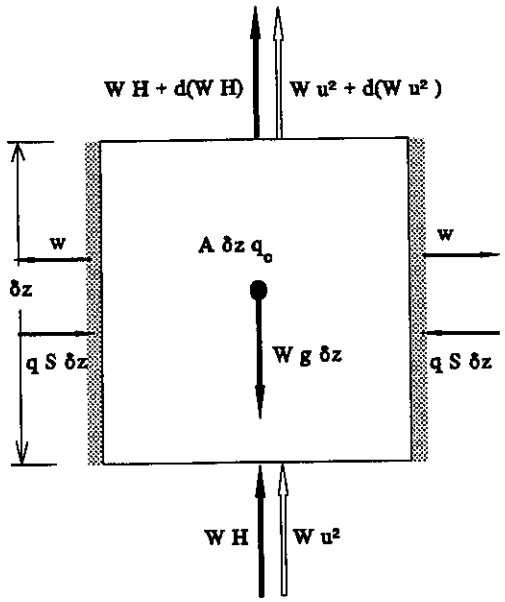

Figure 7.2: An Energy Balance over a Control Volume.

$$\frac{dx}{dz} = \frac{q S_{he}}{W H_{fg}} \tag{7.5}$$

Equation (7.5) can be integrated for a uniformly heated channel and expressed simply as the heat-balance over the channel; i.e.,

$$x = x_{in} + \frac{q\ S_{he}\ z}{W\ H_{fg}} = x_{in} + \frac{Power}{W\ H_{fg}}\ \frac{z}{L_{he}} \tag{7.6}$$

where x_{in} is the inlet quality, and Power is the applied power in W. To account for flashing due to a reduction in saturation temperature, Equation 7.6 is rewritten as

$$x = \frac{H_{in} + (Power/W)\ (z/L_{he}) - H_f}{H_{fg}} \tag{7.7}$$

with H_f and H_{fg} evaluated with the local pressure.

To account for the difference in pressure gradients between a heated and unheated channel in the model, the changes in radial fluid-temperature and void-fraction distributions (especially near the wall) due to the heating effect must be considered. The most significant difference is the near-wall void fraction, which is zero in adiabatic flow but often reaches a maximum in a heated-channel flow. For those flow patterns having similar characteristics in both heated and unheated channels (i.e., single-phase liquid flow and annular flow with no surface boiling), the near-wall viscosity variation due to differences in surface temperature must be included.

This mechanistic model considers the surface/near-wall fluid interaction as the primary cause of pressure gradient inside a channel. This interaction, however, is affected by flow structures at the liquid/vapour interface and the core flow that change the shear-stress and velocity distributions. The same argument was used by Beattie [1973] and Beattie and Whalley [1982] in their development of prediction methods for two-phase pressure gradient. Their comparison against experimental data resulted in the limited success of this approach, and the derivation of equations was restricted to several flow patterns only.

Different equations for predicting pressure gradient are needed for various flow structures. Their derivations are presented in the following sections. They are followed by discussions on transition criteria between these flow structures. While most derivations are analytically based, empirical correlations will also be employed to provide (i) closure relationships and (ii) simplification to complex formulations.

The following basic assumptions are used in the present model:

1) Local parameters are assumed to vary in the radial direction only and not in the azimuthal direction.
2) The same radial velocity distribution is maintained within the control volume.
3) The time-averaged radial void fraction is assumed to be uniform (i.e., homogeneous flow) across the two-phase region (i.e., $d\alpha/dr = 0$).
4) Fluid properties are assumed to be constant within the control volume.

5) The axial gradient in velocity (i.e., du/dz) is independent from the radial variation.
6) The cross-sectional flow structure is assumed to consist of two regions: laminar sublayer and turbulent core.
7) The vapour is assumed incompressible, since $(\delta\rho/\delta P)/\rho << 1$ at high-pressure conditions.

7.2 MODELLING METHODOLOGY

The present model is developed to evaluate the two-phase frictional multiplier by analytically calculating the single-phase and two-phase frictional pressure drops in a smooth channel. Although the analysis of single-phase pressure-drop measurements (to be shown later in Chapter 8) has resulted in a relative roughness value of 0.00103 (a relatively small variation from a smooth tube) for the present test section, it is decided to model a smooth tube, since the effect of tube roughness on pressure drop is beyond the scope of the present study. Also, this would considerably simplify the analysis. As indicated in Section 2.2.5, all recent modelling approaches for single-phase flow suggest a correction to the mixing-length calculation, and appear to contradict the experimental data of Schlichting [1960]. Chisholm [1983] has shown a reduction in two-phase multiplier for a rough tube, compared to that for a smooth tube (due to a much larger increase in pressure drop for single-phase than for two-phase flow; i.e., $(dP_{f,rough} / dP_{f,smooth})_{sp} > (dP_{f,rough} / dP_{f,smooth})_{tp}$). The effect of roughness on the two-phase multiplier becomes less significant at a relative roughness (ε/D) larger than 0.002. Figure 7.3 shows the relation of the coefficient B in the Chisholm correlation (Equation (5.15)) between a rough and smooth tube for various relative-roughness values.

The following approach is used to evaluate the overall pressure drop in a heated channel:

1) Equations for calculating the frictional pressure drop are set up for both single- and two-phase flow. They will be presented and described in later sections of this chapter. While only one sub-model is used for single-phase liquid flow, four different sub-models are prepared for

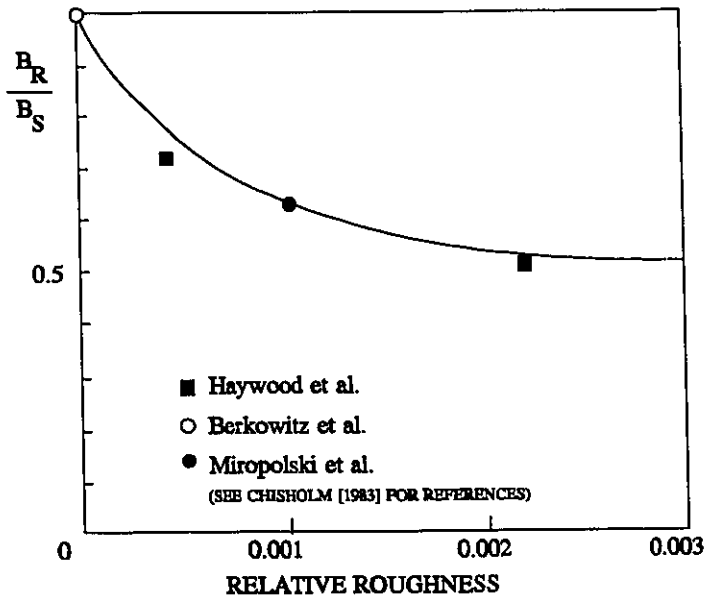

Figure 7.3: Effect of Relative Roughness on Coefficient B in the Chisholm Correlation for Two-Phase Frictional Multiplier [Chisholm, 1983].

two-phase flow, covering the subcooled boiling (near-wall bubbly flow), fully developed bulk boiling (bubbly flow), forced-convective evaporation (annular flow) and film boiling (dispersed droplet flow). The slug, churn, and inverted-annular flows are not encountered at present conditions of interest, and therefore will not be considered. Modifications, however, can be introduced to these sub-models to extend the applications to these flow regimes as well.

2) The channel is divided into small sections to ensure that assumptions (3), (4) and (5) are justified. In each section, the two-phase and single-phase frictional pressure drops are calculated and the two-phase frictional multiplier is the ratio of these two pressure drops. The calculation at each section (a control volume) is based on the upstream pressure and average values of fluid properties, flow, thermodynamic qualities and void fraction. The only exception is the momentum pressure-drop calculation, which is based on the momentum difference over the section, and is therefore calculated with the fluid properties, flow quality and void fraction at both the upstream and downstream points. It is assumed that the inlet

conditions (pressure, mass flow rate, and fluid temperature) and the applied power are known parameters, and the calculation proceeds from the inlet to the outlet end by subtracting various pressure-drop components (i.e., friction, acceleration and gravity) from the upstream pressure at each step.

3) The pressure drops due to acceleration and gravity are calculated separately, with the equations described in Sections 2.3.2 and 3.4.2, and Sections 2.3.3 and 3.4.3, respectively, for single- and two-phase flows.

4) The two-phase pressure drop due to friction is calculated by multiplying the two-phase frictional multiplier (based on the model) with the single-phase pressure drop calculated with the D'Arcy-Weisbach equation (Equation (2.37))

$$\Delta P_{sp} = \frac{f\,\Delta z}{D}\,\frac{\rho_f\,u^2}{2} \tag{7.8}$$

where the empirical friction factor, f, is obtained with the Colebrook-Chen equation (Equation (2.44)). The relative roughness of the section is evaluated from the single-phase pressure-drop data.

5) The effect of the temperature difference between near-wall and bulk fluids (as a result of surface heating) on pressure drop is significant only in single-phase liquid and dispersed droplet flows. In other pre-CHF heat-transfer regimes (mainly saturated boiling), the surface temperature is maintained close to the saturation value, since heat transfer between the heated surface and fluid is very efficient (as indicated by the steep gradient of boiling curve shown in Figure 4.1). Though possible, the radial variation of fluid viscosity is not included in the present model, to simplify the analysis. The effect of radial-temperature variation on the single-phase frictional pressure drop is accounted for with an empirical correction factor, (Equation (2.46), as described in Section 2.3.1.2)

$$\frac{(\Delta P / \Delta z)_{heated}}{(\Delta P / \Delta z)_{unheated}} = \frac{f_{heated}}{f_{unheated}} = \left(\frac{\mu_b}{\mu_w} \right)^m \tag{7.9}$$

where μ_b and μ_w are the dynamic-viscosity values for the bulk and near-wall fluids, respectively. The exponent, m, is determined with the single-phase pressure-drop data of the heated test section for liquid flow. A value of 0.1 (as recommended by Petukhov [1970]), however, is used for single-phase vapour flow, since experimental data of single-phase vapour flow in a heated tube are not available. The near-wall fluid properties are evaluated based on the surface temperature, as predicted with the correlations described in Chapter 4.

6) The transition points between flow patterns (and heat-transfer modes) are predicted based on the correlations described in Chapter 4. They include the ONB point (transition between single-phase liquid and subcooled-boiling heat-transfer regime), the OSV point (transition between single- and two-phase pressure drops) and the CHF point (between forced convective evaporation and film boiling heat-transfer regimes). Differences between ONB and OSV points have been described in Chapter 4. The transition between bubbly (saturated boiling) and annular (forced convective evaporation) flow is estimated with the criterion presented in the Hewitt and Roberts [1969] flow-pattern map (i.e., at a vapour momentum flux, $\rho_g j_g^2$, of 100 as shown in Figure 3.5).

7) The flow quality is calculated with the Kroeger and Zuber [1968] correlation (Equation (3.4)) and the void fraction is determined with the Chexal et al. [1991] correlation (see Section 3.3).

7.3 MODELLING OF SINGLE-PHASE LIQUID FLOW

The pressure gradient at any radial location, r, can be written as (from Equation (7.1))

$$-\frac{dP}{dz} = \frac{2}{r}\tau + G\frac{du}{dz} + \rho g \tag{7.10}$$

based on the assumption that axial pressure gradient is independent of radial location (see Figure 7.1). Hence, the radial shear-stress distribution is written as

$$\begin{aligned}\tau &= -\frac{r}{2}\left(\frac{dP}{dz} + G\frac{du}{dz} + \rho g\right) \\ &= -\frac{r}{2}\left(\frac{dP}{dz}\right)_f\end{aligned} \tag{7.11}$$

Since both the pressure drop and shear-stress distribution are unknown, iterations are required in this analysis. An initial value of pressure drop is assumed. As indicated in Chapter 2, the shear-stress distribution can also be expressed as a function of velocity gradient; i.e.,

$$\tau = \mu_A \frac{du}{dy} \tag{7.12}$$

For laminar flow, the apparent viscosity, μ_A, is equivalent to the liquid or vapour viscosity (μ_l or μ_g) corresponding to respective single-phase flow. The Reynolds number criterion of 2300 is used for the transition from laminar to turbulent flow. Laminar flow is not encountered at the present conditions of interest. As indicated in assumption (6), the buffer layer is not included in the present model.

In turbulent flow, the mixing-length approach is used to calculate the shear stress based on the velocity gradient. As stated in Section 2.2.2, the mixing length represents a hypothetical distance that has to be travelled by the fluid from one lamina to another for assimilation. This approach is the simplest and has been shown valid for tube flow. The apparent viscosity is expressed as

$$\mu_A = \rho\, l^2 \left|\frac{du}{dy}\right| \tag{7.13}$$

where ι is the mixing length. The velocity distribution is obtained by integrating the velocity gradient over the tube radius. It is expressed, for laminar flow as,

$$u = \int_{y=0}^{y} \frac{\tau}{\mu}\, dy = \int_{r=r}^{R} \frac{\tau}{\mu}\, dr \tag{7.14}$$

and, for turbulent flow as,

$$u = \int_{y=y_\delta}^{y} \sqrt{\frac{\tau}{\rho\, l^2}}\, dy + u_{lam,y_\delta} = \int_{r=r}^{R-y_\delta} \sqrt{\frac{\tau}{\rho\, l^2}}\, dr + u_{lam,R-y_\delta} \tag{7.15}$$

where $u_{lam,\, R\text{-}y\delta}$ is the laminar sublayer velocity at the radial location of $R\text{-}y_\delta$. Figure 7.4 shows the velocity distribution inside a tube. While a number of definitions for mixing length have been introduced (see Chapter 2), a simplified form of the Schlichting [1960] empirical equation (Equation (2.22)) is used. It is written as

$$\frac{l}{R} = 0.14 \left(1 - \left(\frac{r}{R} \right)^3 \right) \tag{7.16}$$

This equation provides a correct asymptotic value at the centre of the tube (i.e., $\iota = 0.14$ at R=0), but a slightly larger constant at the near-wall region (0.42 instead of 0.4, as presented by Prandtl's definition). Due to the difference in the present approach compared to those approaches traditionally used in shear-stress modelling (e.g., the mixing length is often defined as, $\iota = 0.4$ y), the non-dimensional laminar sublayer thickness will be determined by comparing the predicted single-phase pressure drops from this model against those from the Blasius equation for a smooth tube. This non-dimensional thickness is expressed as

where y_δ is the laminar sublayer thickness in m, u^* is the friction velocity ($=(\tau_w/\rho)^{0.5}$) in $m.s^{-2}$ and ν is the kinematic viscosity in $m^2.s^{-1}$. It is assumed to be the same in both single- and two-phase flow.

The velocity distribution is evaluated by integrating Equation (7.14) from $r=(R-y_\delta)$ to $r=R$ for the laminar sublayer flow, and Equation (7.15) from $r=0$ to $r=(R-y_\delta)$ for the turbulent core flow. By assuming constant fluid properties, it is expressed, for laminar sublayer flow, as

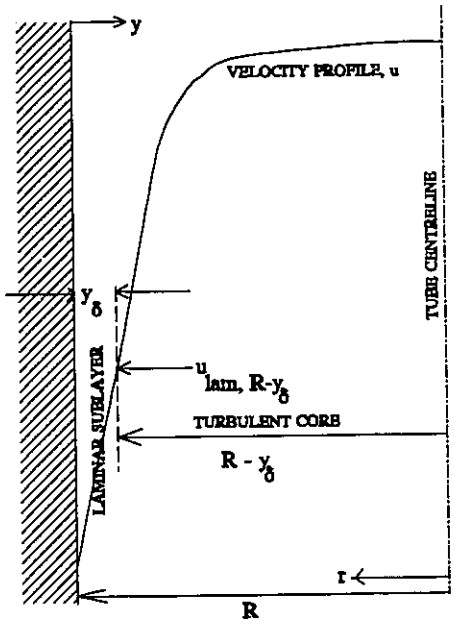

Figure 7.4: Velocity Distribution for Single-Phase Flow in Tubes.

$$y_\delta^+ = \frac{y_\delta\, u^*}{\nu} \tag{7.17}$$

$$u = \int_r^R \frac{\tau}{\mu_l}\, dr = \frac{-1}{2\,\mu_l}\left(\frac{dP}{dz}\right)_f \int_r^R r\, dr$$
$$= \frac{-1}{2\,\mu_l}\left(\frac{dP}{dz}\right)_f \frac{(R^2 - r^2)}{2} \tag{7.18}$$

and, for turbulent core flow, as

$$u = \int_r^{R-y_\delta} \sqrt{\frac{\tau}{\rho_l\, l^2}}\, dr + u_{lam,R-y_\delta}$$
$$= \sqrt{\frac{-1}{2\,\rho_l}\left(\frac{dP}{dz}\right)_f} \int_r^{R-y_\delta} \frac{\sqrt{r}}{l}\, dr + u_{lam,R-y_\delta} \tag{7.19}$$

Since the mixing length (Equation (7.16)) is also a function of radial distance, Equation (7.19) cannot be solved analytically, and is integrated numerically using the trapezoidal rule (see Chapra and Canale [1988] for details of the trapezoidal rule). In brief, the local velocity at any radial location, u_r, is calculated by dividing the distance between the two boundaries (i.e., r and $R-y_\delta$) into a number of sub-divisions. The same local velocity is used for both laminar sublayer and turbulent-core flow at the laminar sublayer thickness (i.e., $r = R-y_\delta$).

As indicated above, an assumed value of frictional pressure gradient is used to initiate the iteration. The convergence criterion (1% difference) is based on a comparison of the predicted and experimental mass fluxes. The predicted mass flux is calculated by multiplying the cross-sectional average velocity with the fluid density, i.e.,

$$G = \frac{2\,\rho_l}{R^2}\int_0^R u\,r\,dr \tag{7.20}$$

As indicated in Section 2.2.4, it has been suggested that different values be used for non-dimensional thicknesses of the laminar sublayer (6.99 and 11.6). To reduce the uncertainty, it has been decided to determine the non-dimensional thickness by comparing the present-model predictions of single-phase pressure drop against the values evaluated using the Blasius Equation. The following steps are used:

1) Assume a value for the non-dimensional thickness of the laminar sublayer.
2) Calculate the pressure drop using the Blasius Equation.
3) Calculate the overall mass flux using the present model.
4) Compare the predicted and experimental mass flux (These procedures are repeated until the two mass fluxes converge).

For a difference of more than 1% in mass flux, the non-dimensional laminar sublayer thickness is adjusted and the procedure is repeated. The calculation is performed for both single-phase

liquid and vapour flow, and the calculated values of non-dimensional laminar sublayer thickness are introduced to the sub-models of two-phase flow.

7.4 MODELLING OF FLOW BOILING

In the present model, the analysis is based primarily on the shear-stress and velocity distributions, as in single-phase flow. It is extended to flow-boiling conditions by including the effects of phase distribution and surface heating on the entrained-liquid fraction. As described in Section 6.4, most studies also use the mixing-length approach in the turbulent two-phase region. Although several studies have introduced modifications to the mixing-length definition, to account for the turbulence-enhancement characteristic of vapour bubbles and turbulence-suppression characteristic of liquid droplets, there is no strong evidence that these characteristics are a dominant factor when the two-phase equivalent properties are used in the analysis. In most cases, these modifications do not provide the correct asymptotic and parametric trends, and hence result in large uncertainties when applied outside their data base. Within the present conditions of interest, the phases tend to be well-mixed in the two-phase region and the homogeneous-flow assumption is probably valid.

The present model analyzes separately the pressure drop in subcooled boiling, bulk boiling, forced-convective evaporation and film boiling. Figure 7.5 illustrates the flow structure in various heat transfer regimes and the anticipated pressure distribution. Among these heat-transfer regimes, the forced-convective evaporation region is the most important, since it is frequently encountered in two-phase equipment. However, it is also the most complex, due to the partially separate (vapour core and liquid film) and partially mixed (vapour and entrained liquid droplets) flow structure. It has been the subject of many extensive investigations (see Chapter 6).

In this model, the basic equations of shear-stress and velocity distributions are similar to those used in single-phase flow. Several flow parameters (such as the laminar sublayer thickness) are

affected by the presence of the two phases. Due to the lack of experimental data for these parameters at the present conditions of interest, derivation of an appropriate modification to these parameters has proven impossible.

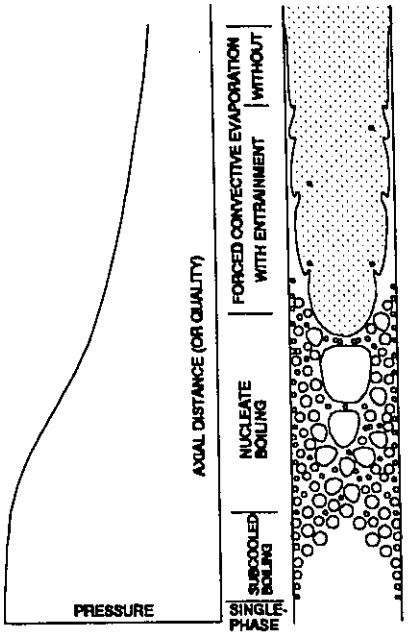

Figure 7.5: Flow Structures of Various Heat-Transfer Regimes at High-Flow Conditions.

The same calculating procedure as in single-phase is therefore used to evaluate the pressure drop, which is also required in the shear-stress equation. A detailed description of the procedure is presented in Section 7.5. In summary, an initial frictional pressure drop is assumed and is introduced into the velocity-gradient equations for various heat-transfer regions. The velocity gradient is then integrated to obtain the velocity distribution, which is in turn integrated to calculate the predicted mass flux. The predicted mass flux has to account for the variation in density; i.e.,

$$G = \frac{2}{R^2} \int_0^R \rho \; u \; r \; dr \tag{7.21}$$

where the density, ρ, represents the liquid or vapour value in single-phase flow and the mixture value in two-phase flow. The estimated frictional pressure gradient is adjusted if the difference between predicted and experimental mass fluxes is more than 1%. The adjustment is based on the following strategy: if the mass flux is overpredicted, the upper-bound value of frictional pressure gradient is replaced with the current estimation; otherwise, the lower bound value is replaced. The overall pressure drop is calculated by adding the pressure drops due to friction,

acceleration and gravity. Chapter 3 describes the equations for pressure drops due to acceleration and gravity.

7.4.1 Subcooled Boiling Flow

In subcooled boiling flow at moderate values of subcooling ($-0.25 < x_{th} < 0$), the flow structure consists of fine bubbles moving in the near-wall region only, and in the single-phase subcooled liquid at the core (see Figure 7.5). In general, the two-phase layer is extended from the heated surface up to a point where fluid achieves the saturation condition, beyond which bubbles will be condensed. This flow pattern is unique to flow boiling and can seldom be encountered in adiabatic flow. The starting point of this boiling region is the point of onset of nucleate boiling (which corresponds generally to conditions where $T_w = T_{sat}$). However, the pressure gradient is not significantly affected until the point of net vapour generation is reached. Therefore, this analysis of subcooled-boiling flow begins at the point of net vapour generation. Prediction of this point has been discussed in Chapter 4.

7.4.1.1 Single-Phase Liquid Core

The analysis for single-phase flow is used at the core where only single-phase liquid is present. It covers the radial locations beyond the thickness of the two-phase bubble layer. For a bubble layer thinner than the laminar sublayer, the single-phase velocity distribution consists of both laminar and turbulent flows, and is represented by Equations (7.18) and (7.19). Otherwise, only the turbulent flows are considered and the velocity distribution is expressed as Equation (7.19).

The thickness of the two-phase bubble layer is the key parameter in the analysis. It is related to the temperature distribution within the fluid, and can be determined by integrating the cross-sectional fluid enthalpy until the local bulk-fluid enthalpy is matched. The local bulk-fluid enthalpy is calculated from

$$H_{fluid} = H_{in} + \frac{Power}{W} \frac{z}{L_{he}} \tag{7.22}$$

where H_{in} is the inlet enthalpy in $J.kg^{-1}$ and W is the mass flow rate in $kg.s^{-1}$. Assuming that, once boiling is initiated, the fluid enthalpy in the core does not vary and is maintained at the same level as the flow at the point of onset of nucleate boiling, H_{ONB}, the bulk-fluid enthalpy can also be approximated to

$$H_{fluid} = \frac{1}{A_F}\left(\alpha A_F H_g + \left((1-\alpha) A_F - \pi (R - \delta_{bub})^2\right) H_f + \pi (R - \delta_{bub})^2 H_{ONB}\right) \tag{7.23}$$

where A_F is the flow area, H_g and H_f are the saturation vapour and liquid enthalpy, respectively, α is the cross-sectional average void fraction, and δ_{bub} is the thickness of the two-phase layer. Re-arranging the above equation, the thickness of the two-phase layer is expressed as

$$\delta_{bub} = R - \sqrt{\frac{A_F (\alpha H_g + (1-\alpha) H_f - H_{fluid})}{\pi (H_f - H_{ONB})}} \tag{7.24}$$

Since the assumption of a constant enthalpy in the core (the same as the flow at the point of onset of nucleate boiling) is probably overly conservative, the thickness of the two-phase layer may be overpredicted.

To simplify further the evaluation process, the thickness of the two-phase layer is assumed to be 0 at the point of onset of nucleate boiling, and reaches the centre of the tube when the thermodynamic quality becomes 0 (see Figure 3.7). For in-between conditions, a linear interpolation is used to determine the thickness; i.e.,

$$\delta_{bub} = \frac{x_{th} - x_{th,ONB}}{0 - x_{th,ONB}} R \tag{7.25}$$

where x_{th} is the thermodynamic quality.

7.4.1.2 Two-Phase Laminar Bubble Layer

The analysis of the bubble layer is similar to that of single-phase flow, but modifications are introduced to account for the presence of two phases. At the near-wall region, a laminar sublayer is assumed and the velocity distribution is calculated with

$$\begin{aligned} u &= \frac{-1}{2\mu_{tp}}\left(\frac{dP}{dz}\right)_f \int_r^R r\, dr \\ &= \frac{-1}{2\mu_{tp}}\left(\frac{dP}{dz}\right)_f \frac{R^2 - r^2}{2} \end{aligned} \tag{7.26}$$

Equation (7.26) is similar to Equation (7.18), except that two-phase viscosity is used. The two-phase viscosity is calculated with (assuming homogeneous flow)

$$\frac{1}{\mu_{tp}} = \frac{x_{bub}}{\mu_g} + \frac{1 - x_{bub}}{\mu_l} \tag{7.27}$$

Due to the high concentration of vapour at the bubbly layer, the local flow quality, x_{bub}, is larger than the cross-sectional flow quality, x_a, predicted by the Kroeger-Zuber correlation (see Section 3.2.1). It is then calculated using

$$x_{bub} = \frac{\alpha_{bub}\ \rho_g}{\rho_f\ (1 - \alpha_{bub}) + \alpha_{bub}\ \rho_g} \tag{7.28}$$

where the local void fraction, α_{bub}, is calculated with

$$\alpha_{bub} = \frac{\alpha\ R^2}{R^2 - (R - \delta_{bub})^2} \tag{7.29}$$

where α is the cross-sectional average void fraction predicted with the Chexal et al. correlation (see Section 3.2.2). As stated in assumption (3), a uniform radial void-fraction distribution is assumed within the two-phase bubble layer.

The thickness of the laminar sublayer in the bubbly layer, on the other hand, is thinner than that of a single-phase liquid, because of the turbulence-enhancement effect of bubbles. Due to the lack of data, the magnitude of this reduction in thickness is unclear, and the single-phase value is assumed to apply.

7.4.1.3 Two-Phase Turbulent Bubble Layer

In the turbulent bubbly layer, the mixing-length approach is also employed to evaluate the shear-stress and velocity distributions. Except in Beattie's work [1972], this approach was not used in previous studies that employed primarily the empirical correlation, the homogeneous-flow model and, recently, the eddy-viscosity approach for adiabatic bubbly flow. The problem of using the empirical correlation was indicated in Chapter 6. The use of the homogeneous-flow model has resulted in some successes in adiabatic bubbly flow, where the homogeneous-flow assumption is valid for most conditions. For low void-fraction conditions where the homogeneous-flow model is invalid, the eddy-viscosity approach has been introduced. However, the eddy viscosity remains empirically based.

The mixing-length approach is selected, because this can provide a smooth transition to the single-phase analysis in the turbulent core. The velocity distribution is expressed as

$$u = \sqrt{\frac{-1}{2\rho_{tp}}\left(\frac{dP}{dz}\right)_f} \int_r^{R-y_{\delta,bub}} \sqrt{\frac{r}{l_{bub}^2}}\, dr + u_{lam,R-y_{\delta,bub}} \tag{7.30}$$

where $y_{\delta,bub}$ is the thickness of the laminar sublayer and l_{bub} is the two-phase mixing length for bubbly flow. As in single-phase flow, this equation is solved numerically using the trapezoid rule. The two-phase density is calculated with the homogeneous-flow assumption and is expressed as

$$\frac{1}{\rho_{tp}} = \frac{x_{bub}}{\rho_g} + \frac{1 - x_{bub}}{\rho_l} \tag{7.31}$$

7.4.1.4 Two-Phase Mixing Length for Bubbly Flow

The use of the mixing-length approach in two-phase bubbly flow may be questioned, due to the presence of an interface boundary between the two phases. However, for a well-mixed bubbly flow having fine bubbles, there is no additional turbulence generated by the gas/vapour phase within the bubbles. Additional turbulence, however, is anticipated in the liquid phase, due to the enhancement effect of the bubbles (primarily caused by the high bubble velocity). The continuity of liquid from the core to the surface allows, therefore, the propagation of eddy fluctuation (which can be accounted for using the mixing-length approach). This approach is expected to become invalid for large bubbles (where internal gas/vapour flow may be present).

The mixing-length approach for two-phase bubbly flow has been used only by Beattie [1972], who expressed the shear stress in bubbly flow as

$$\tau = \rho_l (1 - \alpha) \kappa^2 y^2 \left(\frac{du}{dy}\right)^2 \tag{7.32}$$

Hence, the two-phase mixing length is defined as

$$l_{bub} = (1 - \alpha)^{1/2} \kappa y \tag{7.33}$$

Beattie [1972] indicates that this modification of mixing length provides a good prediction of void fraction in low-pressure air-water flow. However, the $(1-\alpha)^{1/2}$ term appears to correct for the over-estimation of the mixing length in the core region, rather than represent any physical phenomenon. (Beattie used the mixing length definition of κy, which is valid at the near-wall region and overestimates significantly the mixing length at the core.) Based on the two-phase properties, the single-phase mixing length may also be valid for a well-mixed two-phase flow (i.e., no velocity difference between liquid and bubbles and hence no turbulence enhancement). Therefore, no correction of mixing length is introduced in this study.

7.4.1.5 Effect of Bubble Formation on Pressure Gradient

The effect of a bubble layer on pressure gradient has been examined in a number of studies, and has resulted in different conclusions [Bartolomei et al., 1979, Zejgarnik et al., 1983]. Most analyses indicated that this attached-bubble layer increases the relative roughness of the heated surface and hence the pressure gradient. Both Saha and Zuber [1974] and Avdeev [1988] have assumed that the absolute roughness height is similar in magnitude to the bubble diameter. Lu and Jia [1988], on the other hand, suggested that this layer introduces a drag-reducing effect and causes a reduction in pressure gradient. Cumo et al. [1975] observed that a liquid sublayer existed between the bubbly layer and heated surface, except at the bubble-developing locations, for Freon flow inside a rectangular glass channel. This contradicts the fact that a stationary bubbly layer, which acts as surface roughness, is a realistic assumption.

At high pressures and high flows, bubbles tend to be small in size due to the reduced surface tension and efficient heat-transfer rate. If the bubbles remain within the laminar sublayer of the main flow, they will not have any impact on pressure gradient (in analogy to tube roughness as described by Schlichting [1960]). For larger bubbles that protrude into the turbulent sublayer, the following scenarios (depending on the surface-tension force that holds it on the surface, and the dynamic force of free stream that lifts it off) must be considered:

i) At low pressure and low flow conditions (close to stagnation), the surface-tension force dominates. Hence, the bubble remains attached to the surface and the apparent roughness of the surface is increased.
ii) At high pressure and high flow conditions, however, the dynamic force becomes dominant. The bubble is swept into the main stream and condenses. A liquid sublayer, as observed by Cumo et al. [1975], is left between the bubbles and the heated surface. Therefore, there is essentially no increase in apparent roughness at these conditions, and the pressure gradient remains low and similar to that of single-phase flow. The decrease in pressure gradient, as indicated by Lu and Jia [1988], is probably caused by a heating effect similar to that in single-phase flow.

Based on these findings, the effect of bubble formation on pressure gradient in the bubbly region can be assumed to be insignificant, and hence will not be considered in this model.

7.4.1.6 Temperature Gradient

The temperature of the fluid at the heated surface is slightly higher than saturation (super-heated) for bubble formation. It decreases rapidly to the saturation temperature at a short distance from the surface (primarily within the height of the bubble sublayer). At the boundary between two-phase and single-phase flow, the fluid temperature decreases and approaches a fluid temperature similar to the liquid temperature corresponding to the point of onset of nucleate boiling. To simplify the calculation, the thin superheated layer of fluid is ignored and the fluid temperature

is assumed to be maintained at saturation within the two-phase layer but at inlet fluid temperature in the core. Accordingly, the saturated liquid viscosity is used at the two-phase layer, and the liquid viscosity corresponding to the bulk fluid is assumed at the core. The saturated vapour viscosity is used for the vapour phase.

7.4.2 Saturated-Boiling Flow

Saturated-boiling flow begins at the saturation point (i.e., $x_{th} = 0$). It has a similar flow structure to the two-phase bubbly layer in subcooled-boiling flow (see Figure 7.5), and hence can be analyzed using the same procedure:

i) The velocity distribution is expressed as Equation (7.26) for the laminar-sublayer region ($R\text{-}y_{\delta,\,bub} < r < R$), and Equation (7.30) for the turbulent core ($0 < r < R\text{-}y_{\delta,\,bub}$). Two-phase properties are used in the calculations.

ii) The laminar sublayer thickness is assumed to be the same for both single-phase and two-phase flow.

iii) The effect of bubbles on the mixing length is assumed to be negligible. (This region is expected to be small, as the flow changes to annular flow rapidly. Therefore, the size of bubble remains small.)

iv) The effect of attached bubbles at the wall on frictional pressure drop is assumed to be insignificant.

7.4.3 Forced-Convective Evaporation Flow

Forced-convective evaporation is encountered mainly in annular flow, and consists of a two-phase vapour core surrounded by a liquid film. Separate analyses must be introduced for different parts of annular flow. Figure 7.6 illustrates the velocity distribution assumed in the present model.

The most crucial parameter is the entrained liquid fraction, which also controls the CHF phenomenon in flow boiling.

7.4.3.1 Liquid-Film Flow

The liquid film is assumed to consist of single-phase liquid only. This may not be valid at conditions close to the transition point between saturated-boiling and forced-convective evaporation flow, since boiling can still be encountered at the surface. However, the transition region is usually small and this assumption will not have any large impact on the prediction of pressure gradient. Laminar flow is not expected at the present conditions of interest. The velocity distribution in the turbulent liquid-film flow is calculated using the same equations as in single-phase flow (i.e., Equation (7.18) is used for laminar sublayer flow, and Equation (7.19) for turbulent flow).

In general, the thickness of the laminar sublayer flow is calculated with the non-dimensional thickness, y_δ^+, presented for single-phase liquid flow (Equation (7.17)). Abolfadl and Wallis [1985, 1986], however, showed that a thickness criterion based on the Reynolds number ($Re_f = 67$) appears to be more appropriate (see Equation (6.133) in Section 6.4.4). Therefore, the present model uses the maximum thickness of the laminar sublayer calculated between the non-dimensional thickness approach and the Reynolds-number criterion of Abolfadl and Wallis [1986].

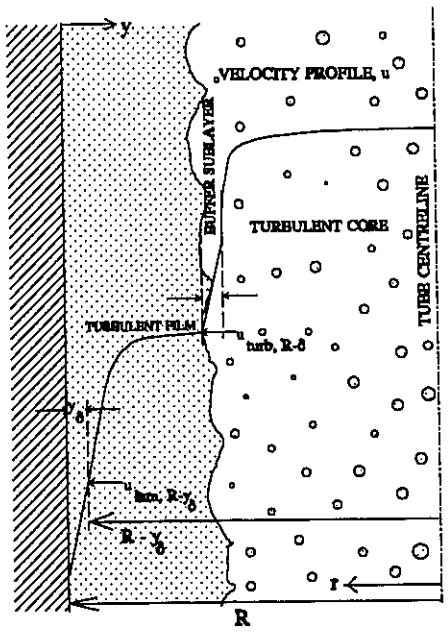

Figure 7.6: Velocity Distribution in Forced Convective Evaporation (Annular Flow).

7.4.3.2 Two-Phase Vapour-Core Flow

The two-phase vapour core consists of a continuous vapour flow and dispersed liquid droplets. It is also separated into two regions: a two-phase buffer zone, which has similar characteristics to the laminar sublayer flow, and a turbulent core (see Figure 7.6). The two-phase buffer zone between the turbulent core and liquid film has been introduced in other models: Levy and Healzer [1981] and Dobran [1983, 1985] considered it as the wavy sublayer between the homogeneous core and liquid film, while Abolfadl and Wallis [1986] treated it as a laminar sublayer of the vapour core flow. In either case, this zone acts as a transition between the liquid film and vapour core, to avoid a steep change in velocity across the liquid/vapour interphase.

Since the flow structure of the two-phase vapour-core flow is the reverse of the two-phase bubbly flow, similar equations of velocity distribution are used (i.e., Equation (7.26) for the (laminar sublayer) two-phase buffer region and Equation (7.30) for the turbulent core). The velocity distribution in the two-phase buffer zone is expressed as

$$\begin{aligned} u &= \frac{-1}{2\,\mu_{core}}\left(\frac{dP}{dz}\right)_f \int_r^R r\,dr + u_{film,\delta_{film}} \\ &= \frac{-1}{2\,\mu_{core}}\left(\frac{dP}{dz}\right)_f \frac{R^2 - r^2}{2} + u_{film,\delta_{film}} \end{aligned} \tag{7.34}$$

and in the turbulent core as

$$u = \sqrt{\frac{-1}{2\,\rho_{core}}\left(\frac{dP}{dz}\right)_f} \int_r^{R-y_{\delta,core}} \sqrt{\frac{r}{l_{drop}^2}}\,dr + u_{buffer,R-y_{\delta,core}} \tag{7.35}$$

The two-phase properties are calculated with a revised void fraction, reflecting only the content within the vapour core. Ignoring the liquid film, the flow quality becomes

$$x_{core} = \frac{x_a}{x_a + (1 - E)(1 - x_a)} \tag{7.36}$$

where E is the entrained liquid fraction (i.e., the fraction of total liquid flow existing as droplets in the vapour core). Assuming no slip between vapour and droplets, the revised void fraction in the core is calculated from

$$\alpha_{core} = \frac{x_{core}\,\rho_f}{x_{core}\,\rho_f + (1 - x_{core})\,\rho_g} \tag{7.37}$$

The mixture density at the core becomes

$$\frac{1}{\rho_{core}} = \frac{x_{core}}{\rho_g} + \frac{1 - x_{core}}{\rho_l} \tag{7.38}$$

and the two-phase viscosity is calculated from

$$\frac{1}{\mu_{core}} = \frac{x_{core}}{\mu_g} + \frac{1 - x_{core}}{\mu_l} \tag{7.39}$$

At the interphase boundary between the liquid film and vapour core, the same velocity is assumed. Due to the difference in velocity gradients, the shear stresses are different at both sides of the interface, and this difference is often referred to as the interfacial shear stress.

7.4.3.3 Mixing Length in Droplet Flow

The single-phase mixing length is often used in the analysis of the droplet flow in the core (e.g., Dobran, [1986]), since a homogeneous flow of mixture is often observed at high flow [Hewitt

et al., 1964, Kirillov et al., 1989]. Support for this approximation comes from the following phenomena:

i) Although an interface is present between vapour and liquid flow, the turbulence fluctuation in the core affects the stability of the interface, which in turn affects also the shear-stress and velocity distribution in the film. Based on this transmission of turbulence fluctuation, the mixing-length approach can be extended from the liquid film to the vapour core.

ii) For annular flow with a thin liquid film (the assumption of most annular-flow analyses), the interface becomes smooth and the transfer of turbulence fluctuation may not be efficient. Since the core consists of a well-mixed droplet flow, the mixing-length approach is valid provided the slip between the vapour and droplets remains small. The interface should be used as the reference point for the mixing length (i.e., ι=0). For a thin liquid film, it approaches the radius of the tube and hence the mixing-length expression becomes the same as the one for single-phase flow. Furthermore, the shear stress at the surface approaches that at the interface.

A number of modified mixing-length expressions were also proposed for droplet flow (see Section 6.4). They were based on the argument that the liquid droplets in a vapour flow tend to decrease the turbulent level and result in a reduction in mixing length. Those expressions developed by Levy [1962, 1966] and Levy and Healzer [1981] were more complex and were based on assumptions with no experimental validation. They were expressed in the form of

$$l_{drop} = \kappa\, y\, (1 - e^{y/F}) \tag{7.40}$$

The damping factor, F, was derived empirically and was presented in graphical form by Levy [1966]. An analytical derivation of this factor was also provided by Levy and Healzer [1981] based on a number of assumptions that were not backed with experimental data (see Section 6.4.1).

Beattie [1972] introduced a modified single-phase mixing length based on the void fraction:

$$l_{drop} = \alpha^{1/2} \kappa y \tag{7.41}$$

Although this was also an assumed function, it resulted in good agreement between predicted and measured void-fraction values in the two-phase vapour core of annular flow. The data were obtained in both adiabatic and boiling flow.

While the above studies have shown some differences in mixing length between single-phase and droplet flow, they were primarily based on the assumption of Prandtl mixing length (i.e., $\iota=\kappa y$). Hence, the modification may serve to compensate for the error introduced by the assumption at the core region (where Prandtl mixing length is invalid).

An empirical mixing length was derived by Abolfadl and Wallis [1986] using experimental data of adiabatic air-water and steam-water flow. It was expressed as

$$l_{drop} = 0.14\ R \left(1 - \left(\frac{r}{R} \right)^2 \right) \tag{7.42}$$

for $-\ln(1-\alpha_{core}) \geq 9$, and

$$l_{drop} = R\ (0.0275 - 0.0125\ ln(1 - \alpha_{core})) \left(1 - \left(\frac{r}{R} \right)^2 \right) \tag{7.43}$$

for $-\ln(1-\alpha_{core}) < 9$. These mixing-length definitions were shown valid for the data base of Abolfadl and Wallis [1986]. However, they also provide an incorrect parametric trend. For a single-phase vapour flow, these equations give a mixing-length constant, κ, of 0.28 at r~R, rather

than 0.4, as observed from experimental data (see Schlichting [1960] for example). Therefore, these equations are not recommended for extrapolation.

Due to the high uncertainty associated with two-phase mixing-length definitions and the lack of an analytical model, the single-phase mixing length is used in the present model (Equation (7.16)). The same approach was used by Skouloudis and Wurtz [1991].

7.4.3.4 Buffer-Zone Thickness in Vapour Core

The buffer-zone thickness in the vapour core is assumed to be the same as the laminar sublayer thickness of single-phase vapour flow for 100% core void fraction. When droplets are entrained into the core, this thickness will be reduced, due to the droplet interaction with the flow. The actual magnitude, however, is difficult to estimate. For a rough interface, the buffer-zone may not be present (i.e., thickness becomes zero). To provide a correct transition to single-phase vapour flow, the laminar-sublayer thickness for the vapour flow is used.

7.4.3.5 Liquid-Entrainment Fraction

One of the most crucial parameters in analyzing annular flow is the amount of liquid entrained into the vapour flow (entrained-liquid fraction) [Manzano-Ruiz, 1988 and Adeniji-Fashola et al., 1986]. Until now, no analytical solution has been available in predicting the entrained-liquid fraction, which relies primarily on the empirical expression (e.g., Ueda [1967a], Hutchinson and Whalley [1973]). Due to the high uncertainty, several models employed experimental data of entrained-liquid fraction as an input parameter when comparing predicted and experimental pressure gradients [Abolfadl and Wallis, 1985 and 1986, Skouloudis and Wurtz, 1991]. This approach is unrealistic, since this fraction will be an unknown factor in the actual application of these models.

A graphical technique, first introduced by Hutchinson and Whalley [1973], was modified by Whalley and Hewitt [1978] with a much wider data base (including several data of high-pressure steam-water flow). The entrainment flux is presented in terms of two-dimensional parameters that are functions of the interfacial shear stress and the film thickness. Since both the interfacial shear stress and the film thickness have to be predicted from the model, this method is difficult to apply. The dimensional parameters may restrict the method's application to the conditions of the data base.

Recently, Ishii and Mishima [1982] derived a correlation for entrained-liquid fraction with a relatively large amount of low-pressure air-water data. Their correlation was based on a force balance at the crest of roll waves, which are the dominant mechanism at most conditions. (Various mechanisms for liquid entrainment have been presented in Ishii [1982]). The entrained liquid fraction, E, is expressed in terms of a correlating parameter, η, and is written as

$$E = \tanh\left(7.25 \times 10^{-7}\ \eta\right) = \tanh\left(7.25 \times 10^{-7}\ We^{1.25}\ Re_f^{0.25}\right) \tag{7.44}$$

$$We = \frac{\rho_g\, j_g^2\, D}{\sigma}\left(\frac{\Delta\rho}{\rho_g}\right)^{1/3} \tag{7.45}$$

$$Re_f = \frac{\rho_f\, j_f\, D}{\mu_f} \tag{7.46}$$

where j_f and j_g are the superficial liquid and gas velocities, respectively. Figure 7.7 shows the comparison between correlation predictions and experimental data. This correlation was used in other analytical studies in the absence of experimental data for the entrained-liquid fraction [Skouloudis and Wurtz, 1991, Manzano-Ruiz, 1988]. It appeared to be valid for the high-pressure, low-flow data of Kirillov et al. [Skouloudis and Wurtz, 1991]. On the other hand, Manzano-Ruiz [1988] showed that this correlation was not applicable for horizontal air-water flow.

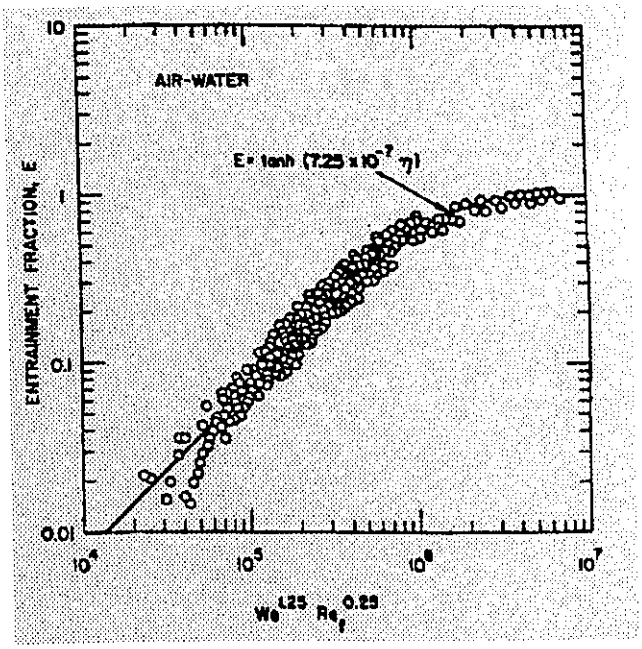

Figure 7.7: Comparison of Ishii-Mishima Correlation with Low-Pressure Air-Water Data [Ishii and Mishima, 1982].

While the number of data for the entrained liquid fraction is scarce at high-pressure conditions, several tests were performed to measure the liquid film thickness by extracting the liquid film using a short porous section. The entrained liquid fraction can be calculated using

$$E = 1 - F \tag{7.47}$$

where F is the fraction of liquid flow travelling in the liquid film. Keeys et al. [1970] focused mainly on the low-flow conditions of pressure 3.5 and 7 MPa. Subbotin et al. [1975] and Nigmatulin et al. [1977] covered a slightly wider range of conditions (mass fluxes of 0.5 to 4 $Mg.m^{-2}.s^{-1}$ and pressures of 1 to 9.8 MPa). While the trends of entrained liquid fraction with respect to various flow parameters were the same in both air-water and steam-water flow at high and low pressures, the variations and the magnitude of the fraction are different. Figure 7.8 shows the differences in entrained fraction between the experimental data and the predictions of the Ishii-Mishima correlation at 7 MPa. (This comparison is presented as an illustration and should not be viewed as discrediting the Ishii-Mishima correlation, which performs well for low-

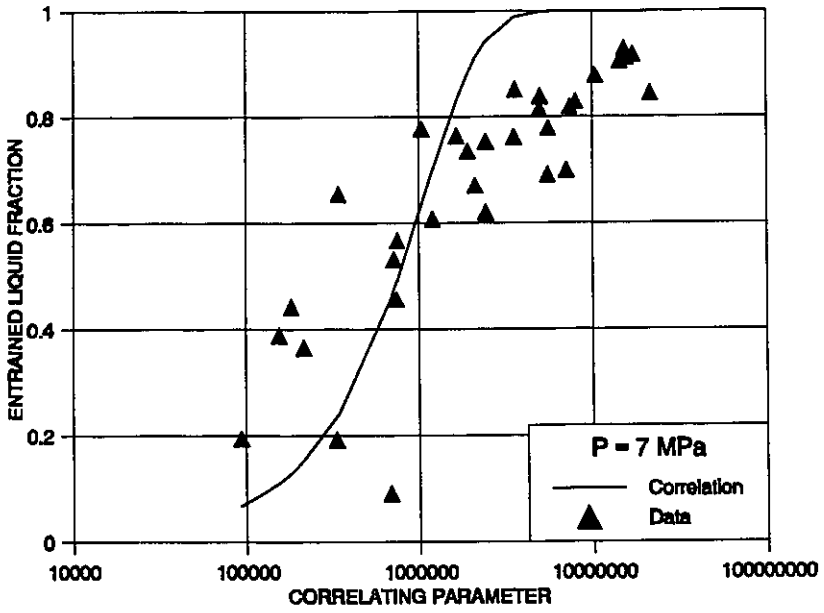

Figure 7.8: Comparison of the Ishii-Mishima Correlation with High-Pressure Steam-Water Data.

pressure air-water flow.) The data are generally underpredicted at small Ishii-Mishima correlating parameters η but overpredicted at large η. This is probably caused by the differences in the liquid-entrainment mechanism between two fluid mixtures. While the shearing-off of the crest of roll waves is the primary mechanism of liquid entrainment in low-pressure air-water flow, the undercutting of surface waves is perhaps a more dominant factor in high-pressure steam-water flow.

Due to the insufficient amount of data, no correlation has been derived for predicting the entrained liquid fraction for high-pressure steam-water flow. This study attempts to correlate the available data for use in the present model, since the Ishii-Mishima correlation is clearly invalid over the conditions of interest. Based on the data of Keeys et al. [1970], Subbotin et al. [1975] and Nigmatulin et al. [1977], a new correlation is optimized in this study for the liquid-film fraction

$$F = 1 - x_a^{\exp(-A_1)} \tag{7.48}$$

where the correlating parameter, A_1, is defined as

$$A_1 = 3.27 x 10^{-6} Re_{tp} \left(1 + \left(\frac{\log(P) - \log(5)}{\log(P_{cr}) - \log(5)} \right)^2 \right)$$

and the two-phase Reynolds number is expressed as

$$Re_{tp} = \frac{G D}{\mu_{tp}} \tag{7.50}$$

Both the pressure, P, and the critical pressure, P_{cr}, are expressed in MPa. Figure 7.9 compares some experimental data and this correlation. Although large differences can be observed at low-flow conditions, this correlation represents a significant improvement over the use of correlations derived using low-pressure data (see Figure 7.8).

The entrained liquid flow rate in annular flow is affected strongly by the heating effect. Figure 7.10 [Bennett et al., 1966] shows that it is much less than the equilibrium value at low qualities. A maximum point is exhibited when the entrained liquid flow rate in flow boiling coincides with the equilibrium value. Beyond this point, the entrained liquid flow rate is reduced and becomes higher than the equilibrium value. Hewitt [1978] noted that there is no prediction method available to account for the heating effect on the entrained liquid flow rate.

Recently, Milashenko et al. [1989] showed a linear relationship between entrainment and heat flux (Figure 7.11). Unlike the data of Bennett et al. [1966], the entrained-liquid fraction in a heated channel was shown to be the same as or higher than that at the equilibrium conditions. Furthermore, no effect of mass flow rate on the entrainment rate was observed. As indicated by Milashenko et al. [1989], this was mainly due to the limited range of mass flow rate covered in their study. They proposed an empirical correlation for predicting the entrained fraction in a heated annular flow. The entrained liquid mass flux, E_t, is expressed in terms of a non-

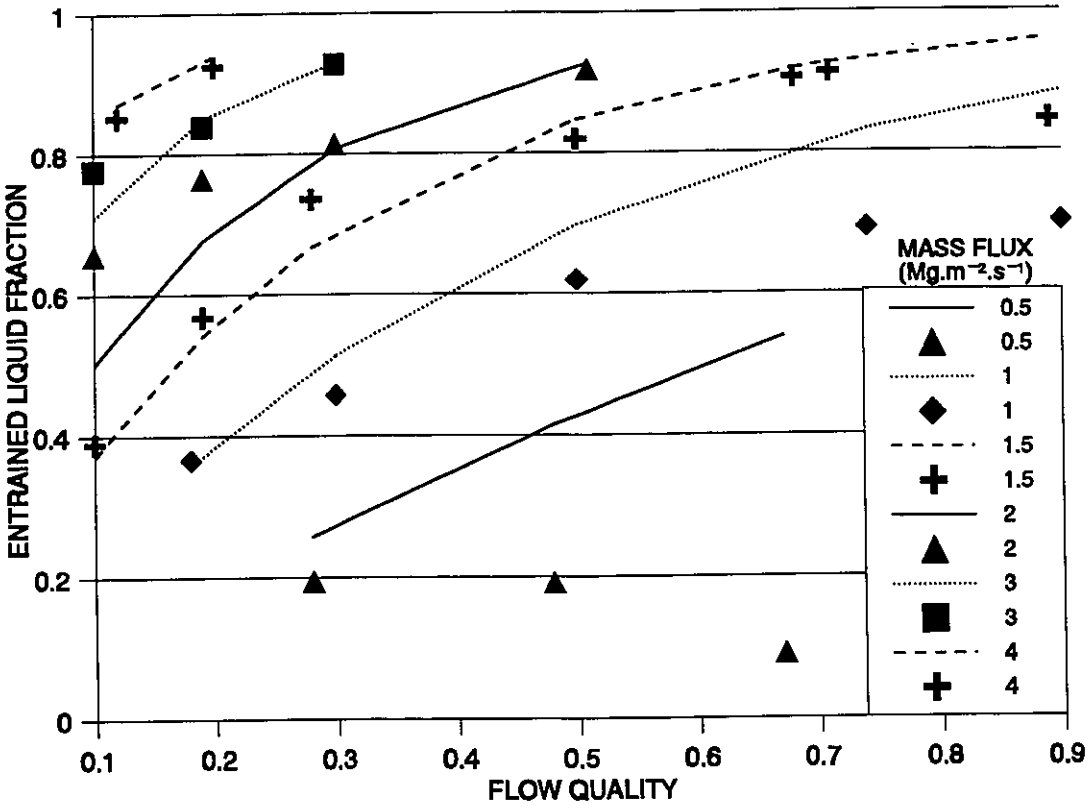

Figure 7.9: Comparison of Proposed Correlation with Some High-Pressure Steam-Water Experimental Data.

dimensional parameter,

$$E_t^+ = \frac{E_t\,(\pi\,D)^2}{W_{lf}} = 1.75\left(\frac{q}{1\,000\,000}\,\frac{\rho_g}{\rho_f}\right)^{1.3} \tag{7.51}$$

where q is the heat flux in $W.m^{-2}$ and W_{lf} is the average liquid-film flow rate in $kg.s^{-1}$. Note that the constant 1.75 is dimensional (in $m^{2.6}.W^{-1.3}$).

Kirillov et al. [1989] also presented an empirical correlation for predicting the liquid-film fraction (i.e., G_{film}/G_l) in boiling annular flow. This correlation is expressed as

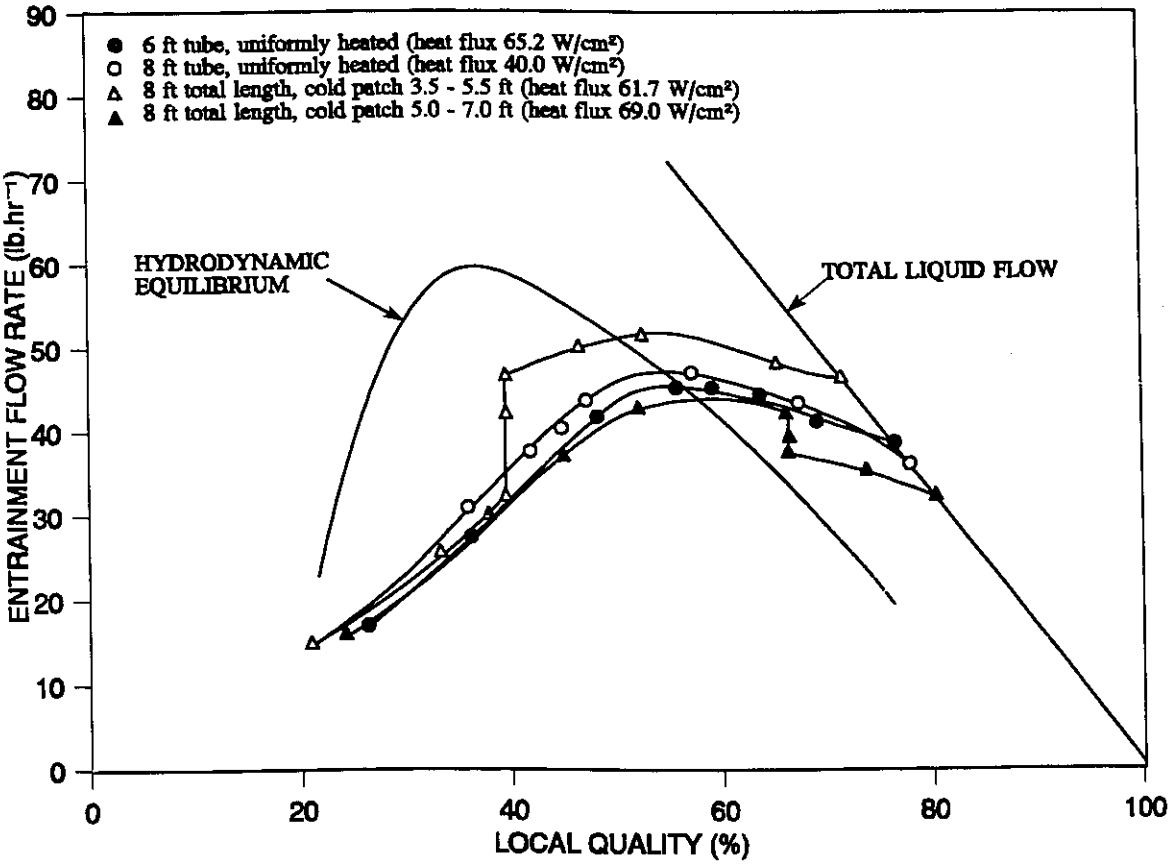

Figure 7.10: Effect of Surface Heating on Entrained Liquid Flow [Bennett et al., 1966].

$$F = 2\,\frac{\delta_{cr}}{D} \tag{7.52}$$

The wave-crest height, δ_{cr}, is defined as

$$\delta_{cr} = C_1\,(C_2 - x)^k \tag{7.53}$$

where

$$C_1 = 0.001\,(0.7 + 2.1\,(0.01\,P - 1.05)^2)\,(0.01\,G)^{0.0179\,p}\,(1 + 200\,q\,((0.01\,p - 0.4)^2 - (0.01\,p - 0.4)^3))^{0.33} \tag{7.54}$$

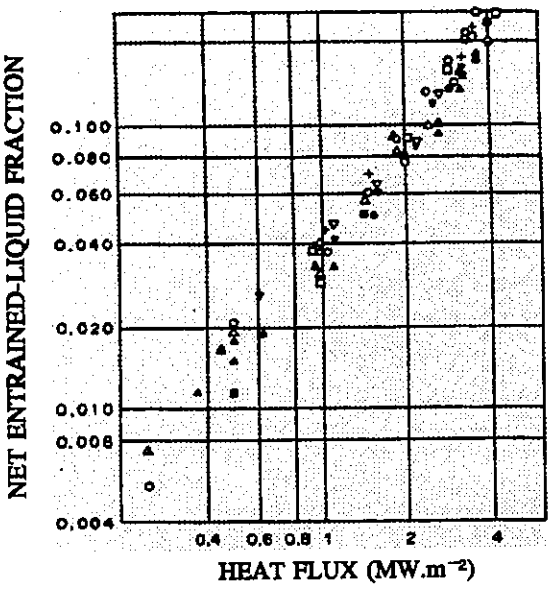

Figure 7.11: Relation Between Entrained Liquid Fraction and Heat Flux [Milashenko et al., 1989].

$$C_2 = \left(0.47 - (1 - 0.01\,p)^2 + \frac{1}{1 + (0.01\,p)^4} \right) \left(\frac{5}{0.01\,G} \right)^{0.00711\,p} - ((0.0015\,q)(1.4 - 0.01\,p))^{0.33} \tag{7.55}$$

$$k = 4.3\ (1\ -\ 0.0044\,p) \tag{7.56}$$

No unit was provided for pressure, mass flux and heat flux. Hence, the correlation cannot be applied.

In view of the strong effect of surface heating on the entrained liquid fraction, a new correlation is derived in this study, using the limited data of Milashenko et al. [1989], since the existing correlation is incapable of predicting the parameter. Unlike other studies correlating either the total entrainment fraction or the net liquid-film fraction, the liquid film fraction in flow boiling is related to the equilibrium liquid film fraction in adiabatic flow, F_{adia}, (as predicted using

Equation (7.48)). Various correlating parameters were tested and the product of the Boiling and Peclet numbers appears to provide a reasonable correlation, which is expressed as

$$F_{boil} = F_{adia} \cos(0.005335\ Bo\ Pe) \tag{7.57}$$

The Boiling and Peclet numbers are defined as

$$Bo = \frac{q}{G\ h_{fg}} \tag{7.58}$$

$$Pe = \frac{G\ D\ C_{pf}}{k_f} \tag{7.59}$$

where k_f is the thermal conductivity of the liquid. Figure 7.12 compares the experimental data and the predictions. The fluctuation at low qualities is caused by a variation in heat flux. Due to the large scattering among the data, this correlation provides only a general trend. Modification is required to improve the prediction accuracy. Furthermore, this equation should be limited to conditions where the cosine term is less than $\pi/2$.

7.4.3.6 Droplet-Deposition Fraction

The droplet deposition fraction accounts for the amount of droplets deposited back to the liquid film from the core. It is primarily a function of the droplet concentration, and is significant in adiabatic flow. At equilibrium conditions, the rate of deposition equals the rate of entrainment.

In a heated channel, however, Doroschuk and Levitan [1971] employed a salt-tracing method and showed that droplet deposition is insignificant. Their finding was questioned by Hewitt [1978], who suggested that the disappearance of salt content in the liquid film was caused by an intense nucleate-boiling phenomena at the dryout point. The salt deposited from the core to the film was

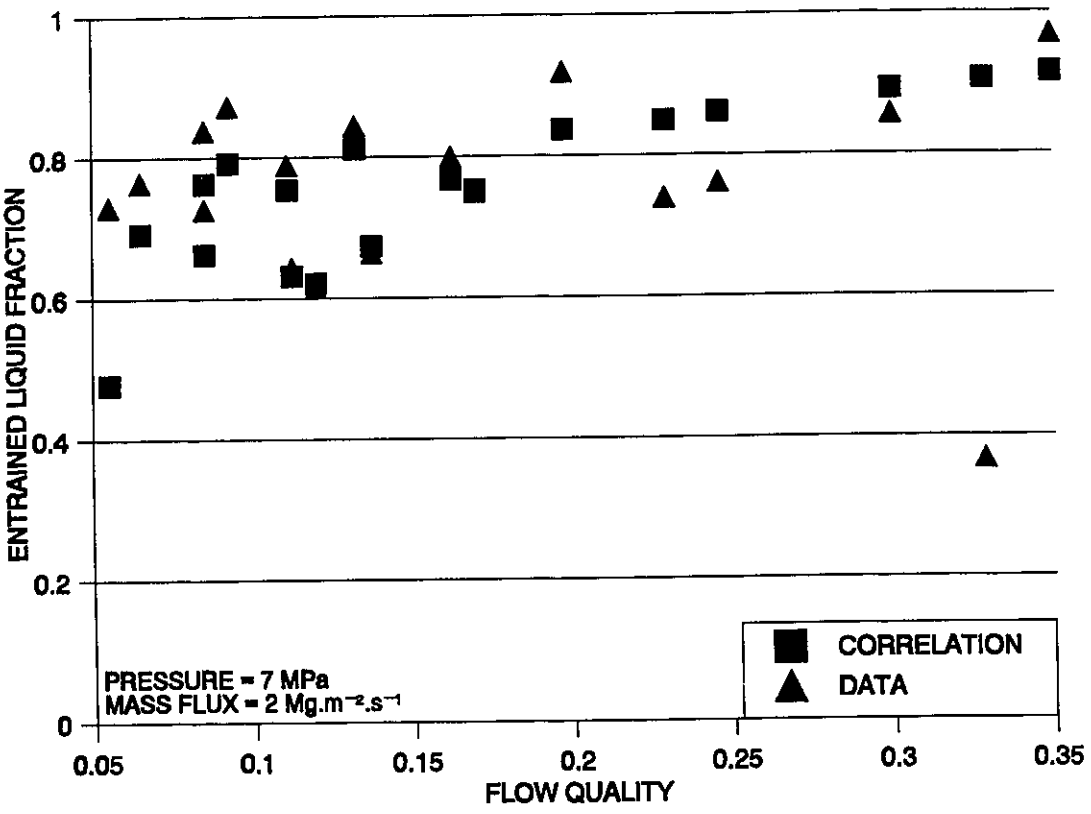

Figure 7.12: Comparison of Proposed Correlation with Experimental Data of Boiling Annular Flow.

ejected back to the core, and hence could not be traced. More experimental data, however, were recently available in support of the argument of insignificant droplet deposition in boiling annular flow [Kirillov et al., 1989]. Since droplet-deposition rate is not available from experiments, it is often assumed to be negligible in flow-boiling analysis anyway [Milashenko et al., 1989]. This assumption of no droplet deposition fraction is also used in this model, based on the following arguments:

i) a net vapour thrust is encountered at the liquid-film/vapour-core interface, due to vaporization, and tends to push the droplets away from the interface,

ii) a transverse force towards the core is experienced by the droplets, due to the velocity gradient in the core flow.

However, this assumption should be limited to the range of conditions covered in this study, since droplet-deposition may become significant at high qualities (greater than 60%).

7.4.4 Dispersed-Droplet Flow

Dispersed-droplet flow is encountered at conditions beyond dryout. Unlike the flow patterns described in previous sections, it has the distinct characteristic of a dry wall (i.e., only vapour/surface contact). Since the dynamic viscosity is much smaller for vapour than for liquid, the pressure gradient is consequently lower in the dispersed droplets flow than the others. On the other hand, a large number of droplets are anticipated to be travelling in the core. While droplet impingement on the heated surface is possible, it is only a small component, as shown in previous studies on post-dryout heat transfer.

The flow structure in dispersed-droplet flow can be viewed as a reverse of the bubbly flow pattern in saturated-flow boiling, except perhaps at the near-wall region: that is, vapour in place of liquid and droplets in place of bubbles. There is no counterpart for the attached bubbles, except perhaps in the transition-boiling region, where liquid wets the surface intermittently.

Until now, only Beattie has analyzed the pressure gradient for dispersed-droplet flow by introducing a special two-phase viscosity into the friction-factor calculation [Beattie, 1973, 1974, 1977, Beattie and Whalley, 1982]. Others simply employed the homogeneous model or the calculation of single-phase vapour flow, neglecting the presence of droplets. While the Beattie correlation has been shown to predict the experimental data well [Kohler and Kastner, 1987], the changing of correlations at the dryout point (from forced-convective evaporation to dispersed-flow film boiling) introduces a discontinuity in the prediction. It is the purpose of this model

to introduce a smooth transition in predicting the pressure gradient from forced-convective evaporation to dispersed-flow film boiling.

7.4.4.1 Velocity Gradient

The same equations used in analyzing the vapour core in forced convective evaporation are extended to dispersed-droplet flow. However, the buffer zone as defined in the vapour core of annular flow is replaced by the laminar-sublayer region. Due to the high surface temperature, droplets are not anticipated in the laminar-sublayer region (neglecting liquid-droplet impingement onto the surface). A single-phase vapour flow is assumed and the velocity gradient is calculated from

$$u = \frac{-1}{2\mu_g}\left(\frac{dP}{dz}\right)_f \int_r^R r\,dr = \frac{-1}{2\mu_g}\left(\frac{dP}{dz}\right)_f \frac{R^2 - r^2}{2} \tag{7.60}$$

In the turbulent two-phase core region, the two-phase density is used and the velocity gradient is expressed as

$$u = \sqrt{\frac{-1}{2\rho_{core}}\left(\frac{dP}{dz}\right)_f} \int_r^{R-y_\delta} \sqrt{\frac{r}{l_{core}^2}}\,dr + u_{lam,R-y_\delta} \tag{7.61}$$

Similar to single-phase flow, the two-phase mixing length is also assumed to be a function of radial distance only (Equation (7.16)).

7.4.4.2 Temperature Gradient

Similar to single-phase flow, the velocity gradient is affected by a large temperature difference between the surface and fluid. Unlike liquid flow, a high surface temperature results in a reduction in the velocity gradient, since the vapour viscosity increases with vapour temperature. This effect, however, is not so distinct, because of a large scatter among experimental data, due to the severe test conditions. The same correction factor to the adiabatic friction factor as in liquid flow is suggested (i.e., Equation (7.9)). A range of exponent values (from -0.1 to -0.52) have been recommended for a turbulent gas flow inside heated tubes [Kakac, 1987].

The effect of fluid-temperature variation on pressure drop in droplet flow is not modelled. Instead, the empirical correction (Equation (7.9)), based on the viscosity ratio, is used to modify the pressure-drop prediction of this model to reflect the difference. A value of 0.1 (as recommended by Petukhov [1970]) is used as the exponent.

7.5 EVALUATION SCHEME

The overall pressure drop along the test section is obtained by calculating separately the pressure drops due to friction, acceleration and gravity over small sub-segments. Only the pressure drop due to friction is calculated with the present model in both single-phase and two-phase flows. A simplified approach (based on a separated-flow model) is used to determine the pressure drops due to acceleration (Sections 2.3.2 and 3.4.2) and gravity (Sections 2.3.3 and 3.4.3).

7.5.1 General Setup

In the present comparison, the test section is divided into 100 segments (or control volumes), with every 20 segments covering each measuring station of the channel in the experiment. Based

on the inlet-flow conditions (i.e., pressure, mass flow rate and fluid temperature), the evaluation is carried out for each segment and continues toward the outlet of the test section. Figure 7.13 shows the flow diagram of the overall setup of this analysis.

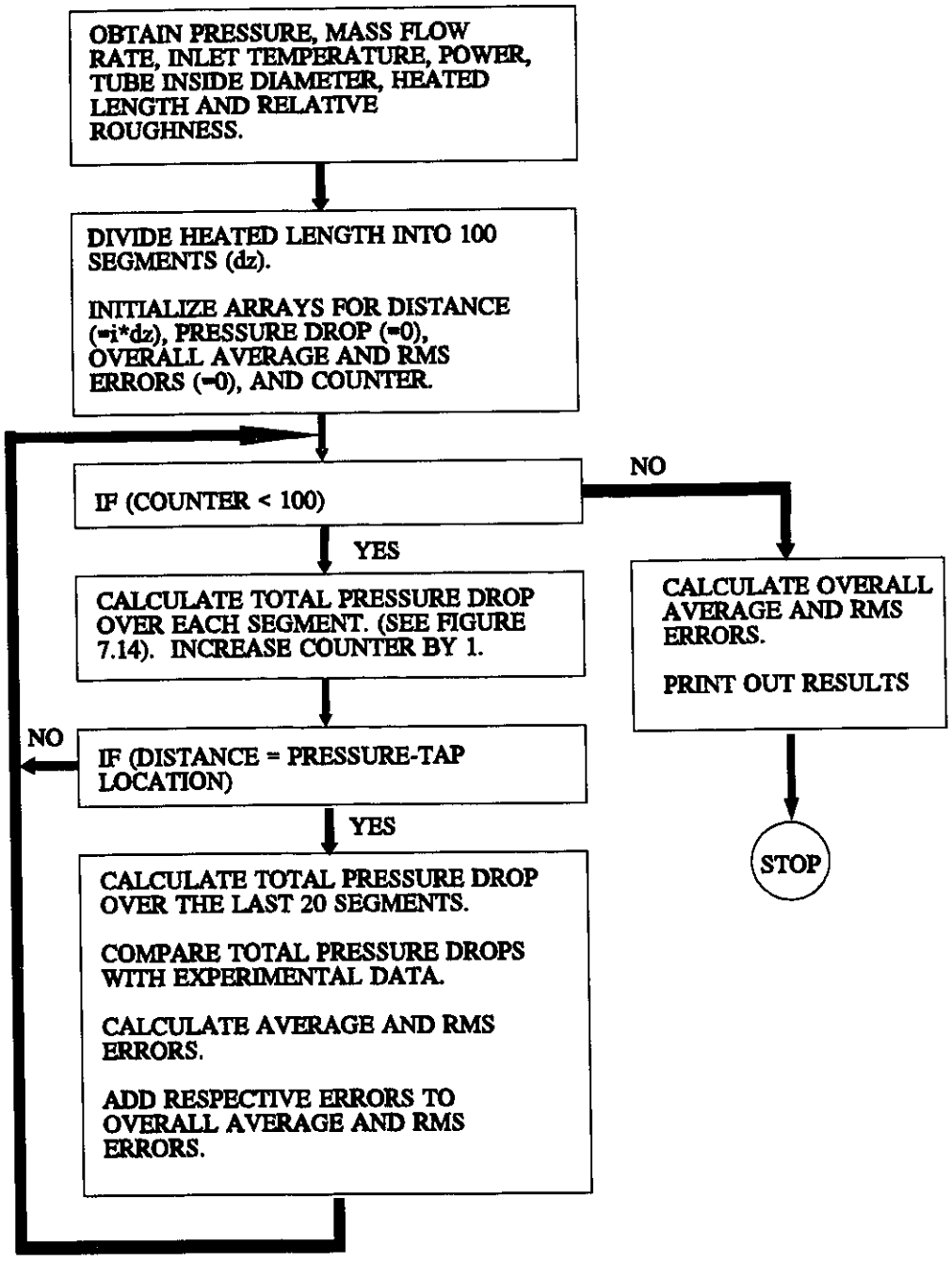

Figure 7.13: General Setup for Present Analysis.

7.5.2 Control Volume Calculations

In each control volume, the upstream pressure is used to evaluate the fluid properties. Based on a heat balance, the thermodynamic quality is calculated for the downstream end. The average fluid properties and two-phase parameters are then calculated. Depending on the flow conditions, the flow-pattern transition is evaluated. The transition from single-phase liquid flow to subcooled boiling is determined with the onset of net vapour-generation criterion. Saturated boiling is assumed when the thermodynamic quality reaches 0. The transition from saturated boiling to forced convective evaporation (i.e., from bubbly to annular flow) is based on the criterion displayed in the Hewitt and Roberts flow-regime map (at a vapour momentum flux, $\rho_g j_g^2$, of 100). The critical heat flux is used to determine whether forced convective evaporation or the dispersed-flow film boiling is encountered inside the control volume. After determining the heat-transfer regime, the appropriate sub-model is used to calculate the frictional pressure drop. The downstream pressure of each control volume is calculated by subtracting the pressure drops due to friction (from the model), acceleration and gravity from the upstream pressure, and in turn is used as the upstream pressure for the subsequent control volume.

For flow boiling, both the single- and two-phase frictional pressure drops are calculated with the present model (using different sub-models). The ratio of these two calculated frictional pressure drops (the two-phase multiplier) is determined. Since the present model is derived for a smooth tube, a modification is introduced for calculating the frictional pressure drop corresponding to the relative roughness of the test section. Assuming the same two-phase multiplier for both smooth and rough tubes (this may result in a slight overprediction of two-phase multiplier in a rough tube), the two-phase frictional pressure drop in the present test section is calculated by multiplying the two-phase multiplier with the empirical single-phase pressure drop. The empirical single-phase pressure drop is evaluated with the D'Arcy-Weisbach equation (Equation (2.37)) using the optimized friction factor from single-phase data. Figure 7.14 shows the flow diagram of the calculation procedure for each control volume.

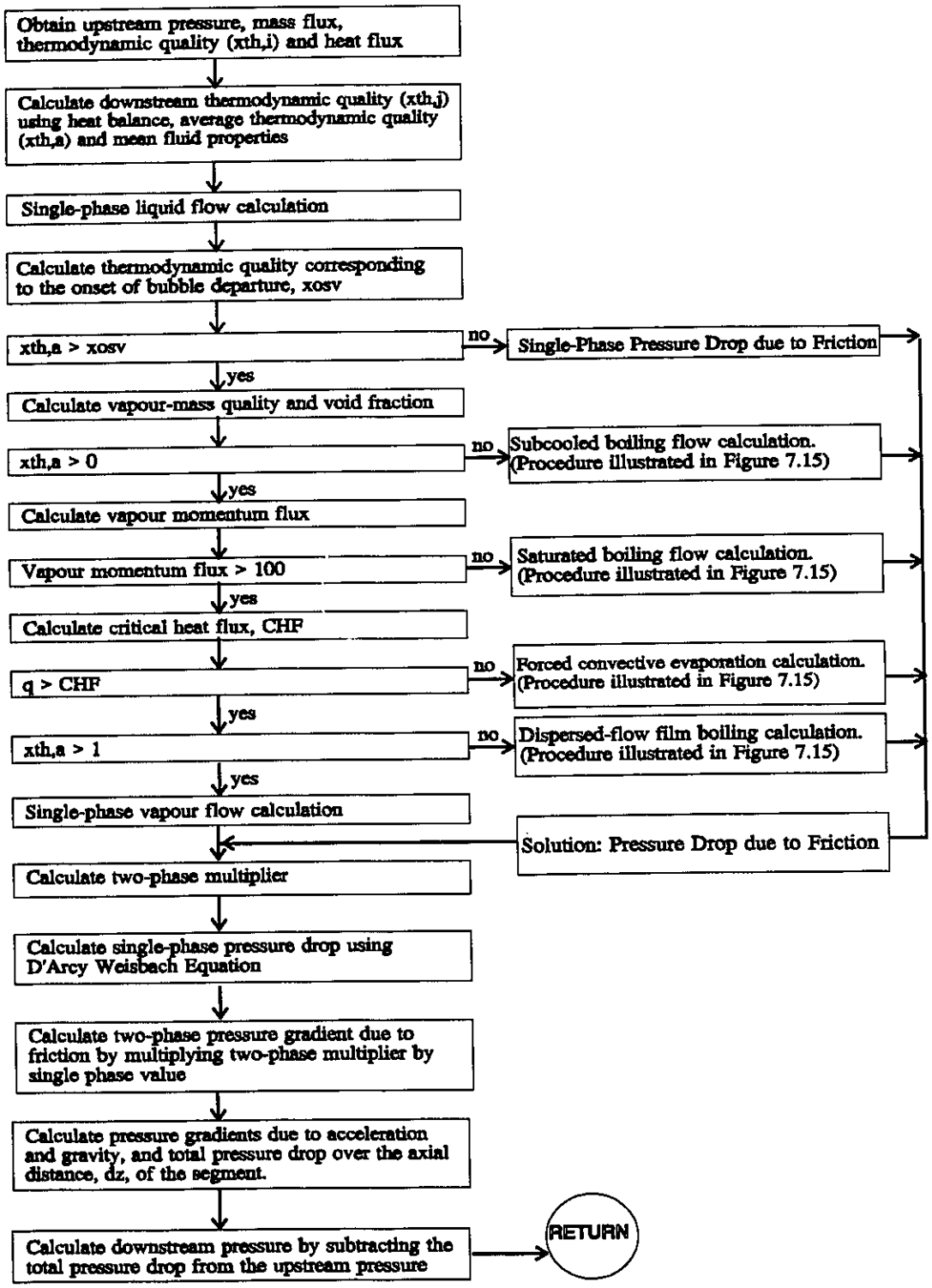

Figure 7.14: Solution Scheme for Calculating Pressure Drop Across Each Control Volume.

7.5.3 Sub-Model Calculations

In each sub-model, the calculation is initiated by assuming two boundary values of frictional pressure gradient (i.e., $(dP/dz)_{f,\,min}$ and $(dP/dz)_{f,\,max}$). In the present analysis, the minimum value $(dP/dz)_{f,\,min}$ is taken as the sum of the pressure gradient due to gravity and acceleration (i.e., $(dP/dz)_a + (dP/dz)_g$), and the maximum value $(dP/dz)_{f,\,max}$ is based on twice the pressure gradient due to friction as predicted by a correlation (i.e., $2x(dP/dz)_{f,\,corr.}$). The Blasius equation is used for single-phase flow and the Friedel correlation [1979] is used for two-phase flow. (The selection of correlation is not crucial, provided it gives an upper bound of the anticipated pressure drop.) The iteration is performed with the bi-sectional method (i.e., $(dP/dz)_{f,\,pred.} = \frac{1}{2}(dP/dz)_{f,\,max} + \frac{1}{2}(dP/dz)_{f,\,min}$).

Using the assumed frictional pressure drop, the velocity distribution is determined by integrating the velocity gradient over a radial distance. The integration is carried out analytically at the laminar-sublayer region (e.g., Equation (7.18)), but numerically at the turbulent-core region (e.g., Equation (7.19)). While a number of numerical-integration techniques are available (see for example, Chapra and Canale [1988] for details), the trapezoidal rule is used in this study for simplicity. Across the flow area, the laminar-sublayer thickness is divided into 20 sub-rings and the turbulent region is divided into 60 sub-rings. The integration procedure using the trapezoidal rule is similar for all sub-models, and is illustrated below for the single-phase liquid flow.

The local velocity at the heated surface (r = R) is initialized as 0 (no-slip conditions). Based on the radial distance (r), the local velocity (u(r)) is calculated with Equation (7.18) for each sub-ring within the laminar sublayer. The same local velocity is assumed at the laminar-sublayer/turbulent-core interface. In the turbulent-core region, the radial distance (dr) between two neighbouring sub-rings (i and i+1) are further sub-divided into 20 sections of distance δr. To calculate the local velocity in each sub-ring, Equation 7.19 is re-formulated into

$$u_{i+1} = u_i + \sqrt{\frac{-1}{2\rho_l}\left(\frac{dP}{dz}\right)_f} \sum_{j=1}^{20} \left(\frac{\sqrt{r_{j-1}}}{0.14R\left(1 - \left(\frac{r_{j-1}}{R}\right)^3\right)} + \frac{\sqrt{r_j}}{0.14R\left(1 - \left(\frac{r_j}{R}\right)^3\right)} \right) \frac{\delta r}{2} \tag{7.62}$$

The velocity distribution is then multiplied by the density and integrated over the flow area to obtain the mass flux (Equation (7.20)). If convergence is achieved when compared with the measured mass flux, the solution is returned to the control-volume calculation. According to the predicted mass flux, the boundaries are adjusted with the following strategy: the maximum pressure gradient is replaced with the average value (i.e., $(dP/dz)_{f,\,pred.}$) if the calculated mass flux is larger than the measured mass flux; otherwise, the minimum pressure gradient is reset. Figure 7.15 shows the flow diagram for the evaluation process in each sub-model.

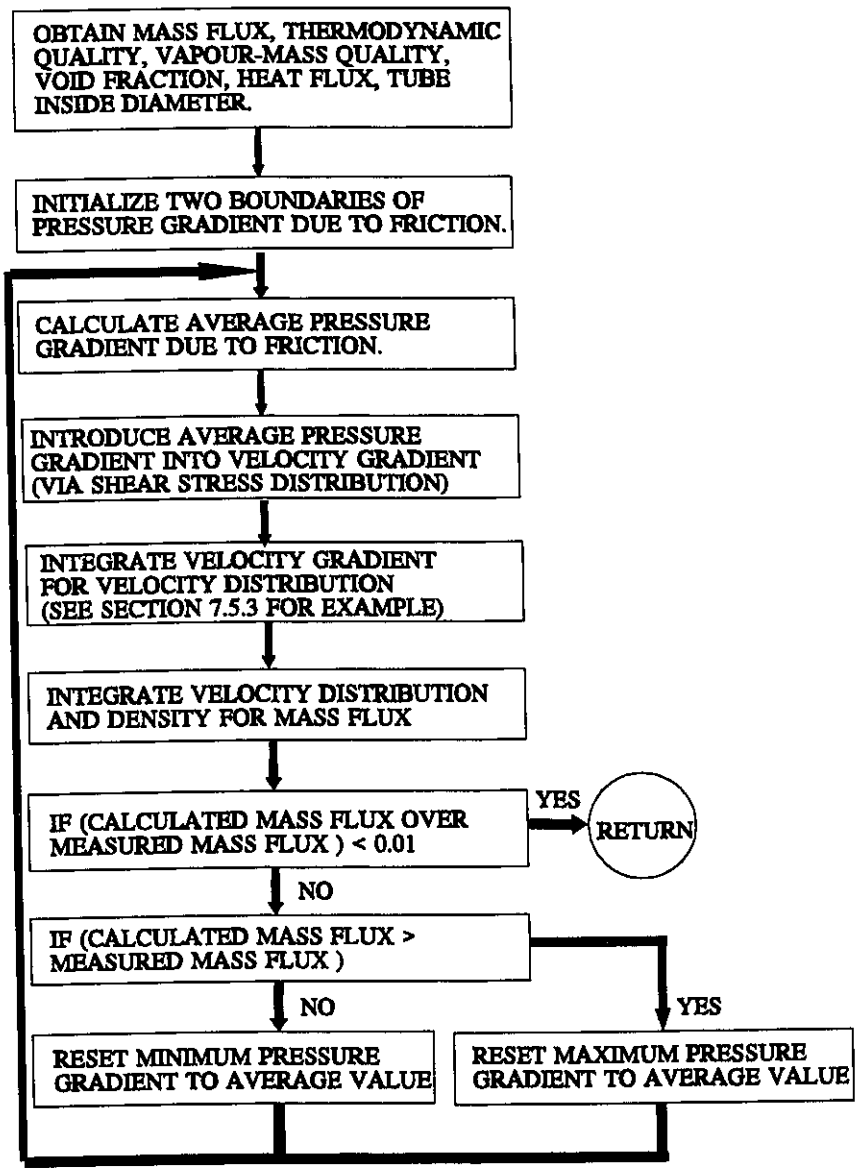

Figure 7.15: Evaluation Procedure in Each Sub-Model.

8. EXPERIMENTAL STUDY

To obtain pressure-drop data for validating the model, an experiment was performed with a heated vertical tube cooled by an upward flow of water. The use of a simple tube geometry in vertical orientation avoided any asymmetric effects of geometry and flow pattern on pressure drop. While the test focused mainly on high-pressure conditions, it covered wide ranges of mass fluxes, inlet subcoolings and heat fluxes.

The test facility for the present experiment is described in Section 8.1. Section 8.2 provides the details of the test section. The data-acquisition system is briefly introduced in Section 8.3, and the test conditions are given in Section 8.4. A description of the experimental procedure is presented in Section 8.5. Several observations made during the test are provided in Section 8.6. The setup of the data base and data correction are shown in Section 8.7, and the calculation of several flow parameters are presented in Section 8.8.

8.1 TEST FACILITY

The experiment was carried out in the high-pressure steam-water test facility (the MR-1 FLARE Loop) at the Chalk River Laboratories. A schematic diagram of the facility, which includes the main flow circuit and the control loops, is shown in Figure 8.1.

The main flow loop consists of two boilers, a condenser, two circulating pumps, a pre-heater and a super-heater. Its system pressure is maintained by the boiler. Water is circulated through the loop by two pumps connected in series. The flow rate is adjusted using the flow-control valves, and is measured with three orifice plates of different calibrated ranges of applications. Pressure drop over each orifice plate is measured using a calibrated Rosemount differential-pressure (DP) cell. The orifice plates cover the low, medium and high ranges of flow rates. A small overlap in ranges is introduced between the orifices, for confirmation purposes. The temperature of the fluid before the orifice plate was measured using a resistance-temperature device (RTD). A pre-

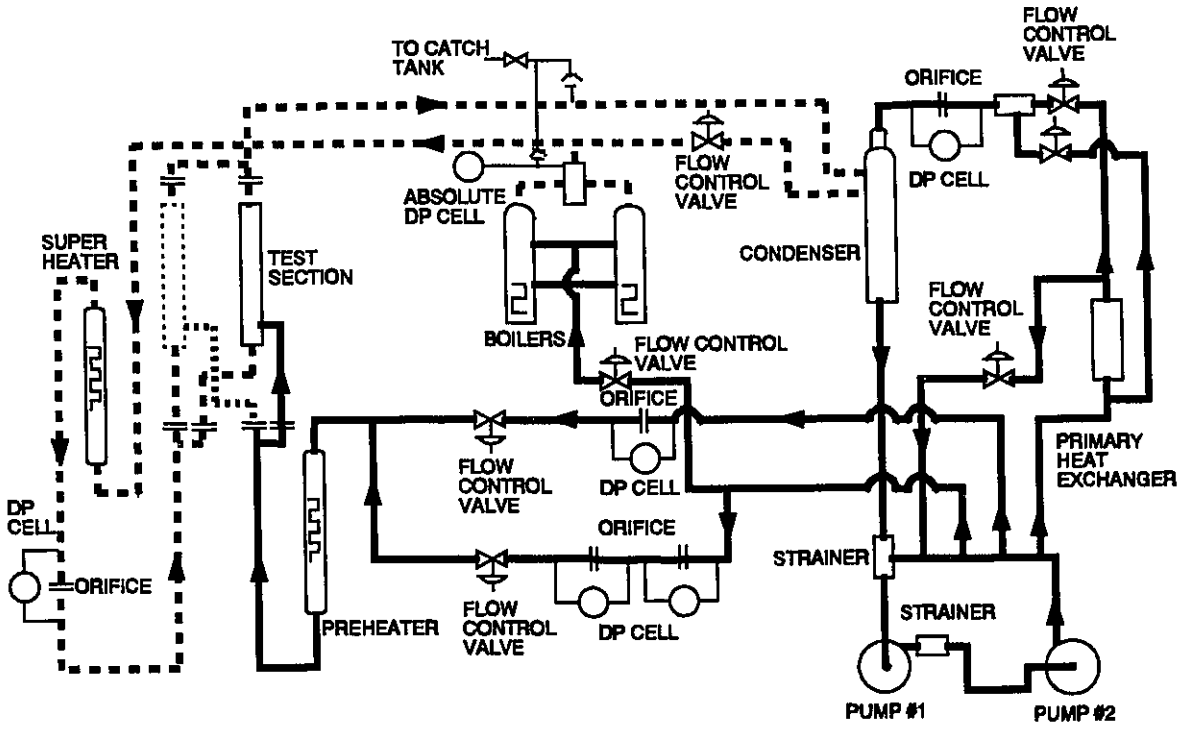

Figure 8.1: Schematic Diagram of MR-1 Loop.

heater is used to raise the temperature of the water to a preset level. The flow is then directed to the test section, which is connected to an external 350 kW (175 VDC and 2000 A) power supply for heating. After exiting the test section, the two-phase mixture is led to the condenser, where heat is removed. The condensed liquid is re-circulated through the loop.

A superheated steam loop is also connected from the boiler to the test-section inlet end. Wet steam is led from the boiler to a superheater, where dry steam is generated through superheating. The dry steam is then directed to the test-section inlet end and mixed with the main water flow. This introduces a two-phase inlet condition to the test section, for studies of adiabatic or high-quality flows. When the present experiment was carried out, however, this loop was unavailable because new heater elements were required in the superheater. Therefore, a test with adiabatic two-phase flow was not performed. The design parameters of the MR-1 loop are:

Fluid:	Light and Heavy Water
Pressure at outiet of test section:	10.3 MPa
Liquid flow rate at test section:	0.05 - 1.7 $kg.s^{-1}$
Steam flow rate at test section:	0.13 - 0.38 $kg.s^{-1}$
Power at test section:	350 kW
Main heat exchanger:	1000 kW
Maximum pressure drop over test section:	1.4 MPa

The control flow loop is used to regulate the flow conditions automatically, by controlling the pressure and liquid-height levels at the condenser and boilers. It includes main components, such as a catch tank and a heat exchanger. The catch tank is installed to relieve any over-pressure conditions in the boiler, and the heat exchanger is used to extract heat from the primary circulating fluid to maintain the same fluid temperature at the inlet of the test section. A make-up pump is used to supply water into the loop and a bleed valve is installed to purge the system.

8.2 TEST SECTION

The test section was constructed with an Inconel-600 tube, having an inside-diameter value of 5.45 mm and a wall-thickness value of 1.25 mm. It is shown schematically in Figure 8.2. Six pressure taps were welded on the test section. A ½-mm hole was drilled through the test section in each pressure tap, to obtain the local system pressure. To avoid burrs on the inside of the test section, a short piece of solid copper rod (of diameter slightly smaller than the inside diameter of the tube) was inserted into the pressure-tap location before drilling. After drilling, a long rod was used to remove any burr around the drilled holes. Two adjacent pressure taps were connected to a calibrated Rosemount differential-pressure cell for measuring the pressure difference. The first and last pressure taps were also connected to a calibrated Rosemount differential-pressure cell, to obtain the overall test-section pressure drop for confirmation of the other measurements. The system pressure at the outlet end of the test section was measured using a calibrated Rosemount absolute-pressure cell, and was maintained by regulating the heated supply to the boilers and the spray-cooling in the condensers. All connections from the pressure taps to the pressure lines directed to the differential-pressure cells were linked via the CONAX (EG-187-A-SS-V) electrical-insulating fitting (4.76 mm in inside diameter). Figure 8.3 shows a schematic diagram of the pressure-tap connection using a CONAX fittings. The temperature distribution along the test section was measured using fifteen ungrounded chromel-alumel (K-type) thermocouples. Each thermocouple was bent around the tube

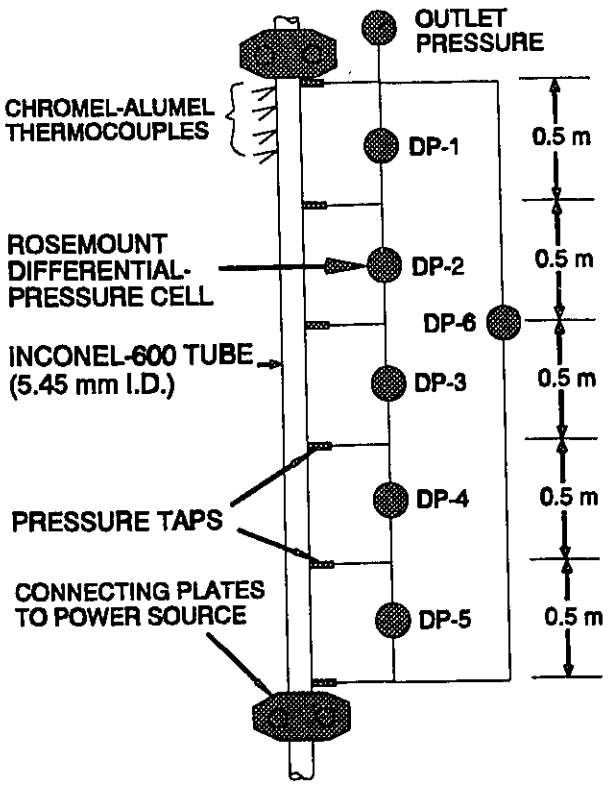

Figure 8.2: Schematic Diagram of Test Section.

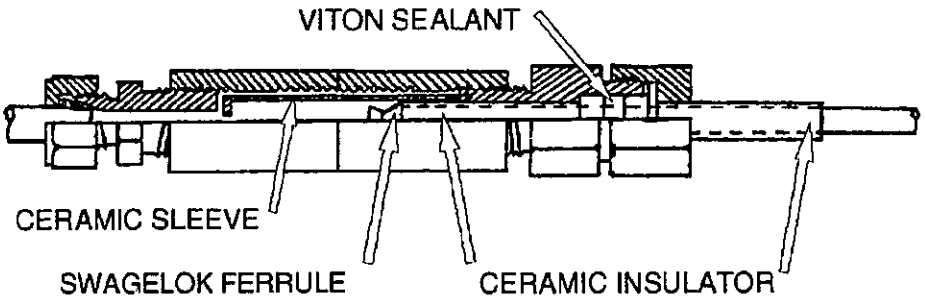

Figure 8.3: Pressure-Tap Connection Using a CONAX Fitting for Electrical Insulation.

contacting about one-third of the circumferential position. This installation technique allows the thermocouple junction to contact a region of constant temperature in the circumferential direction. Hence, it minimizes the heat loss by conduction, which may affect the temperature readings, through the thermocouple. Figure 8.4 illustrates details of this attachment technique. Before the installation, the resistance to ground values for all thermocouple sets were checked, to ensure that there would be no short circuiting between the sheath and the thermocouple wires. After the tests were completed, all thermocouple sets were removed and re-calibrated using a JOFRA temperature calibrator over a range of temperature values from 200°C to 550°C (see Appendix III).

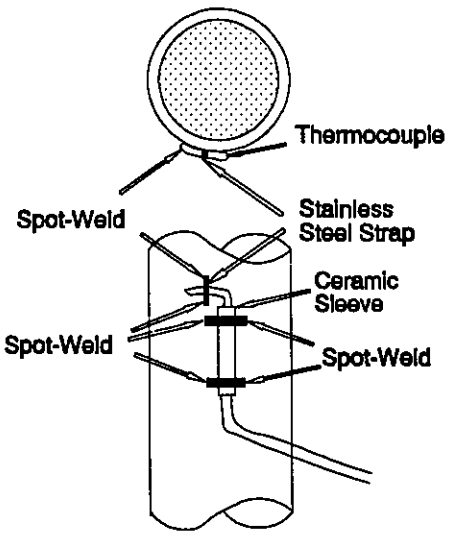

Figure 8.4: Attachment Technique of Thermocouple.

The power to the test section was applied through two connecting clamps installed as shown in Figures 8.2 and 8.5. One of these clamps was situated upstream of the first

pressure tap, while the other was situated downstream of the last pressure tap. The test section was connected to the main flow loop via two CONAX (EG-375-A-SS-L) electrical-insulating fittings (9.525 mm in inside diameter). Two ungrounded chromel-alumel (K-type) thermocouples were installed (one upstream of the CONAX fitting at the inlet end, and the other downstream of the CONAX fitting at the outlet end), to measure the bulk-fluid temperature values at both the inlet and outlet ends. Both sets were calibrated before and after the tests (see Appendix III). Figure 8.5 shows the connection of the test section to the main flow loop. The complete test section was insulated with fibre-glass insulation, to reduce heat loss.

The readings of pressure, flow rate, power, and pressure drop at the last measuring station, and eight thermocouples at the downstream end of test section, were connected also to chart recorders. This allowed the detection of any large flow fluctuation in the system and critical heat-flux conditions at any thermocouple location.

8.3 DATA-ACQUISITION SYSTEM

The conditions of the loop and the test section were monitored by various thermocouples and differential-pressure transducers. Through the analog/digital convertors, these data were collected with a Concurrent mini-computer (Model 3212) and stored on magnetic tape. In this experiment, the following parameters are of primary interest:

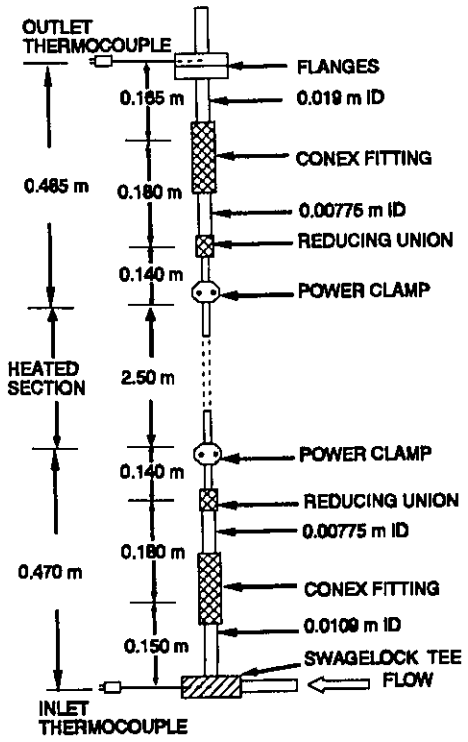

Figure 8.5: Connection of Test Section to Main Flow Loop.

- pressure at the outlet of the test section,
- flow rate of water through the test section,
- power applied to the test section,
- fluid-temperature values at both the inlet and outlet ends of the test section,
- ambient temperature, and
- surface-temperature values and pressure drops along the test section.

8.4 TEST CONDITIONS

The experiment was designed to cover wide ranges of flow conditions. Most tests were performed at a pressure of 9 600 kPa, with various flow rates and inlet-temperature values of water. Selective measurements were also obtained at pressure values of 5 000 and 7 000 kPa, to examine the effect of pressure on frictional pressure drop. The overall test matrix is summarised in Table 8.1. The inlet quality is calculated with

$$x_{in} = \frac{H_{in} - H_f}{H_{fg}} \tag{8.1}$$

where H_{in} and H_f are enthalpy values of liquid at the test-section inlet and of saturated liquid, respectively, and H_{fg} is the latent heat of vaporization in $J.kg^{-1}$.

8.5 EXPERIMENTAL PROCEDURE

With the loop set to the desired pressure, water was circulated through the test section at a constant rate. The differential-pressure transducers, connected to the pressure taps at the test section and to the orifice plates for flow-rate measurements, were adjusted to provide readings of zero pressure drop at stagnant-flow condition. At zero power level, all parameters were

Table 8.1: Test Matrix Included in the Present Experiment.

Mass Flux $kg.m^{-2}.s^{-1}$	Inlet Quality (%)				
	-1	-5	-10	-15	-20
1 000					9 600
2 000	9 600	9 600	9 600	9 600	
3 000	9 600	9 600	9 600	9 600	
4 500	9 600, 7 000	9 600, 5 000	9 600, 7 000	9 600	9 600, 7 000
6 000	9 600, 7 000	9 600, 5 000	9 600, 7 000	9 600	9 600, 7 000
7 000	9 600, 7 000	9 600	9 600, 7 000	9 600	9 600, 7 000
7 500	9 600	9 600	9 600	9 600	9 600
8 500		9 600			
10 000		9 600			

scanned and recorded seven times (the average values of these scans were used in the analysis) at an interval of 10 seconds. The test-section power was then increased in steps of either 5 or 10 kW. After allowing the system to stabilize, the parameters were recorded at each power step. The procedure was repeated until a sharp rise in surface temperature was indicated in any thermocouple. This indicates a critical heat-flux condition at the corresponding location.

After reaching the critical heat-flux condition, the test-section power was reduced by approximately 2 kW. The power was subsequently increased by 1 kW increments until the critical heat-flux point was re-established. This step was performed to confirm the critical heat-flux measurements. Little variation was usually observed between the repeat and the original critical heat-flux values. The difference was primarily caused by the small fluctuation in the system conditions. All parameters were scanned at each increment of power.

Beyond the critical heat flux, the power was increased in 1 kW steps (the increment was reduced to 0.5 kW if a sharp increase in wall temperature was detected). Again, the parameters were

scanned and recorded after each step. The test was terminated whenever any thermocouple recorded a temperature of 650°C (the temperature set for tripping the power supply).

During the experiment, a number of tests were repeated to (i) confirm previous measurements, and (ii) examine the integrity of the experimental equipment.

8.6 OBSERVATIONS

A number of observations were made during the experiment:

a. As the power increased, the mass-flow rate of water decreased at pre-dryout conditions, but increased at post-dryout conditions. Adjustments, were made to maintain a constant flow rate.

b. Pressure drop, across the last 50 cm of the test section, generally increased with increasing power at pre-dryout conditions. It decreased, however, when approaching dryout. Figure 8.6 shows the trace of pressure drop reading from the DP transducers.

c. In the two-phase region, the wall temperature remained nearly constant with increasing power in the pre-dryout regions. At certain power levels, it increased suddenly at a rapid rate. This temperature excursion is used as an indication of dryout. Figure 8.7 shows the temperature

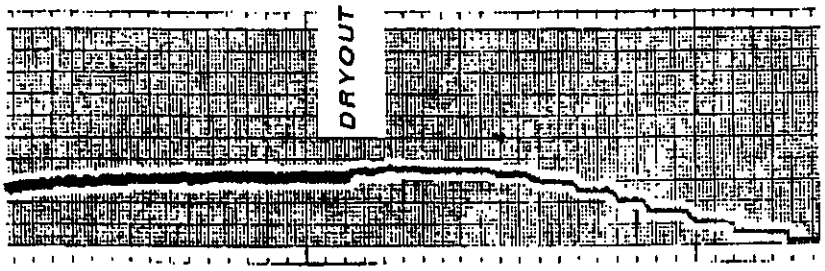

Figure 8.6: Trace of Pressure-Drop Reading Across the Last 50 cm of the Test Section.

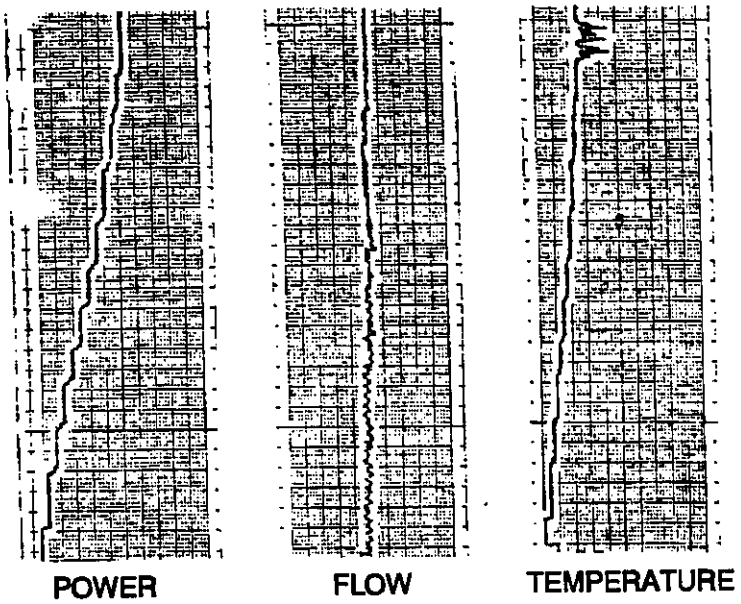

Figure 8.7: Temperature Trace of a Thermocouple Reading Indicating Dryout with Corresponding Variations in Power and Mass Flow Rate .

trace of a thermocouple indicating dryout. With the power remaining at the same level, a fluctuation of wall temperature, together with a slight oscillation in liquid flow rate, was found to correspond to the surface alternating between dryout and rewet.

d. At the dryout point, the magnitude of the temperature excursion depends strongly on the flow conditions. In some cases, the temperature increased rapidly to approximately 600°C. For other cases, however, the increment was hardly noticeable.

e. In most cases, dryout occurred first at the downstream end of the heated length (at the last two positions of the thermocouple). At high mass flux (beyond 7 000 $kg.m^{-2}.s^{-1}$), however, dryout was noticed to occur first upstream of the end of the heated length (about 20 cm away from the end; an insufficient number of thermocouples was available to accurately locate the initial dryout point). Only a slight increase in power is required to expand the dryout region to the end of the heated length. Figure 8.8 shows the traces of several thermocouples and the indication of an upstream dryout.

f. For any location in the post-dryout regions, the wall temperature increased with increasing power until it reached a maximum. Beyond the maximum point, an increase in power caused a decrease in wall temperature at that location. Figure 8.9 shows the temperature traces of thermocouples in the post-dryout regions.

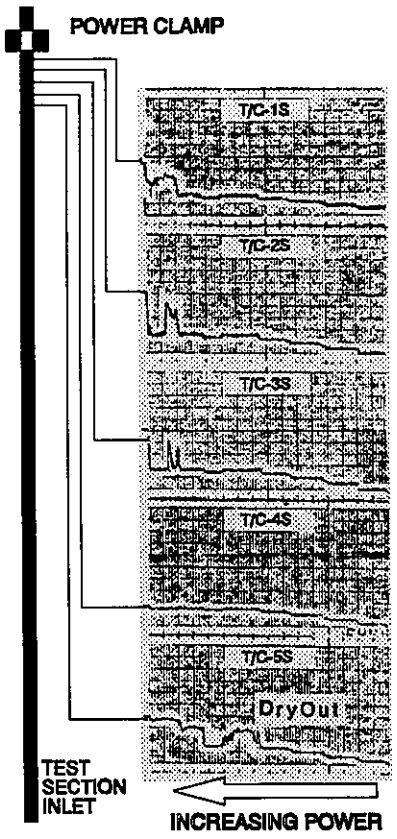

Figure 8.8: Temperature Traces of Thermocouples Indicating Upstream Dryout.

8.7 DATA REDUCTION

The raw data obtained from the experiment are presented in Appendix II. They were not used directly in the analysis, because they included other effects that needed to be eliminated. This section describes the corrections applied to the raw data, transforming them into workable experimental data. The detailed calculations are shown in Appendix III, and the complete set of corrected data is shown in Appendix IV.

8.7.1 Data

Each set of data was assigned with a run-name to present its status and the most important loop parameters. The run name consists of eight alphanumeric characters (i.e., DPxabcde), where:

DP pressure drop tests

x status of the test section: "B" for pre-dryout, "C" for dryout, "P" for post-dryout

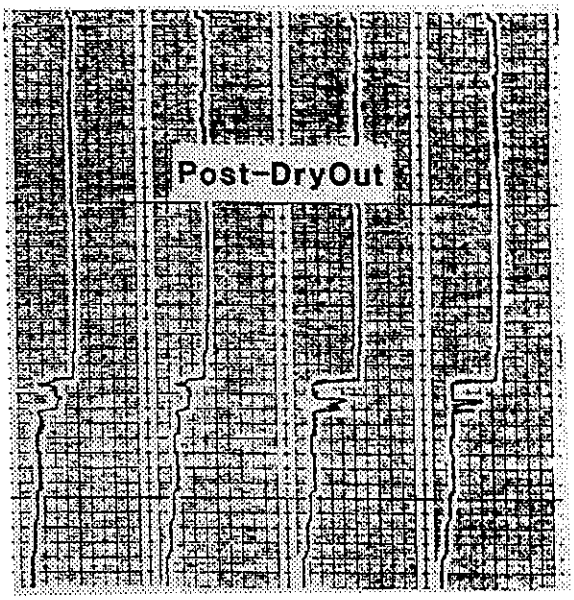

Figure 8.9: Temperature Traces of Thermocouples in the Post-Dryout Region.

a loop pressure: "9" for 9 600, "7" for 7 000, "5" for 5 000 kPa

b mass flux of coolant: "1" for 1 000, 2 for 2 000, "3" for 3 000, "4" for 4 500, "6" for 6 000, "7" for 7 000 or 7 500, "8" for 8 500, and "0" for 10 000 $kg.m^{-2}.s^{-1}$.

c inlet quality: "1" for -1%, "2" for -5%, "3" for -10%, "4" for -15%, "5" for -20%

de power level in 5 kW steps at pre-dryout regions: "00" for zero power, "01" for 5 kW, "02" for 10 kW, etc., or power steps at dryout and post-dryout regions.

The data obtained in the heat-balance tests are identified as "Heat-bal" only.

8.7.2 Data Corrections

A number of corrections to the thermocouple readings of surface and bulk-fluid temperature were introduced. They were based on the calibration tests, despite the small observed differences, as indicated in Appendix III. Calculations were also carried out to obtain the inner surface-temperature value at each location of the thermocouple, which was attached to the outer surface of the test section. Due to the internal heat generation within the wall of the test section,

the temperature was higher at the outer than inner surface. This difference, however, was proportional to the heat generation rate, and hence the power.

The power supply to the test section was corrected based on the heat-balance tests. Despite the thermal insulation of the test section, heat loss was unavoidable. Heat was primarily lost through the connecting clamps attached to the test section. This was caused by the high contact resistance between the two surfaces. Various connecting methods are being examined at Chalk River Laboratories to improve the connection. For the present test, the heat loss was estimated at about 4% of the applied power (see Appendix III).

A correction for static head on the pressure-drop measurement was introduced, to account for the difference in height of pressure taps connected to a differential-pressure cell. Since there was practically no flow inside the pressure-tap lines, the ambient-temperature value was used as the fluid temperature to evaluate the liquid density required in the correction.

8.8 CALCULATION OF FLOW PARAMETERS

The measurements provide mainly the primary flow parameters: diameter, pressure, mass flow rate, inlet temperature and power. Other (secondary) parameters, such as mass flux, heat flux, thermodynamic quality, mass quality and void fraction, are also required in the analysis. The mass flux is calculated with

$$G = \frac{W}{A_F}$$

where W is the mass flow rate in $kg.s^{-1}$, A_F is the flow area in m^2 defined as

$$A_F = \frac{\pi D^2}{4}$$

and D is the inside diameter of the test section in m. The heat flux is calculated using

$$q = \frac{Power}{A_h}$$

where Power is the total applied power in W, A_h is the heated area in m^2 defined as

$$A_h = \pi D L_h$$

and L_h is the heated length in m. The thermodynamic quality at any distance from the start of the heated length, z, is calculated using

$$x_e = \frac{1}{H_{fg}} \left(\frac{Power\ z}{W L_h} + H_{in} - H_f \right)$$

where H_{in} and H_f are the liquid enthalpy at the inlet and saturation, respectively, and H_{fg} is the latent heat of vaporization in $J.kg^{-1}$. Both the saturated liquid enthalpy and latent heat of vaporisation are based on local pressure. The mass quality is calculated using the Kroeger and Zuber [1968] equation, and the void fraction is calculated using the Chexal et al. [1991] correlation. Details of these equations are given in Chapter 3.

9. ANALYSIS OF EXPERIMENTAL RESULTS

The experimental data are analyzed with respect to various flow parameters before the comparison against the predictions of the analytical model is performed. Although the pressure drops, surface temperatures and critical heat flux were measured, only the pressure-drop measurements are analyzed here in detail. The surface temperatures and critical heat flux are mainly used to validate the heat-transfer correlations, which are employed to predict the heat-transfer rate and transition points based on the average conditions over the measuring section. While it is the intention to present as much information from the experimental data as possible, only representative illustrations are provided, to avoid repetition. Some data were presented in Leung and Groeneveld [1991].

Section 9.1 presents a general overview of the overall pressure-drop measurements, which were subsequently separated into various pressure-drop components. The single-phase data is analyzed in Section 9.2. Both the adiabatic and heated conditions are presented. Section 9.3 shows the data of the onset of net-vapour generation. A comparison is made between the data and

predictions of the Saha and Zuber and the Avdeev correlations. The flow-boiling data are analyzed in Section 9.4, showing the effects of various parameters on two-phase frictional pressure drop (expressed as the two-phase multiplier).

9.1 GENERAL

9.1.1 Pressure and Temperature Distributions

The pressure and temperature distributions measured along the test section are illustrated in Figure 9.1 for a specific set of conditions, where dryout has been encountered at the end of the heated length. A sharp rise in surface temperature is indicated at the downstream end. For the

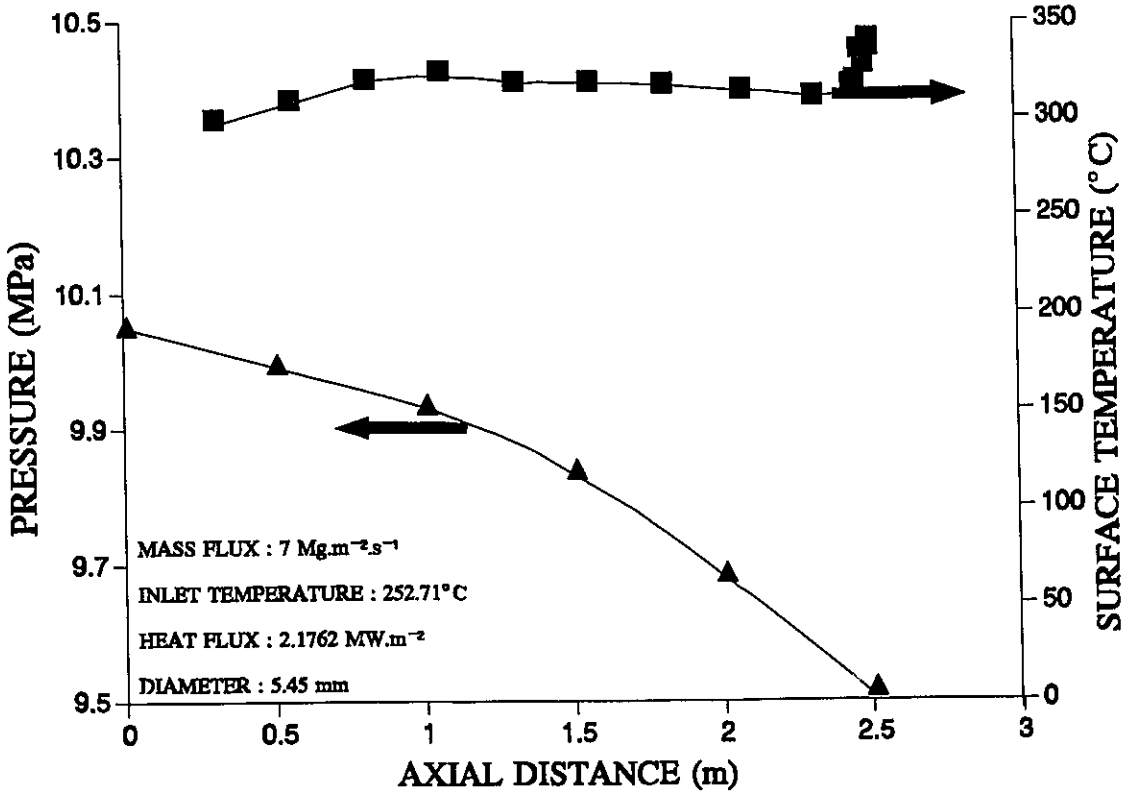

Figure 9.1: Illustrations of Pressure and Surface-Temperature Distributions Along Test Section.

present inlet conditions, single-phase flow is maintained for a 1-m long distance, where a steady increase in surface temperature with respect to axial distance is observed. Once boiling is initiated, the surface temperature becomes stable. A slightly decreasing trend is observed as the axial distance (and hence quality) increases. It corresponds to (i) the forced convective evaporation region, where the heat transfer becomes more efficient with increasing quality (due to both conduction and convection to the liquid film) and (ii) a reduction in saturation temperature. The same trend is illustrated in Collier [1981].

The local pressure, calculated from the pressure-drop measurements, decreases continuously along the test section. This decrease is relatively linear at the inlet end, corresponding to the region of single-phase flow, but tends toward a parabolic profile once boiling is initiated.

9.1.2 Components of Pressure Gradient

Measurements of overall pressure drop between two adjacent pressure taps (over a length of 50 cm) are obtained along the test section. Each of them can be separated into three different components: friction, acceleration and gravity. In single-phase liquid flow, the pressure gradient due to acceleration is calculated from

$$-\left(\frac{dP}{dz}\right)_a = \frac{d(G^2/\rho_l)}{dz} \tag{9.1}$$

and the pressure gradient due to gravity is obtained from

$$-\left(\frac{dP}{dz}\right)_g = \rho_l\, g \tag{9.2}$$

By subtracting these two components from the overall pressure drop (i.e., the measurement), the pressure gradient due to friction is calculated from

$$-\left(\frac{dP}{dz}\right)_f = -\left(\frac{dP}{dz}\right)_l + \left(\frac{dP}{dz}\right)_a + \left(\frac{dP}{dz}\right)_g \tag{9.3}$$

In two-phase flow, the separated-flow model (see Section 3.4.2) is used to evaluate the pressure gradients due to acceleration and gravity, which are expressed, respectively, as

$$-\left(\frac{dP}{dz}\right)_{a,tp} = G^2 \frac{d}{dz}\left(\frac{x_a^2}{\alpha \rho_g} + \frac{(1-x_a)^2}{(1-\alpha)\rho_l}\right) \tag{9.4}$$

and

$$-\left(\frac{dP}{dz}\right)_{g,tp} = (\rho_g \alpha + \rho_f (1-\alpha))\, g \tag{9.5}$$

The two-phase pressure gradient due to friction is calculated in the same manner as Equation (9.3). All fluid properties are evaluated based on the mean bulk-fluid temperature within the measuring section. The vapour-weight quality is calculated from the Kroeger-Zuber correlation (Section 3.2) and the void fraction is obtained from the Chexal et al. correlation (Section 3.3).

9.1.3 Pressure Gradients in Flow Boiling along a Channel with Constant Heat Flux

Figure 9.2 illustrates various components of pressure gradient in flow boiling along the test section (with respect to average thermodynamic qualities) at constant inlet conditions. Over these conditions, the total pressure gradient increases with increasing quality. This increase is gradual in the negative-quality region (single-phase flow), but becomes rapid in the positive-quality region (saturated boiling). At high qualities, the rate of increase is also small. Among the various components, the pressure gradient due to gravity is insignificant and may be neglected. The pressure gradient due to acceleration, however, is small in single-phase flow but becomes

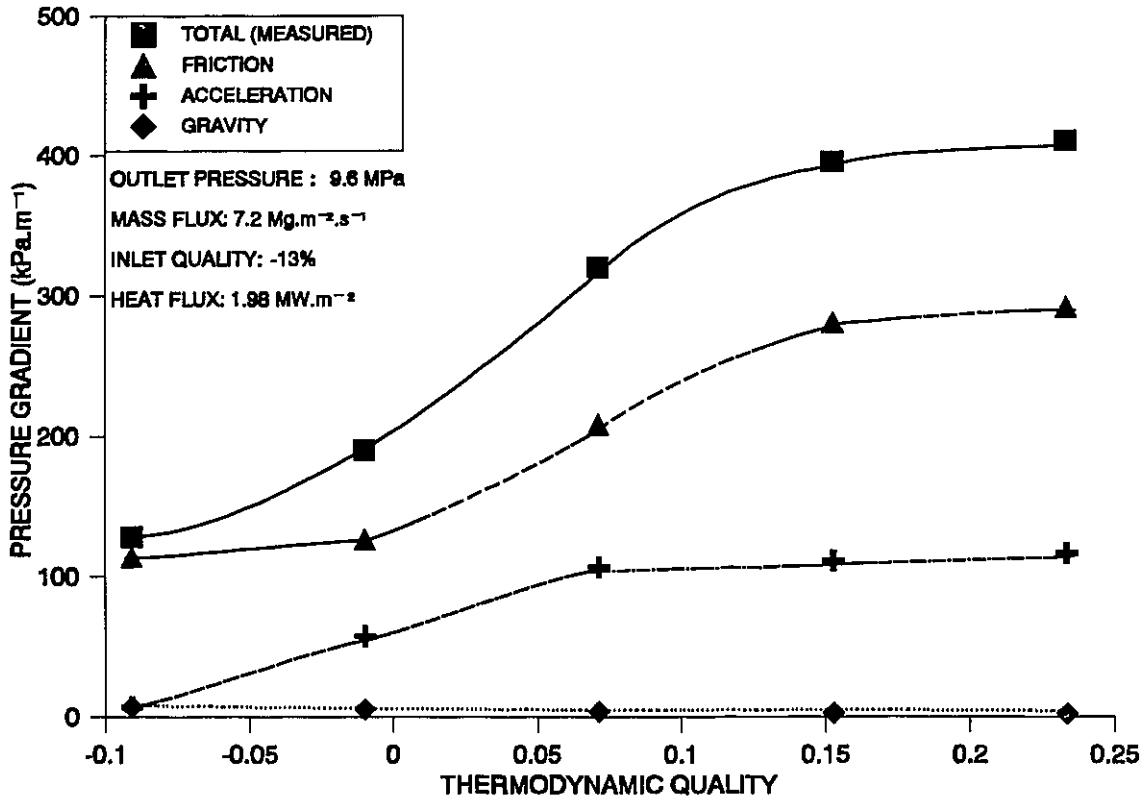

Figure 9.2: Various Pressure Gradients Calculated Along Test Section.

more significant when flow boiling is encountered in the channel. Due to the limited rise in quality, the variation in pressure drops is relatively small over the channel.

9.1.4 Pressure Drops in Flow Boiling along a Channel with Varying Heat Fluxes

Various pressure gradients as a function of thermodynamic quality are shown in Figure 9.2 for a constant heat flux. Only a small variation was observed, due to the narrow range of qualities and limited measured data over the test section. A more detailed presentation, however, can be shown with varying heat fluxes.

Figure 9.3 illustrates various components of pressure drop at the downstream end of the test section (50 cm). The average pressure gradient can be obtained by dividing the pressure drop by the length of the measuring section (i.e., $\Delta P/\Delta z$). The increase in thermodynamic quality in this figure is due to an increase in heat flux, rather than axial location, as was shown in Figure 9.2. Among the three components, the pressure drop due to friction is generally larger than the others, particularly in the subcooled-boiling (negative-quality) regions. When the bulk fluid approaches saturation, the pressure drop due to acceleration increases sharply due to a change in void fraction, once bulk boiling is encountered. The increase becomes gradual and its magnitude is comparable to the frictional component at the high-quality region. Over these conditions, the pressure drop due to gravity is insignificant.

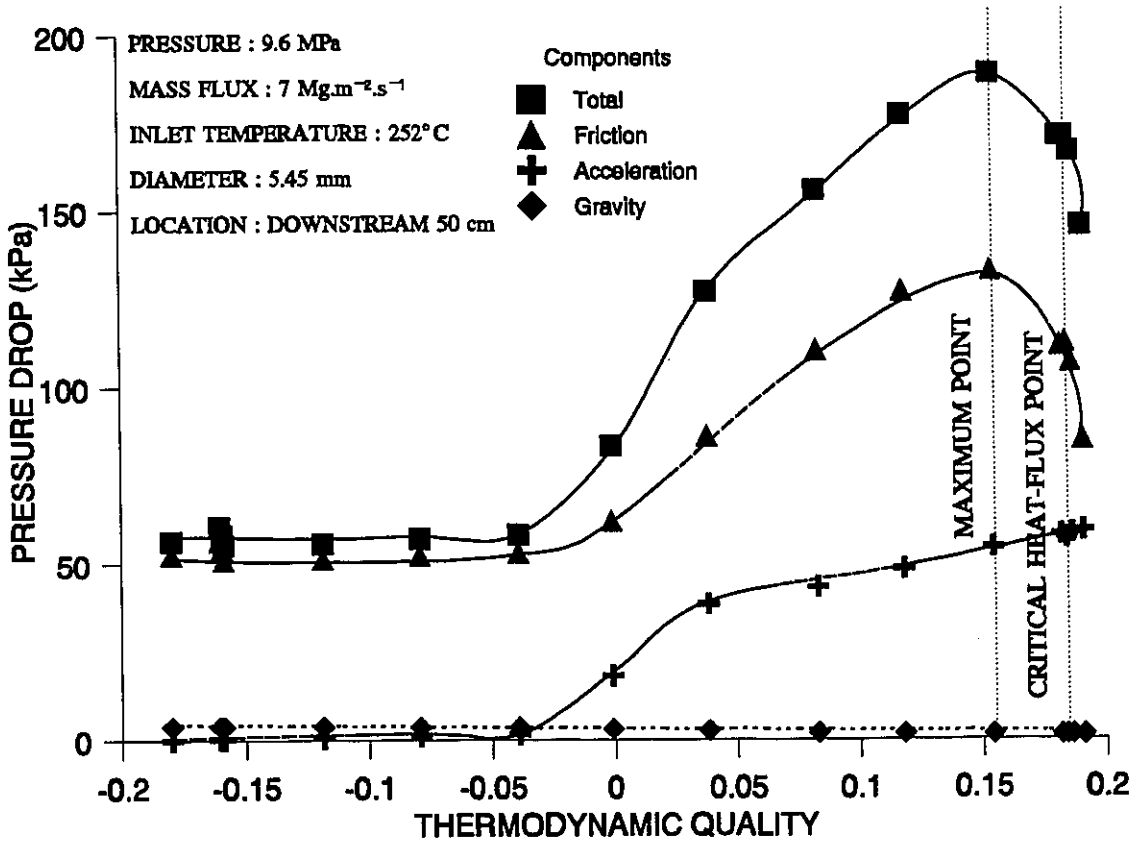

Figure 9.3: Comparison of Various Pressure-Drop Components in a Heated Channel with High Inlet Subcooling.

The pressure drop due to friction is relatively constant in single-phase flow. A small decreasing trend is observed at highly subcooled conditions, but is not noticeable due to the large scale employed for the Y-axis. At low qualities (or heat fluxes), the two-phase pressure drop due to friction increases with increasing qualities. The gradient of this increase is gentle at subcooled conditions, but becomes rapid at low positive qualities. At subcooled conditions, the increase in two-phase frictional pressure drop is caused by the increase in (i) the apparent roughness due to bubble formation at the heated surface, and (ii) the near-wall velocity gradient, due to the relatively high bubble velocity compared to the liquid after the bubbles have departed from the heated surface. Part of this increase, however, is compensated for by the decrease in frictional pressure drop, due to a reduction in near-wall fluid viscosity at high surface temperature.

The frictional pressure drop increases sharply just before the bulk fluid reaches saturation indicating the initiation of bulk boiling (point of net vapour generation) in the channel. Its gradient with respect to quality (i.e., $d(\Delta P)/dx_{th}$) exhibits an increasing trend at regions close to zero quality, but changes to a decreasing trend as the quality is increased. There is insufficient data to locate the transition points accurately, which have been shown to correspond to a change in flow pattern (or heat-transfer regime) [Shoukri, 1983]. At low positive qualities, the bubbles migrate into the main stream and significantly increase the interfacial (due to high void fraction) and wall (due to the reduction of liquid flow area and high vapour velocity) shear stresses. On the other hand, the surface temperature is maintained closely near the saturation temperature, resulting in less severe temperature gradients inside the fluid (i.e., no or little reduction in frictional pressure drop for viscosity variation). These factors bring a sharp rise in frictional pressure drop with increasing qualities.

The frictional pressure-drop gradient with respect to quality (i.e., $d(\Delta P)_f/dx_{th}$) decreases with increasing quality (or heat flux). This decreasing gradient indicates the transition from bubbly to wispy-annular flow. At this transition, the interfacial shear stress is reduced, due to a decrease in the interfacial area. With a further increase in quality, part of the liquid is entrained into the vapour core and results in a reduction in vapour velocity, as well as lowering the core turbulence level. This decreases the velocity gradient at the interface and hence reduces the interfacial shear

stress. Also, a small degree of superheating is anticipated in the near-wall region of the liquid film, and this introduces a further reduction in frictional pressure drop.

At a quality just before the critical heat-flux condition, a maximum point of frictional pressure drop is encountered. Beyond that point, the frictional pressure drop decreases with increasing quality. This decrease is mainly due to the reduction in interfacial shear stress as the liquid film becomes so thin that wave formation and liquid entrainment are terminated. The gradient, $d(\Delta P)_f/dx_{th}$, is steeper at the region after (post-dryout) than before (pre-dryout) the critical heat-flux condition. This is caused by the considerably smaller pressure drop (due to a much smaller vapour viscosity than liquid viscosity) in the post- than pre-dryout regions. Note that the surface temperature at any thermocouple location is limited to a maximum of 650°C (via a high-temperature trip) to avoid damage to the test section in this experiment. This experiment was terminated before the dryout front could spread over the complete measuring section. The local maximum pressure-drop point, though not validated, could be an indication of another flow-pattern transition: from wispy-annular to froth-annular flow.

Figure 9.4 shows the pressure-drop components at the downstream end of the test section (50 cm) for similar flow conditions, but with a lower inlet subcooling than that shown in the previous figure. The pressure drop due to friction remains the most significant component. It increases continuously up to the maximum point within the present range of qualities. The region of single-phase pressure drop is not encountered in this case, due to the low inlet subcooling. However, the pressure-drop trends are similar to those shown in Figure 9.3 for the forced convective evaporation region.

With a further increase in heat flux, the two-phase frictional pressure drop decreases beyond the local maximum point at high qualities. Over this region, a smooth interface between the liquid film and the vapour core is anticipated, resulting in a much smaller interfacial shear stress. It is also expected that the thickness of the liquid film is of the order of the thickness of the laminar sublayer of the vapour flow because the turbulent effect in the mixture core appears to have no influence on the liquid film. Therefore, the velocity of the liquid film is not affected, but the

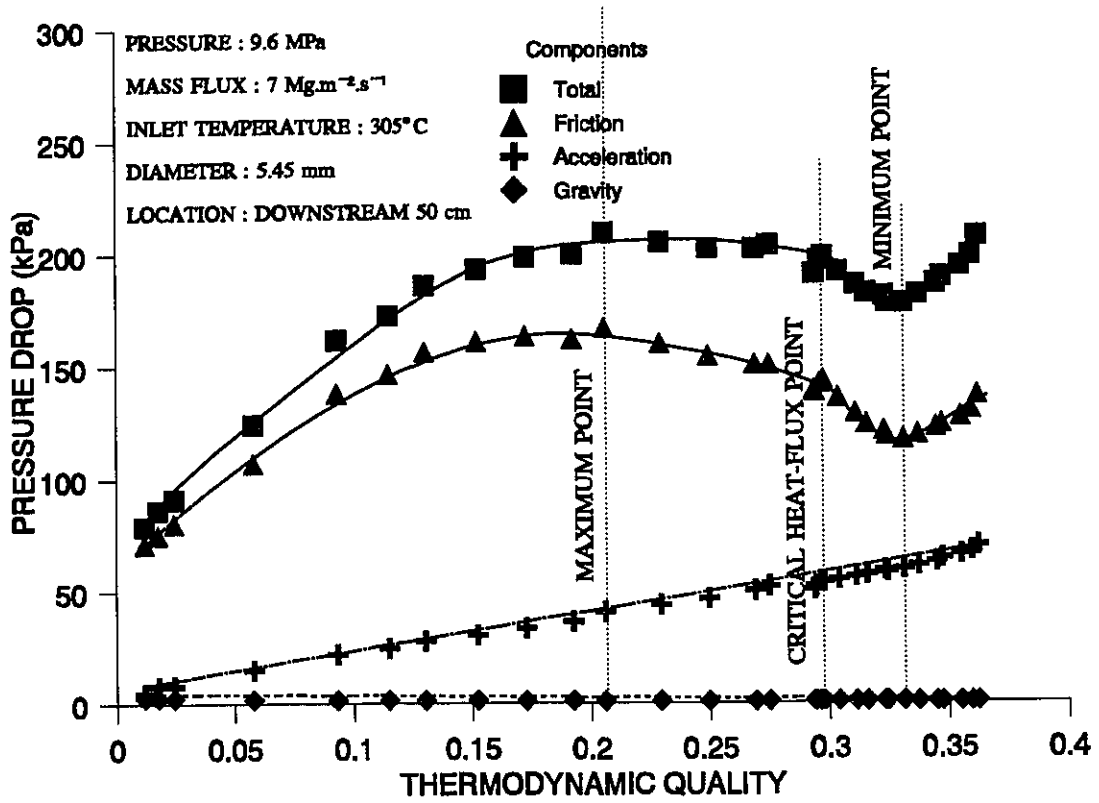

Figure 9.4: Comparison of Various Pressure-Drop Components in a Heated Channel with Low Inlet Subcooling.

film is continuously depleted through vaporization.

The quality difference between the points of maximum pressure drop and critical heat flux is larger for higher inlet temperatures (comparing Figures 9.3 to 9.4). Dryout occurs when the thin liquid film is completely evaporated at a location slightly beyond the local peak. Since the pressure drop is measured over a distance of 50 cm, this decreasing trend continues until the dryout front propagates below the upstream pressure tap and the complete measuring section becomes dry. A local minimum is shown at this point. The frictional pressure-drop gradient, $d(\Delta P)_f/dx_{th}$, is much steeper in the regions before than after the dryout conditions.

After reaching the local minimum point, the two-phase frictional pressure drop increases again with respect to quality. This is caused by the increase in wall shear stress, due to a higher

vapour velocity. The increase in vapour velocity is caused by the rise in vapour temperature and the increase in actual quality due to the evaporation of entrained liquid droplets.

9.2 SINGLE-PHASE FLOW

9.2.1 Experimental Data

The single-phase total pressure drops (including friction and gravity) over the test section are shown in Figure 9.5 for various fluid temperatures and mass flow rates (which correspond to

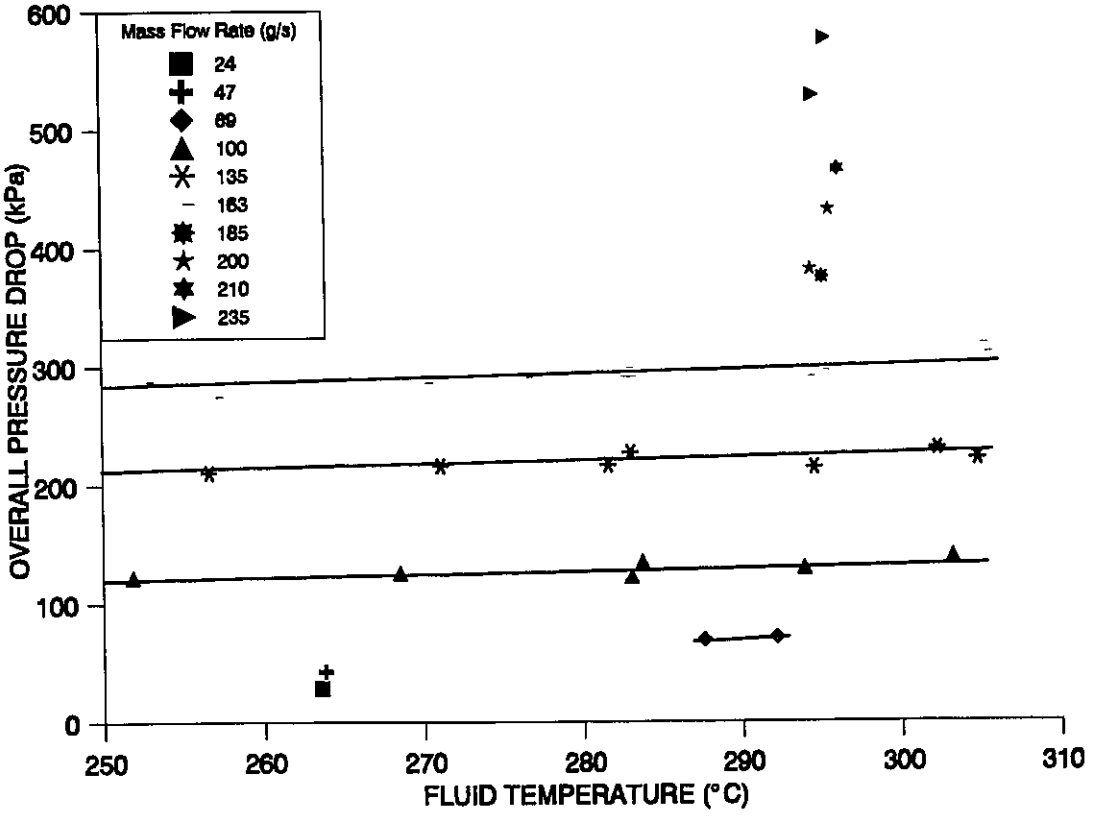

Figure 9.5: Single-Phase Total Pressure Drops for Various Fluid Temperatures and Mass Flow Rates.

mass fluxes of 1.2 to 10 $Mg.m^{-2}.s^{-1}$) at adiabatic conditions. Among data that cover a range of fluid temperatures (i.e., data of 4.5, 6 and 7 $Mg.m^{-2}.s^{-1}$ in mass flux), the effect of fluid temperature is relatively small, but a systematic increase in adiabatic pressure drop is shown with increasing fluid temperature. This appears to contradict the theory that adiabatic pressure drop should decrease with increasing fluid temperature (due to a reduction in fluid viscosity). However, since the mass flow rate (W_l) was maintained constant in this experiment, the fluid velocity increases (as the fluid density decreases) with increasing fluid temperature ($u_l = (W_l/A_f)/\rho_l$), and results in an increase in adiabatic pressure drop. The effect of mass flow rate (or mass flux) on adiabatic pressure drop is strong. As expected (e.g., see Equations (2.37)), a lower adiabatic pressure drop is shown with lower mass flow rates; the increase in adiabatic pressure drop is approximately proportional to the square of the mass flow rate (the pressure drop varies from 20 to 550 kPa when the mass flow rate increases from 24 to 235 $g.s^{-1}$).

9.2.2 Friction Factor (Adiabatic Flow)

The single-phase frictional pressure drop is calculated by subtracting the component due to gravity from the total pressure drop. Although the fluid temperature decreases slightly (due to heat loss) over the test section, the pressure drop due to acceleration is insignificant. The single-phase frictional pressure drop is expressed in terms of the friction factor, which is defined as

$$f = \frac{\Delta P_f D}{z} \frac{2 \rho_l}{G^2} \tag{9.6}$$

where ρ_l is the liquid density based on the average bulk-fluid temperature over the measuring section. Figure 9.6 shows the calculated friction factors with respect to the Reynolds number for adiabatic flow in all measuring sections. Despite some data scatter, the results are generally consistent. The friction factor was optimized, as a function of Reynolds number, as follows:

$$f = 0.0448\ Re^{-0.0709} \tag{9.7}$$

Based on the Colebrook-Chen equation (Equation (2.44)), the calculated value of relative roughness (i.e., ε/D) is 0.00103 for this test section. The friction factors, calculated with Equation (9.7) and the Colebrook-Chen equation using the optimized relative-roughness value, are the same at a high Reynolds number, but slight differences are observed at a low Reynolds number. For comparison, the friction factor of a smooth tube is also shown in the same figure, and is generally smaller than the experimental value.

9.2.3 Effect of Surface Heating

In a heated channel, single-phase flow is assumed when the surface temperature is less than the value corresponding to the onset of nucleate-boiling point (i.e., $T_w < T_{ONB}$). The surface

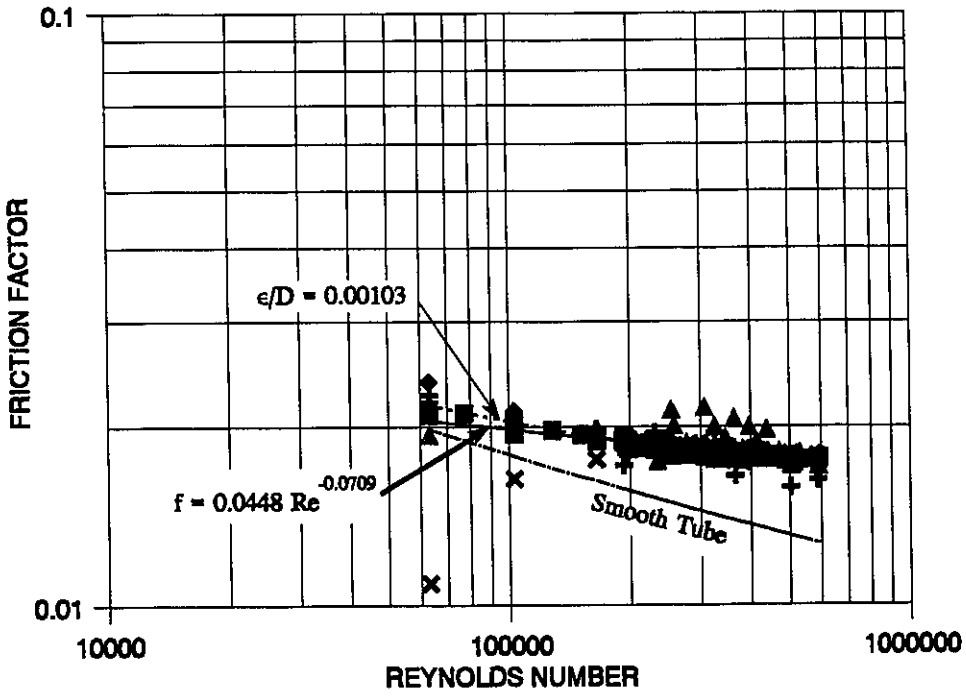

Figure 9.6: Friction Factor of Test Section for Adiabatic Flow.

temperature is calculated with the heat-transfer coefficient predicted from the Gnielinski [1976] equation (Equation 4.7), which was found to agree better with heat-transfer data of the present experiment than other correlations. At the point of onset of nucleate boiling, the corresponding surface temperature is determined from the Davis and Anderson [1966] equation (Equation 4.15).

Figure 9.7 shows the single-phase pressure drops (both the total (i.e., measured) and frictional) for various thermodynamic qualities (an equivalent measure of fluid temperature) and heat fluxes. Since the increase in surface temperature is proportional to heat flux, this figure also presents the trend of increasing surface temperature. The frictional pressure drop is calculated from Equation (9.3) and the pressure drops due to acceleration and gravity have been subtracted from the measurement.

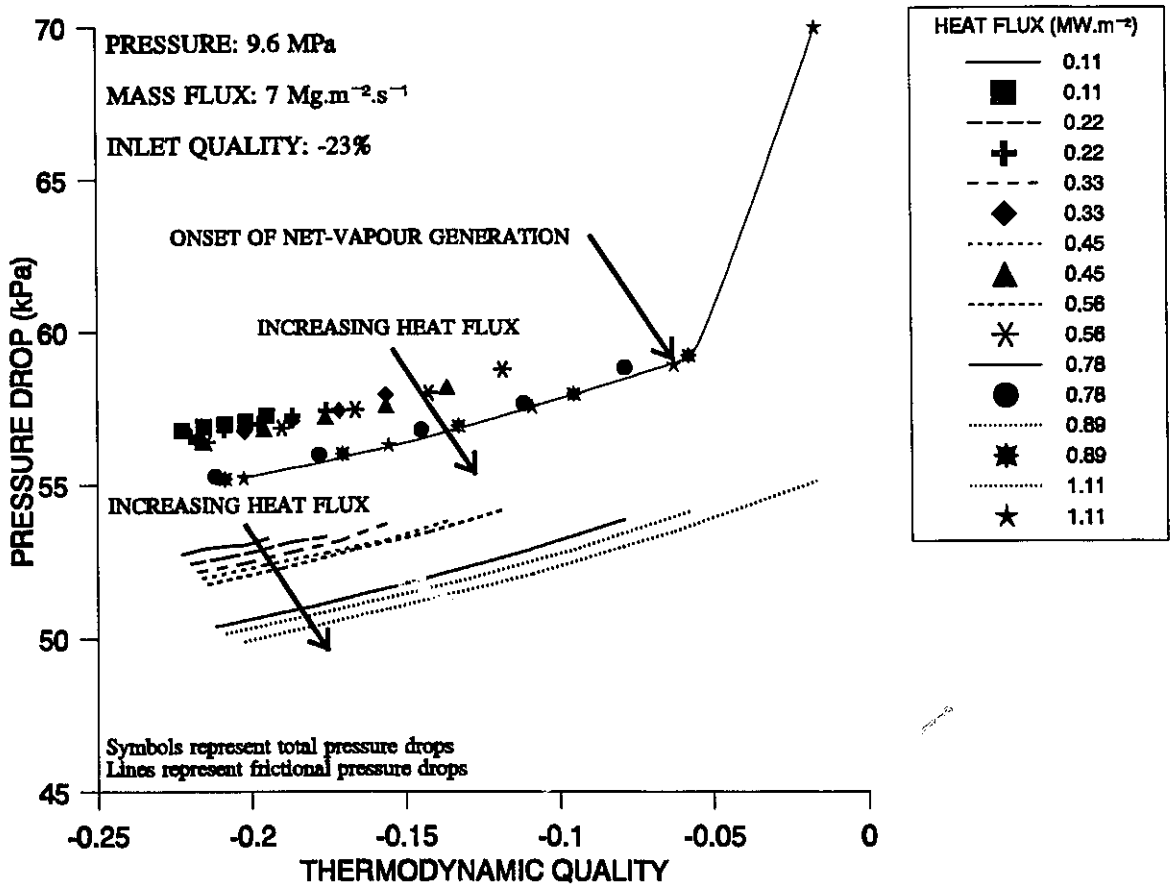

Figure 9.7: Single-Phase Pressure Drops over a Heated Channel.

Similar to the trend exhibited in adiabatic flow, the single-phase pressure drop along a heated tube increases with increasing thermodynamic quality (or bulk-fluid temperature). For the same thermodynamic quality, it decreases with increasing heat flux (or surface temperature). While the majority of the data shown in Figure 9.7 correspond to single-phase flow, several flow-boiling data at high heat fluxes are also presented for comparison. At a thermodynamic quality higher than -5%, a sharp increase in total pressure drop is shown; it signifies the start of flow boiling (or two-phase flow). The increase in frictional pressure drop, however, remains gradual within the same range of quality. This is primarily caused by the high pressure drop due to acceleration resulting in a much steeper increase in total than in frictional pressure drop. The gap exhibited between heat fluxes of 0.56 and 0.78 $MW.m^{-2}$ is caused by a reduction of about 2.3% in mass flux (from 7.10 to 6.94 $Mg.m^{-2}.s^{-1}$).

Similar to other studies, the single-phase frictional pressure drop is presented in terms of a friction-factor ratio between heated and unheated conditions. This ratio is correlated with the viscosity ratio, between the bulk and near-wall fluids, to account for the effect of heating on pressure drop. The correction factor is expressed as (Equation (2.46))

$$\frac{f_{heated}}{f_{unheated}} = \left(\frac{\mu_b}{\mu_w} \right)^n \tag{9.8}$$

In the present analysis, the viscosity of near-wall fluids is evaluated with an average inner surface temperature over the measuring section. Figure 9.8 shows the friction-factor ratio as a function of viscosity ratio. While a large scatter is observed among the data, particularly at viscosity ratios close to 1, the friction-factor ratio decreases with the increasing viscosity ratio. Based on Equation (9.8), the exponent n is optimized to be -0.28. It is bounded between the recommendations of -0.25 by Maurer and Letourneau [1963] and -0.35 by Dormer and Bergles [1964], but is greater than the values of -0.4 and -0.61 by Owen and Schrock [1960] and Rohsenow and Clark [1951], respectively. The same exponent value was found valid for low-pressure (1 to 4 MPa) conditions and large-diameter tubes (13.5 and 22.9 mm) over a much

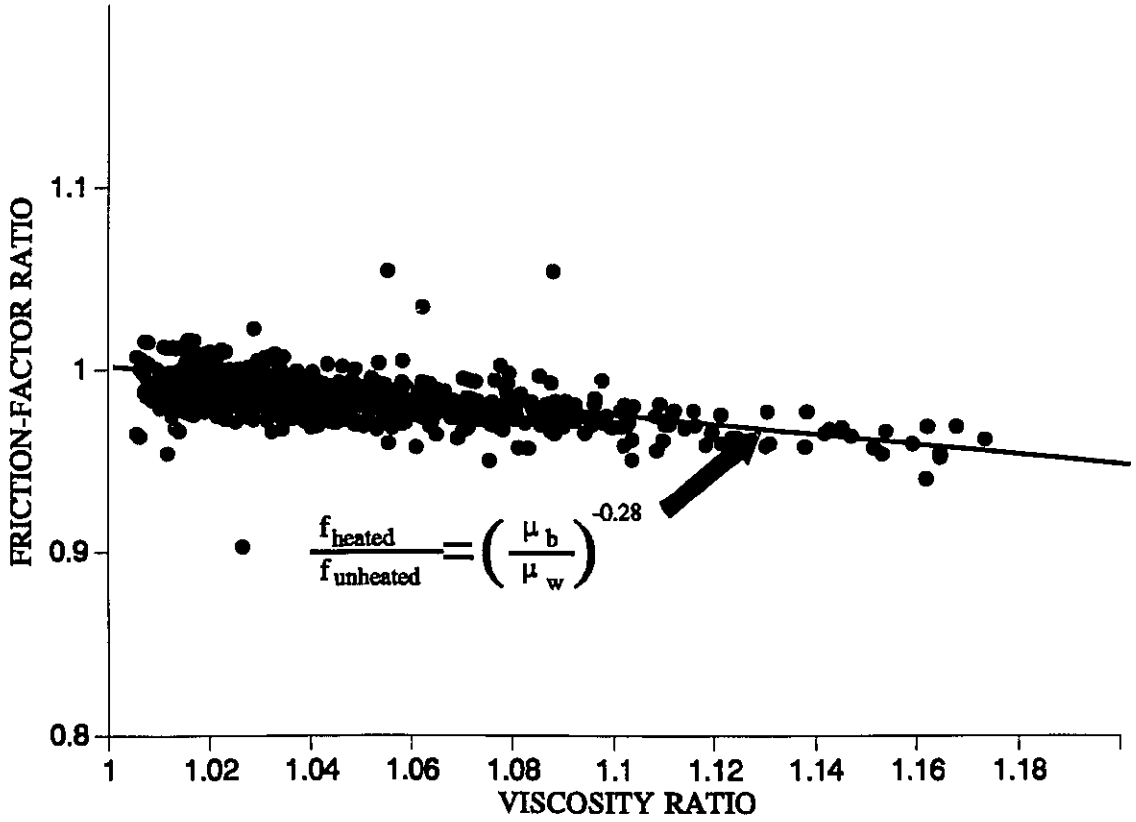

Figure 9.8: Friction-Factor Ratio Between a Heated and Unheated Channel.

wider range of viscosity ratio (up to viscosity ratios of 2.2) in a similar study at Ecole Polytechnique [Leung et al., 1993].

The effect of other parameters (such as mass flow rate and density ratio) on the friction-factor ratio has also been examined in response to the findings of Maurer and Letourneau [1963]. However, none of these parameters displays a noticeable influence on the friction-factor ratio over the present range of test conditions. The correction based on Equation (9.8) is therefore appropriate.

9.3 POINT OF NET-VAPOUR GENERATION

The point of net-vapour generation is the location where a significant amount of vapour volume is generated and maintained in the channel. It is often assumed as the initiation point of two-phase boiling flow, since a rise in pressure drop from the single-phase value is observed from this point on. In the present experiments, this point cannot be accurately determined, due to the relatively large increment in heat flux (or applied power) for each test. Therefore, the last data point of single-phase pressure drop before the deviation occurs is designated as the point of net-vapour generation (see Figure 9.7).

The experimental data obtained in the present study are shown in terms of the Stanton (Equation 4.18) and Peclet numbers (Equation 4.19) in Figure 9.9. They cover mainly the region of high Peclet numbers (beyond 70 000). The data are scattered between 0.001 to 0.1 at the high Peclet numbers. Based on the same approach used by Saha and Zuber [1974] as well as Avdeev [1988], the optimized Stanton number is 0.0041 for the high Peclet numbers. The transition point, however, is located at Peclet numbers of about 100 000, which is different from those recommended by Saha and Zuber [1974] (70 000) and Avdeev [1988] (57 000). Based on the methodologies used by Saha and Zuber [1974] as well as Avdeev [1988], the best-fit equation for the present set of experimental data is expressed as

$$x_{NVG} = -0.0022 \frac{q\ D\ Cp_l}{H_{fg}\ k_l} \tag{9.9}$$

for Peclet numbers less than 100 000, and

$$x_{NVG} = -244 \frac{q}{G\ H_{fg}} \tag{9.10}$$

for Peclet numbers larger than 100 000.

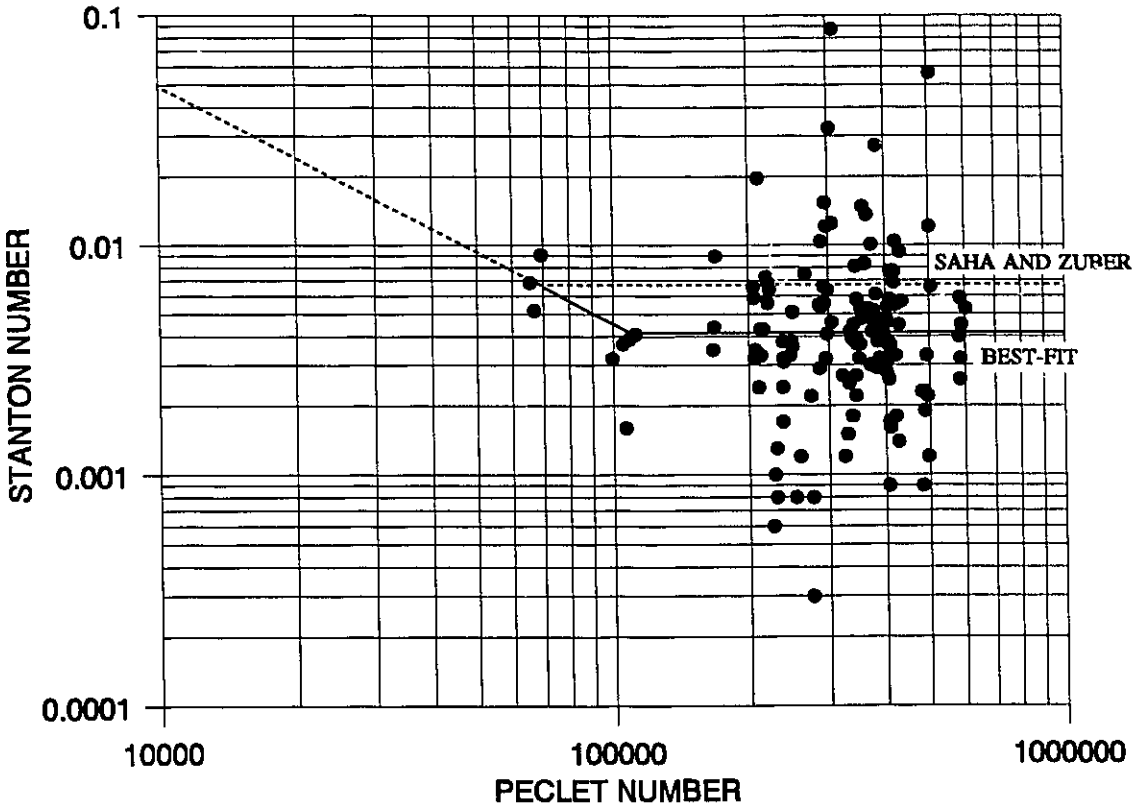

Figure 9.9: Relation Between Stanton and Peclet Numbers for Conditions at Point of Net-Vapour Generation.

An examination of the data reveals that the large scatter among data is independent from pressure, mass flux and heat flux. Figure 9.10 shows the quality at the point of net-vapour generation for a constant pressure and mass flux. Since the flow conditions covered in this test correspond to the high Peclet-number region, it is presented as a function of boiling number, which is defined as

$$Bo = \frac{q}{G\, H_{fg}} \tag{9.11}$$

Both the Saha and Zuber and the Avdeev correlations overpredict the data. The best-fit equation provides a reasonable agreement over this range. However, an underprediction is observed at the

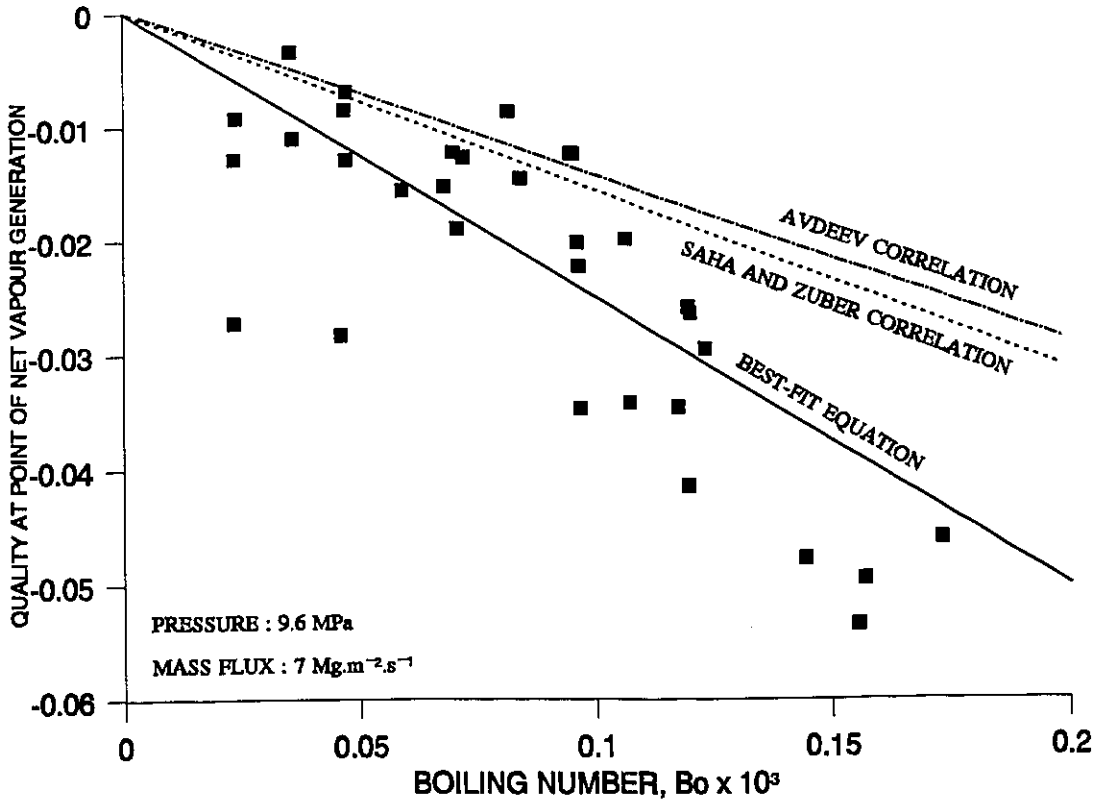

Figure 9.10: Quality at Point of Net-Vapour Generation for Constant Pressure and Mass-Flux Conditions.

small boiling-number region, while overprediction is observed for large boiling-number values. The scattering among these data appears to be a function of inlet temperature. This was also shown by Snoek and Leung [1986] in their analysis of experimental data for the point of net vapour generation in a string of 37-element bundles. They correlated their data with the boiling number and introduced two additional terms which are a function of inlet quality. While the predictions of their correlation agreed reasonably well with their experimental data, their correlation is not suitable for computer-code analysis, which is based solely on local conditions.

Further analysis of the point of net-vapour generation is not attempted, since the focus of this study is on the effect of heating on frictional pressure drop. The best-fit equation described above will be used in a pressure-drop analysis to be presented later. While this introduces some

uncertainty to the analysis of pressure-drop data with low inlet quality, its effect on the overall conclusion is not significant. This is because the data of low inlet quality cover only a narrow range of conditions and the test section remains mostly in the subcooled nucleate-boiling region.

9.4 BOILING TWO-PHASE FLOW

The frictional pressure drop increases sharply (see Figure 9.3) once the point of net-vapour generation is exceeded (i.e., $x_{th} > x_{NVG}$). This increase is mainly caused by:

i) the reduction in flow area for the liquid phase, due to the large volume occupied by the vapour bubbles,
ii) the increase in bulk-fluid velocity, as a result of volume expansion and momentum exchange with the bubbles,
iii) the increase in velocity gradient at the near-wall region, due to the departure of vapour bubbles, and
iv) the increase in interfacial shear stress, due to the increase in interfacial area.

The influence of these factors on frictional pressure drop, however, depends strongly on the flow pattern encountered inside the channel. For example, the second and third factors may be more dominant in bubbly flow, while the fourth factor is crucial in annular flow. At high flows, both the slug and churn flow patterns are either not encountered or occur only over a small range of qualities. Wispy-annular flow is the most common type of flow pattern, especially for saturated flow boiling. Previous studies have indicated that frictional pressure drop generally increases with increasing heat flux in bubbly flow [Tarasova et al., 1965, 1966]. In wispy-annular flow, the frictional pressure-drop gradient with respect to heat flux (or quality) is reduced, compared to the gradient in bubbly flow. This is due to the decrease in interfacial shear stress and velocity gradient in the near-wall region as the vapour phase consolidates in the core of the channel.

9.4.1 FLOW PATTERNS

Flow patterns and their boundaries were not measured in this experiment, because of the non-existence effective measuring techniques for a hostile high-pressure steam-water environment. They are estimated with flow pattern maps.

Two different types of flow-pattern maps are available for vertical two-phase flow (see Section 3.1). The most general one was introduced by Hewitt and Roberts [1969] (Figure 3.5), who present the flow patterns as functions of liquid and vapour momentum flux ($\rho_i\ j_i^2$, where j_i is the superficial velocity of phase i). It was derived with flow-pattern data obtained in low-pressure air-water and high-pressure steam-water (using both heated and unheated channels) experiments. Although it is general in nature, the mass quality must be calculated empirically to obtain the momentum fluxes of a non-equilibrium steam-water flow inside a heated channel. Another type of flow-pattern map shows the transition as a function of thermodynamic quality and mass flux [Bennett et al., 1965, Bergles et al., 1968]. It was derived for flow inside a heated channel, but is restricted to specific geometry and pressure. Until now, this type of flow-pattern map has not been available for the present geometry and range of conditions. While both types of flow-pattern map have their advantages and deficiencies, the one developed by Hewitt and Roberts is often recommended [Collier, 1981, Hewitt, 1982]. Based on the Hewitt and Roberts map, the present experiment covered a wide range of flow patterns (Figure 9.11).

9.4.2 FRICTIONAL PRESSURE DROP

The two-phase frictional pressure drop in flow boiling is investigated in detail, although the total pressure drop (which includes all three components) was measured. It is calculated by subtracting the pressure drops due to acceleration and gravity from the total (measured) pressure drop (Equation (9.3)). As indicated in Section 9.1.3, the separated-flow model is used to calculate the components due to acceleration (Equation (9.4)) and gravity (Equation (9.5)).

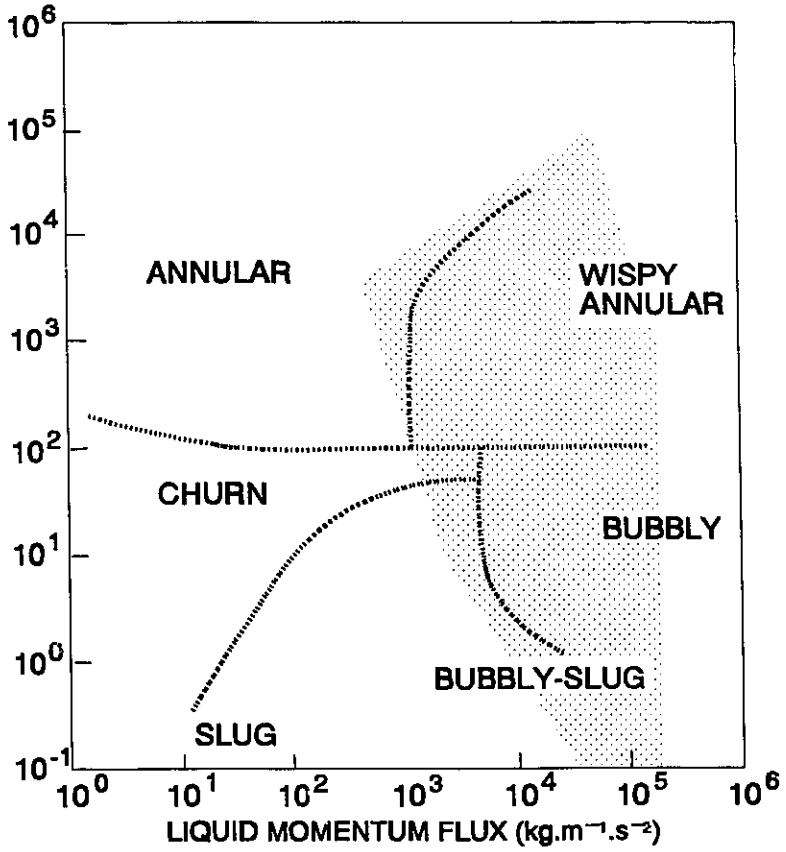

Figure 9.11: Flow Patterns Covered in the Present Experiment (Shaded Area).

The two-phase frictional pressure drop is also presented in terms of the two-phase multiplier

$$\phi_{lo}^2 = \left(\frac{\Delta P_{tp}}{\Delta P_{lo}} \right)_f \tag{9.12}$$

where ΔP_{tp} is the two-phase frictional pressure drop in kPa and ΔP_{lo} is the single-phase frictional pressure drop, in kPa, assuming the total flow is liquid at the bulk-fluid temperature. Various effects on the two-phase multiplier in a heated channel are examined in the following sections, i.e., heat flux, inlet quality, mass flux, system pressure, vapour-weight quality and void fraction. They are shown primarily as a function of thermodynamic quality.

9.4.2.1 EFFECT OF HEAT FLUX

Pre-Dryout Heat-Transfer Regions

The measured (total) and calculated frictional pressure drops are shown in Figure 9.12 for constant inlet conditions and varying heat fluxes. Note that each point represents a pressure-drop datums for an average thermodynamic quality over one measuring section, and every set of (same) symbols represents the pressure drops of five measuring sections along the test section for the same heat flux. They are joined with lines to indicate the effect of heat flux on pressure drop. To avoid overcrowding, the symbols for various heat fluxes are not presented. The range

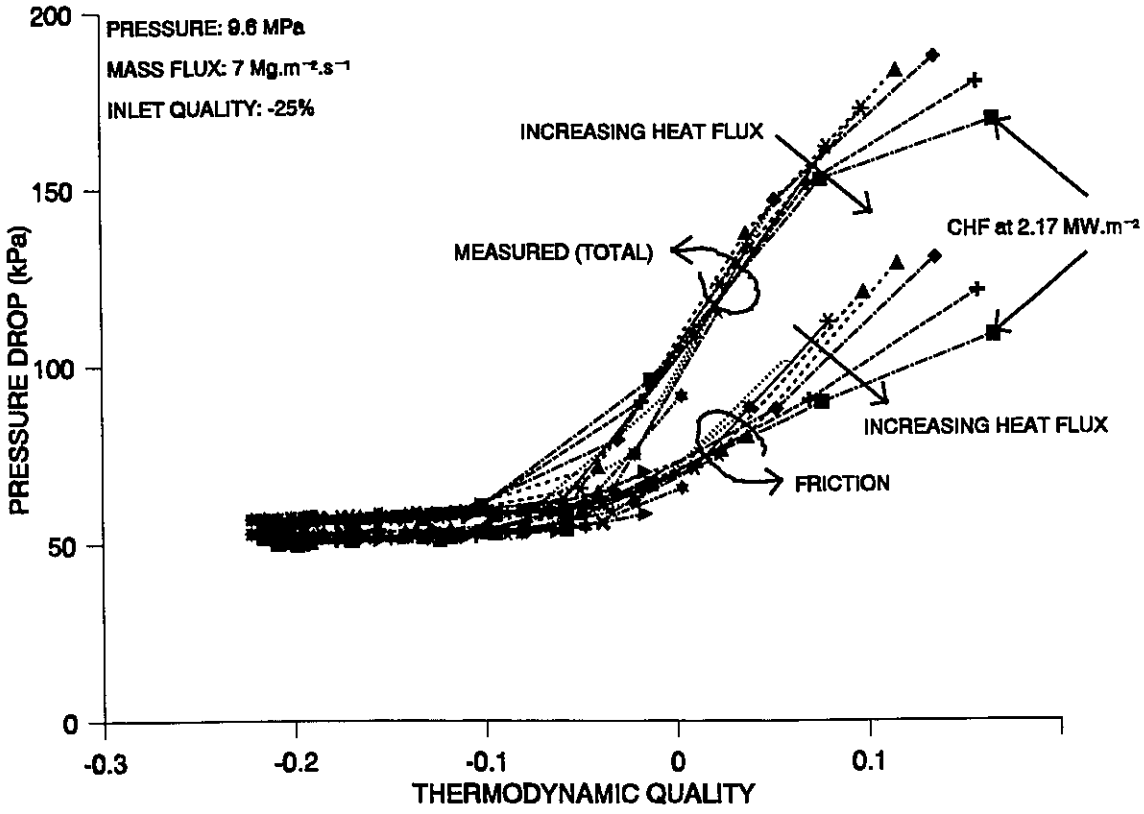

Figure 9.12: Effect of Heat Flux and Thermodynamic Quality on Measured and Frictional Pressure Drops.

of heat fluxes covered in this test is from 0 to 2.11 $MW.m^{-2}$ at an increment of about 0.11 $MW.m^{-2}$. A critical heat flux condition is reached at the end of the test section at a heat flux of 2.17 $MW.m^{-2}$.

The same trend of pressure drops as presented in Figures 9.1 to 9.3 is shown, with a much higher measured (total) than frictional pressure drop. A larger variation is also shown in frictional rather than total pressure drop, with increasing thermodynamic quality. At high qualities, a decreasing trend of pressure drop is shown with increasing heat flux. In both the measured and frictional pressure drops, a local maximum pressure-drop point is exhibited before the occurrence of dryout (i.e., critical heat flux conditions). The specific trend of the heat-flux effect on frictional pressure drops cannot be examined clearly at low qualities, due to the large amount of data included in this figure. A detailed discussion is provided in the next figure, which presents only the frictional pressure drop (in terms of two-phase multiplier).

Figure 9.13 shows the two-phase multipliers as a function of thermodynamic quality for the same heat-flux variation as shown in Figure 9.12. In single-phase flow, a decrease in the two-phase multiplier is shown for increasing heat flux at the same quality. However, the difference is not significant between various heat-flux values. Nucleation starts at a thermodynamic quality of about -10%, depending on heat flux, and an increase in the two-phase multiplier is shown with increasing heat flux in nucleate boiling (bubbly-flow regime). As the thermodynamic quality is increased, an opposite trend, where two-phase multiplier decreases with increasing heat flux, is shown. The transition occurs at a quality close to 0. A local maximum two-phase multiplier is displayed at the two downstream measuring sections. In either section, it occurs at about the same heat flux, but at different average qualities.

Two-phase multipliers obtained at low inlet-subcooling (close to saturation) conditions are shown in Figure 9.14 for various heat fluxes and thermodynamic qualities. (As shown previously in Figures 9.12 and 9.13, both the frictional pressure drop and two-phase multiplier have the same parametric trend with respect to heat flux.) The heat flux varies from 0 to 1.7 $MW.m^{-2}$, and the critical heat flux occurs at 1.71 $MW.m^{-2}$. Due to the low inlet subcoolings, boiling begins at a

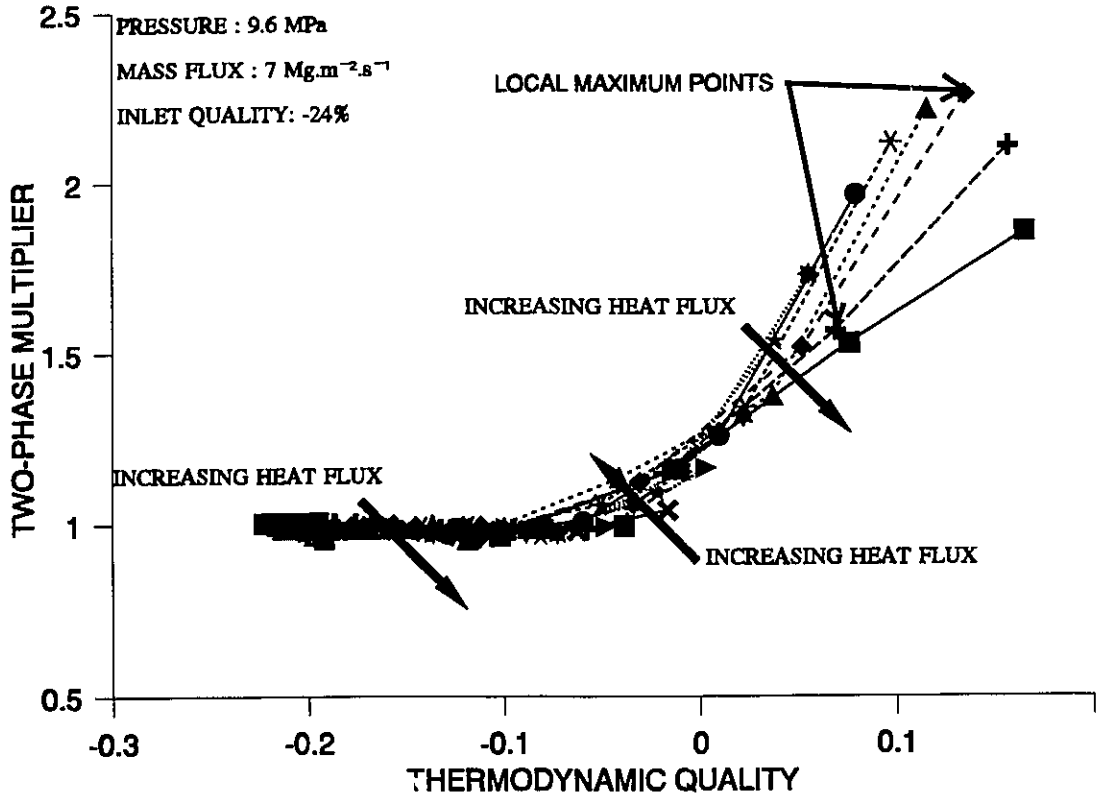

Figure 9.13: Effect of Heat Flux and Thermodynamic Quality on Two-Phase Multipliers.

location close to the inlet end of the test section. Therefore, single-phase flow over a complete measuring section is not encountered at any conditions with heating. Over the range of thermodynamic qualities approximately from -0.02 to 0.03, an increase in the two-phase multiplier is shown for a constant thermodynamic quality with increasing heat flux. This corresponds mostly to the subcooled and saturated nucleate-boiling regions. The two-phase multiplier decreases with increasing heat flux at high thermodynamic qualities (forced convective evaporation region). For the present conditions, three measuring sections display a maximum two-phase multiplier.

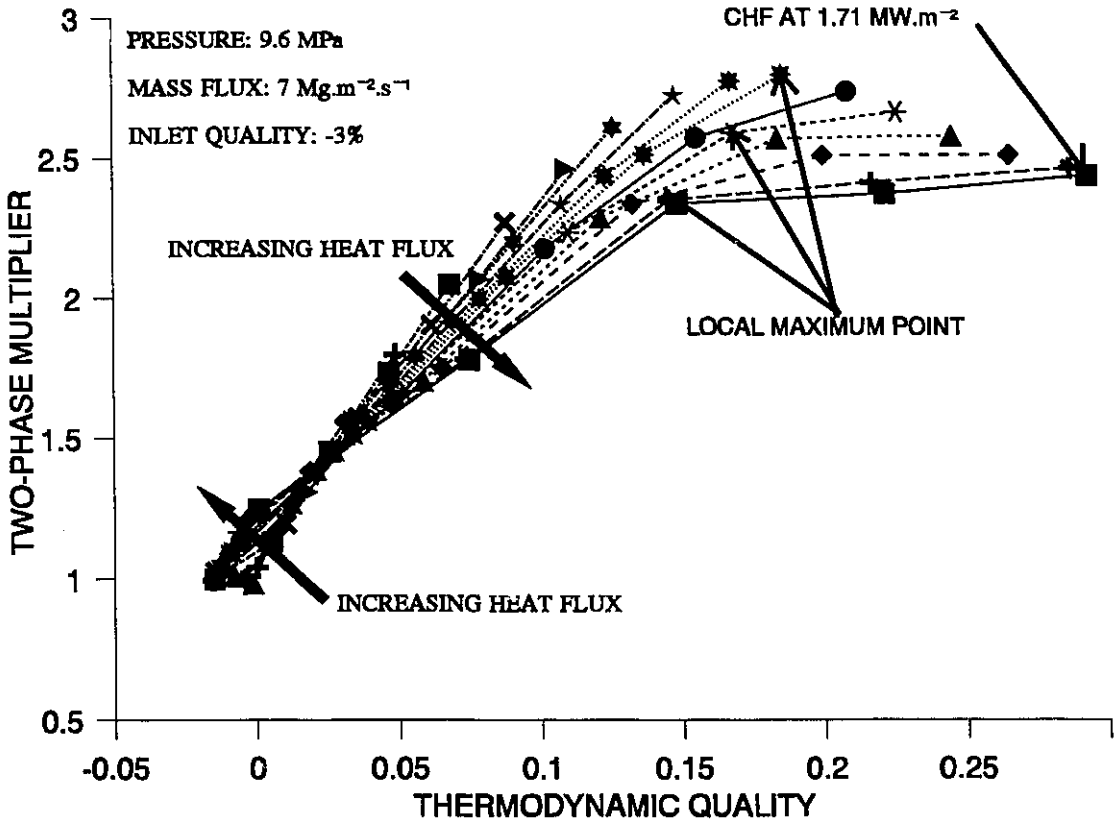

Figure 9.14: Effect of Heat Flux on Two-Phase Multiplier for Low Inlet-Subcooling Conditions.

Post-Dryout Heat-Transfer Region

With a further increase in heat flux, the dryout condition expands upstream from the outlet end of the test section. A significant difference in the phase distribution between pre-dryout and post-dryout (PDO) conditions is the phase in contact with the heated surface. It is the liquid phase that is in contact with the surface at pre-dryout conditions, but the vapour phase at post-dryout conditions. The low viscosity of vapour considerably reduces the wall shear stress and hence the frictional pressure drop.

The frictional pressure drop at post-dryout conditions can be investigated up to the 650°C surface-temperature limit. For tests with high inlet subcoolings, a slight increase in heat flux beyond the critical condition resulted in high PDO temperatures. Therefore, only a narrow range

of post-dryout conditions are encountered for high inlet subcoolings inside the channel. Furthermore, these data may not cover the complete measuring section. Figure 9.15 illustrates the two-phase multipliers for conditions similar to those of Figure 9.13, but including data at high heat fluxes (post-dryout conditions up to 2.22 $MW.m^{-2}$). The data obtained at pre-critical heat-flux conditions were repeat tests and are used to confirm previous results shown in Figure 9.13. Good agreement is observed between these two tests (i.e., Figures 9.13 and 9.15); the same trend of two-phase multipliers is shown. Beyond the critical heat flux, the two-phase multiplier decreases continuously with increasing heat flux (or quality). The gradient of two-phase multiplier with respect to quality is steeper for post-dryout than pre-dryout conditions.

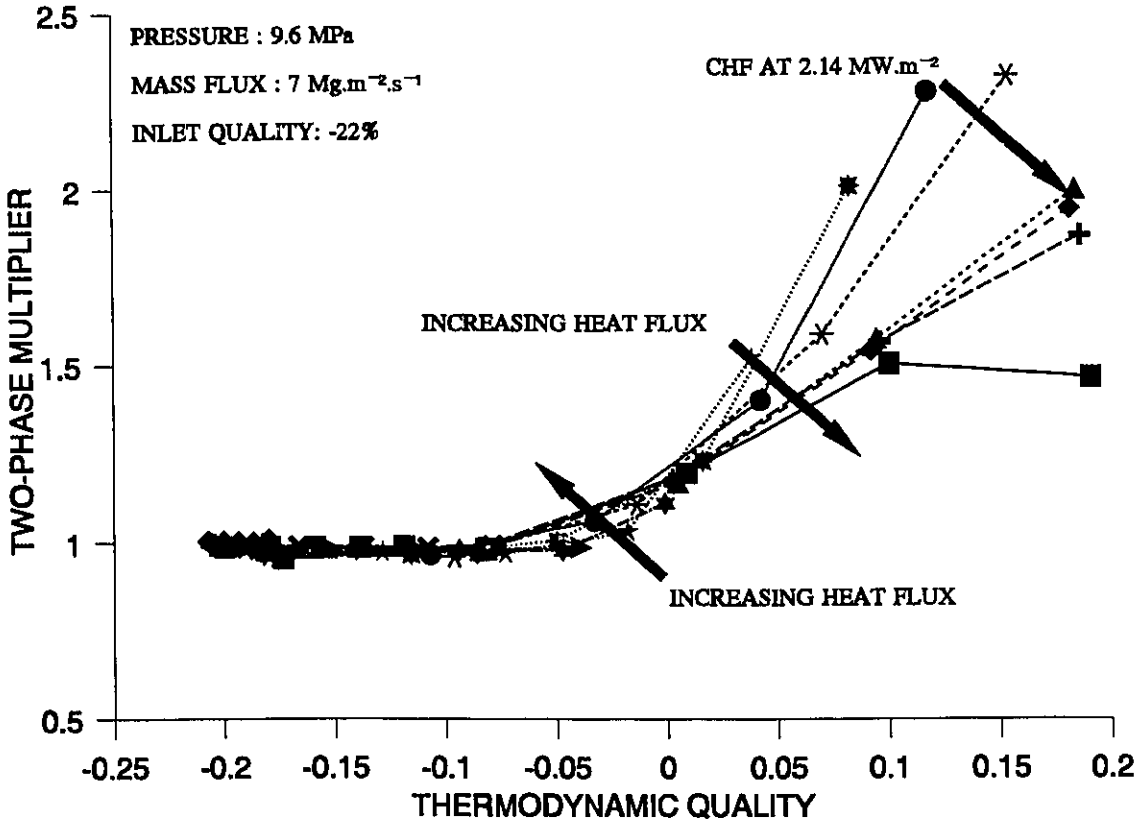

Figure 9.15: Two-Phase Multiplier at Both Pre- and Post-Dryout Conditions with High Inlet Subcooling.

A much wider range of post-dryout conditions (with heat fluxes up to 2.18 $MW.m^{-2}$) can be covered with low inlet subcoolings before the maximum surface temperature of 650°C is reached (Figure 9.16). The change in the gradient of the two-phase multiplier is clearly shown at conditions before and after the critical heat flux for the three downstream measuring sections. This suggests that a significant fraction of the channel was dry and under the post-dryout conditions. A minimum two-phase multiplier, signifying complete dryout of the heated surface over the measuring section, is displayed at two downstream sections. Beyond the minimum point, the two-phase multiplier increases with increasing heat flux. It is caused by an increase in vapour velocity.

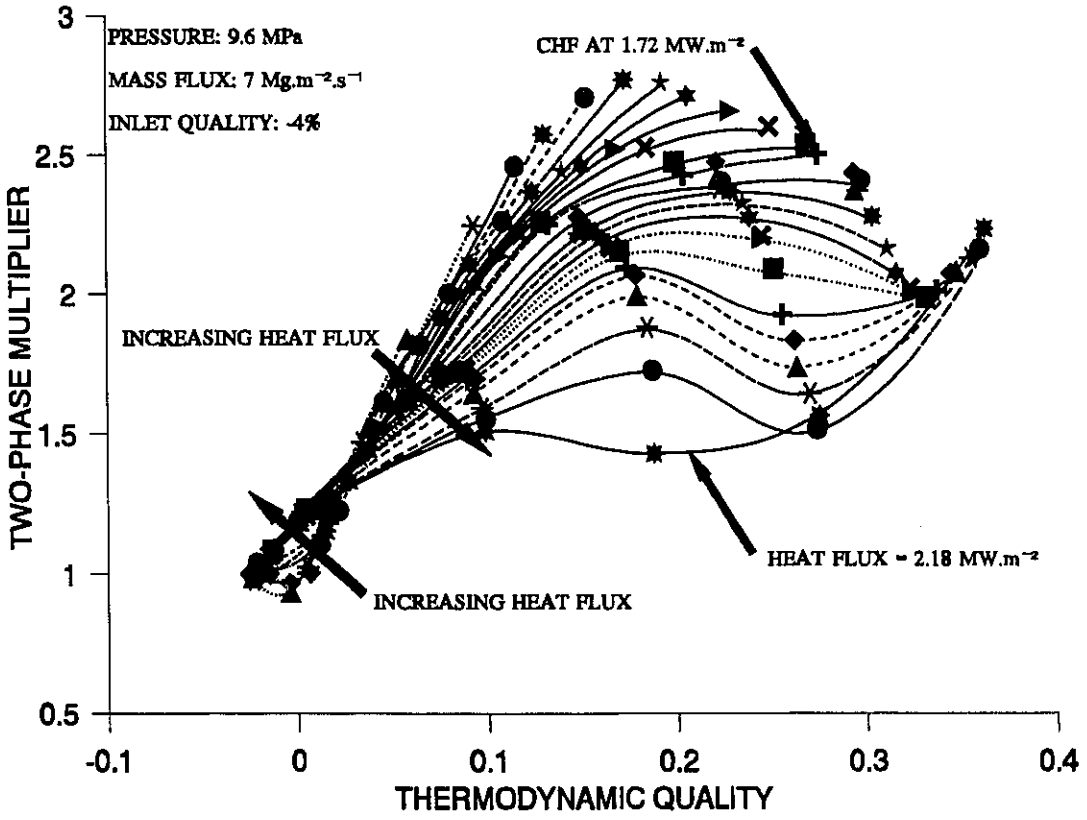

Figure 9.16: Two-Phase Multiplier at Both Pre- and Post-Dryout Conditions with Low Inlet Subcooling.

The thermocouple readings obtained along the test section also confirm the existence of post-dryout conditions over the three downstream sections. Figure 9.17 shows the surface-temperature distributions for heat fluxes from 1.72 (CHF) to 2.18 $MW.m^{-2}$. At heat fluxes lower than 1.72 $MW.m^{-2}$ (corresponding to the pre-dryout heat-transfer region), the surface temperatures are stable and remain close to the saturation temperature. Since the thermodynamic qualities at various thermocouple locations vary with heat flux, the dryout propagation is difficult to examine in a plot of surface temperature versus thermodynamic quality. Therefore, the temperature distribution is shown as a function of axial distance in Figure 9.17, to illustrate the propagation of the dryout region with increasing heat flux.

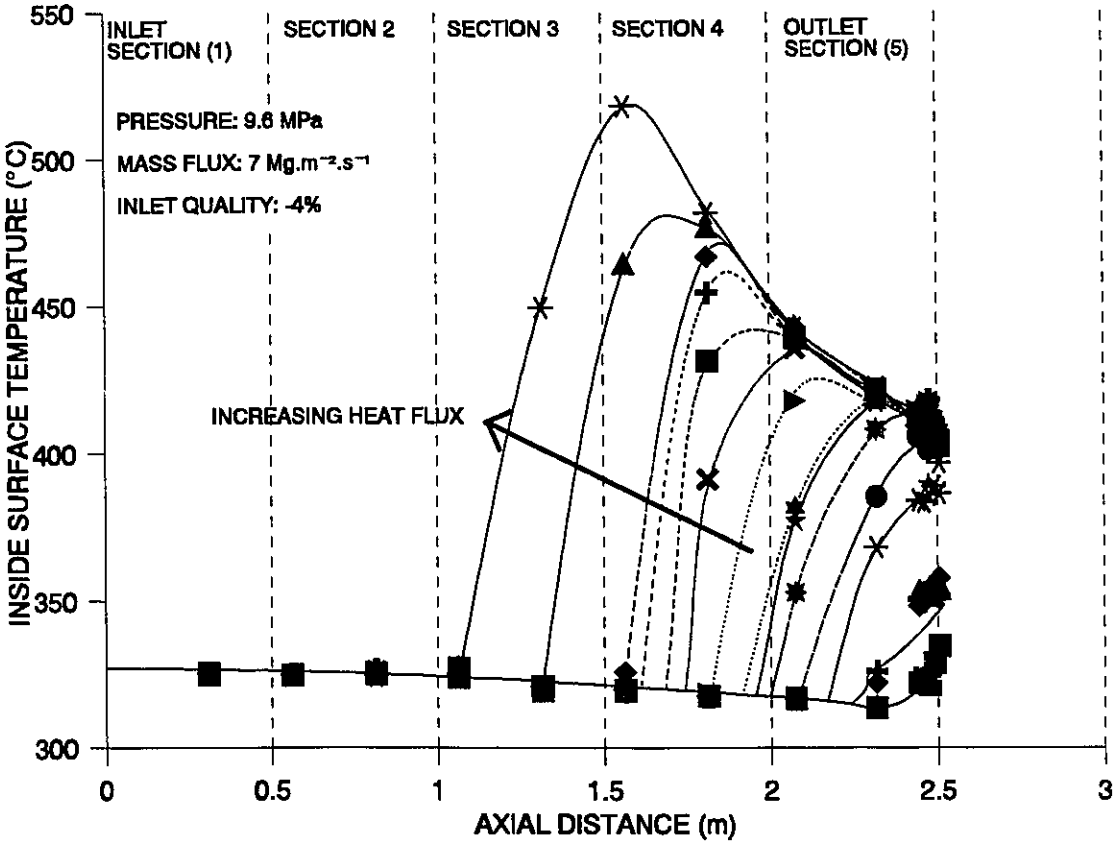

Figure 9.17: Inside Surface-Temperature Distributions at Post-Dryout Conditions.

For small increases in heat flux beyond CHF, a sharp rise in surface temperature was noted at a few thermocouples located at the outlet end. With increasing heat flux, however, the dryout region propagated upstream, and high temperature was detected by more upstream thermocouples. The maximum surface temperature becomes more and more severe as the locations of the upstream thermocouples experience dryout. This is primarily due to the high heat fluxes and low vapour quality leading to a lower vapour velocity and less efficient heat-transfer rate. Hence, the surface temperature increases drastically. As the vapour quality increases toward the downstream end, the surface temperature is reduced and becomes stable. At high heat fluxes, a stable surface temperature of about 400°C is recorded by the downstream thermocouples for the present conditions.

A similar trend of the two-phase multiplier is shown with respect to heat flux for other conditions. The effect is generally more noticeable at high-flow and low inlet-subcooling conditions. As the flow is decreased, the maximum pressure-drop point approaches the critical heat-flux point.

An interesting phenomenon was observed at a mass flux of 9.9 $Mg.m^{-2}.s^{-1}$. At these conditions, the heat flux varies from 0 to 3.07 $MW.m^{-2}$. As shown in Figure 9.18, the two-phase multiplier decreases sharply at both Sections 3 and 4, but remains relatively constant at the outlet section (Section 5). The initial dryout (at a heat flux of 3.06 $Mg.m^{-2}.s^{-1}$) was observed at a distance of approximately 1.75 m from the inlet (at the fourth pressure-drop measuring section (Section 4)), rather than at the outlet of the test section. This phenomenon is encountered mainly at high-flow conditions, and is referred to as an upstream dryout, where the surface of a uniformly heated tube experiences dryout at a location upstream of the exit (where initial dryout often occurs). Groeneveld [1972] studied the upstream-dryout phenomena and offered an explanation from a thermodynamic and heat-transfer point of view. The present author, however, anticipates that the hydrodynamic aspect may be the dominant factor controlling this phenomena. Following the hydrodynamic-dryout mechanism introduced by Beattie [1974] for adiabatic flow, the liquid film is depleted rapidly, due to the high shear force of the vapour. With the high turbulent level at the interfacial boundary, the high-velocity vapour induces a high wave, with a trough cutting

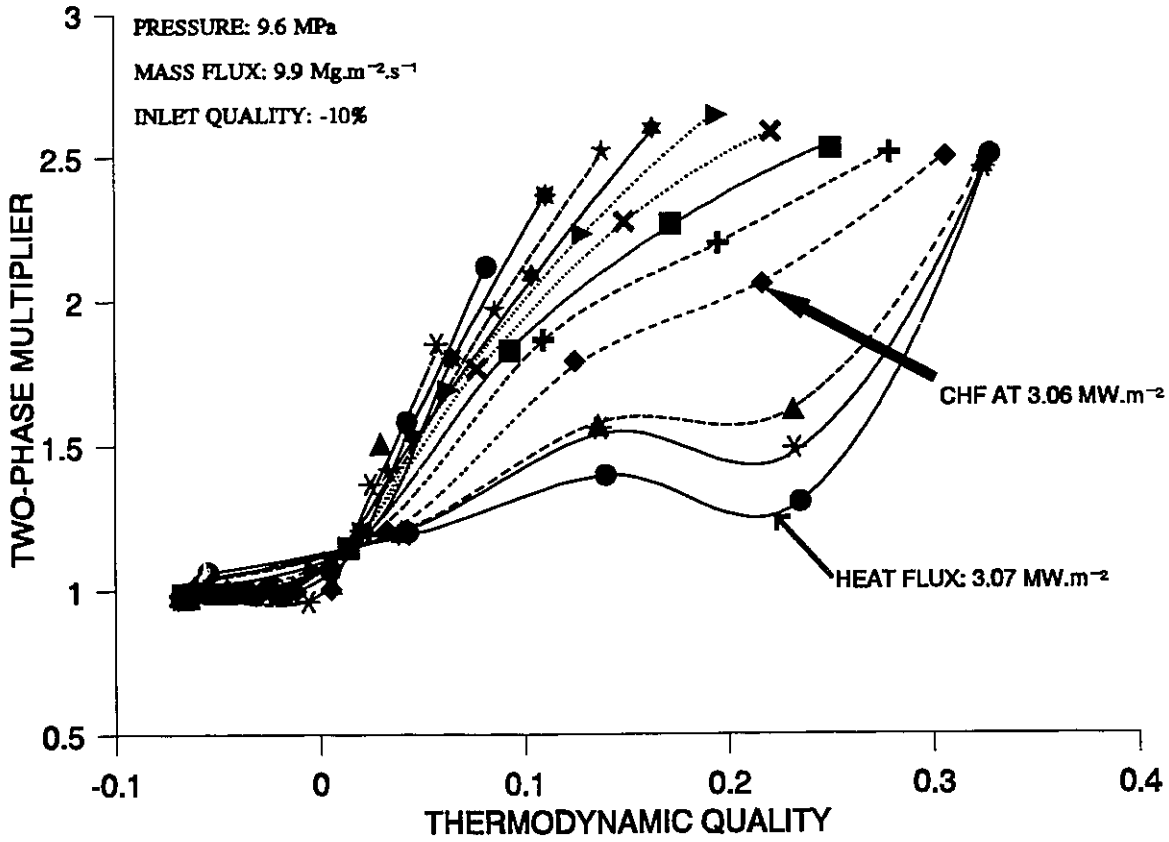

Figure 9.18: Two-Phase Multiplier at Conditions Where Upstream Dryout is Encountered.

deeply into the liquid film. If the velocity is high enough, the thin liquid film can be either (i) stripped or (ii) evaporated away from the surface, creating a dry spot. At the downstream section of this dry spot, the liquid film is less affected, since the amplitude of waves is reduced, due to the thinning of liquid film.

The corresponding inside surface-temperature distributions at both dryout and post-dryout conditions are shown in Figure 9.19. A rise in surface temperature, indicating dryout, is shown at locations between 1.5 and 2 m from the inlet. Based on the data points, the dryout region covers both Sections 3 and 4. This agrees with the rapid decrease in two-phase multiplier as shown in Figure 9.18. Forced convective evaporation is resumed beyond the dryout region at the outlet section (Section 5), and the two-phase multiplier remains high.

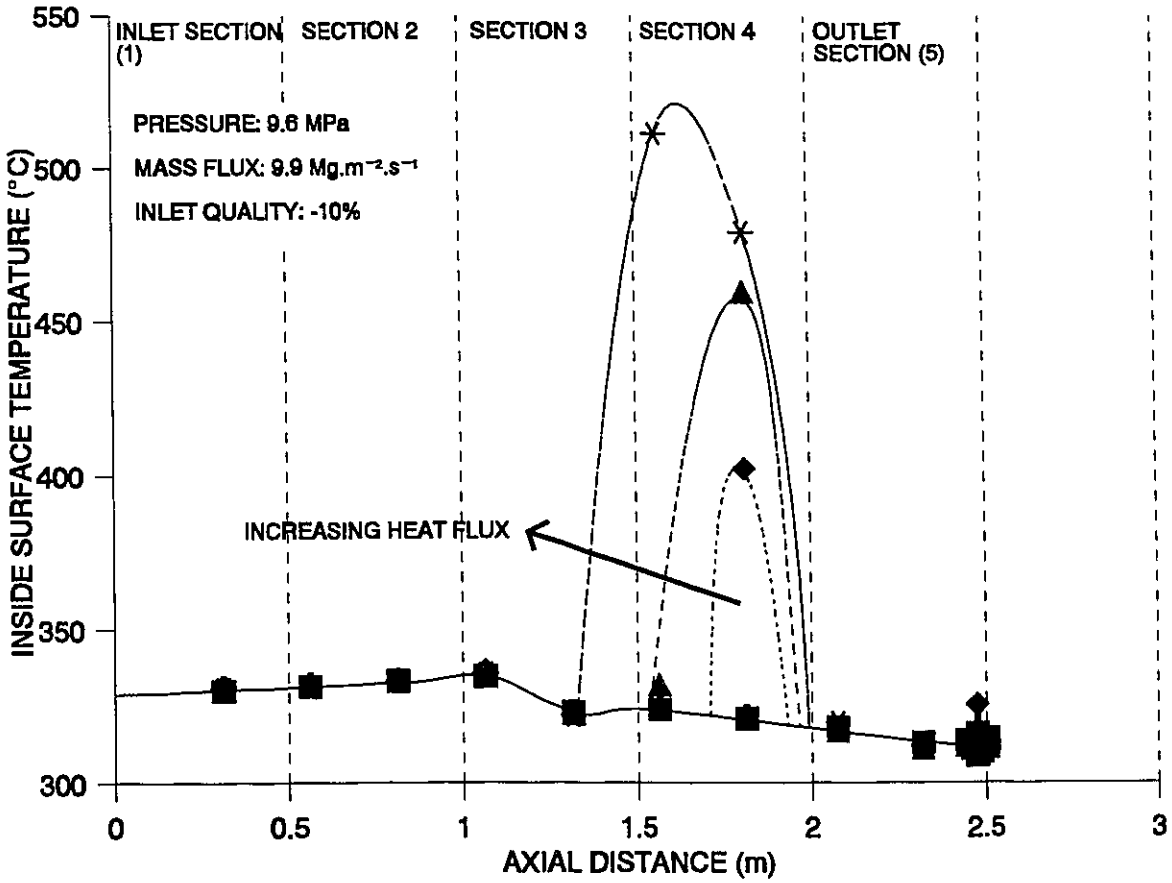

Figure 9.19: Inside Surface-Temperature Distributions for Upstream Dryout Conditions.

9.4.2.2 EFFECT OF INLET QUALITY

The inlet quality is a dimensionless fluid enthalpy at the test-section inlet. As indicated in Section 9.2, it appears to be a factor influencing the point of net vapour generation. Its effect on the frictional pressure drop (in term of two-phase multiplier) is examined in this section.

Figure 9.20 illustrates the total (measured) and frictional (calculated) pressure drops for various inlet qualities at constant pressure, mass flux and heat flux. Both pressure drops display the same parametric trend and do not seem to be affected strongly by the inlet quality. The same trend is shown in Figure 9.21, which displays the variations in two-phase multiplier.

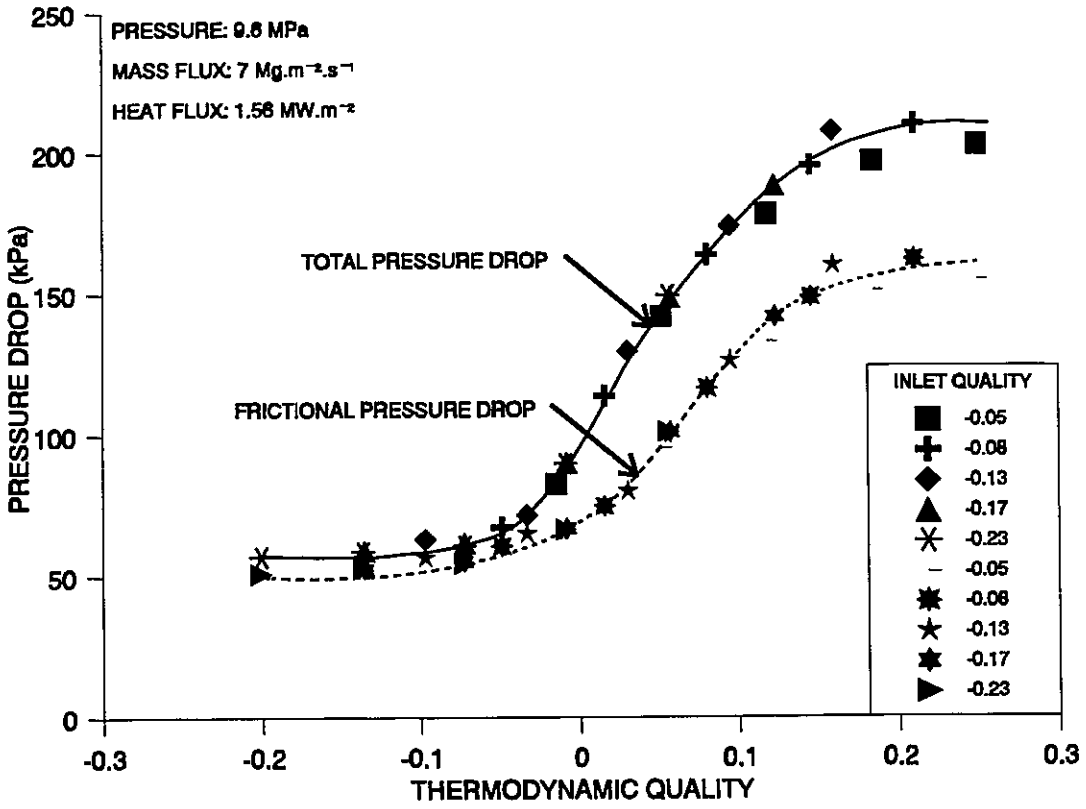

Figure 9.20: Total and Frictional Pressure Drops for Various Inlet Qualities at High Flows.

The effect of inlet quality on two-phase multiplier is also insignificant at medium-flow conditions as shown in Figure 9.22.

Figure 9.23 shows the comparison of the two-phase multiplier for various inlet qualities at both pre-dryout and post-dryout conditions. Similar to the trends shown in Figures 9.21 and 9.22 for pre-dryout conditions, there is no effect of inlet quality on the two-phase multiplier at the post-dryout regions. However, the data scatter increases in the transition region between pre-dryout and post-dryout conditions. This is probably caused by a small fluctuation in the mass flow rate, which can have an effect on the dryout point. The effect of the mass flow rate on pressure drop is examined in the next section.

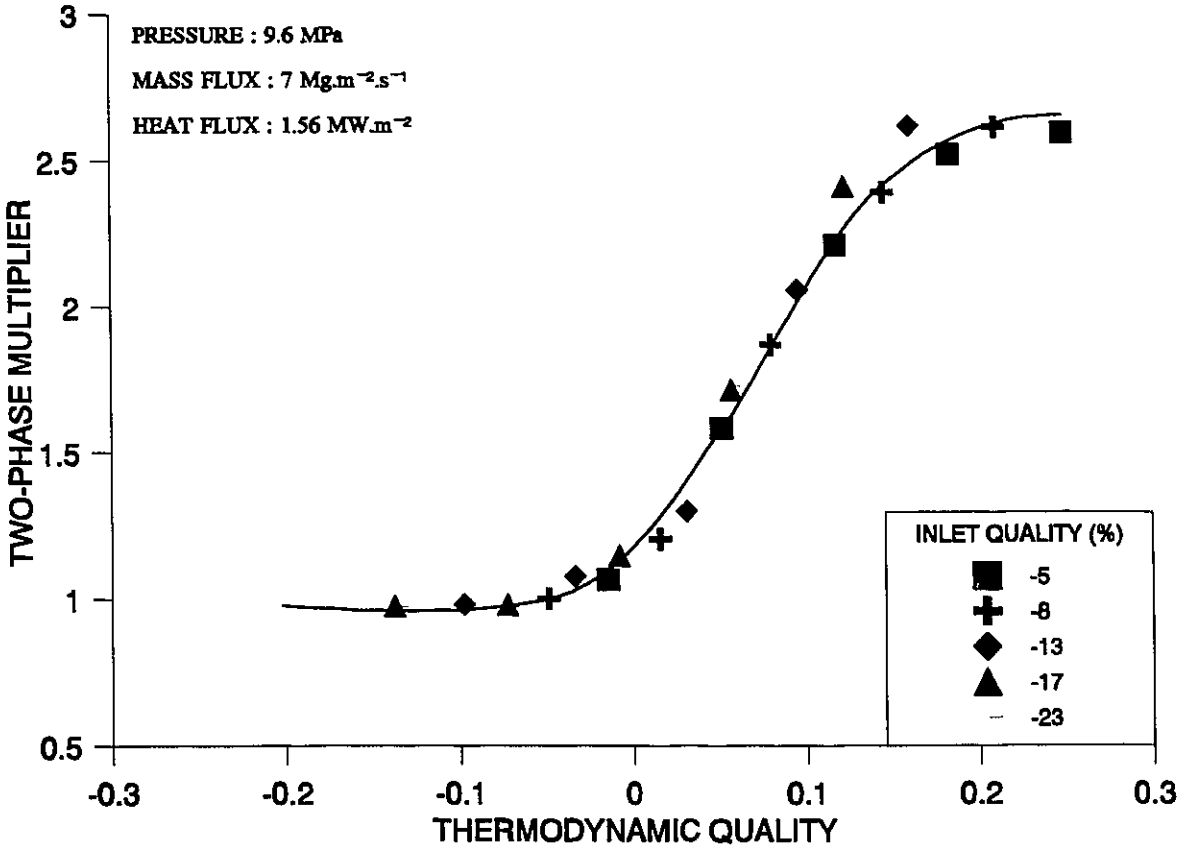

Figure 9.21: Effect of Inlet Quality on Two-Phase Multiplier for High Flows at Pre-Dryout Conditions.

The absence of any significant effect of inlet quality on the two-phase multiplier is also noted for other flow conditions. Therefore, it will not be further discussed.

9.4.2.3 EFFECT OF MASS FLUX

The two-phase pressure drop (or multiplier) is affected significantly by mass flux, primarily due to its strong influence on flow-pattern transition. Therefore, it is difficult to compare and identify this effect. For a heated channel, the complexity increases due to the change in the heat-transfer mode (this is also a change in flow pattern) with varying mass fluxes. To illustrate the differences, the two-phase pressure drop and two-phase multiplier are examined for various heat-

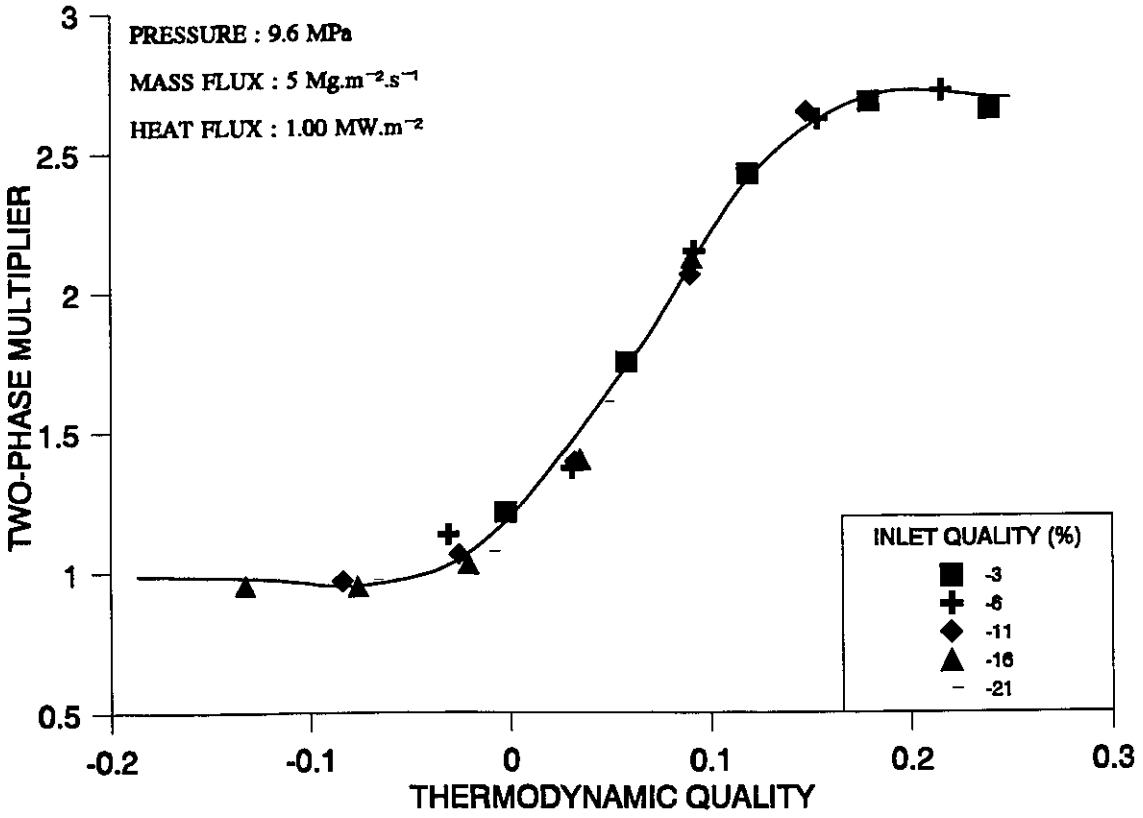

Figure 9.22: Effect of Inlet Quality on Two-Phase Multiplier for Medium Flow Rates at Pre-Dryout Conditions.

flux values. This is necessary because high heat-flux conditions are not feasible at low flow rates, due to the limitation in surface temperature.

The total (measured) pressure drops for various mass fluxes are shown in Figure 9.24. To avoid overcrowding, the calculated frictional pressure drops are not presented. As shown in previous figures (e.g., Figure 9.3), the frictional pressure drop is generally smaller than, but follows the same trend as, the total pressure drop. As shown by all pressure-drop equations, the pressure drop increases significantly with increasing mass fluxes for the same thermodynamic quality. Due to the relatively low heat flux, the high mass-flux data (i.e., 6 and 7 $Mg.m^{-2}.s^{-1}$) cover only the single-phase and nucleate-boiling heat-transfer regimes. Both the pre-dryout and post-dryout conditions, on the other hand, are shown in the data of 1.2 $Mg.m^{-2}.s^{-1}$.

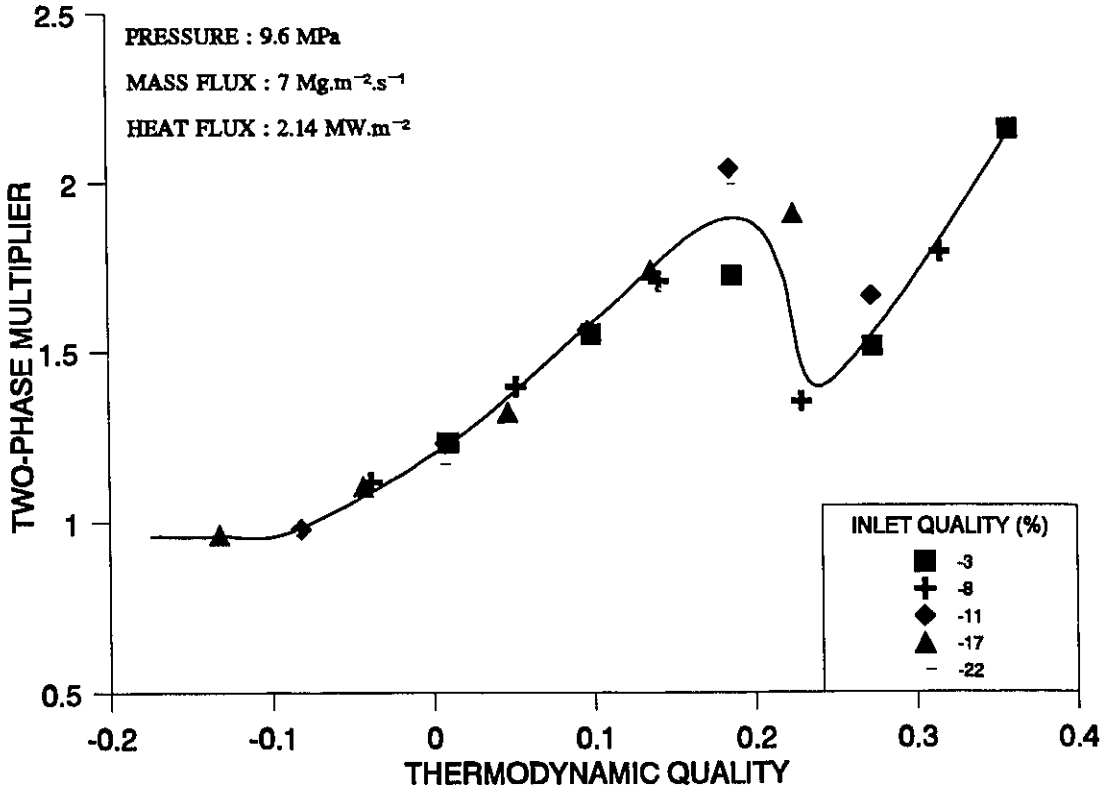

Figure 9.23: Effect of Inlet Quality on Two-Phase Multiplier for High Flows at Pre- and Post-Dryout Conditions.

Figure 9.25 shows the two-phase multiplier for the same conditions as in Figure 9.24. A different trend is presented for various mass fluxes. The two-phase multiplier is much larger for low mass fluxes. This is primarily caused by the relatively high two-phase frictional pressure drops, but small single-phase frictional pressure drops at low mass fluxes (i.e., 1.2 and 1.9 $Mg.m^{-2}.s^{-1}$). The two-phase frictional pressure drops at low mass fluxes, however, may have a high uncertainty, due to the following factors:

a) the simple approach may not be valid for calculating the pressure drops due to acceleration and gravity, which become comparable with the frictional component at low mass fluxes, and
b) the correlation for the onset of net vapour generation point is primarily derived for high mass flux conditions; this may delay the start of the two-phase region and lead to an underprediction of the pressure drop due to acceleration.

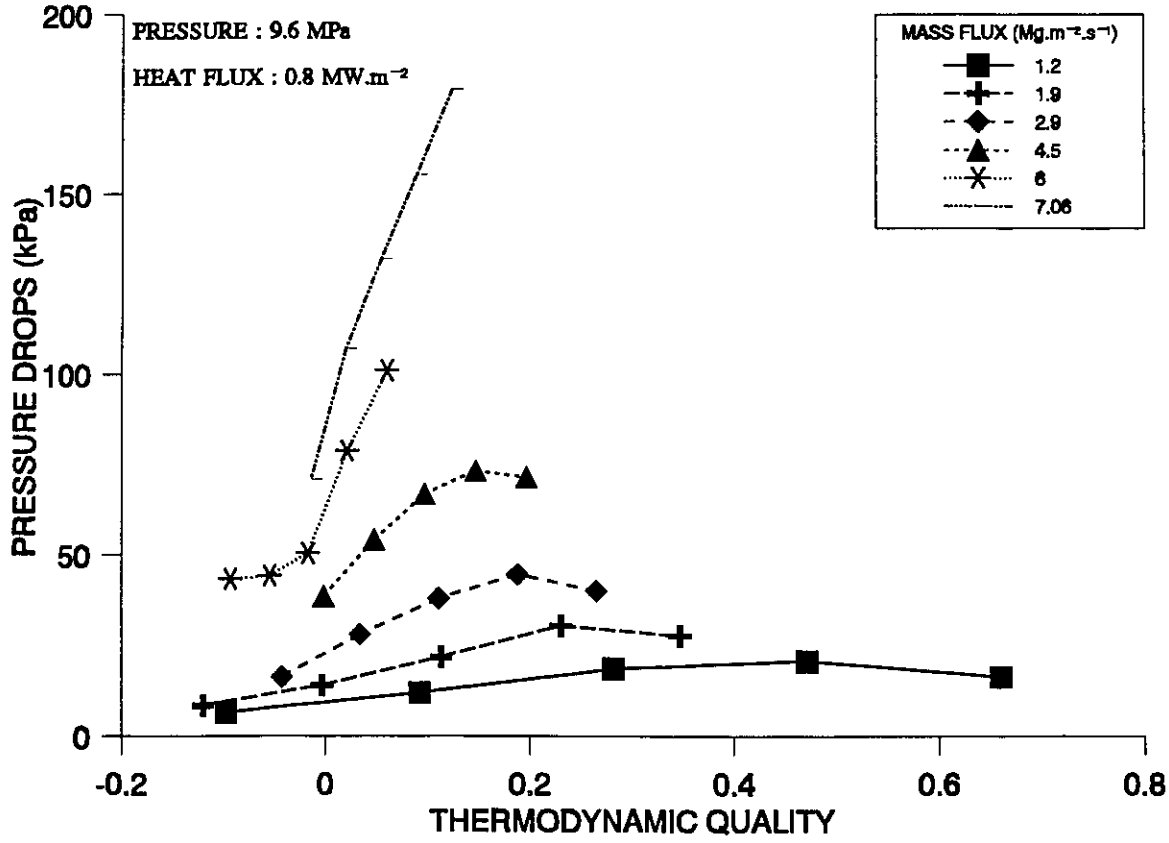

Figure 9.24: Measured Total Pressure Drops over the Test Section for Various Mass Fluxes.

Compared against the values at low flow rates, the variation in the two-phase multiplier becomes insignificant for high flow rates.

The pressure drops at various mass fluxes are shown in Figure 9.26 for a higher heat flux than was shown in Figure 9.24. As in Figure 9.24, the pressure drops increase with increasing mass flux. A large increase in pressure drop from 4.3 to 5.96 $Mg.m^{-2}.s^{-1}$ is shown at a quality of about 0.2. It is caused by the difference in the heat-transfer regime: the data with mass fluxes higher than 4.3 $Mg.m^{-2}.s^{-1}$ are pre-dryout data, while those of 4.3 $Mg.m^{-2}.s^{-1}$ are mainly post-dryout data.

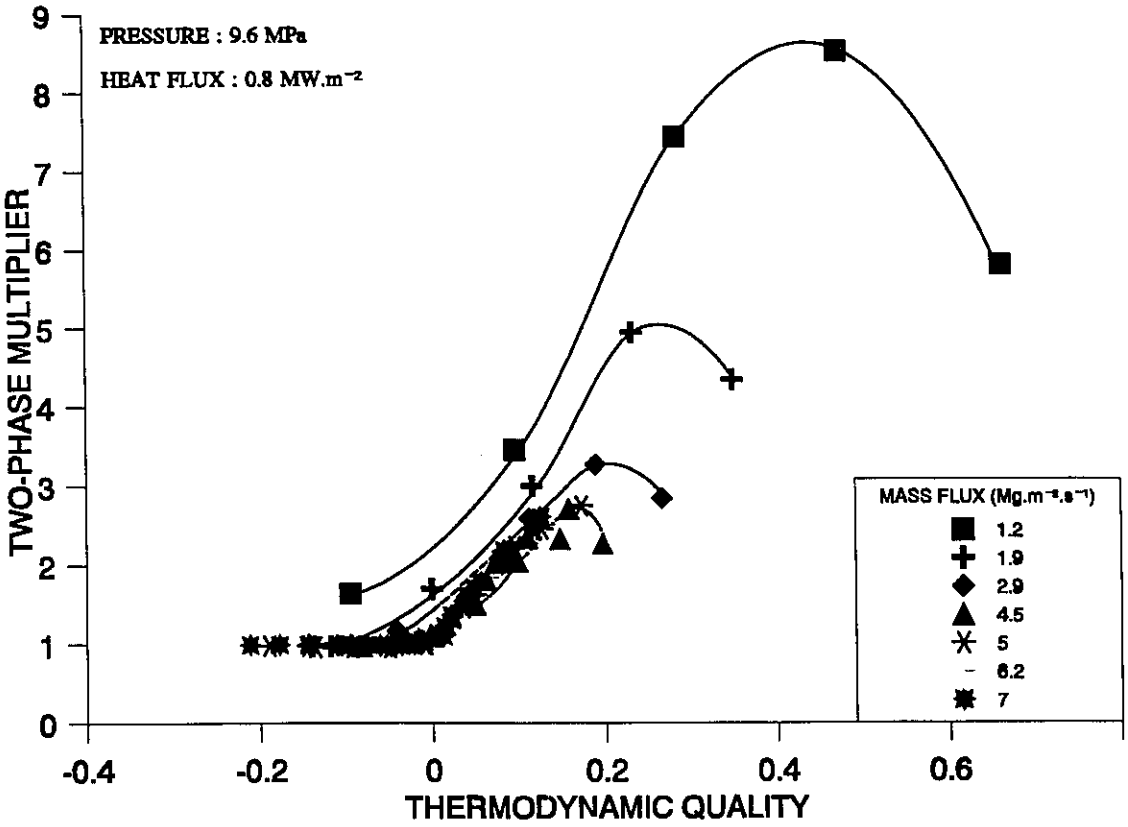

Figure 9.25: Effect of Mass Flux on Two-Phase Multiplier for Low Heat-Flux Conditions.

Figure 9.27 shows the two-phase multiplier with respect to thermodynamic quality. The effect of mass flux on the two-phase multiplier appears to be small for data in the same heat-transfer regime. This agrees with the trend observed in Figure 9.25 for high mass fluxes. However, when the two-phase multiplier for pre-dryout conditions is compared against that of post-dryout conditions, a large difference is shown. This is caused by the much smaller two-phase pressure drop for the post-dryout conditions. Similarly, the effect of mass flux on the two-phase multiplier is also small when only data obtained at post-dryout conditions are compared.

9.4.2.4 EFFECT OF SYSTEM PRESSURE

System pressure affects considerably the void fraction, which in turn has a strong influence on various components of pressure drop (see, for example, Martinelli and Nelson [1949] and Thom

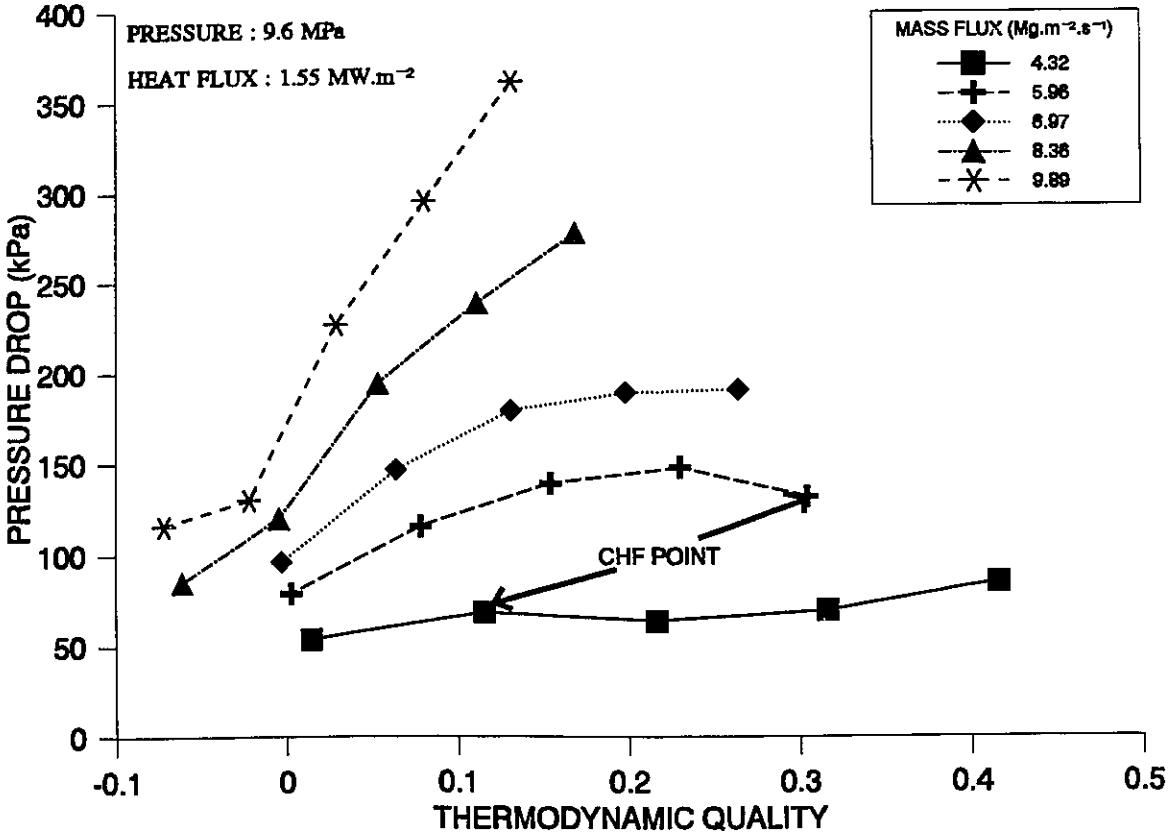

Figure 9.26: Measured Total Pressure Drops for Various Mass Fluxes at a Heat Flux of 1.55 $MW.m^{-2}$.

[1964]). The pressure drop is much higher at low system pressures, and the difference can be several orders in magnitude. This is primarily caused by the high vapour velocity and low vapour density that accelerate the liquid flow and result in an increase in wall shear stress at low system pressure.

In a heated channel, the effect of system pressure on pressure drop could be further complicated, due to the flashing phenomena, where an additional amounts of vapour are generated as a result of a reduction in saturation temperature with pressure drop along the channel (see Groeneveld [1973] and Shoukri [1983]). A rise in vapour quality generally increases the pressure drop. This phenomena, however, is not a significant factor for flow at high pressure.

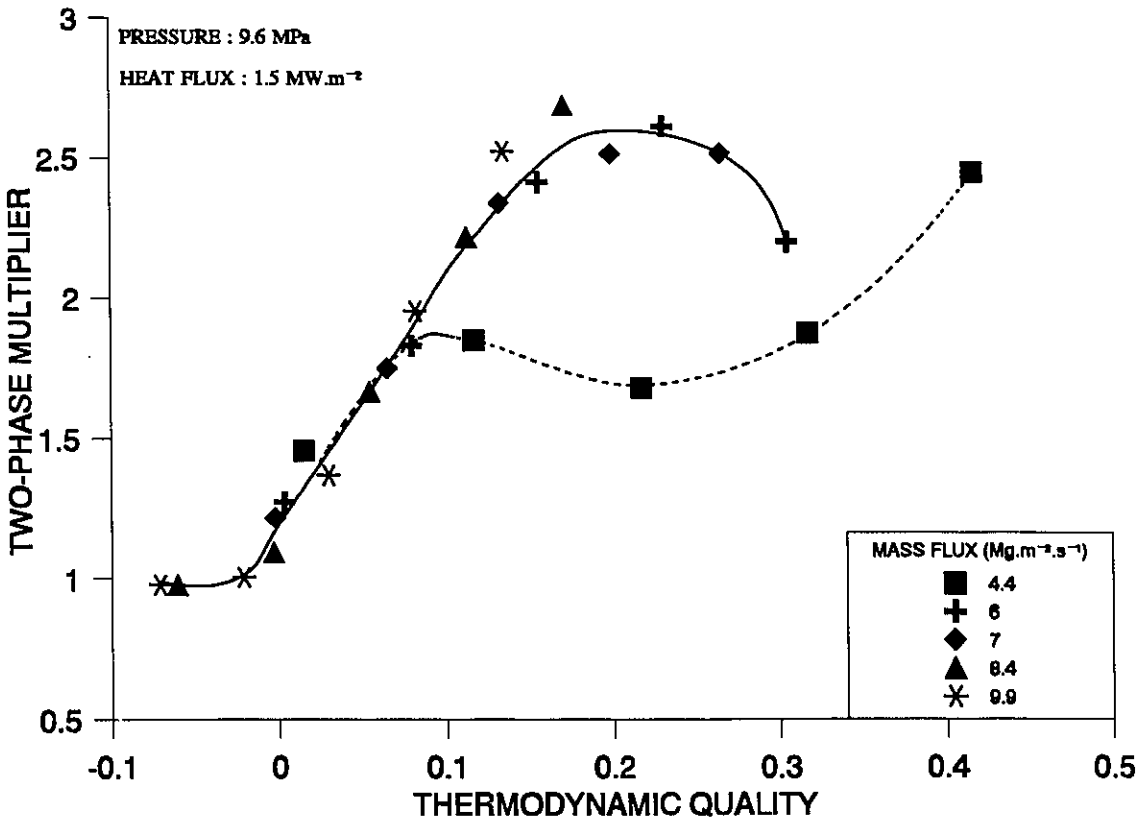

Figure 9.27: Effect of Mass Flux on Two-Phase Multiplier for Medium Heat-Flux Conditions.

The effect of system pressure on two-phase pressure drop (or two-phase multiplier) cannot be examined extensively in this study. This is because the test conditions are limited at pressures less than 9.6 MPa. Nevertheless, a qualitative parametric trend is illustrated.

Figure 9.28 shows the total (measured) pressure drop at various system pressures for a mass flux of 4.4 $Mg.m^{-2}.s^{-1}$. The total pressure drop is much larger at low than at high system pressures. This difference increases with increasing thermodynamic quality, and can be as much as 3 times between pressures (e.g., at $x_{th} = 0.1$). It is even more significant when the pre-dryout data are compared against the post-dryout data (e.g., at $x_{th} = 0.25$). Since only the pre-dryout data are available at the present conditions for low pressure, the difference in two-phase multiplier for post-dryout conditions cannot be examined.

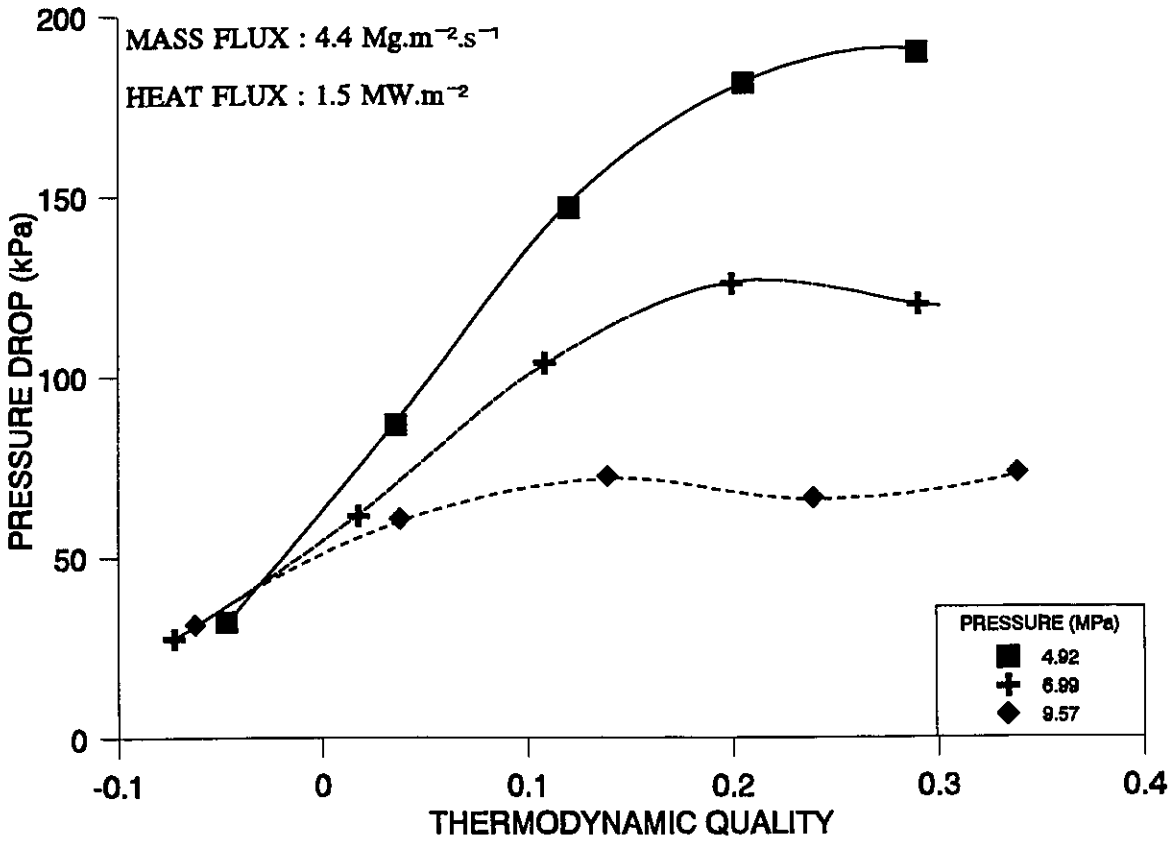

Figure 9.28: Measured Total Pressure Drop versus Thermodynamic Quality for Various Pressures at a Mass Flux of 4.4 $Mg.m^{-2}.s^{-1}$.

Figure 9.29 illustrates the effect of system pressure on the two-phase multiplier at the same conditions as in Figure 9.28. The same trend as in Figure 9.28 is shown with a much larger two-phase multiplier for lower system pressures. The difference in the two-phase multiplier increases with increasing thermodynamic quality.

Only a limited comparison of the two-phase multiplier can be made for post-dryout conditions at low pressure. It is shown in Figure 9.30, where post-dryout conditions have been achieved at high qualities for part of the measuring sections. The same trend of system pressure on the two-phase multiplier was again observed.

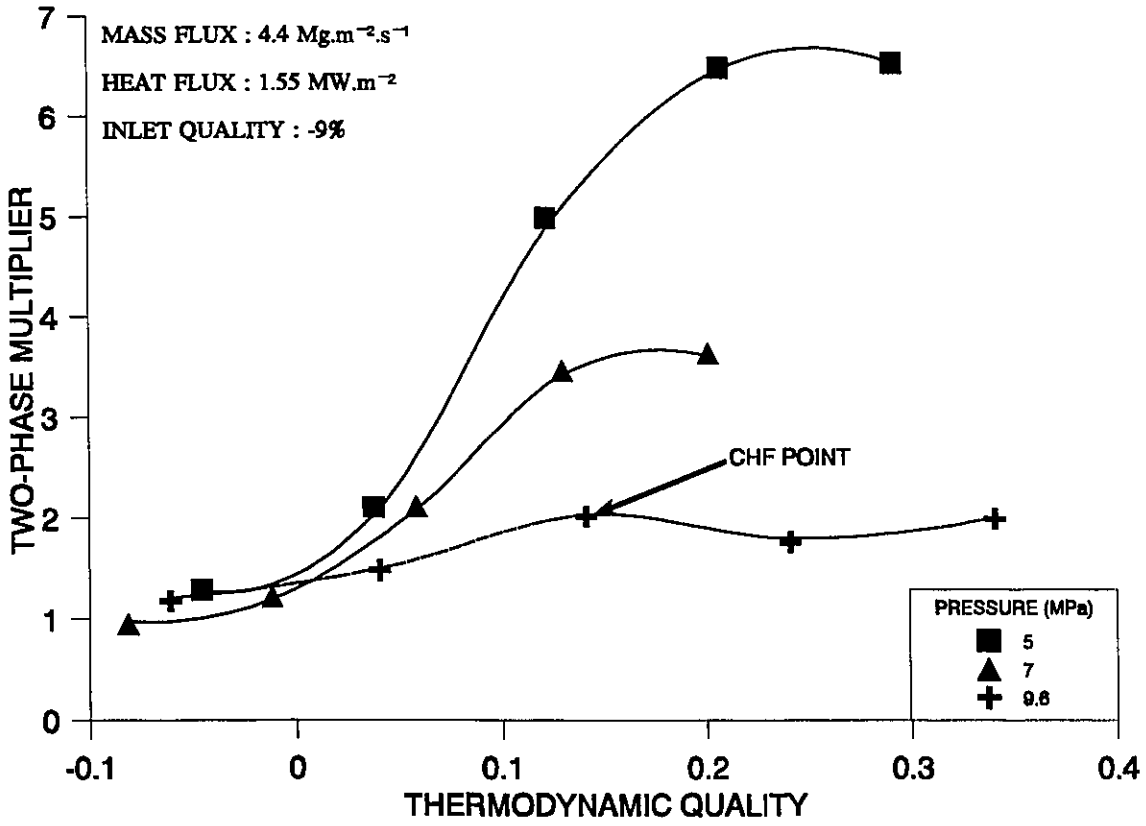

Figure 9.29: Effect of System Pressure on Two-Phase Multiplier at Medium Mass Fluxes and Heat Fluxes.

9.4.2.5 EFFECT OF VAPOUR MASS QUALITY AND VOID FRACTION

Previous discussions focused on the effect of measured parameters on the two-phase frictional pressure drop or two-phase multiplier. For all cases, however, the effects were presented as a function of thermodynamic quality. This may not be a good representation for non-equilibrium conditions since the thermodynamic quality, x_{th}, can differ considerably from the actual vapour mass quality, x_a. Since vapour-mass quality is a physically more significant parameter for calculating the two-phase frictional pressure drop and two-phase multiplier, a different trend may be observed when the two-phase multiplier is shown against the vapour-mass quality (rather than the thermodynamic quality).

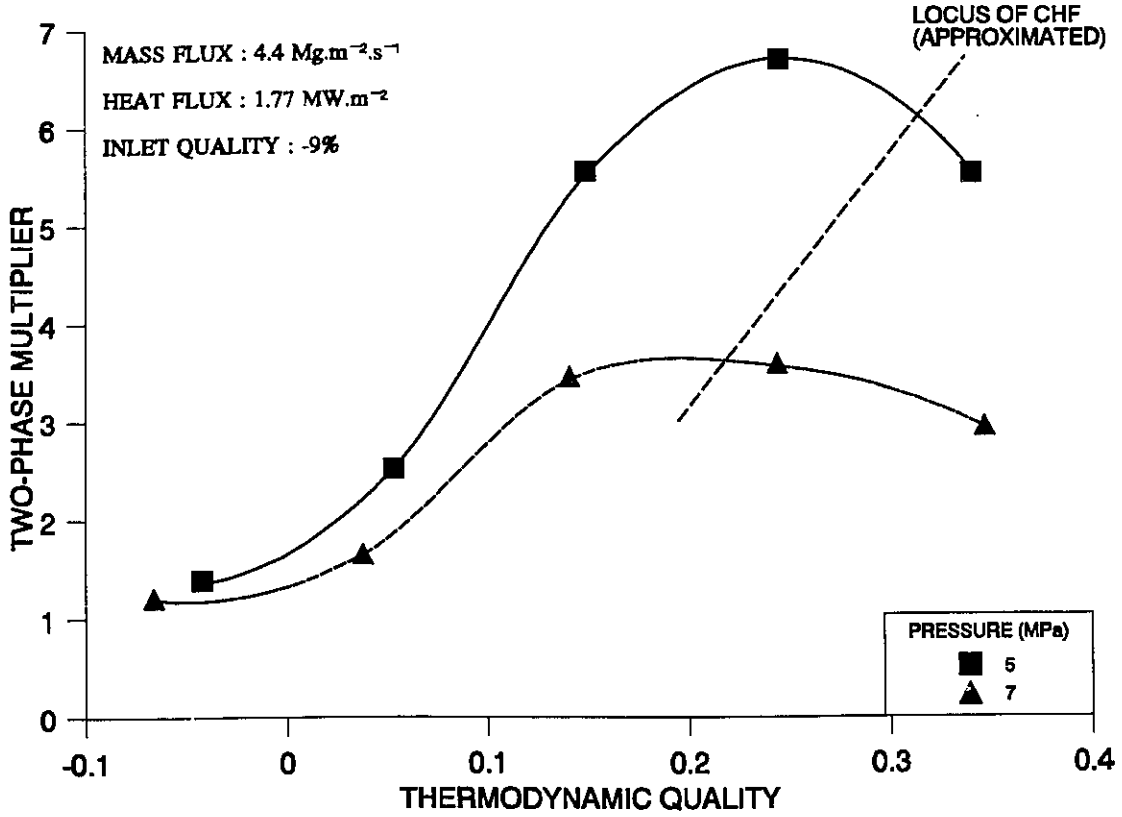

Figure 9.30: Effect of System Pressure on Two-Phase Multiplier, Including Post-Dryout Conditions.

Both the vapour mass and vapour volume are calculated parameters (see Sections 3.2 and 3.3) that involve the measurable parameters. For example, the evaluation of vapour mass quality requires mass flux, heat flux and fluid properties (i.e., pressure). Therefore, the use of these two parameters may include the effect of other factors on two-phase pressure drop.

Figure 9.31 shows the effect of vapour mass quality (calculated from the Kroeger and Zuber correlation, Equation (3.4)) on the two-phase multiplier for the same conditions as shown in Figure 9.16. The heat flux varies from 0 to 2.2 $MW.m^{-2}$. A zero value is introduced for mass quality, which can never be negative, in single-phase flow. The overall trend is quite similar to that exhibited in Figure 9.16, except that the spread of data appears to be reduced. For qualities close to zero, the two-phase multiplier decreases with increasing quality. This is mainly due to

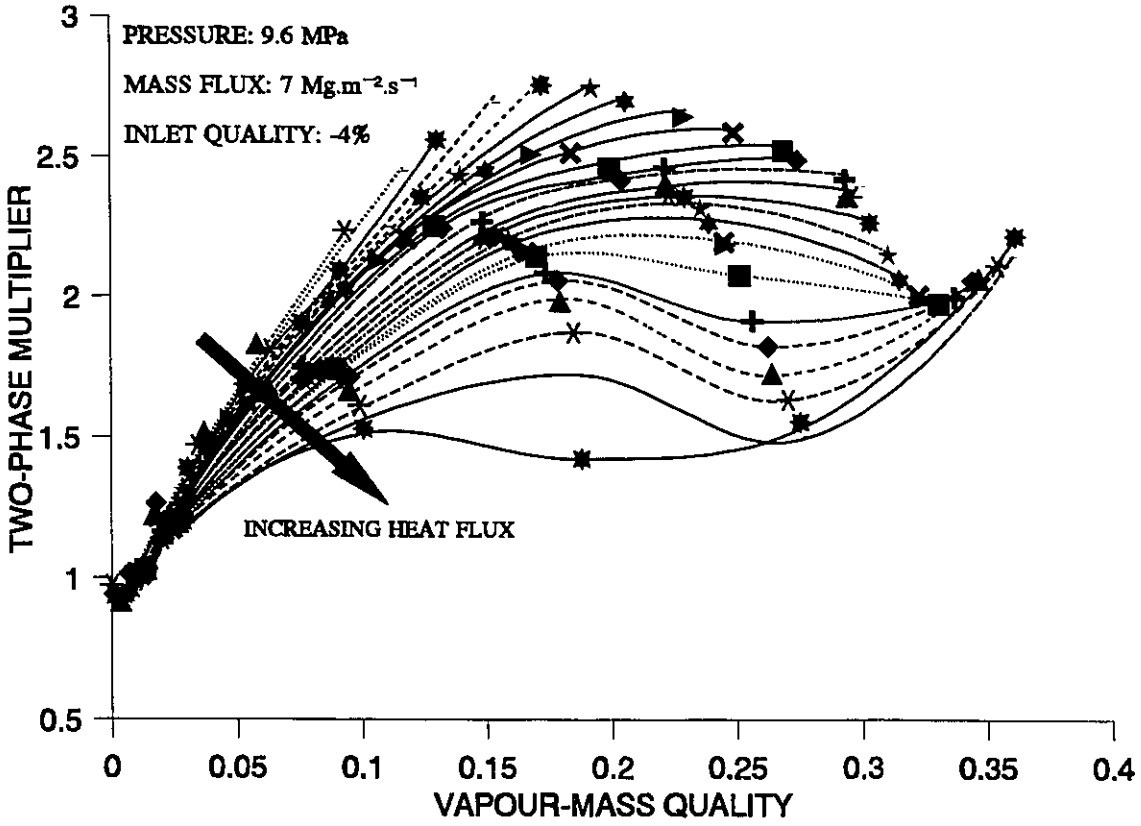

Figure 9.31: Effect of Vapour Mass Quality on Two-Phase Multiplier.

the underprediction of the point of net vapour generation, and boiling is prematurely initiated. The difference, however, is small (about 0.5%) and the pressure-drop calculation is not affected. At low qualities, the increasing trend of two-phase multipliers for increasing heat flux is not exhibited. Comparing Figures 9.31 to 9.16, there is practically no difference in two-phase multipliers with respect to either thermodynamic or vapour mass quality at the high-quality region. This is because the vapour mass quality approaches the thermodynamic quality in that region.

The effect of vapour void fraction (calculated from the Chexal et al. correlation, Equations (3.9) and (3.12)) on the two-phase multiplier is shown in Figure 9.32. While the connecting lines indicate a pattern similar to those shown in Figures 9.16 and 9.31, Figure 9.32 exhibits a different characteristic than the others. At low qualities, the trend of the two-phase multiplier is similar

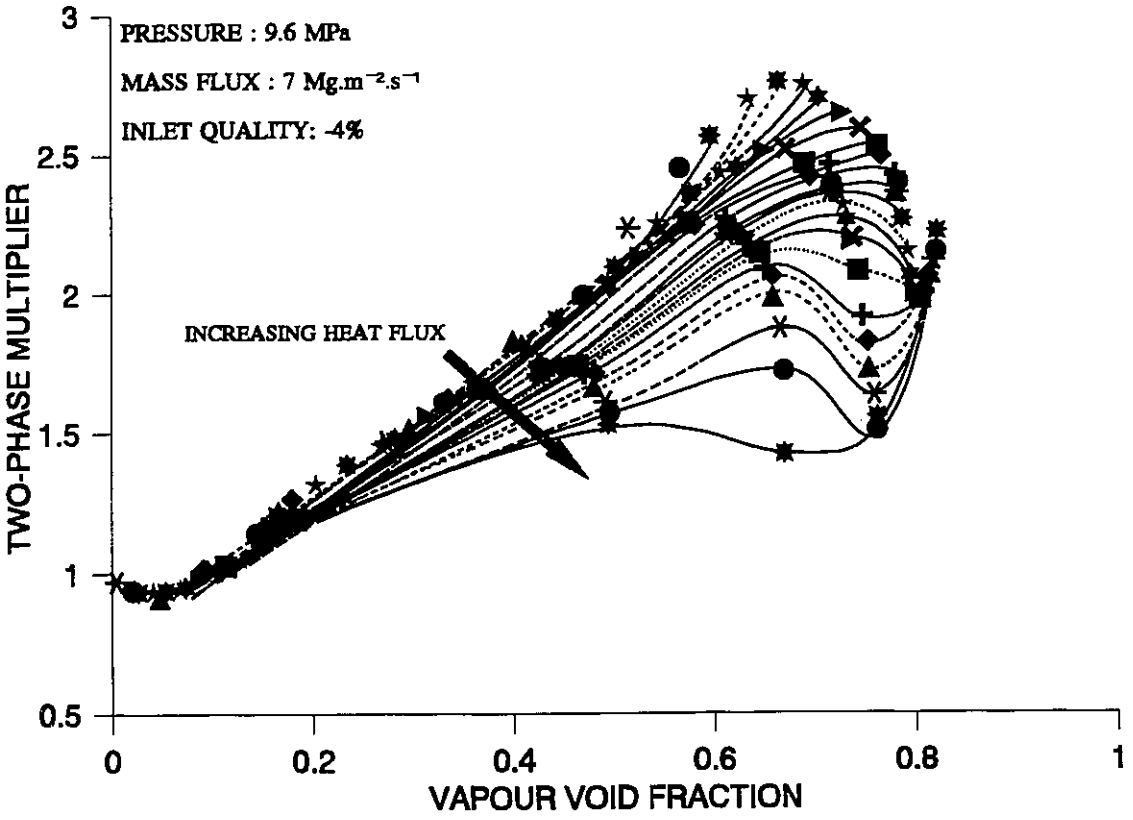

Figure 9.32: Effect of Void Fraction on Two-Phase Multiplier for High Flow and Low Inlet Subcooling Conditions.

to that shown in Figure 9.31. As the void fraction is increased, however, the effect of heat flux on the two-phase multiplier diminishes in the wispy-annular flow region of forced convective evaporation. When the flow approaches the transition point to annular flow, this effect becomes significant again, with larger two-phase multipliers for lower heat fluxes.

9.4.2.6 Summary

The two-phase frictional pressure drop is affected strongly by the heat flux, qualities (both thermodynamic and vapour mass), mass flux and system pressure, but not the inlet quality. A maximum two-phase pressure drop point was observed at high-flow and low inlet-subcooling

conditions. At low flows, it approaches the critical heat flux point. When expressing the two-phase pressure drop in terms of the two-phase multiplier, however, the effect of mass flux appears to diminish at high flows, but remains significant at low flows (the uncertainty among the data is also large). The use of vapour-mass quality appears to reduce the variation of the two-phase multiplier at low-quality flows (bubbly flow). No difference was observed for high qualities. Based on the void fraction, however, the effect of heat flux on the two-phase multiplier becomes small at qualities lower than that corresponding to the maximum pressure-drop point. The pressure-drop measurement can also be used as a detection method for dryout, as it responds strongly to a change in coolant conditions at the heated surface.

10. COMPARISONS BETWEEN MODEL PREDICTIONS AND DATA

The two-phase pressure-drop predictions of the present model (as described in Chapter 7) are compared against the experimental data over each measuring station. In each comparison, the thermodynamic quality and another parameter (either pressure, mass flux or heat flux) are used as the independent variables, while the other two parameters remaining constant. For example: the effect of heat flux is shown with thermodynamic quality and heat flux as the independent variables with constant values for pressure and mass flux. Since the flow conditions vary continuously over a measuring station, a number of flow patterns can be encountered. Most of the data, however, correspond to single-phase liquid flow and annular flow.

The overall comparison is shown in Section 10.1, and is followed by a detailed examination of various effects on the prediction accuracy. Section 10.2 examines the effect of heat flux for each measuring station. The effect of mass flux is shown in Section 10.3, while the effect of pressure is presented in Section 10.4. In each section, only representative comparisons are shown, because

of the large amount of available data (a total of more than 6 000 data). Section 10.5 summarises the results of the comparison.

10.1 OVERALL COMPARISON

The overall pressure drop over each measuring station is calculated using the present model (for pressure drop due to friction) and the simplified separated-flow equation (for pressure drops due to acceleration and gravity). Details of the evaluation procedure have been presented in Section 7.5. The results are presented in terms of the average error

$$Avg.\ Error = \frac{1}{n}\sum_{i=1}^{n}(Error)_i \tag{10.1}$$

and the root-mean-square (rms) error

$$rms\ Error = \left(\frac{1}{n}\sum_{i=1}^{n}(Error)_i^2\right)^{1/2} \tag{10.2}$$

where Error is defined as

$$Error = \frac{Pred.\ \Delta P_{total}}{Expt.\ \Delta P_{total}} - 1 \tag{10.3}$$

where ΔP_{total} is the overall pressure drop which includes the friction, acceleration and gravity components.

The model generally overpredicts the overall pressure drops, compared with the experimental data. For a total of 5085 data, the comparison has resulted in an overall average error of 7.02%

and root-mean-square (rms) error of 12.8%. Figure 10.1 shows the overall comparison of predicted and experimental pressure drops. While relatively good agreement between predictions and data is shown for low pressure drops, the scatter among data becomes high when the pressure drop becomes high. A similar prediction accuracy is also observed at each measuring station. While the average errors differ slightly (with a smaller overprediction at the outlet than the inlet region), the rms errors remain about the same (Table 10.1). The present model is developed with information available in the open literature, and the flow-boiling data obtained in the study have not been used to fine-tune any parameter.

The data at the outlet measuring station (Section 5) are examined further, since they cover all heat-transfer modes (i.e., from single-phase liquid flow to dispersed-flow film boiling)

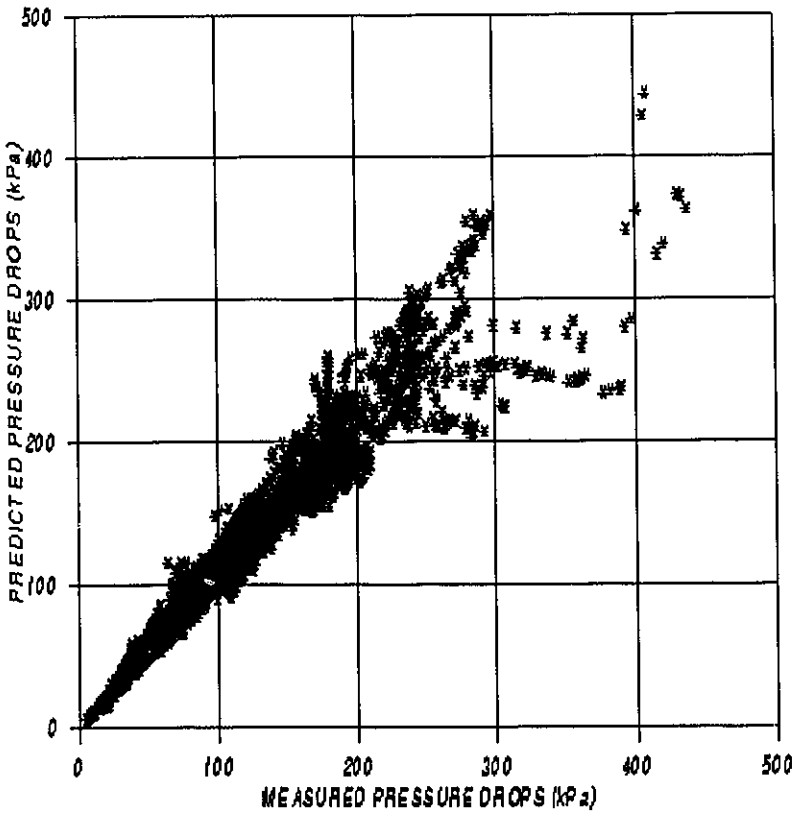

Figure 10.1: Comparison Between Predicted and Measured Pressure Drops.

Table 10.1: Prediction Accuracy of Present Model at Each Measuring Station.

Section	# of Data	Aver. Error	RMS Error
5 (Outlet)	1017	0.0367	0.1293
4	1017	0.0597	0.1261
3	1017	0.0830	0.1304
2	1017	0.0881	0.1275
1 (Inlet)	1017	0.0833	0.1268

encountered in the test section. Figure 10.2 shows the overall prediction error against thermodynamic qualities. An overprediction of the data is observed at qualities close to 0 and 0.3. These regions correspond to bubbly flow and to annular flow with qualities between the maximum pressure-drop and the critical heat flux points.

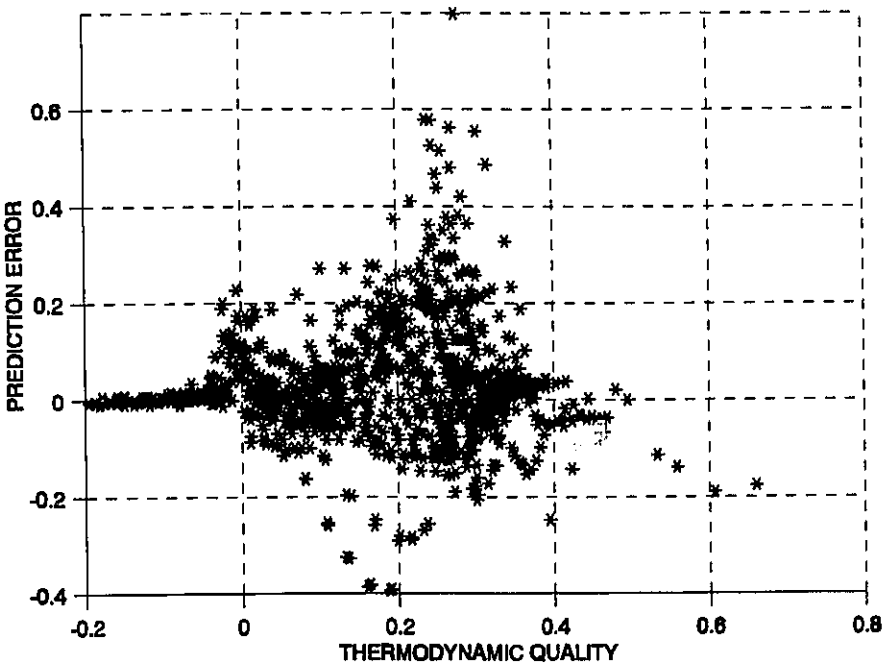

Figure 10.2: Overall Prediction Error with respect to Thermodynamic Quality at the Outlet Section.

Figure 10.3 shows the overall prediction error against mass flux. In general, the data are underpredicted at both low (less than 3 $Mg.m^{-2}.s^{-1}$) and high (greater than 8 $Mg.m^{-2}.s^{-1}$) mass fluxes, but overpredicted in the mid-range. The magnitude of overprediction, however, is larger than that of underprediction. A large overprediction (about 80%) is observed at a mass flux of 5 $Mg.m^{-2}.s^{-1}$; it is caused by the overprediction of critical heat flux, leading to the use of the wrong sub-model (for forced convective evaporation) at post-dryout conditions.

The overall prediction error is shown in Figure 10.4 for various pressures, and in Figure 10.5 for various heat fluxes. Due to the large data scatter, no specific trend can be observed.

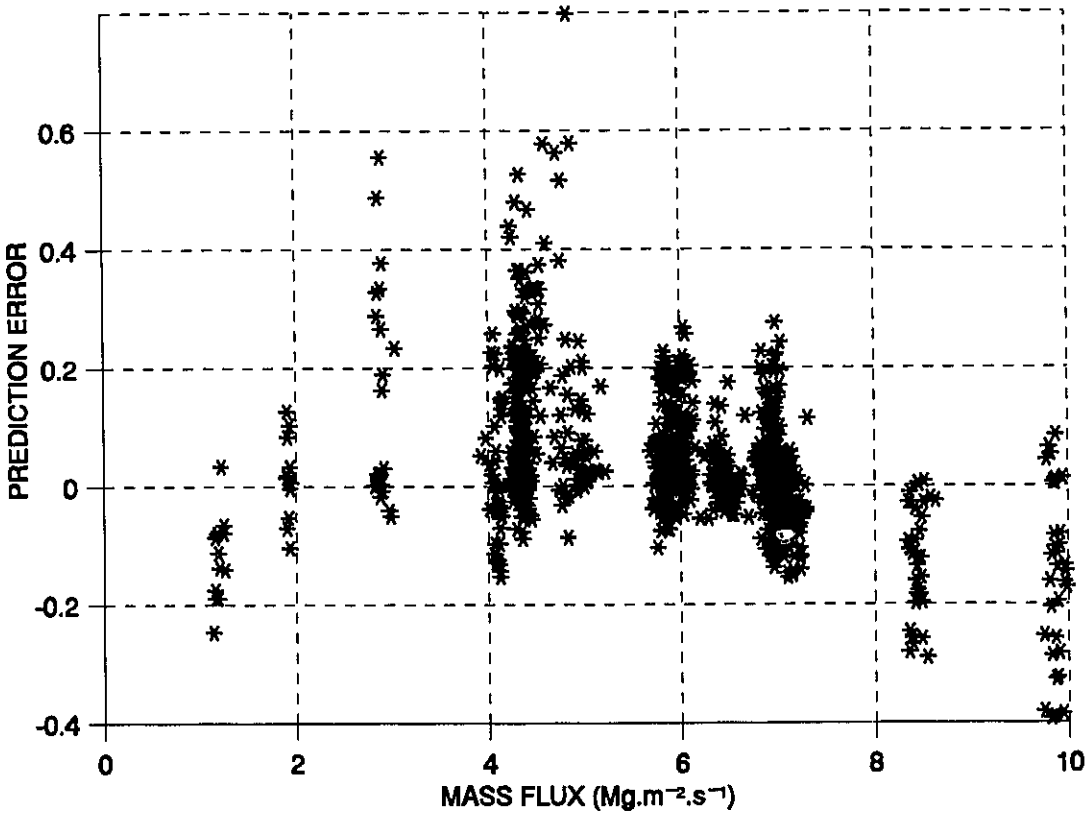

Figure 10.3: Overall Prediction Error with respect to Mass Flux at the Outlet Section.

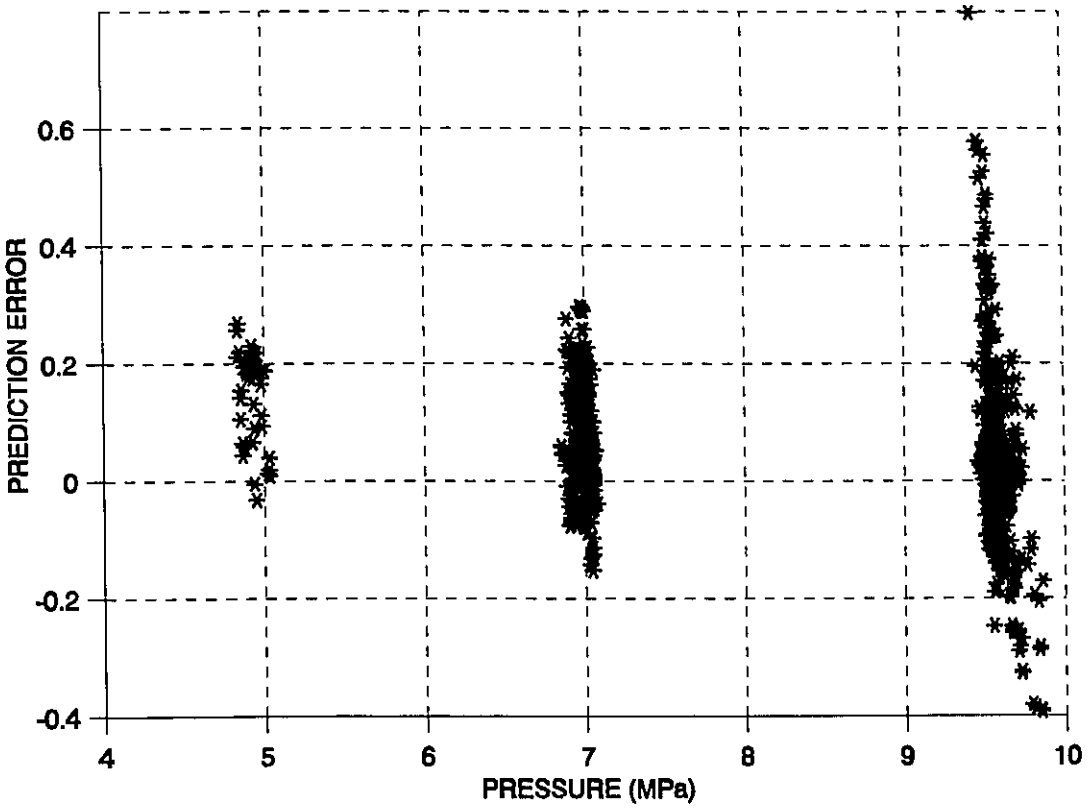

Figure 10.4: Overall Prediction Error with respect to Pressure at the Outlet Section.

10.2 EFFECT OF HEAT FLUX

The comparisons between predictions and data for various heat fluxes are shown in Figure 10.6 for a mass flux of 4.3 $Mg.m^{-2}.s^{-1}$. To avoid overcrowding, the comparisons are shown separately for each measuring station. The heat flux varies from 0 to 1.54 $MW.m^{-2}$. For the two sections at the inlet end, a good prediction is shown at low qualities, but overprediction is observed as the quality is increased. The reduction in pressure drop at high quality is not predicted by the model. At the downstream sections, although a large overprediction is shown over the region close to the maximum pressure-drop point, the decreasing trend of pressure drop is closely followed by the model predictions. At the post-dryout region (beyond the minimum pressure-drop point), the agreement between model prediction and experimental data is good.

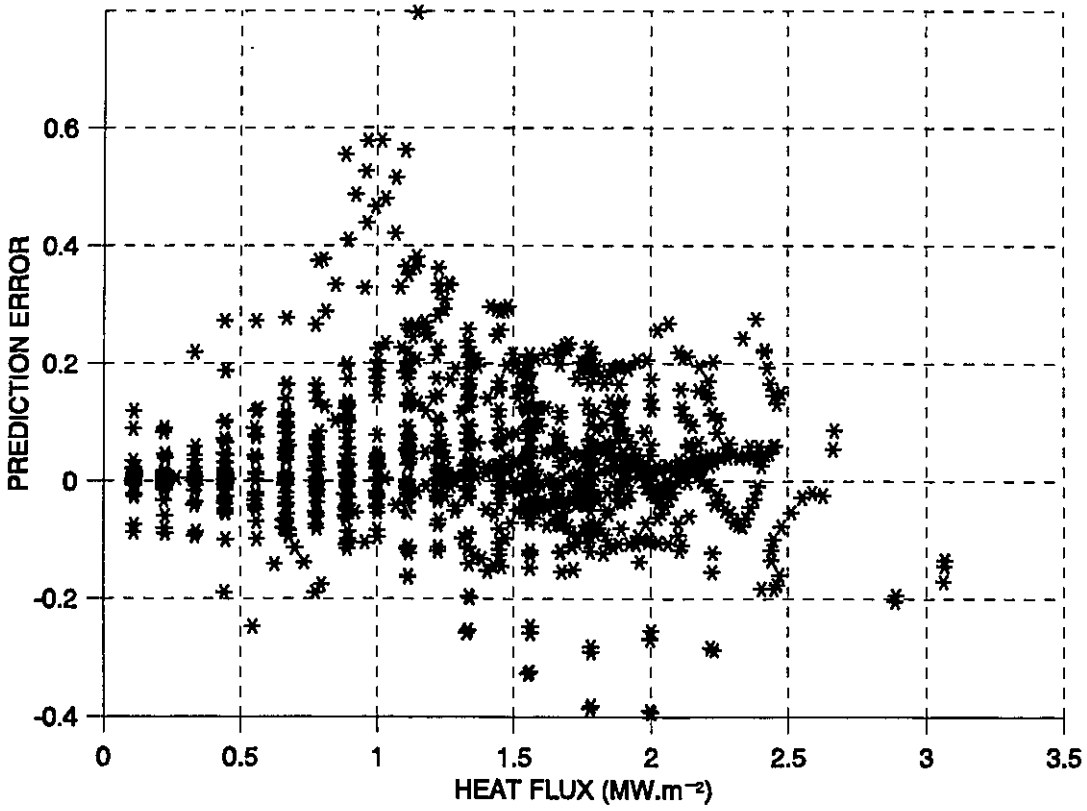

Figure 10.5: Overall Prediction Error with respect to Heat Flux at the Outlet Section.

The overprediction is anticipated to be caused by the underprediction of the entrained liquid fraction, since the correlation was derived based on only a small amount of data. This results in a thick liquid film, which in turn increases the velocity gradient at the liquid/vapour interface and hence the pressure drop. Figure 10.7 shows the comparison for the same set of data illustrated in Figure 10.6, but the correlation for entrained-liquid fraction (i.e., Equation 7.59) is modified to

$$F_{boil} = F_{adia} \cos(3*0.005335\ Bo\ Pe) \tag{10.4}$$

This increases the entrained-liquid fraction in proportion to the heat flux, and results in a better agreement between predictions and data. The improvement is particularly noticeable in Section

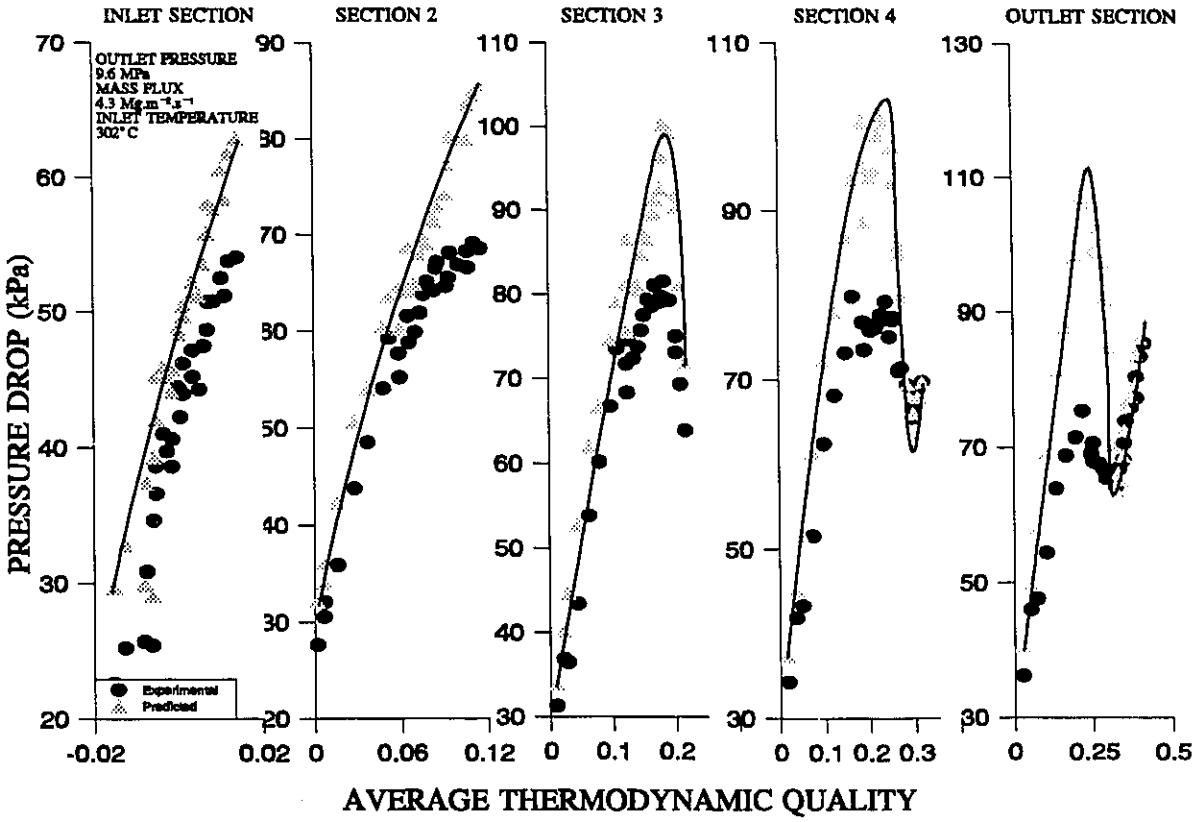

Figure 10.6: Comparison Between Predicted and Measured Pressure Drops for Various Heat Fluxes at a Mass Flux of 4.3 $Mg.m^{-2}.s^{-1}$ and Pressure of 9.6 MPa.

3, where the turn-around point indicated among data is closely followed by the predictions. In other sections, the overprediction is also considerably reduced. Experimental studies are needed to improve the prediction of entrained-liquid fraction at the present conditions of interest (no experimental data are currently available for conditions of interest).

Figure 10.8 shows the comparison for a mass flux of 7 $Mg.m^{-2}.s^{-1}$. The heat flux varies from 0 to 2.18 $MW.m^{-2}$. Although the same trend as in the previous figures is observed in the two inlet sections, a much better agreement between predictions and data is shown in the downstream sections. In particular, the pressure drops measured in Section 4 are predicted closely with the model, including the downward trend. Similarly, the variation of pressure drop with increasing

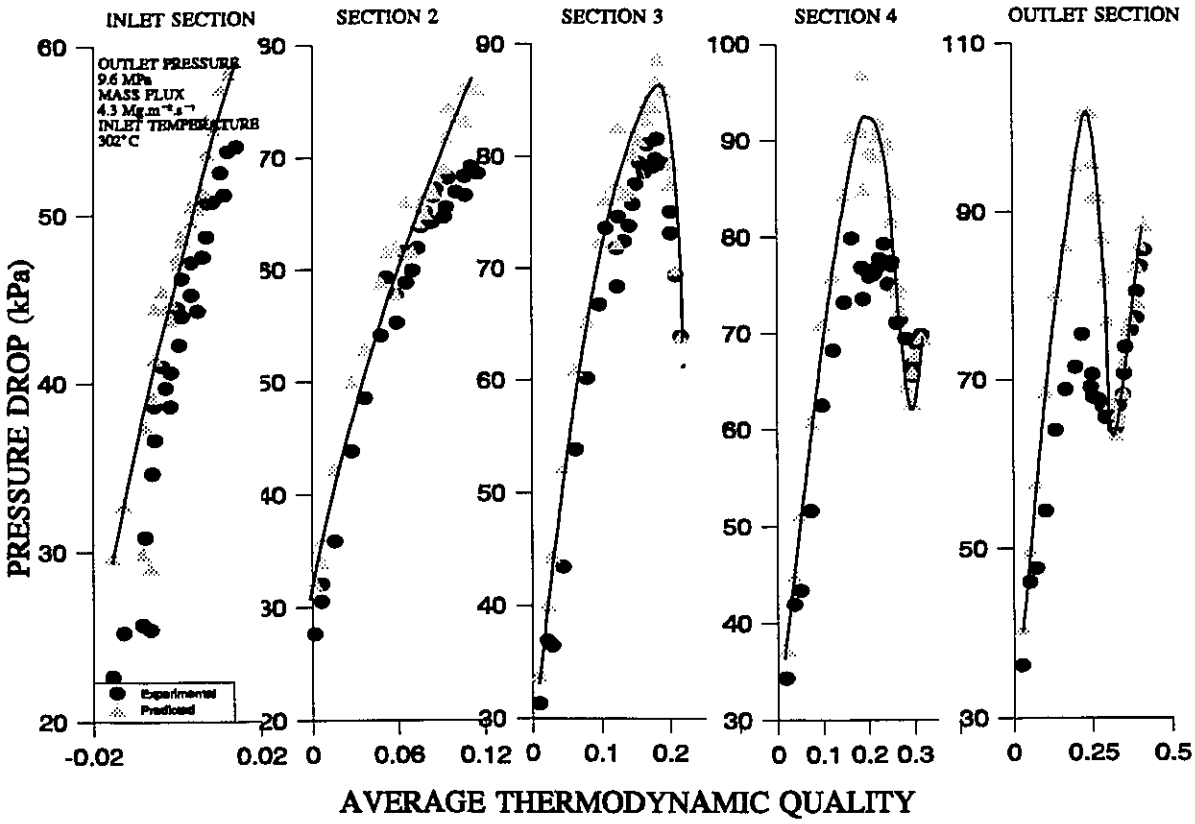

Figure 10.7: Comparison Between Predicted and Measured Pressure Drops for Various Heat Fluxes Using a Modified Correlation for Entrained-Liquid Fraction.

quality is similar to that of the model in the outlet section (Section 5), although the measurements are slightly underpredicted. While the original equation for the entrained-liquid fraction (Equation (7.59)) is valid for most conditions shown in Figure 10.8, these comparisons suggested that the effect of mass flux on the entrained-liquid fraction may have to be further examined. Except for Section 1, the model predictions agree with the measurements at low-quality conditions (before the turn-around point) in these sections.

The same trend is observed at a pressure of 7 MPa for the same mass flux. As indicated in Figure 10.9, the pressure drops are overpredicted at the inlet sections, but good agreement is achieved at the downstream sections. Both the magnitude and trend of the data are relatively

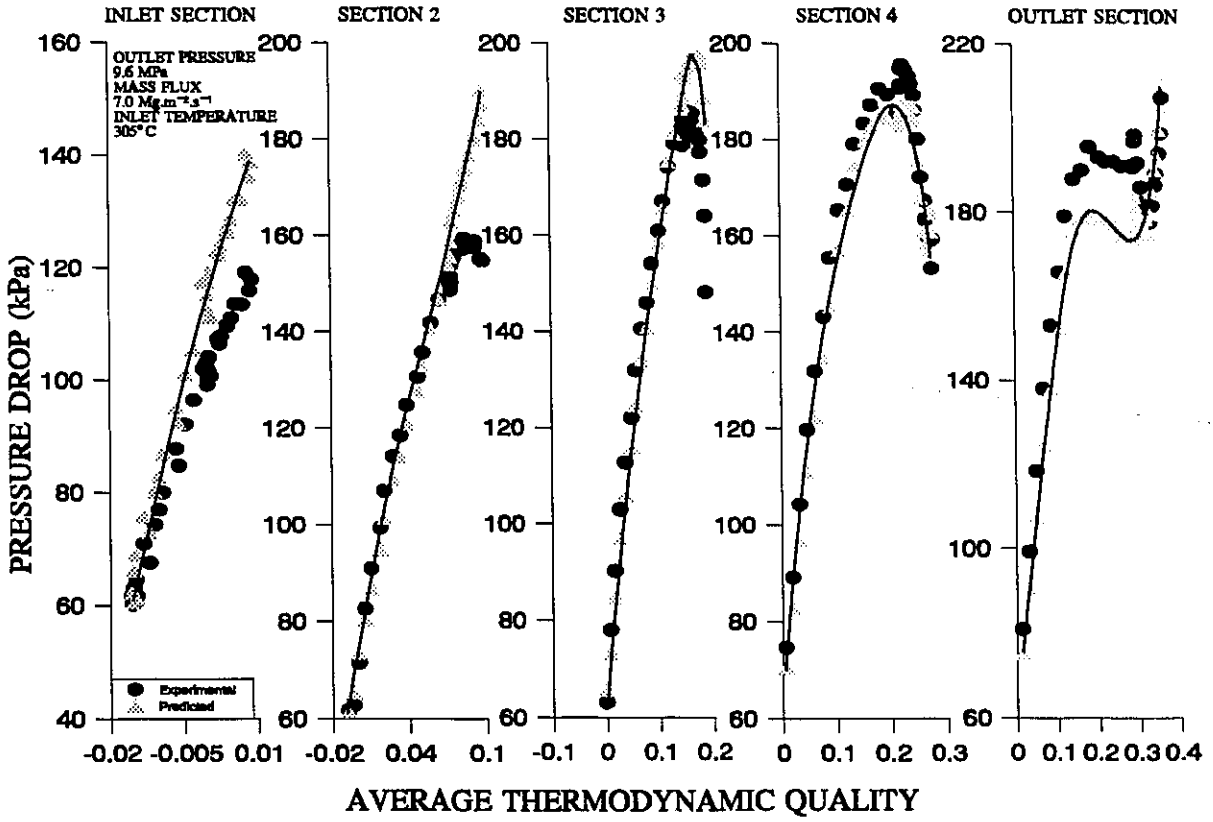

Figure 10.8: Comparison Between Predicted and Measured Pressure Drops for Various Heat Fluxes at a Mass Flux of 7 $Mg.m^{-2}.s^{-1}$ and a Pressure of 9.6 MPa.

well predicted with the model, in particular, at the post-dryout region. The range of heat flux covered in this figure is 0-2.4 $MW.m^{-2}$. Most data obtained at conditions before the turn-around point are predicted with reasonable accuracy.

10.3 EFFECT OF MASS FLUX

To examine the effect of mass flux on two-phase pressure drop, data obtained at constant pressure and heat flux were selected. Figure 10.10 shows the comparison between model predictions and experimental data for a heat flux of 0.8 $MW.m^{-2}$ and a range of mass fluxes

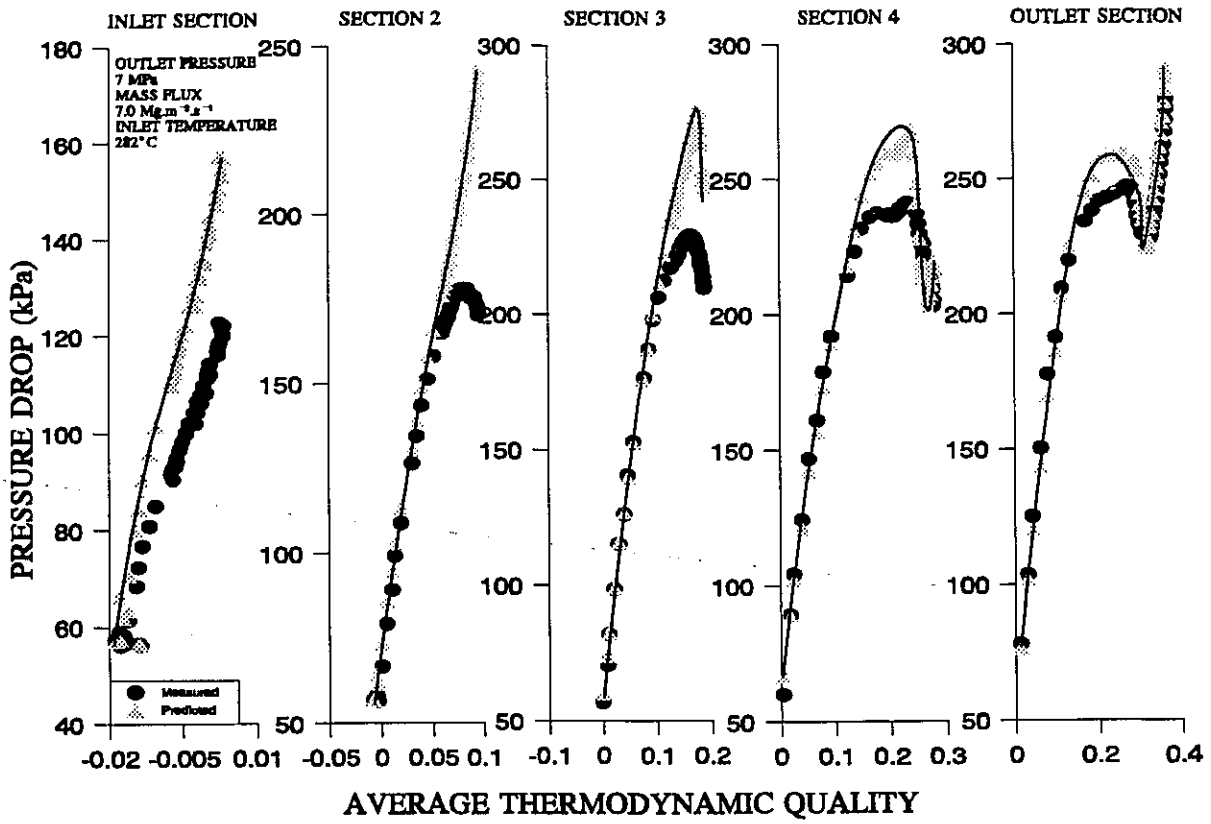

Figure 10.9: Comparison Between Predicted and Measured Pressure Drops for Various Heat Fluxes at a Mass Flux of 7 $Mg.m^{-2}.s^{-1}$ and a Pressure of 7 MPa.

from 1 to 7 $Mg.m^{-2}.s^{-1}$. Over this range, the model predictions agree very well with the data for both low and high mass fluxes. An overprediction, however, is shown for the data of 4.54 $Mg.m^{-2}.s^{-1}$. This agrees with the findings previously shown in Figure 10.6.

Figure 10.11 shows the comparison for the high-flow data at a heat flux of 1.55 $MW.m^{-2}$. A good agreement between predictions and measurements is shown for data of mass fluxes between 4.3 and 7 $Mg.m^{-2}.s^{-1}$. The higher flow data, on the other hand, are underpredicted at high qualities.

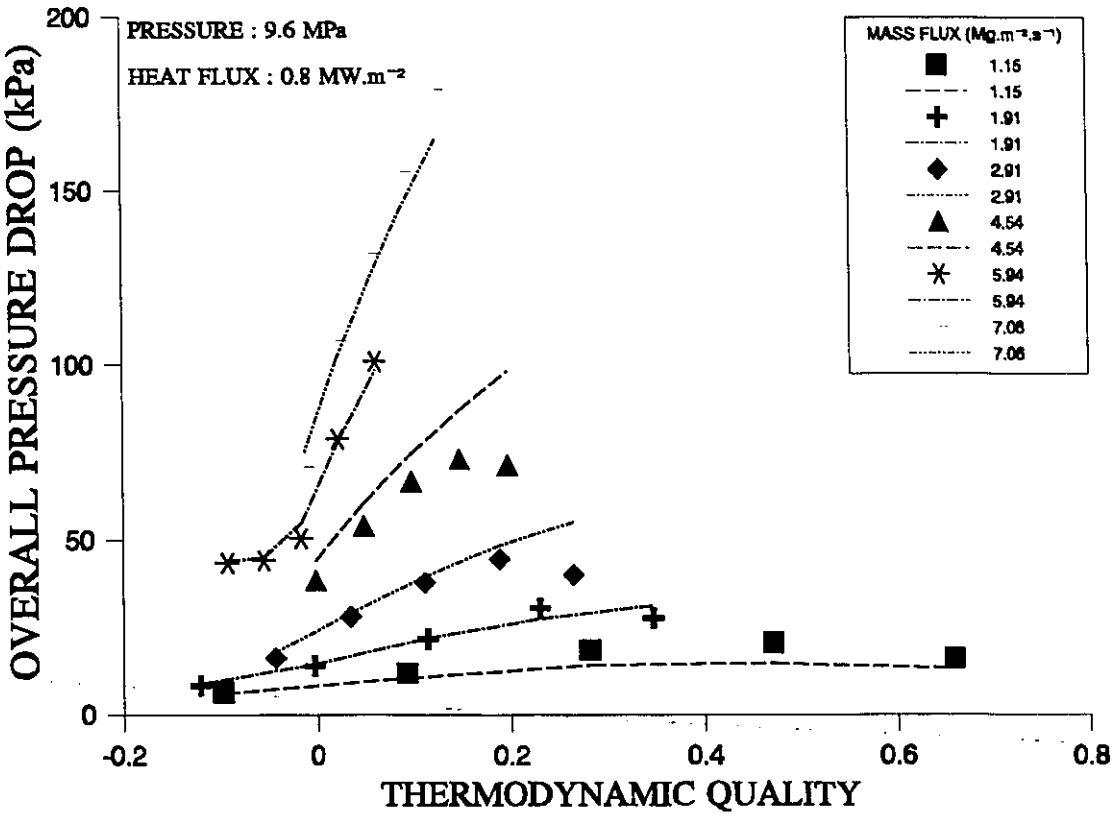

Figure 10.10: Comparison Between Predicted and Measured Pressure Drops for Various Mass Fluxes.

10.4 EFFECT OF SYSTEM PRESSURE

The effect of pressure cannot be examined extensively, since the present experiment covered only limited conditions at low pressures, particularly at 5 MPa. Nevertheless, a qualitative comparison is carried out for a mass flux of 4.3 $Mg.m^{-2}.s^{-1}$ and a heat flux of 1.5 $MW.m^{-2}$. Similar to the trend shown in Figure 9.24, the pressure drop is considerably higher at low pressures (Figure 10.12). The model predictions follow closely the data and exhibit the same trend. However, an overprediction of data is systematically shown at low pressures. It may be caused by the overprediction of single-phase pressure drop at low qualities and entrained-liquid fraction at high qualities. Very good agreement between predictions and measurements is shown at high-pressure and high-quality (dispersed-flow film boiling) conditions.

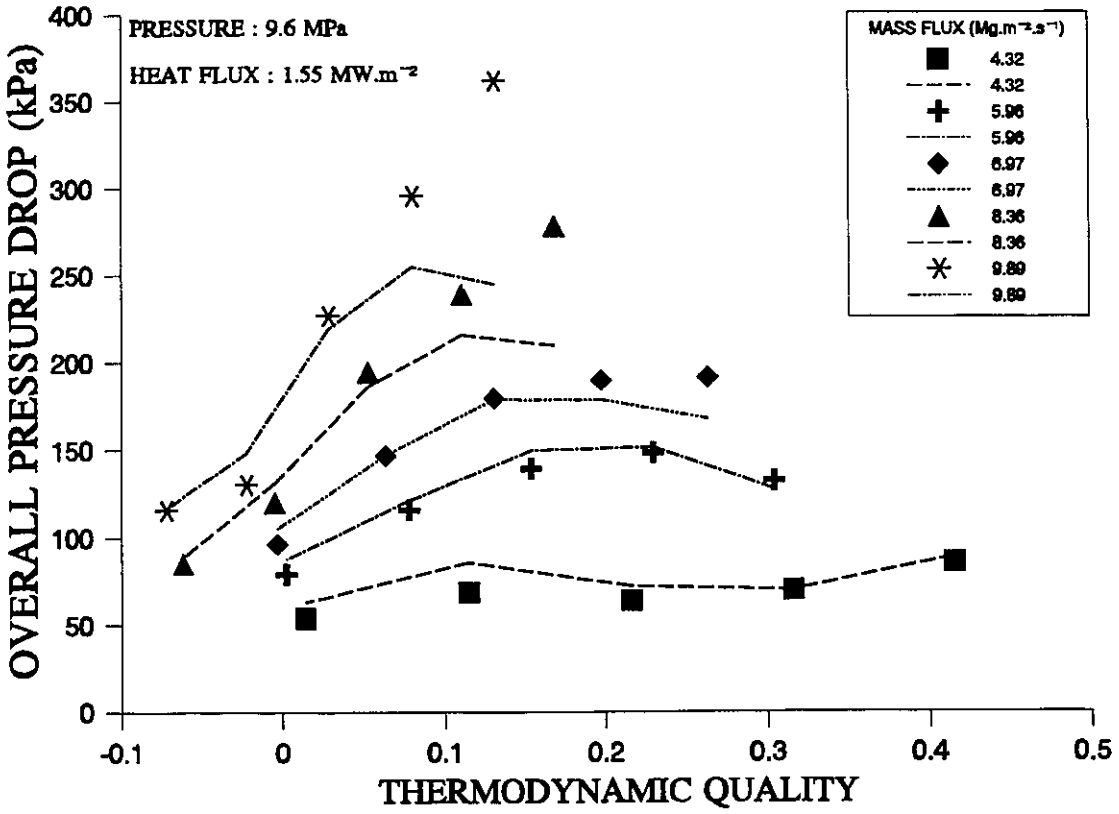

Figure 10.11: Comparison Between Predicted and Measured Pressure Drops for Various Mass Fluxes at a Heat Flux of 1.55 $MW.m^{-2}$.

The same trend is displayed in Figure 10.13 for a mass flux of 6 $Mg.m^{-2}.s^{-1}$ and a heat flux of 1.8 $MW.m^{-2}$. The lower pressure drop shown at low pressures and low qualities is caused by a small variation in mass flux. These pressure-drop data are well-predicted by the model. As in Figure 10.12, the post-dryout data are predicted closely with the model at both 7 and 9.5 MPa in pressure, but the pre-dryout data remain overpredicted. Both the model predictions and experimental data displayed the same parametric trend with respect to quality and pressure.

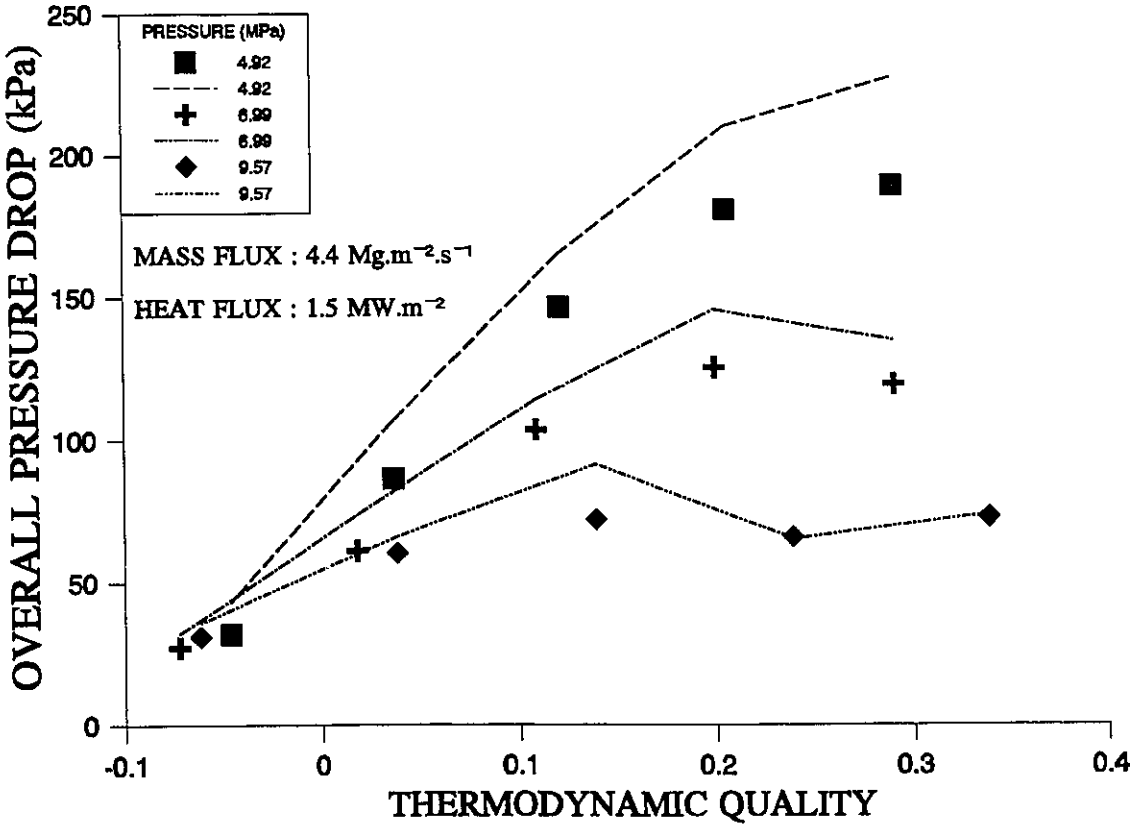

Figure 10.12: Comparison Between Predicted and Measured Pressure Drops for Various Pressures at a Mass Flux of 4.4 $Mg.m^{-2}.s^{-1}$.

10.5 SUMMARY

Relatively good agreement between model predictions and experimental data is shown in the comparison. In particular, the trend of two-phase pressure drop exhibited in the data is closely followed by the model. This increases the confidence in this model whose derivation is based on several simplifying assumptions. A number of improvements can be introduced to enhance the prediction capabilities. They will be presented in Chapter 12. Overall, the model predicts most data (particularly in the dispersed-flow film-boiling region) with good accuracy. The overprediction of data is primarily caused by the underprediction of entrained-liquid fraction with the empirical equation. Nevertheless, the parametric trends of two-phase pressure drop with respect to various flow parameters are closely followed by the model predictions.

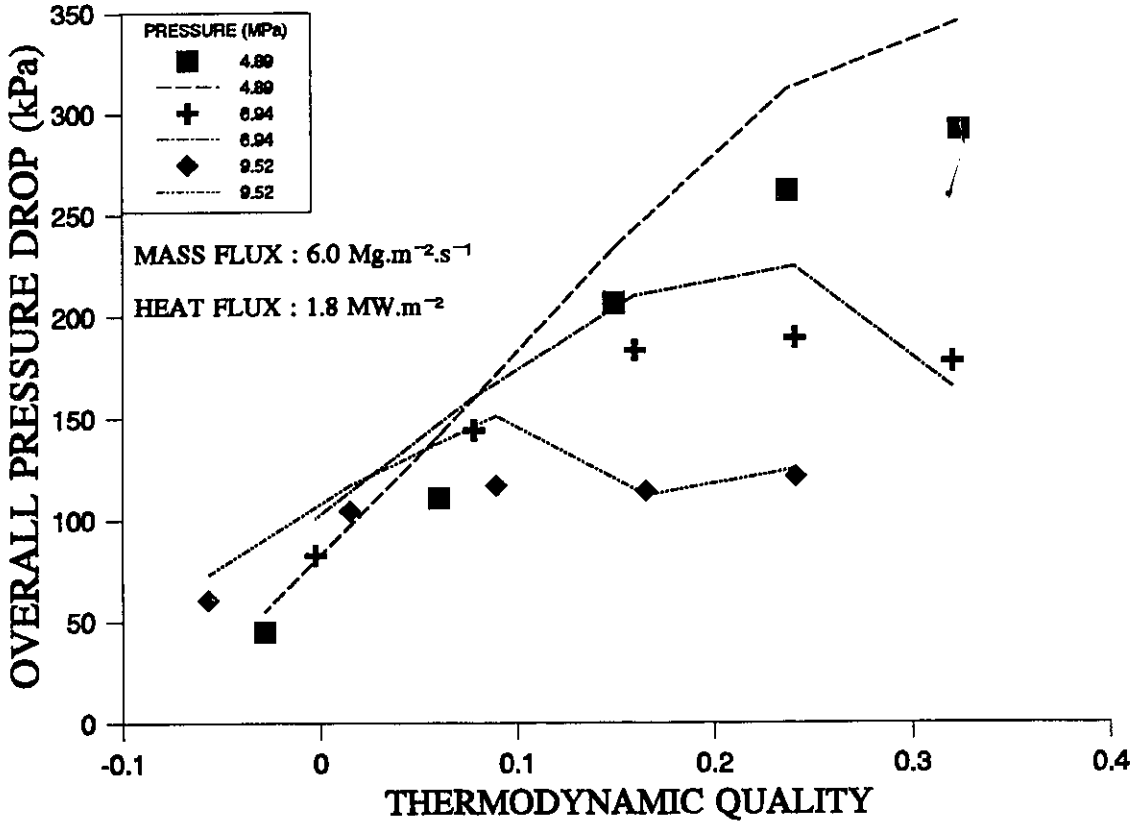

Figure 10.13: Comparison Between Predicted and Measured Pressure Drops for Various Pressures at a Mass Flux of 6 $Mg.m^{-2}.s^{-1}$.

11. ASSESSMENT OF CORRELATIONS

A number of correlations were derived for predicting the pressure gradient in two-phase flow. They have been described in Chapter 5. While most of them were based on adiabatic data, some were shown valid for flow boiling as well. Overall, the Friedel correlation [1979] was derived with the largest number of adiabatic data (over 25 000). Various independent assessments of these correlations, using both adiabatic and flow-boiling data, have generally recommended the Baroczy correlation [1965], the Chisholm correlation [1973] and the homogeneous model, based on the single-phase friction factor (e.g., Dukler et al. [1964], Idsinga et al. [1977], Friedel [1980], Beattie and Whalley [1982] and Chun and Oh [1989]). Kohler and Kastner [1987] found that predictions from the Friedel correlation agreed with their flow-boiling data.

The experimental data obtained in this study (Chapter 9) display a unique trend of the two-phase pressure gradient, which differs from that exhibited in adiabatic flow. This is primarily caused by the variation in flow quality along the heated channel, and the corresponding change in phase distribution due to the heating effect. As indicated in Chapter 5, the approach often used in

predicting the pressure gradient in heated channels is based on an integration of adiabatic pressure gradient with respect to flow quality. The effect of heating on two-phase pressure drop is not accounted for directly in the calculation, but only through the variation of flow quality (which is a function of heat flux). The present set of data were obtained over a relatively short distance, and hence can be used for validating the above approach.

The correlations assessed in this chapter are summarised in Section 11.1. Section 11.2 describes the methodology used in this assessment. The results of an overall assessment of various correlations with the data obtained in this study are presented in Section 11.3. A description of a method to combine various correlations is shown in Section 11.4. The results of the assessment of this multi-correlation method are presented in Section 11.5. An in-depth examination of the prediction capabilities of the best multi-correlation method is discussed in Section 11.6.

11.1 CORRELATIONS

The correlations assessed in this study had been either developed or tested with steam-water data. Others, such as the Bandel and Schlűnder correlation [1974b] (Section 5.4.3) and Muller and Steinhagen correlation [1986] (Section 5.4.4), which had been developed specifically for non-aqueous fluids, were not included. Overall, nineteen correlations are selected; they include three different equations of Beattie [1974] (Table 6.1) for various flow structures (large-bubble, small-bubble and annular flow) in adiabatic flow and homogeneous models (Section 6.1) based on four different definitions of two-phase viscosity (i.e., McAdams et al. [1942], Cicchitti et al. [1960], Owens [1961] and Dukler et al. [1964]). Details of these correlations have been described in Chapters 5 and 6.

The Chisholm [1973] (Section 5.3.1) and the Friedel [1979] (Section 5.3.2) correlations had been derived with a large data base covering various fluid types and flow conditions. However, only limited comparisons were shown for these correlations with steam-water flow at high-pressure

and high-flow conditions in tubes. Chisholm [1973] showed a relatively good agreement between his correlation and the data of Becker et al. [1962a], while Kohler and Kastner [1987] indicated that the Friedel [1979] correlation predicted their data well. The predictions of the Friedel [1979] correlation were also shown to agree closely with the pressure drop data obtained in horizontal bundle geometries [Snoek and Leung, 1986]. Whalley [Hewitt, 1982] recommended that the Friedel correlation should be used for viscosity ratios (μ_l / μ_g) less than 1000, the Chisholm correlation for viscosity ratios greater than 1000 and mass fluxes greater than 0.1 $Mg.m^{-2}.s^{-1}$, and the Martinelli correlations (either Lockhart and Martinelli or Martinelli and Nelson) for viscosity ratios greater than 1000 and mass fluxes less than 0.1 $Mg.m^{-2}.s^{-1}$. For the present conditions of interest (μ_l / μ_g less than 1000), the Friedel correlation should be used.

The present comparison includes also the Beattie and Whalley correlation [1982] (Section 6.4.2), which had been validated with the adiabatic data base of the Heat Transfer and Fluid-flow Service (HTFS). Unlike Beattie's other correlations [Beattie, 1973, 1974], the Beattie and Whalley [1982] correlation is independent of flow structure, making it applicable for a wide range of conditions without the uncertainty introduced by flow-transition predictions. Beattie and Whalley have indicated that the uncertainty of this correlation is expected to be higher for flow-boiling conditions, but no validation was performed.

The graphical methods of Lockhart and Martinelli [1949] (Section 5.2.1), Martinelli and Nelson [1948] (Section 5.2.2), Thom [1964] (Section 5.2.3) and Baroczy [1965] (Section 5.2.4) were not convenient for use in computer applications. However, Chisholm [1967, 1970], Chisholm and Sutherland [1969] and Thom [1964] have derived equations that can provide two-phase multipliers that agree closely with those of the graphical methods. Hence, these equations are used in the comparison.

The assessment includes correlations that were derived either completely or partially with the flow-boiling data: the Becker et al. correlation [1962d] (Section 5.4.1), the Lombardi and Pedrocchi correlation [1972] (Section 5.4.2) and the Reddy et al. correlation [1982] (Section 5.3.4). Although updated versions of the Lombardi and Pedrocchi [1972] correlation have been

proposed (see Section 5.4.2), their prediction capabilities were found to be less satisfactory than the original equation. Therefore, the Lombardi and Pedrocchi correlation [1972] is used. Both the Becker et al. [1962d] and the Reddy et al. [1982] correlations were derived with high-pressure steam-water data. However, the Becker et al. [1962d] correlation was based only on flow-boiling data. On the other hand, the Reddy et al. [1982] correlation was based on both adiabatic and flow-boiling data, and covers a much wider range of conditions, particularly at a high mass flow rate.

Other correlations examined in this assessment are the Levy equation (Section 6.2.1) for simplified annular flow [1966], and the Chisholm and Sutherland correlations [1969] (Section 5.3.1) for both smooth and rough pipes.

11.2 ASSESSMENT METHODOLOGY

The methodology of this assessment is similar to the model assessment described in Chapter 10. A relative comparison is introduced for the pressure gradient between predictions of various correlations and experimental data over the measuring section. It is carried out by dividing the measuring section (about 50 cm) into 20 sub-sections. The flow condition is assumed to be constant in each sub-section, and is used to determine the heat-transfer mode. No attempt is made to distinguish the flow pattern, which is not considered in most correlations. Throughout the comparison, empirical correlations were used in determining various parameters, such as vapour-mass quality (Section 3.2) and void fraction (Section 3.3). Since this comparison focuses mainly on the correlations for the two-phase pressure gradient, the single-phase pressure gradient is predicted with the ad-hoc correlations derived from the present experimental data. The methodology is summarised as follows:

a) Each of the five measuring sections is divided into 20 equal segments. Starting from the segment at the inlet end, the local conditions are calculated in each segment.

b) Since the pressure drop over each segment is unknown, the upstream pressure is used as the local pressure. The uncertainty introduced by this assumption is anticipated to be small, since the pressure drop over each segment is small.

c) The mass flow rate in each segment is constant (conservation of mass).

d) The local enthalpy at the mid-point of each segment is calculated from a heat balance (conservation of energy) where

$$H_{local} = H_{in} + \frac{Power}{W} \frac{z}{L_{he}} \qquad (II.1)$$

e) If the local fluid enthalpy is less than the saturation-liquid value, calculate the point of net-vapour generation based on the local condition. This point is used to determine whether the heat-transfer mode is single-phase forced convection or subcooled boiling. Single-phase flow is assumed at the region between the onset of nucleate boiling and onset of net-vapour generation points.

f) In single-phase flow, the pressure gradient is calculated with the Colebrook-Chen friction factor (Equation (2.44)) based on a relative roughness (i.e., ε/D) of 0.00103. The heating effect is accounted for with the correction factor (Equation (2.46)) which is based on the viscosity ratio to the power of -0.28.

g) At conditions where two-phase flow is anticipated (i.e., subcooled and saturated boiling), the correlation for the two-phase pressure gradient is used.

h) The Chexal et al. correlation (see Section 3.3) is used to calculate the void fraction, the Saha and Zuber correlation (Section 4.3.4) is used to evaluate the onset of net-vapour generation, and the Kroeger and Zuber equation (Section 3.2) is used to determine the actual vapour-mass quality.

i) The pressure gradients due to acceleration and gravity are calculated based on the separated-flow model (Sections 3.4.2 and 3.4.3). For all conditions examined in this study, they represent only a small portion of the overall pressure gradient, which is the sum of the three pressure gradients (friction, acceleration and gravity).

j) The calculated overall pressure gradient in each measuring section is compared against the experimental value.

11.3 RESULTS OF ASSESSMENT OF VARIOUS CORRELATIONS

When the transitions between the heat-transfer regimes are not known, the correlations are often applied over all conditions, even though they may only be valid for a specific heat-transfer regime. This approach is examined in this section, and the predicted overall pressure gradient is compared against the experimental data. The results are presented in terms of the average error

$$Avg.\ Error = \frac{1}{n}\sum_{i=1}^{n}(Error)_i \tag{11.2}$$

and the root-mean-square (rms) error

$$rms\ Error = \left(\frac{1}{n}\sum_{i=1}^{n}(Error)_i^2\right)^{1/2} \tag{11.3}$$

where Error is defined as

$$Error = \frac{Pred.\ \Delta P_{total}}{Expt.\ \Delta P_{total}} - 1 \tag{11.4}$$

where ΔP_{total} is the overall pressure drop, which includes the friction, acceleration and gravity components. Table 11.1 lists the assessment results of various correlations. As a comparison, the prediction accuracy of the present model (Chapter 10) is also shown in the same table; it is

Table II.1: Prediction Accuracy for Various Correlations.

Correlation	No. of Data	Average Error	RMS Error
Reddy et al. [1982]	5085	0.0427	0.1584
Chisholm [1973]	5085	0.0469	0.2009
Lombardi-Pedrocchi [1972]	5085	-0.1376	0.2169
Beattie (annular flow) [1974]	5085	0.0978	0.2558
Homogeneous [Dukler et al., 1964]	5085	0.1076	0.2728
Homogeneous [McAdams et al., 1942]	5085	0.1158	0.2804
Beattie-Whalley [1982]	5085	0.1257	0.2893
Chisholm-Sutherland (smooth) [1969]	5085	0.1234	0.2942
Homogeneous [Cicchitti et al., 1960]	5085	0.1245	0.2924
Homogeneous [Owens, 1961]	5085	0.1299	0.3016
Chisholm-Sutherland (rough) [1969]	5085	0.1386	0.3165
Thom [1964]	5085	0.1404	0.3174
Beattie (large-bubble flow) [1974]	5085	0.1557	0.3357
Beattie (small-bubble flow) [1974]	5085	0.1716	0.3564
Friedel [1979]	5085	0.1906	0.3318
Levy (turbulent-turbulent) [1952]	5085	0.3598	0.6874
Chisholm-Martinelli-Nelson [1983]	5085	0.4960	0.8201
Becker et al. [1962d]	5085	0.7301	1.1990
Chisholm-Lockhart-Martinelli [1967]	5085	1.5812	2.8319
Present Model	5085	0.0702	0.128

better than all assessed correlations. Except for the Lombardi-Pedrocchi correlation, all correlations overpredict the data, most of them by a large margin. Overall, the Reddy et al. correlation [1982] gives the best prediction, with a 4.27% average error and 15.84% rms error, for a total of 5085 data over five measuring sections. Figure 11.1 compares the predicted and experimental pressure drops. Both the Chisholm [1973] and Lombardi-Pedrocchi [1972] correlations predict the data with about the same rms errors. However, the Chisholm correlation gives a much better average error (4.69%), indicating a better fit of data, than the Lombardi-Pedrocchi correlation. All definitions of two-phase viscosity used in the homogeneous flow model result in similar accuracy, but those proposed by Dukler et al. [1964] and McAdams et al. [1942] are slightly better. The correlations representing various graphical methods (such as

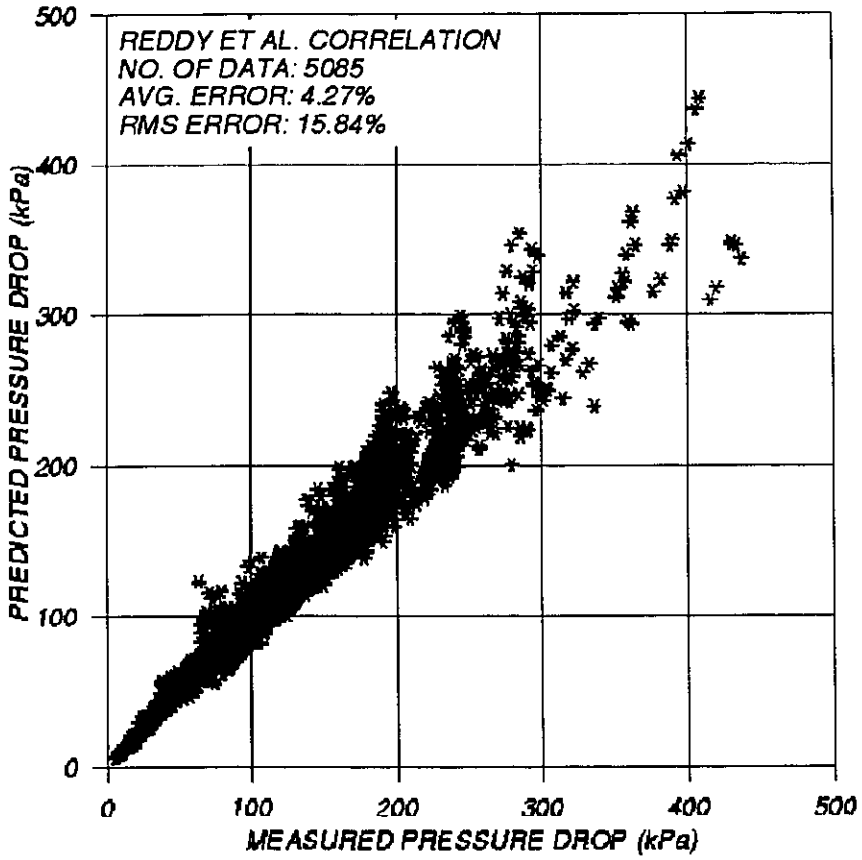

Figure ll.1: Comparison Between Predicted and Experimental Pressure Drops for the Reddy et al. Correlation [1982].

the Chisholm-Lockhart-Martinelli and the Chisholm-Martinelli-Nelson correlations) are not valid for the present conditions of interest.

The above assessment represents the most common approach in using the correlations (i.e., extrapolate them to any conditions despite invalid applications). However, it does not provide a fair comparison, since most of these correlations were developed for adiabatic flow where a liquid/surface contact is often maintained. In film boiling, however, the high surface temperature prevents the liquid from reaching the surface, and only a vapour/surface contact is possible. Due to the low vapour viscosity, the pressure drop is expected to be much smaller for conditions with vapour/surface than liquid/surface contact. Hence, these correlations tend to overpredict the data

(which are shown in Table 11.1). This trend becomes even more noticeable when the prediction errors are separated for various measuring sections.

Table 11.2 shows the prediction errors of the correlations in various measuring sections. A significant difference in prediction errors has been observed between inlet and outlet sections. While the data are overpredicted significantly at the outlet section, the prediction accuracy improves gradually for the sections upstream from the outlet. Since film boiling was normally encountered at the outlet section and at Section 4, the overprediction is therefore caused by the invalid applications of these correlations in this heat-transfer regime. The correlations, on the other hand, appear to predict the data very well at the pre-dryout heat-transfer regimes: single-

Table 11.2: Prediction Accuracy of Correlations at Each Measuring Section.

Correlation	No. of Data	Outlet Section		Section 4		Section 3		Section 2		Inlet Section	
		Ave.	RMS	Ave.	RMS	Ave.	RMS	Ave.	RMS	Ave.	RMS
Reddy et al. [1982]	1017	0.1457	0.2868	0.0340	0.1655	-0.0084	0.0891	0.0083	0.0670	0.0340	0.0582
Chisholm [1973]	1017	0.2018	0.3789	0.0449	0.2023	-0.0231	0.0982	-0.0129	0.0722	0.0237	0.0505
Beattie (annular flow) [1974]	1017	0.3074	0.4833	0.1204	0.2683	0.0236	0.1167	0.0092	0.0714	0.0286	0.0546
Homogeneous [Dukler et al., 1964]	1017	0.3330	0.5163	0.1347	0.2863	0.0302	0.1232	0.0113	0.0726	0.0288	0.0550
Homogeneous [McAdams et al., 1942]	1017	0.3480	0.5308	0.1463	0.2953	0.0385	0.1261	0.0160	0.0719	0.0301	0.0556
Chisholm-Sutherland (smooth) [1969]	1017	0.3719	0.5610	0.1570	0.3069	0.0422	0.1264	0.0163	0.0703	0.0297	0.0554
Beattie-Whalley [1982]	1017	0.3612	0.5402	0.1593	0.3035	0.0505	0.1314	0.0246	0.0734	0.0332	0.0579
Homogeneous [Cicchitti et al., 1960]	1017	0.3685	0.5544	0.1590	0.3080	0.0454	0.1299	0.0188	0.0718	0.0306	0.0559
Homogeneous [Owens, 1961]	1017	0.3835	0.5734	0.1665	0.3167	0.0487	0.1322	0.0199	0.0718	0.0308	0.0560
Chisholm-Sutherland (rough) [1969]	1017	0.4077	0.6041	0.1784	0.3306	0.0539	0.1355	0.0217	0.0714	0.0311	0.0561
Thom [1964]	1017	0.4077	0.6029	0.1815	0.3342	0.0572	0.1404	0.0238	0.0739	0.0317	0.0568
Beattie (large-bubble flow) [1974]	1017	0.4394	0.6370	0.2032	0.3550	0.0710	0.1499	0.0310	0.0760	0.0336	0.0583
Beattie (small-bubble flow) [1974]	1017	0.4728	0.6749	0.2256	0.3783	0.0852	0.1622	0.0386	0.0805	0.0358	0.0604
Friedel [1979]	1017	0.4467	0.6093	0.2349	0.3524	0.1241	0.1782	0.0867	0.1207	0.0605	0.0933
Lombardi-Pedrocchi [1972]	1017	-0.1029	0.2532	-0.1846	0.2491	-0.2008	0.2431	-0.1474	0.1991	-0.0522	0.1021
Levy (turbulent-turbulent) [1952]	1017	0.9547	1.3077	0.4962	0.7226	0.2195	0.3283	0.0862	0.1342	0.0422	0.0670
Chisholm-Martinelli-Nelson [1983]	1017	1.1547	1.4714	0.6979	0.9291	0.3777	0.5079	0.1798	0.2540	0.0697	0.1109
Becker et al. [1962d]	1017	1.7155	2.1724	1.0195	1.3305	0.5584	0.7344	0.2658	0.3710	0.0909	0.1475
Chisholm-Lockhart-Martinelli [1967]	1017	3.7501	5.4420	2.1299	2.6852	1.2552	1.6193	0.6025	0.8554	0.1680	0.2967
Present Model	1017	0.0367	0.1293	0.0597	0.1261	0.0830	0.1304	0.0881	0.1275	0.0833	0.1268

phase liquid flow, boiling flow and forced convective evaporation. This finding suggests that a combination of correlations could improve the prediction accuracy.

11.4 MULTI-CORRELATION METHOD

The assessment results presented in Section 11.3 showed that most of the assessed correlations overpredict the experimental data, and the largest differences occur at the outlet section, where a large amount of film-boiling data were obtained. The overprediction is mainly caused by the assumption in many correlations of a liquid/surface contact, which is not valid in film boiling. To improve the prediction accuracy, a combination of correlations is used to limit the applications of any correlation only to its valid heat-transfer regime. Table 11.2 has shown that most adiabatic correlations are valid for the pre-dryout heat-transfer regime, but not for the post-dryout regime. The most appropriate transition point is the critical heat flux, where the heat-transfer regime changes from a liquid/surface to vapour/surface contact. Hence, an adiabatic correlation is used for conditions up to the critical heat flux, and a separate post-dryout (PDO) correlation is required for conditions beyond that point.

At high-pressure and high-flow conditions, dispersed flow film boiling is the primary PDO heat-transfer regime encountered inside a tube (see Figure 3.2 b). It consists of a continuous vapour flow, which is in contact with the heated surface, and a dispersed flow of entrained droplets. In most conditions, the size of droplets is small and a homogeneous-flow assumption is appropriate. Therefore, the homogeneous-flow model (Equation (6.1)), based on vapour density and vapour friction factor, is often used. For large and closely packed droplets, however, the homogeneous-flow assumption may not be valid, and Beattie [1973, 1975, 1977] proposed a separate correlation for PDO flow. Although this correlation was validated by Beattie [1973, 1975 and 1977] with only a limited data set, its predictions agreed with the data of Kohler and Kastner [1987]. Therefore, the Beattie PDO correlation is used for predicting the pressure gradient in post-dryout flow.

Referring back to the methodology (Section 11.2), an additional step is introduced following Step (g):

g1) The critical heat flux is calculated based on the local conditions. If the local heat flux exceeds the critical heat flux (i.e., post-dryout conditions are present), the Beattie post-dryout correlation is used.

A similar methodology (i.e., combining several correlations for various heat-transfer regimes) was introduced by Beattie [1975, 1977]. It has been described in Section 6.4.3.

11.5 ASSESSMENT RESULTS OF THE MULTI-CORRELATION METHOD

Table 11.3 shows the assessment results of the multi-correlation method (as described in Section 11.4). Both the average and rms errors are improved significantly. Overall, the combination of the Reddy et al. [1982] and Beattie PDO [1974] correlations is the best, with a -0.43% average error and 8.68% rms error for a total of 5085 data over five measuring sections. This is not surprising, since the data used by Reddy et al. (including both adiabatic flow and flow boiling) in deriving their correlation were obtained at high-pressure and high-flow conditions. However, this comparison indicates a much better performance than that presented by Reddy et al. with their data base (about 20% in rms error for 864 flow-boiling data). Figure 11.2 shows the comparison between predicted and experimental pressure drops.

The combination of the Chisholm [1973] and the Beattie PDO [1974] correlations predicts the data very well, with an average error of -1.11% and rms error of 9.88%. This result agrees with the comparison done by Reddy et al. [1982], who showed a similar accuracy between their correlation and the Chisholm correlation. The prediction accuracy, however, is better than expected, since the correlation was primarily derived with adiabatic data (mostly air-water flow),

Table II.3: Prediction Accuracy for Various Combinations of Correlations.

Combination of Correlations	No. of Data	Average Error	RMS Error
Reddy et al. [1982] / Beattie (PDO flow) [1974]	5085	-0.0043	0.0868
Chisholm [1973] / Beattie (PDO flow) [1974]	5085	-0.0111	0.0988
Beattie (annular flow) [1974] / Beattie (PDO flow) [1974]	5085	0.0271	0.1162
Homogeneous [Dukler et al., 1964] / Beattie (PDO flow) [1974]	5085	0.0333	0.1241
Homogeneous [McAdams et al., 1942] / Beattie (PDO flow) [1974]	5085	0.0399	0.1279
Chisholm-Sutherland (smooth) [1969] / Beattie (PDO flow) [1974]	5085	0.0440	0.1319
Beattie-Whalley [1982] / Beattie (PDO flow) [1974]	5085	0.0489	0.1324
Homogeneous [Cicchitti et al., 1960] / Beattie (PDO flow) [1974]	5085	0.0459	0.1336
Homogeneous [Owens, 1961] / Beattie (PDO flow) [1974]	5085	0.0492	0.1376
Chisholm-Sutherland (rough) [1969] / Beattie (PDO flow) [1974]	5085	0.0543	0.1436
Thom [1964] / Beattie (PDO flow) [1974]	5085	0.0565	0.1463
Beattie (large-bubble flow) [1974] / Beattie (PDO flow) [1974]	5085	0.0680	0.1573
Beattie (small-bubble flow) [1974] / Beattie (PDO flow) [1974]	5085	0.0799	0.1704
Friedel [1979] / Beattie (PDO flow) [1974]	5085	0.1067	0.1727
Lombardi-Pedrocchi [1972] / Beattie (PDO flow) [1974]	5085	-0.1622	0.2174
Levy (turbulent-turbulent) [1952] / Beattie (PDO flow) [1974]	5085	0.2049	0.3699
Chisholm-Martinelli-Nelson [1983] / Beattie (PDO flow) [1974]	5085	0.3274	0.5110
Becker et al. [1962d] / Beattie (PDO flow) [1974]	5085	0.4914	0.7544
Chisholm-Lockhart-Martinelli [1967] / Beattie (PDO flow) [1974]	5085	1.0882	1.6201
Present Model	5085	0.0702	0.1280

although it was validated with some of Becker's flow-boiling data. Figure 11.3 compares the predicted and experimental pressure drops. Despite the slightly higher prediction error, this combination of correlations is more favoured, because the Chisholm correlation has a much wider range of applications than the Reddy et al. correlation. The combinations of Beattie PDO and other Chisholm's correlations provide less accurate predictions.

Large differences in prediction accuracy are shown for the combination of various correlations proposed by Beattie [1974]. The combination of the annular-flow and PDO flow equations gives the lowest rms error, despite its assumption of an idealized annular-flow structure (i.e., with no entrainment). This is perhaps the result of compensated errors from various simplified assumptions. However, most of the test conditions correspond primarily to the forced-convective

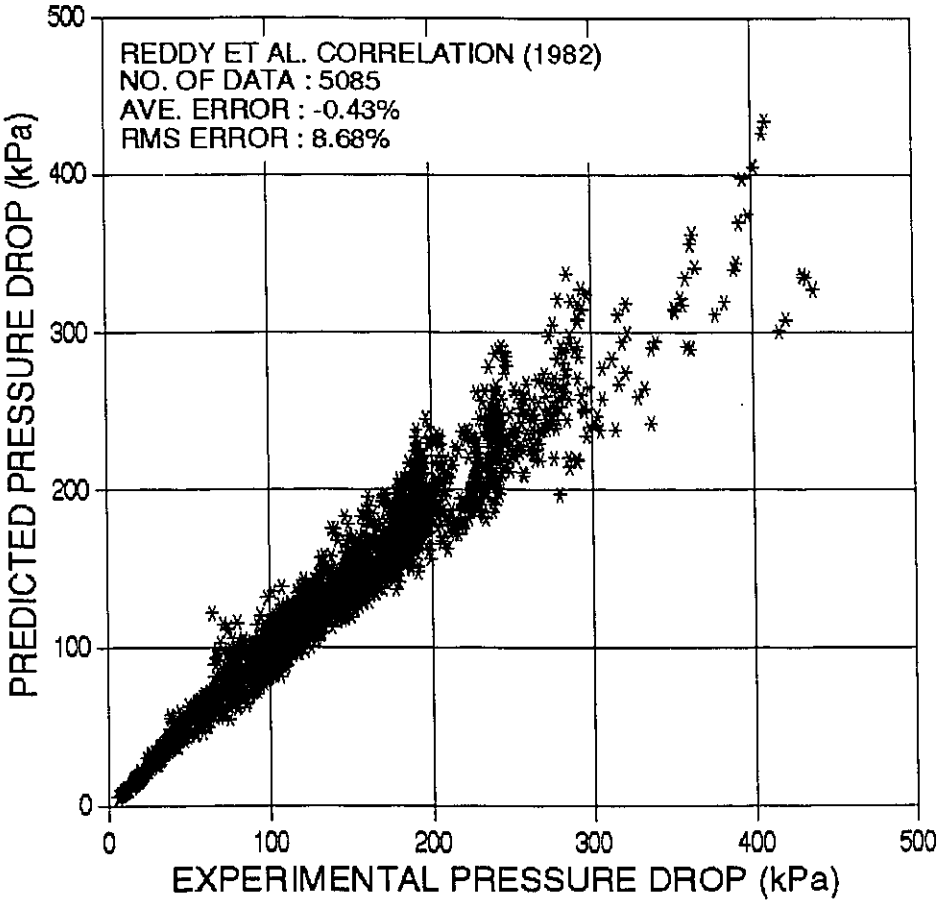

Figure 11.2: Comparison Between Predicted and Experimental Pressure Drops for the Combination of the Reddy et al. and the Beattie PDO Correlations.

evaporation region, which associates with the annular flow pattern. Figure 11.4 presents the comparison between predicted and experimental pressure gradients. The use of equations derived for bubbly flow (for either large or small bubbles) tends to overpredict the pressure gradient. The difference in bubble-size assumption does not have a strong impact on the predictions. Both correlations predict the pressure gradient in about the same magnitude.

The combination of the hybrid equation of Beattie and Whalley [1982] and the Beattie PDO [1974] correlations provides predictions between the correlations for annular and bubbly flows, since its viscosity calculation is based on an optimized expression of these two flow patterns.

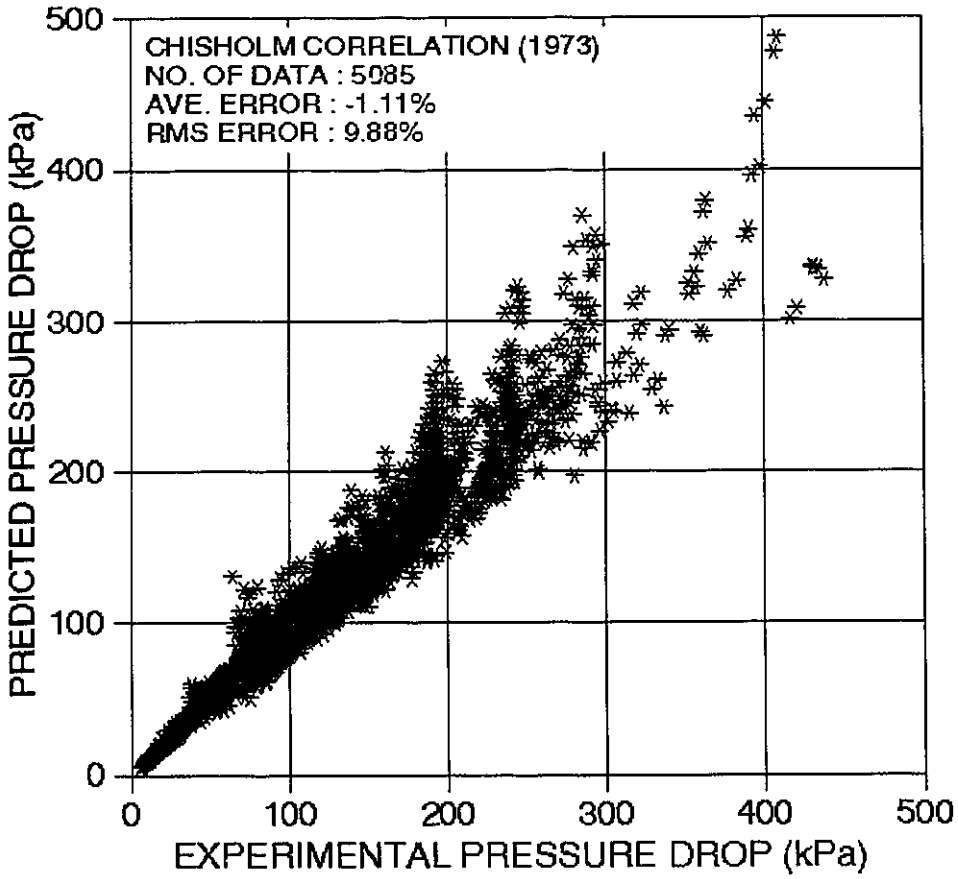

Figure II.3: Comparison Between Predicted and Experimental Pressure Drops for the Combination of the Chisholm and the Beattie PDO Correlations

The prediction accuracy of the homogeneous model depends strongly on the definition of two-phase viscosity. For those examined in this study, the definition by Dukler et al. [1964] provides the best prediction, while the definition by Owens [1961] gives the worst.

The prediction accuracy of the combined Friedel [1979] and Beattie PDO [1974] correlation is much worse than the others, even though this correlation was based on the largest data base. This is primarily caused by the large diversity and scatter among its data base. The combined correlation predicts the present data with an average error of 10.67% and a rms error of 17.27%, which is within the uncertainty limit of its data base for single-component two-phase flow.

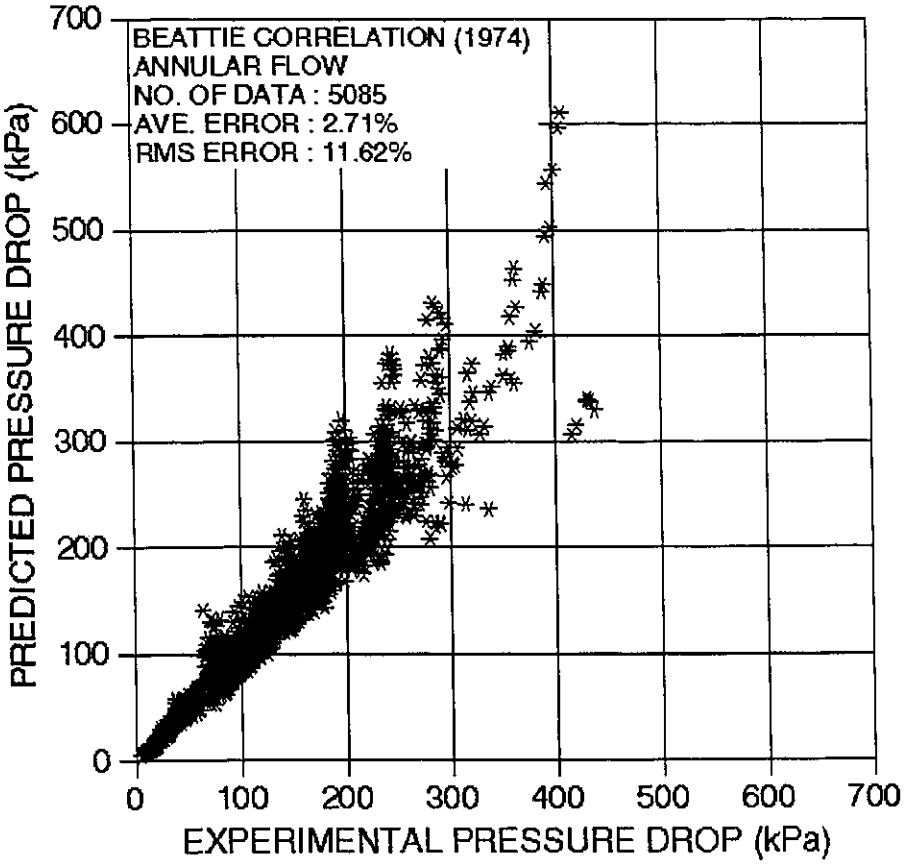

Figure 11.4: Comparison Between Predicted and Experimental Pressure Drops for the Combination of the Beattie Annular-Flow and the Beattie PDO Correlations.

Other correlations based on small data bases (such as the Becker et al. [1962d] and the Lombardi and Pedrocchi [1972] correlations) provide less satisfactory predictions. Similarly, the equations that represent various graphical prediction methods also give poor prediction accuracy. Among them, the Thom equation [1964] is slightly better than the others.

11.6 A CLOSE EXAMINATION OF THE COMPARISON

The comparison presented in Section 11.5 provides only an overall prediction capability of the correlations. While the performance of the best three combinations of correlations appears to be

impressive, a large scatter among the predictions has been observed in Figures 11.2 to 11.4. A number of data are overpredicted by a relatively large margin (close to 100%), and this could be significant in some applications. Therefore, the comparison is examined in detail at each measuring section.

Table 11.4 lists the prediction accuracy of various combinations of correlations (in the same order as in Table 11.3) for each measuring section. To avoid overcrowding, each combination is identified with the correlation which is used for the pre-dryout conditions; the Beattie PDO correlation is used for the post-dryout conditions but is not shown in Table 11.4. For each combination, large differences in prediction accuracy are observed between various measuring sections. The rms error is the smallest at the inlet section, where single-phase liquid flow is

Table 11.4: Prediction Accuracy of Various Combinations of Correlations at Each Measuring Section.

Correlation	No. of Data	Outlet Section		Section 4		Section 3		Section 2		Inlet Section	
		Ave.	RMS	Ave.	RMS	Ave.	RMS	Ave.	RMS	Ave.	RMS
Reddy et al. [1982]	1017	-0.0171	0.1218	-0.0276	0.0906	-0.0175	0.0822	0.0070	0.0673	0.0338	0.0580
Chisholm [1973]	1017	-0.0050	0.1496	-0.0273	0.1017	-0.0328	0.0901	-0.0140	0.0732	0.0235	0.0504
Beattie (annular flow) [1974]	1017	0.0553	0.1853	0.0322	0.1258	0.0121	0.0963	0.0078	0.0713	0.0283	0.0545
Homogeneous [Dukler et al., 1964]	1017	0.0674	0.2000	0.0424	0.1362	0.0183	0.1011	0.0099	0.0723	0.0286	0.0548
Homogeneous [McAdams et al., 1942]	1017	0.0764	0.2074	0.0520	0.1414	0.0264	0.1027	0.0145	0.0714	0.0299	0.0554
Chisholm-Sutherland (smooth) [1969]	1017	0.0862	0.2186	0.0595	0.1451	0.0299	0.1014	0.0149	0.0698	0.0295	0.0552
Beattie-Whalley [1982]	1017	0.0864	0.2138	0.0636	0.1478	0.0382	0.1070	0.0232	0.0726	0.0330	0.0577
Homogeneous [Cicchitti et al., 1960]	1017	0.0869	0.2188	0.0618	0.1490	0.0331	0.1052	0.0174	0.0711	0.0304	0.0557
Homogeneous [Owens, 1961]	1017	0.0934	0.2268	0.0672	0.1537	0.0362	0.1068	0.0185	0.0711	0.0306	0.0558
Chisholm-Sutherland (rough) [1969]	1017	0.1039	0.2397	0.0756	0.1605	0.0411	0.1086	0.0202	0.0707	0.0309	0.0559
Thom [1964]	1017	0.1058	0.2415	0.0784	0.1652	0.0443	0.1136	0.0224	0.0730	0.0315	0.0566
Beattie (large-bubble flow) [1974]	1017	0.1236	0.2602	0.0957	0.1797	0.0577	0.1216	0.0295	0.0748	0.0334	0.0580
Beattie (small-bubble flow) [1974]	1017	0.1422	0.2809	0.1133	0.197	0.0714	0.1327	0.0370	0.0791	0.0356	0.0601
Friedel [1979]	1017	0.1460	0.2564	0.1312	0.1922	0.1110	0.1540	0.0852	0.1189	0.0603	0.0929
Lombardi-Pedrocchi [1972]	1017	-0.1858	0.2432	-0.2175	0.2555	-0.2066	0.2475	-0.1486	0.2006	-0.0524	0.1025
Levy (turbulent-turbulent) [1952]	1017	0.3826	0.6147	0.3157	0.4490	0.2001	0.2880	0.0843	0.1312	0.0420	0.0666
Chisholm-Martinelli-Nelson [1983]	1017	0.5427	0.7764	0.4929	0.6421	0.3545	0.4645	0.1777	0.2503	0.0694	0.1103
Becker et al. [1962d]	1017	0.8317	1.1566	0.7404	0.9418	0.5306	0.6816	0.2635	0.3673	0.0906	0.1469
Chisholm-Lockhart-Martinelli [1967]	1017	1.8109	2.3940	1.6528	2.0500	1.2110	1.5432	0.5985	0.8489	0.1680	0.2958

encountered at most flow conditions. It is the largest at the outlet section, where two-phase flow boiling is usually experienced.

The following detailed examination of prediction accuracy for various flow conditions is based on the combination of the Reddy et al. [1982] and the Beattie PDO [1974] correlations, which has the best prediction accuracy. Figure 11.5 shows the differences between predicted and experimental pressure drops in all measuring sections at an outlet pressure of 9.6 MPa, a mass flux of 4.3 $Mg.m^{-2}.s^{-1}$ and an inlet temperature of 302°C. As shown in both the inlet section and Section 2, the agreement between predicted and experimental pressure drops is good at low qualities. When the heated surface approaches dryout, however, the predicted pressure drops become higher than the experimental values at an average thermodynamic quality of

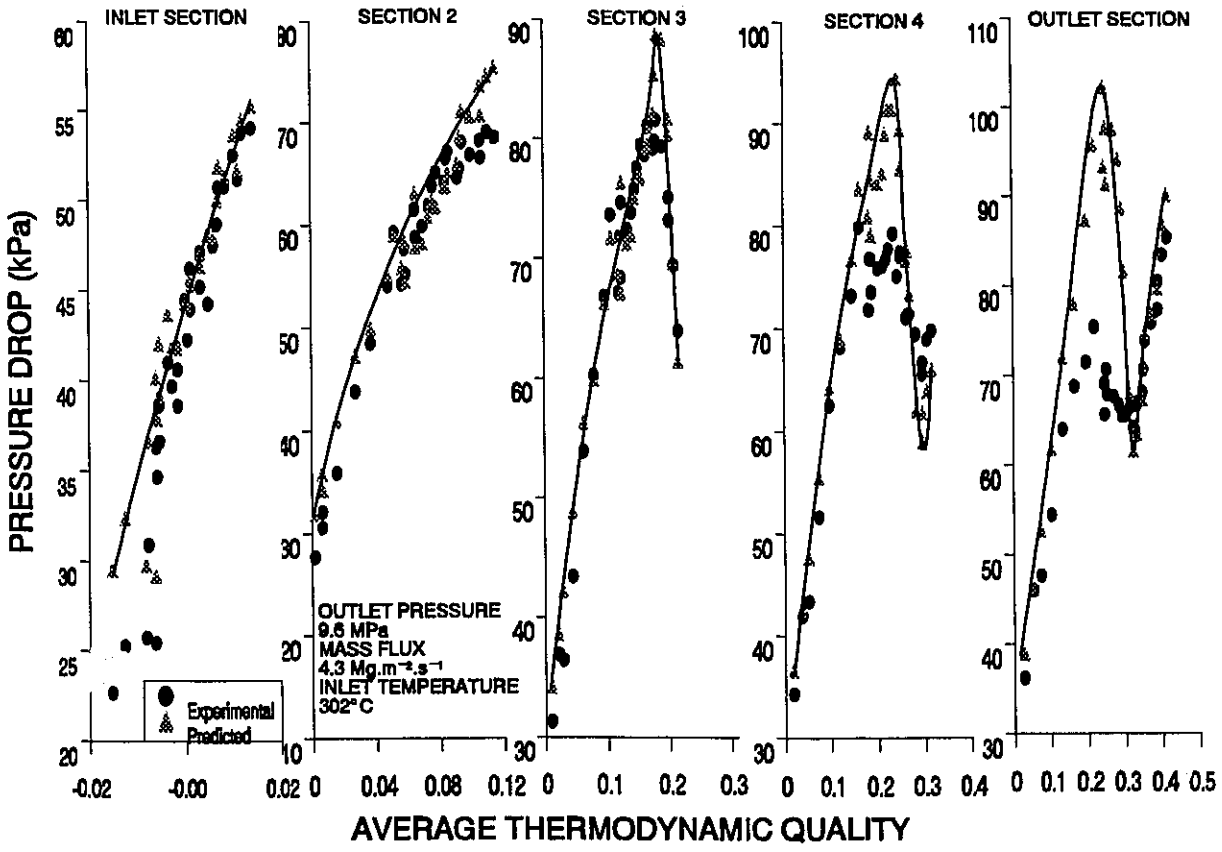

Figure 11.5: Comparison Between Predicted and Experimental Pressure Drops for the Combination of the Reddy et al. and the Beattie PDO Correlations at an Inlet Quality of -3%.

approximately 0.2. The difference is particularly large at the outlet section, where the overprediction is as much as 50% of the experimental values. Beyond dryout, the predictions of the Beattie PDO correlation for post-dryout pressure drop agree very well with the experimental data.

Figure 11.6 shows the comparison at an outlet pressure of 9.6 MPa, a mass flux of 4.3 $Mg.m^{-2}.s^{-1}$ and an inlet temperature of 252°C. A similar trend to that of high inlet temperature (Figure 11.5) is observed, but the overprediction in pressure drops is not as noticeable at conditions where the heated surface is approaching dryout. Furthermore, the pressure drops at pre-dryout conditions in the outlet section appear to be slightly underpredicted by the correlations. Insufficient data

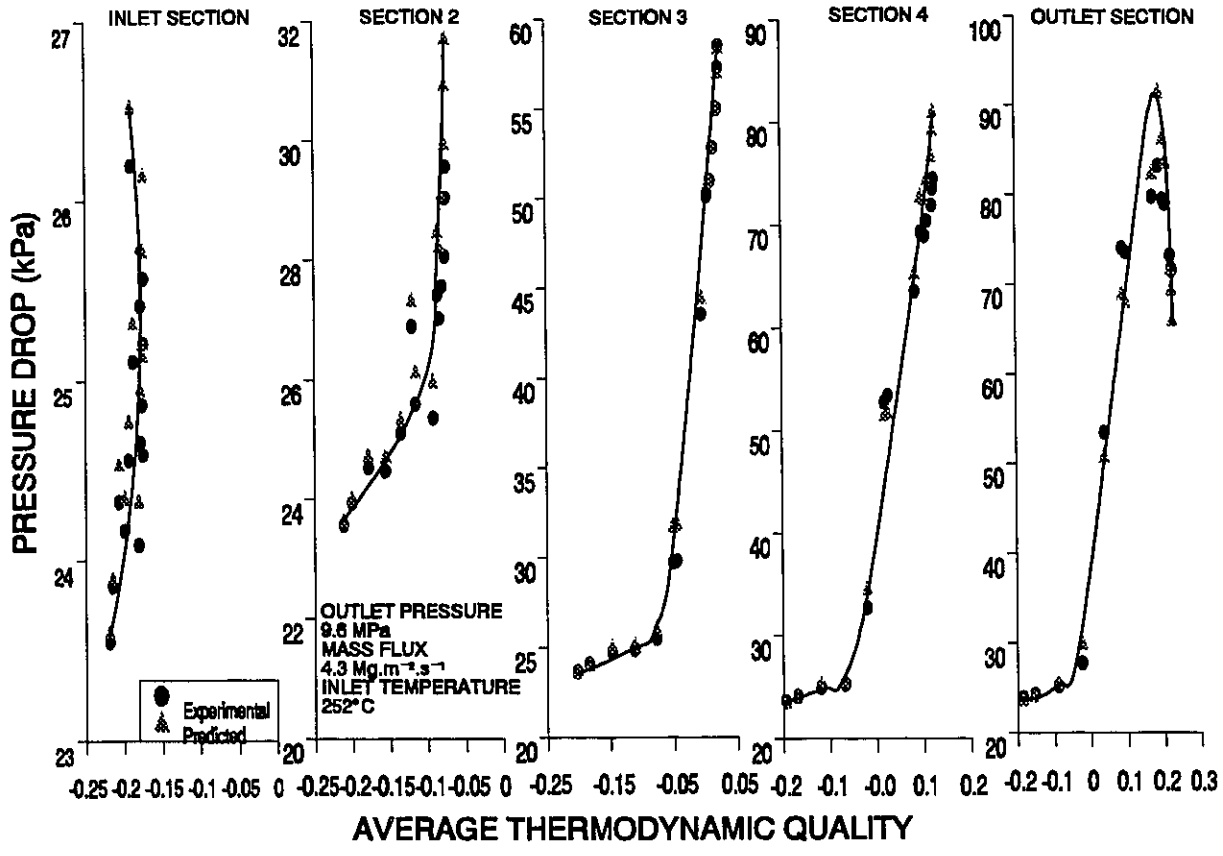

Figure 11.6: Comparison Between Predicted and Experimental Pressure Drops for the Combination of the Reddy et al. and the Beattie PDO Correlations at an Inlet Quality of -22%.

are available to verify the agreement between the predicted and experimental pressure drops at the post-dryout conditions.

A slightly different trend is shown in Figure 11.7 at an outlet pressure of 9.6 MPa, a mass flux of 7.0 $Mg.m^{-2}.s^{-1}$ and an inlet temperature of 302°C. While the single-phase pressure drops are well predicted, the pressure drops are mostly underpredicted at the pre-dryout conditions. Beyond the point of maximum pressure drop, the data are overpredicted. Relatively good agreement between predictions and data is shown for the post-dryout conditions.

An underprediction of pressure drops at pre-dryout conditions is shown at very high mass-flux conditions ($G = 9.9\ Mg.m^{-2}.s^{-1}$) in Figure 11.8. The agreement at conditions beyond the

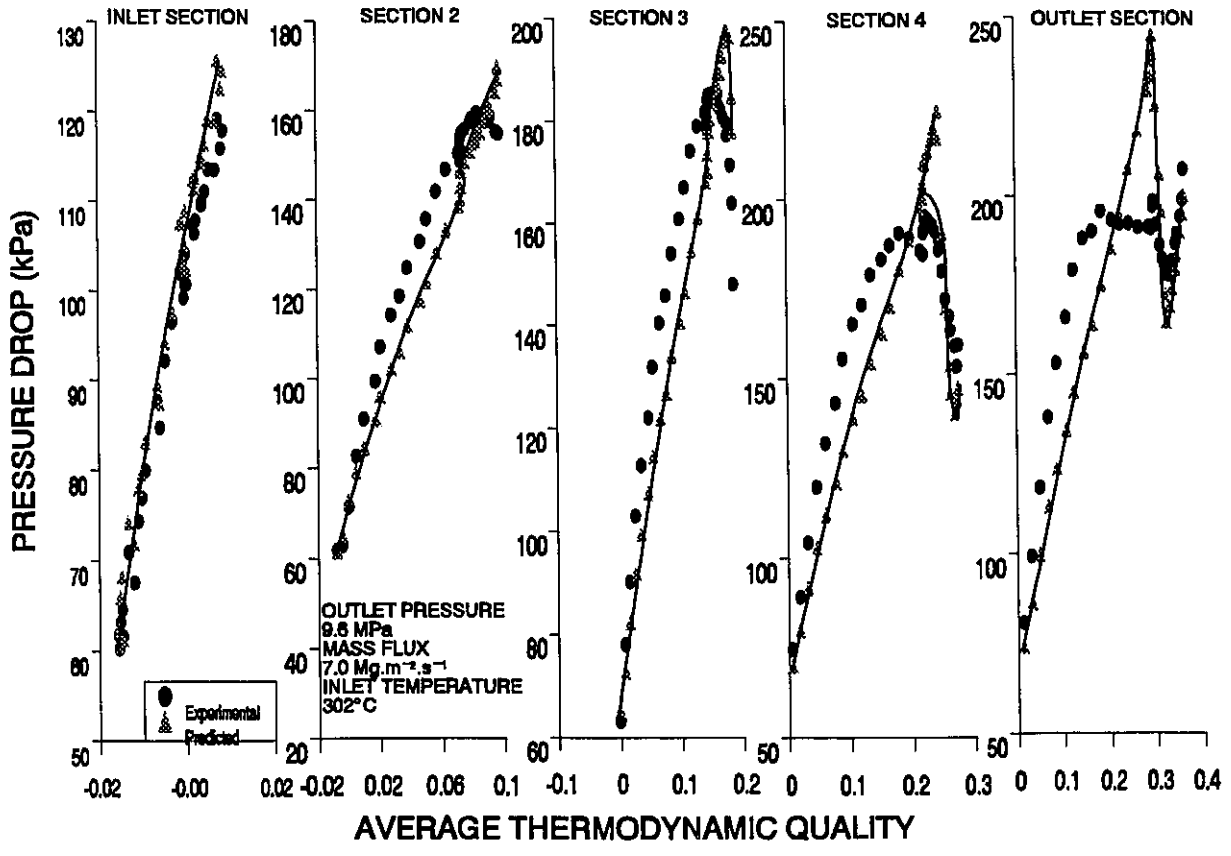

Figure 11.7: Comparison Between Predicted and Experimental Pressure Drops for the Combination of the Reddy et al. and the Beattie PDO Correlations at a Mass flux of 7 $Mg.m^{-2}.s^{-1}$.

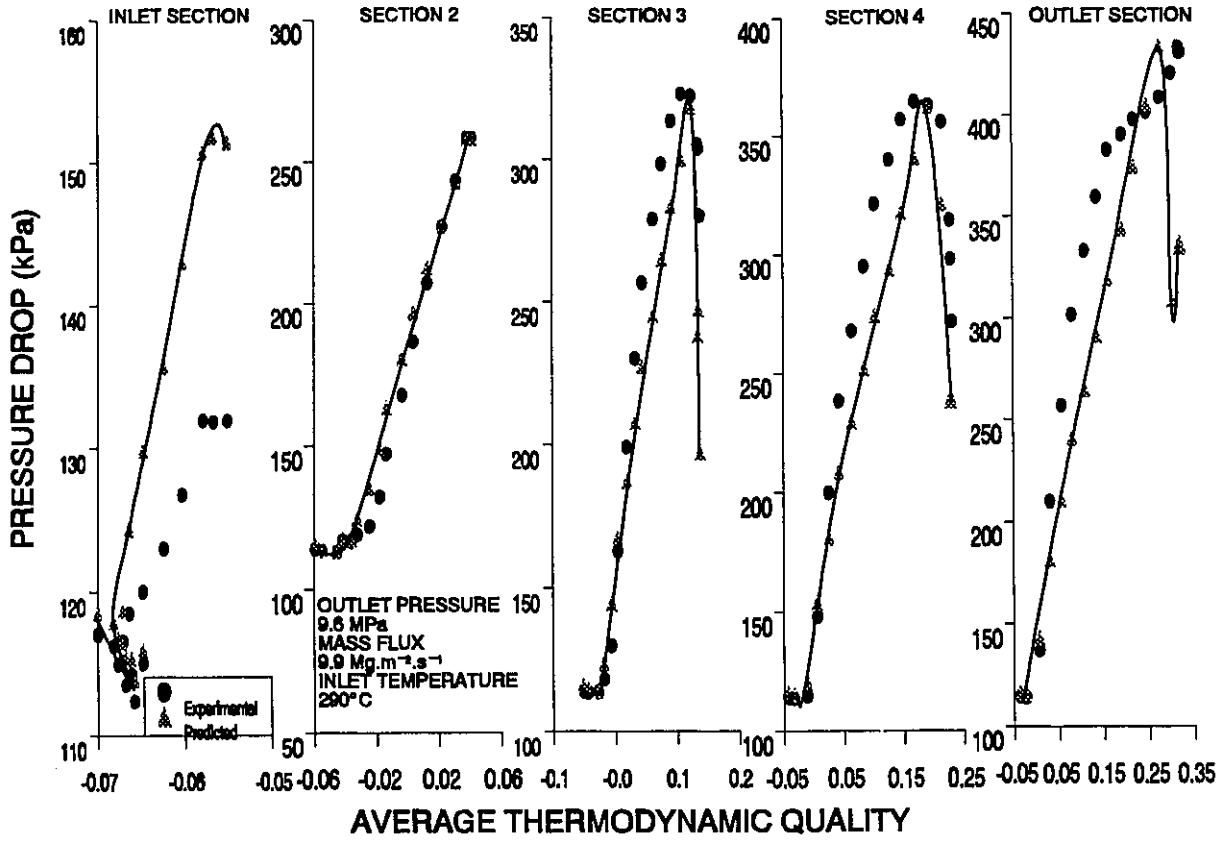

Figure 11.8: Comparison Between Predicted and Experimental Pressure Drops for the Combination of the Reddy et al. and the Beattie PDO Correlations at a Mass flux of 9.9 $Mg.m^{-2}.s^{-1}$

maximum pressure-drop point is apparently good in Sections 3 and 4, which indicate the upstream dryout phenomenon. This is mainly due to the good prediction in critical heat flux leading to the use of the pressure-drop correlation for the post-dryout conditions, rather than the one for the pre-dryout conditions. At these conditions, dryout has not been reached at the end of the tube and the pressure drops remain high at high qualities in the outlet section. This has led to an underprediction in pressure drops, since dryout was predicted by the present method. The uncertainty among data is high at the inlet section, where the entrance effect may be significant at high flows.

An examination of the data for low mass-flux conditions (i.e., 1-3 $Mg.m^{-2}.s^{-1}$) indicates trends similar to those of high mass fluxes. The pressure drops are underpredicted at both the post-

dryout and the pre-dryout conditions before the maximum pressure-drop point, but are overpredicted at the pre-dryout conditions beyond the maximum pressure-drop point.

Figure 11.9 shows the comparison at an outlet pressure of 7 MPa, mass flux of 7 $Mg.m^{-2}.s^{-1}$ and inlet temperature of 280°C (corresponding to an inlet quality of -2%, which is the same as an inlet temperature of 305°C at 9.6 MPa). The pressure drops are overpredicted at the subcooled conditions (mainly at the inlet section), but underpredicted at the positive-quality regions. Similar to the data at high pressure, an overprediction is observed as the heated surface approaches dryout. Beyond dryout, the pressure drops are underpredicted by the correlation.

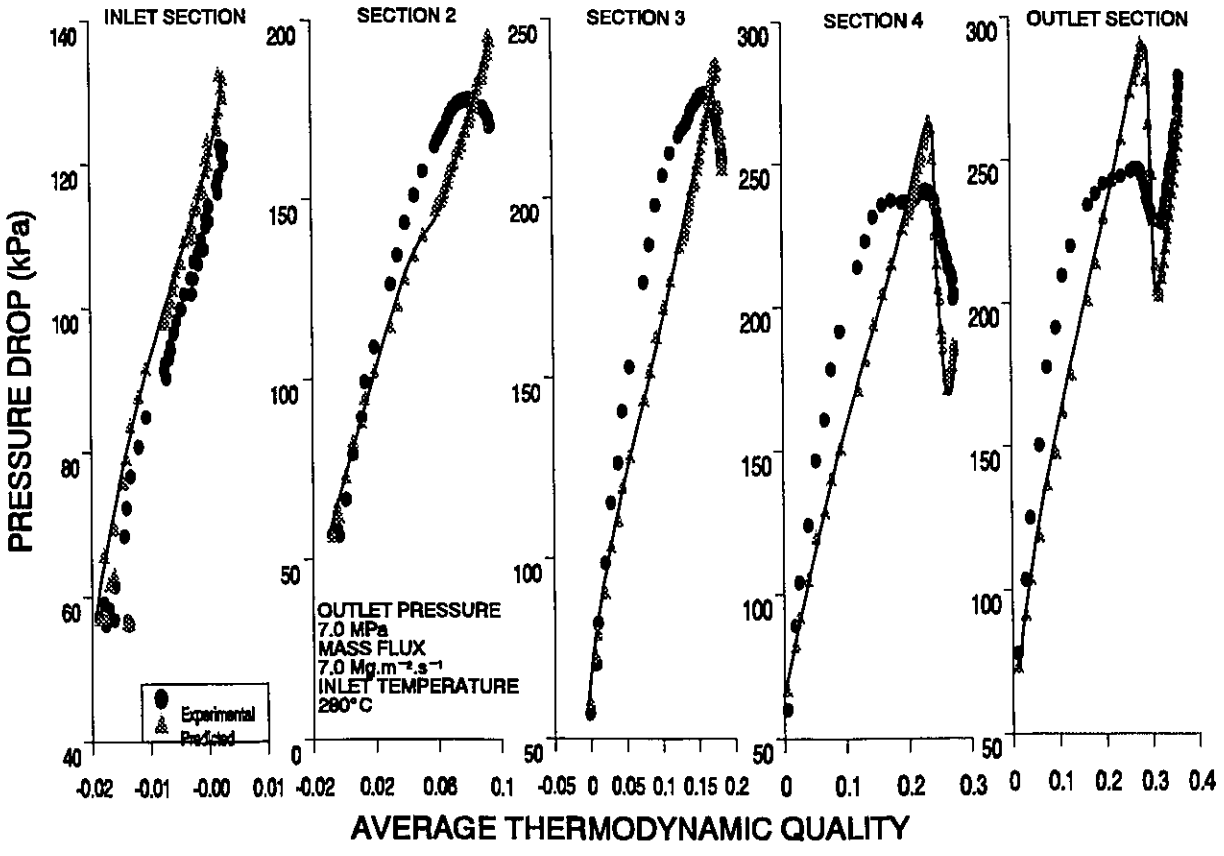

Figure 11.9: Comparison Between Predicted and Experimental Pressure Drops for the Combination of the Reddy et al. and the Beattie PDO Correlations at a Pressure of 7 MPa.

11.7 SUMMARY

In general, the experimental data have been predicted rather closely by the combination of the Reddy et al. [1982] and the Beattie PDO [1974] correlations. However, a systematic trend is shown, with underprediction at conditions before the maximum pressure-drop point and overprediction at conditions between the maximum pressure-drop and the dryout points. At post-dryout conditions, the agreement is good between most data and the predictions of the Beattie correlation; however, underprediction has also been observed for some data.

Although only the predictions of the combination of the Reddy et al. and the Beattie PDO correlations are shown, the same trend is noted for other combinations. The agreement between predictions and experimental data at low qualities was better for some combinations of correlations, which had a high overall average error. Figures 11.10 and 11.11 compare the predicted and experimental pressure drops for the combinations of the Beattie large-bubble and the Beattie PDO correlations (similar results were observed for the Beattie small-bubble correlation). While a systematic underprediction has been shown by the Reddy et al. correlation at the pre-dryout conditions, a close agreement is shown for the Beattie large-bubble correlation at low qualities (up to a thermodynamic quality of about 0.1). The increasing deviation as the quality increases is caused by the transition from bubbly to annular flow, where the correlation becomes invalid. On the other hand, the Beattie correlation for annular flow is also not applicable, because it assumes an idealized annular-flow structure with no liquid entrainment in the vapour core.

In summary, the present model gives a slightly better prediction accuracy than the use of a single correlation to predict flow-boiling pressure drop. It has been shown that none of the assessed correlation is valid for all heat-transfer regimes. By combining the adiabatic-flow and the Beattie PDO correlations, the overall prediction accuracy is significantly improved. However, a significant overprediction of the pressure drop remains at conditions between the maximum pressure-drop and the critical heat flux points. The model, on the other hand, provides a better

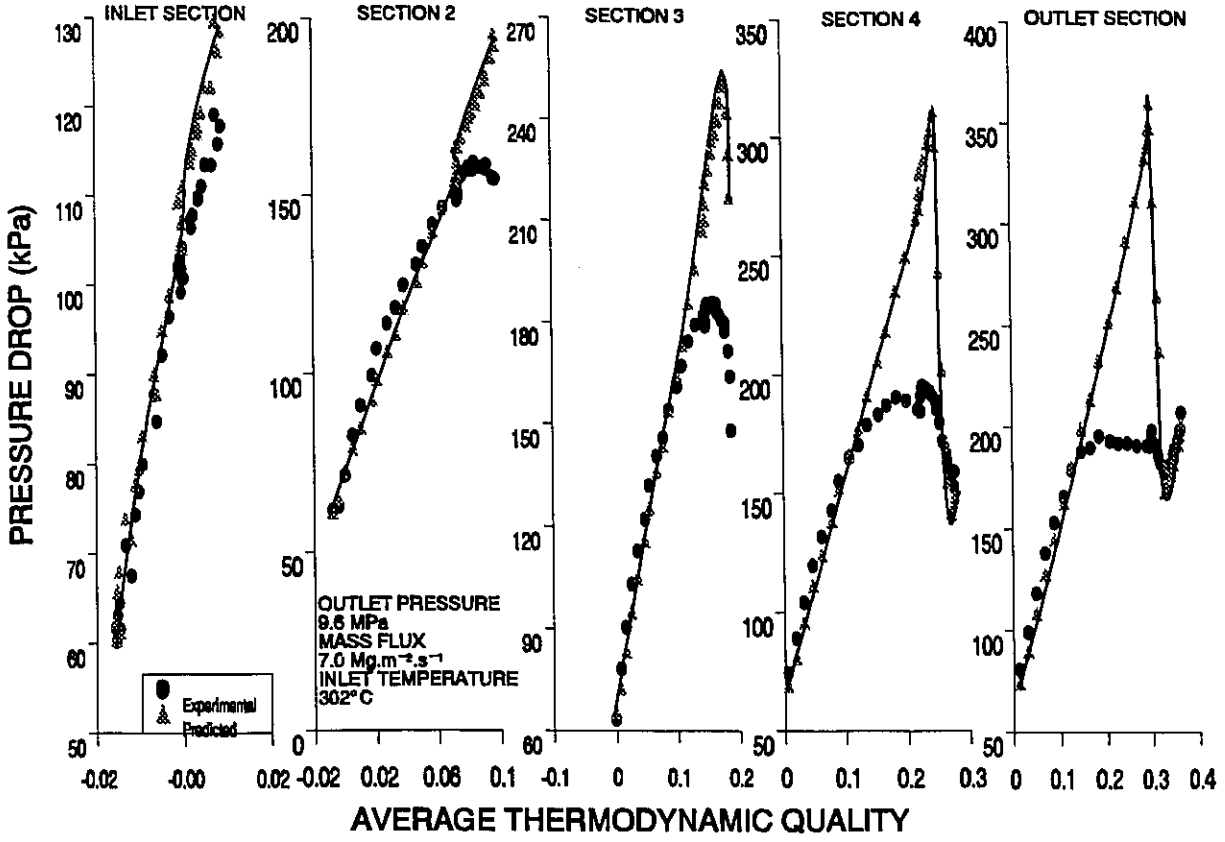

Figure 11.10: Comparison Between Predicted and Experimental Pressure Drops for the Combination of the Beattie Large-Bubble and the Beattie PDO Correlations at a Mass flux of 7 $Mg.m^{-2}.s^{-1}$

prediction accuracy over these conditions and exhibits a similar trends to those shown among the experimental data.

It should be noted that, unlike most correlations, the present model has not been fine-tuned with any available pressure-drop data. The prediction accuracy of the present model can be improved by introducing flow-dependent correction factors derived from experimental data obtained at conditions of interest.

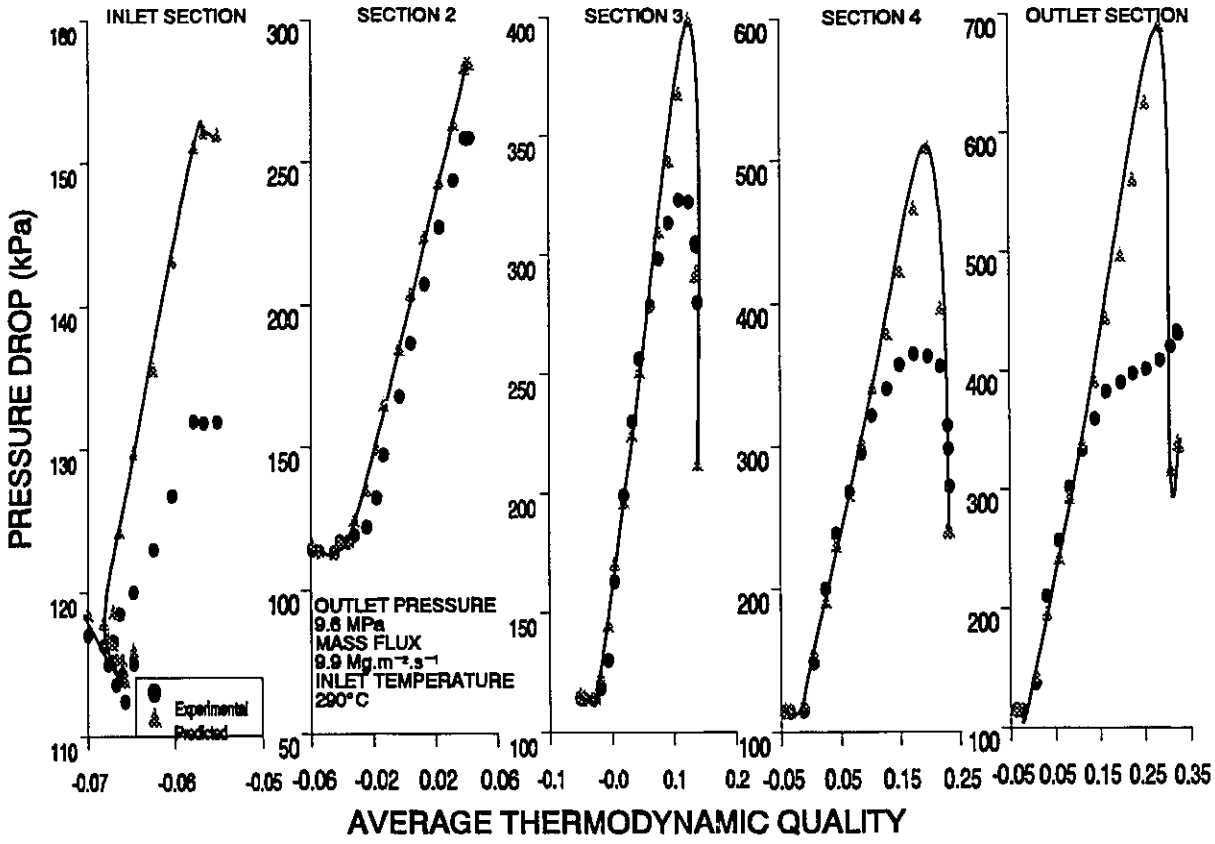

Figure ll.11: Comparison Between Predicted and Experimental Pressure Drops for the Combination of the Beattie Large-Bubble and the Beattie PDO Correlations at a Mass flux of 9.9 $Mg.m^{-2}.s^{-1}$

12. CONCLUSIONS AND FINAL REMARKS

1. A mechanistic model has been presented for predicting two-phase pressure drops in flow boiling at high-pressure and high-flow conditions. It covers heat-transfer modes of single-phase liquid, subcooled boiling, bulk boiling, forced convective evaporation and film boiling. The overall pressure drop is separated into three components: friction, acceleration and gravity. Since both the pressure drops due to acceleration and gravity are relatively small compared to the one due to friction, they are calculated with the separated-flow model. The present model is developed for a smooth tube and focuses on the effect of heating on two-phase pressure drop. An empirical approach has been used to account for the effects of surface roughness and radial temperature variation within the flow.

2. The model is based on the shear-stress/velocity-gradient relationship. Shear-stress expressions are presented as a function of frictional pressure gradients and velocity gradients for both the laminar sublayer and turbulent flow (laminar flow is not expected at the present conditions of interest). The mixing-length approach is used in analyzing the turbulent flow. In flow

boiling, shear-stress expressions similar to those of single-phase flow are used. Modifications are introduced to account for the changes in flow parameters (such as laminar-sublayer thickness and fluid properties) in the presence of two phases. Two empirical correlations are derived for predicting the entrained liquid fraction in high-pressure annular flow for adiabatic and flow-boiling conditions.

3. An experiment was set up to obtain pressure drop data in flow boiling at high-pressure and high-flow conditions to validate the model. It covered a wide range of flow conditions in a vertical tube. A strong effect of surface heating on pressure drop was observed. With increasing heat flux, the pressure drop decreases in single-phase flow, increases in bubbly flow and decreases in annular flow. Based on the experimental data, a correction factor for the adiabatic single-phase pressure drop has been derived for predicting pressure drop in a heated tube. A subsequent comparison showed that this correction factor is also valid for medium-pressure conditions.

4. In flow boiling, the effect of heating was found to be small at subcooled, bulk and film boiling, but becomes significant for forced convective evaporation for the same pressure, mass flux and flow quality (a strong effect is shown when the thermodynamic quality is used as a reference). The presence of a dry wall instead of a wet wall in the film-boiling region, however, was found to have a very strong effect on pressure drop. The pressure drop in forced convective evaporation decreases rapidly with increasing heat flux; a maximum in two-phase pressure drop is encountered at a quality lower than the value that corresponds to the occurrence of dryout. In addition to heating, other flow parameters such as pressure and mass flux were found to have strong effects on two-phase pressure drop.

5. Comparisons of experimental data were made against predictions of the present model and 19 different correlations (18 of them are developed for bulk boiling and forced-convective evaporation and 1 is derived for film boiling). Despite the simplifying assumptions, a relatively good agreement was obtained between model predictions and experimental data. The overall root-mean-square error of the predictions is 12.8% and the average error is 8.7%.

In many cases, the parametric trends of the data (such as the reduction in pressure drop beyond the maximum pressure-drop point) were well-predicted. The overprediction observed for some conditions is primarily caused by the underprediction of the entrained liquid fraction, resulting in a thicker liquid film.

6. The use of the adiabatic correlation for flow boiling overpredicts significantly the pressure drop at film-boiling conditions. A prediction scheme, similar to the one suggested by Beattie [1977], was employed. It uses the adiabatic correlation for pre-dryout conditions and the Beattie PDO correlation [1974] for film boiling. The transition between pre-dryout and post-dryout correlations is based on the critical heat flux criteria. The assessment has shown that some of the adiabatic correlations, when combined with the Beattie PDO correlation [1974], can provide a better prediction (in terms of overall rms error) than the present model. The combination of either the Reddy et al. [1982] or the Chisholm [1973] correlation and the Beattie PDO correlation [1974] resulted in an rms error of less than 10%. A close examination of the comparison, however, showed that this small rms error is primarily due to the compensating effect of underprediction at the low-quality conditions and overprediction at the high-quality conditions in forced-convective evaporation. Furthermore, these correlations did not predict the parametric trend of the flow-boiling pressure drop with respect to heat flux.

7. While the present model covers flow boiling from single-phase up to film boiling, and predicts the present set of data reasonably well, it could be viewed as the foundation for a model to which improvements and enhancements can be introduced to extend its applications. Potential enhancements include:

   - Entrained liquid fraction. The major factor affecting the accuracy of this model is the prediction of entrained liquid fraction, which is based on the correlations derived with a small data base. Strictly speaking, these correlations should not be used for the present conditions of interest, which are well beyond the range of the data base. Therefore, more high-pressure entrainment data are needed to establish a correct trend.

- Effect of temperature variation within the fluid. The presence of a high-temperature surface affects primarily the viscosity of the near-wall fluid, hence the velocity gradient. The same set of equations for calculating the shear-stress and velocity distributions in adiabatic flow can be used for flow inside heated tubes. However, the variation in fluid properties over the cross-sectional flow area must be considered.

- Effect of radial void-fraction variation on pressure drop. For simplicity, the variation of void fraction in the continuous phase is not modelled in this study, since experimental data is scarce and scattered. While an analytical model is needed to provide the void distribution, simplified approaches can be introduced to take into account the void-fraction variation. A power-law relation previously used by Bankoff [1966] can also be attempted. It requires, however, either two boundaries of void distribution or one boundary point and the shape of the void profile.

- Effect of roughness. This model can be extended to rough tubes. Since laminar flow is not affected by surface roughness, no modification is necessary. In turbulent flow, however, correction has to be introduced to account for the increase in turbulent structure due to surface roughness. As indicated in Section 2.2.4, modifications to the mixing-length expression seem inappropriate, based on the experimental evidence of Schlichting [1960]. Therefore, another approach has to be introduced.

- Two-phase mixing length. The definitions for two-phase mixing length in bubbly and droplet flows remain uncertain. While the single-phase mixing-length expression is used in this model, this assumption may become invalid at low-flow and low-pressure conditions, because of the large bubbles and droplets entrained in the continuous phase, and the mixture can no longer be assumed to be a homogeneous flow. Since experimental measurements of turbulence may be difficult under two-phase conditions, another approach may need to be developed.

References

Abolfadl, M. and Wallis, G.B., A Mixing Length Model for Annular Two-Phase Flow, PhysicoChemical Hydrodynamics, Vol. 6, No. 1/2, pp. 49-68, 1985.

Abolfadl, M. and Wallis, G.B., An Improved Mixing-Length Model for Annular Two-Phase Flow with Liquid Entrainment, Nuclear Engineering and Design, Vol. 95, pp. 233-241, 1986.

Abramyan, A.A. and Bartolomei, G.G., An Experimental Investigation of True Volumetric Vapour Content at High Heat Flux Densities, Thermal Engineering, Vol. 32, No. 11, pp. 638-640, 1985.

Abdelmessih, A.H. and Yin, S.T., A Facility for Experimental Investigation of Forced-Convection Boiling Two-Phase Flow, Report UTME-TP 7304, 1973.

Adeniji-Fashola, A.A., Abdelmessih, A.H. and Nejat, Z., Effect of Liquid Entrainment on the Predicted Pressure Drop in Vertical Flow Boiling, Canadian Journal of Chemical Engineering, Vol. 64, pp. 667-679, 1986

Adorni, N., Peterlongo, G., Ravetta and Tacconi, F.A., Large Scale Experiments on Heat Transfer and Hydrodynamics with Steam-Water Mixtures: Phase and Velocity Distribution Measurements in a Round Vertical Tube, CISE-R-91, 1964.

Ahmad, S.Y., Forced Convection Subcooled Boiling - Prediction of the Onset of Bubble Detachment, AECL unpublished report, 1969.

Andeen, G.B. and Griffith, P., Momentum Flux in Two-Phase Flow, J. Heat Transfer, Vol. 90, pp. 211-221, 1968 (also ASME paper 67-HT-32).

Ansari, A.M. and Sylvester, N.D., A Mechanistic Model for Two-Phase Bubble Flow in Vertical Pipes, AIChE Journal, Vol. 34, No. 8, pp. 1392-1394, 1988.

Arkhipov, V.V., Deev, V.I. and Solodovnikov, V.V., Pressure Drop with Two-Phase Helium Flow in the Region of Low Pressures, Thermal Engineering, Vol. 30, No. 3, pp. 125-128, 1983.

Avdeev, A.A., The Boundaries of the Region of the Effect of Surface Boiling on Void Fraction and Hydraulic Resistance, Thermal Engineering, Vol. 35, No. 9, pp. 513-516, 1988.

Bandel, J., Druckverlust und Warmeubergang bei der Verdampfung siedender Kaltemittel im durchstromten waagerechten Rohr. Diss. Univ. Karlsruhe, 1973.

Bandel, J. and Schlűnder, E.U., Pressure Drop and Heat Transfer by Vaporization of Boiling Refrigerants in a Horizontal Pipe, Heat Exchangers, Editors: Afgan, N.H. and Schlűnder, E.U., Scripta Book Company, Washington D.C., 1974a.

Bandel, J. and Schlűnder, E.U., Frictional Pressure Drop and Convective Heat Transfer of Gas-Liquid Flow in Horizontal Tubes, Proc. of the 5th Int. Heat Transfer Conf., Tokyo, Japan, Sept. 3-7, Vol. 4, pp. 190-194, 1974b.

Bankoff, S.G., A Variable Density Single-Fluid Model for Two-Phase Flow with Particular Reference to Steam-Water Flow, J. Heat Transfer, Vol. 82, pp. 265-272, 1960.

Baroczy, C.J., A Systematic Correlation for Two-Phase Pressure Drop, Paper Presented at the Eighth National Heat-Transfer Conference, Los Angeles, California, August 8-11, AIChE Preprint 37, 1965.

Bartolomei, G.G., Brantov, V.G., Molochnikov, Yu.S., Kharitonov, Yu.V., Solodkii, V.A., Batashova, G.N. and Miknailov, V.N., An Experimental Investigation of True Volumetric Vapour Content with Subcooled Boiling in Tubes, Thermal Engineering, Vol. 29., No. 3, pp. 132-135, 1982.

Bartolomei, G.G., Kharitonov, Yu.V., Kovrizhnykh, V.P., Mikhailov, V.N. and Solodkii, V.A., Investigation of the Hydraulic Resistance when Boiling Subcooled Water in a Uniformly Heated Tube, Thermal Engineering, Vol. 26, No. 7, pp. 431-433, 1979.

Bartolomei, C.C. and Chanturiya, V.M., Experimental Study of True Void Fraction When Boiling Subcooled Water in Vertical Tubes, Thermal Engineering, Vol. 14, No. 2, pp.123-128, 1967.

Baumeister, K.J., Graham, R.W. and Henry, R.E., Momentum Flux in Two Phase Two Component Low Quality Flow, Proceedings of the Thirteenth National Heat Transfer Conference, Denver, Colorado, Aug. 6-9, 1972.

Beattie, D.R.H., A Study of Two-Phase Flow Pressure Drop Correlations, Master of Engineering Science Thesis, University of New South Wales, Australia, 1971.

Beattie, D.R.H., Two-Phase Flow Structure and Mixing Length Theory, Nuclear Engineering Design, Vol. 21, pp. 46-64, 1972.

Beattie, D.R.H., A Note on the Calculation of Two-Phase Pressure Losses, Nuclear Engineering and Design, Vol. 25, pp. 395-402, 1973.

Beattie, D.R.H., Drag Reduction Phenomena in Gas-Liquid Systems, Proc. of the International Conference on Drag Reduction, September 4-6, Paper D3, pp. 31-46, 1974.

Beattie, D.R.H., Friction Factors and Regime Transitions in High Pressure Steam-Water Flows, ASME Publication 75-WA/HT-4, 1975.

Beattie, D.R.H., Some Aspects of Two-Phase Flow Drag Reduction, Proc. of the 2nd International Conference on Drag Reduction, Aug. 31-Sept. 2, Paper D1, 1977.

Beattie, D.R.H. and Whalley, P.B., A Simple Two-Phase Frictional Pressure Drop Calculation Method, Int. J. Multiphase Flow, Vol. 8, No. 1, pp. 83-87, 1982.

Becker, K.M., Hernborg, G. and Bode, M., An Experimental Study of Pressure Gradients for Flow of Boiling Water in a Vertical Round Duct, Aktiebolaget Atomenergi Report IPL-89, 1961.

Becker, K.M., Hernborg, G. and Bode, M., An Experimental Study of Pressure Gradients for Flow of Boiling Water in a Vertical Round Duct (Part 1), Aktiebolaget Atomenergi Report AE-69, 1962a.

Becker, K.M., Hernborg, G. and Bode, M., An Experimental Study of Pressure Gradients for Flow of Boiling Water in a Vertical Round Duct (Part 2), Aktiebolaget Atomenergi Report AE-70, 1962b.

Becker, K.M., Hernborg, G. and Bode, M., An Experimental Study of Pressure Gradients for Flow of Boiling Water in a Vertical Round Duct (Part 3), Aktiebolaget Atomenergi Report R4-151, 1962c.

Becker, K.M., Hernborg, G. and Bode, M., An Experimental Study of Pressure Gradients for Flow of Boiling Water in a Vertical Round Duct (Part 4), Aktiebolaget Atomenergi Report AE-86, 1962d.

Bennett, A.W., Hewitt, G.F., Kearsey, H.A., Keeys, R.K.F. and Lacey, P.M.C., Flow Visualization Studies of Boiling at High Pressure, AERE-R 4874, 1965.

Bennett, A.W., Hewitt, G.F., Kearsey, H.A., Keeys, R.K.F. and Pulling, D.J., Studies of Burnout in Boiling Heat Transfer to Water in Round Tubes with Non-Uniform Heating, AERE-R 5076, 1966.

Berenson, D.J., Film Boiling Heat Transfer from a Horizontal Surface, J. of Heat Transfer, pp. 351-358, 1961.

Bergles, A.E. and Rohsenow, W.M., The Determination of Forced Convection Surface Boiling Heat Transfer, Proceedings of the 6th National Heat Transfer Conference, Boston, Aug. 11-14, paper 63-HT-22, 1963.

Bergles, A.E., Roos, J.P. and Bourne, J.G., Investigation of Boiling Flow Regimes and Critical Heat Flux, NYO-3304-13, 1968.

Bertoletti, S., Lesage, J., Lombardi, C., Peterlongo, G., Silvestri, M., Soldaine, G. and Weckermann, F., Heat Transfer and Pressure Drop with Steam-Water Spray; A Critical Survey of Experiments Performed at CISE from November 1, 1959-January 31, 1961, CISE R-36, 1961.

Bhatti, M.S. and Shah, R.K., Turbulent and Transition Flow Convective Heat Transfer in Ducts, Handbook of Single-Phase Convective Heat Transfer (Editors: Kakaç, S., Shah, R.K. and Aung, W.), John Wiley & Sons Publication, New York, 1987.

Bjornard, T.A. and Griffith, P., PWR Blowdown Heat Transfer, Proc. ASME Topical Meeting on Thermal and Hydraulic Aspects of Nuclear Reactor Safety, Atlanta, Vol. 1, pp. 17-41, 1977.

Bonfanti, F., Ceresa, I. and Lombardi, C., Two-Phase Pressure Drops in the Low Flowrate Region, Energia Nucleare, Vol. 26, No. 10, pp. 481-492, 1979.

Boom, R.W., El-Wakil, M., McIntosh, G.E. and Khalil, A., Experimental Investigation of the Helium I Two-Phase Flow Pressure Drop Characteristics in Vertical Tubes, Proc. 7th Cryogenic Engineering, July 4, pp. 468-473, 1978.

Brand, B., Hein, D., Kastner, W. and Kohler, W., Post-CHF Heat Transfer and Pressure Loss in Once-through Boilers, Heat Transfer Science and Technology (Editor: Wang, B.-X.), Hemisphere Publishing Corporation, pp. 371-378, 1987.

Bromley, L.A., Heat Transfer in Stable Film Boiling, Chem. Eng. Prog., Vol. 46, pp. 221-227, 1950.

Buhr, H.O., Horsten, E.A. and Carr, A.D., The Distortion of Turbulent Velocity and Temperature Profiles on Heating, for Mercury in a Vertical Pipe, ASME Publication 72-HT-21, 1972.

Calvert, S. and Williams, B., Upward Cocurrent Annular Flow of Air and Water in Smooth Tubes, AIChE Journal, Vol. 1, No. 1, pp. 78-86, 1955.

Chapra, S.C. and Canale, R.P., Numerical Methods for Engineers, 2nd Edition, McGraw-Hill Book Company, New York, 1988.

Chawla, J.M., Reibungsdruckabfall bei der Strömung von Flüssigkeit/Gas-Gemische bei der Zweiphasenströmung, Chemie-Ing-Techn., Vol. 41, No. 5/6, pp. 328-330, 1969.

Chen, J.C., A Correlation for Boiling Heat Transfer to Saturated Fluids in Convective Flow, ASME Publication 63-HT-34, 1963.

Chen, J.C., Ozkaynak, F.T. and Sundaram, R.K., Vapor Heat Transfer in the Post-CHF Region Including the Effect of Thermodynamic Nonequilibrium, Nuclear Engineering and Design, Vol. 51, pp. 143-155, 1979.

Chen, N.H., An Explicit Equation for Friction Factor in Pipe, Industrial and Engineering Chemistry, Fundamentals, Vol. 18, No. 3, pp. 296-297, 1979.

Chexal, B., Lellouche, G., Horowitz, J., Healzer, J. and Oh, S., The Chexal-Lellouche Void Fraction Correlation for Generalized Applications, NSAC-139, 1991.

Chisholm, D., A Theoretical Basis for the Lockhart-Martinelli Correlation for Two-Phase Flow, Int. J. Heat Mass Transfer, Vol. 10, pp. 1767-1778, 1967.

Chisholm, D., Pressure Gradients During the Flow of Evaporating Two-Phase Mixtures, NEL Report No. 470, 1970.

Chisholm, D., Pressure Gradients due to Friction During the Flow of Evaporating Two-Phase Mixtures in Smooth Tubes and Channels, Int. J. Heat Mass Transfer, Vol. 16, pp. 347-358, 1973.

Chisholm, D., Influence of Pipe Surface Roughness on Friction Pressure Gradient During Two-Phase Flow, J. of Mechanical Engineering Science, Vol. 20, No. 6, pp. 353-354, 1978.

Chisholm, D., Two-Phase Flow in Pipelines and Heat Exchangers, Longman Inc., New York, 1983.

Chisholm, D. and Sutherland, L.A., Prediction of Pressure Gradients in Pipeline Systems During Two-Phase Flow, Inst. Mech. Eng. Symp., Two-Phase Flow Systems, Leeds, Paper No. 4, 1969.

Chun, M.H. and Oh, J.G., A Two-Phase Pressure Drop Calculation Code Based on A New Method with a Correction Factor Obtained from an Assessment of Existing Correlations, J. Korean Nuclear Society, Vol. 21, No. 2, pp. 73-88, 1989.

Cicchitti, A., Lombardi, C., Silvestri, M. and Soldaini, G., Two-Phase Cooling Experiments: Pressure Drop, Heat Transfer and Burnout Measurements, Energia Nucleare, Vol. 7, No. 6, pp. 407-425, 1960.

Colburn, A.P., A Method of Correlating Forced Convection Heat Transfer Data and A Comparison with Fluid Friction, Trans. AIChE J., Vol. 19, pp. 174-210, 1933.

Colebrook, C.F., Turbulent Flow in Pipes with Particular Reference to the Transition Region Between Smooth and Rough Pipe Laws, J. of Inst. Civil Eng., Vol. 11, p. 133, 1939.

Collier, J.G., Heat Transfer and Fluid Dynamic Research as Applied to Fog-Cooled Reactors, AECL Report, AECL-1631, 1962.

Collier, J.G., Convective Boiling and Condensation, McGraw-Hill Book Company, New York, 1981.

Cooper, M.G., Flow Boiling - The 'Apparently Nucleate' Regime, Int. J. Heat Mass Transfer, Vol. 32, No. 3, pp. 459-464, 1989.

Cousins, L.B. and Hewitt, G.F., Liquid Phase Mass Transfer in Annular Two-Phase Flow: Droplet Deposition and Liquid Entrainment, UKAEA Report AERE-R 5657, 1968.

Cravarolo, L., Hassid, A. and Pedrocchi, E., Some Remarks on the Martinelli-Nelson Pressure Loss Correlation in Two-Phase Flow, Energia Nucleare, Vol. 10, No. 7, pp. 395-396, 1963.

Cumo, M., Farello, G.E., Ferrari, G. and Montanari, M., Boiling Sublayers Along Heated Walls, CNEN RT/ING (75) 13, 1975.

Davis, E.S., Heat Transfer and Pressure Drop in Annuli, Trans. ASME, Vol. 65, p. 755, 1943.

Davis, E.J. and Anderson, G.H., The Incipience of Nucleate Boiling in Forced Convection Flow, AIChE J., Vol. 12, No. 4, pp. 774-780, 1966.

Deissler, R.G., Analytical Investigation of Fully Developed Laminar Flow in Tubes with Heat Transfer with Fluid Properties Variable Along the Radius, NACA TN-2410, 1951.

Deissler, R.G., Analytical and Experimental Investigation of Adiabatic Turbulent Flow in Smooth Tubes, NACA-TN-2138, 1952.

Delhaye, J.M., Giot, M. and Riethmuller, M.L., Thermohydraulics of Two-Phase Systems for Industrial Design and Nuclear Engineering, First Edition, McGraw-Hill Book Company, New York, 1981.

Dittus, F.W. and Boelter, L.M.K., Heat Transfer in Automobile Radiators of Tubular Type, Publications in Engineering, University of California, Berkeley, p. 443, 1930.

Dobran, F., Hydrodynamic and Heat Transfer Analysis of Two-Phase Annular Flow with a New Liquid Film Model of Turbulence, Int. J. Heat Mass Transfer, Vol. 26, No. 8, pp. 1159-1171, 1983.

Dobran, F., Heat Transfer in an Annular Two-Phase Flow, J. of Heat Transfer, Vol. 107, pp. 472-476, 1985.

Dormer, T. Jr. and Bergles, A.E., Pressure Drop with Surface Boiling in Small-Diameter Tubes, MIT Report No. 8767-31, 1964.

Doroshchuk, V.E. and Levitan, L.L., Investigation of the Conditions of Precipitation of Drops from the Core of a Dispersed Steam-Water Flow onto a Wall Liquid Film, Thermal Physics, High Temperature, Vol. 9, pp. 591-596, 1971.

Doroshchuk, V.E., Levitan, L.L. and Lantzman, F.P., Investigations into Burnout in Uniformly Heated Tubes, ASME Publication 75-WA/HT-22, 1975.

Dougall, R.S. and Rohsenow, W.M., Film Boiling on the Inside of Vertical Tubes with Upward Flow of the Fluid at Low Qualities, M.I.T. Report 9079-26, 1963.

Dukler, A.E., Wicks, M. and Cleveland, R.G., Frictional Pressure Drop in Two-Phase Flow: B. An Approach through Similarity Analysis, AIChE J., Vol. 10, pp. 44-51, 1964.

Forslund, R.P. and Rohsenow, W.M., Thermal Non-Equilibrium in Dispersed Flow Film Boiling in a Vertical Tube, M.I.T. Report 75312-44, 1966.

Friedel, L., Improved Friction Pressure Drop Correlations for Horizontal and Vertical Two-Phase Pipe Flow, European Two-Phase Flow Group Meeting, Ispra, Italy, paper E2, 1979.

Friedel, L., Pressure Drop during Gas/Vapour-Liquid Flow in Pipes, Int. Chem. Eng., Vol. 20, No. 3, pp. 352-367, 1980.

Fujita, R.K. and Hughes, E.D., Comparison of a Two-Velocity Two-Phase Flow Model with Boiling Two-Phase Flow Data, Proc. of the Multi-Phase Flow and Heat Transfer Symposium-Workshop, Miami Beach, Florida, USA, April 16-18, Vol. 2, pp. 671-709, 1979.

Gaspari, G.P., Lombardi, C. and Peterlongo, G., Pressure Drops in Steam-Water Mixtures, CISE-R-83, 1964.

Gill, L.E. and Hewitt, G.F., Further Data on the Upwards Annular Flow of Air-Water Mixtures, AERE-R-3935, 1962.

Gnielinski, V., New Equations for Heat and Mass Transfer in Turbulent Pipe and Channel Flow, Int. Chem. Eng., Vol. 16, pp. 359-368, 1976.

Gregory, G.A. and Fogarasi, M., Alternate to Standard Friction Factor Equation, Oil & Gas Journal, Vol. 83, No. 13, pp. 125-127, 1985.

Groeneveld, D.C., The Thermal Behaviour of a Heated Surface at and Beyond Dryout, AECL Report, AECL-4309, 1972.

Groeneveld, D.C., Cheng, S.C. and Doan, T., 1986 AECL-UO Critical Heat Flux Look-Up Table, Heat Transfer Engineering, Vol. 7, pp. 46-62, 1986.

Groeneveld, D.C, Cheng, S.C., Leung, L.K.H. and Nguyen, C., Computation of Single- and Two-Phase Heat Transfer Rates Suitable for Water-Cooled Tubes and Subchannels, Nucl. Eng. Design, Vol. 114, pp. 61-77, 1989.

Groeneveld, D.C and Delorme, G.G.J., Prediction of the Thermal Non-Equilibrium in the Post-Dryout Regime, Nuclear Engineering and Design, Vol. 36, pp. 17-26, 1976.

Groeneveld, D.C. and Rousseau, J.C., CHF and Post-CHF Heat Transfer: An Assessment of Prediction Methods and Recommendations for Reactor Safety Codes, Advance in Two-Phase Flow and Heat Transfer (Editors: Kakac, S.C. and Ishii, M.D.), Vol. 1, pp. 203-238, 1983.

Groeneveld, D.C. and Snoek, C.W., A Comprehensive Examination of Heat Transfer Correlation Suitable for Reactor Safety Analysis, Multiphase Science and Technology, Vol. 2, pp. 181-274, 1986.

Groeneveld, D.C., Blumenroehr, D., Cheng, S.C., Cheng, X., Doerffer, S., Erbacher, F.J., Tain, R.M. and Zeggel, W., CHF Fluid-to-Fluid Modelling Studies in Three Different Laboratories Using Different Modelling Fluids, Proceedings of the 5th International Topical Meeting on Nuclear Reactor Thermalhydraulics, Salt Lake City, Utah, USA, September 21-25, 1992.

Groeneveld, D.C., Leung, L.K.H., Kirillov, P.J., Bobkov, V.P., Erbacher, F.J. and Zeggel, W., An Improved Table Look-Up Method for Predicting Critical Heat Flux, Proc. of the 6th International Topical Meeting on Nuclear Reactor Thermalhydraulics, Grenoble, France, Oct. 4-8, Vol. 1, pp. 223-230, 1993.

Guislain, S.J., Friction Factors in Fluid Flow Trough Pipe, Plant Engineering, Vol. 34, No. 12, pp. 134-140, 1980.

Gungor, K.E. and Winterton, R.H.S., A General Correlation for Flow Boiling in Tubes and Annuli, Int. J. Heat Mass Transfer, Vol. 29, No. 3, pp. 351-358, 1987.

Hadaller, G. and Banerjee, S., Heat Transfer to Superheated Steam in Round Tubes, AECL Unpublished Report, 1969.

Han, L.S., A Mixing Length Model for Turbulent Boundary Layers Over Rough Surfaces, Int. J. Heat Mass Transfer, Vol. 14, No. 8, pp. 2053-2062, 1991.

Henstock, W.H. and Hanratty, T.J., The Interfacial Drag and the Height of the Wall Layer in Annular Flows, AIChE J., Vol. 22, pp. 990-995, 1976.

Hewitt, G.F., Flow Patterns, Two-Phase Flow and Heat Transfer (Editors: Butterworth, D. and Hewitt, G.F.), Oxford University Press, 1977.

Hewitt, G.F., Critical Heat Flux in Flow Boiling, Proc. 6th Int. Heat Transfer Conf., Toronto, Canada, Vol. 6, pp. 143-171, 1978.

Hewitt, G.F., Void Fraction, Handbook of Multiphase Flow (Editor: Hetsroni, G.), McGraw-Hill Book Company, New York, 1982.

Hewitt, G.F. and Hall-Taylor, N.S., Annular Two-Phase Flow, Pergamon Press, 1970.

Hewitt, G.F. and Roberts, D.N., Studies of Two-Phase Flow Patterns by Simultaneous X-ray and Flash Photography, AERE-M 2159, 1969.

Hoffman, M.A. and Wong, C.F., Prediction of Pressure Drops in Forced Convection Subcooled Boiling Water Flows, Int. J. Heat Mass Transfer, Vol. 35, No. 12, pp. 3291-3299, 1992.

Hosler, E.R., Visual Study of Boiling at High Pressure, Proc. 6th National Heat Transfer Conference, Boston, Massachusetts, Aug. 11-14, (also WAPD-T-1566), 1963.

Hsu, Y.Y., Preburnout Convective Boiling, Handbook of Multiphase Flow (Editor: Hetsroni, G.), McGraw-Hill Book Company, New York, 1982.

Husain, A., Choe, W.G. and Weisman, J., Applicability of the Homogeneous Flow Model to Two-Phase Pressure Drop in Straight Pipe and Across Area Changes, AIChE Symposium Series, Vol. 74, No. 174, pp. 205-214, 1978.

Hutchinson, P. and Whalley, P.B., A Possible Characterization of Entrainment in Annular Flow, Chemical Engineering Science, Vol. 28, pp. 974-975, 1973.

Idsinga, W., Todreas, N. and Bowring, R., An Assessment of Two-Phase Pressure Drop Correlations for Steam-Water Systems, Int. J. Multiphase Flow, Vol. 3, pp. 401-413, 1977.

Inasaka, F., Nariai, H. and Shimura, T., Pressure Drops in Subcooled Flow Boiling in Narrow Tubes, Heat Transfer-Japanese Research, Vol. 18, No. 1, pp. 70-82, 1989.

Isbin, H.S., Moen, R.H., Wickey, R.O., Mosher, D.R. and Larson, H.C., Two-Phase Steam-Water Pressure Drops, Chem. Eng. Prog. Symp. Series, Vol. 55, No. 23, pp. 75-84, 1959.

Ishii, M. and Mishima, K., Liquid Transfer and Entrainment Correlation for Droplet-Annular Flow, Proc. of the 7th International Heat Transfer Conference, Vol. 5, pp. 307-312, 1982.

Izumi, R., Ishimaru, T. and Matsuzaki, K., Heat Transfer and Pressure Drop for Refrigerant R-12 Evaporating in a Horizontal Tube, Heat Transfer-Japanese Research, Vol. 4, No. 2, pp. 82-91, 1975.

Jens, W.H. and Lottes, P.A., Analysis of Heat Transfer, Burnout, Pressure Drop and Density Data for High-Pressure Water, ANL-4627, 1951.

Jia, D. and Schrock, V.E., A Generalized Procedure for Predicting the Pressure Drop in a Subcooled Boiling Channel, Proc. 4th Int. Symp. on Multi-Phase Transport & Particular Phenomenon, pp. 181-191, 1986.

Kadambi, V., Prediction of Pressure Drop and Void fraction in Annular Two-Phase Flows, Canadian Journal of Chemical Engineering, Vol. 63, No. 5, pp. 728-734, 1985.

Kakaç, S., The Effect of Temperature-Dependent Fluid Properties on Convective Heat Transfer, Handbook of Single-Phase Convective Heat Transfer (Editors: Kakaç, S., Shah, R.K. and Aung, W.), John Wiley & Sons Publication, New York, 1987.

Kandlikar, S.G., A General Correlation for Saturated Flow Boiling Heat Transfer Inside Horizontal and Vertical Tubes, Boiling and Condensation in Heat Transfer Equipment (editors: Ragi, E.G., Rudy, T.M., Rabase, T.J. and Robertson, J.M.), ASME, New York, pp. 9-19, 1987.

Keeys, R.K.F., Ralph, J.C. and Roberts, D.N., Liquid Entrainment in Adiabatic Steam-Water Flow at 500 and 1000 P.S.I.A. (3.447 and 6.894 x 10^6 N/m^2), AERE-R 6293, 1970.

Kenning, D.B.R. and Cooper, M.G., Saturated Flow Boiling of Water in Vertical Tubes, Int. J. Heat Mass Transfer, Vol. 32, No. 3, pp. 445-458, 1989.

Kirillov, P.L., Bobkov, V.P., Boltenko, E.A., Katan, I.B., Smogalev, I.P. and Vinogradov, V.N., New CHF Table for Water in Round Tubes, Report IPPE-2225, Obninsk, Russia, 1991.

Kirillov, P.L., Smogalev, I.P. and Doroshenko, V.A., A Graphical Method of Predicting the Losses of Pressure due to Friction with a Rising Steam-Water Flow in Round Tubes, Thermal Engineering, Vol. 29, No. 3, pp. 171-172, 1982.

Kirillov, P.L., Smogalev, I.P., Shumskii, R.V. and Shtein, Yu, Distribution of Phases Over the Cross Section of a Dispersed-Annular Steam-Water Flow, Thermal Engineering, Vol. 36, No. 1, pp. 26-29, 1989.

Kohler, W. and Kastner, W., Two-Phase Pressure Drop in Boiler Tubes, Two-Phase Flow Heat Exchangers: Thermal-Hydraulic Fundamentals and Design (Editors: Kakac, S., Bergles, A.E. and Fernandes, E.O.), Kluwer Academic Publishers, pp. 575-594, 1987.

Kroeger, P.G. and Zuber, N., An Analysis of the Effects of Various Parameters on the Average Void Fractions in Subcooled Boiling, Int. J. Heat Mass Transfer, Vol. 11, pp. 211-233, 1968.

Kubie, J. and Oates, H.S., Aspects of Two-Phase Frictional Pressure Drop in Tubes, Trans. of Institution of Chemical Engineers, Vol. 56, No. 3, pp. 205-209, 1978.

Lahey, R.T. Jr. and Moody, F.J., The Thermal Hydraulics of Boiling Water Nuclear Reactors, American Nuclear Society, 1975.

Lee, D.H., Studies of Heat Transfer and Pressure Drop Relevant to Subcritical Once-Through Evaporators, IAEA-SM-130/56, IAEA Symposium on Progress in Sodium-Cooled Fast-Reactor Engineering, Monaco, 1970.

Leung, L.K.H., Effect of Flow Obstruction on Pressure Loss, M.A.Sc. Thesis, University of Ottawa, Department of Mechanical Engineering, 1983.

Leung, L.K.H. and Groeneveld, D.C., Frictional Pressure Gradient in the Pre- and Post-CHF Heat-Transfer Regions, Proc. of the Int. Conf. on Multiphase Flows '91-Tsukuba, Sept. 24-27, Vol. 2, pp. 493-496, 1991.

Leung, L.K.H. and Groeneveld, D.C., An Assessment of Prediction Methods of CHF in Tubes with A Large Experimental Data Bank, Proc. of the 4th CNS International Conference on Simulation Methods in Nuclear Engineering, Montreal, June 2-4, 1993.

Leung, L.K.H., Groeneveld, D.C., Aube, F. and Tapucu, A. New Studies of the Effect of Surface Heating on Frictional Pressure Drop in Single- and Two-Phase Flow, Proc. of the 6th International Topical Meeting on Nuclear Reactor Thermalhydraulics, Grenoble, France, Oct. 4-8, Vol. 2, pp. 867-874, 1993.

Levy, S., Theory of Pressure Drop and Heat Transfer for Annular Steady State Two-Phase Two-Component Flow in Pipes, Ohio State University, Engineering Experiment Station, Bulletin 149, pp. 337-348, 1952.

Levy, S., Prediction of Two-Phase Pressure Drop and Density Distribution from Mixing Length Theory, ASME Paper 62-HT-6, 1962.

Levy, S., Steam Slip-Theoretical Prediction from Momentum Model, ASME Paper 59-HT-15, 1959.

Levy, S., Prediction of Two-Phase Annular Flow with Liquid Entrainment, Int. J. Heat Mass Transfer, Vol. 9, pp. 171-188, 1966.

Levy, S., Forced Convection Subcooled Boiling Prediction of Vapour Volumetric Fraction, Int. J. Heat Mass Transfer, Vol. 10, pp. 951-965, 1967.

Levy, S., Prediction of Two-Phase Pressure Drop and Density Distribution from Mixing Length Theory, J. of Heat Transfer, Vol. 85, pp. 1963-1967, 1973.

Levy, S. and Healzer, J.M., Application of Mixing Length Theory to Wavy Turbulent Liquid-Gas Interface, J. of Heat Transfer, Vol. 103, pp. 492-500, 1981.

Lockhart, R.W. and Martinelli, R.C., Proposed Correlation of Data for Isothermal Two-Phase Two-Component Flow in Pipes, Chem. Eng. Prog., Vol. 45, pp. 39-48, 1949.

Lombardi, C. and Ceresa, I., A Generalized Pressure Drop Correlation in Two-Phase Flow, Energia Nucleare, Vol. 25, No. 4, pp. 181-198, 1978.

Lombardi, C. and Pedrocchi, E., A Pressure Drop Correlation in Two-Phase Flow, Energia Nucleare, Vol. 19, No. 2, pp. 91-99, 1972.

Lu, S. and Jia, D., A New Method for Predicting the Pressure Drop in a Subcooled Boiling Channel, Experimental Heat Transfer, Fluid Mechanics, and Thermodynamics (Editors: R.K. Shah, E.N. Ganic and K.T. Yang), pp. 1466-1472, 1988.

Mandhane, J.M., Gregory, G.A. and Aziz, K., A Flow Pattern Map for Gas-Liquid Flow in Horizontal Pipes, Int. J. Multiphase Flow, Vol. 1, No. 4, pp. 537-553, 1974.

Manzano-Ruiz, J.J., A Semi-Empirical Model to Predict Frictional Pressure-Drop in Annular/Wavy Two-Phase Flow Through Horizontal Pipes, Proc. of the Conference on Fundamentals of Gas-Liquid Flows, Nov. 27-Dec. 02, Chicago, pp. 71-78, 1988.

Maroti, L., A Model for Two-Phase Frictional Pressure Drop Calculations, Hungarian Academy of Sciences, Report KFKI-75-31, 1975.

Martinelli, R.C. and Nelson, D.B., Prediction of Pressure Drop During Forced-Circulation Boiling of Water, Trans. ASME, Vol. 79, pp. 695-702, 1948.

Matthew, G.D., Velocity Profiles and Friction Factor Relationships for Turbulent Flow in Smooth Pipes-A Reassessment of Some Earlier Mixing Length Assumptions, Proc. Instn. Civ. Engrs, Part 2, Vol. 81, pp. 277-290, 1986.

Maurer, G.W. and LeTourneau, B.W., Friction Factors for Fully Developed Turbulent Flow in Ducts With and Without Heat Transfer, ASME Paper 63-WA-98, 1963.

McAdams, W.H., Woods, W.K. and Heroman, L.C., Vapourisation Inside Horizontal Tubes, 2: Benzene-Oil Mixtures, Trans. ASME, Vol. 64, pp. 193-200, 1942.

Milashenko, V.I., Nigmatulin, B.I., Petukhov, V.V. and Trubkin, N.I., Burnout and Distribution of Liquid in Evaporative Channels of Various Lengths, Int. J. Multiphase Flow, Vol. 15, No. 3, pp. 393-401, 1989.

Mishima, K. and Ishii, M., Flow Regime Transition Criteria for Upward Two-Phase Flow in Vertical Tubes, Int. J. Heat Mass Transfer, Vol. 27, No. 5, pp. 723-737, 1984.

Moody, L.F., Friction Factors for Pipe Flow, Trans. ASME, Vol. 66, pp. 671-684, 1944.

Müller, H.M. and Steiner, D., Druckverlust bei der Strömung von Argon und Stickstoff in einem horizontalen Verdampferrohr, verfahrenstechnik, Vol. 17, No. 9, pp. 519-523, 1983.

Muller-Steinhagen, H. and Heck, K., A Simple Friction Pressure Drop Correlation for Two-Phase Flow in Pipes, Chemical Engineering and Processing, Vol. 20, No. 6, pp. 297-308, 1986.

Muscettola, M., Two-Phase Pressure Drop - Comparison of the "Momentum Exchange Model" and Martinelli-Nelson's Correlation with Experimental Measurements, AEEW-R 284, 1963.

Ng, K.C., Hawlader, N.A., Chandratilleke, T.T. and Wijeysundera, N.E., An Investigation of Two-Phase Flow Patterns and Pressure Drop in a Horizontal Pipe Using Freon-113, Proceedings of the ASME-Thermal Engineering Joint Conf., Honolulu, Hawaii, USA, March 22-27, pp. 117-124, 1987.

Nicholson, M.K., Nickerson, J.R., Aziz, K. and Gregory, G.A., A Comparison of Flow Regime and Pressure Drop Behaviour in Adiabatic and Diabatic Two-Phase Flow Simulations, Proc. of the 7th International Heat Transfer Conf., Munich, Germany, Sept. 6-10, 1982.

Nigmatulin, B.I., Milashenko, V.I. and Shugaev, Y.Z., Investigation of Liquid Distribution Between the Core and the Film in Annular Dispersed Flow of Steam/Water Mixtures, Thermal Engineering, Vol. 23, No. 5, pp. 66-68, 1977.

Obot, N.T., Wambsganss, M.W., France, D.M. and Jendrzejczyk, J.A., A Generalized Method for Correlation of Adiabatic Two-Phase Flow Frictional Pressure Drop Data, ASME/AIChE/ANS National Heat Transfer Conf., July, Minneapolis, Minnisota, USA, pp. 289-298, 1991.

Owens, W.L., Two-Phase Pressure Gradient, International Developments in Heat Transfer, Part II, Vol. 2, Paper 41, pp. 363-368, 1961.

Owens, W.L. and Schrock, V.E., Local Pressure Gradients for Subcooled Boiling of Water in Vertical Tubes, ASME Paper 60-WA-249, 1960.

Özişik, M.N., Heat Transfer - A Basic Approach, McGraw-Hill Book Company, New York, 1985.

Paliwoda, A., Generalized Method of Pressure Drop and Tube Calculation with Boiling and Condensing Refrigerants within the Entire Zone of Saturation, Int. J. Refrig., Vol. 12, pp. 314-322, 1989.

Petukhov, B.S., Heat Transfer and Friction in Turbulent Pipe Flow with Variable Physical Properties, Advances in Heat Transfer (Editors: J.P. Hartnett and T.F. Irvine), Academic, New York, Vol. 6, pp. 504-564, 1970.

Petukhov, B.S., Zhukov, V.M. and Shieldcret, V.M., Experimental Investigation of Pressure Drop and Critical Heat Flux in the Helium Two-Phase Flow in a Vertical Tube, Proc. 8th Int. Cryog. Eng. Conf., Genoa, Italy, June 3-6, pp. 181-185, 1980.

Reddy, D.G., Sreepada, S.R., Nahavandi, A.N., Two-Phase Friction Multiplier Correlation for High-Pressure Steam-Water Flow, EPRI Report NP-2522, 1982.

Reynolds, J.B., Local Boiling Pressure Drop, ANL-5178, 1954.

Rohsenow, W.M. and Clark, J.A., Heat Transfer and Pressure Drop Data for High Heat Flux Densities to Water at High Subcritical Pressures, 1951 Heat Transfer and Fluid Mechanics Institute, Stanford University Press, Stanford, Calif., 1951 (also MIT report NP-3385).

Rohsenow, W.M. and Hartnett, J.P., Handbook of Heat Transfer, 1973.

Rouhani, S.Z., Subcooled Void Fraction, AB Atomenergi Report AE-RTV-841, 1969.

Saha, P. and Zuber, N., Point of Net Vapour Generation and Vapour Void Fraction in Subcooled Boiling, Proceedings of the 5th Int. Heat Transfer Conference, Tokyo, Vol. 4, pp. 175-179, 1974.

Saito, T., Hughes, E.D. and Carbon, M.W., Multi-Fluid Modelling of Annular Two-Phase Flow, Nuclear Engineering and Design, Vol. 50, pp. 225-271, 1978.

Sami, S.M. and Duong, T., A Subcooled Void Model, Applied Mathematic Modelling, Vol. 11, pp. 264-271, 1987.

Schlichting, H., Boundary Layer Theory, McGraw-Hill Book Company, Inc., New York, 1960.

Schrock, V.E. and Grossman, L.M., Forced Convection Boiling Studies, TID-14632, 1959.

Shah, M.M., Chart Correlation for a Saturated Boiling Heat Transfer: Equation and Further Study, ASHRAE Transactions, Vol. 88, Part 1, pp. 185-206, 1982.

Sher, N.C. and Green, S.J., Boiling Pressure Drop in Thin Rectangular Channels, Chem. Engineering Progress Symposium Series, Vol. 55, No. 23, pp. 61-71, 1959.

Shoukri, M., Effect of Heat Addition on the Pressure Drop in Two-Phase Flow System, Canadian Electrical Association, Research Report on Project 000 G104, 1980.

Shoukri, M., Yanchis, R.J. and Rhodes, E., Effect of Heat Flux on Pressure Drop in Low Pressure Flow Boiling in a Horizontal Tube, Can. J. Chem. Engg., Vol. 59, pp. 149-154, 1981.

Sieder, E.N. and Tate, G.E., Heat Transfer and Pressure Drop of Liquids in Tubes, Industrial and Engineering Chemistry, Vol. 28, pp. 1429-1435, 1936.

Skouloudis, A.N. and Wurtz, J., Film-Thickness, Pressure-Gradient and Turbulent Velocity Profiles in Annular Dispersed Flows, Proc. ASME Winter Meeting, pp. 55-62, 1991.

Smith, R.A., Boiling Inside Tubes: Critical Heat Flux for Upward Flow in Uniformly Heated Tubes, Engineering Science Data Unit International Ltd., ESDU Data Item No. 86032, London, 1986.

Snoek, C.W. and Leung, L.K.H., An Accurate Model for Pressure Drop Prediction in Multi-element CANDU Fuel Channels, Proc. of the 5th Conference on Multiphase Flow and Heat Transfer, Miami, Florida, Dec. 13-16, pp. 193-205, 1986.

Staub, F.W., The Void Fraction in Subcooled Boiling - Prediction of the Initial Point of Net Vapour Generation, ASME Paper 67-HT-36, 1967.

Steen, D.A. and Wallis, G.B., The Transition from Annular to Annular-Mist Concurrent Two-Phase Down Flow, USAEC Report NYO-3114-2, 1964.

Steiner, D. and Schlűnder, E.U., Heat Transfer and Pressure Drop for Boiling Nitrogen Flowing in a Horizontal Tube. I. Saturated Flow Boiling, Cryogenics, Vol. 16, No. 7, pp. 387-398, 1976a.

Steiner, D. and Schlűnder, E.U., Heat Transfer and Pressure Drop for Boiling Nitrogen Flowing in a Horizontal Tube. II. Pressure Drop, Cryogenics, Vol. 16, No. 8 pp. 457-464, 1976b.

Storek, H. and Brauer, H., Reibungsdruckverlust der adiabaten Gas/Flüssigkeit-Strömung in horizontalen und vertikalen Rohren, VDI Forschungsheft, Report 599, 1980.

Streeter, V.L. and Wylie, E.B., Fluid Mechanics, McGraw-Hill Book Company, 1975.

Subbotin, V.I., Sorokin, D.N., Nigmatulin, B.I., Milashenko, V.I. and Nikolayev, V.E., Integrated Investigation into Hydrodynamic Characteristics of Annular-Dispersed Steam-Liquid Flows, Proc. 6th Int. Heat Transfer Conference, Toronto, Vol. 7, pp. 327-332, 1978.

Taitel, Y. and Dukler, A.E., Flow Pattern Transition in Gas-Liquid Systems: Measurement and Modelling, Multiphase Science and Technology, Vol. II, pp. 1-94, 1986.

Taitel, Y., Barnea, D. and Dukler, A.E., Modelling Flow Pattern Transitions for Steady Upward-Gas-Liquid Flow in Vertical Tubes, AIChE J., Vol. 26, No. 3, pp. 345, 1980.

Tarasova, N.V. and Leont'ev, A.I., Hydraulic Resistance with a Steam-Water Mixture Flowing in a Vertical Heated Tube, Teplo. Vyso Temp., Vol. 3, No. 1, pp. 115-123, 1965.

Tarasova, N.V., Leont'ev, A.I., Hlopuskin, V.I. and Orlov, V.M., Pressure Drop of Boiling Subcooled Water and Steam-Water Mixture Flowing in Heated Channels, Proc. of the 3rd International Heat Transfer Conference, Chicago, USA, Vol. 4, pp. 178-183, 1966.

Thom, J.R.S., Prediction of Pressure Drop During Forced Circulation Boiling of Water, Int. J. Heat Mass Transfer, Vol. 7, pp. 709-724, 1964.

Thom, J.R.S., Walker, W.M., Fallon, T.A. and Resising, G.F.S., Boiling in Subcooled Water During Flow Up Heated Tubes or Annuli, Paper 6 presented at the Symposium on Boiling Heat Transfer in Steam Generating Units and Heat Exchangers, Manchester, IMechE (London), Sept. 15-16, 1965.

Tong, L.S., Boiling Crisis and Critical Heat Flux, USAEC Report, TID-25887, 1972.

Tong, L.S. and Young, J.D., A Phenomenological Transition and Film Boiling Heat Transfer Correlation, Proc. of the 5th International Heat Transfer Conf., Tokyo, Vol. 4, paper B3.9, 1974.

Ueda, T., On Upward Flow of Gas-Liquid Mixtures in Vertical Tubes (1st Report, Experimental data of Frictional Pressure Drop and Void Fraction), Bulletin of JSME, Vol. 10, No. 42, pp. 989-1000, 1967b.

Ueda, T., On Upward Flow of Gas-Liquid Mixtures in Vertical Tubes (2nd Report, Consideration of Frictional Pressure Drop and Void Fraction), Bulletin of JSME, Vol. 10, No. 42, pp. 1000-1007, 1967a.

Wallis, G.B., Annular Two-Phase Flow-Part I: A Simple Theory, ASME Publication 69-FE-45, 1969a.

Wallis, G.B., Annular Two-Phase Flow-Part II: Additional Effects, ASME Publication 69-FE-46, 1969b.

Weisman, J. and Du, L., Computation of the Effect of Heat Addition on Interfacial Shear in Bubbly Flow, Int. J. Multiphase Flow, Vol. 18, No. 4, pp. 623-631, 1992.

Whalley, P.B. and Hewitt, G.F., The Correlation of Liquid Entrainment Fraction and Entrainment Rate in Annular Two-Phase Flow, AERE-R9187, 1978.

Yamazaki, Y. and Yamaguchi, K., Void Fraction Correlation for Boiling and Non-Boiling Vertical Two-Phase Flows in Tube, J. Nuclear Science and Technology, Vol. 13, No. 12, pp. 701-707, 1976.

Yao, S.C. and Sylvester, N.D., A Mechanistic Model for Two-Phase Annular-Mist Flow in Vertical Pipes, AIChE Journal, Vol. 33, No. 6, pp. 1008-1012, 1987.

Yelin, N.N., Concerning the Drag Coefficient in Annular Pipe Flow of Gas-Liquid Mixtures, Fluid Mechanics-Soviet Research, Vol. 14, No. 1, pp. 66-71, 1985.

Ying, A. and Weisman, J., The Relationship Between Interfacial Shear and Flow Patterns in Vertical Flow, Int. J. Multiphase Flow, Vol. 15, No. 1, pp. 23-34, 1989.

Zeigarnik, Yu. A., Kirillova, I.V., Klimov, A.I. and Smirnova, E.G., Some Measurements of Hydraulic Resistance in Boiling Water Heated to Below the Saturation Temperature, Teplofiz. Vys. Temp., Vol. 21, No. 2, pp. 303-308, 1983.

Zivi, S.M., Estimation of Steady State Steam Void Fraction by Means of the Principle of Minimum Entropy Production, J. Heat Transfer, Vol. 86, pp. 247-252, 1964.

Zuber, N. and Findlay, J.A., Average Volumetric Concentration in Two-Phase Flow Systems, J. Heat Transfer, Vol. 87, pp. 453-468, 1965.

Zyatnina, O.A., Ivashkevich, A.A. and Mitrofanova, T.V., Analytical Determination of the Onset of Nucleate Boiling of Subcooled Water in Pipes, Heat-Transfer-Soviet Research, Vol. 21, No. 6, pp. 742-752, 1989.

I. PART OF CHF LOOK-UP TABLE FOR TUBES OF 8-mm INSIDE DIAMETER

(CHF IN $kW.m^{-2}$)

P	G	Dryout Quality																						
kPa	kg.m⁻².s⁻¹	-0.5	-0.4	-0.3	-0.2	-0.15	-0.1	-0.05	0	0.05	0.1	0.15	0.2	0.25	0.3	0.35	0.4	0.45	0.5	0.6	0.7	0.8	0.9	1
1000	0	ice	ice	5727	4604	4043	3482	2920	2359	811	589	479	410	360	321	289	262	239	218	180	147	115	79	0
1000	50	ice	ice	6546	5510	4783	4473	3954	3436	1845	1695	1599	1521	1451	1384	1318	1251	1183	1111	955	852	642	375	0
1000	100	ice	ice	7365	6416	5523	5464	4988	4513	2879	2800	2718	2632	2542	2447	2346	2240	2126	2004	1729	1556	1168	671	0
1000	300	ice	ice	7630	7620	7610	7600	7590	7580	7570	6000	5620	5230	4840	4450	4200	3680	3290	2900	2405	1735	1239	722	0
1000	500	ice	ice	7642	7630	7620	7609	7580	7570	7560	5900	5600	4900	4400	4300	4200	3395	2829	2701	2016	1383	966	514	0
1000	1000	ice	ice	7674	7660	7550	7631	7570	7560	7550	5700	5500	4700	4345	4265	4189	3262	2685	2096	1283	731	477	351	0
1000	1500	ice	ice	7706	7690	7680	7653	7560	7550	7540	5490	5452	4657	4248	4092	3847	2956	2020	1353	739	453	294	147	0
1000	2000	ice	ice	7864	7857	7826	7676	7550	7540	7530	5290	5204	4652	4105	3695	3274	2112	1396	859	585	399	180	90	0
1000	2500	ice	ice	8708	8025	7971	7698	7540	7530	7520	5080	4791	4454	3861	3673	3211	1959	1272	501	500	420	69	35	0
1000	3000	ice	ice	9484	8192	8117	7720	7530	7520	7510	4879	4411	4022	3654	3339	2929	1950	1200	900	530	430	51	26	0
1000	3500	ice	ice	10211	8922	8263	7742	7520	7510	7505	4871	4246	3816	3230	2787	1862	1817	1150	950	560	440	77	38	0
1000	4000	ice	ice	10897	9462	8408	7850	7510	7500	6377	4870	3961	3319	2918	1756	1692	1681	1288	1000	592	450	106	53	0
1000	4500	ice	ice	11555	9974	9123	7789	7500	7490	5803	4412	3900	3300	2900	1700	1600	1560	1232	1032	638	460	129	65	0
1000	5000	ice	ice	12184	10463	9620	7809	7490	7480	5240	4301	3800	3200	2800	1650	1630	1629	1376	1143	736	470	167	84	0
1000	5500	ice	ice	12763	10932	10021	8222	7030	7020	4900	4258	3750	3000	1900	1850	1800	1727	1477	1244	827	492	214	107	0
1000	6000	ice	ice	13310	11383	10407	8741	6419	6100	4113	3776	3284	2928	2631	2346	2073	1814	1568	1335	913	554	263	132	0
1000	6500	ice	ice	13840	11780	10782	9286	5883	4351	4085	3748	3259	2966	2682	2408	2144	1891	1649	1418	993	622	312	156	0
1000	7000	ice	ice	14358	12167	11105	9786	6249	4664	4100	3770	3277	2998	2726	2462	2207	1960	1722	1494	1068	688	361	181	0
1000	7500	ice	ice	14864	12543	11419	10228	7175	5636	4120	3790	3291	3024	2764	2510	2262	2022	1789	1564	1138	751	410	205	0
1000	8000	ice	ice	15362	12911	11724	10583	7450	6361	4140	3810	3302	3047	2797	2552	2312	2078	1849	1627	1204	811	458	229	0
3000	0	6475	5825	5174	4524	4199	3874	3549	3224	1531	1100	879	737	636	557	494	441	395	355	285	224	167	107	0
3000	50	7363	6613	5974	5373	5072	4771	4470	4169	2505	2244	2086	1966	1863	1769	1680	1592	1503	1413	1220	1012	824	481	0
3000	100	8251	7400	6773	6222	5945	5668	5391	5114	3478	3388	3293	3194	3090	2981	2865	2742	2611	2471	2154	1800	1481	854	0
3000	300	8403	7490	7250	7240	7230	7220	7210	7200	7190	5710	5480	5260	5030	4810	4580	4350	4130	3900	3191	2594	1784	1023	0
3000	500	8554	7580	7364	7282	7247	7229	7220	7190	7180	5800	5600	5500	5200	4829	4599	4450	4228	3972	3206	2397	1677	917	0
3000	1000	8933	7806	7648	7386	7291	7251	7230	7180	7160	6640	6110	5578	5171	4775	4310	4288	3733	3347	2548	1679	1301	647	0
3000	1500	9312	8032	7933	7490	7334	7274	7240	7170	7152	6640	5885	5297	4860	4581	4237	3742	3075	2522	1807	1325	1251	620	0
3000	2000	10765	9828	8217	7594	7378	7296	7250	7160	6471	5938	5531	5063	4550	4240	3712	2982	2719	2306	1495	982	231	116	0
3000	2500	11855	10919	9571	7698	7570	7318	7260	7150	5931	5490	5149	4720	4204	3995	3333	2799	2710	2272	1389	589	101	51	0
3000	3000	12871	11779	10692	8550	7640	7490	7270	7140	5735	5188	4809	4429	3924	3596	3280	2609	2585	1590	972	443	74	37	0
3000	3500	13834	12590	11371	9378	8231	7680	7280	7130	5612	5011	4741	4341	3786	2797	2005	1829	1751	1416	821	460	94	47	0
3000	4000	14752	13362	11999	10288	8853	7840	7290	6914	5445	5008	4712	4109	3771	2484	1674	1578	1272	1110	608	470	112	56	0
3000	4500	15638	14101	12597	11047	9379	7974	7300	6553	5434	4884	4642	4002	3672	2095	1619	1493	1329	1140	698	480	127	63	0
3000	5000	16494	14816	13171	11597	10110	8859	7310	5739	4898	4441	4390	3782	3484	2000	1950	1687	1386	1182	778	490	149	75	0
3000	5500	17326	15507	13724	12020	10771	9260	7320	5731	4895	4358	4246	3700	2400	2050	2037	1756	1492	1246	839	500	158	79	0
3000	6000	18136	16176	14260	12427	11354	9381	7550	6000	4099	3762	3700	3600	2730	2410	2122	1847	1587	1342	896	540	209	105	0
3000	6500	18929	16831	14781	12820	11848	9721	7750	6200	4070	3733	3600	3500	2764	2475	2196	1928	1673	1429	980	588	260	130	0
3000	7000	19703	17473	15288	13204	12231	10079	8000	6400	4116	3779	3645	3546	2810	2531	2261	2001	1750	1508	1059	657	312	156	0
3000	7500	20466	18098	15783	13573	12544	10572	8369	6555	4420	3807	3673	3574	2849	2581	2320	2066	1819	1581	1132	723	363	182	0
3000	8000	21212	18711	16266	13934	12849	11037	9094	7280	4620	3830	3696	3597	3350	2860	2371	2124	1883	1648	1200	786	413	207	0
5000	0	5811	5352	4893	4434	4205	3976	3746	3517	1978	1447	1156	965	827	720	633	561	499	444	351	270	196	121	0
5000	50	6627	6091	5650	5225	5013	4800	4587	4374	2886	2572	2376	2227	2103	1991	1886	1784	1683	1581	1365	1065	844	499	0
5000	100	7442	6829	6406	6016	5820	5623	5427	5231	3793	3696	3595	3489	3378	3261	3138	3007	2867	2717	2378	1860	1492	876	0
5000	300	7653	6973	6860	6850	6840	6830	6820	6810	6800	5420	5240	5070	4890	4720	4540	4400	4190	4012	3168	2616	1908	1129	0
5000	500	7864	7116	6998	6921	6888	6837	6826	6810	6250	5490	5210	5170	5082	4861	4437	4387	4057	3677	3043	2568	1886	1127	0
5000	1000	8391	7475	7341	7099	7009	6855	6842	6800	5700	5550	5108	4898	4672	4033	3678	3622	3370	3108	2525	1889	1594	1026	0
5000	1500	8918	7834	7685	7277	7130	6873	6800	6763	5671	5178	4811	4507	4195	3753	3363	3087	2903	2437	1713	1638	1494	1000	0
5000	2000	10509	9426	8029	7454	7251	6891	6400	6234	5084	4650	4369	3996	3589	3403	3129	2546	2202	1934	1480	1184	149	75	0
5000	2500	11531	10648	9198	7632	7560	7280	6300	5900	4772	4420	4051	3627	3271	3123	2851	2380	2080	1878	1292	639	118	59	0
5000	3000	12483	11453	10312	8389	7630	7480	6299	5500	4616	4192	3739	3455	3268	2837	2351	1886	1429	861	860	470	98	49	0
5000	3500	13381	12210	11088	9088	8167	7670	6298	5149	4504	4043	3563	3406	3205	2768	2107	1560	1098	731	730	480	111	56	0
5000	4000	14241	12930	11675	9931	8709	7830	6297	5032	4258	3706	3543	3173	3005	2455	1656	1354	1255	1165	760	490	118	59	0
5000	4500	15067	13618	12232	10664	9149	8045	6330	5021	4229	3624	3527	2967	2792	2108	1638	1425	1325	1183	790	500	124	62	0
5000	5000	15865	14281	12766	11273	9820	8841	6480	4890	4169	3367	3367	2855	2575	2050	1765	1612	1438	1221	820	510	132	66	0
5000	5500	16638	14922	13281	11745	10430	9241	6548	4961	4120	3310	3233	3200	2500	1850	1800	1753	1471	1248	850	520	155	78	0
5000	6000	17394	15545	13780	12128	11450	9500	7140	5033	3950	3340	3280	3255	2788	2373	1850	1834	1568	1316	880	530	197	99	0
5000	6500	18129	16152	14262	12496	11820	9870	7730	5600	4000	3370	3320	3316	3000	2477	2191	1917	1655	1405	944	542	206	103	0
5000	7000	18853	16744	14733	12854	11894	10300	8450	5940	4100	3400	3370	3334	3050	2535	2258	1991	1733	1486	1024	612	258	129	0
5000	7500	19557	17324	15192	13202	12254	10700	8650	6080	4400	3816	3648	3350	3100	2585	2317	2057	1804	1560	1099	679	309	155	0
5000	8000	20251	17892	15640	13540	12553	11800	9310	6490	4600	4015	3708	3400	3340	2850	2370	2116	1868	1628	1169	744	360	180	0

P	G	Dryout Quality																						
kPa	kg.m^{-2}.s^{-1}	-0.5	-0.4	-0.3	-0.2	-0.15	-0.1	-0.05	0	0.05	0.1	0.15	0.2	0.25	0.3	0.35	0.4	0.45	0.5	0.6	0.7	0.8	0.9	1
6000	0	5537	5142	4748	4354	4157	3960	3763	3566	2132	1578	1264	1055	903	785	689	609	540	479	376	288	207	126	0
6000	50	6320	5856	5453	5088	4905	4722	4539	4356	2910	2574	2359	2197	2061	1939	1834	1735	1637	1538	1334	1125	990	668	0
6000	100	7103	6569	6157	5822	5653	5483	5314	5145	3688	3569	3453	3339	3218	3093	2979	2860	2733	2597	2291	1962	1772	1209	0
6000	300	7327	6723	6480	6470	6460	6450	6440	6430	6420	5130	4980	4820	4670	4510	4360	4200	4050	3891	3468	2443	1827	1143	0
6000	500	7551	6877	6516	6484	6478	6230	6210	6193	5940	5190	5000	5000	4953	4524	4390	4261	4048	3620	2965	2336	1711	988	0
6000	1000	8112	7262	6604	6523	6518	6100	6000	5900	5600	5496	4861	4371	4191	3814	3589	3429	3239	2767	2178	1556	1117	885	0
6000	1500	8673	7647	6693	6567	6553	6200	6106	5861	5095	4742	4344	3971	3640	3271	3103	2867	2621	1923	1243	1105	913	876	0
6000	2000	10231	9164	7839	6730	6612	6587	6204	5566	4698	4222	3858	3520	3083	2868	2563	2008	1596	1299	1026	634	145	73	0
6000	2500	11209	10362	8961	7570	7544	7265	6211	5476	4543	4160	3648	3293	2775	2444	2068	1678	1346	1174	786	147	118	59	0
6000	3000	12121	11139	10019	8200	7615	7468	6226	5382	4524	3955	3299	2961	2606	2204	1684	1143	894	628	610	393	110	55	0
6000	3500	12981	11863	10791	8887	7720	7660	6254	5006	4347	3909	3218	2859	2589	2140	1665	1067	799	524	464	403	120	60	0
6000	4000	13800	12550	11353	9686	7830	7819	6260	4388	3650	3207	2983	2731	2315	1948	1546	1266	1239	1219	469	413	121	61	0
6000	4500	14588	13209	11886	10378	7940	7880	6270	4420	3639	3105	2949	2721	2310	1848	1411	1305	1260	1230	512	423	122	61	0
6000	5000	15351	13842	12397	10961	8050	7950	6291	4637	3699	3096	2900	2644	2217	1678	1498	1325	1280	1240	554	433	123	62	0
6000	5500	16089	14454	12889	11431	9187	8000	6489	4740	3801	3151	2991	2981	2839	2283	1780	1749	1300	1250	634	443	152	76	0
6000	6000	16809	15047	13363	11804	11790	11780	7100	4797	3841	3158	3024	2983	2846	2336	1838	1760	1327	1260	713	453	184	92	0
6000	6500	17513	15626	13824	12157	11800	11790	7710	5124	3952	3245	3085	3022	2969	2398	2099	1770	1430	1270	790	463	217	109	0
6000	7000	18200	16190	14273	12499	11810	11800	8892	5487	4056	3275	3194	3048	2976	2495	2179	1785	1528	1290	867	519	252	126	0
6000	7500	18874	16744	14709	12831	11925	11810	8929	5606	4383	3825	3623	3151	3091	2604	2262	1883	1623	1379	941	575	287	144	0
6000	8000	19535	17286	15136	13154	12224	11820	9524	5700	4575	4200	3720	3380	3330	2840	2340	1978	1714	1465	1014	631	324	162	0
7000	0	5275	4934	4593	4252	4081	3911	3740	3570	2248	1684	1355	1132	968	840	737	650	575	509	397	302	215	129	0
7000	50	6026	5622	5245	4929	4770	4612	4453	4295	2916	2563	2333	2161	2013	1882	1779	1682	1587	1493	1169	1116	1018	770	0
7000	100	6776	6310	5896	5606	5459	5312	5165	5019	3584	3441	3311	3190	3058	2924	2820	2713	2599	2477	1940	1930	1821	1410	0
7000	300	7010	6470	6090	6080	6070	6060	6050	6040	6030	4840	4710	4580	4440	4310	4180	4050	3920	3783	2375	2311	1804	1230	0
7000	500	7244	6630	6170	6129	6117	5880	5860	5846	5620	4880	4802	4357	4318	3972	3686	3506	3386	3283	2624	2124	1580	955	0
7000	1000	7828	7030	6369	6252	6234	5800	5700	5600	5500	5421	4460	3798	3668	3353	3073	2883	2700	2452	2031	1512	974	857	0
7000	1500	8413	7431	6568	6375	6351	5900	5719	5071	4608	4270	3843	3493	3207	2886	2718	2539	2125	1594	1100	961	899	822	0
7000	2000	9914	8886	7622	6498	6469	6000	5790	4876	4243	3770	3379	3121	2830	2627	2239	1691	1333	1015	855	625	137	69	0
7000	2500	10854	10036	8710	7350	7307	6759	5797	4857	4037	3526	3161	2887	2563	2256	1836	1401	1098	874	487	133	114	57	0
7000	3000	11726	10790	9711	7982	7492	6915	5807	4589	3959	3316	2868	2651	2399	1947	1411	944	707	532	470	316	107	54	0
7000	3500	12546	11482	10459	8668	7580	7224	5818	4550	3916	3292	2820	2602	2368	1925	1408	875	615	444	442	326	116	58	0
7000	4000	13330	12139	11002	9421	7660	7542	5957	4318	3500	2730	2523	2412	2053	1654	1314	851	847	815	445	336	117	59	0
7000	4500	14084	12767	11512	10075	7740	7680	6157	4323	3359	2620	2438	2364	2016	1521	1257	1000	900	816	475	346	118	59	0
7000	5000	14810	13371	12000	10629	7827	7825	6267	4520	3245	2487	2428	2385	1946	1441	1348	1100	1010	821	505	356	119	60	0
7000	5500	15517	13956	12470	11086	8941	7834	6441	4649	3565	2497	2470	2400	2071	1598	1500	1300	1115	917	580	366	139	70	0
7000	6000	16201	14522	12924	11452	11440	11430	7010	4732	3599	2610	2489	2418	2187	1695	1600	1442	1216	1010	653	373	169	85	0
7000	6500	16872	15073	13364	11791	11450	11440	7590	4753	3731	2817	2545	2481	2246	2208	2007	1545	1314	1100	726	425	200	100	0
7000	7000	17528	15613	13794	12118	11460	11450	8163	4904	3827	2823	2674	2558	2341	2215	2100	1643	1407	1187	798	478	232	116	0
7000	7500	18171	16138	14211	12436	11560	11460	8381	4972	4226	3213	3043	2932	2787	2675	2207	1737	1497	1272	868	531	265	133	0
7000	8000	18801	16653	14618	12745	11854	11470	8403	5008	4400	3580	3400	3370	3320	2830	2309	1827	1583	1353	937	583	299	150	0
8000	0	5016	4720	4425	4129	3981	3833	3685	3537	2329	1768	1429	1196	1023	887	777	684	604	534	415	313	222	131	0
8000	50	5736	5382	5034	4752	4614	4477	4339	4201	2904	2541	2299	2118	1960	1822	1719	1625	1535	1446	1266	1025	949	777	0
8000	100	6455	6043	5642	5375	5247	5120	4992	4864	3479	3314	3169	3040	2897	2756	2661	2566	2465	2357	2117	1736	1676	1422	0
8000	300	6696	6208	5753	5700	5690	5680	5670	5660	5650	4550	4440	4340	4230	4120	4010	3910	3780	3690	1970	1712	1509	1180	0
8000	500	6938	6372	5864	5779	5761	5540	5520	5497	5300	4580	4492	3884	3658	3468	3411	3288	3121	2879	2166	1628	1295	732	0
8000	1000	7542	6784	5977	5943	5939	5100	5000	4980	4960	4944	4443	3361	3092	2783	2702	2557	2372	2127	1529	987	650	395	0
8000	1500	8146	7195	6419	6175	6117	5100	5050	4939	4518	4162	3551	3171	2915	2467	2383	2182	1659	1237	654	451	331	267	0
8000	2000	9576	8599	7387	6373	6295	5300	5100	4784	4165	3643	3027	2760	2497	2147	1877	1426	973	508	317	167	130	65	0
8000	2500	10483	9693	8447	7210	7200	6559	5154	4757	4003	3093	2679	2391	2116	1879	1550	962	784	497	418	126	110	55	0
8000	3000	11318	10423	9392	7728	7420	6889	5391	4305	3671	2897	2426	2147	1971	1633	1155	893	689	491	419	239	104	52	0
8000	3500	12103	11085	10111	8425	7500	6900	5440	4066	3669	2865	2369	2111	1908	1588	992	686	605	420	420	250	112	56	0
8000	4000	12853	11713	10638	9131	7590	7140	5940	4024	3177	2528	2235	2093	1907	1559	1193	742	730	573	421	260	113	57	0
8000	4500	13573	12313	11127	9743	7730	7390	6122	4170	3123	2162	2072	2071	1808	1508	1195	952	834	669	422	270	114	57	0
8000	5000	14268	12891	11595	10266	7800	7760	6265	4348	3240	2210	2162	2100	1872	1422	1267	959	939	763	470	280	115	58	0
8000	5500	14941	13450	12044	10702	8700	7800	6372	4371	3278	2464	2210	2197	1930	1495	1415	1227	1040	855	540	299	130	65	0
8000	6000	15598	13991	12480	11057	11050	10940	6540	4474	3385	2485	2239	2209	2127	1606	1516	1347	1137	944	611	348	158	79	0
8000	6500	16237	14518	12900	11381	11060	10950	6700	4670	3500	2629	2528	2467	2239	1971	1813	1447	1230	1030	680	398	187	94	0
8000	7000	16863	15032	13312	11693	11070	10960	6864	4858	3623	2816	2640	2505	2287	2052	1898	1542	1321	1114	749	448	217	109	0
8000	7500	17476	15533	13710	11996	11161	10970	6901	4919	3671	3145	3007	2845	2654	2067	1999	1633	1408	1196	816	499	249	125	0
8000	8000	18078	16026	14100	12291	11444	10980	7100	4990	3868	3513	3390	3360	3310	2820	2096	1721	1491	1275	883	550	282	141	0

P	G	Dryout Quality																						
kPa	kg.m^{-2}.s^{-1}	-0.5	-0.4	-0.3	-0.2	-0.15	-0.1	-0.05	0	0.05	0.1	0.15	0.2	0.25	0.3	0.35	0.4	0.45	0.5	0.6	0.7	0.8	0.9	1
9000	0	4757	4500	4243	3986	3857	3729	3600	3472	2377	1828	1486	1247	1067	926	810	712	628	555	429	322	226	132	0
9000	50	5444	5133	4830	4556	4436	4316	4196	4076	2876	2508	2257	2069	1902	1757	1656	1566	1480	1396	1230	1021	906	786	0
9000	100	6131	5766	5416	5125	5014	4903	4791	4679	3374	3187	3027	2890	2737	2588	2502	2419	2331	2237	2030	1720	1585	1439	0
9000	300	6378	5932	5533	5310	5300	5290	5280	5270	5260	4300	4210	4120	4030	3950	3860	3770	3680	3590	1719	1496	1292	1030	0
9000	500	6625	6099	5650	5416	5335	5180	5160	5141	4990	4278	3513	3431	3097	3096	2880	2746	2513	1880	1556	1345	856	560	0
9000	1000	7243	6516	5912	5683	5423	4850	4700	4500	4400	4062	3291	3097	2729	2346	2302	1962	1735	1264	856	668	517	366	0
9000	1500	7861	6932	6236	5949	5512	4890	4745	4447	4302	3729	3263	2902	2451	2197	1845	1474	1019	813	616	420	137	83	0
9000	2000	9213	8290	7113	6215	5600	5216	4875	4067	3353	2969	2643	2284	1998	1669	1285	1057	762	442	275	160	124	62	0
9000	2500	10084	9320	8157	7110	7100	6043	5050	4017	3287	2825	2404	2079	1807	1416	1019	847	718	376	274	118	107	54	0
9000	3000	10879	10020	9039	7445	7340	6347	5108	3977	3203	2411	2045	1806	1568	1283	968	828	662	318	300	162	102	51	0
9000	3500	11630	10652	9717	8158	7400	6354	5191	3974	3164	2406	2019	1778	1550	1270	960	635	565	390	301	163	109	55	0
9000	4000	12344	11250	10222	8817	7530	6730	5254	3921	3140	2228	1896	1741	1504	1329	1029	730	610	537	308	164	110	55	0
9000	4500	13031	11823	10688	9388	7720	7108	5378	4169	2918	2095	1800	1796	1545	1341	1105	748	740	629	375	193	111	55	0
9000	5000	13693	12373	11133	9876	7780	7686	5452	4271	2951	2133	1862	1842	1593	1344	1105	862	860	720	443	237	112	56	0
9000	5500	14335	12904	11561	10289	8450	7772	5639	4351	3220	2184	1902	1891	1623	1448	1399	1011	983	808	511	283	123	62	0
9000	6000	14962	13420	11974	10629	10620	10140	5660	4460	3281	2343	2126	2038	1673	1555	1457	1277	1078	895	579	330	149	75	0
9000	6500	15571	13921	12375	10937	10630	10150	5690	4563	3490	2624	2511	2258	2225	1845	1624	1375	1169	979	646	378	178	89	0
9000	7000	16170	14411	12764	11235	10640	10160	5714	4664	3570	2745	2515	2345	2274	1861	1768	1468	1257	1061	713	427	207	104	0
9000	7500	16754	14890	13144	11524	10727	10170	5768	4904	3661	3109	2954	2813	2578	2008	1778	1558	1343	1141	779	476	238	119	0
9000	8000	17327	15359	13514	11805	10998	10180	5787	4972	3800	3432	3376	3350	3300	2810	1920	1645	1425	1218	844	525	269	135	0
10000	0	4494	4271	4048	3825	3713	3602	3490	3379	2395	1867	1527	1285	1101	956	836	734	647	570	439	328	229	132	0
10000	50	5147	4874	4610	4344	4240	4136	4031	3927	2833	2464	2206	2013	1839	1688	1590	1503	1422	1344	1191	1014	892	698	0
10000	100	5800	5476	5172	4863	4766	4669	4571	4475	3270	3060	2885	2740	2577	2419	2343	2272	2197	2117	1943	1700	1554	1263	0
10000	300	6050	5642	5293	4930	4920	4910	4900	4890	4880	4100	4030	3950	3880	3800	3730	3650	3580	3500	1700	1400	1145	828	0
10000	500	6300	5808	5414	5058	4985	4840	4820	4799	4680	4060	3383	3209	3064	3002	2793	2582	2458	1857	1458	1212	732	439	0
10000	1000	6925	6223	5717	5379	5147	4600	4382	4270	4210	3963	3147	2914	2676	2211	2119	1756	1504	1026	823	416	381	245	0
10000	1500	7550	6638	6020	5700	5310	4630	4520	4216	3959	3481	3066	2735	2215	1934	1576	1176	707	664	568	293	129	65	0
10000	2000	8810	7957	6822	6021	5472	4650	4588	4048	3310	2914	2364	1910	1644	1344	952	720	552	205	145	117	117	59	0
10000	2500	9638	8916	7840	7020	7000	5839	4608	4008	3256	2704	2187	1756	1501	1132	722	525	343	293	268	111	103	52	0
10000	3000	10392	9580	8657	7260	7163	6275	4642	3917	3153	2278	1801	1508	1267	1016	691	371	310	295	294	133	99	50	0
10000	3500	11103	10178	9288	7863	7300	6349	4646	3915	3083	2262	1777	1487	1300	1034	786	463	441	370	295	138	105	53	0
10000	4000	11779	10745	9765	8473	7460	6680	4738	3603	2898	2044	1618	1469	1334	1107	1021	650	490	393	296	143	106	53	0
10000	4500	12429	11287	10206	9000	7710	7020	4781	3547	2897	2076	1569	1563	1380	1254	1049	676	670	598	368	183	107	53	0
10000	5000	13058	11808	10628	9454	7750	7629	4871	3880	2890	2094	1670	1661	1397	1258	1075	715	710	686	422	226	108	54	0
10000	5500	13666	12311	11032	9838	8200	7770	5058	4023	3176	2112	1901	1747	1421	1344	1209	736	730	720	488	270	117	59	0
10000	6000	14258	12800	11423	10160	10150	9330	5070	4130	3259	2129	2049	1926	1461	1368	1251	1224	1033	858	555	316	143	72	0
10000	6500	14836	13274	11802	10452	10160	9340	5080	4240	3434	2612	2355	2250	2056	1758	1620	1321	1123	941	621	363	171	86	0
10000	7000	15401	13736	12169	10734	10170	9350	5084	4241	3469	2620	2362	2301	2214	1812	1660	1413	1210	1021	686	411	199	100	0
10000	7500	15952	14189	12529	11008	10264	9360	5354	4279	3597	2913	2821	2529	2525	1984	1694	1503	1295	1100	751	459	229	115	0
10000	8000	16496	14633	12877	11274	10517	9370	5372	4623	3763	3345	3186	2869	2852	2798	1900	1620	1410	1177	815	507	260	130	0
11000	0	4224	4032	3839	3646	3549	3453	3357	3260	2384	1883	1550	1309	1124	976	854	750	660	581	446	332	230	131	0
11000	50	4842	4604	4374	4138	4024	3933	3843	3753	2775	2408	2147	1950	1771	1614	1519	1438	1362	1289	1151	1006	891	591	0
11000	100	5459	5176	4908	4630	4498	4413	4329	4245	3165	2932	2744	2591	2417	2251	2183	2125	2063	1997	1855	1680	1552	1050	0
11000	300	5710	5347	5031	4682	4530	4520	4510	4500	4490	3790	3760	3730	3700	3670	3640	3610	3577	3377	1650	1050	950	547	0
11000	500	5960	5518	5154	4735	4622	4546	4519	4440	4360	3682	3192	3110	3059	2739	2698	2001	1617	1487	1180	504	432	283	0
11000	1000	6586	5945	5461	4866	4850	4300	4278	4030	4027	3351	3118	2730	2391	2100	1820	1254	861	835	607	380	318	159	0
11000	1500	7212	6372	5768	4998	4600	4472	4321	3856	3266	2911	2674	2196	1853	1501	1115	836	687	550	500	235	121	61	0
11000	2000	8370	7589	6554	5787	5300	4575	4372	3806	3247	2710	2095	1582	1300	951	693	580	491	200	142	110	110	50	0
11000	2500	9146	8471	7492	6920	6899	5769	4378	3744	3140	2419	1771	1356	1115	818	582	482	290	260	244	103	99	49	0
11000	3000	9856	9090	8241	7200	7184	5937	4547	3684	3038	2118	1508	1194	971	746	474	271	270	270	245	104	96	48	0
11000	3500	10525	9653	8820	7532	7200	6047	4581	3660	3008	2028	1394	1151	1012	846	560	396	370	340	246	105	101	50	0
11000	4000	11161	10186	9266	8092	7400	6459	4656	3455	2760	1980	1389	1179	1016	1004	861	631	376	360	279	137	102	51	0
11000	4500	11772	10695	9680	8575	7700	6751	4718	3493	2837	1938	1481	1384	1281	1212	938	666	390	390	360	176	103	51	0
11000	5000	12362	11184	10076	8990	7730	6819	4833	3849	2861	1959	1484	1429	1375	1232	990	672	440	440	408	217	104	52	0
11000	5500	12934	11656	10456	9343	7960	6946	5055	3941	3133	2034	1851	1549	1378	1287	1136	700	470	460	450	261	113	57	0
11000	6000	13489	12114	10822	9642	9630	8520	5060	4020	3238	2218	1948	1567	1498	1349	1300	1184	999	829	536	306	138	69	0
11000	6500	14032	12560	11178	9917	9640	8530	5070	4095	3389	2446	2326	2171	2056	1729	1599	1280	1088	911	602	352	165	83	0
11000	7000	14561	12995	11523	10181	9650	8540	5080	4129	3464	2565	2348	2272	2115	1789	1638	1373	1175	992	666	399	194	97	0
11000	7500	15080	13418	11859	10439	9771	8647	5100	4133	3537	2887	2780	2467	2459	1859	1680	1462	1260	1071	731	447	223	112	0
11000	8000	15589	13834	12186	10688	10009	8921	5200	4330	3757	3071	2782	2717	2641	2567	1880	1610	1400	1147	795	495	253	127	0

II. MEASURED PRESSURE-DROP DATA

Runname	Date	Pressure	T/S Temp	T/S Temp	Temp	Flow	Power	Pressure	Pressure	Pressure	Pressure	Pressure	Pressure
		Outlet	Inlet	Outlet	Ambient	Water	T/S	Diff.01	Diff.02	Diff.03	Diff.04	Diff.05	Diff.06
		MPa	°C	°C	°C	g/s	kW	kPa	kPa	kPa	kPa	kPa	kPa
DPB94403	12/05/89	9.71	271.02	295.12	30.83	104.41	15.04	32.80	32.09	32.13	32.30	31.83	159.97
DPB94404	12/05/89	9.70	271.37	303.83	30.75	101.90	20.51	32.51	31.71	31.55	31.60	31.03	156.51
DPB94405	12/05/89	9.70	271.43	310.09	30.73	103.78	25.43	35.57	32.82	32.55	32.46	31.81	164.01
DPB94406	12/05/89	9.70	271.23	310.83	31.22	105.98	30.47	51.04	34.82	33.90	33.70	32.95	185.36
DPB94407	12/05/89	9.71	271.77	311.04	31.27	108.25	35.14	66.85	42.29	34.98	34.71	33.83	212.49
DPB94408	12/05/89	9.70	271.77	310.97	31.35	106.06	40.45	78.86	56.83	35.78	34.12	33.11	238.75
DPB94409	12/05/89	9.70	271.77	310.97	31.40	106.29	45.12	89.71	67.53	40.52	34.12	33.23	265.30
DPB94410	12/05/89	9.71	271.84	311.04	31.43	103.09	50.04	97.50	75.03	48.56	33.62	32.43	288.09
DPB94411	12/05/89	9.71	271.71	311.17	31.42	103.74	55.10	103.61	82.42	57.83	34.66	32.38	312.33
DPB94412	12/05/89	9.71	271.91	311.24	31.42	102.75	60.16	104.19	88.42	66.33	36.64	32.01	329.36
DPB94413	12/05/89	9.70	271.91	311.17	31.51	107.68	65.10	109.96	96.73	74.88	40.87	33.91	357.64
DPC94414	12/05/89	9.71	271.91	311.24	31.51	103.30	66.66	100.51	92.30	74.68	41.80	32.01	342.57
DPB94300	12/05/89	9.71	284.28	285.23	31.58	99.43	0.00	30.26	29.93	30.24	30.59	30.38	149.87
DPB94303	12/05/89	9.73	284.35	307.20	31.83	103.64	15.04	33.67	33.05	33.01	33.11	32.64	164.30
DPB94304	12/05/89	9.71	284.28	310.97	31.77	101.85	20.02	44.00	32.94	32.55	32.53	31.96	172.67
DPB94305	12/05/89	9.71	284.28	310.97	31.81	101.20	25.14	58.95	42.79	32.74	32.43	31.73	197.77
DPB94306	12/05/89	9.71	284.42	310.83	31.76	104.28	30.08	71.99	56.44	37.09	33.63	32.87	232.40
DPB94307	12/05/89	9.71	284.28	311.04	31.82	101.58	35.14	82.38	64.99	45.67	32.97	31.96	258.66
DPB94308	12/05/89	9.71	284.35	311.04	31.79	103.48	40.08	93.11	74.41	55.52	35.00	32.74	290.98
DPB94309	12/05/89	9.71	284.35	311.24	31.70	102.66	45.12	99.40	82.42	63.99	38.22	32.48	317.53
DPB94310	12/05/89	9.71	284.28	311.04	31.80	102.03	50.18	103.21	90.19	70.72	43.00	32.64	341.77
DPB94311	12/05/89	9.71	284.28	311.24	31.78	102.61	55.10	102.52	96.04	76.18	48.61	32.79	358.21
DPB94312	12/05/89	9.72	284.28	311.24	31.72	102.83	60.16	99.98	100.23	80.91	54.74	33.44	371.49
DPC94313	12/05/89	9.71	284.28	311.24	31.91	101.85	60.72	99.11	100.19	81.30	55.52	33.52	372.07
DPB94500	15/05/89	9.63	253.74	254.70	30.52	96.14	0.00	29.46	29.13	29.28	29.68	29.44	150.74
DPB94506	15/05/89	9.62	256.14	304.44	30.60	96.97	29.94	32.11	31.21	30.97	30.90	30.22	159.10
DPB94507	15/05/89	9.62	256.14	310.16	30.68	98.90	35.14	38.80	32.21	31.90	31.63	30.95	168.92
DPB94508	15/05/89	9.63	256.27	310.23	30.69	96.52	40.19	55.66	33.55	31.48	31.16	30.38	186.52
DPB94509	15/05/89	9.63	256.20	310.23	30.73	96.79	45.04	68.35	41.44	31.55	31.26	30.35	207.30
DPB94510	15/05/89	9.62	256.27	310.30	30.80	95.99	50.10	79.38	53.79	32.78	31.44	30.43	232.40
DPB94511	15/05/89	9.62	256.20	310.30	30.81	94.52	55.10	88.15	64.49	35.98	30.59	29.73	254.33
DPB94512	15/05/89	9.62	256.14	310.30	30.87	94.05	60.04	94.96	71.22	42.83	30.51	29.52	273.95
DPB94513	15/05/89	9.63	256.34	310.30	30.94	94.95	65.08	96.52	76.03	51.02	31.47	29.88	290.40
DPC94514	15/05/89	9.63	256.61	310.30	31.00	93.79	69.55	91.90	78.61	58.87	32.33	29.60	297.04
DPB94200	15/05/89	9.62	296.61	297.62	31.20	96.94	0.00	31.36	30.94	31.21	31.57	31.37	160.55
DPB94201	15/05/89	9.63	296.34	304.98	31.27	99.17	5.06	32.69	32.17	32.32	32.61	32.30	166.03
DPB94202	15/05/89	9.63	296.61	309.96	31.36	98.19	10.00	38.75	32.05	32.01	32.20	31.81	171.22
DPB94203	15/05/89	9.63	296.74	310.23	31.47	94.76	15.08	52.19	44.21	33.63	31.21	30.66	196.33
DPB94204	15/05/89	9.63	296.27	310.30	31.51	95.01	20.10	63.74	53.25	42.71	31.86	30.72	227.49
DPB94205	15/05/89	9.63	296.07	310.36	31.67	95.25	24.88	74.99	62.22	51.56	35.70	30.87	260.97
DPB94206	15/05/89	9.62	296.07	310.30	31.75	93.83	30.08	83.01	70.76	58.45	41.78	30.74	290.69
DPB94207	15/05/89	9.63	296.61	310.36	31.75	92.51	35.14	87.23	77.57	64.56	48.43	31.08	315.51
DPB94208	15/05/89	9.62	296.54	310.36	31.79	92.60	40.08	91.84	84.38	71.45	54.32	32.82	341.77
DPB94209	15/05/89	9.62	296.14	310.43	31.91	91.71	44.98	90.28	87.30	75.99	58.19	34.07	352.15
DPB94210	15/05/89	9.63	296.54	310.50	31.93	97.01	50.04	96.00	95.84	85.42	65.72	38.09	389.09
DPC94211	15/05/89	9.62	296.34	310.50	32.02	95.60	53.05	91.73	94.88	87.53	67.39	39.13	388.51
DPB94100	16/05/89	9.60	304.25	305.58	32.30	85.20	0.00	33.68	33.25	33.57	33.98	33.65	172.76
DPB94103	16/05/89	9.54	302.82	309.69	32.48	96.06	14.92	63.04	54.52	47.90	38.48	31.26	242.21
DPB94104	16/05/89	9.61	302.68	310.30	32.58	96.20	20.10	73.14	62.95	54.21	43.81	31.86	273.09
DPB94105	16/05/89	9.62	303.22	310.16	32.76	96.21	25.02	83.19	72.68	62.41	51.15	34.61	311.47
DPB94106	16/05/89	9.60	302.42	310.23	32.75	95.76	30.08	87.74	78.84	67.80	55.00	35.96	333.11
DPB94107	16/05/89	9.61	302.89	310.30	32.79	99.84	35.14	98.48	89.49	77.95	62.94	40.95	378.41
DPB94108	16/05/89	9.62	303.16	310.23	32.88	97.26	40.02	97.61	92.30	82.68	66.63	43.78	391.98
DPB94109	16/05/89	9.63	303.36	310.30	32.82	94.48	45.12	92.77	93.03	86.69	69.70	46.66	396.88
DPC94110	16/05/89	9.61	303.22	310.30	33.22	98.47	50.86	93.63	96.04	93.34	75.54	51.15	418.81
DPB96200	17/05/89	9.63	295.66	297.08	29.71	144.53	0.00	53.81	53.06	53.52	54.12	53.67	275.11

DPB96204	17/05/89	9.67	295.93	310.43	29.61	139.82	20.23	89.36	71.10	53.40	52.35	51.34	325.90
DPB96205	17/05/89	9.63	295.86	310.16	30.01	137.51	24.88	103.61	84.99	62.37	51.29	50.14	361.68
DPB96206	17/05/89	9.63	295.66	310.36	30.16	136.34	30.22	118.68	96.80	75.72	52.53	50.04	403.52
DPB96207	17/05/89	9.63	295.73	310.36	30.06	137.03	35.04	129.65	105.96	85.95	56.14	49.03	437.28
DPB96208	17/05/89	9.64	295.80	310.50	30.32	142.73	39.94	150.59	123.47	100.61	64.76	54.04	504.23
DPB96209	17/05/89	9.63	295.93	310.36	30.22	142.17	45.06	159.25	132.74	109.35	72.19	53.47	538.57
DPB96210	17/05/89	9.64	295.73	310.50	30.15	139.98	50.18	163.35	139.74	115.58	79.41	52.84	562.52
DPB96211	17/05/89	9.63	295.66	310.36	30.19	140.29	54.96	167.62	147.86	123.01	86.84	53.80	591.37
DPB96212	17/05/89	9.64	295.86	310.50	30.19	138.82	60.02	165.31	152.67	129.09	94.32	54.69	608.69
DPB96213	17/05/89	9.64	295.80	310.50	30.25	138.56	65.22	163.18	157.02	135.74	101.38	56.56	626.58
DPB96214	17/05/89	9.63	295.73	310.50	30.07	138.03	70.39	159.94	158.14	141.59	107.95	58.92	638.99
DPC96214	17/05/89	9.64	296.00	310.63	30.15	138.32	71.86	158.96	157.87	142.86	109.69	59.72	641.58
DPB96100	17/05/89	9.63	304.24	305.65	30.21	137.68	0.00	52.37	51.56	51.94	52.63	52.17	268.47
DPB96104	17/05/89	9.64	304.71	310.16	30.19	143.26	20.10	118.45	100.88	87.42	67.39	55.15	439.01
DPB96105	17/05/89	9.64	305.04	310.36	30.14	139.16	25.02	128.32	108.58	94.11	75.28	53.62	470.47
DPB96106	17/05/89	9.63	304.91	310.23	30.09	137.25	30.08	138.59	117.66	101.50	82.14	54.82	505.67
DPB96107	17/05/89	9.63	303.76	310.36	30.16	136.71	35.02	145.69	123.97	106.12	84.32	54.45	525.58
DPB96108	17/05/89	9.63	304.64	310.36	30.17	140.87	40.06	159.14	137.59	118.35	95.20	59.83	582.43
DPB96109	17/05/89	9.64	302.01	310.50	30.05	140.39	44.98	165.72	143.90	122.39	94.97	57.98	596.86
DPB96110	17/05/89	9.63	303.16	310.43	30.03	138.89	49.88	166.52	150.44	130.59	104.32	62.97	628.31
DPB96111	17/05/89	9.64	303.36	310.43	30.16	138.27	54.96	164.39	154.63	136.74	109.77	66.43	644.18
DPB96112	17/05/89	9.63	303.56	310.50	30.04	139.85	64.94	162.02	159.94	149.75	121.20	75.28	681.69
DPC96113	17/05/89	9.63	303.16	310.70	30.17	139.73	68.22	161.10	159.17	152.09	123.20	76.53	685.16
DPB96300	17/05/89	9.63	282.38	283.74	30.28	137.83	0.00	48.62	47.94	48.29	48.95	48.56	249.14
DPB96301	17/05/89	9.65	282.32	289.64	30.40	138.11	5.06	49.25	48.44	48.71	49.21	48.74	252.02
DPB96302	17/05/89	9.65	282.66	295.53	30.44	142.73	10.04	52.83	51.75	51.94	52.35	51.70	268.76
DPB96303	17/05/89	9.66	283.20	301.81	30.46	142.05	15.04	52.89	51.67	51.64	51.96	51.18	266.16
DPB96304	17/05/89	9.62	281.98	305.65	30.47	143.77	19.96	54.16	52.83	52.71	52.87	51.96	272.22
DPB96305	17/05/89	9.64	282.18	310.09	30.54	144.98	25.04	61.48	54.25	53.94	54.01	52.95	285.21
DPB96306	17/05/89	9.64	282.32	310.30	30.59	142.43	30.04	85.49	55.98	53.02	52.77	51.62	307.14
DPB96307	17/05/89	9.64	282.32	310.23	30.68	140.02	34.94	102.58	70.49	52.25	51.73	50.48	336.00
DPB96308	17/05/89	9.64	282.38	310.36	30.61	143.97	40.04	120.01	88.11	56.71	54.24	52.74	381.01
DPB96310	17/05/89	9.64	282.25	310.36	30.65	139.83	49.90	143.55	112.12	75.07	52.51	50.66	443.63
DPB96311	17/05/89	9.64	282.32	310.43	30.75	138.42	54.98	152.56	121.28	87.38	53.18	49.96	475.08
DPB96312	17/05/89	9.63	282.25	310.50	30.73	137.45	60.02	157.98	129.70	98.07	55.70	49.39	502.21
DPB96313	17/05/89	9.63	282.38	310.50	30.78	140.75	64.98	167.27	141.40	108.89	60.92	51.31	541.45
DPB96314	17/05/89	9.63	282.38	310.57	30.79	141.57	70.14	170.10	150.56	118.16	66.92	52.04	569.44
DPB96315	17/05/89	9.63	282.38	310.50	30.78	140.85	75.20	165.37	155.33	124.08	73.57	51.70	582.14
DPC96316	17/05/89	9.63	282.25	310.50	30.73	140.63	79.43	161.62	157.83	128.12	79.54	52.04	591.08
DPB96400	17/05/89	9.64	268.37	269.46	30.68	138.47	0.00	47.92	47.25	47.71	48.17	47.78	246.25
DPB96401	17/05/89	9.63	273.61	309.83	30.60	137.44	29.98	53.98	49.37	49.06	48.87	47.86	256.93
DPB96407	17/05/89	9.63	273.34	310.23	30.70	136.02	35.00	73.78	49.90	48.90	48.58	47.47	275.97
DPB96408	17/05/89	9.63	273.75	310.16	30.59	140.30	40.06	96.69	58.87	51.67	51.26	49.93	316.66
DPB96409	17/05/89	9.64	274.43	310.30	30.60	139.64	44.98	113.54	76.34	52.10	51.23	49.73	352.15
DPB96410	17/05/89	9.64	274.50	310.43	30.66	136.88	49.90	125.66	92.19	54.91	49.70	48.27	380.15
DPB96411	17/05/89	9.63	272.66	310.36	30.63	136.29	55.10	135.30	101.31	59.29	49.52	48.06	403.52
DPB96412	17/05/89	9.62	271.30	310.23	30.62	144.06	60.02	150.31	112.16	64.60	53.73	52.12	443.34
DPB96413	17/05/89	9.63	271.37	310.43	30.66	140.02	65.06	157.46	121.08	75.49	52.27	50.35	467.58
DPB96414	17/05/89	9.63	271.43	310.36	30.72	136.66	70.04	158.90	127.32	87.30	51.62	48.48	484.89
DPB96415	17/05/89	9.63	271.37	310.50	30.87	137.71	74.92	161.85	135.24	97.42	53.93	48.95	508.56
DPB96416	17/05/89	9.63	271.77	310.50	30.88	138.30	79.88	161.44	142.01	107.81	57.54	49.41	529.33
DPC96417	17/05/89	9.64	271.84	310.77	30.87	137.96	83.61	156.19	142.05	113.27	60.35	49.31	532.22
DPB96500	17/05/89	9.63	260.44	261.40	30.88	144.40	0.00	50.12	49.37	49.83	50.35	49.93	257.50
DPB96506	17/05/89	9.65	259.97	297.22	30.96	140.95	29.98	51.79	50.33	50.10	49.96	49.03	258.66
DPB96507	17/05/89	9.63	259.90	302.68	30.98	141.30	35.00	52.54	50.87	50.40	50.25	49.13	260.97
DPB96508	17/05/89	9.63	259.56	308.28	30.94	140.21	40.06	54.10	50.75	50.25	49.88	48.66	260.97
DPB96509	17/05/89	9.63	259.49	310.30	30.94	141.88	44.98	66.39	52.10	51.48	50.95	49.65	278.86
DPB96510	17/05/89	9.63	259.42	310.23	31.03	135.98	50.04	90.92	52.37	49.02	48.38	47.05	295.88
DPB96511	17/05/89	9.63	259.08	310.30	31.11	137.56	54.96	108.23	61.48	50.10	49.62	48.04	325.90

DPB96512	17/05/89	9.64	259.42	310.36	31.17	139.05	59.88	122.03	75.07	51.13	50.22	48.56	355.91
DPB96513	17/05/89	9.63	259.35	310.30	31.22	141.21	64.98	136.97	91.11	54.14	51.80	50.04	394.00
DPB96514	17/05/89	9.63	259.49	310.30	31.28	141.47	70.00	148.69	106.04	57.91	52.01	50.25	425.45
DPB96515	17/05/89	9.63	259.49	310.30	31.44	139.41	75.02	156.48	117.16	64.91	50.95	49.26	449.40
DPB96516	17/05/89	9.63	259.49	310.36	31.42	138.05	80.12	159.54	123.85	75.07	50.77	48.61	469.02
DPB96517	17/05/89	9.63	259.49	310.43	31.47	138.69	84.94	158.21	128.24	85.65	52.12	49.05	483.74
DPC96518	17/05/89	9.63	259.90	310.63	31.49	140.20	88.87	150.65	129.63	94.04	53.78	49.93	489.80
DPB97100	31/05/89	9.55	302.75	303.70	27.69	162.99	0.00	63.68	63.22	63.10	63.80	63.34	324.45
DPB97102	31/05/89	9.56	302.75	309.49	27.69	160.64	9.96	86.53	70.91	62.79	63.18	62.43	353.89
DPB97104	31/05/89	9.55	302.89	309.56	27.73	159.19	20.10	124.80	105.89	87.61	65.00	61.39	454.59
DPB97106	31/05/89	9.55	303.02	309.69	27.79	163.76	29.94	162.25	135.86	114.39	82.94	64.61	570.89
DPB97107	31/05/89	9.55	303.09	309.62	27.76	160.95	34.98	172.99	145.44	122.62	91.20	63.96	607.82
DPB97108	31/05/89	9.55	302.75	309.62	27.93	162.79	39.79	186.38	157.48	132.66	99.64	66.01	654.57
DPB97109	31/05/89	9.55	302.75	309.69	27.83	160.74	44.98	193.24	166.25	140.40	107.77	67.02	686.89
DPB97110	31/05/89	9.56	302.75	309.83	27.77	160.17	50.16	198.78	174.37	147.94	114.76	68.95	717.76
DPB97111	31/05/89	9.54	302.75	309.69	27.81	159.72	54.96	200.11	180.53	154.63	121.43	71.41	740.85
DPB97112	31/05/89	9.54	302.68	309.76	27.89	163.87	60.02	209.64	192.99	166.87	131.40	76.37	791.35
DPB97113	31/05/89	9.56	302.75	309.76	27.75	161.90	65.39	205.31	195.65	172.52	137.01	79.20	803.47
DPB97114	31/05/89	9.55	302.68	309.89	27.78	160.69	70.08	202.54	196.23	177.60	142.00	82.68	815.59
DPB97115	31/05/89	9.55	302.55	309.96	27.75	160.78	75.31	202.48	196.34	183.30	147.35	86.24	829.73
DPC97116	31/05/89	9.55	302.62	309.96	27.73	161.83	77.23	204.04	196.88	185.84	150.15	88.37	839.25
DPB97200	31/05/89	9.56	295.39	296.41	27.22	160.23	0.00	60.97	60.41	60.29	61.13	60.63	310.60
DPB97202	31/05/89	9.54	293.70	304.98	27.25	160.25	9.98	62.52	61.60	60.98	61.57	60.82	314.93
DPB97204	31/05/89	9.55	294.99	309.56	27.27	159.69	19.96	98.36	73.03	61.68	61.88	60.82	363.70
DPB97206	31/05/89	9.57	295.19	309.76	27.21	164.08	30.02	139.11	112.39	78.76	65.47	64.06	469.31
DPB97207	31/05/89	9.56	294.78	309.62	27.23	162.24	34.86	152.85	123.89	91.84	65.15	62.92	507.11
DPB97208	31/05/89	9.54	295.19	309.56	27.38	159.59	39.92	165.89	135.24	106.69	68.32	61.28	548.38
DPB97209	31/05/89	9.57	294.95	309.75	27.43	164.84	44.91	184.23	150.81	119.35	1.95	64.98	605.37
DPB97208	31/05/89	9.57	294.58	309.62	26.80	160.54	40.12	165.95	134.86	104.62	67.34	62.17	545.78
DPB97208	31/05/89	9.54	294.72	309.83	26.81	162.20	40.19	167.73	136.36	105.92	68.37	62.74	551.84
DPB97209	31/05/89	9.56	294.31	309.69	26.84	161.91	44.98	180.43	147.71	117.16	73.10	63.18	593.39
DPB97210	31/05/89	9.55	294.65	309.62	26.86	161.28	50.02	190.94	159.02	128.66	81.36	62.94	635.52
DPB97211	31/05/89	9.54	294.38	309.62	27.01	159.94	55.10	196.19	167.10	135.94	88.03	62.30	661.78
DPB97212	31/05/89	9.55	294.44	309.76	26.98	160.13	60.02	201.09	175.99	144.28	96.37	62.97	693.24
DPB97213	31/05/89	9.55	294.65	309.62	27.05	163.31	65.02	208.42	187.38	154.90	105.74	65.52	735.08
DPB97214	31/05/89	9.56	294.65	309.83	27.17	163.47	70.10	209.86	194.69	163.06	114.08	67.10	762.49
DPB97215	31/05/89	9.57	294.78	310.03	27.10	161.89	75.16	205.13	196.69	168.79	122.52	68.14	775.19
DPB97216	31/05/89	9.55	294.65	309.89	27.13	163.44	79.98	205.94	200.15	175.91	130.42	70.55	797.12
DPC97217	31/05/89	9.56	294.65	309.89	26.90	163.24	82.17	205.54	200.03	177.91	133.12	71.20	801.45
DPB97300	31/05/89	9.56	280.28	281.09	26.77	164.50	0.00	61.08	60.79	60.60	61.36	60.89	311.47
DPB97302	31/05/89	9.58	279.12	290.93	26.77	161.51	9.98	61.37	60.72	60.29	60.76	60.09	310.31
DPB97304	31/05/89	9.56	280.28	302.21	26.78	163.53	20.10	63.85	62.95	62.18	62.43	61.39	320.12
DPB97306	31/05/89	9.56	280.42	309.49	26.76	166.37	30.06	79.26	66.30	65.22	65.05	63.83	347.83
DPB97308	31/05/89	9.55	281.30	309.62	26.76	160.62	40.14	129.01	88.42	62.72	62.01	60.32	411.31
DPB97309	31/05/89	9.56	281.77	309.69	26.76	163.48	44.96	148.17	108.81	68.10	64.06	62.24	460.65
DPB97310	31/05/89	9.56	281.91	309.69	26.76	163.43	50.08	164.27	126.12	76.76	64.17	62.32	503.65
DPB97311	31/05/89	9.54	281.84	309.56	26.79	161.78	55.12	176.62	138.40	89.30	63.57	61.15	540.01
DPB97312	31/05/89	9.56	281.77	309.69	26.76	164.34	60.04	190.94	151.36	101.69	66.32	63.05	584.45
DPB97313	31/05/89	9.54	281.91	309.62	26.76	165.91	65.22	203.52	164.44	116.47	69.46	64.24	630.33
DPB97314	31/05/89	9.56	281.91	309.83	26.81	163.01	70.14	206.11	172.02	127.89	71.39	62.82	651.68
DPB97314	31/05/89	9.53	281.91	309.35	26.76	164.63	70.14	207.33	173.52	129.09	72.01	62.92	656.88
DPB97315	31/05/89	9.55	281.91	309.83	26.78	162.23	74.96	205.71	179.26	137.51	75.72	61.98	672.17
DPB97316	31/05/89	9.56	281.91	309.76	26.78	162.37	80.06	205.94	186.95	146.44	81.93	62.37	696.12
DPB97317	31/05/89	9.55	282.32	309.89	26.81	164.14	85.06	208.71	195.92	155.94	89.88	64.09	727.00
DPC97318	31/05/89	9.55	282.25	309.83	26.77	164.20	89.10	205.31	197.38	159.67	95.54	64.19	735.08
DPB97500	20/09/89	9.52	252.78	254.22	28.76	167.05	0.00	56.64	57.83	57.18	57.18	55.62	288.09
DPB97505	20/09/89	9.52	252.71	260.38	28.77	165.83	5.04	56.75	57.75	57.02	56.95	55.26	286.65
DPB97510	20/09/89	9.52	252.78	266.18	28.76	165.57	9.98	56.93	57.95	57.02	56.84	55.08	286.07
DPB97515	20/09/89	9.52	252.78	271.91	28.74	165.59	15.00	57.44	58.10	57.14	56.79	54.95	286.94

DPB97520	20/09/89	9.52	252.64	277.63	28.77	164.83	20.14	57.68	58.29	57.25	56.87	54.89	287.80
DPB97525	20/09/89	9.52	252.50	283.00	28.76	165.00	24.96	58.25	58.68	57.48	56.89	54.87	288.96
DPB97530	20/09/89	9.52	252.30	288.56	28.86	165.12	29.94	58.83	58.95	57.79	57.10	54.92	290.11
DPB97535	20/09/89	9.55	252.30	294.24	28.98	162.28	35.06	58.31	58.33	56.83	56.01	53.75	287.23
DPB97540	20/09/89	9.53	252.30	299.72	29.03	162.49	40.18	58.71	58.64	56.94	56.04	53.67	287.80
DPB97545	20/09/89	9.52	252.44	304.50	29.08	163.35	45.04	60.62	59.98	58.10	56.95	54.43	293.58
DPB97550	20/09/89	9.52	252.78	308.55	29.11	162.01	50.04	69.45	59.60	57.56	56.32	53.70	301.08
DPB97555	20/09/89	9.52	252.78	308.88	29.21	162.14	55.10	90.86	61.18	58.45	56.97	54.14	325.90
DPB97560	20/09/89	9.52	252.78	308.88	29.30	162.41	60.16	114.12	65.72	58.48	57.08	54.14	354.46
DPB97565	20/09/89	9.52	252.37	308.88	29.28	163.13	64.96	132.41	75.72	59.02	57.57	54.48	384.47
DPB97570	20/09/89	9.52	252.30	308.88	29.32	164.46	70.08	148.57	90.38	60.75	58.69	55.44	418.81
DPB97575	20/09/89	9.52	252.50	308.88	29.39	162.43	75.22	160.98	106.39	62.14	57.80	54.71	448.82
DPB97580	20/09/89	9.52	252.30	309.02	29.44	162.35	80.00	171.60	123.35	65.37	57.73	54.58	477.68
DPB97581	20/09/89	9.52	252.50	309.02	29.50	163.88	85.18	182.57	137.86	71.57	58.69	55.52	511.44
DPB97590	20/09/89	9.52	252.44	309.08	29.61	163.34	89.98	186.26	147.13	79.22	58.82	55.18	531.93
DPB97595	20/09/89	9.52	252.64	309.22	29.74	162.89	95.00	179.16	151.71	89.76	59.41	55.13	540.30
DPC97597	20/09/89	9.52	252.71	309.29	29.91	164.30	97.85	168.48	152.94	95.88	60.53	55.78	538.57
DPB97400	20/09/89	9.52	270.21	271.71	30.23	163.92	0.00	56.17	57.71	56.60	56.58	55.02	286.36
DPB97405	20/09/89	9.53	270.00	277.56	30.29	163.27	5.06	56.75	58.21	57.02	56.92	55.26	288.67
DPB97410	20/09/89	9.52	270.34	283.33	30.35	163.02	9.96	57.10	58.48	57.10	56.95	55.08	288.96
DPB97415	20/09/89	9.52	270.28	288.96	30.32	162.88	15.04	57.73	58.83	57.29	57.00	55.10	289.82
DPB97420	20/09/89	9.54	270.41	294.24	30.35	163.16	20.04	58.31	59.21	57.60	57.10	55.08	291.56
DPB97425	20/09/89	9.53	270.34	299.51	30.36	162.51	24.98	58.89	59.71	57.95	57.28	55.15	293.00
DPB97430	20/09/89	9.53	270.48	304.64	30.41	163.73	30.08	60.45	61.02	59.10	58.32	55.98	299.35
DPB97435	20/09/89	9.52	270.48	308.28	30.41	162.91	35.10	68.93	61.06	58.91	57.93	55.49	307.14
DPB97440	20/09/89	9.52	270.48	308.68	30.46	163.36	40.18	93.17	62.95	59.41	58.32	55.72	334.55
DPB97445	20/09/89	9.51	270.48	308.82	30.51	162.09	44.84	114.12	71.45	59.25	58.09	55.34	363.41
DPB97450	20/09/89	9.52	270.48	308.88	30.52	163.35	50.04	132.47	88.30	60.75	59.08	56.12	402.08
DPB97455	20/09/89	9.53	270.48	308.88	30.62	163.96	54.96	148.69	106.81	63.99	59.67	56.71	441.32
DPB97460	20/09/89	9.52	270.55	308.88	30.62	163.76	59.92	162.60	123.35	69.72	59.62	56.61	476.81
DPB97465	20/09/89	9.52	270.48	308.88	30.71	163.60	65.12	175.58	137.24	79.15	59.98	56.76	514.04
DPB97470	20/09/89	9.53	270.48	309.02	30.86	164.83	70.22	187.36	149.44	90.03	61.62	57.70	552.13
DPB97475	20/09/89	9.52	270.68	309.02	30.87	164.58	74.90	193.70	158.48	101.50	62.30	57.41	579.54
DPB97480	20/09/89	9.53	270.75	309.29	30.83	164.39	80.12	197.34	168.02	114.12	64.22	57.46	607.53
DPB97485	20/09/89	9.52	270.96	309.22	30.86	162.49	85.04	193.76	173.76	124.82	66.48	56.56	621.10
DPB97490	20/09/89	9.53	270.96	309.29	30.99	163.65	90.02	193.13	179.57	134.28	70.53	57.36	640.72
DPC97495	20/09/89	9.53	270.96	309.35	30.95	164.14	94.43	187.70	177.37	140.98	75.05	57.52	645.05
DPB97300	21/09/89	9.51	282.86	284.76	30.25	164.56	0.00	58.08	58.21	58.33	58.43	57.72	298.48
DPB97305	21/09/89	9.52	282.86	290.39	30.21	163.82	5.04	58.25	58.41	58.37	58.27	57.47	298.48
DPB97310	21/09/89	9.51	283.00	295.66	30.15	164.21	10.10	59.52	59.37	59.25	59.10	58.12	303.10
DPB97315	21/09/89	9.52	283.00	300.86	30.20	164.16	15.08	60.04	59.75	59.41	59.08	58.01	303.39
DPB97320	21/09/89	9.51	283.20	305.99	30.27	163.94	20.08	60.50	60.02	59.60	59.08	57.88	304.54
DPB97325	21/09/89	9.51	283.13	308.41	30.23	162.94	24.94	72.91	60.25	59.56	58.92	57.57	317.53
DPB97330	21/09/89	9.52	283.27	308.82	30.20	164.12	30.00	99.29	66.87	61.33	60.40	58.87	354.75
DPB97335	21/09/89	9.52	283.27	308.88	30.26	162.73	35.14	118.04	83.72	61.14	59.78	58.14	389.09
DPB97340	21/09/89	9.52	283.27	308.88	30.22	164.04	40.06	135.99	103.27	65.80	60.71	58.87	413.82
DPB97345	21/09/89	9.52	283.27	308.95	30.26	164.87	44.98	151.81	118.89	74.72	61.36	59.46	475.66
DPB97350	21/09/89	9.51	283.33	308.88	30.22	163.52	50.04	165.43	131.78	87.80	61.18	58.69	514.33
DPB97355	21/09/89	9.51	283.27	308.88	30.15	163.40	55.08	177.78	143.36	100.69	62.87	58.84	552.99
DPB97360	21/09/89	9.52	283.20	309.22	29.81	164.22	60.00	188.28	154.75	112.89	65.93	59.52	591.37
DPB97365	21/09/89	9.51	283.33	308.95	29.81	162.66	65.08	193.24	163.98	123.97	69.85	58.71	619.94
DPB97370	21/09/89	9.52	283.27	309.29	29.72	164.34	70.12	198.73	174.22	134.13	75.62	59.60	651.97
DPB97375	21/09/89	9.53	283.20	309.29	29.72	161.97	75.06	196.13	180.41	141.21	81.77	59.26	669.00
DPB97380	21/09/89	9.52	283.40	309.22	29.78	163.62	80.04	195.67	187.53	149.32	89.90	60.06	692.08
DPB97385	21/09/89	9.52	283.33	309.15	29.78	163.31	85.12	191.28	189.22	153.90	97.70	60.17	702.18
DPC97390	21/09/89	9.51	283.33	309.35	29.74	162.86	87.87	188.97	188.41	155.86	102.29	60.50	706.51
DPB97200	21/09/89	9.52	295.19	296.61	30.87	162.73	0.00	58.19	58.37	58.64	58.74	57.96	299.64
DPB97205	21/09/89	9.52	295.05	302.15	30.91	162.11	5.06	58.95	58.95	58.91	58.97	58.04	301.66
DPB97210	21/09/89	9.53	295.12	307.00	30.84	162.20	9.98	59.87	59.71	59.48	59.39	58.27	303.96

DPB97215	21/09/89	9.52	295.12	308.61	30.94	164.98	15.06	80.88	62.91	61.91	61.54	60.32	335.42
DPB97220	21/09/89	9.52	295.12	308.82	30.95	164.19	19.94	101.71	80.53	61.99	60.95	59.60	372.35
DPB97225	21/09/89	9.52	294.99	308.75	30.96	162.88	25.10	120.01	98.84	70.76	60.63	59.10	417.95
DPB97230	21/09/89	9.52	294.78	308.88	30.97	163.16	30.02	135.82	112.08	83.88	61.28	59.21	461.23
DPB97235	21/09/89	9.53	294.92	308.95	30.99	165.06	34.94	153.94	126.86	98.50	65.52	61.02	515.48
DPB97240	21/09/89	9.52	295.05	308.88	31.09	163.43	39.94	166.18	137.82	110.20	70.61	59.93	554.44
DPB97245	21/09/89	9.53	295.05	309.08	31.10	164.22	45.04	178.41	149.59	120.70	77.70	60.69	597.15
DPB97250	21/09/89	9.51	295.12	308.88	31.12	164.98	50.00	189.20	161.33	130.97	86.34	61.41	638.59
DPB97255	21/09/89	9.52	294.92	309.15	31.15	161.49	54.96	190.65	167.45	136.86	93.59	60.40	659.19
DPB97260	21/09/89	9.52	295.05	309.15	31.13	164.98	60.00	199.42	179.64	147.59	102.68	63.13	703.05
DPBP7265	21/09/89	9.53	294.85	309.35	31.22	163.92	64.96	195.90	183.99	153.21	109.72	63.52	717.19
DPB97270	21/09/89	9.52	294.99	309.29	31.18	162.92	70.12	191.11	187.15	159.44	117.35	64.79	730.46
DPB97275	21/09/89	9.53	294.72	309.35	31.28	162.58	75.04	189.55	189.11	165.18	123.46	66.48	744.31
DPB97280	21/09/89	9.52	294.78	309.35	31.39	163.89	79.96	191.63	191.61	172.14	130.73	69.59	765.96
DPC97285	21/09/89	9.52	294.72	309.29	31.51	164.06	82.48	192.61	192.07	175.30	134.47	71.28	776.92
DPB97100	21/09/89	9.52	305.38	307.00	31.99	163.81	0.00	60.50	60.95	60.87	61.15	60.24	311.18
DPB97105	21/09/89	9.52	305.52	308.82	31.99	163.44	5.04	80.59	74.76	63.18	62.12	61.02	349.56
DPB97110	21/09/89	9.51	305.11	308.82	31.83	162.04	10.14	98.94	89.26	78.07	63.18	59.62	397.17
DPB97115	21/09/89	9.52	305.11	308.88	31.96	163.99	15.00	118.10	104.39	90.30	71.80	61.10	454.02
DPB97120	21/09/89	9.51	305.11	308.82	31.99	165.28	20.08	137.78	119.89	103.04	83.02	62.53	515.48
DPB97125	21/09/89	9.51	305.04	308.88	32.07	164.68	25.18	152.79	132.05	112.81	91.30	63.91	561.94
DPB97130	21/09/89	9.51	305.52	308.75	32.04	163.98	30.08	165.54	143.32	122.16	99.72	66.97	607.53
DPB97135	21/09/89	9.51	305.11	308.95	32.00	164.93	35.02	178.87	155.60	132.01	107.33	70.32	653.70
DPB97140	21/09/89	9.52	305.45	308.95	32.12	164.47	40.19	187.70	165.41	140.67	114.45	73.75	692.08
DPB97145	21/09/89	9.51	305.18	309.02	32.13	162.77	45.00	189.78	170.76	146.05	118.78	76.35	711.13
DPB97150	21/09/89	9.51	305.11	309.02	32.12	163.38	49.90	195.38	179.18	154.25	125.12	79.39	743.16
DPB97155	21/09/89	9.51	305.45	309.22	32.16	162.42	54.98	192.90	183.45	161.02	130.94	84.16	762.49
DPB97160	21/09/89	9.52	305.04	309.22	32.18	162.49	59.86	191.80	187.34	167.18	136.00	87.15	779.81
DPB97165	21/09/89	9.51	305.04	309.15	32.18	163.22	65.06	191.92	190.72	174.33	142.18	91.57	800.58
DPB97170	21/09/89	9.52	305.04	309.29	32.22	162.87	70.14	190.76	189.45	179.18	147.01	95.88	812.99
DPB97175	21/09/89	9.51	305.25	309.35	32.22	162.45	75.06	190.82	185.88	181.80	150.73	100.11	819.63
DPC97180	21/09/89	9.52	305.04	309.35	32.32	162.55	76.97	190.94	184.88	182.30	151.84	101.17	821.36
DPB96300	21/09/89	9.51	283.06	284.42	32.74	139.91	0.00	43.77	44.48	44.33	44.43	43.70	227.21
DPB96305	21/09/89	9.53	283.54	291.87	32.79	140.74	5.18	44.40	44.86	44.63	44.58	43.81	228.65
DPB96310	21/09/89	9.52	283.40	297.69	32.80	140.20	10.12	44.63	45.02	44.63	44.48	43.55	229.23
DPB96315	21/09/89	9.52	282.93	303.22	32.76	139.95	15.02	45.21	45.29	44.71	44.53	43.49	230.38
DPB96320	21/09/89	9.52	282.18	308.08	32.79	139.29	19.92	46.83	45.63	44.98	44.58	43.44	232.69
DPB96325	21/09/89	9.51	282.38	308.61	32.83	138.89	25.02	68.64	47.10	45.25	44.71	43.44	256.64
DPB96330	21/09/89	9.53	282.86	308.88	32.77	139.41	30.08	86.36	62.26	45.86	45.16	43.70	291.27
DPB96335	21/09/89	9.51	282.79	308.88	33.01	137.40	35.12	100.27	78.91	50.37	44.25	42.74	324.45
DPB96340	21/09/89	9.51	283.00	308.82	33.01	139.41	40.29	116.43	92.88	61.52	45.78	44.07	368.89
DPB96345	21/09/89	9.51	283.40	308.82	33.03	141.25	44.98	130.16	104.85	73.91	48.04	45.26	410.16
DPB96350	21/09/89	9.52	283.27	308.88	32.87	139.78	50.04	138.07	113.66	84.11	49.83	44.66	439.30
DPB96355	21/09/89	9.51	283.33	308.88	32.85	141.49	55.16	147.19	125.05	94.92	54.66	45.47	475.95
DPB96360	21/09/89	9.52	283.27	309.15	32.88	139.53	59.88	146.61	131.05	101.00	59.18	44.53	491.24
DPB96365	21/09/89	9.51	283.33	308.95	32.85	142.40	64.94	151.34	141.44	110.04	66.32	46.19	524.14
DPB96370	21/09/89	9.53	283.20	309.22	32.90	141.00	70.00	145.92	145.02	114.93	72.81	46.14	534.24
DPC96375	21/09/89	9.52	283.33	309.29	32.82	141.20	75.06	141.24	146.48	119.24	80.32	46.77	542.89
DPB94300	22/09/89	9.55	283.06	284.15	30.07	98.54	0.00	24.20	24.97	24.89	24.64	24.09	122.74
DPB94305	22/09/89	9.56	282.79	293.43	30.15	98.25	5.10	24.66	25.32	25.09	24.90	24.22	124.48
DPB94310	22/09/89	9.55	283.00	301.74	30.15	97.65	9.98	24.84	25.43	25.13	24.79	24.09	124.48
DPB94315	22/09/89	9.56	282.86	308.61	30.14	97.09	15.04	27.90	25.51	25.13	24.74	23.88	127.65
DPB94320	22/09/89	9.55	282.79	308.95	30.18	98.80	19.94	42.50	31.32	26.09	25.60	24.77	151.02
DPB94325	22/09/89	9.54	283.00	308.95	30.18	101.10	25.00	55.14	44.75	29.74	26.87	25.91	183.34
DPB94330	22/09/89	9.54	282.79	309.02	30.25	98.57	29.98	64.26	52.44	37.40	26.12	24.90	206.14
DPB94335	22/09/89	9.54	282.72	309.15	30.30	97.96	34.98	71.01	60.14	45.40	27.68	24.43	230.38
DPB94340	22/09/89	9.55	283.20	309.35	30.29	101.07	40.04	79.20	70.14	53.48	32.46	25.78	262.70
DPB94345	22/09/89	9.55	282.86	309.35	30.37	97.95	44.96	76.95	74.11	57.71	36.77	24.64	271.36
DPB94350	22/09/89	9.55	283.13	309.35	30.41	100.35	50.06	78.86	81.18	64.26	42.82	26.04	295.31

DPB94355	22/09/89	9.55	282.93	309.22	30.45	101.56	55.10	78.16	85.61	69.30	48.30	27.11	310.31
DPB94355	22/09/89	9.55	283.27	309.29	30.48	105.23	51.46	88.90	87.49	68.68	45.08	28.09	320.41
DPB94355	22/09/89	9.56	283.33	309.35	30.48	104.49	53.34	86.94	88.19	69.99	46.95	28.12	321.85
DPB94355	22/09/89	9.54	283.13	309.22	30.47	103.94	54.92	85.96	89.30	71.72	49.10	28.38	327.05
DPB94355	22/09/89	9.55	283.27	309.35	30.50	104.47	56.07	84.80	89.53	72.18	50.01	28.51	326.76
DPB94355	22/09/89	9.56	283.13	309.35	30.52	104.46	56.97	83.24	89.73	72.61	50.82	28.61	327.05
DPB94355	22/09/89	9.57	283.33	309.35	30.53	104.86	57.01	83.44	89.85	72.53	50.86	28.68	327.63
DPC94355	22/09/89	9.55	282.79	309.22	30.57	104.03	56.80	82.55	89.11	72.10	50.63	28.46	324.74
DPB94100	22/09/89	9.56	303.22	304.50	31.14	97.46	0.00	27.49	28.55	28.05	27.99	27.37	139.77
DPB94105	22/09/89	9.55	306.06	309.02	31.19	97.18	5.06	35.74	34.90	31.40	27.68	24.82	154.49
DPB94110	22/09/89	9.54	304.98	309.15	31.10	96.76	9.94	45.56	42.52	36.98	32.07	25.11	182.77
DPB94115	22/09/89	9.54	302.48	309.02	30.95	96.77	15.00	47.17	43.94	36.55	30.56	22.04	180.17
DPB94120	22/09/89	9.55	302.68	309.08	30.91	97.65	19.94	53.98	52.21	43.52	35.88	24.64	209.89
DPB94125	22/09/89	9.54	303.36	309.08	30.91	99.45	25.08	63.51	63.10	53.94	43.83	30.27	255.20
DPB94130	22/09/89	9.55	303.16	309.22	30.92	97.20	30.08	68.35	68.80	60.29	48.56	34.04	280.59
DPB94135	22/09/89	9.55	303.56	309.35	30.80	98.15	35.27	71.01	73.80	66.87	54.12	38.01	304.83
DPB94140	22/09/89	9.55	302.62	309.29	30.87	99.40	40.18	74.93	80.45	73.68	59.31	40.40	330.22
DPC94145	22/09/89	9.55	304.03	309.29	30.79	100.04	43.42	68.64	77.38	74.72	61.57	43.67	327.05
DPB74500	26/09/89	7.01	223.39	224.29	24.23	99.07	0.00	23.39	22.97	23.39	22.95	22.90	107.74
DPB74501	26/09/89	7.03	222.91	234.77	24.27	98.13	4.98	23.16	22.78	23.20	22.74	22.69	106.01
DPB74502	26/09/89	7.02	222.91	244.20	24.20	101.14	9.98	24.84	24.36	24.66	24.14	24.04	112.93
DPB74503	26/09/89	7.02	222.91	254.83	24.30	98.26	14.90	23.86	23.36	23.63	23.11	22.98	106.01
DPB74504	26/09/89	7.05	222.77	264.89	24.24	99.38	20.04	24.43	23.74	24.01	23.31	23.16	106.59
DPB74505	26/09/89	7.03	223.32	275.52	24.18	97.53	25.02	23.91	23.20	23.36	22.74	22.51	103.70
DPB74506	26/09/89	7.02	223.39	283.74	24.26	99.93	30.18	25.30	24.47	24.59	23.83	23.60	108.32
DPB74507	26/09/89	7.03	223.88	288.01	24.23	99.30	35.00	36.38	24.36	24.63	23.75	23.50	119.57
DPB74508	26/09/89	7.03	223.74	288.01	24.39	100.95	40.12	55.48	27.93	24.97	24.40	23.94	143.52
DPB74509	26/09/89	7.02	223.81	287.88	24.53	99.43	44.98	73.61	39.90	24.63	24.01	23.52	172.96
DPB74510	26/09/89	7.03	223.81	288.08	24.69	101.01	50.02	89.65	52.48	26.97	24.31	24.25	205.85
DPB74511	26/09/89	7.02	223.88	288.08	24.97	100.87	55.08	103.27	67.60	31.67	24.33	24.09	249.14
DPB74512	26/09/89	7.02	223.88	288.01	25.11	99.39	60.10	112.04	81.07	40.13	24.17	23.73	280.59
DPB74513	26/09/89	7.03	223.53	288.15	25.01	98.41	65.00	118.39	92.00	48.90	24.43	23.21	309.16
DPB74514	26/09/89	7.03	223.74	288.15	25.05	99.07	70.00	124.85	102.42	57.87	26.14	23.37	345.52
DPB74515	26/09/89	7.02	223.88	288.22	24.88	97.70	74.98	125.49	109.62	67.64	27.99	22.95	361.39
DPC74515	26/09/89	7.03	224.15	288.22	25.07	98.55	76.50	124.74	111.89	70.49	28.98	23.00	367.45
DPC74515	26/09/89	7.03	224.15	288.15	25.17	98.21	76.23	125.61	112.08	70.03	28.90	23.11	371.49
DPC74515	26/09/89	7.03	224.44	288.32	25.29	99.47	78.50	128.08	116.20	74.01	30.38	23.65	403.71
DPB77300	26/09/89	7.02	256.82	258.26	25.78	164.00	0.00	55.66	55.60	55.60	55.52	55.31	258.37
DPB77301	26/09/89	7.03	255.65	263.32	25.73	165.09	5.04	56.41	55.94	55.91	55.80	55.47	259.52
DPB77302	26/09/89	7.03	255.11	268.84	25.77	164.27	10.10	56.52	55.98	55.75	55.57	55.18	260.10
DPB77303	26/09/89	7.03	255.31	274.77	25.68	164.03	15.04	56.98	56.29	55.94	55.62	55.08	259.81
DPB77304	26/09/89	7.03	255.59	280.48	25.75	164.03	20.10	57.62	56.75	56.33	55.83	55.28	261.83
DPB77305	26/09/89	7.03	255.31	286.05	25.71	163.09	25.02	57.73	56.91	56.29	55.78	55.02	262.12
DPB77306	26/09/89	7.03	255.18	288.01	25.70	161.53	30.12	77.99	56.37	55.83	55.10	54.22	280.30
DPB77307	26/09/89	7.03	255.18	288.01	25.71	160.44	34.92	110.37	61.45	55.41	54.61	53.73	316.66
DPB77308	26/09/89	7.03	255.11	288.01	25.73	162.16	40.06	137.55	81.95	56.25	55.67	54.61	366.87
DPB77309	26/09/89	7.03	255.18	288.08	25.64	162.03	45.00	163.98	106.62	58.87	56.06	55.10	421.99
DPB77310	26/09/89	7.03	255.45	288.08	25.63	161.90	50.04	187.01	128.82	67.14	55.78	54.97	474.79
DPB77311	26/09/89	7.02	255.52	288.01	25.66	162.85	55.02	206.63	148.40	79.72	56.19	55.41	527.89
DPB77312	26/09/89	7.03	255.52	288.08	25.69	161.19	60.04	219.56	165.79	94.38	56.14	54.61	571.46
DPB77313	26/09/89	7.03	255.65	288.15	25.68	160.77	65.08	230.70	182.84	108.93	57.72	54.48	615.90
DPB77314	26/09/89	7.03	255.59	288.22	25.71	160.81	70.22	238.84	198.96	123.66	60.71	54.30	657.74
DPB77315	26/09/89	7.03	255.59	288.42	25.77	162.04	75.04	245.65	212.69	136.74	65.28	54.74	696.70
DPB77316	26/09/89	7.03	255.65	288.49	25.81	161.62	80.10	248.88	224.39	149.71	71.33	54.71	730.46
DPB77317	26/09/89	7.03	255.65	288.56	25.76	161.60	85.08	249.69	232.16	159.90	78.48	54.63	755.57
DPB77318	26/09/89	7.03	255.65	288.56	25.77	162.06	89.96	252.23	239.28	168.10	86.50	55.47	782.98
DPB77319	26/09/89	7.03	255.65	288.62	25.78	162.56	95.10	253.55	241.43	173.45	95.33	56.27	801.74
DPC77319	26/09/89	7.03	255.65	288.62	25.75	164.22	96.15	256.27	243.78	175.26	97.30	57.10	811.26
DPP77320	26/09/89	7.03	255.72	288.62	25.77	164.20	96.93	256.09	243.90	175.80	98.86	57.05	812.70

DPP77321	26/09/89	7.03	256.07	288.76	25.75	164.10	97.60	253.90	243.78	176.53	100.47	57.36	812.99
DPP77322	26/09/89	7.03	256.07	288.69	25.78	164.21	98.34	251.94	244.01	177.14	101.62	57.39	813.57
DPP77323	26/09/89	7.03	256.00	288.62	25.83	164.18	99.02	249.74	243.97	177.95	103.17	57.70	814.43
DPP77324	26/09/89	7.02	255.93	288.69	25.82	164.74	99.65	247.67	243.59	178.72	104.45	58.01	813.57
DPP77325	26/09/89	7.03	255.93	288.62	25.75	163.60	100.37	243.86	242.40	178.30	105.59	57.93	810.10
DPP77326	26/09/89	7.02	256.14	288.62	25.70	164.11	100.90	243.11	242.36	178.99	106.99	58.19	810.97
DPP77327	26/09/89	7.02	256.07	288.62	25.73	164.20	101.50	241.84	242.51	179.53	108.24	58.43	812.41
DPP77328	26/09/89	7.03	256.00	288.76	25.79	164.68	102.13	241.61	241.59	179.49	109.25	58.51	812.13
DPP77329	26/09/89	7.03	256.14	288.76	25.78	165.16	102.87	240.22	241.09	180.07	110.50	58.71	812.41
DPP77330	26/09/89	7.03	256.14	288.76	25.80	165.17	103.50	239.82	240.47	179.64	111.72	59.10	811.84
DPP77331	26/09/89	7.03	256.14	288.76	25.80	165.80	104.20	238.26	239.66	180.26	113.22	59.34	812.41
DPP77332	26/09/89	7.02	256.14	288.90	25.86	164.69	104.86	233.82	237.20	179.76	114.50	59.02	806.35
DPP77333	26/09/89	7.03	256.14	288.83	25.75	164.84	105.53	232.55	236.78	179.84	115.64	59.10	805.49
DPP77334	26/09/89	7.03	256.14	288.83	25.75	166.02	106.19	231.56	237.24	180.57	116.73	59.83	807.22
DPP77335	26/09/89	7.03	256.14	288.83	25.69	166.02	106.88	230.93	236.24	180.45	118.11	60.01	807.51
DPP77336	26/09/89	7.03	256.07	288.76	25.71	166.60	107.40	228.39	234.32	180.37	119.28	60.40	804.04
DPP77337	26/09/89	7.03	256.14	288.76	25.72	166.60	108.01	223.02	232.05	180.64	121.09	60.76	798.85
DPP77338	26/09/89	7.02	256.14	288.56	25.73	166.47	108.69	222.04	221.62	180.45	122.73	60.27	788.17
DPP77339	26/09/89	7.03	256.14	288.76	25.68	166.97	109.39	223.60	214.92	180.80	124.37	61.18	787.31
DPP77340	26/09/89	7.03	256.14	288.83	25.77	166.55	110.02	223.54	205.11	180.10	125.56	61.08	776.63
DPP77341	26/09/89	7.03	256.14	288.76	25.79	166.70	110.33	224.47	202.31	180.18	126.55	61.34	776.34
DPB74300	27/09/89	7.04	254.15	255.18	22.88	105.17	0.00	26.74	24.89	26.55	26.33	26.20	129.09
DPB74301	27/09/89	7.05	254.30	265.94	22.84	95.65	4.99	23.31	21.22	23.11	22.77	22.65	110.82
DPB74302	27/09/89	7.04	254.63	275.18	22.93	99.88	9.96	25.18	23.20	24.93	24.53	24.35	120.44
DPB74302	27/09/89	7.05	254.70	275.25	22.85	100.11	9.96	25.13	23.20	24.93	24.56	24.30	119.86
DPB74303	27/09/89	7.05	255.11	284.69	22.75	100.12	15.02	25.36	23.20	24.89	24.48	24.20	119.86
DPB74304	27/09/89	7.05	255.11	288.15	22.85	100.14	20.06	37.82	23.47	25.20	24.69	24.33	134.00
DPB74305	27/09/89	7.04	255.38	288.08	22.83	100.29	24.64	56.06	35.21	25.36	24.87	24.43	164.30
DPB74306	27/09/89	7.05	255.59	288.15	22.79	101.54	30.02	74.82	51.60	30.59	25.21	24.85	205.56
DPB74306	27/09/89	7.05	255.65	288.15	22.81	99.81	30.22	73.66	51.33	30.82	24.53	24.20	202.39
DPB74307	27/09/89	7.04	255.59	288.15	22.94	100.53	35.10	88.09	65.60	41.02	25.13	24.64	242.50
DPB74308	27/09/89	7.04	255.52	288.15	22.99	99.76	40.08	97.04	78.45	51.14	26.90	24.27	275.97
DPB74308	27/09/89	7.04	255.45	288.08	23.07	99.71	40.16	97.04	78.38	51.10	26.92	24.22	275.97
DPB74309	27/09/89	7.05	255.52	288.42	23.15	100.45	44.96	104.71	89.49	61.14	30.77	24.48	308.87
DPB74310	27/09/89	7.05	255.65	288.35	23.26	101.13	50.16	112.27	99.54	71.95	36.82	24.66	343.21
DPB74311	27/09/89	7.05	255.65	288.49	23.26	100.75	54.71	116.89	106.31	80.45	42.43	24.90	369.76
DPB74312	27/09/89	7.05	255.65	288.49	23.30	99.98	60.00	119.26	112.81	89.38	48.92	25.26	394.28
DPC74312	27/09/89	7.05	255.59	288.56	23.33	99.49	63.56	117.76	116.66	94.53	53.13	25.75	406.11
DPC74313	27/09/89	7.04	255.65	288.42	23.30	100.45	64.63	119.43	118.97	97.19	54.89	26.30	415.35
DPP74313	27/09/89	7.06	255.65	288.56	23.28	100.49	65.24	119.20	119.62	97.61	55.41	26.30	416.79
DPP74314	27/09/89	7.05	255.86	288.49	23.31	100.16	66.00	119.37	120.12	98.81	56.45	26.43	419.97
DPP74315	27/09/89	7.04	255.93	288.49	23.32	101.30	66.52	120.87	121.97	100.31	57.57	26.92	426.32
DPP74316	27/09/89	7.04	255.79	288.56	23.44	100.80	67.32	120.06	121.93	100.77	58.19	26.82	426.32
DPP74317	27/09/89	7.05	256.07	288.56	23.38	100.34	67.95	119.03	122.24	101.46	59.05	27.08	427.18
DPP74318	27/09/89	7.04	255.86	288.49	23.26	99.47	68.50	117.12	122.24	102.04	59.83	27.13	426.60
DPP74319	27/09/89	7.04	255.86	288.42	23.21	101.95	68.48	123.12	124.55	103.31	59.96	27.65	436.41
DPP74320	27/09/89	7.04	256.00	288.49	23.13	99.48	67.62	118.74	121.55	100.88	59.13	26.79	425.74
DPP74320	27/09/89	7.04	256.14	288.56	23.11	102.52	68.48	125.66	125.62	104.15	60.61	27.78	442.47
DPP74321	27/09/89	7.04	256.07	288.49	23.08	99.86	69.18	118.51	122.51	102.51	60.76	26.98	429.78
DPP74322	27/09/89	7.05	256.14	288.56	23.05	101.05	69.73	120.30	124.39	104.00	61.49	27.44	436.99
DPP74323	27/09/89	7.05	256.00	288.49	23.14	101.36	70.41	118.91	125.16	104.89	62.22	27.73	437.57
DPP74324	27/09/89	7.05	256.00	288.62	23.05	101.07	71.11	115.33	125.47	105.92	63.28	27.99	436.99
DPP74325	27/09/89	7.05	256.14	288.69	23.21	101.04	71.78	114.00	125.82	106.35	64.09	28.20	437.57
DPP74326	27/09/89	7.05	256.07	288.56	23.14	100.98	72.44	112.91	126.35	106.89	64.76	28.22	438.15
DPP74327	27/09/89	7.04	255.93	288.56	23.16	101.12	73.07	115.68	127.24	107.16	65.49	28.38	441.90
DPP74328	27/09/89	7.05	256.00	288.56	23.14	99.85	73.69	112.45	125.93	107.00	66.17	28.46	438.72
DPP74329	27/09/89	7.05	256.14	288.56	23.16	100.09	74.36	111.70	126.28	107.69	66.95	28.72	439.88
DPP74330	27/09/89	7.04	256.14	288.56	23.16	101.18	74.92	112.85	127.66	108.85	67.78	29.00	444.78
DPP74331	27/09/89	7.05	256.06	288.56	23.27	101.27	75.61	111.98	128.68	109.51	68.62	29.35	447.14

DPP74331	27/09/89	7.04	256.07	288.56	23.26	99.51	75.59	109.96	127.12	108.43	68.48	29.39	441.32
DPP74332	27/09/89	7.04	256.14	288.56	23.22	101.17	76.33	112.91	129.55	110.31	69.59	29.65	450.27
DPP74333	27/09/89	7.05	255.79	288.56	23.21	100.58	76.91	111.12	128.28	110.16	69.85	29.70	448.53
DPP74334	27/09/89	7.04	255.79	288.56	23.24	100.80	77.66	104.77	122.85	109.93	69.28	31.50	436.42
DPP74335	27/09/89	7.05	256.07	288.69	23.25	101.16	78.14	106.27	122.51	110.70	70.19	32.01	436.70
DPP74336	27/09/89	7.04	256.00	288.56	23.30	102.01	78.83	106.79	123.51	112.50	72.16	33.42	445.94
DPP74337	27/09/89	7.05	256.07	288.56	23.30	100.93	79.35	106.10	114.31	111.47	71.23	30.98	446.80
DPP74338	27/09/89	7.04	256.00	288.56	23.38	100.75	80.06	110.02	115.81	112.16	71.15	31.05	441.90
DPB76300	27/09/89	7.05	258.05	259.15	24.09	133.14	0.00	38.92	39.02	38.75	38.66	38.45	189.98
DPB76301	27/09/89	7.05	257.91	266.66	24.09	133.24	5.02	39.32	39.40	38.90	38.74	38.53	191.71
DPB76302	27/09/89	7.05	257.98	273.82	24.08	134.43	10.10	40.31	40.21	39.79	39.44	39.05	194.89
DPB76303	27/09/89	7.05	257.98	280.75	24.18	134.72	15.02	40.82	40.63	40.13	39.65	39.26	196.62
DPB76304	27/09/89	7.05	257.98	287.07	24.14	137.19	19.90	42.56	42.48	41.79	41.31	40.77	205.27
DPB76305	27/09/89	7.04	258.05	288.08	24.21	133.66	25.14	66.10	40.98	40.44	39.75	39.13	222.88
DPB76306	27/09/89	7.04	257.91	288.15	24.22	136.71	30.04	90.63	55.94	42.09	41.55	40.79	267.60
DPB76307	27/09/89	7.05	257.85	288.15	24.21	134.26	35.27	112.39	78.72	43.71	40.07	39.36	310.60
DPB76308	27/09/89	7.05	257.91	288.28	24.13	136.21	39.98	132.30	96.42	52.87	41.21	40.77	359.66
DPB76309	27/09/89	7.05	257.71	288.22	24.15	133.78	44.88	144.71	112.20	65.37	40.25	39.36	397.46
DPB76309	27/09/89	7.04	257.98	288.15	24.29	133.35	44.96	144.71	112.58	65.95	40.04	39.10	397.75
DPB76309	27/09/89	7.05	257.85	288.28	24.25	132.93	50.29	155.90	129.66	79.45	41.99	38.90	440.74
DPB76310	27/09/89	7.05	257.57	288.42	24.21	132.29	50.31	156.54	129.74	79.41	42.09	38.97	441.61
DPB76311	27/09/89	7.03	258.05	288.15	24.37	133.92	54.94	166.52	144.75	91.92	45.96	39.42	482.87
DPB76312	27/09/89	7.05	258.05	288.56	24.27	135.10	60.04	175.70	158.06	104.58	51.52	39.81	523.56
DPB76313	27/09/89	7.05	257.91	288.49	24.41	135.19	65.04	181.99	168.72	116.31	58.38	39.96	559.34
DPB76314	27/09/89	7.05	258.05	288.56	24.45	134.82	70.08	183.89	175.80	126.20	65.88	39.99	585.03
DPB76314	27/09/89	7.05	258.05	288.56	24.37	134.62	70.04	183.55	175.76	126.12	66.01	39.96	584.74
DPB76315	27/09/89	7.05	258.05	288.56	24.41	134.63	75.04	185.34	182.45	135.36	73.88	40.45	610.42
DPC76315	27/09/89	7.05	258.05	288.56	24.43	135.64	79.73	185.74	187.68	142.09	81.13	41.52	631.48
DPP76314	27/09/89	7.04	258.12	288.56	24.58	136.38	78.52	190.13	189.45	142.09	79.80	41.81	636.68
DPP76315	27/09/89	7.05	258.53	288.56	25.03	136.03	79.24	189.44	189.41	142.36	80.63	41.93	637.26
DPP76316	27/09/89	7.04	258.46	288.56	25.07	135.76	79.82	188.91	189.88	143.55	82.03	42.17	639.28
DPP76317	27/09/89	7.04	258.33	288.56	25.20	135.83	80.43	187.65	189.69	144.05	82.76	42.01	638.99
DPP76318	27/09/89	7.04	258.46	288.62	25.38	135.33	81.21	187.65	189.95	144.21	83.75	42.04	640.43
DPP76319	27/09/89	7.05	258.39	288.62	25.48	135.33	81.74	186.61	189.91	143.90	84.47	42.14	639.85
DPP76320	27/09/89	7.04	258.46	288.62	25.59	136.51	82.32	190.88	193.11	146.67	85.85	42.77	652.55
DPP76321	27/09/89	7.04	258.39	288.69	25.75	136.80	83.22	189.61	193.88	147.21	86.89	43.03	653.70
DPP76322	27/09/89	7.04	258.46	288.56	25.92	136.41	83.67	189.15	193.92	148.09	88.14	43.26	655.72
DPP76323	27/09/89	7.06	258.53	288.69	26.12	136.91	84.34	187.88	194.46	147.90	88.63	43.47	655.15
DPP76324	27/09/89	7.05	258.46	288.56	26.25	135.46	85.02	178.99	192.22	147.90	90.03	42.97	646.20
DPP76325	27/09/89	7.05	258.46	288.62	26.42	135.49	85.80	177.14	192.22	148.40	90.99	43.16	644.47
DPP76326	27/09/89	7.05	258.53	288.56	26.55	135.48	86.41	175.99	192.69	149.09	92.14	43.41	646.78
DPP76327	27/09/89	7.04	258.46	288.56	26.75	135.50	87.17	175.47	193.30	150.13	93.51	43.57	649.09
DPP76328	27/09/89	7.04	258.53	288.56	27.07	135.74	87.75	174.60	193.15	150.63	94.45	43.62	649.95
DPP76329	27/09/89	7.03	258.53	288.56	27.27	135.70	88.32	173.16	193.15	151.44	95.67	43.96	650.24
DPP76330	27/09/89	7.05	258.53	288.69	27.35	135.61	89.10	172.41	192.80	151.98	96.53	44.09	650.82
DPP76331	27/09/89	7.05	258.53	288.76	27.38	136.73	89.75	174.37	194.99	153.29	97.43	44.53	657.17
DPP76332	27/09/89	7.04	258.60	288.76	27.44	136.53	90.47	172.81	194.07	153.90	98.86	44.77	657.74
DPP76333	27/09/89	7.06	258.53	288.90	27.62	135.47	91.09	166.98	189.76	152.56	99.23	44.14	645.33
DPP76334	27/09/89	7.06	258.53	288.83	27.64	135.44	91.74	167.16	189.88	153.25	100.11	44.53	647.93
DPP76335	27/09/89	7.04	258.53	288.62	27.82	135.03	92.40	166.75	189.61	154.02	101.36	44.66	649.38
DPP76336	27/09/89	7.05	258.53	288.76	27.93	134.96	92.97	165.60	187.99	154.10	102.06	44.82	648.22
DPP76337	27/09/89	7.04	258.53	288.76	27.97	134.45	93.59	165.43	187.07	154.63	103.12	44.95	648.51
DPP76338	27/09/89	7.05	258.53	288.90	27.98	135.12	94.34	164.73	185.99	154.71	104.01	45.10	647.93
DPP76339	27/09/89	7.05	258.53	288.83	27.98	134.86	94.92	163.87	184.88	155.21	105.17	45.49	648.22
DPP76340	27/09/89	7.04	258.60	288.69	28.05	134.29	95.53	164.79	183.26	155.75	106.29	45.60	649.09
DPP76341	27/09/89	7.05	258.67	288.96	28.14	134.76	96.25	166.41	179.41	155.48	107.07	45.86	647.64
DPP76342	27/09/89	7.04	258.53	288.76	28.14	134.40	96.91	168.02	176.56	155.94	108.21	46.07	648.51
DPP76343	27/09/89	7.06	258.60	288.76	28.15	135.19	97.52	169.64	174.22	155.98	109.17	46.27	649.66
DPP76344	27/09/89	7.05	258.74	289.03	28.19	135.64	98.20	171.20	175.87	156.33	110.37	46.77	651.40

DPP76345	27/09/89	7.04	258.87	288.69	28.22	135.86	98.85	172.76	174.02	156.64	111.51	47.05	653.13
DPB74100	27/09/89	7.04	281.30	282.18	29.85	102.24	0.00	17.74	17.97	17.93	17.60	17.50	85.23
DPB74101	27/09/89	7.04	281.03	288.01	29.84	99.28	4.86	29.97	25.63	22.93	22.43	22.25	118.99
DPB74102	27/09/89	7.05	282.18	288.22	29.99	100.55	10.21	53.06	47.10	37.98	28.79	24.95	187.38
DPB74103	27/09/89	7.05	283.13	288.22	30.04	100.70	15.04	65.58	61.72	48.67	37.99	25.86	235.57
DPB74104	27/09/89	7.05	280.96	288.06	30.18	99.00	19.94	80.13	75.03	58.18	43.03	28.07	279.44
DPB74105	27/09/89	7.04	283.74	288.15	30.32	99.36	25.02	89.42	85.99	71.68	53.96	34.25	330.22
DPB74106	27/09/89	7.05	284.22	288.15	30.50	97.98	30.04	95.30	91.96	79.68	60.74	38.74	361.68
DPB74107	27/09/89	7.04	285.03	288.28	30.48	102.46	35.00	104.60	100.65	89.42	69.70	44.25	403.81
DPB74108	27/09/89	7.05	284.76	288.28	30.57	101.23	40.04	107.19	103.69	93.19	74.16	46.27	419.68
DPB74109	27/09/89	7.05	285.10	288.35	30.64	100.32	45.10	109.39	109.23	97.96	79.93	49.70	441.61
DPB74109	27/09/89	7.04	285.10	288.35	30.66	101.22	45.12	107.94	107.96	97.15	79.02	49.15	437.28
DPC74110	27/09/89	7.04	285.10	288.42	30.66	99.89	50.25	106.39	111.12	100.31	83.38	51.83	449.11
DPP74108	27/09/89	7.04	285.03	288.42	30.69	99.82	49.02	108.75	111.00	99.58	82.84	51.60	449.40
DPP74109	27/09/89	7.05	282.38	288.18	30.64	96.92	49.77	120.79	120.95	106.89	84.66	49.90	479.93
DPP74110	27/09/89	7.05	285.10	288.35	30.71	102.52	50.37	118.45	118.24	105.04	87.62	54.53	480.57
DPP74111	27/09/89	7.04	283.06	288.22	30.68	102.03	51.62	121.22	121.20	106.73	87.05	52.04	484.32
DPP74112	27/09/89	7.06	281.91	288.49	30.81	102.34	53.01	122.55	122.78	107.93	86.63	50.30	486.63
DPP74113	27/09/89	7.04	282.86	288.42	30.76	102.22	54.24	121.57	123.35	109.23	89.41	53.05	492.97
DPP74114	27/09/89	7.04	283.00	288.35	30.76	100.13	55.14	118.51	121.55	108.23	89.44	53.26	488.07
DPP74115	27/09/89	7.05	282.93	288.49	30.81	100.80	55.90	118.74	121.97	108.77	89.82	53.39	490.09
DPP74116	27/09/89	7.04	282.86	288.35	30.96	100.49	56.52	119.26	122.39	109.35	90.53	53.78	492.40
DPP74117	27/09/89	7.04	282.72	288.49	30.83	100.56	57.13	119.66	123.47	110.50	91.33	54.12	496.44
DPP74118	27/09/89	7.04	282.72	288.35	30.90	100.36	58.03	119.37	123.51	111.00	92.29	54.69	498.75
DPP74119	27/09/89	7.05	283.27	288.56	30.91	100.67	59.04	118.[illegible]	123.47	111.58	93.38	55.78	500.48
DPP74120	27/09/89	7.05	282.52	288.49	30.84	100.43	59.88	117.93	124.05	112.31	93.46	55.31	501.05
DPP74121	27/09/89	7.05	283.00	288.56	30.85	100.70	61.06	113.31	124.55	113.89	95.75	57.31	503.36
DPP74122	27/09/89	7.04	282.86	288.49	30.73	101.66	62.15	113.72	126.28	115.66	97.43	57.91	509.13
DPP74123	27/09/89	7.05	283.06	288.56	30.80	102.33	63.03	111.81	125.70	116.39	98.45	58.95	510.00
DPP74124	27/09/89	7.04	282.93	288.56	30.68	101.69	64.08	109.45	124.74	116.97	98.97	59.21	507.69
DPP74125	27/09/89	7.05	282.72	288.56	30.66	101.51	65.02	108.64	124.55	117.78	99.75	59.46	509.42
DPP74126	27/09/89	7.04	282.79	288.49	30.59	101.83	66.17	108.23	124.70	119.01	101.07	60.35	512.31
DPP74127	27/09/89	7.04	283.06	288.56	30.62	102.10	66.93	107.31	123.85	120.01	102.50	61.67	514.62
DPP74128	27/09/89	7.05	282.66	288.49	30.72	102.11	68.07	107.25	121.81	120.62	102.58	61.62	512.88
DPP74129	27/09/89	7.05	282.66	288.49	30.88	101.72	68.97	109.39	118.35	121.01	103.25	62.43	513.75
DPP74130	27/09/89	7.05	282.79	288.56	30.96	101.84	70.00	110.66	115.97	121.35	103.67	62.79	514.33
DPP74131	27/09/89	7.04	282.79	288.56	30.97	102.12	70.96	112.79	114.47	122.16	104.81	63.91	518.08
DPP74132	27/09/89	7.05	282.86	288.56	30.76	102.34	72.01	114.06	111.89	122.35	104.45	64.35	516.92
DPP74133	27/09/89	7.05	282.18	288.56	30.69	101.60	72.99	115.91	111.89	122.89	104.37	64.06	518.65
DPP74134	27/09/89	7.04	283.00	288.56	30.47	100.94	73.97	117.87	108.89	122.28	104.47	65.54	519.23
DPP74135	27/09/89	7.05	282.72	288.56	30.50	101.51	75.10	120.58	110.04	123.51	105.12	65.93	525.00
DPP74136	27/09/89	7.04	282.79	288.56	30.44	102.18	76.00	123.07	109.43	123.78	105.80	66.89	529.33
DPP74137	27/09/89	7.04	282.66	288.35	30.43	101.49	77.05	124.91	108.58	122.97	105.90	67.18	529.91
DPP74138	27/09/89	7.04	282.38	288.49	30.50	100.96	77.72	126.36	107.73	122.55	105.90	67.23	530.78
DPP74139	27/09/89	7.05	282.79	288.56	30.43	100.94	78.83	128.95	107.58	121.85	106.42	67.96	534.24
DPP74140	27/09/89	7.04	282.72	288.49	30.36	100.96	80.08	131.84	107.69	121.51	107.61	68.74	538.28
DPP74140	27/09/89	7.04	282.79	288.42	30.37	100.64	79.16	130.28	108.50	122.55	107.36	68.63	537.70
DPB77500	28/09/89	7.04	223.39	224.36	29.99	160.23	0.00	51.50	48.06	51.37	51.52	51.47	261.55
DPB77501	28/09/89	7.04	223.88	232.09	29.93	160.93	5.08	52.08	48.67	51.87	51.96	51.86	264.14
DPB77502	28/09/89	7.04	223.88	238.56	29.85	161.12	10.19	52.02	48.33	51.48	51.49	51.23	263.57
DPB77503	28/09/89	7.04	223.88	244.82	29.99	160.41	14.98	52.60	48.79	51.79	51.70	51.44	264.14
DPB77504	28/09/89	7.03	224.08	250.79	30.28	160.41	19.77	53.12	49.29	52.21	52.12	51.80	265.87
DPB77505	28/09/89	7.04	224.22	257.57	30.73	160.41	25.16	53.58	49.67	52.44	52.22	51.83	267.60
DPB77506	28/09/89	7.04	224.29	263.59	30.72	160.64	30.06	54.04	49.98	52.71	52.35	51.88	268.18
DPB77507	28/09/89	7.04	224.22	269.12	30.80	162.33	34.98	55.37	51.21	53.71	53.28	52.69	273.95
DPB77500	28/09/89	7.03	224.22	225.32	30.78	159.50	0.00	50.92	51.67	50.87	51.03	51.00	258.95
DPB77501	28/09/89	7.04	224.01	232.02	30.71	162.48	5.00	53.35	53.94	52.98	53.00	52.89	269.05
DPB77502	28/09/89	7.04	224.22	238.84	30.73	162.38	10.35	53.58	54.06	52.94	52.95	52.82	268.76
DPB77503	28/09/89	7.04	224.15	244.68	30.83	162.00	15.16	53.98	54.60	53.33	53.31	53.05	270.20

DPB77503	28/09/89	7.05	224.29	251.27	30.78	162.29	20.20	54.44	54.67	53.44	53.28	53.00	271.36
DPB77505	28/09/89	7.04	224.29	257.09	30.66	162.58	25.04	54.67	54.94	53.48	53.23	52.79	271.36
DPB77506	28/09/89	7.05	224.22	263.25	30.73	161.79	29.94	54.96	55.33	53.48	53.23	52.69	272.51
DPB77507	28/09/89	7.04	224.29	269.25	30.74	161.94	35.25	55.60	55.83	53.75	53.36	52.77	273.66
DPB77508	28/09/89	7.03	224.29	275.11	30.79	161.22	40.16	55.77	55.91	53.79	53.23	52.58	273.66
DPB77509	28/09/89	7.04	224.29	280.62	30.83	161.53	45.00	55.77	56.25	53.91	53.31	52.53	274.24
DPB77510	28/09/89	7.06	224.29	286.66	30.86	160.02	50.02	58.14	55.87	53.41	52.61	51.80	274.53
DPB77510	28/09/89	7.03	224.36	286.66	30.89	159.28	50.02	58.89	56.06	53.44	52.58	51.78	275.11
DPB77511	28/09/89	7.03	224.29	288.01	30.93	159.54	55.08	78.97	56.44	53.91	53.00	52.01	297.04
DPB77512	28/09/89	7.03	224.22	287.95	30.90	160.69	60.04	107.25	58.18	54.29	53.44	52.35	328.20
DPB77512	28/09/89	7.05	224.29	288.08	30.93	160.24	60.10	106.39	58.37	54.21	53.44	52.38	327.63
DPB77513	28/09/89	7.03	224.01	288.01	30.85	161.36	64.94	134.15	65.10	54.60	54.09	52.84	363.41
DPB77514	28/09/89	7.04	224.29	288.08	31.00	163.63	70.00	160.23	78.84	56.10	55.62	54.30	408.14
DPB77515	28/09/89	7.03	224.84	288.08	31.00	160.90	75.04	185.97	103.54	55.56	53.70	52.63	452.86
DPB77517	28/09/89	7.03	224.15	288.08	31.08	163.00	84.98	221.41	139.74	61.33	54.97	53.88	531.64
DPB77518	28/09/89	7.04	224.15	288.08	31.22	159.52	90.10	230.06	157.90	67.99	53.44	52.35	560.79
DPB77519	28/09/89	7.03	224.01	288.08	31.09	163.48	94.88	241.90	171.18	75.57	55.67	54.45	597.72
DPB77520	28/09/89	7.04	224.29	288.42	31.03	162.13	100.14	242.41	182.99	88.42	55.62	54.01	621.96
DPB77521	28/09/89	7.03	224.29	288.35	30.47	164.06	104.94	243.80	191.22	100.27	57.15	54.89	645.91
DPC77521	28/09/89	7.04	224.36	288.56	30.52	162.70	108.55	235.95	192.30	111.08	57.54	54.17	649.66
DPP77520	28/09/89	7.03	224.36	288.56	30.66	162.86	107.15	239.01	192.22	107.27	57.28	54.06	647.93
DPP77521	28/09/89	7.03	224.36	288.56	30.73	163.08	108.53	236.12	192.22	111.31	57.67	54.12	648.80
DPP77522	28/09/89	7.03	224.36	288.56	30.53	162.63	108.97	236.82	193.15	112.58	57.65	54.12	652.26
DPP77523	28/09/89	7.04	224.36	288.56	30.55	162.45	109.51	236.93	193.69	113.74	57.65	54.01	653.70
DPP77524	28/09/89	7.03	224.36	288.56	30.75	162.48	110.08	236.88	194.53	115.66	57.72	53.73	656.01
DPP77525	28/09/89	7.03	224.36	288.56	30.71	162.96	110.61	235.20	195.03	116.81	57.91	53.80	656.88
DPP77526	28/09/89	7.03	224.43	288.56	30.77	163.47	111.27	228.33	196.23	118.58	58.40	54.32	653.70
DPB77100	29/09/89	7.03	261.81	262.84	32.38	162.52	0.00	54.85	54.17	54.48	54.69	54.69	279.44
DPB77101	29/09/89	7.04	261.40	269.05	32.38	162.28	5.02	55.48	54.75	54.94	55.08	54.92	280.30
DPB77100	29/09/89	7.04	283.81	285.50	31.92	163.77	0.00	57.73	56.91	57.37	57.54	57.60	292.71
DPB77101	29/09/89	7.04	283.74	288.01	31.97	161.72	5.02	78.34	59.45	56.75	56.84	56.69	314.06
DPB77102	29/09/89	7.04	283.94	287.88	31.85	160.92	10.08	103.85	88.80	70.41	56.61	56.32	382.17
DPB77103	29/09/89	7.04	282.45	288.01	31.69	162.07	14.88	125.43	103.73	81.80	58.40	57.28	433.24
DPB77104	29/09/89	7.04	282.86	288.01	31.69	160.57	20.10	150.65	123.74	98.46	66.71	56.22	503.07
DPB77105	29/09/89	7.03	283.20	287.95	31.65	163.46	25.00	177.89	146.21	115.16	79.23	58.35	583.87
DPB77106	29/09/89	7.03	283.27	288.01	31.71	160.51	30.08	191.63	160.44	126.16	89.23	56.89	632.06
DPB77107	29/09/89	7.04	282.93	288.08	31.67	162.14	35.18	209.69	178.14	140.51	99.28	59.15	694.68
DPB77108	29/09/89	7.03	283.27	288.08	31.72	161.48	39.90	220.08	191.22	152.86	108.89	61.57	743.45
DPB77110	29/09/89	7.03	283.27	288.28	31.47	159.95	50.25	234.45	213.58	176.41	126.39	68.50	828.00
DPB77111	29/09/89	7.04	283.27	288.35	31.24	160.28	55.00	238.38	222.54	186.91	134.49	72.40	863.78
DPB77112	29/09/89	7.04	283.27	288.42	31.45	161.39	60.04	242.01	231.08	197.92	143.51	76.79	900.43
DPB77113	29/09/89	7.04	283.27	288.56	31.22	160.92	65.20	243.22	235.24	206.23	151.14	80.89	925.53
DPB77114	29/09/89	7.05	283.33	288.56	31.24	160.53	70.10	244.61	236.82	212.46	157.92	85.02	946.60
DPB77115	29/09/89	7.03	283.67	288.56	31.28	160.11	75.06	246.28	236.05	217.12	164.78	90.45	964.49
DPC77115	29/09/89	7.04	283.33	288.56	31.14	159.15	78.50	246.98	236.01	219.35	167.61	92.47	972.57
DPP77114	29/09/89	7.03	283.33	288.56	31.19	159.53	77.11	247.26	236.32	218.66	166.34	91.54	969.39
DPP77115	29/09/89	7.04	283.54	288.56	31.08	159.16	78.46	247.09	235.74	219.43	167.97	93.10	972.57
DPP77116	29/09/89	7.03	283.33	288.56	31.10	158.95	79.34	247.26	236.09	219.97	168.83	93.62	975.45
DPP77117	29/09/89	7.03	283.33	288.62	31.30	159.05	80.39	246.51	236.05	220.47	169.32	94.14	976.03
DPP77118	29/09/89	7.04	283.27	288.62	31.28	159.30	81.48	244.78	236.66	221.50	170.26	94.86	976.90
DPP77119	29/09/89	7.04	283.33	288.69	31.16	159.12	82.60	242.65	237.28	222.43	171.94	96.55	980.65
DPP77120	29/09/89	7.03	283.20	288.62	31.11	159.59	83.53	240.57	238.39	223.66	172.44	96.78	981.51
DPP77121	29/09/89	7.04	283.33	288.76	31.05	160.08	84.49	236.59	238.63	224.62	173.87	98.32	981.80
DPP77122	29/09/89	7.03	283.33	288.56	31.03	159.62	85.59	233.82	239.20	225.51	175.35	99.95	983.53
DPP77123	29/09/89	7.04	283.27	288.76	30.66	159.59	86.50	232.55	239.86	226.20	175.35	100.01	983.82
DPP77124	29/09/89	7.04	283.74	288.90	30.55	160.12	87.38	229.89	239.63	226.77	176.85	102.08	984.97
DPP77125	29/09/89	7.04	283.27	288.96	30.57	160.44	88.59	229.60	240.59	227.58	176.57	102.03	985.84
DPP77126	29/09/89	7.04	283.60	288.76	30.55	159.89	89.45	229.03	239.16	227.85	177.50	104.21	987.86
DPP77127	29/09/89	7.03	283.27	288.69	30.55	160.46	90.53	229.31	240.13	228.66	177.06	104.24	988.15

DPP77128	29/09/89	7.03	283.54	288.83	30.53	160.73	91.60	228.91	238.89	228.24	177.84	106.21	990.17
DPP77129	29/09/89	7.04	283.33	288.83	30.46	160.90	92.54	228.85	238.55	229.05	177.53	106.55	990.46
DPP77130	29/09/89	7.03	283.60	288.83	30.39	160.80	93.53	228.22	237.32	229.12	178.02	108.26	990.75
DPP77131	29/09/89	7.04	283.33	288.96	30.37	161.23	94.47	229.49	236.74	229.05	177.14	107.88	990.17
DPP77132	29/09/89	7.04	283.33	288.90	30.46	160.90	95.47	232.49	232.78	228.39	177.42	109.67	990.17
DPP77133	29/09/89	7.03	283.40	288.76	30.48	161.59	96.50	235.72	229.24	228.47	177.81	111.36	992.19
DPP77134	29/09/89	7.03	283.40	288.83	30.52	161.51	97.48	238.61	226.35	227.54	177.01	112.13	990.46
DPP77135	29/09/89	7.04	283.33	288.96	30.54	162.23	98.46	241.55	224.97	226.66	176.54	112.63	992.77
DPP77136	29/09/89	7.04	283.33	288.96	30.64	162.39	99.59	245.59	221.93	225.51	176.28	114.08	993.63
DPP77137	29/09/89	7.04	283.27	289.03	30.73	163.08	100.49	248.19	220.58	224.04	175.71	114.32	993.92
DPP77138	29/09/89	7.04	283.54	288.96	30.80	162.39	101.45	251.76	217.16	222.04	175.76	116.13	993.06
DPP77139	29/09/89	7.03	283.33	288.96	30.83	162.77	102.54	256.15	215.93	220.89	175.43	117.15	994.79
DPP77140	29/09/89	7.03	283.33	288.90	30.94	163.50	103.42	259.33	213.39	218.58	174.59	118.06	994.50
DPP77141	29/09/89	7.04	283.33	289.03	30.95	163.02	104.47	262.79	212.19	216.69	173.69	118.55	994.21
DPP77142	29/09/89	7.03	283.33	288.90	31.05	163.31	105.55	267.58	210.42	213.85	172.57	120.05	994.50
DPP77143	29/09/89	7.04	283.33	289.03	31.01	164.28	106.50	272.02	208.54	211.96	171.61	121.35	996.52
DPP77144	29/09/89	7.04	283.33	289.03	31.01	164.65	107.46	276.24	204.57	210.54	170.49	122.26	995.65
DPP77145	29/09/89	7.04	283.13	289.03	31.51	165.58	107.99	279.64	202.50	209.65	170.26	122.76	995.65
DPP77136	29/09/89	7.04	283.33	288.96	31.98	161.61	98.97	242.18	225.47	226.20	175.50	112.16	992.19
DPB94300	11/10/89	9.56	283.74	284.76	29.63	101.94	0.00	25.41	29.63	26.09	26.17	26.22	135.15
DPC94311	11/10/89	9.56	283.47	309.42	29.57	100.87	55.08	78.51	89.15	69.72	48.95	27.88	354.75
DPC94311	11/10/89	9.56	283.81	309.42	29.60	100.06	56.04	75.80	88.49	70.18	50.12	27.99	374.37
DPP94312	11/10/89	9.56	283.81	309.49	29.52	99.48	57.05	71.64	87.30	69.60	50.48	27.83	484.32
DPP94313	11/10/89	9.55	283.25	309.43	29.61	101.16	58.90	73.87	90.66	71.94	52.71	28.89	578.77
DPP94314	11/10/89	9.56	283.88	309.56	29.71	102.99	60.16	74.12	92.11	73.45	54.82	29.81	383.61
DPP94315	11/10/89	9.56	283.54	309.42	29.70	101.36	61.39	70.55	89.84	72.22	55.34	29.60	374.66
DPP94316	11/10/89	9.55	283.47	309.49	29.78	101.40	62.89	70.08	89.07	72.14	56.43	29.96	372.93
DPP94317	11/10/89	9.56	283.67	309.49	29.93	102.57	64.28	70.60	89.15	73.11	58.12	30.74	376.68
DPP94318	11/10/89	9.56	283.67	309.49	29.83	101.78	65.64	70.08	86.22	73.57	59.02	31.03	366.29
DPP94319	11/10/89	9.55	283.54	309.42	29.91	101.35	67.74	71.53	75.91	73.45	60.24	31.39	354.46
DPP94320	11/10/89	9.56	283.33	309.62	29.88	99.53	69.41	72.51	69.76	72.18	60.61	31.42	345.52
DPP94321	11/10/89	9.55	283.47	309.49	29.91	103.01	71.07	76.20	71.53	74.03	63.62	32.95	354.46
DPP94317	11/10/89	9.56	283.33	309.49	30.13	99.95	57.95	73.66	88.76	70.18	51.47	28.33	334.84
DPP94316	11/10/89	9.56	283.67	309.49	30.06	101.61	55.23	79.78	89.19	69.53	49.13	27.91	336.86
DPP94315	11/10/89	9.55	283.54	309.35	30.11	101.28	52.77	81.80	88.92	68.26	47.00	27.68	332.24
DPB96300	11/10/89	9.55	281.64	309.49	29.90	133.28	0.00	39.84	44.17	40.32	40.61	40.61	216.82
DPC96315	11/10/89	9.55	281.91	309.49	30.09	135.05	73.59	130.28	139.51	108.66	73.02	43.41	508.56
DPP96316	11/10/89	9.56	281.70	309.56	30.06	134.65	75.92	123.35	138.59	109.50	76.24	43.86	505.96
DPP96317	11/10/89	9.55	282.32	309.56	30.09	133.84	77.75	116.49	135.40	109.31	79.75	44.27	499.03
DPP96318	11/10/89	9.56	282.38	309.62	30.15	134.61	79.28	113.14	132.47	108.89	81.83	44.61	495.86
DPP96319	11/10/89	9.56	282.38	309.69	30.22	135.61	81.05	111.64	130.93	110.20	84.55	45.73	497.88
DPP96320	11/10/89	9.56	282.38	309.76	30.11	136.51	82.81	110.14	115.12	108.43	86.99	46.22	484.03
DPP96321	11/10/89	9.55	282.38	309.69	30.20	136.24	83.87	111.12	105.08	106.39	88.45	46.53	477.39
DPB97300	12/10/89	9.56	283.00	284.69	30.75	163.97	0.00	56.69	61.52	56.91	57.39	57.26	291.56
DPB97300	12/10/89	9.57	282.86	290.11	30.75	163.99	5.04	57.33	61.95	57.21	57.54	57.23	294.15
DPB97300	12/10/89	9.56	276.54	278.10	30.90	164.51	0.00	56.75	63.37	56.75	57.28	57.02	291.27
DPB97300	12/10/89	9.57	282.52	284.22	30.86	163.32	0.00	56.75	63.33	56.71	57.23	57.05	291.84
DPB97305	12/10/89	9.57	282.86	289.98	30.87	163.73	5.06	57.27	63.79	56.98	57.41	57.10	292.71
DPB97302	12/10/89	9.57	282.93	295.59	31.03	162.80	9.96	57.91	64.10	57.21	57.41	57.08	293.86
DPB97303	12/10/89	9.57	282.93	298.03	30.96	162.54	12.03	58.08	64.41	57.44	57.60	57.10	295.31
DPC97317	12/10/89	9.57	283.20	309.89	30.94	161.27	87.52	182.97	197.57	149.48	98.42	59.00	683.14
DPP97318	12/10/89	9.57	283.00	309.83	30.92	162.10	89.41	177.55	197.99	151.17	101.41	59.60	683.43
DPP97319	12/10/89	9.58	282.86	309.83	30.98	163.03	91.09	173.56	197.49	151.86	103.72	60.19	681.98
DPP97320	12/10/89	9.57	282.93	309.83	30.97	163.33	92.72	169.29	194.73	151.86	106.66	60.79	679.67
DPP97321	12/10/89	9.58	282.86	309.83	30.97	164.03	94.36	164.10	190.95	150.86	109.25	61.26	672.17
DPP97322	12/10/89	9.57	283.00	309.83	31.01	164.56	95.96	157.58	184.22	150.52	112.47	62.06	663.51
DPP97323	12/10/89	9.57	283.20	309.83	31.03	165.46	97.62	157.98	164.41	150.82	115.90	63.05	650.82
DPP97324	12/10/89	9.57	283.20	309.89	31.11	166.01	99.55	161.16	142.05	148.09	119.54	64.11	636.68
DPB97100	12/10/89	9.56	305.11	306.66	30.80	164.67	0.00	62.23	69.26	61.98	62.79	62.56	318.97

DPB97101	12/10/89	9.57	305.85	309.08	30.78	163.51	5.06	78.51	79.91	61.37	60.89	60.43	340.32
DPB97102	12/10/89	9.57	304.30	309.42	30.84	161.77	9.96	90.75	89.19	67.18	59.31	58.76	364.85
DPC97115	12/10/89	9.57	305.31	309.83	31.19	160.76	77.03	190.42	197.38	178.10	148.86	99.10	810.68
DPP97116	12/10/89	9.57	305.38	309.83	31.29	162.42	77.93	190.76	197.92	179.22	150.39	100.58	817.32
DPP97117	12/10/89	9.57	305.25	309.83	31.19	164.74	79.67	196.59	201.38	183.61	153.95	101.90	837.81
DPP97117	12/10/89	9.58	305.45	309.83	31.27	164.31	79.69	198.09	202.11	184.53	154.93	102.78	841.56
DPP97118	12/10/89	9.57	305.31	309.83	31.21	164.40	81.35	191.45	201.27	184.65	155.71	104.01	836.36
DPP97119	12/10/89	9.57	305.58	309.83	31.20	164.41	82.99	185.68	199.77	184.84	157.30	106.32	833.77
DPP97120	12/10/89	9.57	305.38	309.89	31.22	164.73	84.53	181.99	198.19	185.07	158.18	107.20	831.75
DPP97121	12/10/89	9.56	305.52	309.83	31.30	164.97	86.41	180.66	195.88	184.76	159.56	109.46	830.88
DPP97121	12/10/89	9.58	305.25	309.83	31.23	163.69	86.39	177.60	192.69	182.68	157.45	107.74	819.05
DPP97122	12/10/89	9.57	305.25	309.83	31.31	163.49	87.99	177.37	186.72	181.80	158.41	109.74	815.01
DPP97123	12/10/89	9.58	305.31	309.96	31.20	163.99	89.84	181.24	178.84	180.22	158.26	110.97	811.26
DPP97124	12/10/89	9.56	305.52	309.83	31.21	163.83	91.37	186.09	174.02	179.18	158.96	113.38	813.28
DPP97125	12/10/89	9.57	305.11	309.89	31.31	164.46	92.89	188.86	170.06	176.68	157.79	113.43	809.53
DPP97126	12/10/89	9.57	305.58	309.96	31.40	164.65	94.49	193.70	165.72	170.87	155.43	115.77	804.04
DPP97127	12/10/89	9.57	305.52	309.89	31.33	165.36	96.13	198.50	159.98	163.44	154.96	117.77	799.43
DPP97129	12/10/89	9.59	305.25	310.03	31.50	166.59	97.91	206.98	165.98	147.59	155.09	119.07	794.23
DPB96100	12/10/89	9.58	304.84	306.46	31.84	134.43	0.00	42.96	49.52	43.06	43.62	43.55	222.01
DPB96100	12/10/89	9.58	302.28	303.90	31.92	139.77	0.00	44.63	51.21	44.75	45.26	45.10	230.38
DPB96101	12/10/89	9.57	302.75	308.75	32.06	139.33	5.16	51.44	52.25	45.40	45.81	45.49	239.90
DPB96101	12/10/89	9.57	303.16	309.22	31.86	137.25	10.18	69.62	70.37	51.79	44.92	44.43	279.72
DPC96113	12/10/89	9.57	304.17	309.83	31.90	139.65	65.45	138.88	153.71	136.24	112.63	76.27	615.04
DPP96114	12/10/89	9.57	304.17	309.69	32.18	138.72	66.43	137.20	153.40	136.78	113.17	76.61	613.02
DPP96115	12/10/89	9.57	304.17	309.83	32.18	139.35	68.09	133.74	153.63	138.13	114.84	78.06	614.75
DPP96116	12/10/89	9.57	304.10	309.76	31.98	139.69	69.55	131.72	154.25	138.86	115.95	79.13	615.33
DPP96117	12/10/89	9.56	304.17	309.76	31.94	139.48	71.27	127.68	152.98	139.55	117.17	80.66	614.75
DPP96118	12/10/89	9.57	304.17	309.83	32.05	141.25	72.85	127.45	152.29	140.40	118.94	82.45	618.21
DPP96119	12/10/89	9.56	304.17	309.83	32.18	140.36	74.51	126.30	150.17	140.32	119.54	83.62	615.90
DPP96120	12/10/89	9.57	303.97	309.83	32.01	141.35	76.15	127.45	145.59	140.01	119.64	84.14	613.59
DPP96121	12/10/89	9.57	304.17	309.83	32.01	141.10	77.81	130.80	138.24	138.82	120.24	86.16	611.00
DPP96122	12/10/89	9.58	304.10	309.83	32.25	141.09	79.45	133.68	133.47	137.24	119.17	86.89	608.11
DPP96123	12/10/89	9.57	304.17	309.76	32.44	140.23	81.02	137.20	130.97	134.28	118.50	88.37	606.67
DPP96124	12/10/89	9.57	304.17	309.83	32.25	140.83	82.97	141.59	126.39	129.24	116.52	89.67	600.61
DPP96125	12/10/89	9.57	304.17	309.83	32.28	141.28	84.61	145.11	123.58	116.47	114.76	91.18	591.08
DPP96126	12/10/89	9.57	304.17	309.83	32.38	142.10	86.07	149.67	125.89	101.85	112.73	92.66	579.54
DPB94100	12/10/89	9.58	304.57	305.99	32.64	105.03	0.00	32.63	38.67	32.90	33.34	33.21	170.65
DPB94101	12/10/89	9.58	303.63	308.95	32.76	101.47	4.98	40.02	40.44	31.44	31.47	31.37	173.82
DPB94102	12/10/89	9.58	306.59	309.22	32.70	101.28	10.08	50.46	52.67	40.90	36.79	30.20	210.76
DPC94109	12/10/89	9.57	302.75	309.62	32.71	101.71	45.74	72.57	87.57	75.88	62.27	42.97	339.75
DPC94109	13/10/89	9.58	301.13	309.69	31.25	100.67	43.13	65.29	73.76	67.10	54.48	36.43	296.75
DPC94109	13/10/89	9.57	301.10	309.35	31.23	99.57	43.27	67.55	75.49	68.35	55.47	36.74	304.40
DPP94110	12/10/89	9.57	302.82	309.56	32.73	99.37	48.13	73.66	88.84	78.53	64.97	44.95	349.84
DPP94111	12/10/89	9.57	303.09	309.49	32.58	98.42	49.63	70.55	87.61	79.03	66.06	46.17	348.40
DPP94112	12/10/89	9.57	303.49	309.56	32.56	98.59	51.48	79.03	95.65	85.69	71.49	49.99	379.86
DPP94112	12/10/89	9.57	303.76	309.56	32.51	101.47	51.52	63.51	82.22	77.38	66.35	47.75	335.71
DPP94110	13/10/89	9.58	301.33	309.62	31.21	101.92	44.69	70.26	78.76	71.76	57.93	38.74	316.95
DPP94111	13/10/89	9.59	301.54	309.69	31.26	99.56	46.33	67.26	77.80	72.41	59.02	39.83	315.51
DPP94112	13/10/89	9.59	301.47	309.69	31.30	98.57	47.97	66.39	78.03	73.76	60.12	40.74	318.10
DPP94113	13/10/89	9.59	301.81	309.89	31.21	100.53	49.73	65.12	78.68	75.72	62.11	42.38	324.74
DPP94114	13/10/89	9.58	301.74	309.76	31.25	100.24	51.21	65.12	79.65	77.49	64.04	44.07	330.22
DPP94115	13/10/89	9.58	301.07	309.69	31.28	98.99	52.91	65.99	81.18	79.38	65.34	44.58	335.71
DPP94116	13/10/89	9.59	301.67	309.69	31.30	99.69	54.43	63.85	77.03	78.57	64.40	45.34	329.07
DPP94117	13/10/89	9.58	301.41	309.59	31.45	100.15	56.17	66.40	78.99	81.01	67.37	47.26	340.76
DPP94117	13/10/89	9.59	300.86	309.83	31.36	98.35	56.19	66.60	79.35	81.06	66.74	46.32	339.07
DPP94118	13/10/89	9.58	301.60	309.76	31.45	98.35	57.93	67.78	72.99	79.11	64.87	47.60	333.11
DPP94119	13/10/89	9.58	301.74	309.76	31.51	101.31	59.47	70.32	73.22	79.76	65.75	48.79	337.73
DPP94120	13/10/89	9.58	301.74	309.69	31.65	102.74	61.25	73.49	73.34	81.53	68.32	50.84	347.25
DPP94121	13/10/89	9.58	301.54	309.76	31.63	100.48	62.89	75.51	71.37	79.30	67.10	50.89	343.21

DPP94122	13/10/89	9.58	301.67	309.62	31.72	98.93	64.53	76.95	67.49	75.03	66.82	51.29	336.57
DPP94123	13/10/89	9.58	301.47	309.83	31.56	101.32	66.31	80.07	68.60	73.11	68.48	52.61	343.50
DPP94124	13/10/89	9.58	301.60	309.69	31.91	100.25	67.91	83.07	70.87	69.37	69.33	53.86	346.96
DPP94125	13/10/89	9.59	301.81	309.83	31.59	99.88	69.45	85.03	71.72	63.91	68.79	54.14	343.79
DPB94200	13/10/89	9.59	293.90	295.19	31.89	101.03	0.00	25.36	27.67	25.70	25.96	25.86	129.96
DPB94201	13/10/89	9.58	293.97	303.49	31.88	98.85	4.88	25.07	27.32	25.24	25.44	25.26	127.94
DPB94201	13/10/89	9.58	294.17	309.22	31.91	101.20	10.23	32.05	28.55	26.24	26.33	26.07	138.62
DPC94210	13/10/89	9.59	294.38	309.83	31.56	102.45	48.81	78.05	87.30	74.18	56.66	32.59	328.20
DPC94210	13/10/89	9.58	294.17	309.69	31.73	100.90	50.18	75.63	86.19	74.68	57.08	32.97	325.03
DPP94211	13/10/89	9.58	294.58	309.76	31.61	100.55	51.46	72.05	84.80	75.53	58.06	33.88	323.88
DPP94212	13/10/89	9.58	294.58	309.76	31.58	100.46	53.05	69.91	84.72	76.53	58.79	34.56	323.59
DPP94213	13/10/89	9.58	294.65	309.83	31.57	101.26	54.71	69.22	85.80	78.61	60.53	35.86	329.36
DPP94214	13/10/89	9.59	294.44	309.83	31.10	99.54	56.29	65.47	82.45	77.03	59.91	35.88	319.55
DPP94215	13/10/89	9.58	295.12	309.76	30.83	101.03	57.81	67.78	84.26	79.41	62.32	38.07	331.67
DPP94216	13/10/89	9.59	294.78	309.89	30.91	100.09	59.73	67.89	83.03	77.18	62.32	38.48	328.20
DPP94217	13/10/89	9.58	294.78	309.89	30.89	100.94	61.25	69.33	81.45	77.95	63.52	39.65	332.24
DPP94218	13/10/89	9.59	294.92	309.83	30.85	98.74	62.89	70.49	73.03	75.80	62.87	39.88	322.43
DPP94219	13/10/89	9.58	294.58	309.89	30.93	99.16	64.59	72.74	71.14	75.72	63.96	40.51	323.88
DPP94220	13/10/89	9.59	294.99	309.89	30.90	101.60	66.31	75.86	69.72	75.80	66.19	42.53	331.38
DPP94221	13/10/89	9.58	294.72	309.76	30.99	99.04	67.79	76.89	67.03	72.03	66.01	42.74	324.74
DPP94222	13/10/89	9.58	294.58	309.89	30.98	100.30	67.77	77.47	68.03	73.30	66.58	42.82	328.49
DPP94222	13/10/89	9.58	295.12	309.83	30.93	100.31	70.14	81.05	69.53	67.41	68.09	44.69	331.95
DPB96200	13/10/89	9.58	294.58	296.00	31.34	135.67	0.00	42.27	44.90	42.29	42.79	42.61	214.51
DPB96201	13/10/89	9.58	294.58	302.28	31.26	135.69	5.18	42.56	45.02	42.32	42.71	42.35	214.22
DPB96202	13/10/89	9.57	294.51	308.48	31.31	134.52	10.12	43.13	45.52	42.67	42.97	42.51	216.53
DPB96204	13/10/89	9.60	294.38	309.56	31.24	133.56	19.94	76.09	66.22	43.63	42.58	41.86	269.91
DPB96206	13/10/89	9.58	294.44	309.49	31.31	132.97	30.04	103.33	89.49	67.49	45.03	41.29	346.09
DPB96208	13/10/89	9.58	294.44	309.49	31.34	133.55	39.69	124.74	110.96	85.11	57.70	42.38	419.97
DPB96209	13/10/89	9.59	294.24	309.49	31.09	133.29	44.98	132.13	120.89	93.07	64.82	43.16	452.86
DPB96210	13/10/89	9.58	294.31	309.56	31.16	134.58	50.37	136.51	130.43	101.27	73.26	44.35	484.32
DPB96211	13/10/89	9.59	294.24	309.69	31.26	135.14	55.51	136.63	137.01	107.85	79.57	45.73	504.52
DPB96212	13/10/89	9.58	294.44	309.76	31.38	134.18	60.00	134.55	140.51	113.54	85.51	47.47	519.81
DPB96213	13/10/89	9.58	294.44	309.83	31.31	135.03	65.18	133.16	142.94	119.51	91.28	49.83	534.81
DPC96213	13/10/89	9.58	294.72	309.89	31.29	135.54	67.85	131.20	142.01	122.12	94.32	51.57	539.72
DPP96214	13/10/89	9.58	294.65	309.83	31.20	134.84	69.57	128.72	142.05	123.58	95.82	52.43	541.45
DPP96215	13/10/89	9.58	294.58	309.83	31.01	134.88	71.09	123.76	141.55	124.39	97.18	53.39	538.57
DPP96216	13/10/89	9.57	294.72	309.83	31.05	134.89	72.93	120.58	140.44	125.35	98.99	54.77	538.85
DPP96217	13/10/89	9.59	294.65	309.83	31.13	136.30	74.49	118.45	139.44	125.74	100.03	55.57	537.70
DPP96218	13/10/89	9.59	294.31	309.83	31.13	136.61	76.11	117.12	138.13	125.24	101.23	56.48	535.97
DPP96219	13/10/89	9.58	294.38	309.83	31.21	136.05	77.91	116.02	134.59	123.24	102.39	57.72	532.79
DPP96220	13/10/89	9.58	294.65	309.83	31.33	136.40	79.57	117.81	122.97	119.31	103.23	59.39	520.96
DPP96221	13/10/89	9.57	294.72	309.83	31.26	136.55	81.07	120.87	116.47	116.58	104.53	60.84	517.79
DPP96222	13/10/89	9.59	294.65	309.96	31.28	137.45	82.97	123.07	102.46	107.27	105.15	61.93	500.48
DPP96223	13/10/89	9.57	294.72	309.83	31.44	136.86	83.67	124.39	103.92	97.46	104.91	62.87	493.55
DPB97200	16/10/89	9.57	295.19	296.61	30.15	163.24	0.00	58.31	61.60	57.98	58.76	58.35	296.46
DPB97201	16/10/89	9.57	295.12	301.94	30.15	162.72	5.04	58.95	62.18	58.29	58.97	58.40	298.48
DPC97216	16/10/89	9.57	294.72	309.83	30.37	160.24	80.90	184.70	190.95	163.94	126.34	67.18	733.92
DPB97200	26/10/89	9.57	294.24	295.86	30.62	162.31	0.00	57.62	58.95	57.41	58.04	57.83	290.98
DPB97201	26/10/89	9.57	294.31	301.33	30.65	162.66	5.14	58.60	59.64	57.95	58.45	58.14	294.15
DPB98200	26/10/89	9.57	295.19	296.61	31.40	185.82	0.00	74.24	76.14	73.72	74.76	74.32	375.24
DPB99200	26/10/89	9.57	296.27	297.89	31.59	210.02	0.00	92.48	94.80	91.46	92.79	92.50	466.42
DPC97216	26/10/89	9.56	293.77	309.83	31.73	163.26	83.73	192.20	196.92	169.79	130.31	69.41	760.18
DPP97215	26/10/89	9.57	293.77	309.83	31.63	163.54	82.87	193.88	198.38	169.29	129.04	68.84	760.76
DPP97216	26/10/89	9.56	293.77	309.83	31.85	164.40	84.63	192.61	197.84	170.91	131.46	69.70	764.80
DPP97217	26/10/89	9.57	293.77	309.83	31.99	163.62	86.41	183.49	196.19	171.33	132.94	70.48	756.43
DPP97218	26/10/89	9.57	293.77	309.83	31.96	163.21	88.07	179.22	194.73	172.49	135.38	71.67	755.85
DPP97219	26/10/89	9.57	293.77	309.83	31.86	164.73	89.69	177.49	194.34	173.22	137.01	72.53	757.88
DPP97220	26/10/89	9.57	293.77	309.83	31.99	164.21	91.05	173.51	192.57	173.14	138.34	73.39	754.41
DPP97221	26/10/89	9.56	293.77	309.83	32.14	163.26	92.83	167.33	184.03	168.56	138.75	74.11	737.39

DPP97222	26/10/89	9.57	293.77	309.83	32.03	163.55	94.61	169.76	176.45	165.95	140.55	75.41	732.77
DPP97223	26/10/89	9.57	293.77	309.83	32.14	165.21	96.13	168.54	139.36	158.57	143.92	78.14	694.68
DPP97224	26/10/89	9.57	293.70	309.83	32.18	162.14	96.89	172.52	135.09	137.78	140.00	76.92	671.31
DPB97500	27/10/89	9.58	257.09	258.53	30.22	161.24	0.00	53.35	52.48	53.33	54.04	53.83	275.11
DPB97501	27/10/89	9.58	257.43	264.75	30.55	164.55	5.06	56.35	55.06	55.91	56.56	56.24	287.52
DPB97502	27/10/89	9.59	257.57	270.89	30.78	170.79	10.39	60.50	58.87	59.68	60.22	59.80	306.85
DPB97502	27/10/89	9.58	257.50	270.96	30.84	167.03	10.39	58.19	56.71	57.48	58.09	57.62	296.17
DPB97502	27/10/89	9.58	257.37	271.30	30.85	162.25	10.35	55.14	53.83	54.56	55.02	54.69	281.17
DPB97504	27/10/89	9.59	257.57	282.72	30.87	161.49	20.22	55.54	54.02	54.44	54.71	54.17	281.17
DPB97506	27/10/89	9.59	257.43	293.84	30.68	161.13	30.18	56.98	54.98	55.17	55.23	54.35	284.05
DPB97508	27/10/89	9.59	257.57	304.30	30.59	160.55	39.92	58.08	55.71	55.67	55.39	54.38	286.36
DPB97510	27/10/89	9.58	257.57	309.29	30.72	162.17	49.92	83.24	57.91	57.33	56.76	55.47	319.26
DPB97512	27/10/89	9.58	257.85	309.42	30.50	162.57	59.81	127.11	70.53	58.10	57.49	55.91	378.70
DPB97514	27/10/89	9.55	257.57	309.35	30.65	160.14	70.18	155.73	104.08	59.75	56.38	54.69	442.47
DPB97516	27/10/89	9.58	257.43	309.42	30.26	161.28	79.84	177.20	129.28	69.18	57.78	55.91	502.50
DPB97518	27/10/89	9.58	257.57	309.62	30.22	163.36	89.90	188.86	147.71	88.46	59.60	57.08	555.88
DPC97519	27/10/89	9.58	257.98	309.83	30.36	163.79	96.70	171.14	148.44	105.08	61.05	57.18	558.19
DPP97518	27/10/89	9.57	258.05	309.76	30.27	162.12	96.17	171.14	147.48	104.35	60.48	56.61	554.44
DPP97519	27/10/89	9.58	257.85	309.76	30.27	163.44	97.77	166.70	149.75	107.85	61.70	57.57	557.90
DPP97520	27/10/89	9.58	258.05	309.83	30.23	164.61	99.39	145.63	148.59	112.23	62.45	57.88	541.45
DPB96500	27/10/89	9.58	256.61	258.05	28.21	138.31	0.00	41.00	40.25	40.98	41.49	41.29	211.05
DPB96501	27/10/89	9.57	256.00	264.27	28.52	138.25	5.10	41.75	41.06	41.67	42.14	41.88	215.09
DPB96502	27/10/89	9.58	256.00	271.23	28.50	141.00	10.16	43.13	42.36	42.86	43.23	42.90	220.57
DPB96504	27/10/89	9.59	256.07	284.49	28.56	140.85	20.22	44.11	42.94	43.33	43.55	43.03	223.17
DPB96506	27/10/89	9.59	256.14	297.01	28.40	140.89	30.08	45.10	43.59	43.67	43.65	42.95	224.90
DPB96508	27/10/89	9.59	256.00	308.41	28.57	139.60	40.00	48.85	44.06	43.83	43.55	42.61	229.52
DPB96510	27/10/89	9.57	256.14	309.35	28.20	138.66	50.29	87.05	49.63	44.09	43.65	42.51	275.11
DPB96512	27/10/89	9.58	256.07	309.42	26.47	140.70	60.23	114.99	73.99	46.52	45.16	43.78	333.98
DPB96514	27/10/89	9.59	256.07	309.62	26.55	139.97	70.06	135.18	99.19	54.21	44.51	43.26	387.07
DPB96516	27/10/89	9.58	256.07	309.62	26.64	138.08	79.98	136.28	110.50	72.60	44.90	42.71	418.81
DPC96517	27/10/89	9.58	256.14	309.83	26.76	138.40	83.67	125.78	111.31	80.34	45.78	42.82	417.95
DPP96516	27/10/89	9.58	256.14	309.83	26.72	138.14	83.01	128.84	111.39	78.84	45.62	42.71	418.52
DPP96517	27/10/89	9.58	256.34	309.83	26.21	138.97	84.75	124.05	111.97	82.42	46.27	42.95	418.52
DPP96518	27/10/89	9.59	256.55	309.83	25.93	139.16	86.19	111.29	111.58	85.34	46.89	43.26	410.44
DPB94500	27/10/89	9.58	251.82	252.71	-	99.36	0.00	23.45	23.43	23.74	23.99	23.86	123.03
DPB94501	27/10/89	9.58	251.89	263.25	-	97.60	5.16	23.51	23.24	23.55	23.70	23.55	121.88
DPB94502	27/10/89	9.58	252.16	272.46	-	98.47	9.96	23.86	23.70	23.97	24.07	23.86	124.19
DPB94504	27/10/89	9.58	252.71	290.93	-	99.38	19.94	24.84	24.55	24.63	24.66	24.33	127.94
DPB94506	27/10/89	9.58	252.71	308.21	-	98.80	30.08	27.38	24.86	24.78	24.61	24.17	130.25
DPB94508	27/10/89	9.57	252.71	309.29	-	99.36	40.19	53.12	32.28	25.40	25.24	24.56	166.32
DPB94510	27/10/89	9.59	252.98	309.49	-	103.19	50.06	73.61	52.33	29.63	27.03	26.20	215.95
DPB94510	27/10/89	9.58	253.26	309.42	-	100.45	50.04	73.20	52.98	29.71	25.73	25.11	213.93
DPB94512	27/10/89	9.58	253.19	309.69	-	97.57	60.12	79.32	63.10	43.44	25.50	24.09	243.36
DPC94513	27/10/89	9.59	253.26	309.76	-	99.01	65.31	79.03	68.49	50.87	27.16	24.66	258.66
DPP94512	27/10/89	9.58	253.60	309.69	-	100.75	64.65	82.78	68.83	50.02	27.55	25.42	263.57
DPP94513	27/10/89	9.58	253.74	309.69	-	99.46	66.31	78.51	69.95	52.71	27.70	24.87	262.12
DPP94514	27/10/89	9.58	253.60	309.76	-	99.78	68.20	72.80	71.45	54.87	28.20	24.59	260.68
DPP94515	27/10/89	9.58	253.60	309.83	-	100.99	69.69	71.35	73.07	57.18	29.18	25.21	264.72
DPP94516	27/10/89	9.58	253.74	309.83	-	101.00	70.55	71.12	74.03	58.41	29.70	25.57	267.89
DPB94400	27/10/89	9.57	268.50	269.46	-	98.94	0.00	23.80	23.70	24.01	24.35	24.17	125.92
DPB94401	27/10/89	9.55	269.18	279.33	-	101.30	4.90	25.01	24.93	25.20	25.42	25.18	131.40
DPB94402	27/10/89	9.56	269.12	288.56	-	99.72	10.10	24.89	24.63	24.82	25.00	24.74	129.67
DPB94404	27/10/89	9.56	268.91	305.52	-	99.33	19.92	25.24	24.82	24.89	24.92	24.48	130.25
DPB94406	27/10/89	9.55	269.46	309.22	-	101.52	30.08	49.60	32.59	26.40	26.25	25.68	168.05
DPB94408	27/10/89	9.56	268.98	309.29	-	99.12	39.92	69.05	52.40	32.59	25.60	25.00	213.35
DPB94410	27/10/89	9.56	269.39	309.35	-	100.94	50.02	82.55	67.87	48.56	27.96	25.78	262.41
DPB94412	27/10/89	9.55	269.39	309.35	-	99.82	60.00	80.01	75.68	59.68	34.30	25.16	285.21
DPC94412	27/10/89	9.55	269.25	309.35	-	98.98	60.29	79.09	75.14	59.68	34.43	24.98	283.76
DPP94411	27/10/89	9.55	269.25	309.35	-	98.30	59.79	78.91	74.68	59.14	34.12	24.79	282.61

DPP94412	27/10/89	9.55	269.53	309.35	-	100.37	61.29	82.32	77.57	61.68	35.75	25.83	295.02
DPP94412	27/10/89	9.55	269.46	309.35	-	100.18	61.50	80.82	77.26	61.72	36.17	25.68	292.42
DPP94413	27/10/89	9.56	269.25	309.42	-	98.67	63.13	73.84	76.64	61.76	37.31	25.08	286.65
DPP94414	27/10/89	9.54	269.46	309.35	-	99.3(	64.78	71.87	77.95	63.33	39.10	25.29	290.98
DPP94415	27/10/89	9.56	269.87	309.42	-	102.90	66.41	74.59	80.84	66.68	41.03	26.72	31..18
DPP94416	27/10/89	9.55	270.00	309.35	-	102.84	68.09	70.84	79.65	67.87	42.87	26.74	316.37
DPP94417	27/10/89	9.54	269.93	309.42	33.04	102.62	69.57	68.76	77.49	68.91	44.66	26.87	335.13
DPP94418	27/10/89	9.55	270.00	309.35	33.02	102.35	71.37	69.3(	71.30	69.68	46.30	26.98	263.57
DPB97400	31/10/89	9.56	268.57	270.00	31.85	166.98	0.00	57.27	56.06	57.02	57.67	57.65	291.27
DPB97400	31/10/89	9.56	268.50	275.86	31.82	164.22	5.04	56.69	55.91	56.68	57.26	57.18	290.11
DPB97401	31/10/89	9.55	268.50	276.00	31.91	164.65	5.06	56.93	55.83	56.56	57.21	57.10	289.25
DPB97402	31/10/89	9.56	268.57	281.70	31.98	164.24	10.16	57.39	56.21	56.83	57.39	57.13	290.11
DPB97404	31/10/89	9.55	268.57	292.21	32.01	163.54	19.88	58.31	56.75	57.18	57.47	57.00	292.71
DPB97406	31/10/89	9.55	268.57	302.95	32.05	163.28	29.86	59.70	57.60	57.75	57.72	57.00	294.73
DPB97408	31/10/89	9.58	268.57	309.69	32.02	163.32	40.04	77.99	59.18	58.91	58.63	57.57	317.82
DPB97410	31/10/89	9.55	268.57	309.35	31.86	159.98	50.00	123.76	75.34	57.25	56.69	55.44	375.82
DPB97412	31/10/89	9.56	268.57	309.35	31.90	159.78	59.88	152.15	108.50	62.02	56.87	55.39	443.92
DPB97414	31/10/89	9.55	268.64	309.42	32.05	161.13	70.00	177.43	135.13	79.99	58.04	56.45	518.65
DPB97416	31/10/89	9.55	268.84	309.35	31.98	163.45	80.12	193.07	154.98	103.65	61.08	57.83	583.01
DPB97418	31/10/89	9.56	269.05	309.76	32.08	162.16	89.96	188.86	164.91	125.70	65.57	57.67	616.77
DPC97419	31/10/89	9.56	269.53	309.83	32.06	164.81	95.00	182.57	159.98	135.24	70.30	58.71	621.38
DPP97418	31/10/89	9.55	269.39	309.62	32.03	163.37	94.61	182.97	160.64	134.63	70.06	58.48	619.37
DPP97419	31/10/89	9.55	269.39	309.62	32.07	164.19	96.21	168.43	156.90	137.36	71.96	58.66	606.09
DPP97420	31/10/89	9.54	269.53	309.56	32.02	165.04	97.75	150.94	154.86	140.09	74.11	59.36	593.10
DPP97421	31/10/89	9.55	269.46	309.76	32.09	166.15	99.65	142.57	145.05	142.63	75.75	60.24	578.97
DPP97422	31/10/89	9.54	269.53	309.62	32.09	166.55	100.35	143.73	138.74	143.94	77.10	60.43	576.37
DPB96400	02/11/89	9.59	271.09	272.25	27.96	138.68	0.00	42.04	41.13	41.75	42.43	42.74	216.24
DPB96400	02/11/89	9.60	270.55	278.92	28.03	138.12	5.04	42.38	41.36	41.79	42.48	42.66	216.24
DPB96401	02/11/89	9.59	270.68	278.92	28.01	138.47	5.00	42.27	41.32	41.79	42.45	42.61	216.82
DPB96402	02/11/89	9.57	270.75	285.50	27.98	138.38	9.96	42.84	41.67	42.13	42.69	42.79	218.55
DPB96404	02/11/89	9.60	270.75	298.50	28.21	137.39	20.02	43.31	42.02	42.21	42.56	42.51	219.41
DPB96406	02/11/89	9.58	271.02	309.22	28.18	141.26	29.92	50.06	45.25	45.17	45.29	44.97	238.46
DPB96408	02/11/89	9.52	270.96	309.22	27.96	137.90	40.06	90.11	56.06	44.25	44.17	43.57	287.80
DPB96410	02/11/89	9.59	270.89	309.69	27.88	141.35	49.88	116.49	84.07	49.60	45.93	45.18	353.02
DPB96412	02/11/89	9.58	270.96	309.56	28.10	139.41	60.27	138.76	106.46	67.87	45.83	44.56	417.66
DPB96414	02/11/89	9.59	270.89	309.76	28.04	138.48	70.12	145.34	121.24	87.96	48.38	44.22	463.54
DPB96415	02/11/89	9.58	270.96	309.83	28.03	139.65	79.78	140.55	127.66	103.58	55.86	44.84	488.93
DPC96415	02/11/89	9.58	271.09	309.83	28.02	137.58	80.25	132.24	122.32	102.54	56.51	43.60	471.33
DPP96414	02/11/89	9.58	271.37	309.76	28.15	139.32	79.65	140.73	127.66	103.54	56.14	44.64	488.93
DPP96415	02/11/89	9.58	271.43	309.89	28.15	139.60	81.21	137.84	126.05	105.46	58.01	44.92	487.78
DPP96416	02/11/89	9.58	271.30	309.83	28.20	140.24	82.81	128.61	123.32	107.04	59.78	45.23	479.41
DPP96417	02/11/89	9.60	271.30	310.03	28.15	141.15	84.43	117.06	119.47	108.43	61.41	45.47	467.58
DPP96418	02/11/89	9.58	270.96	309.83	28.13	138.65	85.55	104.25	100.34	106.69	62.56	44.43	434.11
DPB74500	02/11/89	7.03	223.39	224.22	29.86	100.42	0.00	23.63	23.36	23.70	23.86	23.91	114.67
DPB74501	02/11/89	7.04	222.91	234.50	30.94	100.16	5.04	23.51	23.32	23.59	23.73	23.73	114.95
DPB74502	02/11/89	7.04	222.84	244.61	31.18	99.83	10.21	23.68	23.43	23.70	23.78	23.81	115.53
DPB74504	02/11/89	7.04	222.35	263.45	29.82	100.80	20.22	24.49	24.20	24.32	24.30	24.25	118.42
DPB74506	02/11/89	7.04	222.42	281.57	29.17	101.26	30.08	25.13	24.55	24.66	24.53	24.40	119.86
DPB74508	02/11/89	7.04	222.42	288.35	28.95	99.95	40.19	50.58	25.90	24.51	24.38	24.14	147.56
DPB74512	02/11/89	7.03	222.22	288.15	28.68	100.74	60.23	110.77	76.18	36.05	24.74	24.56	272.80
DPB74514	02/11/89	7.04	221.94	288.49	28.51	99.30	70.10	123.53	97.38	53.91	25.29	23.94	326.18
DPC74515	02/11/89	7.04	221.94	288.56	28.52	101.47	79.49	130.74	113.70	70.95	29.31	24.77	372.07
DPP74514	02/11/89	7.03	222.22	288.56	28.54	101.67	79.16	131.03	113.43	70.57	29.13	24.74	372.07
DPP74515	02/11/89	7.04	222.35	288.56	28.50	100.36	80.96	127.91	115.58	74.03	30.04	24.22	374.95
DPP74516	02/11/89	7.03	222.42	288.56	28.56	99.96	82.44	125.55	118.31	76.95	31.24	24.14	379.57
DPP74517	02/11/89	7.04	222.42	288.56	28.44	100.55	84.06	124.16	120.66	79.34	32.20	24.30	383.90
DPB96400	02/11/89	9.59	271.09	272.25	27.96	138.68	0.00	42.04	41.13	41.75	42.43	42.74	216.24
DPB96400	02/11/89	9.60	270.55	278.92	28.03	138.12	5.04	42.38	41.36	41.79	42.48	42.66	216.24
DPB96401	02/11/89	9.59	270.68	278.92	28.01	138.47	5.00	42.27	41.32	41.79	42.45	42.61	216.82

DPB96402	02/11/89	9.57	270.75	285.50	27.98	138.38	9.96	42.84	41.67	42.13	42.69	42.79	218.55
DPB96404	02/11/89	9.60	270.75	298.50	28.21	137.39	20.02	43.31	42.02	42.21	42.56	42.51	219.41
DPB96406	02/11/89	9.58	271.02	309.22	28.18	141.26	29.92	50.06	45.25	45.17	45.29	44.97	238.46
DPB96408	02/11/89	9.52	270.96	309.22	27.96	137.90	40.06	90.11	56.06	44.25	44.17	43.57	287.80
DPB96410	02/11/89	9.59	270.89	309.69	27.88	141.35	49.88	116.49	84.07	49.60	45.93	45.18	353.02
DPB96412	02/11/89	9.58	270.96	309.56	28.10	139.41	60.27	138.76	106.46	67.87	45.83	44.56	417.66
DPB96414	02/11/89	9.59	270.89	309.76	28.04	138.48	70.12	145.34	121.24	87.96	48.38	44.22	463.54
DPB96415	02/11/89	9.58	270.96	309.83	28.03	139.65	79.78	140.55	127.66	103.58	55.86	44.84	488.93
DPC96415	02/11/89	9.58	271.09	309.83	28.02	137.58	80.25	132.24	122.32	102.54	56.51	43.60	471.33
DPP96414	02/11/89	9.58	271.37	309.76	28.15	139.32	79.65	140.73	127.66	103.54	56.14	44.64	488.93
DPP96415	02/11/89	9.58	271.43	309.89	28.15	139.60	81.21	137.84	126.05	105.46	58.01	44.92	487.78
DPP96416	02/11/89	9.58	271.30	309.83	28.20	140.24	82.81	128.61	123.32	107.04	59.78	45.23	479.41
DPP96417	02/11/89	9.60	271.30	310.03	28.15	141.15	84.43	117.06	119.47	108.43	61.41	45.47	467.58
DPP96418	02/11/89	9.58	270.96	309.83	28.13	138.65	85.55	104.25	100.34	106.69	62.56	44.43	434.11
DPB74500	02/11/89	7.03	223.39	224.22	29.86	100.42	0.00	23.63	23.36	23.70	23.86	23.91	114.67
DPB74501	02/11/89	7.04	222.91	234.50	30.94	100.16	5.04	23.51	23.32	23.59	23.73	23.73	114.95
DPB74502	02/11/89	7.04	222.84	244.61	31.18	99.83	10.21	23.68	23.43	23.70	23.78	23.81	115.53
DPB74504	02/11/89	7.04	222.35	263.45	29.82	100.80	20.22	24.49	24.20	24.32	24.30	24.25	118.42
DPB74506	02/11/89	7.04	222.42	281.57	29.17	101.26	30.08	25.13	24.55	24.66	24.53	24.40	119.86
DPB74508	02/11/89	7.04	222.42	288.35	28.95	99.95	40.19	50.58	25.90	24.51	24.38	24.14	147.56
DPB74512	02/11/89	7.03	222.22	288.15	28.68	100.74	60.23	110.77	76.18	36.05	24.74	24.56	272.80
DPB74514	02/11/89	7.04	221.94	288.49	28.51	99.30	70.10	123.53	97.38	53.91	25.29	23.94	326.18
DPC74515	02/11/89	7.04	221.94	288.56	28.52	101.47	79.49	130.74	113.70	70.95	29.31	24.77	372.07
DPP74514	02/11/89	7.03	222.22	288.56	28.54	101.67	79.16	131.03	113.43	70.57	29.13	24.74	372.07
DPP74515	02/11/89	7.04	222.35	288.56	28.50	100.36	80.96	127.91	115.58	74.03	30.04	24.22	374.95
DPP74516	02/11/89	7.03	222.42	288.56	28.56	99.96	82.44	125.55	118.31	76.95	31.24	24.14	379.57
DPP74517	02/11/89	7.04	222.42	288.56	28.44	100.55	84.06	124.16	120.66	79.34	32.20	24.30	383.90
DPB76500	03/11/89	7.00	225.32	226.29	28.73	141.42	0.00	41.00	40.25	40.90	41.29	41.49	208.45
DPB76501	03/11/89	7.00	224.70	233.53	29.03	138.84	4.90	40.25	39.48	40.06	40.40	40.58	205.27
DPB76502	03/11/89	7.00	224.70	240.63	28.93	142.70	10.10	42.44	41.56	42.06	42.40	42.45	215.38
DPB76504	03/11/89	7.00	224.77	254.22	28.84	142.42	19.84	42.79	41.71	42.13	42.33	42.27	215.66
DPB76506	03/11/89	7.00	224.70	268.09	28.84	141.53	29.94	43.42	42.09	42.36	42.30	42.19	217.68
DPB76508	03/11/89	7.00	224.50	281.03	28.65	141.98	40.00	44.63	43.13	43.13	43.05	42.66	221.44
DPB76510	03/11/89	7.00	224.22	288.01	28.77	137.92	49.94	73.26	42.06	41.86	41.39	40.92	244.81
DPB76512	03/11/89	7.00	224.56	287.88	28.73	141.67	59.75	121.68	58.48	43.17	43.18	42.43	316.08
DPB76514	03/11/89	7.00	224.36	288.08	29.63	138.04	70.16	162.77	95.11	45.25	41.44	40.97	394.57
DPB76515	03/11/89	7.00	224.29	288.08	29.86	138.40	75.04	177.55	111.16	50.33	41.78	41.26	432.09
DPB76516	03/11/89	7.00	224.36	288.01	29.77	139.80	80.14	189.90	126.01	58.64	42.40	41.81	469.31
DPB76517	03/11/89	7.00	224.36	288.08	29.86	138.84	85.24	195.67	137.32	69.95	42.30	41.42	497.59
DPB76518	03/11/89	7.00	224.36	288.08	30.01	137.57	90.06	197.28	146.98	81.80	42.66	41.05	521.54
DPB76519	03/11/89	7.00	224.84	288.15	30.28	139.60	95.10	202.77	157.48	92.53	44.97	42.22	552.13
DPB76520	03/11/89	7.00	224.77	288.08	29.88	141.55	100.04	204.56	165.64	104.31	47.10	43.13	576.95
DPC76520	03/11/89	7.00	224.77	288.15	30.11	140.26	99.92	199.53	164.48	105.12	46.51	42.14	570.02
DPP76519	03/11/89	7.00	224.77	288.08	30.00	139.93	99.04	200.63	163.52	103.04	45.99	41.88	566.56
DPP76520	03/11/89	7.00	224.77	288.15	29.87	138.79	100.76	194.23	164.71	107.73	46.17	41.26	566.56
DPP76521	03/11/89	7.00	224.84	288.22	29.90	140.12	102.13	192.61	166.48	110.46	47.36	41.91	571.46
DPB76100	03/11/89	6.97	282.52	283.67	29.90	136.87	0.00	41.23	40.40	41.06	41.57	41.67	211.34
DPB76101	03/11/89	7.00	280.89	287.67	29.89	140.82	4.92	47.17	43.63	44.33	44.71	44.71	229.23
DPB76102	03/11/89	7.00	282.18	287.81	29.88	138.56	10.39	80.82	67.83	53.48	43.91	43.88	296.46
DPB76104	03/11/89	7.00	282.52	287.88	29.90	137.38	20.10	121.05	101.04	81.65	58.32	43.55	414.48
DPB76106	03/11/89	6.99	282.45	287.81	29.88	138.15	29.98	147.82	130.20	107.08	77.91	46.22	520.39
DPB76108	03/11/89	6.99	282.79	287.88	29.99	138.86	40.18	169.18	150.98	130.20	94.86	53.67	611.86
DPB76110	03/11/89	7.00	280.28	288.15	29.83	138.91	50.04	183.84	166.48	145.25	103.62	55.60	668.71
DPB76112	03/11/89	7.00	280.28	288.22	29.91	138.25	60.02	189.38	178.53	160.87	117.90	62.53	723.83
DPB76114	03/11/89	7.00	280.48	288.28	29.87	138.50	70.00	195.49	186.03	173.99	132.57	71.65	775.77
DPC76114	03/11/89	7.01	281.16	288.35	29.79	139.84	71.80	198.09	189.30	178.14	137.09	75.26	793.08
DPP76113	03/11/89	7.00	280.96	288.22	29.83	140.40	71.23	199.30	189.19	177.64	136.42	74.63	793.08
DPP76114	03/11/89	7.00	281.03	288.28	29.97	139.69	72.73	198.21	189.80	179.22	138.31	76.06	797.41
DPP76115	03/11/89	7.00	280.96	288.28	29.85	140.00	74.51	196.30	190.19	180.30	139.87	77.46	800.58

DPP76116	03/11/89	7.00	280.96	288.35	29.97	139.66	75.88	192.26	191.03	181.72	141.17	78.32	800.58
DPP76117	03/11/89	7.00	280.96	288.42	29.90	139.79	77.79	186.43	191.19	183.22	143.19	80.40	800.01
DPP76118	03/11/89	7.00	281.16	288.56	29.86	139.56	79.36	181.64	190.84	183.57	144.47	81.96	797.70
DPP76119	03/11/89	7.00	280.96	288.42	29.96	138.46	81.07	177.60	188.22	182.88	144.36	83.02	791.35
DPP76120	03/11/89	7.00	281.03	288.56	29.87	139.55	82.70	179.16	189.69	185.18	145.45	84.53	799.43
DPP76121	03/11/89	7.00	280.75	288.42	29.92	138.67	84.43	177.43	187.68	185.26	144.94	85.13	796.54
DPP76122	03/11/89	7.00	280.96	288.62	29.84	140.94	86.00	180.49	189.88	188.49	147.56	87.77	809.82
DPP76123	03/11/89	7.00	281.16	288.62	29.95	140.54	87.72	183.32	183.14	188.26	148.31	89.57	808.37
DPP76124	03/11/89	7.00	281.09	288.62	29.86	140.68	89.26	186.66	177.72	187.53	148.23	90.71	806.64
DPP76125	03/11/89	7.00	281.09	288.62	29.99	140.56	91.05	191.40	174.30	186.99	148.60	92.09	809.24
DPP76126	03/11/89	7.00	281.30	288.76	30.13	140.36	92.70	196.36	171.56	186.34	149.66	93.85	813.28
DPP76127	03/11/89	6.99	281.37	288.62	30.04	140.55	94.47	200.92	167.72	184.38	149.84	95.15	813.86
DPP76128	03/11/89	7.00	280.96	288.69	30.11	140.82	96.11	205.19	165.10	182.22	149.77	96.03	815.01
DPP76129	03/11/89	7.00	281.23	288.62	30.05	141.25	97.60	210.90	163.44	180.14	150.39	97.82	817.90
DPB56200	03/11/89	5.03	242.07	243.03	29.95	141.41	0.00	42.56	42.13	42.75	43.05	43.00	217.68
DPB56201	03/11/89	5.03	243.99	252.44	30.09	140.83	5.19	42.15	41.71	42.36	42.48	42.38	214.80
DPB56202	03/11/89	5.02	244.41	259.49	30.03	139.47	9.96	42.15	41.59	42.17	42.22	42.04	213.93
DPB56204	03/11/89	5.03	244.61	266.73	29.49	139.61	20.10	80.18	43.21	42.13	42.04	41.70	253.47
DPB56206	03/11/89	5.02	244.48	266.59	29.28	139.88	30.02	147.88	96.46	48.63	42.82	42.66	386.20
DPB56208	03/11/89	5.03	244.61	266.73	29.28	141.32	40.06	198.67	146.59	82.49	43.52	43.10	524.72
DPB56210	03/11/89	5.03	245.37	266.80	29.05	140.07	49.49	228.27	186.07	120.70	54.27	42.35	644.18
DPB56212	03/11/89	5.03	245.09	266.87	28.95	140.54	60.12	262.56	217.43	154.40	72.11	42.61	762.49
DPB56214	03/11/89	5.03	245.30	267.21	28.98	141.31	69.71	285.76	241.16	182.80	90.11	43.73	858.29
DPB56215	03/11/89	5.03	245.16	267.34	29.02	138.95	80.12	291.30	260.83	206.31	110.84	45.31	930.44
DPC56217	03/11/89	5.03	245.09	267.48	28.99	138.94	84.80	291.53	269.41	215.96	119.80	46.71	960.16
DPP56216	03/11/89	5.03	245.09	267.27	28.96	138.90	84.36	291.88	268.37	214.58	118.63	46.45	956.98
DPP56217	03/11/89	5.03	245.16	267.62	29.01	139.52	85.98	294.47	272.98	219.23	122.08	47.39	973.43
DPP56218	03/11/89	5.03	245.30	267.55	29.20	140.80	87.64	297.42	276.95	222.97	124.89	48.25	988.15
DPP56219	03/11/89	5.03	245.09	267.62	29.03	139.37	89.28	293.72	277.25	224.81	127.53	48.58	989.01
DPP56220	03/11/89	5.02	245.16	267.62	28.88	139.58	91.05	285.24	280.10	228.58	131.74	49.39	991.32
DPP56221	03/11/89	5.03	245.09	267.62	28.64	139.18	92.83	279.29	281.18	231.12	134.47	50.01	993.34
DPP56222	03/11/89	5.03	245.09	267.62	28.61	138.99	94.45	276.29	283.10	233.97	137.48	50.84	998.83
DPP56223	03/11/89	5.02	245.09	267.62	28.59	139.30	95.98	273.41	283.87	237.09	140.78	51.91	1004.02
DPP56224	03/11/89	5.03	245.09	267.68	28.60	138.88	97.73	270.75	284.22	238.89	143.12	52.66	1007.19
DPP56225	03/11/89	5.03	245.16	267.62	28.52	141.35	99.38	278.54	291.61	244.51	146.70	53.86	1032.59
DPP56226	03/11/89	5.03	245.09	267.82	28.46	140.88	101.03	275.60	289.14	246.32	149.45	54.71	1031.43
DPP56227	03/11/89	5.03	245.16	267.82	28.47	139.66	102.79	272.71	286.49	246.97	152.31	55.75	1032.59
DPP56228	03/11/89	5.03	245.09	267.68	28.47	139.68	104.28	272.43	286.33	249.21	155.27	56.66	1037.78
DPP56229	03/11/89	5.03	245.09	267.62	28.46	138.81	106.07	273.06	282.72	250.63	158.02	57.65	1039.22
DPP56230	03/11/89	5.03	245.09	267.68	28.40	138.48	107.64	278.20	276.56	252.05	160.93	58.84	1043.84
DPB54200	03/11/89	5.02	242.69	243.65	28.62	102.66	0.00	24.72	24.82	25.16	25.18	25.03	127.36
DPB54201	03/11/89	5.03	242.76	253.87	28.43	101.83	5.22	24.78	24.78	25.09	25.05	24.90	127.36
DPB54202	03/11/89	5.03	243.03	263.38	28.51	102.02	10.21	25.01	25.01	25.24	25.18	24.95	127.94
DPB54204	03/11/89	5.03	242.69	266.73	28.56	101.01	20.08	67.03	41.59	25.51	25.11	24.82	187.96
DPB54206	03/11/89	5.02	242.76	266.59	28.71	102.70	30.16	111.81	84.42	50.44	26.27	25.44	304.25
DPB54208	03/11/89	5.02	242.69	266.59	28.57	103.56	39.88	141.94	117.70	78.38	37.62	25.60	409.58
DPB54210	03/11/89	5.03	242.96	266.66	28.57	101.60	50.08	164.97	141.67	105.69	53.86	25.60	501.34
DPB54212	03/11/89	5.03	242.89	267.07	28.59	103.07	59.94	187.65	163.33	128.70	70.11	28.35	589.06
DPB54214	03/11/89	5.02	242.69	267.14	28.73	100.93	69.53	189.20	180.91	146.75	86.81	32.12	647.07
DPC54214	03/11/89	5.03	242.89	267.14	28.66	101.75	70.06	187.93	182.26	147.32	87.72	32.40	649.09
DPP54213	03/11/89	5.03	242.76	267.14	28.71	101.33	69.59	188.80	181.95	146.59	86.81	32.27	648.51
DPP54213	03/11/89	5.03	242.76	267.14	28.73	100.81	69.59	188.28	181.49	146.52	86.92	32.17	647.35
DPP54214	03/11/89	5.03	242.82	267.14	28.70	101.52	71.09	187.76	184.03	149.17	89.10	32.90	655.15
DPP54215	03/11/89	5.03	242.96	267.14	28.69	101.25	72.73	188.86	186.76	152.25	91.77	33.91	666.40
DPP54216	03/11/89	5.03	242.69	267.14	28.77	101.45	74.51	188.34	189.07	155.60	94.01	34.66	674.19
DPP54217	03/11/89	5.03	242.69	267.34	28.99	101.55	75.86	182.45	191.19	158.14	96.68	35.62	676.21
DPP54218	03/11/89	5.03	242.76	267.34	29.03	101.68	77.83	179.91	193.96	161.98	99.36	36.79	683.71
DPP54219	03/11/89	5.03	242.82	267.14	28.95	101.56	79.43	176.97	194.65	164.94	101.90	37.96	688.91
DPP54220	03/11/89	5.03	242.69	267.48	28.96	101.28	81.05	173.85	193.61	167.02	103.33	38.74	688.62

DPP54221	03/11/89	5.02	242.69	267.21	28.97	102.02	82.72	175.30	196.53	171.52	106.42	40.01	701.89
DPP54222	03/11/89	5.02	242.82	267.41	28.94	101.74	84.43	173.85	194.69	174.02	108.29	41.10	705.07
DPP54223	03/11/89	5.03	242.69	267.55	28.73	100.77	86.13	172.99	192.53	175.99	109.88	41.91	706.51
DPB98200	06/11/89	9.54	294.44	296.07	28.52	200.59	0.00	84.97	82.53	83.76	85.25	85.57	381.88
DPB98201	06/11/89	9.55	294.11	300.39	28.58	199.76	5.08	85.44	82.84	83.99	85.25	85.36	383.32
DPB98202	06/11/89	9.55	294.17	304.57	28.40	197.85	10.06	86.24	83.38	84.30	85.44	85.38	385.63
DPB98203	06/11/89	9.55	294.17	309.22	28.54	197.49	19.96	113.43	83.61	83.95	84.74	84.27	412.46
DPB98206	06/11/89	9.55	294.11	309.42	28.58	197.40	30.49	167.73	127.28	87.80	85.77	84.94	522.12
DPB98208	06/11/89	9.54	294.17	309.35	28.66	197.71	39.92	206.52	162.60	113.58	87.36	86.14	629.75
DPB98210	06/11/89	9.54	294.24	309.35	28.82	198.40	49.90	238.49	190.61	146.17	91.54	86.06	731.33
DPB98212	06/11/89	9.55	294.24	309.42	28.86	200.78	60.00	268.73	219.08	174.26	104.32	88.50	839.25
DPB98214	06/11/89	9.54	294.24	309.56	29.01	197.66	70.14	278.49	236.86	193.73	121.20	86.45	904.47
DPB98216	06/11/89	9.56	294.24	309.69	29.02	197.59	80.06	283.80	253.25	211.31	139.30	87.75	966.22
DPB98218	06/11/89	9.56	294.24	309.89	29.02	198.41	89.82	284.03	263.10	225.85	157.14	90.01	1014.70
DPB98220	06/11/89	9.55	294.24	310.03	29.12	200.50	99.96	292.68	269.75	240.36	175.35	94.24	1070.10
DPB98222	06/11/89	9.54	294.24	310.03	29.14	200.20	110.08	291.76	261.02	241.13	190.46	98.21	1078.76
DPC98222	06/11/89	9.54	294.24	309.89	29.10	199.73	110.57	291.01	261.25	241.78	191.81	98.84	1076.74
DPP98223	06/11/89	9.55	294.24	310.03	29.26	199.17	111.02	286.10	261.06	240.97	191.99	98.89	1069.81
DPB90200	06/11/89	9.54	294.72	296.47	29.55	234.33	0.00	113.60	110.39	111.93	113.90	114.42	528.76
DPB90201	06/11/89	9.54	294.65	300.32	29.54	233.69	5.06	114.58	111.00	112.43	114.19	114.50	531.93
DPB90202	06/11/89	9.56	294.72	303.70	29.50	233.03	9.98	115.16	111.27	112.47	114.03	114.16	532.79
DPB90204	06/11/89	9.54	294.65	309.08	29.75	232.14	20.08	130.45	112.62	113.39	114.37	114.06	551.26
DPB90206	06/11/89	9.56	294.65	309.35	29.70	233.30	30.45	206.23	139.28	116.77	117.22	116.39	667.84
DPB90208	06/11/89	9.55	294.72	309.35	29.58	234.08	40.06	258.46	196.15	127.59	118.39	117.09	795.10
DPB90210	06/11/89	9.54	294.58	309.35	29.55	232.25	50.00	297.24	231.62	158.37	117.61	115.93	901.58
DPB90212	06/11/89	9.54	294.72	309.35	29.60	230.77	59.88	329.85	261.90	194.15	120.83	115.15	1007.77
DPB90214	06/11/89	9.54	294.51	309.42	29.76	234.12	70.00	362.52	292.95	225.89	131.38	117.67	1120.60
DPB90216	06/11/89	9.54	294.72	309.56	29.77	230.84	80.04	377.98	315.00	252.09	146.60	116.37	1201.40
DPB90218	06/11/89	9.56	294.72	309.76	29.68	232.40	89.96	389.93	335.08	273.33	163.27	117.64	1274.69
DPB90220	06/11/89	9.55	294.72	309.89	29.70	232.70	100.22	393.39	350.40	292.80	184.90	118.37	1338.75
DPB90222	06/11/89	9.54	294.72	309.89	29.76	232.69	109.65	395.35	356.44	306.30	204.36	119.56	1383.19
DPB90224	06/11/89	9.55	294.72	310.09	29.86	232.64	119.75	407.47	359.44	318.61	223.94	122.81	1440.04
DPB90226	06/11/89	9.55	294.72	310.30	29.97	232.46	129.86	417.28	349.82	316.34	242.79	125.51	1468.32
DPC90227	06/11/89	9.55	294.72	310.23	29.92	236.43	137.72	438.41	334.35	306.23	256.84	130.73	1518.24
DPB93200	06/11/89	9.54	292.15	293.09	30.10	69.01	0.00	13.81	13.78	13.93	14.17	13.08	71.09
DPB93200	06/11/89	9.55	287.61	288.22	30.13	69.11	0.00	13.35	13.28	13.47	13.65	12.61	69.07
DPB93201	06/11/89	9.55	288.15	302.01	30.18	69.43	5.04	13.41	13.28	13.55	13.68	12.59	69.07
DPB93202	06/11/89	9.55	288.62	309.08	30.17	69.09	10.08	18.66	14.62	13.62	13.73	12.61	76.00
DPB93204	06/11/89	9.55	288.01	309.08	30.07	70.25	20.08	33.96	28.43	22.70	15.57	13.19	117.84
DPB93206	06/11/89	9.55	289.03	309.15	30.03	70.05	30.08	41.86	39.44	32.40	24.04	13.68	156.22
DPC93207	06/11/89	9.56	289.37	309.29	30.07	70.10	36.13	40.02	44.48	37.98	28.35	15.47	171.51
DPP93206	06/11/89	9.54	288.62	309.15	30.06	69.85	34.90	42.33	43.63	36.75	27.39	14.87	169.20
DPP93207	06/11/89	9.55	287.13	309.29	30.15	68.78	36.50	41.69	44.25	37.17	27.31	14.74	169.49
DPP93208	06/11/89	9.55	286.25	309.29	30.13	69.65	38.13	41.81	45.86	38.52	28.17	14.95	174.40
DPP93209	06/11/89	9.54	289.91	309.22	30.01	69.93	39.79	37.82	46.87	41.52	31.18	17.08	179.88
DPP93210	06/11/89	9.55	288.35	309.22	30.21	69.26	41.43	37.77	47.71	42.09	31.44	16.95	181.04
DPP93211	06/11/89	9.54	290.11	309.22	29.99	68.94	42.93	37.07	47.37	43.98	33.11	18.48	184.79
DPP93212	06/11/89	9.55	292.15	309.35	29.95	70.21	44.86	36.78	44.90	45.90	34.64	20.38	187.96
DPP93213	06/11/89	9.55	290.30	309.43	29.99	73.11	46.35	38.05	46.58	46.72	34.89	19.86	190.61
DPP93213	06/11/89	9.55	290.79	309.35	30.05	69.00	46.35	38.46	46.75	47.13	35.44	20.35	193.15
DPP93214	06/11/89	9.55	292.96	309.42	30.02	71.65	48.13	40.31	41.83	48.90	36.64	22.25	194.89
DPP93215	06/11/89	9.55	288.71	309.43	29.75	71.97	49.77	41.15	44.29	48.83	35.95	20.17	195.32
DPP93216	06/11/89	9.54	289.10	309.42	29.95	69.47	51.54	41.92	40.56	49.56	36.30	20.77	194.02
DPP93217	06/11/89	9.54	289.10	309.35	29.63	69.91	53.03	43.48	40.82	50.83	37.47	21.47	199.50
DPP93218	06/11/89	9.54	289.57	309.35	29.78	69.79	54.82	45.38	40.52	51.98	38.87	22.59	204.99
DPP93219	06/11/89	9.54	292.69	309.29	29.58	68.75	56.33	47.23	39.32	50.75	40.77	24.92	208.45
DPP93220	06/11/89	9.54	291.40	309.35	29.76	68.04	57.83	49.19	40.86	52.37	41.70	25.11	214.51
DPB92200	06/11/89	9.54	263.79	263.89	29.81	46.82	0.00	8.16	8.16	8.43	8.56	7.47	42.81
DPB92201	06/11/89	9.56	263.32	283.33	29.78	46.61	4.92	8.16	8.16	8.43	8.53	7.47	42.81

DPB92202	06/11/89	9.54	263.38	302.21	29.76	46.88	9.98	8.27	8.24	8.43	8.62	7.52	42.81
DPB92204	06/11/89	9.51	263.67	309.00	29.69	45.82	20.06	18.86	14.89	10.31	8.56	7.47	63.01
DPB92206	06/11/89	9.58	263.59	309.56	29.55	45.86	30.06	29.11	23.63	17.39	10.74	7.29	92.16
DPC92207	06/11/89	9.54	263.70	309.17	29.64	46.01	35.52	28.36	29.60	21.25	13.80	7.47	104.62
DPP92206	06/11/89	9.54	263.56	309.12	29.66	45.88	34.73	29.67	28.76	20.68	13.38	7.43	103.41
DPP92207	06/11/89	9.55	263.64	309.28	29.61	45.93	36.37	27.62	30.38	21.89	14.29	7.56	105.43
DPP92208	06/11/89	9.57	263.56	309.35	29.55	46.56	38.14	26.14	31.66	23.11	15.11	7.65	106.95
DPP92209	06/11/89	9.55	263.32	309.35	29.41	46.61	39.76	25.46	32.62	24.45	15.89	7.84	110.48
DPP92210	06/11/89	9.56	263.08	309.47	29.44	46.30	41.43	24.82	33.14	25.73	16.61	7.97	112.00
DPP92211	06/11/89	9.54	263.12	309.17	29.40	46.55	42.93	25.13	33.37	27.17	17.43	8.13	115.53
DPB91500	06/11/89	9.55	263.56	261.80	29.30	24.28	0.00	5.60	5.47	5.74	5.84	4.75	28.67
DPB91501	06/11/89	9.54	263.51	293.11	29.32	24.73	4.92	5.33	5.47	5.74	5.84	4.75	28.67
DPB91502	06/11/89	9.55	261.40	308.61	29.42	23.68	10.08	7.41	6.20	5.58	5.81	4.75	31.85
DPB91503	06/11/89	9.55	259.49	309.15	29.23	23.26	15.18	11.16	8.97	7.08	5.71	4.75	40.22
DPB91504	06/11/89	9.55	257.85	309.15	29.28	23.44	19.90	15.31	11.97	9.24	6.38	4.75	50.60
DPB91505	06/11/89	9.54	258.12	309.29	29.33	22.79	24.45	18.20	15.62	11.39	7.94	4.75	60.99
DPC91506	06/11/89	9.55	259.01	309.22	29.31	25.44	29.59	18.37	19.93	14.78	9.91	5.11	71.09
DPP91505	06/11/89	9.55	259.56	309.22	29.35	25.64	28.16	19.53	19.05	13.93	9.47	5.11	69.94
DPP91506	06/11/89	9.55	260.38	309.29	29.23	25.40	29.65	18.14	20.12	15.01	10.10	5.13	71.67
DPP91507	06/11/89	9.55	259.15	309.15	29.22	24.01	31.45	16.70	20.55	15.85	10.59	5.19	71.67
DPP91508	06/11/89	9.55	258.46	309.15	29.31	24.28	32.97	16.24	21.05	16.85	11.06	5.29	73.69
DPP91509	06/11/89	9.55	258.94	309.22	29.32	24.06	34.73	16.07	21.13	17.97	11.70	5.47	75.13
DPP91510	06/11/89	9.55	259.69	309.15	29.10	23.24	35.82	16.24	20.59	18.74	12.20	5.65	76.57
DPB98200	07/11/89	9.57	295.66	297.28	29.37	200.22	0.00	85.03	82.68	83.99	85.44	85.07	432.09
DPB98201	07/11/89	9.57	295.12	301.00	29.24	199.31	4.92	85.67	83.18	84.26	85.54	85.02	433.24
DPB98202	07/11/89	9.57	295.05	305.31	29.12	200.56	10.39	87.34	84.49	85.42	86.47	85.75	438.72
DPB98204	07/11/89	9.56	294.99	309.22	29.15	198.31	20.02	119.78	84.65	84.53	85.23	84.16	468.44
DPB98206	07/11/89	9.57	294.65	309.49	29.08	198.34	30.45	170.16	129.70	89.11	86.71	85.23	573.48
DPB98208	07/11/89	9.57	295.19	309.42	29.00	197.35	40.19	208.36	164.83	118.20	86.94	85.07	678.52
DPB98210	07/11/89	9.57	295.19	309.56	28.90	199.69	50.18	242.88	194.53	150.75	93.70	86.45	784.42
DPB98212	07/11/89	9.58	295.19	309.62	29.08	198.29	60.16	264.75	217.73	176.18	107.46	85.57	868.97
DPB98214	07/11/89	9.56	294.92	309.76	28.74	199.93	70.12	285.24	241.90	198.23	124.00	88.03	955.54
DPB98216	07/11/89	9.57	295.05	309.83	29.01	201.23	80.06	291.82	259.40	216.81	143.61	89.41	1021.91
DPB98218	07/11/89	9.57	295.19	309.89	28.84	197.49	89.96	281.43	261.83	226.43	160.44	89.23	1040.38
DPB98220	07/11/89	9.56	295.12	309.96	28.81	198.82	100.06	288.01	264.60	238.74	178.44	93.43	1084.24
DPC98221	07/11/89	9.57	295.19	310.03	28.80	198.81	108.01	286.33	257.36	238.93	189.11	96.84	1090.88
DPP98223	07/11/89	9.56	295.19	310.09	28.79	198.75	109.63	276.81	255.75	238.01	191.48	97.93	1080.78
DPP98224	07/11/89	9.56	295.05	310.23	28.83	199.34	111.29	265.61	257.17	238.93	194.49	99.59	1076.74
DPP98225	07/11/89	9.56	295.19	310.09	28.61	199.97	112.93	265.56	253.32	236.59	196.49	100.53	1074.43
DPP98226	07/11/89	9.57	295.12	310.16	28.68	200.43	114.71	265.61	247.01	234.01	199.32	102.11	1067.79
DPP98227	07/11/89	9.57	294.99	310.30	28.63	202.10	116.35	271.44	233.47	230.70	201.84	103.62	1062.31
DPP98228	07/11/89	9.56	294.85	310.30	28.75	203.37	118.13	281.08	199.30	227.58	204.59	105.36	1040.38
DPB90200	07/11/89	9.60	295.53	297.15	28.53	235.33	0.00	114.99	111.81	113.08	116.34	113.28	576.95
DPB90201	07/11/89	9.57	295.66	301.00	28.65	235.31	5.19	115.68	112.00	113.12	116.45	112.65	576.95
DPB90202	07/11/89	9.58	295.59	304.64	28.70	233.30	10.23	115.27	111.73	112.66	115.82	111.49	574.64
DPB90204	07/11/89	9.55	295.66	309.35	28.65	231.30	20.23	138.30	112.43	112.81	115.41	110.78	597.15
DPB90206	07/11/89	9.57	295.53	309.49	28.44	234.62	30.20	211.08	145.82	117.20	119.30	114.13	719.50
DPB90208	07/11/89	9.62	295.86	309.89	28.49	233.32	40.19	258.06	197.73	128.82	119.02	113.36	829.44
DPB90210	07/11/89	9.56	295.19	309.49	28.59	235.57	50.04	302.67	236.32	161.79	121.46	115.36	950.64
DPB90212	07/11/89	9.57	295.66	309.69	28.73	233.38	59.61	334.12	265.75	197.99	124.31	114.24	1052.50
DPB90214	07/11/89	9.56	295.53	309.56	28.70	233.44	69.69	360.61	292.91	228.97	134.60	114.06	1147.15
DPB90216	07/11/89	9.58	295.26	309.83	28.69	235.07	79.84	383.70	319.31	255.52	149.58	116.13	1242.37
DPB90218	07/11/89	9.57	295.66	309.89	28.73	232.93	89.69	391.37	337.97	277.72	170.07	115.67	1312.21
DPB90220	07/11/89	9.57	295.66	310.03	28.83	234.38	99.67	398.70	354.90	297.22	188.72	117.61	1377.13
DPB90222	07/11/89	9.57	295.66	310.30	28.82	234.42	110.02	402.51	362.48	312.23	209.34	119.12	1426.77
DPB90224	07/11/89	9.56	295.66	310.30	28.68	233.65	119.90	409.72	360.82	321.85	229.16	122.11	1464.57
DPB90226	07/11/89	9.57	295.66	310.50	28.75	234.10	130.02	421.61	353.93	321.12	245.44	125.85	1489.10
DPC90227	07/11/89	9.57	295.46	310.36	28.56	235.86	137.91	434.37	312.50	304.03	260.35	131.04	1464.86
DPP90228	07/11/89	9.56	295.46	310.43	28.63	235.72	137.93	432.00	295.99	302.57	260.19	130.94	1443.79

DPP90229	07/11/89	9.57	295.39	310.50	28.38	233.91	138.11	431.94	269.60	279.02	260.35	131.02	1394.16
DPB97100	23/11/89	9.58	305.52	307.00	27.94	174.98	0.00	67.20	-	-	-	-	-
DPB97101	23/11/89	9.59	305.04	309.62	28.14	173.75	4.92	76.09	-	-	-	-	-
DPB97102	23/11/89	9.56	304.64	309.56	28.03	173.75	10.33	103.73	-	-	-	-	-
DPB97104	23/11/89	9.59	305.11	309.89	28.30	173.96	20.23	142.63	-	-	-	-	-
DPB97106	23/11/89	9.59	305.18	309.96	28.41	175.10	29.94	176.85	-	-	-	-	-
DPB97108	23/11/89	9.58	305.11	309.96	28.58	173.85	40.27	200.98	-	-	-	-	-
DPB97110	23/11/89	9.59	305.11	309.96	28.66	174.69	50.04	217.66	-	-	-	-	-
DPB97112	23/11/89	9.59	305.11	310.03	28.70	173.46	60.43	220.54	-	-	-	-	-
DPB97114	23/11/89	9.59	305.18	310.16	28.50	173.56	70.96	219.16	-	-	-	-	-
DPB97116	23/11/89	9.58	305.25	310.30	28.43	175.33	80.12	227.76	-	-	-	-	-
DPC97117	23/11/89	9.59	305.11	310.30	28.38	175.25	86.31	226.77	-	-	-	-	-
DPP97116	23/11/89	9.58	305.31	310.30	28.45	174.72	85.00	228.45	-	-	-	-	-
DPP97117	23/11/89	9.59	305.11	310.30	28.39	175.28	86.68	226.14	-	-	-	-	-
DPP97118	23/11/89	9.59	305.04	310.30	28.45	175.42	88.24	218.64	-	-	-	-	-
DPP97119	23/11/89	9.58	305.04	310.30	28.42	174.88	89.84	211.25	-	-	-	-	-
DPP97120	23/11/89	9.60	304.98	310.30	28.54	175.38	91.60	209.00	-	-	-	-	-
DPP97121	23/11/89	9.60	304.84	310.30	28.49	176.36	93.22	208.31	-	-	-	-	-
DPP97123	23/11/89	9.58	305.11	310.30	28.42	176.57	94.88	206.58	-	-	-	-	-
DPP97124	23/11/89	9.59	305.25	310.30	28.47	175.82	96.52	208.36	-	-	-	-	-
DPP97125	23/11/89	9.60	304.98	310.30	28.42	175.47	98.16	212.00	-	-	-	-	-
DPP97126	23/11/89	9.58	305.04	310.30	28.50	175.48	99.84	217.94	-	-	-	-	-
DPP97127	23/11/89	9.60	305.11	310.36	28.55	175.67	101.72	222.56	-	-	-	-	-
DPP97128	23/11/89	9.57	304.71	310.30	28.48	176.64	103.22	228.62	-	-	-	-	-
DPP97129	23/11/89	9.60	305.11	310.43	28.51	176.68	104.84	234.28	-	-	-	-	-
DPB97300	23/11/89	9.59	282.79	284.22	28.73	173.45	0.00	63.85	-	-	-	-	-
DPB97301	23/11/89	9.59	282.52	289.50	28.81	176.86	5.27	65.93	-	-	-	-	-
DPB97302	23/11/89	9.59	282.79	294.58	29.02	175.59	10.21	66.45	-	-	-	-	-
DPB97304	23/11/89	9.60	282.72	304.17	28.79	173.76	20.10	66.74	-	-	-	-	-
DPB97306	23/11/89	9.60	282.79	309.89	28.53	175.54	30.08	88.03	-	-	-	-	-
DPB97308	23/11/89	9.59	282.66	309.89	28.96	170.69	40.06	134.38	-	-	-	-	-
DPB97308	23/11/89	9.60	282.38	309.96	28.81	173.26	40.08	135.24	-	-	-	-	-
DPB97310	23/11/89	9.59	282.59	309.89	28.76	175.09	50.04	170.04	-	-	-	-	-
DPB97312	23/11/89	9.59	282.59	310.03	28.77	175.89	60.43	200.69	-	-	-	-	-
DPB97314	23/11/89	9.59	282.38	309.96	28.51	173.10	69.84	213.79	-	-	-	-	-
DPB97316	23/11/89	9.60	283.06	310.30	29.02	175.63	80.18	223.43	-	-	-	-	-
DPB97318	23/11/89	9.58	282.38	310.23	29.05	174.66	90.51	218.69	-	-	-	-	-
DPC97319	23/11/89	9.58	282.38	310.30	29.02	173.02	95.84	213.56	-	-	-	-	-
DPP97318	23/11/89	9.60	282.38	310.30	29.08	173.43	95.02	214.02	-	-	-	-	-
DPP97318	23/11/89	9.59	282.38	310.30	28.87	175.79	96.80	219.10	-	-	-	-	-
DPP97318	23/11/89	9.58	282.45	310.30	28.94	175.81	98.42	209.17	-	-	-	-	-
DPP97320	23/11/89	9.58	282.38	310.30	28.94	175.07	100.08	194.40	-	-	-	-	-
DPP97321	23/11/89	9.59	282.45	310.30	29.05	175.37	101.74	184.18	-	-	-	-	-
DPP97322	23/11/89	9.58	282.38	310.30	29.06	175.75	103.36	178.47	-	-	-	-	-
DPP97323	23/11/89	9.59	282.38	310.30	29.10	176.01	105.02	176.97	-	-	-	-	-
DPP97324	23/11/89	9.59	282.38	310.30	29.39	174.27	105.47	176.33	-	-	-	-	-
DPB97500	23/11/89	9.35	255.65	257.02	28.61	176.43	0.00	61.95	-	-	-	-	-
DPB97501	23/11/89	9.39	254.42	261.26	28.75	174.57	5.04	61.60	-	-	-	-	-
DPB97502	23/11/89	9.53	254.01	267.55	29.12	172.85	10.94	61.08	-	-	-	-	-
DPB97502	23/11/89	9.59	254.22	267.62	29.02	173.59	10.96	61.37	-	-	-	-	-
DPB97504	23/11/89	9.63	254.90	277.97	28.96	174.35	19.92	63.33	-	-	-	-	-
DPB97506	23/11/89	9.60	255.52	289.03	29.00	175.57	30.06	65.24	-	-	-	-	-
DPB97508	23/11/89	9.59	255.52	298.84	28.65	174.03	39.77	65.87	-	-	-	-	-
DPB97510	23/11/89	9.59	255.52	308.82	28.58	174.35	50.43	72.16	-	-	-	-	-
DPB97512	23/11/89	9.59	255.77	309.83	28.46	186.78	59.88	106.13	-	-	-	-	-
DPB97512	23/11/89	9.60	254.01	309.83	28.59	176.27	60.29	104.31	-	-	-	-	-
DPB97514	23/11/89	9.57	255.65	309.83	28.63	172.71	70.55	157.00	-	-	-	-	-
DPB97514	23/11/89	9.58	255.65	309.83	28.65	173.62	70.55	157.29	-	-	-	-	-
DPB97514	23/11/89	9.58	255.24	309.83	28.88	172.71	80.12	182.05	-	-	-	-	-

DPB97514	23/11/89	9.58	255.38	309.83	28.91	172.10	80.18	181.99	-	-	-	-	-
DPB97516	23/11/89	9.59	255.18	309.89	28.92	172.93	89.96	200.75	-	-	-	-	-
DPB97520	23/11/89	9.59	255.59	310.09	29.14	173.55	100.00	200.00	-	-	-	-	-
DPC97521	23/11/89	9.58	255.65	310.03	29.08	173.95	103.14	190.59	-	-	-	-	-
DPP97520	23/11/89	9.58	255.65	309.96	29.20	173.88	101.86	196.42	-	-	-	-	-
DPP97521	23/11/89	9.59	255.65	310.16	29.25	173.52	103.13	189.26	-	-	-	-	-
DPP97522	23/11/89	9.59	255.65	310.16	29.37	174.09	104.18	187.88	-	-	-	-	-
DPP97523	23/11/89	9.58	255.72	310.23	29.47	174.84	105.02	177.43	-	-	-	-	-
DPP97524	23/11/89	9.59	256.00	310.30	29.44	175.36	105.94	168.14	-	-	-	-	-
Heat Bal	22/11/89	9.60	204.98	204.01	30.01	23.34	0.00	6.20	-	-	-	-	-
Heat Bal	22/11/89	9.60	204.70	237.67	29.46	23.21	4.92	6.14	-	-	-	-	-
Heat Bal	22/11/89	9.61	204.50	271.09	29.55	23.21	10.12	6.02	-	-	-	-	-
Heat Bal	22/11/89	9.60	204.90	294.72	29.62	25.58	15.20	6.14	-	-	-	-	-
Heat Bal	22/11/89	9.60	204.98	309.35	29.10	25.34	19.82	8.97	-	-	-	-	-
Heat Bal	22/11/89	9.60	204.98	309.83	29.04	23.68	25.29	13.81	-	-	-	-	-
Heat Bal	22/11/89	9.35	221.21	221.13	29.21	68.14	0.00	13.14	-	-	-	-	-
Heat Bal	22/11/89	9.43	221.94	238.44	29.17	66.68	5.19	12.94	-	-	-	-	-
Heat Bal	22/11/89	9.64	222.67	252.42	28.99	71.38	10.15	13.92	-	-	-	-	-
Heat Bal	22/11/89	9.68	222.91	253.19	29.02	70.58	10.18	13.76	-	-	-	-	-
Heat Bal	22/11/89	9.62	222.98	268.09	28.92	71.38	15.59	14.10	-	-	-	-	-
Heat Bal	22/11/89	9.60	223.31	282.07	28.99	70.41	20.64	14.08	-	-	-	-	-
Heat Bal	22/11/89	9.60	223.39	295.66	29.12	69.00	25.29	13.76	-	-	-	-	-
Heat Bal	22/11/89	9.60	223.88	307.94	28.98	69.16	30.19	15.83	-	-	-	-	-
Heat Bal	22/11/89	9.60	224.36	309.83	28.96	71.25	34.86	23.74	-	-	-	-	-
Heat Bal	22/11/89	9.14	229.95	230.64	29.16	114.46	0.00	27.49	-	-	-	-	-
Heat Bal	22/11/89	9.10	229.67	239.80	29.22	115.39	5.16	28.01	-	-	-	-	-
Heat Bal	22/11/89	9.15	229.67	249.42	29.16	115.75	10.39	28.36	-	-	-	-	-
Heat Bal	22/11/89	9.26	229.67	257.78	29.05	116.14	15.16	28.70	-	-	-	-	-
Heat Bal	22/11/89	9.39	229.67	265.91	29.07	116.11	19.96	29.11	-	-	-	-	-
Heat Bal	22/11/89	9.56	229.67	274.57	29.03	115.65	25.02	29.17	-	-	-	-	-
Heat Bal	22/11/89	9.67	229.67	283.33	29.00	115.23	30.16	29.57	-	-	-	-	-
Heat Bal	22/11/89	9.49	230.09	290.72	29.07	115.27	34.55	29.86	-	-	-	-	-
Heat Bal	22/11/89	9.69	230.64	300.46	29.02	115.35	40.47	30.32	-	-	-	-	-
Heat Bal	22/11/89	9.61	231.60	308.21	29.08	115.13	45.21	33.96	-	-	-	-	-
Heat Bal	22/11/89	9.59	231.81	309.83	29.02	114.42	50.02	46.42	-	-	-	-	-
Heat Bal	22/11/89	8.91	231.60	232.57	28.82	164.58	0.00	53.98	-	-	-	-	-
Heat Bal	22/11/89	8.92	231.60	238.90	28.68	163.20	5.14	53.98	-	-	-	-	-
Heat Bal	22/11/89	8.99	231.60	245.09	28.68	164.27	9.98	54.50	-	-	-	-	-
Heat Bal	22/11/89	9.11	231.60	251.34	28.63	163.97	15.04	54.67	-	-	-	-	-
Heat Bal	22/11/89	9.37	231.60	257.91	28.71	164.21	20.37	54.96	-	-	-	-	-
Heat Bal	22/11/89	9.67	232.57	264.55	28.52	162.92	25.16	55.31	-	-	-	-	-
Heat Bal	22/11/89	9.35	233.53	271.57	28.50	164.83	30.63	56.87	-	-	-	-	-
Heat Bal	22/11/89	9.39	234.91	277.90	28.66	165.83	35.10	57.73	-	-	-	-	-
Heat Bal	22/11/89	9.54	234.98	283.60	28.52	164.88	40.16	58.02	-	-	-	-	-
Heat Bal	22/11/89	9.70	234.98	288.96	28.51	164.27	44.98	58.60	-	-	-	-	-
Heat Bal	22/11/89	9.61	235.74	295.59	28.55	163.93	50.43	59.23	-	-	-	-	-
Heat Bal	22/11/89	9.60	236.56	301.40	28.53	163.30	54.96	59.64	-	-	-	-	-
Heat Bal	22/11/89	9.61	236.91	306.66	28.64	163.18	60.02	62.87	-	-	-	-	-
Heat Bal	22/11/89	9.60	236.91	309.83	28.61	163.25	65.20	74.47	-	-	-	-	-
Heat Bal	22/11/89	8.81	232.78	233.95	28.45	213.57	0.00	86.94	-	-	-	-	-
Heat Bal	22/11/89	8.83	232.43	238.63	28.33	214.34	5.14	87.40	-	-	-	-	-
Heat Bal	22/11/89	8.94	232.29	243.44	28.38	214.12	10.37	87.80	-	-	-	-	-
Heat Bal	22/11/89	9.09	232.36	248.73	28.31	211.94	15.72	86.88	-	-	-	-	-
Heat Bal	22/11/89	9.37	233.12	253.87	28.32	208.82	20.10	85.32	-	-	-	-	-
Heat Bal	22/11/89	9.65	234.50	260.44	28.42	209.57	25.82	86.53	-	-	-	-	-
Heat Bal	22/11/89	9.45	235.81	266.46	28.39	209.37	30.86	87.34	-	-	-	-	-
Heat Bal	22/11/89	9.66	237.05	276.06	28.36	209.79	40.04	88.55	-	-	-	-	-
Heat Bal	22/11/89	9.61	237.18	280.89	28.30	208.10	45.25	89.25	-	-	-	-	-
Heat Bal	22/11/89	9.62	238.01	286.52	28.28	208.83	50.68	90.00	-	-	-	-	-

Heat Bal	22/11/89	9.60	238.15	286.59	28.33	209.98	50.70	90.57	-	-	-	-	-
Heat Bal	22/11/89	9.60	238.42	290.86	28.33	209.63	55.51	91.15	-	-	-	-	-
Heat Bal	22/11/89	9.60	238.35	295.73	28.38	208.31	61.11	91.67	-	-	-	-	-
Heat Bal	22/11/89	9.60	238.56	298.50	28.39	210.63	65.22	94.09	-	-	-	-	-
Heat Bal	22/11/89	9.60	238.49	298.57	28.38	210.99	65.22	94.44	-	-	-	-	-
Heat Bal	22/11/89	9.60	238.56	302.48	28.24	210.84	70.08	95.71	-	-	-	-	-
Heat Bal	22/11/89	9.60	238.63	306.66	28.42	210.52	75.06	98.82	-	-	-	-	-
Heat Bal	22/11/89	9.60	238.70	309.83	28.48	210.22	79.92	109.16	-	-	-	-	-
Heat Bal	22/11/89	8.53	231.67	233.05	28.81	258.70	0.00	123.99	-	-	-	-	-
Heat Bal	22/11/89	8.61	231.67	237.39	28.84	257.95	5.47	123.35	-	-	-	-	-
Heat Bal	22/11/89	8.69	231.60	241.11	28.91	256.34	10.25	123.70	-	-	-	-	-
Heat Bal	22/11/89	8.85	231.95	245.37	28.93	257.18	15.04	124.34	-	-	-	-	-
Heat Bal	22/11/89	9.01	232.71	249.90	28.87	257.18	20.00	124.34	-	-	-	-	-
Heat Bal	22/11/89	9.23	233.47	254.83	28.80	257.55	25.37	125.84	-	-	-	-	-
Heat Bal	22/11/89	9.53	234.70	259.97	28.79	254.23	30.33	123.76	-	-	-	-	-
Heat Bal	22/11/89	9.69	235.74	260.72	28.81	255.62	30.31	125.84	-	-	-	-	-
Heat Bal	22/11/89	9.26	237.67	266.32	28.56	255.49	35.00	125.55	-	-	-	-	-
Heat Bal	22/11/89	9.32	237.18	269.73	28.56	254.58	40.02	126.76	-	-	-	-	-
Heat Bal	22/11/89	9.45	237.46	273.27	28.52	257.95	45.00	129.99	-	-	-	-	-
Heat Bal	22/11/89	9.64	238.22	277.97	28.45	257.70	50.43	130.80	-	-	-	-	-
Heat Bal	22/11/89	9.65	238.90	282.32	28.45	256.76	55.23	131.26	-	-	-	-	-
Heat Bal	22/11/89	9.60	239.94	286.59	28.46	256.00	59.88	132.07	-	-	-	-	-
Heat Bal	22/11/89	9.60	240.14	290.72	28.36	255.62	65.63	133.40	-	-	-	-	-
Heat Bal	22/11/89	9.60	240.21	294.04	28.31	256.84	70.27	134.32	-	-	-	-	-
Heat Bal	22/11/89	9.60	240.14	297.28	28.29	258.08	75.74	136.74	-	-	-	-	-
Heat Bal	22/11/89	9.59	240.21	300.25	28.38	258.53	80.25	138.59	-	-	-	-	-
Heat Bal	22/11/89	9.60	240.35	303.56	28.39	258.47	85.18	140.49	-	-	-	-	-
Heat Bal	22/11/89	9.60	240.35	306.93	28.46	257.57	90.04	143.73	-	-	-	-	-
Heat Bal	22/11/89	9.60	240.21	309.62	28.50	257.47	95.57	156.65	-	-	-	-	-

III. CALIBRATION OF EQUIPMENT AND CORRECTION TO MEASUREMENTS

III.1 CALIBRATION OF THERMOCOUPLES MEASURING BULK-FLUID TEMPERATURES

The Chromel-Alumel (K-type) thermocouples were used to measure the bulk-fluid temperatures at both the inlet and the outlet, and the surface temperatures at various locations along the test section. All of them were the ungrounded type, of which the chromel and alumel wires are packed with magnesium oxide inside a stainless-steel sheath. This type of thermocouple shields the wires from the high voltage exhibited by the test section during experiment, and hence reduces the interference to the recording signal. During operation, the voltage difference, V, in (mV) between the two wires is recorded, and converted into temperature readings with

$$\begin{aligned} T = {} & 0.226584602 + 24152.109\ V + 67233.4248\ V^2 + 2210340.682\ V^3 \\ & - 860963914.9\ V^4 + 4.83506x10^{10}\ V^5 - 1.18452x10^{12}\ V^6 \\ & + 1.3869x10^{13}\ V^7 - 6.33708x10^{13}\ V^8 \end{aligned} \qquad \text{(III.1)}$$

The thermocouple used to measure the bulk-fluid temperature at the inlet (identified as #1525) was 15.25 cm long, and its outer diameter was 0.32 cm. It was inserted into the flow through a Swagelok fitting at a distance of 0.470 m upstream of the heated section (see Figure III.1). Before installation, this thermocouple was calibrated for the ranges of temperature between 100 and 400°C at a 100°C increments, and the maximum deviation was 0.5°C. After the experiment, it was re-calibrated over the test ranges of 200 to 400°C at a 20°C intervals using a JOFRA temperature calibrator (Model 650SE, S/N 92157). Table III.1 shows the measurements taken from the re-calibration of this thermocouple. The recorded readings were slightly lower than the actual (i.e., calibrated) temperatures.

At the outlet of the test section, the thermocouple identified as #1718 was used for measuring the bulk-fluid temperature. It was 30.5 cm long and 0.16 cm in diameter. This thermocouple was installed at a distance of 0.485 m from the end of the heated section (see Figure III.1). Before the installation, it was calibrated at an interval of 100°C over the range of 8.5 to 406.5°C with a maximum deviation of 1°C. It was also re-calibrated with the JOFRA temperature calibrator over the ranges of 200 to

Table III.1: Calibration of Inlet Thermocouple

Actual Temperature (°C)	Measured Temperature (°C)	Difference (°C)
200	199.6	-0.4
220	219.3	-0.7
240	239.3	-0.7
260	259.4	-0.6
280	279.4	-0.6
300	299.3	-0.7
320	319.2	-0.8
340	339.1	-0.9
360	358.9	-1.1
380	378.9	-1.1
400	398.7	-1.3

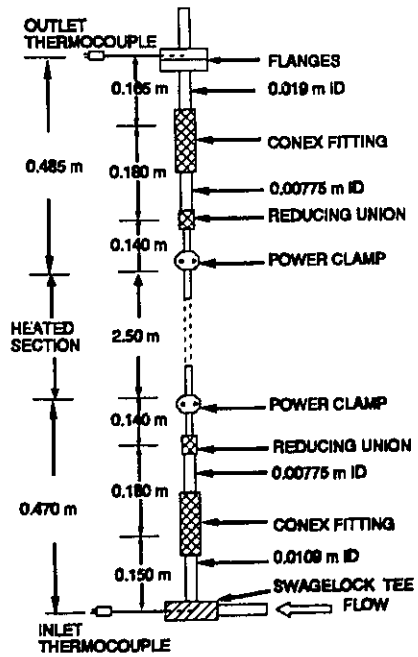

Figure III.1: Locations of Thermocouples Measuring Bulk-Fluid Temperatures.

400°C at increments of 20°C after the completion of the experiment. As shown in Table III.2, the measurements were higher than the actual temperature.

Although differences between the measured and the reference temperatures are small, these calibrations were used to correct the measured temperatures. The measurements of bulk-fluid temperature for adiabatic flow (i.e., no power is applied to the test section) were then used to confirm the validity of these corrections during operation. Figure III.2 shows the temperature

Table III.2: Calibration of Outlet Thermocouple.

Actual Temperature (°C)	Measured Temperature (°C)	Difference (°C)
200	201.6	1.6
220	221.4	1.4
240	241.6	1.6
260	261.6	1.6
280	282.0	2.0
300	302.0	2.0
320	322.1	2.1
340	342.1	2.1
360	362.2	2.2
380	382.4	2.4
400	402.6	2.6

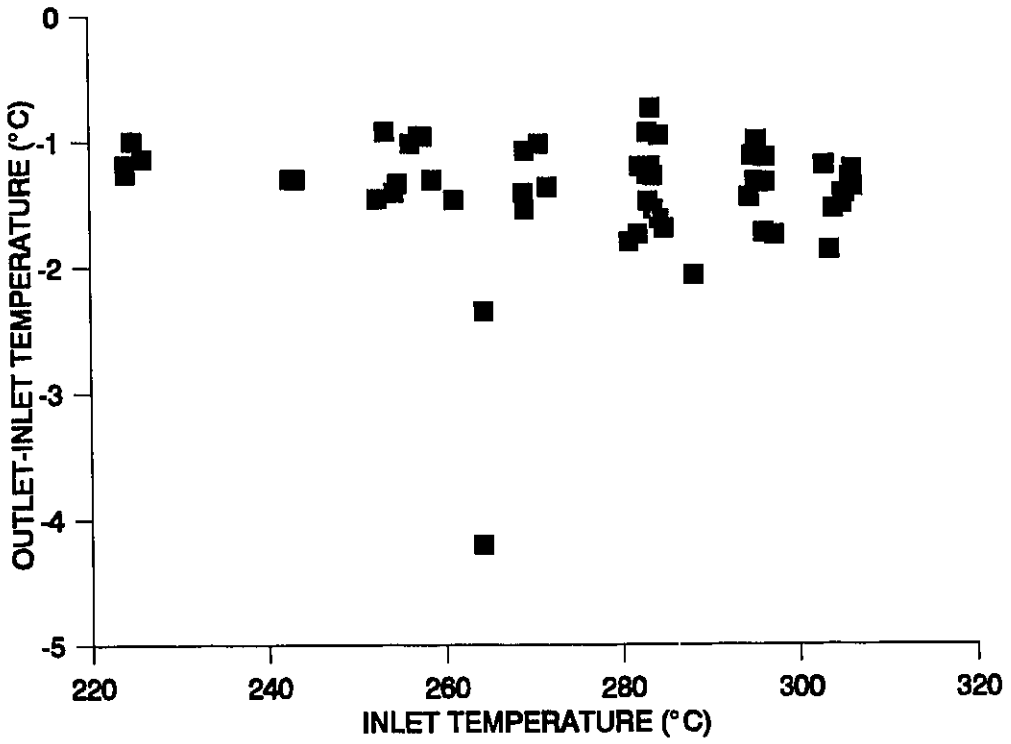

Figure III.2: Difference in Measured Temperature Between the Inlet and the Outlet Thermocouples.

difference between the outlet and inlet flows. A constant offset of about 1°C is noted in the results. While heat loss is anticipated, a drop of 1°C over the test section seems to be exaggerated. The difference is also presented in Figure III.3 as a function of the bulk-fluid Reynolds number

$$Re_b = \frac{G\ D}{\mu_b} \tag{III.2}$$

where G is the mass flux of fluid in $kg.m^{-2}.s^{-1}$, D is the inside diameter of the tube in m and μ_b is the bulk-fluid dynamic viscosity in $kg.m^{-1}.s^{-1}$. Since the temperature difference should

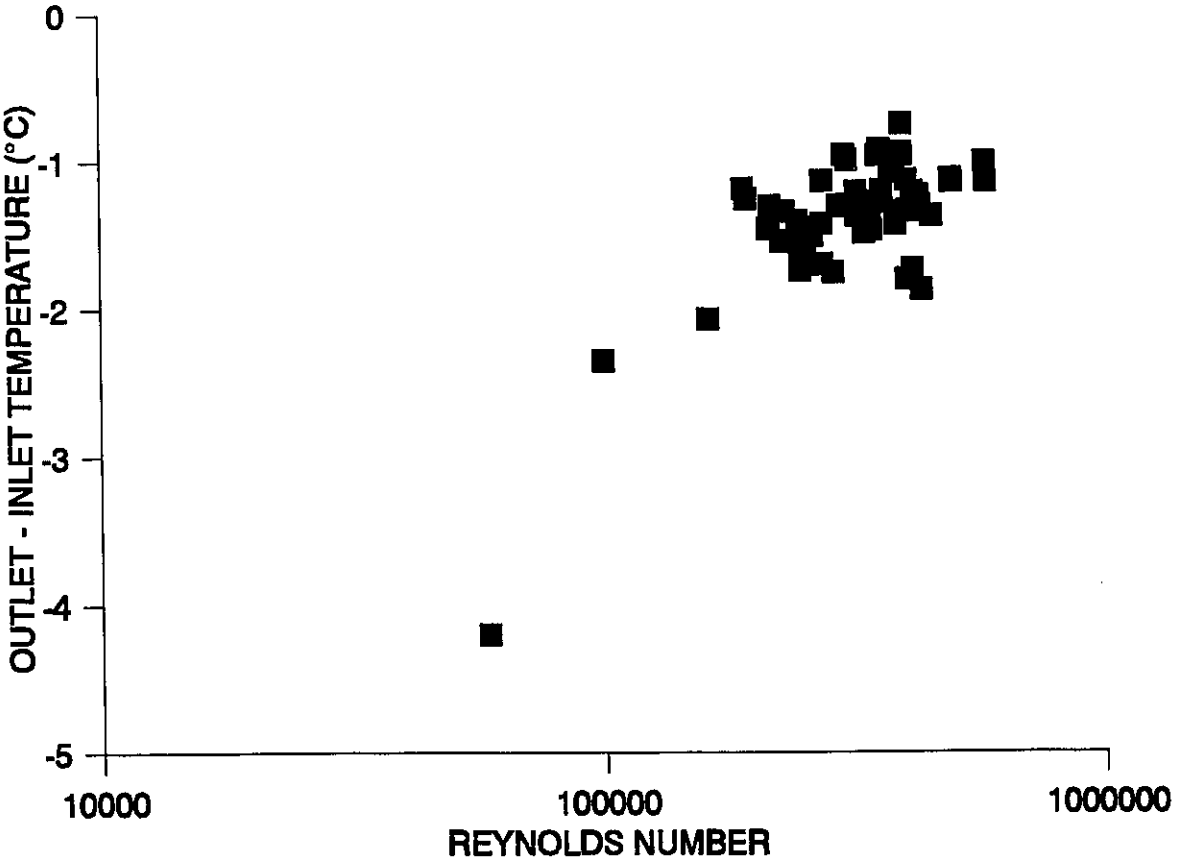

Figure III.3: Temperature Drop over the Test Section at Adiabatic Flow as a function of Reynolds Number.

approach 0 at high Reynolds numbers, the correction based on calibrated results may not be valid for the operating conditions.

A correction factor to the thermocouple's reading is derived from the results of adiabatic flow. It is applied to the outlet thermocouple, which has been shown from the calibration to have higher uncertainty than the inlet thermocouple. Figure III.4 shows the difference in measurements between the outlet and the inlet thermocouples as a function of the outlet temperature. Note that no correction is applied to the measurements. A linear relation between the temperature difference and the outlet temperature is derived by optimising the data with the largest difference. It is also shown in Figure III.4 and is expressed as

$$T_{out} - T_{in} = 0.0058\ T_{out} \qquad \text{(III.3)}$$

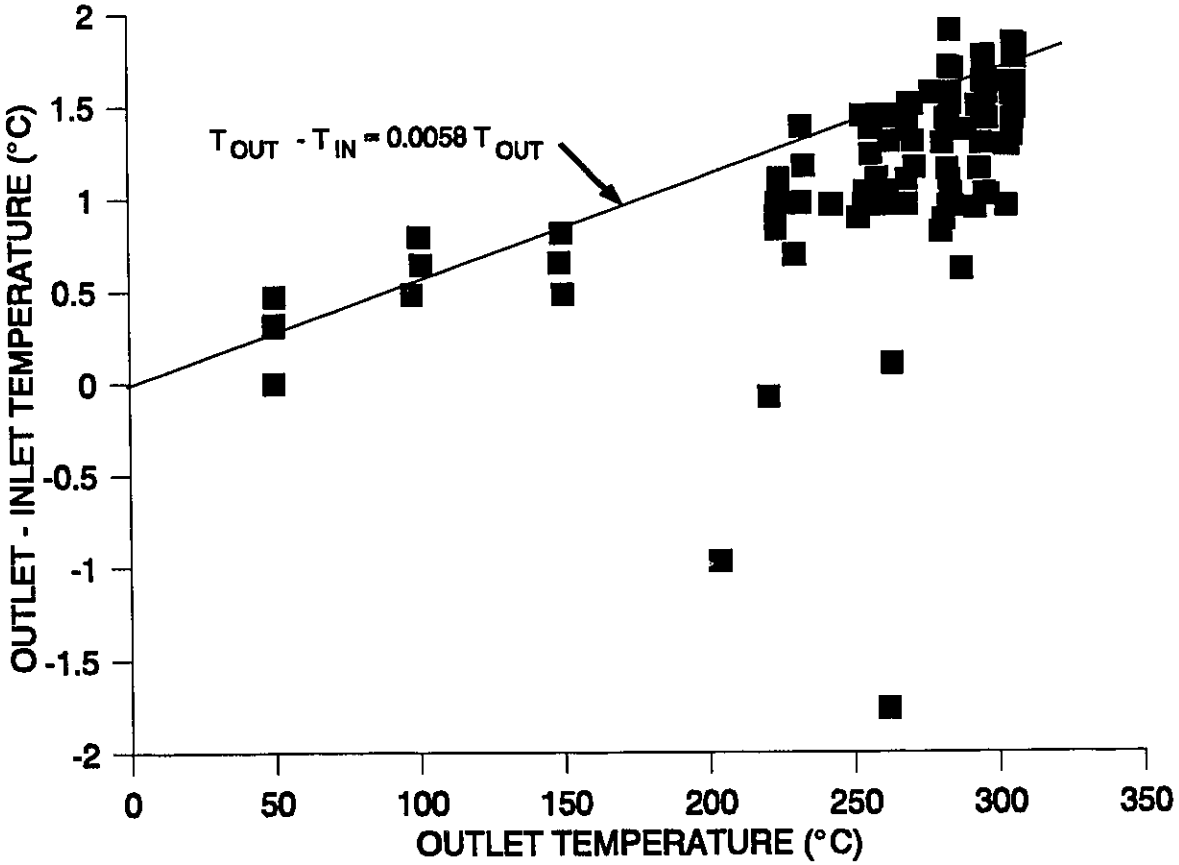

Figure III.4: Difference in Measured Temperature Between Inlet and Outlet Thermocouples.

The largest difference is selected as the criterion, because it provides the maximum correction, which represents the ideal case of negligible heat loss from the test section. Over the range of operating temperature (i.e., between 220 and 320°C), the correction varies from 1.3 to 1.9°C, which is similar to results from the calibration (see Table III.2). Unless specified, the outlet temperature, as indicated from here on, represents the corrected value based on Equation (III.3);

$$T_{out,act.} = 0.9942\ T_{out,meas.} \tag{III.4}$$

III.2 CALCULATION OF POWER LOSS FROM TEST SECTION AND POWER-SOURCE CONNECTORS

Part of the power applied to the test section was lost through the insulation, the connecting cables, and the power clamps. While the power loss through the insulation is expected to be small, the other two components can be quite significant. In this study, no attempt is made to separate the individual loss in the heated section, but the overall power loss is calculated and correlated in terms of the applied power.

The differences between outlet and inlet temperatures in adiabatic flow were examined to assess the heat loss through insulation. They are shown in Figure III.5 and appear to have no definite trend as a function of the mean bulk-fluid temperature. Negative value signifies heat loss in the test section. While the data ranged between -3.5°C and 0.5°C, a majority of them lie within the range of -1 to 0°C. Figure III.6 shows the data with respect to the Reynolds number. The temperature difference is large for the flow of low Reynolds numbers and asymptotically approaches 0 as the Reynolds number increases. When the temperature difference is expressed in terms of heat loss, the dependence on the Reynolds number is not indicated in Figure III.7. Note that heat gain is calculated with

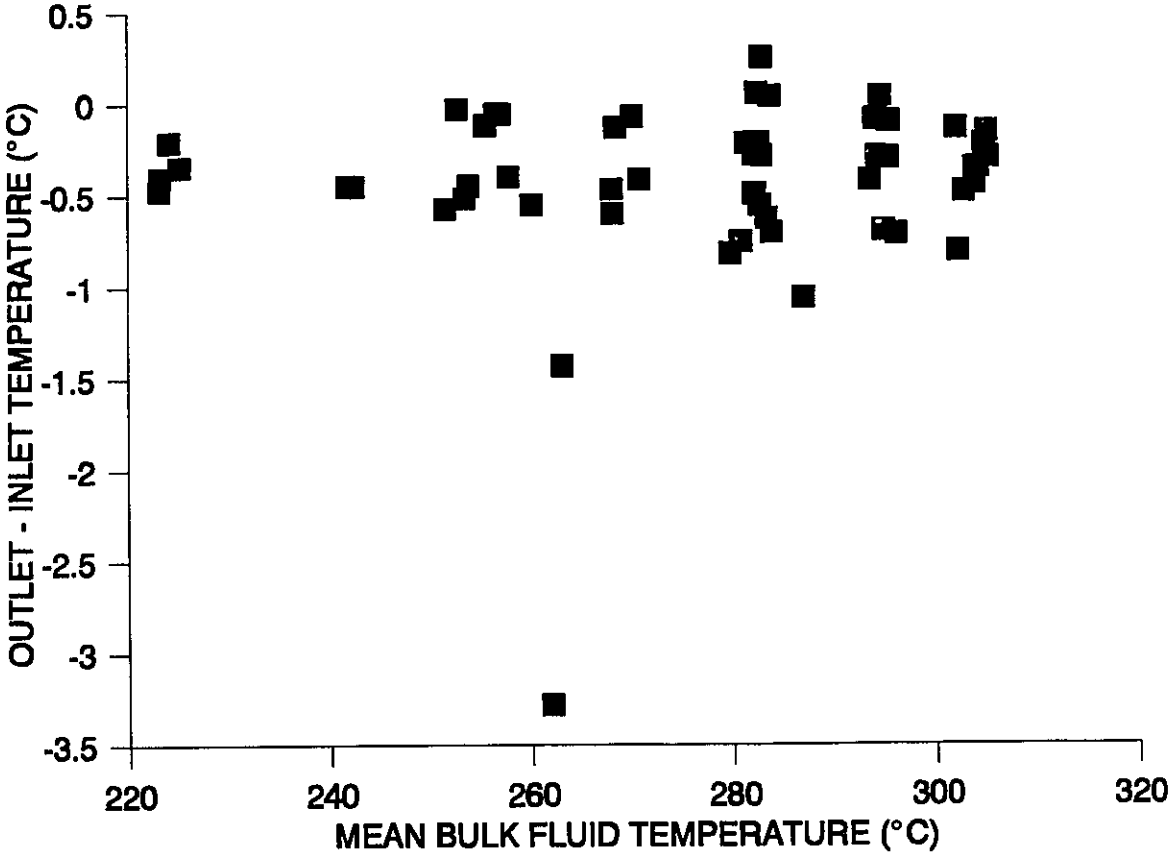

Figure III.5: Differences Between Inlet and Outlet Temperatures.

$$Heat\ Gain = (H_{out} - H_{in})W \tag{III.5}$$

where W is the mass flow rate in $kg.m^{-1}$, and H_{in} and H_{out} are the fluid-enthalpy values in $J.kg^{-1}$ at the inlet and outlet, respectively. Negative values signify heat loss from the test section through the insulation. No specific trend is displayed for the heat loss either when plotted as a function of temperature (Figure III.8). The results scatter over the range of -0.5 and 0.5 kW. Hence, the heat loss at adiabatic flow can be considered to be negligible.

The correction factor for the outlet thermocouple is derived based on the criterion that the minimum drop in fluid temperature over the test section is 0. A simple one-dimensional analysis of heat transfer by conduction is carried out to justify this limit. It considers that heat is

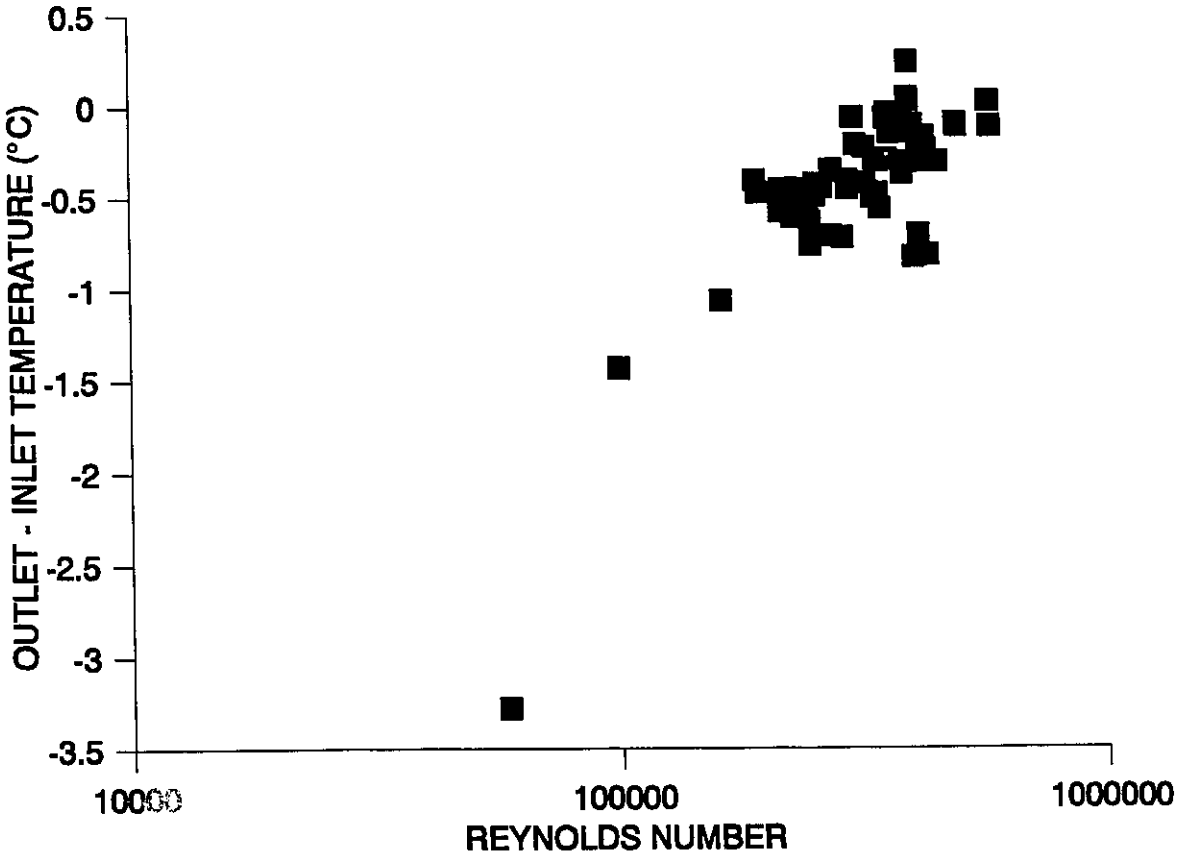

Figure III.6: Difference Between Inlet and Outlet Temperatures as a function of Reynolds Number.

transferred from

i) the fluid to the inner channel wall (through forced convection),

ii) the inner to the outer channel wall (through conduction),

iii) the outer channel wall to the outer surface of a 3.81-cm thick insulation (through conduction), and

iv) the outer surface of the insulation to the environment (through natural convection).

The basic assumptions employed in this analysis are that

i) heat is transferred through the radial direction only (no axial heat transfer),

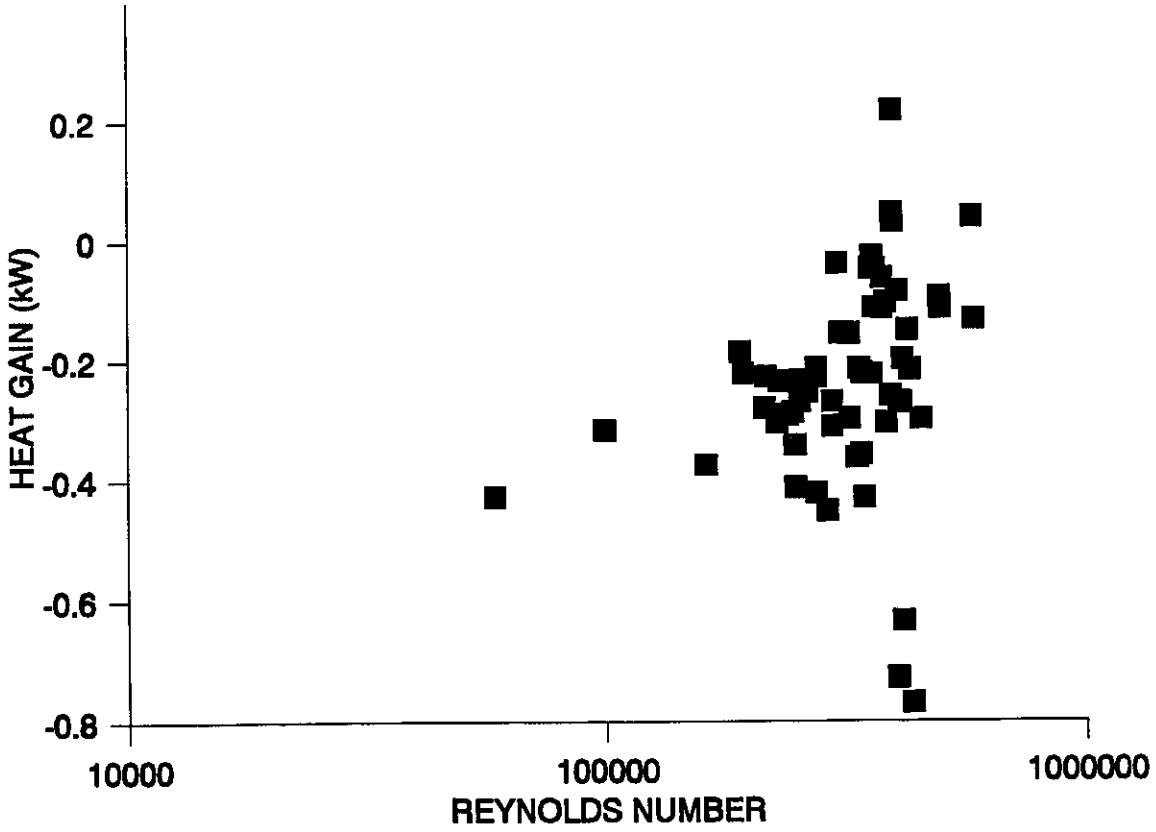

Figure III.7: Heat Loss from the Test Section in Adiabatic Flow.

ii) the thermal expansion of the test section is negligible,

iii) heat transfer by radiation is neglected, since the surface of the insulation is covered with an aluminum-foil paper, and

iv) fluid properties are constant.

The axial length of the test section was sub-divided into 10 sections, so that the temperature drop in each section can be considered negligible, to ensure the validity of the last assumption. In each section, the heat loss, Q, is presented in Equations (III.6) to (III.9) (see Figure III.9).

At the inner tube surface, the heat is transferred through forced convection from the fluid to the surface and is expressed as

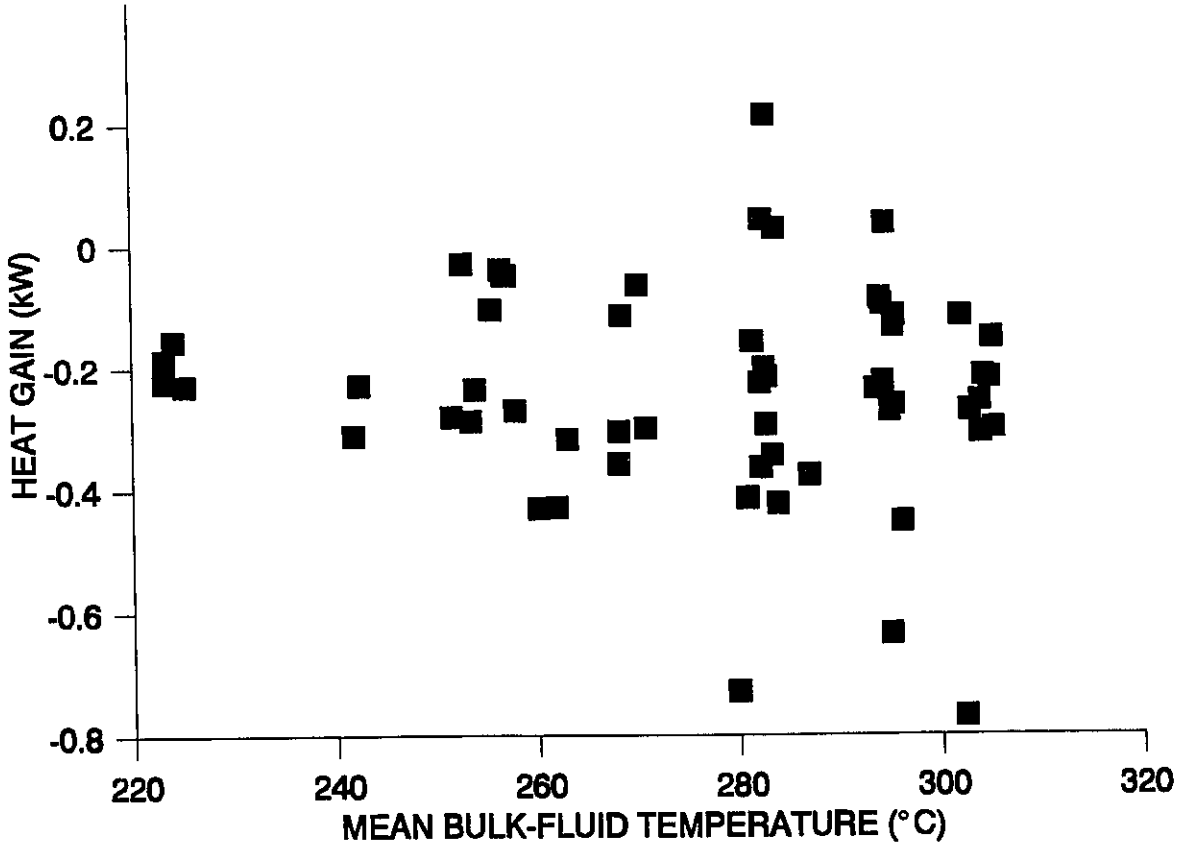

Figure III.8: Heat Loss from the Test Section in Adiabatic Flow as a function of Inlet Temperature.

$$Q = h_{FC} (T_b - T_{w,i}) \pi D_i Z \tag{III.6}$$

where h_{FC} is the heat-transfer coefficient for forced convection in $W.m^{-2}.K^{-1}$, T_b is the bulk-fluid temperature in K, $T_{w,i}$ is the temperature at the inner wall in K, D_i is the inner diameter of the tube in m, and Z is the axial length of the section in m.

At the outer tube surface, the heat is transferred through conduction from the inner to outer surface and is expressed as

$$Q = \frac{2 \pi k_{T/S} Z}{ln(D_o / D_i)} (T_{w,i} - T_{w,o}) \tag{III.7}$$

where $k_{T/S}$ is the thermal conductivity of the test section in $W.m^{-1}.K^{-1}$, D_o is the outer diameter of the tube in m, and $T_{w,o}$ is the temperature at the outer surface in K.

The same temperature is assumed for both the outer surface of tube and the inner surface of insulation.

At the outer surface of insulation, the heat is transferred through conduction from the inner to outer surface of insulation and is expressed as

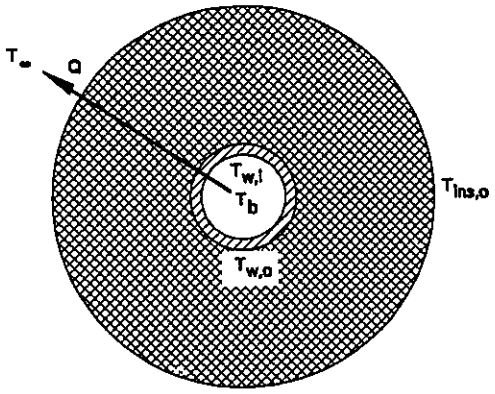

Figure III.9: Analysis of Heat Loss from the Test Section.

$$Q = \frac{2\,\pi\,k_{F/G}\,Z}{ln(D_{ins}\,/\,D_o)}\,(T_{w,o} - T_{ins,o}) \qquad \text{(III.8)}$$

where $k_{F/G}$ is the thermal conductivity of the fiberglass insulation in $W.m^{-1}.K^{-1}$, D_{ins} is the outer diameter of the insulation in m, and $T_{ins,o}$ is the temperature at the outer surface of the insulation in K.

The heat transfer through natural convection from the outer surface of insulation to the environment is expressed as

$$Q = h_{NC}\,(T_{ins,o} - T_\infty)\,\pi\,D_{ins}\,Z \qquad \text{(III.9)}$$

where h_{NC} is the heat-transfer coefficient for natural convection in $W.m^{-2}.K^{-1}$, and T_∞ is the ambient temperature in K. Combining Equations (III.6) to (III.9), the heat loss from the fluid to the environment is expressed

$$Q = \frac{T_b - T_\infty}{\frac{1}{h_{FC}\ \pi\ D_i\ Z} + \frac{ln(D_o\ /\ D_i)}{2\ \pi\ k_{T/S}\ Z} + \frac{\ln(D_{ins}\ /\ D_o)}{2\ \pi\ k_{F/G}\ Z} + \frac{1}{h_{NC}\ \pi\ D_{ins}\ Z}} \qquad \text{(III.10)}$$

The heat-transfer coefficient for forced convective cooling is calculated using the Dittus-Boelter equation [Dittus and Boelter, 1930]

$$h_{FC} = 0.024\ Re_b^{0.8}\ Pr_b^{0.3} \qquad \text{(III.11)}$$

where Pr_b is the bulk-fluid Prandtl number

$$Pr_b = \frac{\mu_b\ Cp_b}{k_b} \qquad \text{(III.12)}$$

with Cp_b being the specific heat in $J.kg^{-1}.K^{-1}$ and k_b the thermal conductivity of bulk fluid in $W.m^{-1}.K^{-1}$.

The values for thermal conductivity of Inconel-600 (which is the material of the test section) and fibreglass insulation are obtained from data provided by the Huntington Alloy, Inc. (Figure III.10) and the Manville Fibre Glass Group (Figure III.11), respectively.

The heat-transfer coefficient for natural convection to air at atmospheric pressure is expressed as

$$h_{NC} = 1.42 \left(\frac{T_{ins,o} - T_\infty}{Z} \right)^{1/4} \qquad \text{(III.13)}$$

for ranges of $(Gr_z.Pr)_{air}$ between 10^4 to 10^9, and

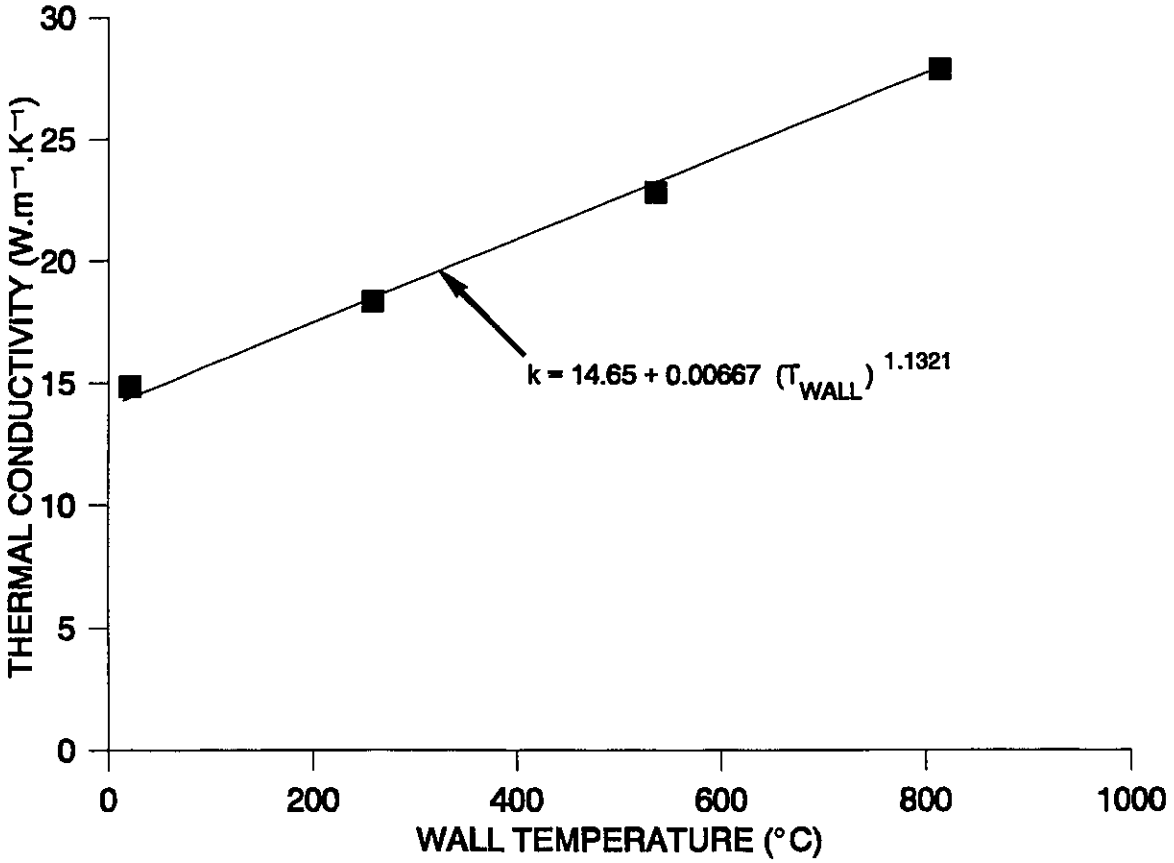

Figure III.10: Thermal Conductivity of Inconel-600.

$$h_{nc} = 0.95\ (T_{ins,o} - T_{\infty})^{1/3} \qquad \text{(III.14)}$$

for ranges of $(Gr_z.Pr)_{air}$ between 10^9 to 10^{13}. The Grashof number, Gr_z, for air is defined as

$$Gr_z = \frac{g\ \beta\ (T_{ins,o} - T_{\infty})\ Z^3}{\nu^2} \qquad \text{(III.15)}$$

where g is the acceleration due to gravity (9.806 $m.s^{-2}$), ν is the kinematic viscosity of air in $m^2.s^{-1}$,

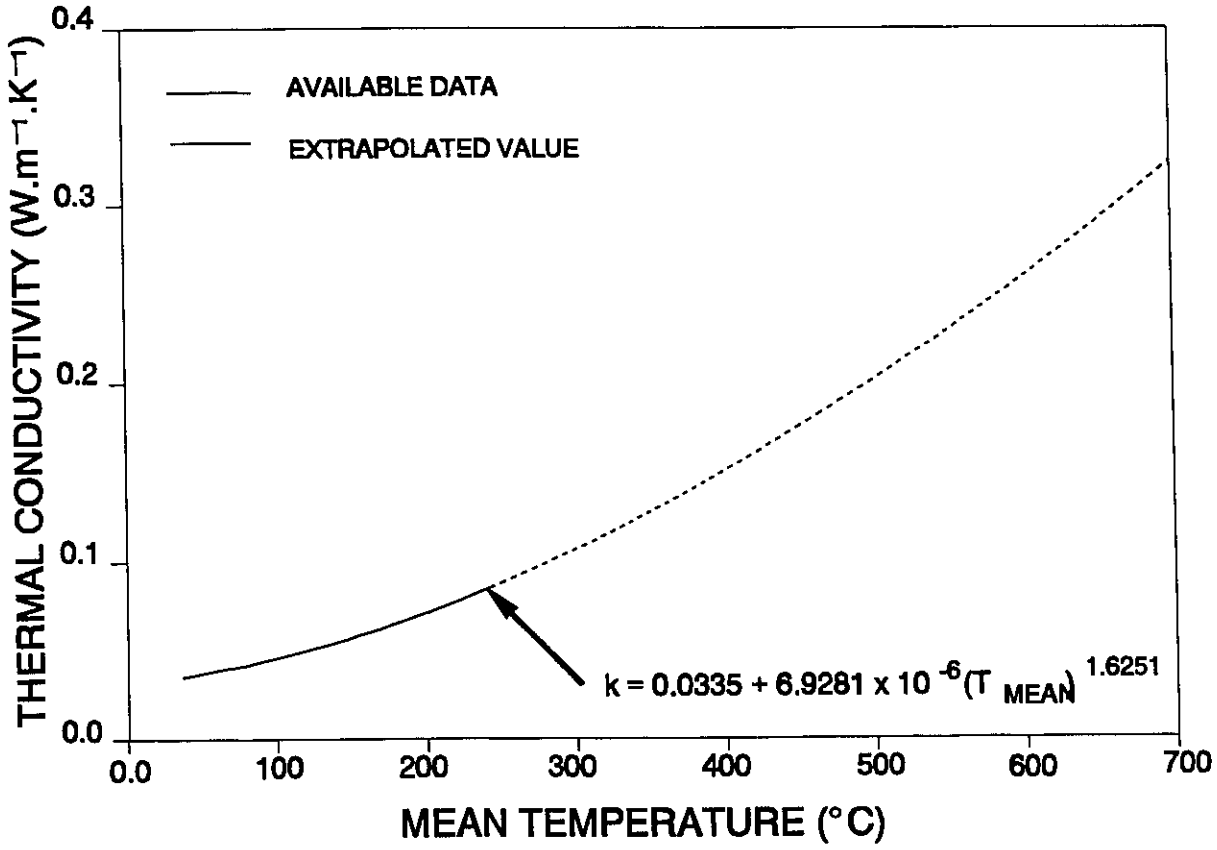

Figure III.11: Thermal Conductivity of the Fibreglass Insulation.

$$\beta = \frac{1}{T^*_{mean}} \tag{III.16}$$

and

$$T^*_{mean} = \frac{T_{ins,o} + T_\infty}{2} + 273.15 \tag{III.17}$$

The Prandtl number, Pr_{air}, of air is defined as

$$Pr_{air} = \left(\frac{\mu\ Cp}{k}\right)_{air} \tag{III.18}$$

The heat loss at adiabatic flow is shown in Figure III.12. It depends strongly on the temperature where larger heat loss corresponds to higher temperature. As a function of the Reynolds number, no definite trend is displayed in Figure III.13. Although there is some uncertainty for using a simplified-conduction model, this analysis has shown that the heat loss through the insulation can be considered as negligible.

For flow inside a heated channel, the power loss is determined based on a heat balance from data having a subcooled outlet flow (i.e., bulk-fluid temperature is less than saturation). To further eliminate those data with subcooled boiling, a criterion of 2°C below the saturation is employed. Figure III.14 shows the difference between the applied power to the test section and the

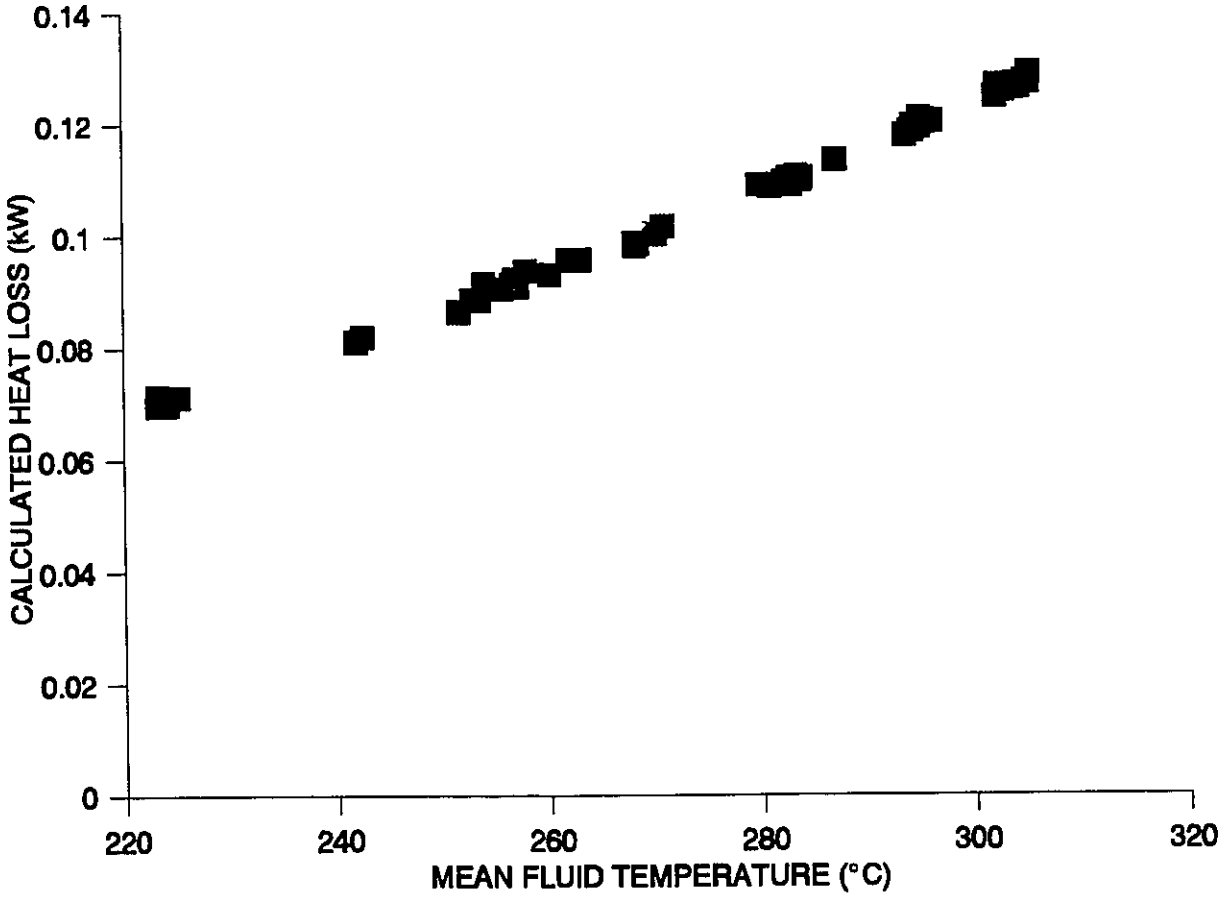

Figure III.12: Calculated Heat Loss as a function of Inlet Temperature Based on 1-Dimensional Conduction Model.

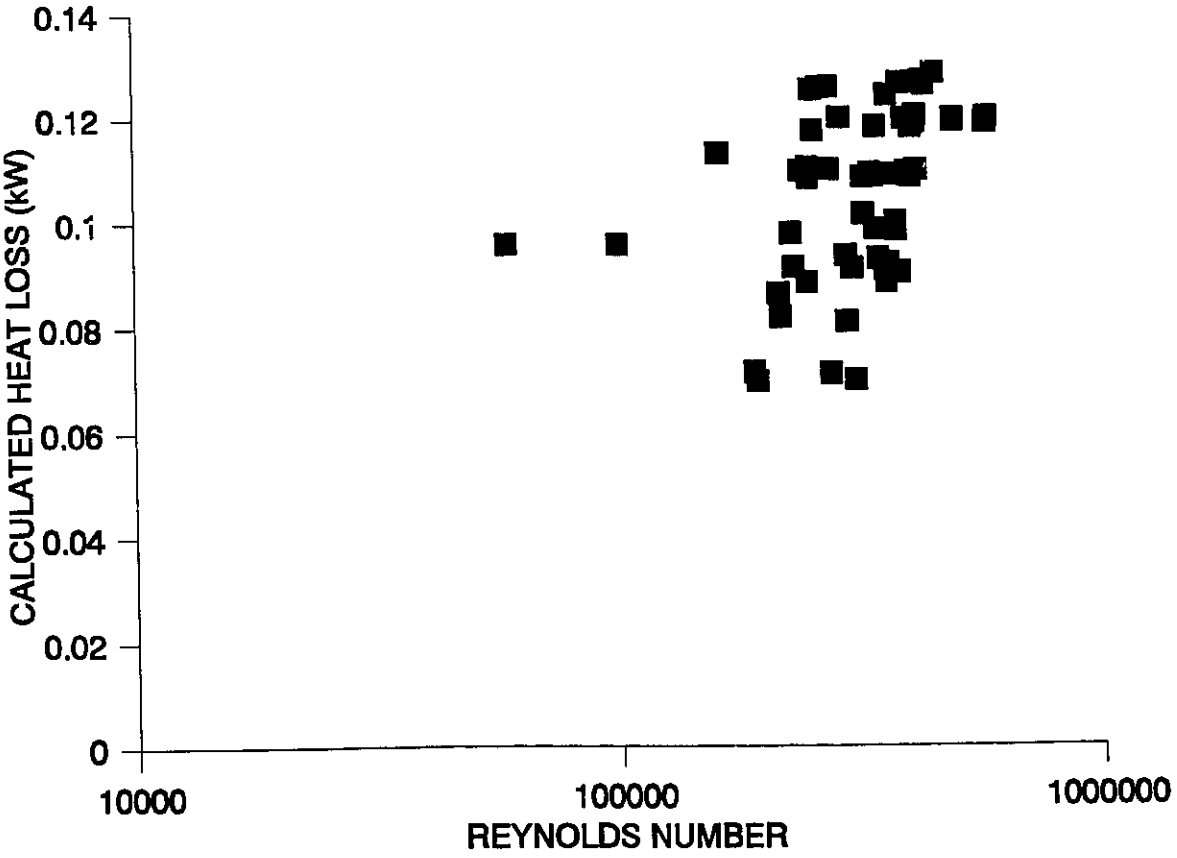

Figure III.13: Calculated Heat Loss as a function of Reynolds Number.

calculated power based on a heat balance of the inlet and outlet flows. Although the data are quite scattered, it indicates only a small power loss (about 2 kW for 50 kW of applied power). This power loss is primarily caused by the heat dissipation through the power connecting clamps, and possible errors in the power-supply and fluid-temperature measurements. These data can be correlated into

$$Q_{Loss} = 0.0407\ Q_{Applied} \tag{III.19}$$

Figures III.15 and III.16 show the power loss as functions of the mean bulk-fluid temperature (i.e., $\frac{1}{2}(T_{in} + T_{out})$) and the Reynolds number, respectively. No definite trend is exhibited in either figure. Hence, it is concluded that the power loss is related to the applied power, and

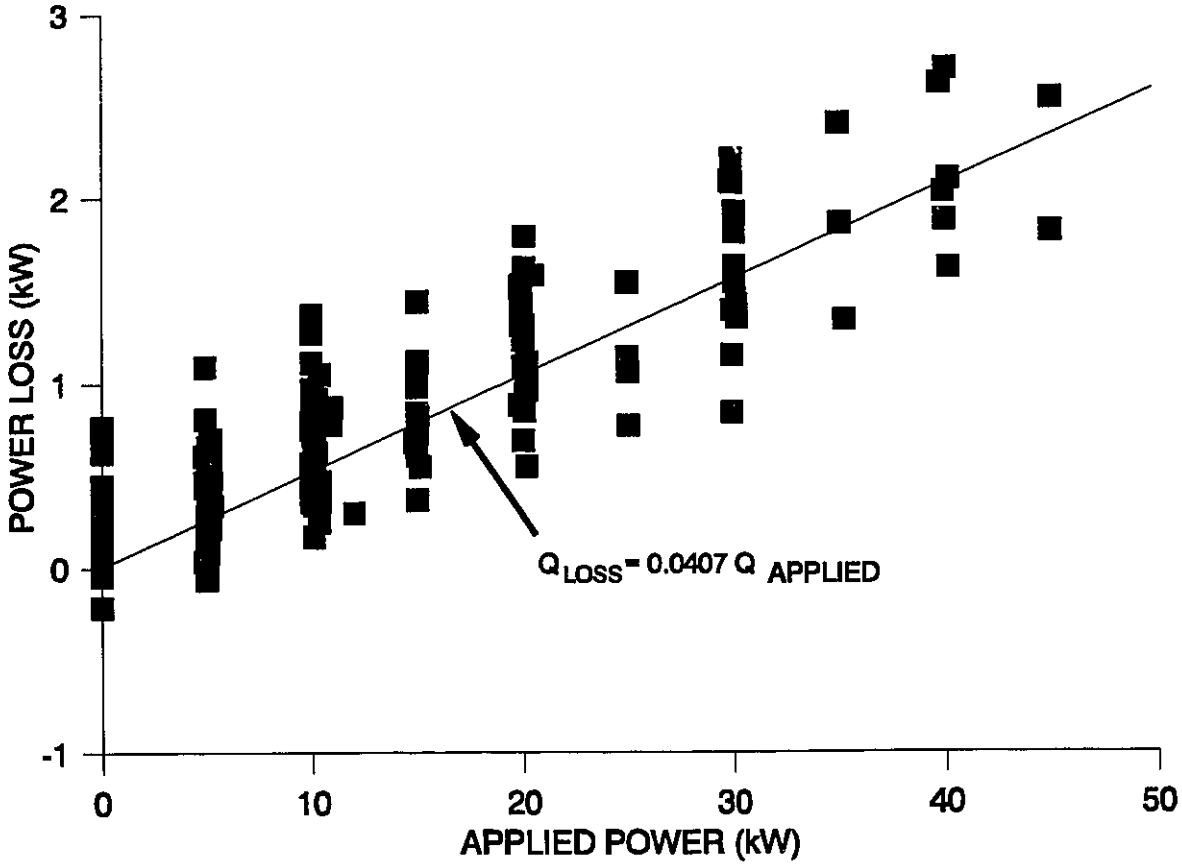

Figure III.14: Power Loss for Flow Inside a Heated Test Section.

Equation (III.19) should be adequate.

III.3 CALIBRATION OF THERMOCOUPLES THAT MEASURE THE TEMPERATURE OF A HEATED SURFACE

The thermocouples used to measure the surface temperature were not calibrated before the installation. They were bent and spot-welded at the tip onto the test section (Figure 8.4). This reduced the heat loss due to conduction through the thermocouples. A small strip of stainless steel was used to anchor the thermocouple on the test section to reduce excess force on the weld due to vibration during operation. This attachment method has been used in a number of experiments performed at the Chalk River Laboratories, and appears to have no significant effect

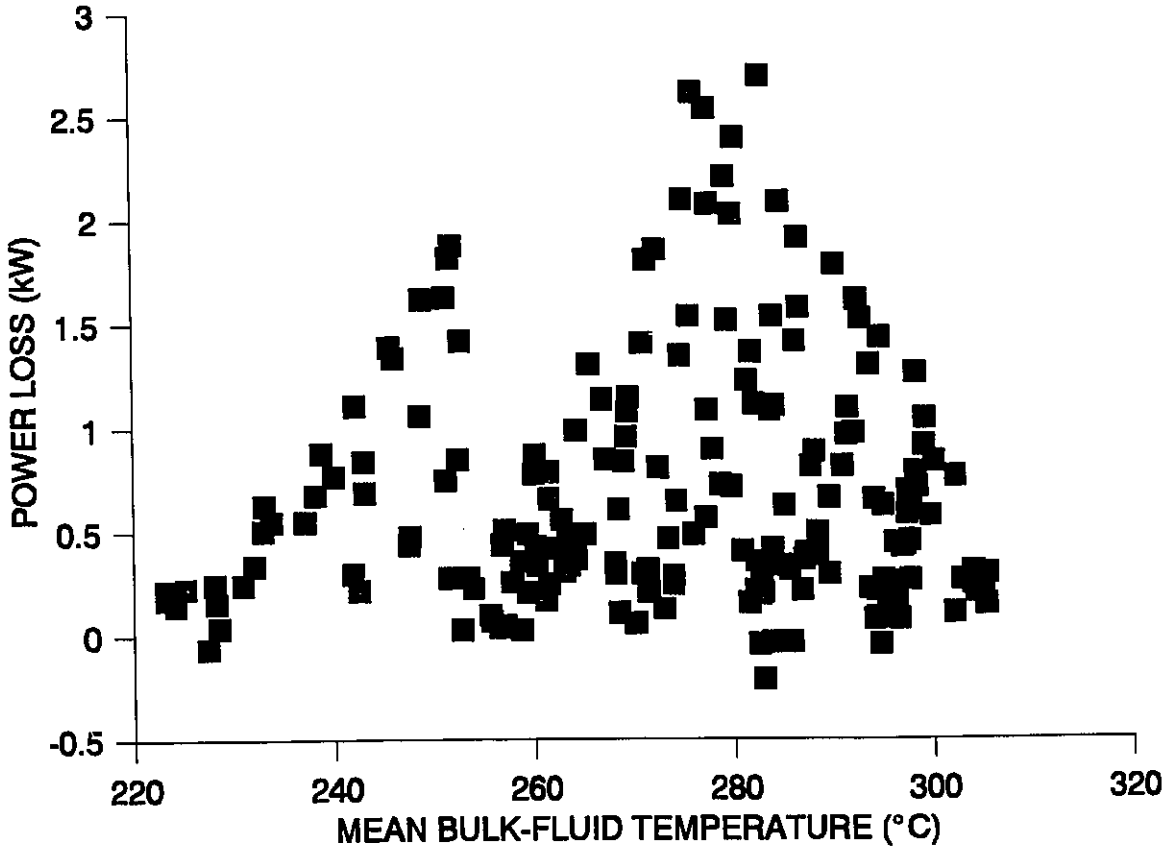

Figure III.15: Power Loss as a function of Mean Bulk-Fluid Temperature.

on the accuracy of the measurements. During the experiment, a large scatter in temperature readings was observed for thermocouple No. 4. It was later found that this thermocouple had detached from the test section and the scatter was caused by intermittent contacts. The readings from this thermocouple were therefore discarded. After the completion of the experiment, all thermocouples were carefully removed from the test section and calibrated with the JOFRA temperature calibrator. This will generally indicate the accuracy of the readings and the reliability of the thermocouple.

Although the thermocouples were twisted, bent and subjected to severe changes in temperature, they consistently provided accurate readings, with a maximum deviation of about 1% at high temperature. The measurements from the calibration are presented in Table III.3.

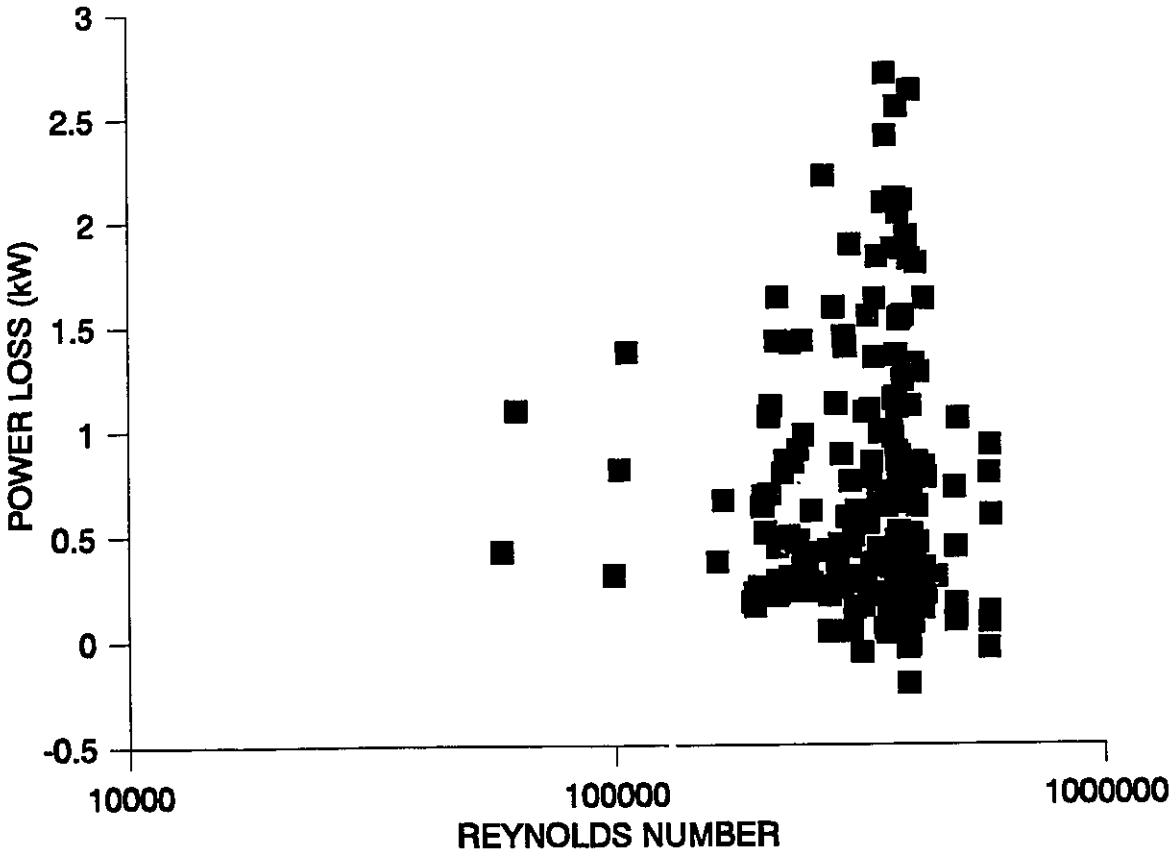

Figure III.16: Power Loss as a function of Reynolds Number.

Despite the small temperature difference, as indicated from the calibration, the temperature readings were corrected to improve the accuracy of the measurements. These corrections, however, were introduced based on the temperature recorded with adiabatic flow, rather than the measurements from the calibration. This provides a better reflection of the differences during operation, and not the close-to-ideal conditions that the thermocouples experienced inside the calibrator.

The temperature readings of the thermocouples were compared against the bulk-fluid temperature of adiabatic flow. In general, the relation between the bulk-fluid temperature and the thermocouple's reading is expressed as

Table III.3: Calibration of Thermocouples Measuring Surface Temperature.

T/C	Location	Actual Temperature (°C)							
	(m)	200.	250.	300.	350.	400.	450.	500.	550.
1	2.505	200.7	250.3	300.0	349.2	398.8	448.1	497.4	547.1
2	2.505	200.4	250.7	300.1	350.2	400.2	450.7	499.5	549.3
3	2.490	199.0	249.9	298.6	348.4	399.1	449.8	498.4	547.0
4	2.475	-	-	-	-	-	-	-	-
5	2.460	199.0	248.3	297.8	347.1	397.3	447.1	496.7	546.1
6	2.445	199.9	249.6	298.3	348.2	397.6	447.6	496.8	546.8
7	2.318	199.6	248.7	298.1	347.7	397.4	446.6	496.3	545.7
8	2.074	199.6	249.3	298.6	347.8	398.0	448.3	497.6	547.8
9	1.812	202.7	248.1	297.4	347.1	396.7	447.7	497.1	544.9
10	1.562	199.4	249.1	298.2	347.8	398.0	447.6	496.7	545.7
11	1.313	200.8	250.6	299.6	349.2	400.2	450.6	500.0	549.9
12	1.062	201.1	251.3	300.7	350.8	400.3	450.3	499.8	548.4
13	0.813	201.1	251.1	300.4	350.1	400.8	450.7	500.1	548.2
14	0.560	200.5	250.3	299.6	348.6	400.1	448.6	498.7	548.0
15	0.310	201.1	251.1	299.8	349.7	397.4	450.1	499.9	549.6

$$T_{b,i} = a_i + b_i T_{w,i} \tag{III.20}$$

The coefficients a_i and b_i are shown for each thermocouple in Table III.4.

III.4 TEMPERATURE CALCULATION AT INNER SURFACE

The temperature at the inner surface is evaluated based on the conduction theory using the temperature measurements obtained at the outer surface, $T_{w,o}$. Based on a one-dimensional approach and by assuming that heat is only transferred radially, the conduction equation with internal energy generation is expressed in cylindrical coordinates as

$$\frac{1}{r}\frac{d}{dr}\left(r\frac{dT}{dr}\right)+\frac{q_o}{k_{T/S}}=0 \qquad \text{(III.21)}$$

with the boundary conditions of

$T = T_{w,i}$ at $r = r_i$

$T = T_{w,o}$ at $r = r_o$

$dT/dr = 0$ at $r = r_o$

where q_o is the internal heat generation in $W.m^{-3}$, $k_{T/S}$ is the thermal conductivity of the test section in $W.m^{-1}.K^{-1}$, r_i and r_o are the radii of the inner and outer surfaces in m, respectively. After integrating Equation (III.21), the temperature at the inner surface is expressed as

Table III.4: Coefficients to be Used for Thermocouple's Correction.

T/C	a_i	b_i
1	-2.0307	1.0022
2	-0.4794	0.9982
3	-0.4807	0.9982
4	-0.9161	1.0000
5	-0.8146	1.0078
6	-2.0255	1.0114
7	-1.6665	1.0146
8	-2.4817	1.0190
9	-1.1401	1.0084
10	-0.6657	1.0043
11	-1.1587	1.0042
12	-1.2550	0.9982
13	-0.8832	1.0001
14	-1.2709	0.9996
15	-2.0099	1.0171

$$T_{w,i} = T_{w,o} - \frac{q_o\,(r_o^2 - r_i^2)}{2\,k_{T/S}}\left(\frac{r_o^2\,ln\left(\frac{r_o}{r_i}\right)}{r_o^2 - r_i^2} - \frac{1}{2}\right) \qquad \text{(III.22)}$$

For a tube with thin wall thickness, Equation (III.22) can be written as

$$T_{w,i} = T_{w,o} - \frac{q\,r_i}{k_{T/S}}\left(\frac{r_o^2\,ln\left(\frac{r_o}{r_i}\right)}{r_o^2 - r_i^2} - \frac{1}{2}\right) \qquad \text{(III.23)}$$

III.5 SINGLE-PHASE PRESSURE DROP

The single-phase pressure drop is established with tests of adiabatic flow (i.e., no power is applied). Except for a small difference due to the variation of fluid temperature along the test section, the pressure drop over each sub-region is about the same. Furthermore, the sum of these pressure drops agrees with the measurements over the whole test section. Therefore, the pressure drop over the test section is used to calculate the single-phase friction factor.

For a vertical flow of single-phase liquid, the overall pressure drop is primarily due to friction and gravity (the acceleration component is negligible, since there is no change in density and flow area). The frictional pressure drop, $\Delta P_{fric.}$, is calculated by subtracting the gravitational component from the overall pressure drop measured in the experiment

$$\Delta P_{fric.} = \Delta P_{meas.} - \Delta P_{grav.} \tag{III.24}$$

and the gravitational pressure drop, $\Delta P_{grav.}$ is calculated with

$$\Delta P_{grav.} = \rho_{l,ave}\, g\, \Delta z \tag{III.25}$$

where Δz is the length of the channel in m, g is the acceleration due to gravity (9.806 $m.s^{-2}$), and $\rho_{l,ave}$ is the average liquid density in $kg.m^{-3}$. Using the D'Arcy-Weisbach equation, the friction factor, f, is expressed as

$$f = \frac{\Delta P_{fric.}}{\Delta Z}\,\frac{D}{}\,\frac{2\,\rho_{l,ave}}{G^2} \tag{III.26}$$

where D is the inside diameter of the tube in m and G is the mass flux of fluid in $kg.m^{-2}.s^{-1}$. As shown in Figure III.17, the calculated friction factor is larger than that of a smooth tube. The friction factor for a smooth tube was calculated with

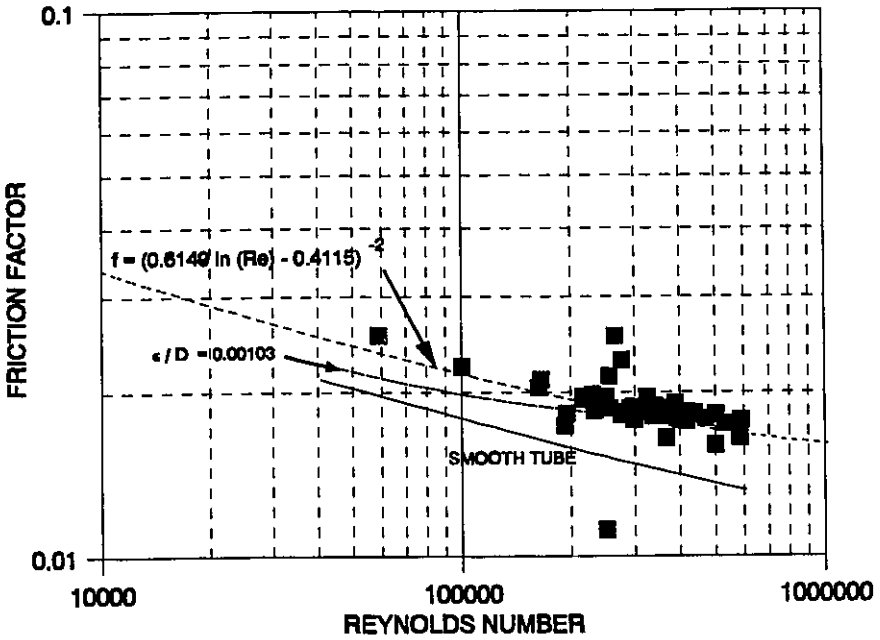

Figure III.17: Friction Factor of the Test Section.

$$f = (1.82 \log(Re) - 1.64)^{-2} \tag{III.27}$$

and the present data were optimized as

$$f = (0.6149\ ln(Re) - 0.4115)^{-2} \tag{III.28}$$

The friction factor was also expressed in terms of relative roughness, ε/D,

$$\frac{1}{f^{1/2}} = -2 \log\left(\frac{\varepsilon/D}{3.7} + \frac{2.51}{f^{1/2}\ Re}\right) \tag{III.29}$$

Based on Equation (III.29), the average relative roughness of the test section is 0.00103. The friction factors calculated based on Equations (III.27), (III.28) and (III.29) are also presented in Figure III.17.

The friction factors as calculated from the measurements of pressure drop in each sub-region are shown in Figure III.18. They display a similar pattern as in Figure III.17, and follow closely Equations (III.28) and (III.29).

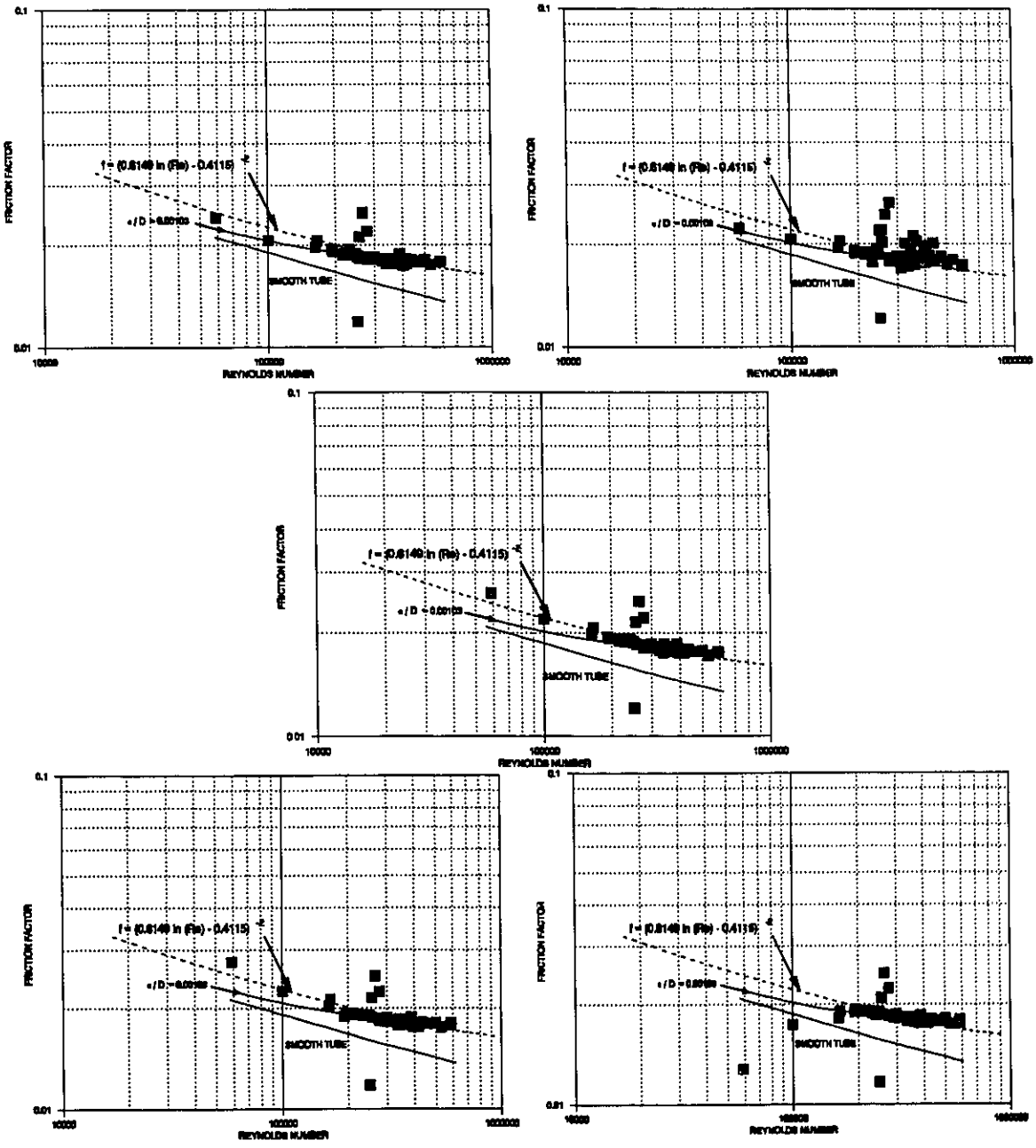

Figure III.18: Friction Factor for each Sub-Region of the Test Section.

All measurements of pressure drop have to be aligned with that of the entire test section, so that the results can be compared systematically in other heat-transfer modes. Since the differential-pressure (DP) cells were calibrated before the installation, the uncertainty is probably caused by the adjustment of the zero reading at the start of each test, which introduces a constant shift in measurement. Based on the relative roughness and Equation (III.29), the difference between the measured and predicted pressure drop at adiabatic flow is included in all measurements for the same test. This correction affects slightly the magnitude of the measurements (since the correction is small compared to the high pressure drop encountered in two-phase flow), and does not alter the trend of the data.

The friction factors calculated based on the corrected measurements of pressure drop are shown in Figures III.19, which combines the friction factors for each sub-region as well as those for the entire test section. As expected, the data agree with those calculated from Equation III.29.

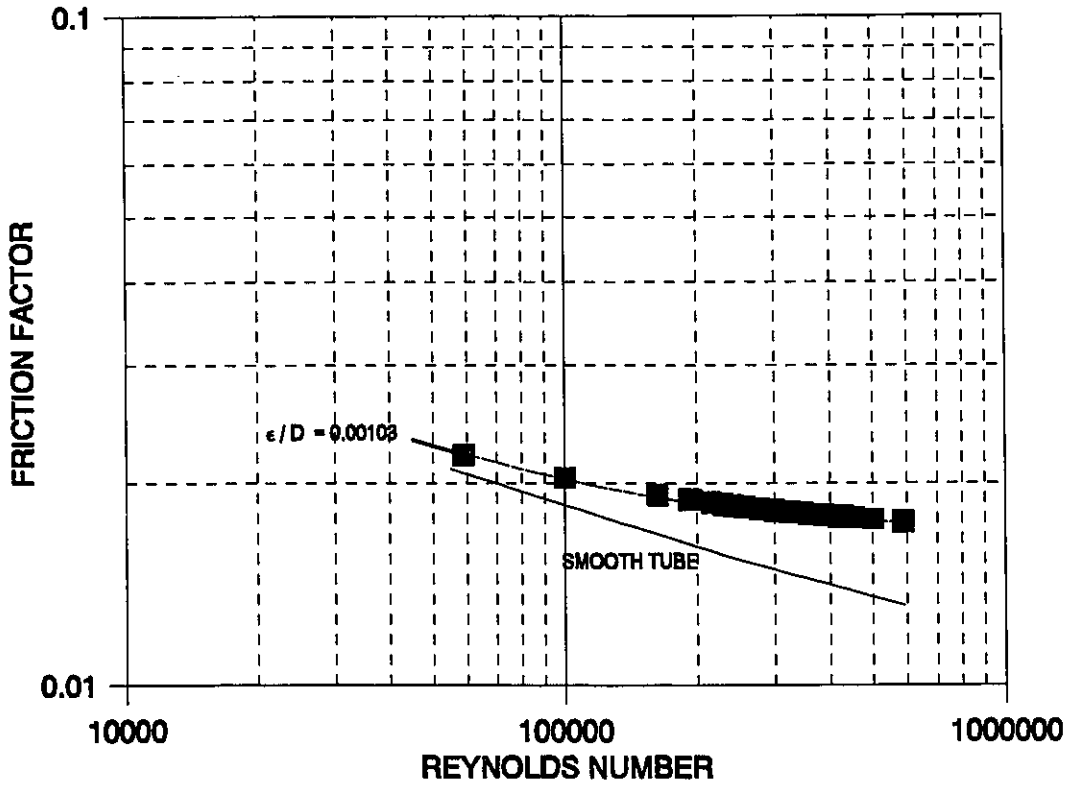

Figure III.19: Friction Factor Based on Corrected Measurements of Single-Phase Pressure Drop.

REFERENCES

Dittus, F.W. and Boelter, L.M.K., Heat Transfer in Automobile Radiators of Tubular Type, Publications in Engineering, University of California, Berkeley, p. 443, 1930.

Handbook of Huntington Alloys, the International Nickel Company of Canada, Limited, 1965.

Manville Fibre Glass Group, Information Sheet for "Micro-Lok" Fibre Glass Pipe Insulation.

Holman, J.P., Heat Transfer, 4th Edition, McGraw-Hill Book Company, 1976.

Colebrook, C.F., Turbulent Flow in Pipes with Particular Reference to the Transition Region between the Smooth and Rough Pipes Laws, J. Inst. Civ. Eng., Vol. 11, pp. 133-156, 1939.

IV. CORRECTED PRESSURE-DROP DATA

Runname	Date	PT-108	TE-103	TE-105	TE-133	FT-1/2	JS-100	PDT-01	PDT-02	PDT-03	PDT-04	PDT-05	PDT-06
		Pressure	T/S Temp	T/S Temp	Temp	Flowrate	Power	Pressure	Pressure	Pressure	Pressure	Pressure	Pressure
		Outlet	Inlet	Outlet	Ambient	Water	T/S	Diff	Diff.	Diff.	Diff.	Diff.	Diff.
		MPa	°C	°C	°C	g/s	kW	kPa	kPa	kPa	kPa	kPa	kPa
DPB94300	12/05/89	9.71	284.28	285.23	31.58	112.97	0.00	30.29	30.29	30.29	30.29	30.29	151.47
DPB94303	12/05/89	9.73	284.35	307.20	31.83	117.26	75.04	33.70	33.41	33.06	32.81	32.55	165.90
DPB94304	12/05/89	9.71	284.28	310.97	31.77	115.44	20.02	44.03	33.30	32.60	32.23	31.87	174.27
DPB94305	12/05/89	9.71	284.28	310.97	31.81	115.06	25.14	58.98	43.15	32.79	32.13	31.64	199.37
DPB94306	12/05/89	9.71	284.42	310.83	31.76	117.54	30.08	72.02	56.80	37.14	33.33	32.78	234.00
DPB94307	12/05/89	9.71	284.28	311.04	31.82	114.83	35.14	82.41	65.35	45.72	32.67	31.87	260.26
DPB94308	12/05/89	9.71	284.35	311.04	31.79	116.67	40.08	93.14	74.77	55.57	34.70	32.65	292.58
DPB94309	12/05/89	9.71	284.35	311.24	31.70	115.91	45.12	99.43	82.78	64.04	37.92	32.39	319.13
DPB94310	12/05/89	9.71	284.28	311.04	31.80	115.78	50.18	103.24	90.55	70.77	42.70	32.55	343.37
DPB94311	12/05/89	9.71	284.28	311.24	31.78	115.75	55.10	102.55	96.40	76.23	48.31	32.70	359.81
DPB94312	12/05/89	9.72	284.28	311.24	31.72	116.04	60.16	100.01	100.59	80.96	54.44	33.35	373.09
DPC94313	12/05/89	9.71	284.28	311.24	31.91	116.18	60.72	99.14	100.55	81.35	55.22	33.43	373.67
DPB94403	12/05/89	9.71	271.02	295.12	30.83	117.30	15.04	32.83	32.45	32.18	32.00	31.74	161.57
DPB94404	12/05/89	9.70	271.37	303.83	30.75	114.92	20.51	32.54	32.07	31.60	31.30	30.94	158.11
DPB94405	12/05/89	9.70	271.43	310.09	30.73	117.21	25.43	35.60	33.18	32.60	32.16	31.72	165.61
DPB94406	12/05/89	9.70	271.23	310.83	31.22	119.09	30.47	51.07	35.18	33.95	33.40	32.86	186.96
DPB94407	12/05/89	9.71	271.77	311.04	31.27	121.60	35.14	66.88	42.65	35.03	34.41	33.74	214.09
DPB94408	12/05/89	9.70	271.77	310.97	31.35	119.34	40.45	78.89	57.19	35.83	33.82	33.02	240.35
DPB94409	12/05/89	9.70	271.77	310.97	31.40	120.04	45.12	89.74	67.89	40.57	33.82	33.14	266.90
DPB94410	12/05/89	9.71	271.84	311.04	31.43	117.45	50.04	97.53	75.39	48.61	33.32	32.34	289.69
DPB94411	12/05/89	9.71	271.71	311.17	31.42	116.89	55.10	103.64	82.78	57.88	34.36	32.29	313.93
DPB94412	12/05/89	9.71	271.91	311.24	31.42	116.17	60.16	104.22	88.78	66.38	36.34	31.92	330.96
DPB94413	12/05/89	9.70	271.91	311.17	31.51	120.65	65.10	109.99	97.09	74.93	40.57	33.82	359.24
DPC94414	12/05/89	9.71	271.91	311.24	31.51	116.73	66.66	100.54	92.66	74.73	41.50	31.92	344.17
DPB94500	15/05/89	9.63	253.74	254.70	30.52	113.90	0.00	29.47	29.47	29.47	29.47	29.47	147.32
DPB94506	15/05/89	9.62	256.14	304.44	30.60	114.36	29.94	32.12	31.55	31.15	30.68	30.24	155.68
DPB94507	15/05/89	9.62	256.14	310.16	30.68	115.96	35.14	38.81	32.54	32.08	31.41	30.98	165.50
DPB94508	15/05/89	9.63	256.27	310.23	30.69	114.43	40.19	55.67	33.89	31.66	30.94	30.40	183.10
DPB94509	15/05/89	9.63	256.20	310.23	30.73	114.02	45.04	68.35	41.78	31.73	31.05	30.38	203.88
DPB94510	15/05/89	9.62	256.27	310.30	30.80	114.04	50.10	79.38	54.13	32.96	31.23	30.45	228.98
DPB94511	15/05/89	9.62	256.20	310.30	30.81	111.75	55.10	88.15	64.82	36.17	30.38	29.75	250.91
DPB94512	15/05/89	9.62	256.14	310.30	30.87	111.05	60.04	94.96	71.56	43.01	30.30	29.55	270.54
DPB94513	15/05/89	9.63	256.34	310.30	30.94	112.54	65.08	96.52	76.36	51.21	31.25	29.90	286.98
DPC94514	15/05/89	9.63	256.61	310.30	31.00	110.95	69.55	91.90	78.94	59.06	32.12	29.63	293.63
DPB94200	15/05/89	9.62	296.61	297.62	31.20	113.81	0.00	31.38	31.38	31.38	31.38	31.38	156.89
DPB94201	15/05/89	9.63	296.34	304.98	31.27	115.73	5.06	32.71	32.61	32.49	32.42	32.31	162.37
DPB94202	15/05/89	9.63	296.61	309.96	31.36	114.79	10.00	38.77	32.49	32.18	32.01	31.82	167.56
DPB94203	15/05/89	9.63	296.74	310.23	31.47	111.44	15.08	52.21	44.65	33.80	31.02	30.67	192.67
DPB94204	15/05/89	9.63	296.27	310.30	31.51	111.39	20.10	63.76	53.69	42.88	31.67	30.73	221.83
DPB94205	15/05/89	9.63	296.07	310.36	31.67	111.11	24.88	75.01	62.66	51.73	35.51	30.88	257.31
DPB94206	15/05/89	9.62	296.07	310.30	31.75	110.40	30.08	83.03	71.20	58.62	41.59	30.75	287.03
DPB94207	15/05/89	9.63	296.61	310.36	31.75	108.98	35.14	87.25	78.01	64.73	48.24	31.09	311.85
DPB94208	15/05/89	9.62	296.54	310.36	31.79	109.39	40.08	91.86	84.82	71.62	54.13	32.83	338.11
DPB94209	15/05/89	9.62	296.14	310.43	31.91	108.50	44.98	90.30	87.74	76.16	58.00	34.08	348.49
DPB94210	15/05/89	9.63	296.54	310.50	31.93	113.43	50.04	96.02	96.28	85.59	65.53	38.10	385.43
DPC94211	15/05/89	9.62	296.34	310.50	32.02	112.18	53.05	91.75	95.32	87.70	67.20	39.14	384.85
DPB94100	16/05/89	9.60	304.25	305.58	32.30	117.54	0.00	33.72	33.72	33.72	33.72	33.72	168.60
DPB94103	16/05/89	9.54	302.82	309.69	32.48	112.83	14.92	63.08	54.99	48.05	38.22	31.33	238.05
DPB94104	16/05/89	9.61	302.68	310.30	32.58	112.74	20.10	73.18	63.42	54.36	43.55	31.93	268.93
DPB94105	16/05/89	9.62	303.22	310.16	32.76	112.02	25.02	83.23	73.15	62.56	50.89	34.68	307.31
DPB94106	16/05/89	9.60	302.42	310.23	32.75	112.26	30.08	87.78	79.31	67.95	54.74	36.03	328.95
DPB94107	16/05/89	9.61	302.89	310.30	32.79	115.95	35.14	98.52	89.96	78.10	62.68	41.02	374.25
DPB94108	16/05/89	9.62	303.16	310.23	32.88	114.42	40.02	97.65	92.77	82.83	66.37	43.85	387.82
DPB94109	16/05/89	9.63	303.36	310.30	32.82	111.35	45.12	92.81	93.50	86.84	69.44	46.73	392.72
DPC94110	16/05/89	9.61	303.22	310.30	33.22	115.37	50.86	93.67	96.51	93.49	75.28	51.22	414.65

DPB96200	17/05/89	9.63	295.66	297.08	29.71	154.60	0.00	53.78	53.78	53.78	53.78	53.78	268.90
DPB96204	17/05/89	9.67	295.93	310.43	29.61	149.89	20.23	89.33	71.82	53.66	52.01	51.45	319.69
DPB96205	17/05/89	9.63	295.86	310.16	30.01	147.58	24.88	103.58	85.71	62.63	50.95	50.25	355.47
DPB96206	17/05/89	9.63	295.66	310.36	30.16	146.41	30.22	118.65	97.52	75.98	52.19	50.15	397.31
DPB96207	17/05/89	9.63	295.73	310.36	30.06	144.47	35.04	129.62	106.68	86.21	55.80	49.14	431.07
DPB96208	17/05/89	9.64	295.80	310.50	30.32	152.80	39.94	150.56	124.19	100.87	64.42	54.15	498.02
DPB96209	17/05/89	9.63	295.93	310.36	30.22	152.24	45.06	159.22	133.46	109.61	71.85	53.58	532.36
DPB96210	17/05/89	9.64	295.73	310.50	30.15	150.05	50.18	163.32	140.46	115.84	79.07	52.95	556.31
DPB96211	17/05/89	9.63	295.66	310.36	30.19	150.36	54.96	167.59	148.58	123.27	86.50	53.91	585.16
DPB96212	17/05/89	9.64	295.86	310.50	30.19	148.89	60.02	165.28	153.39	129.35	93.98	54.80	602.48
DPB96213	17/05/89	9.64	295.80	310.50	30.25	148.63	65.22	163.15	157.74	136.00	101.04	56.67	620.37
DPB96214	17/05/89	9.63	295.73	310.50	30.07	148.10	70.39	159.91	158.86	141.85	107.61	59.03	632.78
DPC96214	17/05/89	9.64	296.00	310.63	30.15	148.39	71.86	158.93	158.59	143.12	109.35	59.83	635.37
DPB96100	17/05/89	9.63	304.24	305.65	30.21	150.61	0.00	52.28	52.28	52.28	52.28	52.28	261.39
DPB96104	17/05/89	9.64	304.71	310.16	30.19	156.19	20.10	118.36	101.60	87.76	67.04	55.26	431.93
DPB96105	17/05/89	9.64	305.04	310.36	30.14	152.09	25.02	128.23	109.30	94.45	74.93	53.73	463.39
DPB96106	17/05/89	9.63	304.91	310.23	30.09	150.18	30.08	138.50	118.38	101.84	81.79	54.93	498.59
DPB96107	17/05/89	9.63	303.76	310.36	30.16	149.64	35.02	145.60	124.69	106.46	83.97	54.56	518.50
DPB96108	17/05/89	9.63	304.64	310.36	30.17	153.80	40.06	159.05	138.31	118.69	94.85	59.94	575.35
DPB96109	17/05/89	9.64	302.01	310.50	30.05	153.32	44.98	165.63	144.62	122.73	94.62	58.09	589.78
DPB96110	17/05/89	9.63	303.16	310.43	30.03	151.82	49.88	166.43	151.16	130.93	103.97	63.08	621.23
DPB96111	17/05/89	9.64	303.36	310.43	30.16	151.20	54.96	164.30	155.35	137.08	109.42	66.54	637.10
DPB96112	17/05/89	9.63	303.56	310.50	30.04	152.78	64.94	161.93	160.66	150.09	120.85	75.39	674.61
DPC96113	17/05/89	9.63	303.16	310.70	30.17	152.66	68.22	161.01	159.89	152.43	122.85	76.64	678.08
DPB96300	17/05/89	9.63	282.38	283.74	30.28	148.35	0.00	48.60	48.60	48.60	48.60	48.60	243.02
DPB96301	17/05/89	9.65	282.32	289.64	30.40	148.63	5.06	49.24	49.10	49.02	48.86	48.78	245.90
DPB96302	17/05/89	9.65	282.66	295.53	30.44	153.25	10.04	52.82	52.42	52.25	52.00	51.74	262.65
DPB96303	17/05/89	9.66	283.20	301.81	30.46	152.57	15.04	52.88	52.33	51.95	51.61	51.22	260.04
DPB96304	17/05/89	9.62	281.98	305.65	30.47	154.29	19.96	54.15	53.50	53.02	52.52	52.00	266.10
DPB96305	17/05/89	9.64	282.18	310.09	30.54	155.50	25.04	61.47	54.92	54.25	53.66	52.99	279.09
DPB96306	17/05/89	9.64	282.32	310.30	30.59	152.95	30.04	85.47	56.65	53.33	52.42	51.66	301.03
DPB96307	17/05/89	9.64	282.32	310.23	30.68	150.54	34.94	102.57	71.15	52.56	51.38	50.52	329.89
DPB96308	17/05/89	9.64	282.38	310.36	30.61	154.49	40.04	120.00	88.78	57.02	53.90	52.78	374.90
DPB96310	17/05/89	9.64	282.25	310.36	30.65	150.35	49.90	143.54	112.79	75.38	52.16	50.70	437.52
DPB96311	17/05/89	9.64	282.32	310.43	30.75	148.94	54.98	152.54	121.94	87.69	52.83	50.00	468.96
DPB96312	17/05/89	9.63	282.25	310.50	30.73	147.97	60.02	157.96	130.36	98.38	55.35	49.43	496.09
DPB96313	17/05/89	9.63	282.38	310.50	30.78	151.27	64.98	167.26	142.07	109.21	60.57	51.35	535.34
DPB96314	17/05/89	9.63	282.38	310.57	30.79	152.09	70.14	170.09	151.23	118.48	66.57	52.08	563.33
DPB96315	17/05/89	9.63	282.38	310.50	30.78	151.37	75.20	165.35	155.99	124.40	73.22	51.74	576.03
DPC96316	17/05/89	9.63	282.25	310.50	30.73	151.15	79.43	161.60	158.49	128.43	79.19	52.08	584.97
DPB96400	17/05/89	9.64	268.37	269.46	30.68	149.18	0.00	47.89	47.89	47.89	47.89	47.89	239.47
DPB96401	17/05/89	9.63	273.61	309.83	30.60	148.15	29.98	53.95	50.01	49.24	48.59	47.97	250.15
DPB96407	17/05/89	9.63	273.34	310.23	30.70	146.73	35.00	73.75	50.54	49.08	48.31	47.58	269.19
DPB96408	17/05/89	9.63	273.75	310.16	30.59	151.01	40.06	96.67	59.51	51.85	50.98	50.04	309.88
DPB96409	17/05/89	9.64	274.43	310.30	30.60	150.35	44.98	113.51	76.98	52.28	50.95	49.84	345.37
DPB96410	17/05/89	9.64	274.50	310.43	30.66	147.59	49.90	125.64	92.83	55.09	49.42	48.38	373.37
DPB96411	17/05/89	9.63	272.66	310.36	30.63	147.00	55.10	135.27	101.95	59.47	49.24	48.17	396.74
DPB96412	17/05/89	9.62	271.30	310.23	30.62	154.77	60.02	150.29	112.81	64.78	53.45	52.23	436.56
DPB96413	17/05/89	9.63	271.37	310.43	30.66	150.73	65.06	157.43	121.72	75.67	51.99	50.46	460.80
DPB96414	17/05/89	9.63	271.43	310.36	30.72	147.37	70.04	158.88	127.96	87.49	51.34	48.59	478.11
DPB96415	17/05/89	9.63	271.37	310.50	30.87	148.42	74.92	161.83	135.89	97.60	53.65	49.06	501.78
DPB96416	17/05/89	9.63	271.77	310.50	30.88	149.01	79.88	161.42	142.65	107.99	57.26	49.52	522.55
DPC96417	17/05/89	9.64	271.84	310.77	30.87	148.67	83.61	156.17	142.70	113.45	60.07	49.42	525.44
DPB96500	17/05/89	9.63	260.44	261.40	30.88	153.90	0.00	50.06	50.06	50.06	50.06	50.06	250.29
DPB96506	17/05/89	9.65	259.97	297.22	30.96	150.45	29.98	51.73	51.02	50.33	49.67	49.16	251.45
DPB96507	17/05/89	9.63	259.90	302.68	30.98	150.80	35.00	52.48	51.56	50.63	49.96	49.26	253.76
DPB96508	17/05/89	9.63	259.56	308.28	30.94	149.71	40.06	54.04	51.44	50.48	49.59	48.79	253.76
DPB96509	17/05/89	9.63	259.49	310.30	30.94	151.38	44.98	66.33	52.79	51.71	50.66	49.78	271.65
DPB96510	17/05/89	9.63	259.42	310.23	31.03	145.48	50.04	90.86	53.06	49.25	48.09	47.18	288.67

DPB96511	17/05/89	9.63	259.08	310.30	31.11	147.06	54.96	108.17	62.17	50.33	49.33	48.17	318.69
DPB96512	17/05/89	9.64	259.42	310.36	31.17	148.55	59.88	121.97	75.76	51.36	49.93	48.69	348.70
DPB96513	17/05/89	9.63	259.35	310.30	31.22	150.71	64.98	136.91	91.80	54.37	51.51	50.17	386.79
DPB96514	17/05/89	9.63	259.49	310.30	31.28	150.97	70.00	148.63	106.73	58.14	51.72	50.38	418.24
DPB96515	17/05/89	9.63	259.49	310.30	31.44	148.91	75.02	156.42	117.85	65.14	50.66	49.39	442.19
DPB96516	17/05/89	9.63	259.49	310.36	31.42	147.55	80.12	159.48	124.54	75.30	50.48	48.74	461.81
DPB96517	17/05/89	9.63	259.49	310.43	31.47	148.19	84.94	158.15	128.93	85.88	51.83	49.18	476.53
DPC96518	17/05/89	9.63	259.90	310.63	31.49	149.70	88.87	150.59	130.32	94.27	53.49	50.06	482.59
DPB97100	31/05/89	9.55	302.75	303.70	27.69	167.79	0.00	63.43	63.43	63.43	63.43	63.43	317.14
DPB97102	31/05/89	9.56	302.75	309.49	27.69	165.44	9.96	86.28	71.12	63.12	62.81	62.52	346.58
DPB97104	31/05/89	9.55	302.89	309.56	27.73	163.99	20.10	124.55	106.10	87.94	64.63	61.48	447.28
DPB97106	31/05/89	9.55	303.02	309.69	27.79	168.56	29.94	162.00	136.07	114.72	82.57	64.70	563.58
DPB97107	31/05/89	9.55	303.09	309.62	27.76	165.75	34.98	172.74	145.65	122.95	90.83	64.05	600.51
DPB97108	31/05/89	9.55	302.75	309.62	27.93	167.59	39.79	186.13	157.69	132.99	99.27	66.10	647.26
DPB97109	31/05/89	9.55	302.75	309.69	27.83	165.54	44.98	192.99	166.46	140.73	107.40	67.11	679.58
DPB97110	31/05/89	9.56	302.75	309.83	27.77	164.97	50.16	198.53	174.58	148.27	114.39	69.04	710.45
DPB97111	31/05/89	9.54	302.75	309.69	27.81	164.52	54.96	199.86	180.74	154.96	121.06	71.50	733.54
DPB97112	31/05/89	9.54	302.68	309.76	27.89	168.67	60.02	209.39	193.20	167.20	131.03	76.46	784.04
DPB97113	31/05/89	9.56	302.75	309.76	27.75	166.70	65.39	205.06	195.86	172.85	136.64	79.29	796.16
DPB97114	31/05/89	9.55	302.68	309.89	27.78	165.49	70.08	202.29	196.44	177.93	141.63	82.77	808.28
DPB97115	31/05/89	9.55	302.55	309.96	27.75	165.58	75.31	202.23	196.55	183.63	146.98	86.33	822.42
DPC97116	31/05/89	9.55	302.62	309.96	27.73	166.63	77.23	203.79	197.09	186.17	149.78	88.46	831.94
DPB97200	31/05/89	9.56	295.39	296.41	27.22	165.45	0.00	60.79	60.79	60.79	60.79	60.79	303.03
DPB97202	31/05/89	9.54	293.70	304.98	27.25	165.47	9.98	62.34	61.98	61.48	61.23	60.98	308.26
DPB97204	31/05/89	9.55	294.99	309.56	27.27	164.91	19.96	98.18	73.40	62.18	61.54	60.98	357.03
DPB97206	31/05/89	9.57	295.19	309.76	27.21	169.30	30.02	138.93	112.76	79.26	65.13	64.21	462.64
DPB97207	31/05/89	9.56	294.78	309.62	27.23	167.46	34.86	152.67	124.26	92.33	64.81	63.08	500.43
DPB97208	31/05/89	9.54	295.19	309.56	27.38	164.81	39.92	165.71	135.62	107.19	67.98	61.44	541.71
DPB97209	31/05/89	9.57	294.95	309.75	27.43	170.06	44.91	184.04	151.18	119.85	74.60	65.14	598.70
DPB97208	31/05/89	9.57	294.58	309.62	26.80	165.76	40.12	165.76	135.24	105.12	66.99	62.33	539.11
DPB97208	31/05/89	9.54	294.72	309.83	26.81	167.42	40.19	167.54	136.74	106.42	68.03	62.90	545.17
DPB97209	31/05/89	9.56	294.31	309.69	26.84	167.13	44.98	180.24	148.09	117.66	72.76	63.34	586.72
DPB97210	31/05/89	9.55	294.65	309.62	26.86	166.50	50.02	190.76	159.40	129.15	81.01	63.10	628.85
DPB97211	31/05/89	9.54	294.38	309.62	27.01	165.16	55.10	196.01	167.48	136.43	87.68	62.46	655.11
DPB97212	31/05/89	9.55	294.44	309.76	26.98	165.35	60.02	200.90	176.37	144.77	96.03	63.13	686.57
DPB97213	31/05/89	9.55	294.65	309.62	27.05	168.53	65.02	208.24	187.76	155.39	105.40	65.68	728.41
DPB97214	31/05/89	9.56	294.65	309.83	27.17	168.69	70.10	209.68	195.07	163.55	113.74	67.26	755.82
DPB97215	31/05/89	9.57	294.78	310.03	27.10	167.11	75.16	204.95	197.07	169.29	122.18	68.29	768.52
DPB97216	31/05/89	9.55	294.65	309.89	27.13	168.66	79.98	205.76	200.52	176.40	130.07	70.71	790.45
DPC97217	31/05/89	9.56	294.65	309.89	26.90	168.46	82.17	205.35	200.40	178.40	132.77	71.35	794.78
DPB97300	31/05/89	9.56	280.28	281.09	26.77	168.70	0.00	61.03	61.03	61.03	61.03	61.03	305.15
DPB97302	31/05/89	9.58	279.12	290.93	26.77	165.71	9.98	61.32	60.96	60.72	60.43	60.23	303.99
DPB97304	31/05/89	9.56	280.28	302.21	26.78	167.73	20.10	63.80	63.19	62.61	62.10	61.53	313.80
DPB97306	31/05/89	9.56	280.42	309.49	26.76	170.57	30.06	79.21	66.54	65.65	64.72	63.97	341.51
DPB97308	31/05/89	9.55	281.30	309.62	26.76	164.82	40.14	128.96	88.66	63.15	61.68	60.46	404.99
DPB97309	31/05/89	9.56	281.77	309.69	26.76	167.68	44.96	148.12	109.05	68.53	63.73	62.38	454.33
DPB97310	31/05/89	9.56	281.91	309.69	26.76	167.63	50.08	164.22	126.36	77.19	63.84	62.46	497.33
DPB97311	31/05/89	9.54	281.84	309.56	26.79	165.98	55.12	176.57	138.64	89.73	63.24	61.29	533.69
DPB97312	31/05/89	9.56	281.77	309.69	26.76	168.54	60.04	190.89	151.60	102.12	65.99	63.19	578.13
DPB97313	31/05/89	9.54	281.91	309.62	26.76	170.11	65.22	203.47	164.68	116.90	69.13	64.38	624.01
DPB97314	31/05/89	9.56	281.91	309.83	26.81	167.21	70.14	206.06	172.26	128.32	71.06	62.96	645.36
DPB97314	31/05/89	9.53	281.91	309.35	26.76	168.83	70.14	207.28	173.76	129.52	71.68	63.06	650.56
DPB97315	31/05/89	9.55	281.91	309.83	26.78	166.43	74.96	205.66	179.50	137.94	75.39	62.12	665.85
DPB97316	31/05/89	9.56	281.91	309.76	26.78	166.57	80.06	205.89	187.19	146.87	81.60	62.51	689.80
DPB97317	31/05/89	9.55	282.32	309.89	26.81	168.34	85.06	208.66	196.16	156.37	89.55	64.23	720.68
DPC97318	31/05/89	9.55	282.25	309.83	26.77	168.40	89.10	205.26	197.62	160.10	95.21	64.33	728.76
DPB97500	20/09/89	9.52	252.78	254.22	28.76	166.75	0.00	57.15	57.15	57.15	57.15	57.15	285.77
DPB97501	20/09/89	9.52	252.71	260.38	28.77	165.53	5.04	57.26	57.07	56.99	56.92	56.79	284.33
DPB97502	20/09/89	9.52	252.78	266.18	28.76	165.27	9.98	57.44	57.27	56.99	56.81	56.61	283.75

DPB97503	20/09/89	9.52	252.78	271.91	28.74	165.29	15.00	57.95	57.42	57.11	56.76	56.48	284.62
DPB97504	20/09/89	9.52	252.64	277.63	28.77	164.53	20.14	58.19	57.61	57.22	56.84	56.42	285.48
DPB97505	20/09/89	9.52	252.50	283.00	28.76	164.70	24.96	58.76	58.00	57.45	56.86	56.40	286.64
DPB97506	20/09/89	9.52	252.30	288.56	28.86	164.82	29.94	59.34	58.27	57.76	57.07	56.45	287.79
DPB97506	20/09/89	9.55	252.30	294.24	28.98	161.98	35.06	58.82	57.65	56.80	55.98	55.28	284.91
DPB97508	20/09/89	9.53	252.30	299.72	29.03	162.19	40.18	59.22	57.96	56.91	56.01	55.20	285.48
DPB97509	20/09/89	9.52	252.44	304.50	29.08	163.05	45.04	61.13	59.30	58.07	56.92	55.96	291.26
DPB97510	20/09/89	9.52	252.78	308.55	29.11	161.71	50.04	69.96	58.92	57.53	56.29	55.23	298.76
DPB97511	20/09/89	9.52	252.78	308.88	29.21	161.84	55.10	91.37	60.50	58.42	56.94	55.67	323.58
DPB97512	20/09/89	9.52	252.78	308.88	29.30	162.11	60.16	114.63	65.04	58.45	57.05	55.67	352.14
DPB97513	20/09/89	9.52	252.37	308.88	29.28	162.83	64.96	132.92	75.04	58.99	57.54	56.01	382.15
DPB97514	20/09/89	9.52	252.30	308.88	29.32	164.16	70.08	149.08	89.70	60.72	58.66	56.97	416.49
DPB97515	20/09/89	9.52	252.50	308.88	29.39	162.13	75.22	161.49	107.71	62.11	57.77	56.24	446.50
DPB97516	20/09/89	9.52	252.30	309.02	29.44	162.05	80.00	172.11	122.67	65.34	57.70	56.11	475.36
DPB97517	20/09/89	9.52	252.50	309.02	29.50	163.58	85.18	183.08	137.18	71.54	58.66	57.05	509.12
DPB97518	20/09/89	9.52	252.44	309.08	29.61	163.04	89.98	186.77	146.45	79.19	58.79	56.71	529.61
DPB97519	20/09/89	9.52	252.64	309.22	29.74	162.59	95.00	179.67	151.03	89.73	59.38	56.66	537.98
DPC97519	20/09/89	9.52	252.71	309.29	29.91	164.00	97.85	168.99	152.26	95.85	60.50	57.31	536.25
DPB97400	20/09/89	9.52	270.21	271.71	30.23	163.49	0.00	56.66	56.66	56.66	56.66	56.66	283.28
DPB97401	20/09/89	9.53	270.00	277.56	30.29	162.84	5.06	57.24	57.16	57.08	57.00	56.90	285.59
DPB97402	20/09/89	9.52	270.34	283.33	30.35	162.59	9.96	57.59	57.43	57.16	57.03	56.72	285.88
DPB97403	20/09/89	9.52	270.28	288.96	30.32	162.45	15.04	58.22	57.78	57.35	57.08	56.74	286.74
DPB97404	20/09/89	9.54	270.41	294.24	30.35	162.73	20.04	58.80	58.16	57.66	57.18	56.72	288.48
DPB97405	20/09/89	9.53	270.34	299.51	30.36	162.08	24.98	59.38	58.66	58.01	57.36	56.79	289.92
DPB97406	20/09/89	9.53	270.48	304.64	30.41	163.30	30.08	60.94	59.97	59.16	58.40	57.62	296.27
DPB97407	20/09/89	9.52	270.48	308.28	30.41	162.48	35.10	69.42	60.01	58.97	58.01	57.13	304.06
DPB97408	20/09/89	9.52	270.48	308.68	30.46	162.93	40.18	93.66	61.90	59.47	58.40	57.36	331.47
DPB97409	20/09/89	9.51	270.48	308.82	30.51	161.66	44.84	114.61	70.40	59.31	58.17	56.98	360.33
DPB97410	20/09/89	9.52	270.48	308.88	30.52	162.92	50.04	132.96	87.25	60.81	59.16	57.76	399.00
DPB97411	20/09/89	9.53	270.48	308.88	30.62	163.53	54.96	149.18	105.76	64.05	59.75	58.35	438.24
DPB97412	20/09/89	9.52	270.55	308.88	30.62	163.33	59.92	163.09	122.30	69.78	59.70	58.25	473.73
DPB97413	20/09/89	9.52	270.48	308.88	30.71	163.17	65.12	176.07	136.19	79.21	60.06	58.40	510.96
DPB97414	20/09/89	9.53	270.48	309.02	30.86	164.40	70.22	187.85	148.39	90.09	61.70	59.34	549.05
DPB97415	20/09/89	9.52	270.68	309.02	30.87	164.15	74.90	194.19	157.43	101.56	62.38	59.05	576.46
DPB97416	20/09/89	9.53	270.75	309.29	30.83	163.96	80.12	197.83	166.97	114.18	64.30	59.10	604.45
DPB97417	20/09/89	9.52	270.96	309.22	30.86	162.06	85.04	194.25	172.71	124.88	66.56	58.20	618.02
DPB97418	20/09/89	9.53	270.96	309.29	30.99	163.22	90.02	193.62	178.52	134.34	70.61	59.00	637.64
DPC97419	20/09/89	9.53	270.96	309.35	30.95	163.71	94.43	188.19	176.32	141.04	75.13	59.16	641.97
DPB97300	21/09/89	9.51	282.86	284.76	30.25	163.94	0.00	58.26	58.26	58.26	58.26	58.26	291.31
DPB97301	21/09/89	9.52	282.86	290.39	30.21	163.20	5.04	58.43	58.46	58.30	58.10	58.01	291.31
DPB97302	21/09/89	9.51	283.00	295.66	30.15	163.59	10.10	59.70	59.42	59.18	58.93	58.66	295.93
DPB97303	21/09/89	9.52	283.00	300.86	30.20	163.54	15.08	60.22	59.80	59.34	58.91	58.55	296.22
DPB97304	21/09/89	9.51	283.20	305.99	30.27	163.32	20.08	60.68	60.07	59.53	58.91	58.42	297.37
DPB97305	21/09/89	9.51	283.13	308.41	30.23	162.32	24.94	73.09	60.30	59.49	58.75	58.11	310.36
DPB97306	21/09/89	9.52	283.27	308.82	30.20	163.50	30.00	99.47	66.92	61.26	60.23	59.41	347.58
DPB97307	21/09/89	9.52	283.27	308.88	30.26	162.11	35.14	118.22	83.77	61.07	59.61	58.68	381.92
DPB97308	21/09/89	9.52	283.27	308.88	30.22	163.42	40.06	136.17	103.32	65.73	60.54	59.41	426.65
DPB97309	21/09/89	9.52	283.27	308.95	30.26	164.25	44.98	151.99	118.94	74.65	61.19	60.00	468.49
DPB97310	21/09/89	9.51	283.33	308.88	30.22	162.90	50.04	165.61	131.83	87.73	61.01	59.23	507.16
DPB97311	21/09/89	9.51	283.27	308.88	30.15	162.78	55.08	177.96	143.41	100.62	62.70	59.38	545.82
DPB97312	21/09/89	9.52	283.20	309.22	29.81	163.60	60.00	188.46	154.80	112.82	65.76	60.06	584.20
DPB97313	21/09/89	9.51	283.33	308.95	29.81	162.04	65.08	193.42	164.03	123.90	69.68	59.25	612.77
DPB97314	21/09/89	9.52	283.27	309.29	29.72	163.72	70.12	198.91	174.27	134.06	75.45	60.14	644.80
DPB97315	21/09/89	9.53	283.20	309.29	29.72	161.35	75.06	196.31	180.46	141.14	81.60	59.80	661.83
DPB97316	21/09/89	9.52	283.40	309.22	29.78	163.00	80.04	195.85	187.58	149.25	89.73	60.60	684.91
DPB97317	21/09/89	9.52	283.33	309.15	29.78	162.69	85.12	191.46	189.27	153.83	97.53	60.71	695.01
DPC97318	21/09/89	9.51	283.33	309.35	29.74	162.24	87.87	189.15	188.46	155.79	102.12	61.04	699.34
DPB97200	21/09/89	9.52	295.19	296.61	30.87	161.99	0.00	58.49	58.49	58.49	58.49	58.49	292.42
DPB97201	21/09/89	9.52	295.05	302.15	30.91	161.37	5.06	59.25	59.07	58.76	58.72	58.57	294.44

DPB97202	21/09/89	9.53	295.12	307.00	30.84	161.46	9.98	60.17	59.83	59.33	59.13	58.80	296.74
DPB97203	21/09/89	9.52	295.12	308.61	30.94	164.24	15.06	81.18	63.03	61.76	61.28	60.85	328.20
DPB97204	21/09/89	9.52	295.12	308.82	30.95	163.45	19.94	102.01	80.65	61.84	60.69	60.13	365.13
DPB97205	21/09/89	9.52	294.99	308.75	30.96	162.14	25.10	120.31	98.96	70.61	60.38	59.63	410.73
DPB97206	21/09/89	9.52	294.78	308.88	30.97	162.42	30.02	136.12	112.20	83.72	61.02	59.74	454.01
DPB97207	21/09/89	9.53	294.92	308.95	30.99	164.32	34.94	154.24	126.98	98.35	65.26	61.55	508.26
DPB97208	21/09/89	9.52	295.05	308.88	31.09	162.69	39.94	166.47	137.94	110.04	70.35	60.46	547.22
DPB97209	21/09/89	9.53	295.05	309.08	31.10	163.48	45.04	178.71	149.71	120.54	77.44	61.22	589.93
DPB97210	21/09/89	9.51	295.12	308.88	31.12	164.24	50.00	189.49	161.45	130.82	86.08	61.94	631.77
DPB97211	21/09/89	9.52	294.92	309.15	31.15	160.75	54.96	190.94	167.57	136.71	93.33	60.93	651.97
DPB97212	21/09/89	9.52	295.05	309.15	31.13	164.24	60.00	199.71	179.76	147.43	102.43	63.66	695.83
DPBP7213	21/09/89	9.53	294.85	309.35	31.22	163.18	64.96	196.19	184.11	153.06	109.46	64.04	709.97
DPB97214	21/09/89	9.52	294.99	309.29	31.18	162.18	70.12	191.40	187.26	159.29	117.10	65.32	723.34
DPB97215	21/09/89	9.53	294.72	309.35	31.28	161.84	75.04	189.85	189.23	165.02	123.21	67.01	737.09
DPB97216	21/09/89	9.52	294.78	309.35	31.39	163.15	79.96	191.93	191.73	171.99	130.47	70.11	758.74
DPC97217	21/09/89	9.52	294.72	309.29	31.51	163.32	82.48	192.90	192.19	175.15	134.21	71.81	769.70
DPB97100	21/09/89	9.52	305.38	307.00	31.99	163.38	0.00	60.87	60.87	60.87	60.87	60.87	304.34
DPB97101	21/09/89	9.52	305.52	308.82	31.99	163.01	5.04	80.96	74.68	63.18	61.84	61.65	342.72
DPB97102	21/09/89	9.51	305.11	308.82	31.83	161.61	10.14	99.31	89.18	78.07	62.90	60.25	390.33
DPB97103	21/09/89	9.52	305.11	308.88	31.96	163.56	15.00	118.47	104.31	90.30	71.52	61.73	447.18
DPB97104	21/09/89	9.51	305.11	308.82	31.99	164.85	20.08	138.15	119.81	103.04	82.74	63.16	508.64
DPB97105	21/09/89	9.51	305.04	308.88	32.07	164.25	25.18	153.16	131.97	112.81	91.02	64.54	555.10
DPB97106	21/09/89	9.51	305.52	308.75	32.04	163.55	30.08	165.91	143.24	122.16	99.44	67.60	600.69
DPB97107	21/09/89	9.51	305.11	308.95	32.00	164.50	35.02	179.24	155.52	132.01	107.05	70.95	646.86
DPB97108	21/09/89	9.52	305.45	308.95	32.12	164.04	40.19	188.07	165.33	140.67	114.17	74.38	685.24
DPB97109	21/09/89	9.51	305.18	309.02	32.13	162.34	45.00	190.15	170.61	146.05	118.50	76.98	704.29
DPB97110	21/09/89	9.51	305.11	309.02	32.12	162.95	49.90	195.75	179.10	154.25	124.84	80.02	736.32
DPB97111	21/09/89	9.51	305.45	309.22	32.16	161.99	54.98	193.27	183.37	161.02	130.66	84.79	755.65
DPB97112	21/09/89	9.52	305.04	309.22	32.18	162.06	59.86	192.17	187.26	167.18	135.72	87.78	772.97
DPB97113	21/09/89	9.51	305.04	309.15	32.18	162.79	65.06	192.29	190.64	174.33	141.90	92.20	793.74
DPB97114	21/09/89	9.52	305.04	309.29	32.22	162.44	70.14	191.13	189.37	179.18	146.73	96.51	806.15
DPB97115	21/09/89	9.51	305.25	309.35	32.22	162.02	75.06	191.19	185.80	181.80	150.45	100.74	812.79
DPC97116	21/09/89	9.52	305.04	309.35	32.32	162.12	76.97	191.31	184.80	182.30	151.56	101.80	814.52
DPB96300	21/09/89	9.51	283.06	284.42	32.74	140.91	0.00	44.41	44.41	44.41	44.41	44.41	222.07
DPB96301	21/09/89	9.53	283.54	291.87	32.79	141.74	5.18	45.04	44.79	44.71	44.56	44.52	223.51
DPB96302	21/09/89	9.52	283.40	297.69	32.80	141.20	10.12	45.27	44.95	44.71	44.46	44.26	224.09
DPB96303	21/09/89	9.52	282.93	303.22	32.76	140.95	15.02	45.85	45.22	44.79	44.51	44.20	225.24
DPB96304	21/09/89	9.52	282.18	308.08	32.79	140.29	19.92	47.47	45.56	45.06	44.56	44.15	227.55
DPB96305	21/09/89	9.51	282.38	308.61	32.83	139.89	25.02	69.28	47.03	45.33	44.69	44.15	251.50
DPB96306	21/09/89	9.53	282.86	308.88	32.77	140.41	30.08	87.00	62.19	45.94	45.14	44.41	286.13
DPB96307	21/09/89	9.51	282.79	308.88	33.01	138.40	35.12	100.91	78.84	50.45	44.23	43.45	319.31
DPB96308	21/09/89	9.51	283.00	308.82	33.01	140.41	40.29	117.07	92.81	61.60	45.76	44.78	363.75
DPB96309	21/09/89	9.51	283.40	308.82	33.03	142.25	44.98	130.80	104.78	73.99	48.02	45.97	405.02
DPB96310	21/09/89	9.52	283.27	308.88	32.87	140.78	50.04	138.71	113.59	84.19	49.81	45.37	434.16
DPB96311	21/09/89	9.51	283.33	308.88	32.85	142.49	55.16	147.83	124.98	95.00	54.64	46.18	470.81
DPB96312	21/09/89	9.52	283.27	309.15	32.88	140.53	59.88	147.25	130.98	101.08	59.16	45.24	486.10
DPB96313	21/09/89	9.51	283.33	308.95	32.85	143.40	64.94	151.98	141.37	110.12	66.30	46.90	519.00
DPB96314	21/09/89	9.53	283.20	309.22	32.90	142.00	70.00	146.56	144.95	115.01	72.79	46.85	529.10
DPC96315	21/09/89	9.52	283.33	309.29	32.82	142.20	75.06	141.88	146.41	119.32	80.30	47.48	537.75
DPB94300	22/09/89	9.55	283.06	284.15	30.07	99.72	0.00	24.59	24.59	24.59	24.59	24.59	122.97
DPB94301	22/09/89	9.56	282.79	293.43	30.15	99.70	5.10	25.05	24.94	24.79	24.85	24.72	124.71
DPB94302	22/09/89	9.55	283.00	301.74	30.15	98.80	9.98	25.23	25.05	24.83	24.74	24.59	124.71
DPB94303	22/09/89	9.56	282.86	308.61	30.14	98.71	15.04	28.29	25.13	24.83	24.69	24.38	127.88
DPB94304	22/09/89	9.55	282.79	308.95	30.18	99.91	19.94	42.89	30.94	25.79	25.55	25.27	151.25
DPB94305	22/09/89	9.54	283.00	308.95	30.18	102.93	25.00	55.53	44.37	29.44	26.82	26.41	183.57
DPB94306	22/09/89	9.54	282.79	309.02	30.25	100.34	29.98	64.65	52.06	37.10	26.07	25.40	206.37
DPB94307	22/09/89	9.54	282.72	309.15	30.30	99.03	34.98	71.40	59.76	45.10	27.63	24.93	230.61
DPB94308	22/09/89	9.55	283.20	309.35	30.29	102.13	40.04	79.59	69.76	53.18	32.41	26.28	262.93
DPB94309	22/09/89	9.55	282.86	309.35	30.37	99.29	44.96	77.34	73.73	57.41	36.72	25.14	271.59

DPB94310	22/09/89	9.55	283.13	309.35	30.41	101.28	50.06	79.25	80.80	63.96	42.77	26.54	295.54
DPB94311	22/09/89	9.55	282.93	309.22	30.45	102.66	55.10	78.55	85.23	69.00	48.25	27.61	310.54
DPB94310	22/09/89	9.55	283.27	309.29	30.48	106.07	51.46	89.29	87.11	68.38	45.03	28.59	320.64
DPB94311	22/09/89	9.56	283.33	309.35	30.48	105.75	53.34	87.33	87.81	69.69	46.90	28.62	322.08
DPB94311	22/09/89	9.54	283.13	309.22	30.47	105.64	54.92	86.35	88.92	71.42	49.05	28.88	327.28
DPB94311	22/09/89	9.55	283.27	309.35	30.50	105.76	56.07	85.19	89.15	71.88	49.96	29.01	326.99
DPC94311	22/09/89	9.56	283.13	309.35	30.52	105.46	56.97	83.63	89.35	72.31	50.77	29.11	327.28
DPC94311	22/09/89	9.57	283.33	309.35	30.53	106.00	57.01	83.83	89.47	72.23	50.81	29.18	327.86
DPC94311	22/09/89	9.55	282.79	309.22	30.57	104.76	56.80	82.94	88.73	71.80	50.58	28.96	324.97
DPB94100	22/09/89	9.56	303.22	304.50	31.14	105.66	0.00	28.00	28.00	28.00	28.00	28.00	139.99
DPB94101	22/09/89	9.55	306.06	309.02	31.19	105.97	5.06	36.25	34.35	31.35	27.69	25.45	154.71
DPB94102	22/09/89	9.54	304.98	309.15	31.10	104.45	9.94	46.07	41.97	36.93	32.08	25.74	182.99
DPB94103	22/09/89	9.54	302.48	309.02	30.95	104.26	15.00	47.68	43.39	36.50	30.57	22.67	180.39
DPB94104	22/09/89	9.55	302.68	309.08	30.91	105.43	19.94	54.49	51.66	43.47	35.89	25.27	210.11
DPB94105	22/09/89	9.54	303.36	309.08	30.91	107.12	25.08	64.02	62.55	53.89	43.84	30.90	255.42
DPB94106	22/09/89	9.55	303.16	309.22	30.92	104.95	30.08	68.86	68.25	60.24	48.57	34.67	280.81
DPB94107	22/09/89	9.55	303.56	309.35	30.80	105.82	35.27	71.52	73.25	66.82	54.13	38.64	305.05
DPB94108	22/09/89	9.55	302.62	309.29	30.87	107.43	40.18	75.44	79.90	73.63	59.32	41.03	330.44
DPC94109	22/09/89	9.55	304.03	309.29	30.79	107.20	43.42	69.15	76.83	74.67	61.58	44.30	327.27
DPB94300	11/10/89	9.56	283.74	284.76	29.63	103.60	0.00	26.18	26.18	26.18	26.18	26.18	130.92
DPC94311	11/10/89	9.56	283.47	309.42	29.57	102.26	55.08	79.28	85.70	69.81	48.96	27.84	350.52
DPC94311	11/10/89	9.56	283.81	309.42	29.60	101.96	56.04	76.57	85.04	70.27	50.13	27.95	370.14
DPP94312	11/10/89	9.56	283.81	309.49	29.52	100.52	57.05	72.41	83.85	69.69	50.49	27.79	480.09
DPP94313	11/10/89	9.55	283.25	309.43	29.61	102.84	58.90	74.64	87.21	72.03	52.72	28.85	574.54
DPP94314	11/10/89	9.56	283.88	309.56	29.71	104.23	60.16	74.89	88.66	73.54	54.83	29.77	379.38
DPP94315	11/10/89	9.56	283.54	309.42	29.70	103.00	61.39	71.32	86.39	72.31	55.35	29.56	370.43
DPP94316	11/10/89	9.55	283.47	309.49	29.78	102.55	62.89	70.85	85.62	72.23	56.44	29.92	368.70
DPP94317	11/10/89	9.56	283.67	309.49	29.93	103.76	64.28	71.37	85.70	73.20	58.13	30.70	372.45
DPP94318	11/10/89	9.56	283.67	309.49	29.83	103.23	65.64	70.85	82.77	73.66	59.03	30.99	362.06
DPP94319	11/10/89	9.55	283.54	309.42	29.91	102.16	67.74	72.30	72.46	73.54	60.25	31.35	350.23
DPP94320	11/10/89	9.56	283.33	309.62	29.88	100.95	69.41	73.28	66.31	72.27	60.62	31.38	341.29
DPP94321	11/10/89	9.55	283.47	309.49	29.91	103.72	71.07	76.97	68.08	74.12	63.63	32.91	350.23
DPP94317	11/10/89	9.56	283.33	309.49	30.13	101.64	57.95	74.43	85.31	70.27	51.48	28.29	330.61
DPP94316	11/10/89	9.56	283.67	309.49	30.06	102.40	55.23	80.55	85.74	69.62	49.14	27.87	332.63
DPP94315	11/10/89	9.55	283.54	309.35	30.11	102.70	52.77	82.57	85.47	68.35	47.01	27.64	328.01
DPB96300	11/10/89	9.55	281.64	283.06	29.90	133.69	0.00	40.35	40.35	40.35	40.35	40.35	201.73
DPC96315	11/10/89	9.55	281.91	309.49	30.09	135.46	73.59	130.79	135.68	108.69	72.75	43.15	493.46
DPP96316	11/10/89	9.56	281.70	309.56	30.06	135.06	75.92	123.85	134.76	109.53	75.97	43.60	490.86
DPP96317	11/10/89	9.55	282.32	309.56	30.09	134.25	77.75	116.99	131.57	109.33	79.49	44.01	483.93
DPP96318	11/10/89	9.56	282.38	309.62	30.15	135.02	79.28	113.65	128.65	108.92	81.57	44.35	480.76
DPP96319	11/10/89	9.56	282.38	309.69	30.22	136.02	81.05	112.15	127.10	110.22	84.29	45.47	482.79
DPP96320	11/10/89	9.56	282.38	309.76	30.11	136.92	82.81	110.65	111.30	108.46	86.72	45.96	468.93
DPP96321	11/10/89	9.55	282.38	309.69	30.20	136.65	83.87	111.63	101.26	106.42	88.18	46.26	462.30
DPB97300	12/10/89	9.57	282.52	284.22	30.86	162.39	0.00	57.22	57.22	57.22	57.22	57.22	286.11
DPB97301	12/10/89	9.57	282.86	289.98	30.87	162.80	5.06	57.74	57.68	57.49	57.40	57.27	286.98
DPB97302	12/10/89	9.57	282.93	295.59	31.03	161.87	9.96	58.38	57.99	57.72	57.40	57.25	288.13
DPB97303	12/10/89	9.57	282.93	298.03	30.96	161.61	12.03	58.55	58.30	57.95	57.59	57.27	289.58
DPC97317	12/10/89	9.57	283.20	309.89	30.94	160.34	87.52	183.44	191.46	149.99	98.41	59.17	677.41
DPP97318	12/10/89	9.57	283.00	309.83	30.92	161.17	89.41	178.02	191.88	151.68	101.40	59.77	677.70
DPP97319	12/10/89	9.58	282.86	309.83	30.98	162.10	91.09	174.03	191.38	152.37	103.71	60.36	676.25
DPP97320	12/10/89	9.57	282.93	309.83	30.97	162.40	92.72	169.76	188.62	152.37	106.65	60.96	673.94
DPP97321	12/10/89	9.58	282.86	309.83	30.97	163.10	94.36	164.57	184.84	151.37	109.24	61.43	666.44
DPP97322	12/10/89	9.57	283.00	309.83	31.01	163.63	95.96	158.05	178.11	151.03	112.46	62.23	657.78
DPP97323	12/10/89	9.57	283.20	309.83	31.03	164.53	97.62	158.45	158.30	151.33	115.89	63.22	645.09
DPP97324	12/10/89	9.57	283.20	309.89	31.11	165.08	99.55	161.63	135.94	148.60	119.53	64.28	630.95
DPB97100	12/10/89	9.56	305.11	306.66	30.80	166.14	0.00	62.67	62.67	62.67	62.67	62.67	313.35
DPB97101	12/10/89	9.57	305.85	309.08	30.78	164.98	5.06	78.95	73.32	62.06	60.77	60.54	334.70
DPB97102	12/10/89	9.57	304.30	309.42	30.84	163.24	9.96	91.19	82.60	67.87	59.19	58.87	359.23
DPC97115	12/10/89	9.57	305.31	309.83	31.19	162.23	77.03	190.86	190.79	178.79	148.74	99.21	805.06

DPP97116	12/10/89	9.57	305.38	309.83	31.29	163.89	77.93	191.20	191.33	179.91	150.27	100.69	811.70
DPP97117	12/10/89	9.57	305.25	309.83	31.19	166.21	79.67	197.03	194.79	184.30	153.83	102.01	832.19
DPP97117	12/10/89	9.58	305.45	309.83	31.27	165.78	79.69	198.53	195.52	185.22	154.81	102.89	835.94
DPP97118	12/10/89	9.57	305.31	309.83	31.21	165.87	81.35	191.89	194.68	185.34	155.59	104.12	830.74
DPP97119	12/10/89	9.57	305.58	309.83	31.20	165.88	82.99	186.12	193.18	185.53	157.18	106.43	828.15
DPP97120	12/10/89	9.57	305.38	309.89	31.22	166.20	84.53	182.43	191.60	185.76	158.06	107.31	826.13
DPP97121	12/10/89	9.56	305.52	309.83	31.30	166.44	86.41	181.10	189.29	185.45	159.44	109.57	825.26
DPP97121	12/10/89	9.58	305.25	309.83	31.23	165.16	86.39	178.04	186.10	183.37	157.33	107.85	813.43
DPP97122	12/10/89	9.57	305.25	309.83	31.31	164.96	87.99	177.81	180.13	182.49	158.29	109.85	809.39
DPP97123	12/10/89	9.58	305.31	309.96	31.20	165.46	89.84	181.68	172.25	180.91	158.14	111.08	805.64
DPP97124	12/10/89	9.56	305.52	309.83	31.21	165.30	91.37	186.53	167.43	179.87	158.84	113.49	807.66
DPP97125	12/10/89	9.57	305.11	309.89	31.31	165.93	92.89	189.30	163.47	177.37	157.67	113.54	803.91
DPP97126	12/10/89	9.57	305.58	309.96	31.40	166.12	94.49	194.14	159.13	171.56	155.31	115.88	798.42
DPP97127	12/10/89	9.57	305.52	309.89	31.33	166.83	96.13	198.94	153.39	164.13	154.84	117.88	793.81
DPP97129	12/10/89	9.59	305.25	310.03	31.50	168.06	97.91	207.42	159.39	148.28	154.97	119.18	788.61
DPB96100	12/10/89	9.58	302.28	303.90	31.92	139.13	0.00	45.16	45.16	45.16	45.16	45.16	225.82
DPB96101	12/10/89	9.57	302.75	308.75	32.06	138.69	5.16	51.97	46.20	45.81	45.71	45.55	235.34
DPB96101	12/10/89	9.57	303.16	309.22	31.86	136.61	10.18	70.15	64.32	52.20	44.82	44.49	275.16
DPC96113	12/10/89	9.57	304.17	309.83	31.90	139.01	65.45	139.41	147.66	136.65	112.53	76.33	610.48
DPP96114	12/10/89	9.57	304.17	309.69	32.18	138.08	66.43	137.73	147.35	137.19	113.07	76.67	608.46
DPP96115	12/10/89	9.57	304.17	309.83	32.18	138.71	68.09	134.27	147.58	138.54	114.74	78.12	610.19
DPP96116	12/10/89	9.57	304.10	309.76	31.98	139.05	69.55	132.25	148.20	139.27	115.85	79.19	610.77
DPP96117	12/10/89	9.56	304.17	309.76	31.94	138.84	71.27	128.21	146.93	139.96	117.07	80.72	610.19
DPP96118	12/10/89	9.57	304.17	309.83	32.05	140.61	72.85	127.98	146.24	140.81	118.84	82.51	613.65
DPP96119	12/10/89	9.56	304.17	309.83	32.18	139.72	74.51	126.83	144.12	140.73	119.44	83.68	611.34
DPP96120	12/10/89	9.57	303.97	309.83	32.01	140.71	76.15	127.98	139.54	140.42	119.54	84.20	609.03
DPP96121	12/10/89	9.57	304.17	309.83	32.01	140.46	77.81	131.33	132.19	139.23	120.14	86.22	606.44
DPP96122	12/10/89	9.58	304.10	309.83	32.25	140.45	79.45	134.21	127.42	137.65	119.07	86.95	603.55
DPP96123	12/10/89	9.57	304.17	309.76	32.44	139.59	81.02	137.73	124.92	134.69	118.40	88.43	602.11
DPP96124	12/10/89	9.57	304.17	309.83	32.25	140.19	82.97	142.12	120.34	129.65	116.42	89.73	596.05
DPP96125	12/10/89	9.57	304.17	309.83	32.28	140.64	84.61	145.64	117.53	116.88	114.66	91.24	586.52
DPP96126	12/10/89	9.57	304.17	309.83	32.38	141.46	86.07	150.20	119.84	102.26	112.63	92.72	574.98
DPB94100	12/10/89	9.58	304.57	305.99	32.64	116.54	0.00	33.24	33.24	33.24	33.24	33.24	166.21
DPB94101	12/10/89	9.58	303.63	308.95	32.76	112.52	4.98	40.63	35.01	31.78	31.37	31.40	169.38
DPB94102	12/10/89	9.58	306.59	309.22	32.70	112.59	10.08	51.07	47.24	41.24	36.69	30.23	206.32
DPC94109	12/10/89	9.57	302.75	309.62	32.71	113.61	45.74	73.18	82.14	76.22	62.17	43.00	335.31
DPP94110	12/10/89	9.57	302.82	309.56	32.73	111.24	48.13	74.27	83.41	78.87	64.87	44.98	345.40
DPP94111	12/10/89	9.57	303.09	309.49	32.58	110.11	49.63	71.16	82.18	79.37	65.96	46.20	343.96
DPP94112	12/10/89	9.57	303.49	309.56	32.56	110.82	51.48	79.64	90.22	86.03	71.39	50.02	375.42
DPP94112	12/10/89	9.57	303.76	309.56	32.51	113.02	51.52	64.12	76.79	77.72	66.25	47.78	331.27
DPB94200	13/10/89	9.59	293.90	295.19	31.89	101.51	0.00	25.77	25.77	25.77	25.77	25.77	128.87
DPB94201	13/10/89	9.58	293.97	303.49	31.88	99.81	4.88	25.48	25.42	25.31	25.25	25.17	126.85
DPB94201	13/10/89	9.58	294.17	309.22	31.91	101.49	10.23	32.46	26.65	26.31	26.14	25.98	137.53
DPC94210	13/10/89	9.59	294.38	309.83	31.56	102.78	48.81	78.46	85.40	74.25	56.47	32.50	327.11
DPC94210	13/10/89	9.58	294.17	309.69	31.73	101.15	50.18	76.04	84.29	74.75	56.89	32.88	323.94
DPP94211	13/10/89	9.58	294.58	309.76	31.61	101.00	51.46	72.46	82.90	75.60	57.87	33.79	322.79
DPP94212	13/10/89	9.58	294.58	309.76	31.58	100.98	53.05	70.32	82.82	76.60	58.60	34.47	322.50
DPP94213	13/10/89	9.58	294.65	309.83	31.57	101.48	54.71	69.63	83.90	78.68	60.34	35.77	328.27
DPP94214	13/10/89	9.59	294.44	309.83	31.10	99.93	56.29	65.88	80.55	77.10	59.72	35.79	318.46
DPP94215	13/10/89	9.58	295.12	309.76	30.83	101.37	57.81	68.19	82.36	79.48	62.13	37.98	330.58
DPP94216	13/10/89	9.59	294.78	309.89	30.91	100.94	59.73	68.30	81.13	77.25	62.13	38.39	327.11
DPP94217	13/10/89	9.58	294.78	309.89	30.89	101.80	61.25	69.74	79.55	78.02	63.33	39.56	331.15
DPP94218	13/10/89	9.59	294.92	309.83	30.85	99.91	62.89	70.90	71.13	75.87	62.68	39.79	321.34
DPP94219	13/10/89	9.58	294.58	309.89	30.93	99.87	64.59	73.15	69.24	75.79	63.77	40.42	322.79
DPP94220	13/10/89	9.59	294.99	309.89	30.90	101.50	66.31	76.27	67.82	75.87	66.00	42.44	330.29
DPP94221	13/10/89	9.58	294.72	309.76	30.99	99.87	67.79	77.30	65.13	72.10	65.82	42.65	323.65
DPP94222	13/10/89	9.58	294.58	309.89	30.98	100.80	67.77	77.88	66.13	73.37	66.39	42.73	327.40
DPP94222	13/10/89	9.58	295.12	309.83	30.93	101.52	70.14	81.46	67.63	67.48	67.90	44.60	330.86
DPC94109	13/10/89	9.58	301.13	309.69	31.25	101.14	43.13	65.70	71.86	67.17	54.29	36.34	295.66

DPC94109	13/10/89	9.57	301.10	309.35	31.23	98.82	43.27	67.96	73.59	68.42	55.28	36.65	303.31
DPP94110	13/10/89	9.58	301.33	309.62	31.21	103.16	44.69	70.67	76.86	71.83	57.74	38.65	315.86
DPP94111	13/10/89	9.59	301.54	309.69	31.26	100.22	46.33	67.67	75.90	72.48	58.83	39.74	314.42
DPP94112	13/10/89	9.59	301.47	309.69	31.30	99.06	47.97	66.80	76.13	73.83	59.93	40.65	317.01
DPP94113	13/10/89	9.59	301.81	309.89	31.21	100.55	49.73	65.53	76.78	75.79	61.92	42.29	323.65
DPP94114	13/10/89	9.58	301.74	309.76	31.25	101.16	51.21	65.53	77.75	77.56	63.85	43.98	329.13
DPP94115	13/10/89	9.58	301.07	309.69	31.28	99.36	52.91	66.40	79.28	79.45	65.15	44.49	334.62
DPP94116	13/10/89	9.59	301.67	309.69	31.30	100.03	54.43	64.26	75.13	78.64	64.21	45.25	327.98
DPP94117	13/10/89	9.58	301.41	309.59	31.45	100.29	56.17	66.81	77.09	81.08	67.18	47.17	339.67
DPP94117	13/10/89	9.59	300.86	309.83	31.36	99.16	56.19	67.01	77.45	81.13	66.55	46.23	337.98
DPP94118	13/10/89	9.58	301.60	309.76	31.45	99.36	57.93	68.19	71.09	79.18	64.68	47.51	332.02
DPP94119	13/10/89	9.58	301.74	309.76	31.51	101.26	59.47	70.73	71.32	79.83	65.56	48.70	336.64
DPP94120	13/10/89	9.58	301.74	309.69	31.65	103.00	61.25	73.90	71.44	81.60	68.13	50.75	346.16
DPP94121	13/10/89	9.58	301.54	309.76	31.63	100.92	62.89	75.92	69.47	79.37	66.91	50.80	342.12
DPP94122	13/10/89	9.58	301.67	309.62	31.72	99.32	64.53	77.36	65.59	75.10	66.63	51.20	335.48
DPP94123	13/10/89	9.58	301.47	309.83	31.56	101.71	66.31	80.48	66.70	73.18	68.29	52.52	342.41
DPP94124	13/10/89	9.58	301.60	309.69	31.91	101.31	67.91	83.48	68.97	69.44	69.14	53.77	345.87
DPP94125	13/10/89	9.59	301.81	309.83	31.59	100.81	69.45	85.44	69.82	63.98	68.60	54.05	342.70
DPB96200	13/10/89	9.58	294.58	296.00	31.34	135.85	0.00	42.57	42.57	42.57	42.57	42.57	212.86
DPB96201	13/10/89	9.58	294.58	302.28	31.26	135.87	5.18	42.86	42.69	42.60	42.49	42.31	212.57
DPB96202	13/10/89	9.57	294.51	308.48	31.31	134.70	10.12	43.43	43.19	42.95	42.75	42.47	214.88
DPB96204	13/10/89	9.60	294.38	309.56	31.24	133.74	19.94	76.39	63.89	43.91	42.36	41.82	268.26
DPB96206	13/10/89	9.58	294.44	309.49	31.31	133.15	30.04	103.63	87.16	67.77	44.81	41.25	344.44
DPB96208	13/10/89	9.58	294.44	309.49	31.34	133.73	39.69	125.04	108.63	85.39	57.48	42.34	418.32
DPB96209	13/10/89	9.59	294.24	309.49	31.09	133.47	44.98	132.43	118.56	93.35	64.60	43.12	451.21
DPB96210	13/10/89	9.58	294.31	309.56	31.16	134.76	50.37	136.81	128.10	101.55	73.04	44.31	482.67
DPB96211	13/10/89	9.59	294.24	309.69	31.26	135.32	55.51	136.93	134.68	108.13	79.35	45.69	502.87
DPB96212	13/10/89	9.58	294.44	309.76	31.38	134.36	60.00	134.85	138.18	113.82	85.29	47.43	518.16
DPB96213	13/10/89	9.58	294.44	309.83	31.31	135.21	65.18	133.46	140.61	119.79	91.06	49.79	533.16
DPC96213	13/10/89	9.58	294.72	309.89	31.29	135.72	67.85	131.50	139.68	122.40	94.10	51.53	538.07
DPP96214	13/10/89	9.58	294.65	309.83	31.20	135.02	69.57	129.02	139.72	123.86	95.60	52.39	539.80
DPP96215	13/10/89	9.58	294.58	309.83	31.01	135.06	71.09	124.06	139.22	124.67	96.96	53.35	536.92
DPP96216	13/10/89	9.57	294.72	309.83	31.05	135.07	72.93	120.88	138.11	125.63	98.77	54.73	537.20
DPP96217	13/10/89	9.59	294.65	309.83	31.13	136.48	74.49	118.75	137.11	126.02	99.81	55.53	536.05
DPP96218	13/10/89	9.59	294.31	309.83	31.13	136.79	76.11	117.42	135.80	125.52	101.01	56.44	534.32
DPP96219	13/10/89	9.58	294.38	309.83	31.21	136.23	77.91	116.32	132.26	123.52	102.17	57.68	531.14
DPP96220	13/10/89	9.58	294.65	309.83	31.33	136.58	79.57	118.11	120.64	119.59	103.01	59.35	519.31
DPP96221	13/10/89	9.57	294.72	309.83	31.26	136.73	81.07	121.17	114.14	116.86	104.31	60.80	516.14
DPP96222	13/10/89	9.59	294.65	309.96	31.28	137.63	82.97	123.37	100.13	107.55	104.93	61.89	498.83
DPP96223	13/10/89	9.57	294.72	309.83	31.44	137.04	83.67	124.69	101.59	97.74	104.69	62.83	491.90
DPB97200	16/10/89	9.57	295.19	296.61	30.15	162.15	0.00	58.54	58.54	58.54	58.54	58.54	292.69
DPB97201	16/10/89	9.57	295.12	301.94	30.15	161.63	5.04	59.18	59.12	58.85	58.75	58.59	294.71
DPC97216	16/10/89	9.57	294.72	309.83	30.37	159.15	80.90	184.93	187.89	164.50	126.12	67.37	730.15
DPB97200	26/10/89	9.57	294.24	295.86	30.62	161.25	0.00	57.92	57.92	57.92	57.92	57.92	289.61
DPB97201	26/10/89	9.57	294.31	301.33	30.65	161.60	5.14	58.90	58.61	58.46	58.33	58.23	292.78
DPC97216	26/10/89	9.56	293.77	309.83	31.73	162.20	83.73	192.50	195.89	170.30	130.19	69.50	758.81
DPP97215	26/10/89	9.57	293.77	309.83	31.63	162.48	82.87	194.18	197.35	169.80	128.92	68.93	759.39
DPP97216	26/10/89	9.56	293.77	309.83	31.85	163.34	84.63	192.91	196.81	171.42	131.34	69.79	763.43
DPP97217	26/10/89	9.57	293.77	309.83	31.99	162.56	86.41	183.79	195.16	171.84	132.82	70.57	755.06
DPP97218	26/10/89	9.57	293.77	309.83	31.96	162.15	88.07	179.52	193.70	173.00	135.26	71.76	754.48
DPP97219	26/10/89	9.57	293.77	309.83	31.86	163.67	89.69	177.79	193.31	173.73	136.89	72.62	756.51
DPP97220	26/10/89	9.57	293.77	309.83	31.99	163.15	91.05	173.81	191.54	173.65	138.22	73.48	753.04
DPP97221	26/10/89	9.56	293.77	309.83	32.14	162.20	92.83	167.63	183.00	169.07	138.63	74.20	736.02
DPP97222	26/10/89	9.57	293.77	309.83	32.03	162.49	94.61	170.06	175.42	166.46	140.43	75.50	731.40
DPP97223	26/10/89	9.57	293.77	309.83	32.14	164.15	96.13	168.84	138.33	159.18	143.80	78.23	693.31
DPP97224	26/10/89	9.57	293.70	309.83	32.18	161.08	96.89	172.82	134.06	138.29	139.88	77.01	669.94
DPB97500	27/10/89	9.58	257.09	258.53	30.22	160.35	0.00	53.64	53.64	53.64	53.64	53.64	268.19
DPB97501	27/10/89	9.58	257.43	264.75	30.55	163.66	5.06	56.64	56.22	56.22	56.16	56.05	280.60
DPB97502	27/10/89	9.59	257.57	270.89	30.78	169.90	10.39	60.79	60.03	59.99	59.82	59.61	299.93

DPB97502	27/10/89	9.58	257.50	270.96	30.84	166.14	10.39	58.48	57.87	57.79	57.69	57.43	289.25
DPB97502	27/10/89	9.58	257.37	271.30	30.85	161.36	10.35	55.43	54.99	54.87	54.62	54.50	274.25
DPB97504	27/10/89	9.59	257.57	282.72	30.87	160.60	20.22	55.83	55.18	54.75	54.31	53.98	274.25
DPB97506	27/10/89	9.59	257.43	293.84	30.68	160.24	30.18	57.27	56.14	55.48	54.83	54.16	277.13
DPB97508	27/10/89	9.59	257.57	304.30	30.59	159.66	39.92	58.37	56.87	55.98	54.99	54.19	279.44
DPB97510	27/10/89	9.58	257.57	309.29	30.72	161.28	49.92	83.53	59.07	57.64	56.36	55.28	312.34
DPB97512	27/10/89	9.58	257.85	309.42	30.50	161.68	59.81	127.40	71.69	58.41	57.09	55.72	371.78
DPB97514	27/10/89	9.55	257.57	309.35	30.65	159.25	70.18	156.02	105.24	60.06	55.98	54.50	435.55
DPB97516	27/10/89	9.58	257.43	309.42	30.26	160.39	79.84	177.49	130.44	69.49	57.38	55.72	495.58
DPB97518	27/10/89	9.58	257.57	309.62	30.22	162.47	89.90	189.15	148.87	88.77	59.20	56.89	548.96
DPC97519	27/10/89	9.58	257.98	309.83	30.36	162.90	96.70	171.43	149.60	105.39	60.65	56.99	551.27
DPP97518	27/10/89	9.57	258.05	309.76	30.27	161.23	96.17	171.43	148.64	104.66	60.08	56.42	547.52
DPP97519	27/10/89	9.58	257.85	309.76	30.27	162.55	97.77	166.99	150.91	108.16	61.30	57.38	550.98
DPP97520	27/10/89	9.58	258.05	309.83	30.23	163.72	99.39	145.92	149.75	112.54	62.05	57.69	534.53
DPB96500	27/10/89	9.58	256.61	258.05	28.21	138.22	0.00	41.19	41.19	41.19	41.19	41.19	205.95
DPB96501	27/10/89	9.57	256.00	264.27	28.52	138.16	5.10	41.94	42.00	41.88	41.84	41.78	209.99
DPB96502	27/10/89	9.58	256.00	271.23	28.50	140.91	10.16	43.32	43.30	43.07	42.93	42.80	215.47
DPB96504	27/10/89	9.59	256.07	284.49	28.56	140.76	20.22	44.30	43.88	43.54	43.25	42.93	218.07
DPB96506	27/10/89	9.59	256.14	297.01	28.40	140.80	30.08	45.29	44.53	43.88	43.35	42.85	219.80
DPB96508	27/10/89	9.59	256.00	308.41	28.57	139.51	40.00	49.04	45.00	44.04	43.25	42.51	224.42
DPB96510	27/10/89	9.57	256.14	309.35	28.20	138.57	50.29	87.24	50.57	44.30	43.35	42.41	270.01
DPB96512	27/10/89	9.58	256.07	309.42	26.47	140.61	60.23	115.18	74.93	46.73	44.86	43.68	328.88
DPB96514	27/10/89	9.59	256.07	309.62	26.55	139.88	70.06	135.37	100.13	54.42	44.21	43.16	381.97
DPB96516	27/10/89	9.58	256.07	309.62	26.64	137.99	79.98	136.47	111.44	72.81	44.60	42.61	413.71
DPC96517	27/10/89	9.58	256.14	309.83	26.76	138.31	83.67	125.97	112.25	80.55	45.48	42.72	412.85
DPP96516	27/10/89	9.58	256.14	309.83	26.72	138.05	83.01	129.03	112.33	79.05	45.32	42.61	413.42
DPP96517	27/10/89	9.58	256.34	309.83	26.21	138.88	84.75	124.24	112.91	82.63	45.97	42.85	413.42
DPP96518	27/10/89	9.59	256.55	309.83	25.93	139.07	86.19	111.48	112.52	85.55	46.59	43.16	405.34
DPP96518	27/10/89	9.58	251.82	252.71	-12.43	100.22	0.00	23.86	23.86	23.86	23.86	23.86	119.32
DPB94501	27/10/89	9.58	251.89	263.25	-12.41	99.37	5.16	23.92	23.67	23.67	23.57	23.55	118.17
DPB94502	27/10/89	9.58	252.16	272.46	-12.42	100.01	9.96	24.27	24.13	24.09	23.94	23.86	120.48
DPB94504	27/10/89	9.58	252.71	290.93	-12.44	101.26	19.94	25.25	24.98	24.75	24.53	24.33	124.23
DPB94506	27/10/89	9.58	252.71	308.21	-12.42	100.39	30.08	27.79	25.29	24.90	24.48	24.17	126.54
DPB94508	27/10/89	9.57	252.71	309.29	-12.42	101.11	40.19	53.53	32.71	25.52	25.11	24.56	162.61
DPB94510	27/10/89	9.59	252.98	309.49	-12.42	105.05	50.06	74.02	52.76	29.75	26.90	26.20	212.24
DPB94510	27/10/89	9.58	253.26	309.42	-12.41	102.07	50.04	73.61	53.41	29.83	25.60	25.11	210.22
DPB94512	27/10/89	9.58	253.19	309.69	-12.42	99.04	60.12	79.73	63.53	43.56	25.37	24.09	239.65
DPC94513	27/10/89	9.59	253.26	309.76	-12.43	100.40	65.31	79.44	68.92	50.99	27.03	24.66	254.95
DPP94512	27/10/89	9.58	253.60	309.69	-12.41	102.34	64.65	83.19	69.26	50.14	27.42	25.42	259.86
DPP94513	27/10/89	9.58	253.74	309.69	-12.41	100.93	66.31	78.92	70.38	52.83	27.57	24.87	258.41
DPP94514	27/10/89	9.58	253.60	309.76	-12.42	100.66	68.20	73.21	71.88	54.99	28.07	24.59	256.97
DPP94515	27/10/89	9.58	253.60	309.83	-12.41	102.06	69.69	71.76	73.50	57.30	29.05	25.21	261.01
DPP94516	27/10/89	9.58	253.74	309.83	-12.42	103.09	70.55	71.53	74.46	58.53	29.57	25.57	264.18
DPB94400	27/10/89	9.57	268.50	269.46	-12.42	99.64	0.00	24.08	24.08	24.08	24.08	24.08	120.41
DPB94401	27/10/89	9.55	269.18	279.33	-12.42	102.17	4.90	25.29	25.31	25.27	25.15	25.09	125.89
DPB94402	27/10/89	9.56	269.12	288.56	-12.42	100.69	10.10	25.17	25.01	24.89	24.73	24.65	124.16
DPB94404	27/10/89	9.56	268.91	305.52	-12.42	99.93	19.92	25.52	25.20	24.96	24.65	24.39	124.74
DPB94406	27/10/89	9.55	269.46	309.22	-12.42	102.40	30.08	49.88	32.97	26.47	25.98	25.59	162.54
DPB94408	27/10/89	9.56	268.98	309.29	-12.42	100.18	39.92	69.33	52.78	32.66	25.33	24.91	207.84
DPB94410	27/10/89	9.56	269.39	309.35	-12.44	101.37	50.02	82.83	68.25	48.63	27.69	25.69	256.90
DPB94412	27/10/89	9.55	269.39	309.35	-12.42	99.69	60.00	80.29	76.06	59.75	34.03	25.07	279.70
DPC94412	27/10/89	9.55	269.25	309.35	-12.44	99.52	60.29	79.37	75.52	59.75	34.16	24.89	278.25
DPP94411	27/10/89	9.55	269.25	309.35	-12.42	99.24	59.79	79.19	75.06	59.21	33.85	24.70	277.10
DPP94412	27/10/89	9.55	269.53	309.35	-12.45	101.64	61.29	82.60	77.95	61.75	35.48	25.74	289.51
DPP94412	27/10/89	9.55	269.46	309.35	-12.42	101.18	61.50	81.10	77.64	61.79	35.90	25.59	286.91
DPP94413	27/10/89	9.56	269.25	309.42	-12.43	99.72	63.13	74.12	77.02	61.83	37.04	24.99	281.14
DPP94414	27/10/89	9.54	269.46	309.35	-12.43	99.72	64.78	72.15	78.33	63.40	38.83	25.20	285.47
DPP94415	27/10/89	9.56	269.87	309.42	-12.42	103.60	66.41	74.87	81.22	66.75	40.76	26.63	305.67
DPP94416	27/10/89	9.55	270.00	309.35	-12.42	103.58	68.09	71.12	80.03	67.94	42.60	26.65	310.86

DPP94417	27/10/89	9.54	269.93	309.42	33.04	102.97	69.57	69.04	77.87	68.98	44.39	26.78	329.62
DPP94418	27/10/89	9.55	270.00	309.35	33.02	103.04	71.37	69.67	71.68	69.75	46.03	26.89	258.06
DPB97400	31/10/89	9.56	268.57	270.00	31.85	164.91	0.00	57.40	57.40	57.40	57.40	57.40	287.01
DPB97400	31/10/89	9.56	268.50	275.86	31.82	162.15	5.04	56.82	57.25	57.06	56.99	56.93	285.85
DPB97401	31/10/89	9.55	268.50	276.00	31.91	162.58	5.06	57.06	57.17	56.94	56.94	56.85	284.99
DPB97402	31/10/89	9.56	268.57	281.70	31.98	162.17	10.16	57.52	57.55	57.21	57.12	56.88	285.85
DPB97404	31/10/89	9.55	268.57	292.21	32.01	161.47	19.88	58.44	58.09	57.56	57.20	56.75	288.45
DPB97406	31/10/89	9.55	268.57	302.95	32.05	161.21	29.86	59.83	58.94	58.13	57.45	56.75	290.47
DPB97408	31/10/89	9.58	268.57	309.69	32.02	161.25	40.04	78.12	60.52	59.29	58.36	57.32	313.56
DPB97410	31/10/89	9.55	268.57	309.35	31.86	157.91	50.00	123.89	76.68	57.63	56.42	55.19	371.56
DPB97412	31/10/89	9.56	268.57	309.35	31.90	157.71	59.88	152.28	109.84	62.40	56.60	55.14	439.66
DPB97414	31/10/89	9.55	268.64	309.42	32.05	159.06	70.00	177.56	136.47	80.37	57.77	56.20	514.39
DPB97416	31/10/89	9.55	268.84	309.35	31.98	161.38	80.12	193.20	156.32	104.03	60.81	57.58	578.75
DPB97418	31/10/89	9.56	269.05	309.76	32.08	160.09	89.96	188.99	166.25	126.08	65.30	57.42	612.51
DPC97419	31/10/89	9.56	269.53	309.83	32.06	162.34	95.00	182.70	161.32	135.62	70.03	58.46	617.12
DPP97418	31/10/89	9.55	269.39	309.62	32.03	161.30	94.61	183.10	161.98	135.01	69.79	58.23	615.11
DPP97419	31/10/89	9.55	269.39	309.62	32.07	162.12	96.21	168.56	158.24	137.74	71.69	58.41	601.83
DPP97420	31/10/89	9.54	269.53	309.56	32.02	162.97	97.75	151.07	156.20	140.47	73.84	59.11	588.84
DPP97421	31/10/89	9.55	269.46	309.76	32.09	164.08	99.65	142.70	146.39	143.01	75.48	59.99	574.71
DPP97422	31/10/89	9.54	269.53	309.62	32.09	164.48	100.35	143.86	140.08	144.32	76.83	60.18	572.11
DPB96400	02/11/89	9.59	271.09	272.25	27.96	138.59	0.00	42.24	42.24	42.24	42.24	42.24	211.20
DPB96400	02/11/89	9.60	270.55	278.92	28.03	138.03	5.04	42.58	42.47	42.28	42.29	42.16	211.20
DPB96401	02/11/89	9.59	270.68	278.92	28.01	138.38	5.00	42.47	42.43	42.28	42.26	42.11	211.78
DPB96402	02/11/89	9.57	270.75	285.50	27.98	138.29	9.96	43.04	42.78	42.62	42.50	42.29	213.51
DPB96404	02/11/89	9.60	270.75	298.50	28.21	137.30	20.02	43.51	43.13	42.70	42.37	42.01	214.37
DPB96406	02/11/89	9.58	271.02	309.22	28.18	141.17	29.92	50.26	46.36	45.66	45.10	44.47	233.42
DPB96408	02/11/89	9.52	270.96	309.22	27.96	137.81	40.06	90.31	57.17	44.74	43.98	43.07	282.76
DPB96410	02/11/89	9.59	270.89	309.69	27.88	141.26	49.88	116.69	85.18	50.09	45.74	44.68	347.98
DPB96412	02/11/89	9.58	270.96	309.56	28.10	139.32	60.27	138.96	107.57	68.36	45.64	44.06	412.62
DPB96414	02/11/89	9.59	270.89	309.76	28.04	138.39	70.12	145.54	122.35	88.45	48.19	43.72	458.50
DPB96415	02/11/89	9.58	270.96	309.83	28.03	139.56	79.78	140.75	128.77	104.07	55.67	44.34	483.89
DPC96415	02/11/89	9.58	271.09	309.83	28.02	137.49	80.25	132.44	123.43	103.03	56.32	43.10	466.29
DPP96414	02/11/89	9.58	271.37	309.76	28.15	139.23	79.65	140.93	128.77	104.03	55.95	44.14	483.89
DPP96415	02/11/89	9.58	271.43	309.89	28.15	139.51	81.21	138.04	127.16	105.95	57.82	44.42	482.74
DPP96416	02/11/89	9.58	271.30	309.83	28.20	140.15	82.81	128.81	124.43	107.53	59.59	44.73	474.37
DPP96417	02/11/89	9.60	271.30	310.03	28.15	141.06	84.43	117.26	120.58	108.92	61.22	44.97	462.54
DPP96418	02/11/89	9.58	270.96	309.83	28.13	138.56	85.55	104.45	101.45	107.18	62.37	43.93	429.07
DPB98200	06/11/89	9.54	294.44	296.07	28.52	197.72	0.00	84.42	84.42	84.42	84.42	84.42	422.08
DPB98201	06/11/89	9.55	294.11	300.39	28.58	196.89	5.08	84.89	84.73	84.65	84.42	84.21	423.52
DPB98202	06/11/89	9.55	294.17	304.57	28.40	194.98	10.06	85.69	85.27	84.96	84.61	84.23	425.83
DPB98203	06/11/89	9.55	294.17	309.22	28.54	194.62	19.96	112.88	85.50	84.61	83.91	83.12	452.66
DPB98206	06/11/89	9.55	294.11	309.42	28.58	194.53	30.49	167.18	129.17	88.46	84.94	83.79	562.32
DPB98208	06/11/89	9.54	294.17	309.35	28.66	194.84	39.92	205.97	164.49	114.24	86.53	84.99	669.95
DPB98210	06/11/89	9.54	294.24	309.35	28.82	195.53	49.90	237.94	192.50	146.83	90.71	84.91	771.53
DPB98212	06/11/89	9.55	294.24	309.42	28.86	197.91	60.00	268.18	220.97	174.92	103.49	87.35	879.45
DPB98214	06/11/89	9.54	294.24	309.56	29.01	194.79	70.14	277.94	238.75	194.39	120.37	85.30	944.67
DPB98216	06/11/89	9.56	294.24	309.69	29.02	194.72	80.06	283.25	255.14	211.97	138.47	86.60	1006.42
DPB98218	06/11/89	9.56	294.24	309.89	29.02	195.54	89.82	283.48	264.99	226.51	156.31	88.86	1054.90
DPB98220	06/11/89	9.55	294.24	310.03	29.12	197.63	99.96	292.13	271.64	241.02	174.52	93.09	1110.30
DPB98222	06/11/89	9.54	294.24	310.03	29.14	197.33	110.08	291.21	262.91	241.79	189.63	97.06	1118.96
DPC98222	06/11/89	9.54	294.24	309.89	29.10	196.86	110.57	290.46	263.14	242.44	190.98	97.69	1116.94
DPP98223	06/11/89	9.55	294.24	310.03	29.26	196.30	111.02	285.55	262.95	241.63	191.16	97.74	1110.01
DPB90200	06/11/89	9.54	294.72	296.47	29.55	230.74	0.00	112.85	112.85	112.85	112.85	112.85	564.24
DPB90201	06/11/89	9.54	294.65	300.32	29.54	230.10	5.06	113.83	113.46	113.35	113.14	112.93	567.41
DPB90202	06/11/89	9.56	294.72	303.70	29.50	229.44	9.98	114.41	113.73	113.39	112.98	112.59	568.27
DPB90204	06/11/89	9.54	294.65	309.08	29.75	228.55	20.08	129.70	115.08	114.31	113.32	112.49	586.74
DPB90206	06/11/89	9.56	294.65	309.35	29.70	229.71	30.45	205.48	141.74	117.69	116.17	114.82	703.32
DPB90208	06/11/89	9.55	294.72	309.35	29.58	230.49	40.06	257.71	198.61	128.51	117.34	115.52	830.58
DPB90210	06/11/89	9.54	294.58	309.35	29.55	228.66	50.00	296.49	234.08	159.29	116.56	114.36	937.06

DPB90212	06/11/89	9.54	294.72	309.35	29.60	227.18	59.88	329.10	264.36	195.07	119.78	113.58	1043.25
DPB90214	06/11/89	9.54	294.51	309.42	29.76	230.53	70.00	361.77	295.41	226.81	130.33	116.10	1156.08
DPB90216	06/11/89	9.54	294.72	309.56	29.77	227.25	80.04	377.23	317.46	253.01	145.55	114.80	1236.88
DPB90218	06/11/89	9.56	294.72	309.76	29.68	228.81	89.96	389.18	337.54	274.25	162.22	116.07	1310.17
DPB90220	06/11/89	9.55	294.72	309.89	29.70	229.11	100.22	392.64	352.86	293.72	183.85	116.80	1374.23
DPB90222	06/11/89	9.54	294.72	309.89	29.76	229.10	109.65	394.60	358.90	307.22	203.31	117.99	1418.67
DPB90224	06/11/89	9.55	294.72	310.09	29.86	229.05	119.75	406.72	361.90	319.53	222.89	121.24	1475.52
DPB90226	06/11/89	9.55	294.72	310.30	29.97	228.87	129.86	416.53	352.28	317.26	241.74	123.94	1503.80
DPC90227	06/11/89	9.55	294.72	310.23	29.92	232.84	137.72	437.66	336.81	307.15	255.79	129.16	1553.72
DPB93200	06/11/89	9.55	287.61	288.22	30.13	66.75	0.00	13.44	13.44	13.44	13.44	13.44	67.19
DPB93201	06/11/89	9.55	288.15	302.01	30.18	67.07	5.04	13.50	13.44	13.52	13.47	13.42	67.19
DPB93202	06/11/89	9.55	288.62	309.08	30.17	66.73	10.08	18.75	14.78	13.59	13.52	13.44	74.12
DPB93204	06/11/89	9.55	288.01	309.08	30.07	67.89	20.08	34.05	28.59	22.67	15.36	14.02	115.96
DPB93206	06/11/89	9.55	289.03	309.15	30.03	67.69	30.08	41.95	39.60	32.37	23.83	14.51	154.34
DPC93207	06/11/89	9.56	289.37	309.29	30.07	67.74	36.13	40.11	44.64	37.95	28.14	16.30	169.63
DPP93206	06/11/89	9.54	288.62	309.15	30.06	67.49	34.90	42.42	43.79	36.72	27.18	15.70	167.32
DPP93207	06/11/89	9.55	287.13	309.29	30.15	66.42	36.50	41.78	44.41	37.14	27.10	15.57	167.61
DPP93208	06/11/89	9.55	286.25	309.29	30.13	67.29	38.13	41.90	46.02	38.49	27.96	15.78	172.52
DPP93209	06/11/89	9.54	289.91	309.22	30.01	67.57	39.79	37.91	47.03	41.49	30.97	17.91	178.00
DPP93210	06/11/89	9.55	288.35	309.22	30.21	66.90	41.43	37.86	47.87	42.06	31.23	17.78	179.16
DPP93211	06/11/89	9.54	290.11	309.22	29.99	66.58	42.93	37.16	47.53	43.95	32.90	19.31	182.91
DPP93212	06/11/89	9.55	292.15	309.35	29.95	67.85	44.86	36.87	45.06	45.87	34.43	21.21	186.08
DPP93213	06/11/89	9.55	290.30	309.43	29.99	70.75	46.35	38.14	46.74	46.69	34.68	20.69	188.73
DPP93213	06/11/89	9.55	290.79	309.35	30.05	66.64	46.35	38.55	46.91	47.10	35.23	21.18	191.27
DPP93214	06/11/89	9.55	292.96	309.42	30.02	69.29	48.13	40.40	41.99	48.87	36.43	23.08	193.01
DPP93215	06/11/89	9.55	288.71	309.43	29.75	69.61	49.77	41.24	44.45	48.80	35.74	21.00	193.44
DPP93216	06/11/89	9.54	289.10	309.42	29.95	67.11	51.54	42.01	40.72	49.53	36.09	21.60	192.14
DPP93217	06/11/89	9.54	289.10	309.35	29.63	67.55	53.03	43.57	40.98	50.80	37.26	22.30	197.62
DPP93218	06/11/89	9.54	289.57	309.35	29.78	67.43	54.82	45.47	40.68	51.95	38.66	23.42	203.11
DPP93219	06/11/89	9.54	292.69	309.29	29.58	66.39	56.33	47.32	39.48	50.72	40.56	25.75	206.57
DPP93220	06/11/89	9.54	291.40	309.35	29.76	65.68	57.83	49.28	41.02	52.34	41.49	25.94	212.63
DPB92200	06/11/89	9.54	263.79	263.89	29.81	45.39	0.00	8.37	8.37	8.37	8.37	8.37	41.87
DPB92201	06/11/89	9.56	263.32	283.33	29.78	45.18	4.92	8.37	8.37	8.37	8.34	8.37	41.87
DPB92202	06/11/89	9.54	263.38	302.21	29.76	45.45	9.98	8.48	8.45	8.37	8.43	8.42	41.87
DPB92204	06/11/89	9.51	263.67	309.00	29.69	44.39	20.06	19.07	15.10	10.25	8.37	8.37	62.07
DPB92206	06/11/89	9.58	263.59	309.56	29.55	44.43	30.06	29.32	23.84	17.33	10.55	8.19	91.22
DPC92207	06/11/89	9.54	263.70	309.17	29.64	44.58	35.52	28.57	29.81	21.19	13.61	8.37	103.68
DPP92206	06/11/89	9.54	263.56	309.12	29.66	44.45	34.73	29.88	28.97	20.62	13.19	8.33	102.47
DPP92207	06/11/89	9.55	263.64	309.28	29.61	44.50	36.37	27.83	30.59	21.83	14.10	8.46	104.49
DPP92208	06/11/89	9.57	263.56	309.35	29.55	45.13	38.14	26.35	31.87	23.05	14.92	8.55	106.01
DPP92209	06/11/89	9.55	263.32	309.35	29.41	45.18	39.76	25.67	32.83	24.39	15.70	8.74	109.54
DPP92210	06/11/89	9.56	263.08	309.47	29.44	44.87	41.43	25.03	33.35	25.67	16.42	8.87	111.06
DPP92211	06/11/89	9.54	263.12	309.17	29.40	45.12	42.93	25.34	33.58	27.11	17.24	9.03	114.59
DPB91500	06/11/89	9.55	263.56	261.80	29.30	27.96	0.00	5.68	5.68	5.68	5.68	5.68	28.38
DPB91501	06/11/89	9.54	263.51	293.11	29.32	28.41	4.92	5.41	5.68	5.68	5.68	5.68	28.38
DPB91502	06/11/89	9.55	261.40	308.61	29.42	27.36	10.08	7.49	6.41	5.52	5.65	5.68	31.56
DPB91503	06/11/89	9.55	259.49	309.15	29.23	26.94	15.18	11.24	9.18	7.02	5.55	5.68	39.93
DPB91504	06/11/89	9.55	257.85	309.15	29.28	27.12	19.90	15.39	12.18	9.18	6.22	5.68	50.31
DPB91505	06/11/89	9.54	258.12	309.29	29.33	26.47	24.45	18.28	15.83	11.33	7.78	5.68	60.70
DPC91506	06/11/89	9.55	259.01	309.22	29.31	29.12	29.59	18.45	20.14	14.72	9.75	6.04	70.80
DPP91505	06/11/89	9.55	259.56	309.22	29.35	29.32	28.16	19.61	19.26	13.97	9.31	6.04	69.65
DPP91506	06/11/89	9.55	260.38	309.29	29.23	29.08	29.65	18.22	20.33	14.95	9.94	6.06	71.38
DPP91507	06/11/89	9.55	259.15	309.15	29.22	27.69	31.45	16.78	20.76	15.79	10.43	6.12	71.38
DPP91508	06/11/89	9.55	258.46	309.15	29.31	27.96	32.97	16.32	21.26	16.79	10.90	6.22	73.40
DPP91509	06/11/89	9.55	258.94	309.22	29.32	27.74	34.73	16.15	21.34	17.91	11.54	6.40	74.84
DPP91510	06/11/89	9.55	259.69	309.15	29.10	26.92	35.82	16.32	20.80	18.68	12.04	6.58	76.28
DPB98200	07/11/89	9.57	295.66	297.28	29.37	198.10	0.00	84.88	84.88	84.88	84.88	84.88	424.41
DPB98201	07/11/89	9.57	295.12	301.00	29.24	197.19	4.92	85.52	85.38	85.15	84.98	84.83	425.56
DPB98202	07/11/89	9.57	295.05	305.31	29.12	198.44	10.39	87.19	86.69	86.31	85.91	85.56	431.04

DPB98204	07/11/89	9.56	294.99	309.22	29.15	196.19	20.02	119.63	86.85	85.42	84.67	83.97	460.76
DPB98206	07/11/89	9.57	294.65	309.49	29.08	196.22	30.45	170.01	131.90	90.00	86.15	85.04	565.80
DPB98208	07/11/89	9.57	295.19	309.42	29.00	195.23	40.19	208.21	167.03	119.09	86.38	84.88	670.84
DPB98210	07/11/89	9.57	295.19	309.56	28.90	197.57	50.18	242.73	196.73	151.64	93.14	86.26	776.74
DPB98212	07/11/89	9.58	295.19	309.62	29.08	196.17	60.16	264.60	219.93	177.07	106.90	85.38	861.29
DPB98214	07/11/89	9.56	294.92	309.76	28.74	197.81	70.12	285.09	244.10	199.12	123.44	87.84	947.86
DPB98216	07/11/89	9.57	295.05	309.83	29.01	199.11	80.06	291.67	261.60	217.70	143.05	89.22	1014.23
DPB98218	07/11/89	9.57	295.19	309.89	28.84	195.37	89.96	281.28	264.03	227.32	159.88	89.04	1032.70
DPB98220	07/11/89	9.56	295.12	309.96	28.81	196.70	100.06	287.86	266.80	239.63	177.88	93.24	1076.56
DPC98221	07/11/89	9.57	295.19	310.03	28.80	196.69	108.01	286.18	259.56	239.82	188.55	96.65	1083.20
DPP98223	07/11/89	9.56	295.19	310.09	28.79	196.63	109.63	276.66	257.95	238.90	190.92	97.74	1073.10
DPP98224	07/11/89	9.56	295.05	310.23	28.83	197.22	111.29	265.46	259.37	239.82	193.93	99.40	1069.06
DPP98225	07/11/89	9.56	295.19	310.09	28.61	197.85	112.93	265.41	255.52	237.48	195.93	100.34	1066.75
DPP98226	07/11/89	9.57	295.12	310.16	28.68	198.31	114.71	265.46	249.21	234.90	198.76	101.92	1060.11
DPP98227	07/11/89	9.57	294.99	310.30	28.63	199.98	116.35	271.29	235.67	231.59	201.28	103.43	1054.63
DPP98228	07/11/89	9.56	294.85	310.30	28.75	201.25	118.13	280.93	201.50	228.47	204.03	105.17	1032.70
DPB90200	07/11/89	9.60	295.53	297.15	28.53	231.96	0.00	114.19	114.19	114.19	114.19	114.19	570.93
DPB90201	07/11/89	9.57	295.66	301.00	28.65	231.94	5.19	114.88	114.38	114.23	114.30	113.56	570.93
DPB90202	07/11/89	9.58	295.59	304.64	28.70	229.93	10.23	114.47	114.11	113.77	113.67	112.40	568.62
DPB90204	07/11/89	9.55	295.66	309.35	28.65	227.93	20.23	137.50	114.81	113.92	113.26	111.69	591.13
DPB90206	07/11/89	9.57	295.53	309.49	28.44	231.25	30.20	210.28	148.20	118.31	117.15	115.04	713.48
DPB90208	07/11/89	9.62	295.86	309.89	28.49	229.95	40.19	257.26	200.11	129.93	116.87	114.27	823.42
DPB90210	07/11/89	9.56	295.19	309.49	28.59	232.20	50.04	301.87	238.70	162.89	119.31	116.27	944.62
DPB90212	07/11/89	9.57	295.66	309.69	28.73	230.01	59.61	333.32	268.13	199.10	122.16	115.15	1046.48
DPB90214	07/11/89	9.56	295.53	309.56	28.70	230.07	69.69	359.80	295.29	230.08	132.45	114.97	1141.13
DPB90216	07/11/89	9.58	295.26	309.83	28.69	231.70	79.84	382.90	321.68	256.63	147.43	117.04	1236.34
DPB90218	07/11/89	9.57	295.66	309.89	28.73	229.56	89.69	390.57	340.35	278.83	167.92	116.58	1306.19
DPB90220	07/11/89	9.57	295.66	310.03	28.83	231.01	99.67	397.90	357.27	298.33	186.57	118.52	1371.10
DPB90222	07/11/89	9.57	295.66	310.30	28.82	231.05	110.02	401.71	364.86	313.34	207.18	120.03	1420.75
DPB90224	07/11/89	9.56	295.66	310.30	28.68	230.28	119.90	408.92	363.20	322.96	227.01	123.02	1458.54
DPB90226	07/11/89	9.57	295.66	310.50	28.75	230.73	130.02	420.80	356.30	322.23	243.29	126.76	1483.07
DPC90227	07/11/89	9.57	295.46	310.36	28.56	232.49	137.91	433.57	314.88	305.14	258.20	131.95	1458.83
DPP90228	07/11/89	9.56	295.46	310.43	28.63	232.35	137.93	431.20	298.36	303.68	258.04	131.85	1437.77
DPP90229	07/11/89	9.57	295.39	310.50	28.38	230.54	138.11	431.14	271.98	280.13	258.20	131.93	1388.14
DPB97100	23/11/89	9.58	305.52	307.00	27.94	172.59	0.00	67.20	0.00	0.00	0.00	0.00	0.00
DPB97101	23/11/89	9.59	305.04	309.62	28.14	171.36	4.92	76.09	0.00	0.00	0.00	0.00	0.00
DPB97102	23/11/89	9.56	304.64	309.56	28.03	171.36	10.33	103.73	0.00	0.00	0.00	0.00	0.00
DPB97104	23/11/89	9.59	305.11	309.89	28.30	171.57	20.23	142.63	0.00	0.00	0.00	0.00	0.00
DPB97106	23/11/89	9.59	305.18	309.96	28.41	172.71	29.94	176.85	0.00	0.00	0.00	0.00	0.00
DPB97108	23/11/89	9.58	305.11	309.96	28.58	171.46	40.27	200.98	0.00	0.00	0.00	0.00	0.00
DPB97110	23/11/89	9.59	305.11	309.96	28.66	172.30	50.04	217.66	0.00	0.00	0.00	0.00	0.00
DPB97112	23/11/89	9.59	305.11	310.03	28.70	171.07	60.43	220.54	0.00	0.00	0.00	0.00	0.00
DPB97114	23/11/89	9.59	305.18	310.16	28.50	171.17	70.96	219.16	0.00	0.00	0.00	0.00	0.00
DPB97116	23/11/89	9.58	305.25	310.30	28.43	172.94	80.12	227.76	0.00	0.00	0.00	0.00	0.00
DPC97117	23/11/89	9.59	305.11	310.30	28.38	172.86	86.31	226.77	0.00	0.00	0.00	0.00	0.00
DPP97116	23/11/89	9.58	305.31	310.30	28.45	172.33	85.00	228.45	0.00	0.00	0.00	0.00	0.00
DPP97117	23/11/89	9.59	305.11	310.30	28.39	172.89	86.68	226.14	0.00	0.00	0.00	0.00	0.00
DPP97118	23/11/89	9.59	305.04	310.30	28.45	173.03	88.24	218.64	0.00	0.00	0.00	0.00	0.00
DPP97119	23/11/89	9.58	305.04	310.30	28.42	172.49	89.84	211.25	0.00	0.00	0.00	0.00	0.00
DPP97120	23/11/89	9.60	304.98	310.30	28.54	172.99	91.60	209.00	0.00	0.00	0.00	0.00	0.00
DPP97121	23/11/89	9.60	304.84	310.30	28.49	173.97	93.22	208.31	0.00	0.00	0.00	0.00	0.00
DPP97123	23/11/89	9.58	305.11	310.30	28.42	174.18	94.88	206.58	0.00	0.00	0.00	0.00	0.00
DPP97124	23/11/89	9.59	305.25	310.30	28.47	173.43	96.52	208.36	0.00	0.00	0.00	0.00	0.00
DPP97125	23/11/89	9.60	304.98	310.30	28.42	173.08	98.16	212.00	0.00	0.00	0.00	0.00	0.00
DPP97126	23/11/89	9.58	305.04	310.30	28.50	173.09	99.84	217.94	0.00	0.00	0.00	0.00	0.00
DPP97127	23/11/89	9.60	305.11	310.36	28.55	173.28	101.72	222.56	0.00	0.00	0.00	0.00	0.00
DPP97128	23/11/89	9.57	304.71	310.30	28.48	174.25	103.22	228.62	0.00	0.00	0.00	0.00	0.00
DPP97129	23/11/89	9.60	305.11	310.43	28.51	174.29	104.84	234.28	0.00	0.00	0.00	0.00	0.00
DPB97300	23/11/89	9.59	282.79	284.22	28.73	172.60	0.00	63.85	0.00	0.00	0.00	0.00	0.00

DPB97301	23/11/89	9.59	282.52	289.50	28.81	176.01	5.27	65.93	0.00	0.00	0.00	0.00	0.00
DPB97302	23/11/89	9.59	282.79	294.58	29.02	174.74	10.21	66.45	0.00	0.00	0.00	0.00	0.00
DPB97304	23/11/89	9.60	282.72	304.17	28.79	172.91	20.10	66.74	0.00	0.00	0.00	0.00	0.00
DPB97306	23/11/89	9.60	282.79	309.89	28.53	174.69	30.08	88.03	0.00	0.00	0.00	0.00	0.00
DPB97308	23/11/89	9.59	282.66	309.89	28.96	169.84	40.06	134.38	0.00	0.00	0.00	0.00	0.00
DPB97308	23/11/89	9.60	282.38	309.96	28.81	172.41	40.08	135.24	0.00	0.00	0.00	0.00	0.00
DPB97310	23/11/89	9.59	282.59	309.89	28.76	174.24	50.04	170.04	0.00	0.00	0.00	0.00	0.00
DPB97312	23/11/89	9.59	282.59	310.03	28.77	175.04	60.43	200.69	0.00	0.00	0.00	0.00	0.00
DPB97314	23/11/89	9.59	282.38	309.96	28.51	172.25	69.84	213.79	0.00	0.00	0.00	0.00	0.00
DPB97316	23/11/89	9.60	283.06	310.30	29.02	174.78	80.18	223.43	0.00	0.00	0.00	0.00	0.00
DPB97318	23/11/89	9.58	282.38	310.23	29.05	173.81	90.51	218.69	0.00	0.00	0.00	0.00	0.00
DPC97319	23/11/89	9.58	282.38	310.30	29.02	172.17	95.84	213.56	0.00	0.00	0.00	0.00	0.00
DPP97318	23/11/89	9.60	282.38	310.30	29.08	172.58	95.02	214.02	0.00	0.00	0.00	0.00	0.00
DPP97318	23/11/89	9.59	282.38	310.30	28.87	174.94	96.80	219.10	0.00	0.00	0.00	0.00	0.00
DPP97318	23/11/89	9.58	282.45	310.30	28.94	174.96	98.42	209.17	0.00	0.00	0.00	0.00	0.00
DPP97320	23/11/89	9.58	282.38	310.30	28.94	174.22	100.08	194.40	0.00	0.00	0.00	0.00	0.00
DPP97321	23/11/89	9.59	282.45	310.30	29.05	174.52	101.74	184.18	0.00	0.00	0.00	0.00	0.00
DPP97322	23/11/89	9.58	282.38	310.30	29.06	174.90	103.36	178.47	0.00	0.00	0.00	0.00	0.00
DPP97323	23/11/89	9.59	282.38	310.30	29.10	175.16	105.02	176.97	0.00	0.00	0.00	0.00	0.00
DPP97324	23/11/89	9.59	282.38	310.30	29.39	173.42	105.47	176.33	0.00	0.00	0.00	0.00	0.00
DPB97500	23/11/89	9.35	255.65	257.02	28.61	174.02	0.00	61.95	0.00	0.00	0.00	0.00	0.00
DPB97501	23/11/89	9.39	254.42	261.26	28.75	172.16	5.04	61.60	0.00	0.00	0.00	0.00	0.00
DPB97502	23/11/89	9.53	254.01	267.55	29.12	170.44	10.94	61.08	0.00	0.00	0.00	0.00	0.00
DPB97502	23/11/89	9.59	254.22	267.62	29.02	171.18	10.96	61.37	0.00	0.00	0.00	0.00	0.00
DPB97504	23/11/89	9.63	254.90	277.97	28.96	171.94	19.92	63.33	0.00	0.00	0.00	0.00	0.00
DPB97506	23/11/89	9.60	255.52	289.03	29.00	173.16	30.06	65.24	0.00	0.00	0.00	0.00	0.00
DPB97508	23/11/89	9.59	255.52	298.84	28.65	171.62	39.77	65.87	0.00	0.00	0.00	0.00	0.00
DPB97510	23/11/89	9.59	255.52	308.82	28.58	171.94	50.43	72.16	0.00	0.00	0.00	0.00	0.00
DPB97512	23/11/89	9.59	255.77	309.83	28.46	184.37	59.88	106.13	0.00	0.00	0.00	0.00	0.00
DPB97512	23/11/89	9.60	254.01	309.83	28.59	173.86	60.29	104.31	0.00	0.00	0.00	0.00	0.00
DPB97514	23/11/89	9.57	255.65	309.83	28.63	170.30	70.55	157.00	0.00	0.00	0.00	0.00	0.00
DPB97514	23/11/89	9.58	255.65	309.83	28.65	171.21	70.55	157.29	0.00	0.00	0.00	0.00	0.00
DPB97514	23/11/89	9.58	255.24	309.83	28.88	170.30	80.12	182.05	0.00	0.00	0.00	0.00	0.00
DPB97514	23/11/89	9.58	255.38	309.83	28.91	169.69	80.18	181.99	0.00	0.00	0.00	0.00	0.00
DPB97516	23/11/89	9.59	255.18	309.89	28.92	170.52	89.96	200.75	0.00	0.00	0.00	0.00	0.00
DPB97520	23/11/89	9.59	255.59	310.09	29.14	171.14	100.00	200.00	0.00	0.00	0.00	0.00	0.00
DPC97521	23/11/89	9.58	255.65	310.03	29.08	171.54	103.14	190.59	0.00	0.00	0.00	0.00	0.00
DPP97520	23/11/89	9.58	255.65	309.96	29.20	171.47	101.86	196.42	0.00	0.00	0.00	0.00	0.00
DPP97521	23/11/89	9.59	255.65	310.16	29.25	171.11	103.13	189.26	0.00	0.00	0.00	0.00	0.00
DPP97522	23/11/89	9.59	255.65	310.16	29.37	171.68	104.18	187.88	0.00	0.00	0.00	0.00	0.00
DPP97523	23/11/89	9.58	255.72	310.23	29.47	172.43	105.02	177.43	0.00	0.00	0.00	0.00	0.00
DPP97524	23/11/89	9.59	256.00	310.30	29.44	172.95	105.94	168.14	0.00	0.00	0.00	0.00	0.00
DPB74500	26/09/89	7.01	223.39	224.29	24.23	99.64	0.00	23.12	23.12	23.12	23.12	23.12	115.60
DPB74501	26/09/89	7.03	222.91	234.77	24.27	98.89	4.98	22.89	22.93	22.93	22.91	22.91	113.87
DPB74502	26/09/89	7.02	222.91	244.20	24.20	103.02	9.98	24.57	24.51	24.39	24.31	24.26	120.79
DPB74503	26/09/89	7.02	222.91	254.83	24.30	99.59	14.90	23.59	23.51	23.36	23.28	23.20	113.87
DPB74504	26/09/89	7.05	222.77	264.89	24.24	100.43	20.04	24.16	23.89	23.74	23.48	23.38	114.45
DPB74505	26/09/89	7.03	223.32	275.52	24.18	98.60	25.02	23.64	23.35	23.09	22.91	22.73	111.56
DPB74506	26/09/89	7.02	223.39	283.74	24.26	100.98	30.18	25.03	24.62	24.32	24.00	23.82	116.18
DPB74507	26/09/89	7.03	223.88	288.01	24.23	100.52	35.00	36.11	24.51	24.36	23.92	23.72	127.43
DPB74508	26/09/89	7.03	223.74	288.01	24.39	101.99	40.12	55.21	28.08	24.70	24.57	24.16	151.38
DPB74509	26/09/89	7.02	223.81	287.88	24.53	100.36	44.98	73.34	40.05	24.36	24.18	23.74	180.82
DPB74510	26/09/89	7.03	223.81	288.08	24.69	102.40	50.02	89.38	52.63	26.70	24.68	24.47	213.71
DPB74511	26/09/89	7.02	223.88	288.08	24.97	102.12	55.08	103.00	67.75	31.40	24.50	24.31	257.00
DPB74512	26/09/89	7.02	223.88	288.01	25.11	100.49	60.10	111.77	81.22	39.86	24.34	23.95	288.45
DPB74513	26/09/89	7.03	223.53	288.15	25.01	99.41	65.00	118.12	92.15	48.63	24.60	23.43	317.02
DPB74514	26/09/89	7.03	223.74	288.15	25.05	100.21	70.00	124.58	102.57	57.60	26.31	23.59	353.38
DPB74515	26/09/89	7.02	223.88	288.22	24.88	98.93	74.98	125.22	109.77	67.37	28.16	23.17	369.25
DPC74515	26/09/89	7.03	224.15	288.22	25.07	99.29	76.50	124.47	112.04	70.22	29.15	23.22	375.31

DPC74515	26/09/89	7.03	224.15	288.15	25.17	99.55	76.23	125.34	112.23	69.76	29.07	23.33	379.35
DPC74515	26/09/89	7.03	224.44	288.32	25.29	100.87	78.50	127.81	116.35	73.74	30.55	23.87	411.57
DPB77300	26/09/89	7.02	256.82	258.26	25.78	163.57	0.00	55.54	55.54	55.54	55.54	55.54	277.69
DPB77301	26/09/89	7.03	255.65	263.32	25.73	164.66	5.04	56.29	55.88	55.85	55.82	55.70	278.84
DPB77302	26/09/89	7.03	255.11	268.84	25.77	163.84	10.10	56.40	55.92	55.69	55.59	55.41	279.42
DPB77303	26/09/89	7.03	255.31	274.77	25.68	163.60	15.04	56.86	56.23	55.88	55.64	55.31	279.13
DPB77304	26/09/89	7.03	255.59	280.48	25.75	163.60	20.10	57.50	56.69	56.27	55.85	55.51	281.15
DPB77305	26/09/89	7.03	255.31	286.05	25.71	162.66	25.02	57.61	56.85	56.23	55.80	55.25	281.44
DPB77306	26/09/89	7.03	255.18	288.01	25.70	161.10	30.12	77.87	56.31	55.77	55.12	54.45	299.62
DPB77307	26/09/89	7.03	255.18	288.01	25.71	160.01	34.92	110.25	61.39	55.35	54.63	53.96	335.98
DPB77308	26/09/89	7.03	255.11	288.01	25.73	161.73	40.06	137.43	81.89	56.19	55.69	54.84	386.19
DPB77309	26/09/89	7.03	255.18	288.08	25.64	161.60	45.00	163.86	106.56	58.81	56.08	55.33	441.31
DPB77310	26/09/89	7.03	255.45	288.08	25.63	161.47	50.04	186.89	128.76	67.08	55.80	55.20	494.11
DPB77311	26/09/89	7.02	255.52	288.01	25.66	162.42	55.02	206.51	148.34	79.66	56.21	55.64	547.21
DPB77312	26/09/89	7.03	255.52	288.08	25.69	160.76	60.04	219.44	165.73	94.32	56.16	54.84	590.78
DPB77313	26/09/89	7.03	255.65	288.15	25.68	160.34	65.08	230.58	182.78	108.87	57.74	54.71	635.22
DPB77314	26/09/89	7.03	255.59	288.22	25.71	160.38	70.22	238.72	198.90	123.60	60.73	54.53	677.06
DPB77315	26/09/89	7.03	255.59	288.42	25.77	161.61	75.04	245.53	212.63	136.68	65.30	54.97	716.02
DPB77316	26/09/89	7.03	255.65	288.49	25.81	161.19	80.10	248.76	224.33	149.65	71.35	54.94	749.78
DPB77317	26/09/89	7.03	255.65	288.56	25.76	161.17	85.08	249.57	232.10	159.84	78.50	54.86	774.89
DPB77318	26/09/89	7.03	255.65	288.56	25.77	161.63	89.96	252.11	239.22	168.04	86.52	55.70	802.30
DPB77319	26/09/89	7.03	255.65	288.62	25.78	162.13	95.10	253.43	241.37	173.39	95.35	56.50	821.06
DPC77319	26/09/89	7.03	255.65	288.62	25.75	163.79	96.15	256.15	243.72	175.20	97.32	57.33	830.58
DPP77320	26/09/89	7.03	255.72	288.62	25.77	163.77	96.93	255.97	243.84	175.74	98.88	57.28	832.02
DPP77321	26/09/89	7.03	256.07	288.76	25.75	163.67	97.60	253.78	243.72	176.47	100.49	57.59	832.31
DPP77322	26/09/89	7.03	256.07	288.69	25.78	163.78	98.34	251.82	243.95	177.08	101.64	57.62	832.89
DPP77323	26/09/89	7.03	256.00	288.62	25.83	163.75	99.02	249.62	243.91	177.89	103.19	57.93	833.75
DPP77324	26/09/89	7.02	255.93	288.69	25.82	164.31	99.65	247.55	243.53	178.66	104.47	58.24	832.89
DPP77325	26/09/89	7.03	255.93	288.62	25.75	163.17	100.37	243.74	242.34	178.24	105.61	58.16	829.42
DPP77326	26/09/89	7.02	256.14	288.62	25.70	163.68	100.90	242.99	242.30	178.93	107.01	58.42	830.29
DPP77327	26/09/89	7.02	256.07	288.62	25.73	163.77	101.50	241.72	242.45	179.47	108.26	58.66	831.73
DPP77328	26/09/89	7.03	256.00	288.76	25.79	164.25	102.13	241.49	241.53	179.43	109.27	58.74	831.45
DPP77329	26/09/89	7.03	256.14	288.76	25.78	164.73	102.87	240.10	241.03	180.01	110.52	58.94	831.73
DPP77330	26/09/89	7.03	256.14	288.76	25.80	164.74	103.50	239.70	240.41	179.58	111.74	59.33	831.16
DPP77331	26/09/89	7.03	256.14	288.76	25.80	165.37	104.20	238.14	239.60	180.20	113.24	59.57	831.73
DPP77332	26/09/89	7.02	256.14	288.90	25.86	164.26	104.86	233.70	237.14	179.70	114.52	59.25	825.67
DPP77333	26/09/89	7.03	256.14	288.83	25.75	164.41	105.53	232.43	236.72	179.78	115.66	59.33	824.81
DPP77334	26/09/89	7.03	256.14	288.83	25.75	165.59	106.19	231.44	237.18	180.51	116.75	60.06	826.54
DPP77335	26/09/89	7.03	256.14	288.83	25.69	165.59	106.88	230.81	236.18	180.39	118.13	60.24	826.83
DPP77336	26/09/89	7.03	256.07	288.76	25.71	166.17	107.40	228.27	234.26	180.31	119.30	60.63	823.36
DPP77337	26/09/89	7.03	256.14	288.76	25.72	166.17	108.01	222.90	231.99	180.58	121.11	60.99	818.17
DPP77338	26/09/89	7.02	256.14	288.56	25.73	166.04	108.69	221.92	221.56	180.39	122.75	60.50	807.49
DPP77339	26/09/89	7.03	256.14	288.76	25.68	166.54	109.39	223.48	214.86	180.74	124.39	61.41	806.63
DPP77340	26/09/89	7.03	256.14	288.83	25.77	166.12	110.02	223.42	205.05	180.04	125.58	61.31	795.95
DPP77341	26/09/89	7.03	256.14	288.76	25.79	166.27	110.33	224.35	202.25	180.12	126.57	61.57	795.66
DPB74300	27/09/89	7.04	254.15	255.18	22.88	106.09	0.00	26.22	26.22	26.22	26.22	26.22	131.12
DPB74301	27/09/89	7.05	254.30	265.94	22.84	96.54	4.99	22.79	22.55	22.78	22.66	22.67	112.85
DPB74302	27/09/89	7.04	254.63	275.18	22.93	100.68	9.96	24.66	24.53	24.60	24.42	24.37	122.47
DPB74302	27/09/89	7.05	254.70	275.25	22.85	101.25	9.96	24.61	24.53	24.60	24.45	24.32	121.89
DPB74303	27/09/89	7.05	255.11	284.69	22.75	100.79	15.02	24.84	24.53	24.56	24.37	24.22	121.89
DPB74304	27/09/89	7.05	255.11	288.15	22.85	100.93	20.06	37.30	24.80	24.87	24.58	24.35	136.03
DPB74305	27/09/89	7.04	255.38	288.08	22.83	100.87	24.84	55.54	36.54	25.03	24.76	24.45	166.33
DPB74306	27/09/89	7.05	255.59	288.15	22.79	101.74	30.02	74.30	52.93	30.26	25.10	24.87	207.59
DPB74306	27/09/89	7.05	255.65	288.15	22.81	99.92	30.22	73.14	52.66	30.49	24.42	24.22	204.42
DPB74307	27/09/89	7.04	255.59	288.15	22.94	101.09	35.10	87.57	66.93	40.69	25.02	24.66	244.53
DPB74308	27/09/89	7.04	255.52	288.15	22.99	100.24	40.08	96.52	79.78	50.81	26.79	24.29	278.00
DPB74308	27/09/89	7.04	255.45	288.08	23.07	100.32	40.16	96.52	79.71	50.77	26.81	24.24	278.00
DPB74309	27/09/89	7.05	255.52	288.42	23.15	101.10	44.96	104.19	90.82	60.81	30.66	24.50	310.90
DPB74310	27/09/89	7.05	255.65	288.35	23.26	101.84	50.16	111.75	100.87	71.62	36.71	24.68	345.24

DPB74311	27/09/89	7.05	255.65	288.49	23.26	101.33	54.71	116.37	107.64	80.12	42.32	24.92	371.79
DPB74312	27/09/89	7.05	255.65	288.49	23.30	100.53	60.00	118.74	114.14	89.05	48.81	25.28	396.31
DPC74312	27/09/89	7.05	255.59	288.56	23.33	100.04	63.56	117.24	117.99	94.20	53.02	25.77	408.14
DPC74313	27/09/89	7.04	255.65	288.42	23.30	100.95	64.63	118.91	120.30	96.86	54.78	26.32	417.38
DPP74313	27/09/89	7.06	255.65	288.56	23.28	100.68	65.24	118.68	120.95	97.28	55.30	26.32	418.82
DPP74314	27/09/89	7.05	255.86	288.49	23.31	100.36	66.00	118.85	121.45	98.48	56.34	26.45	422.00
DPP74315	27/09/89	7.04	255.93	288.49	23.32	101.56	66.52	120.35	123.30	99.98	57.46	26.94	428.35
DPP74316	27/09/89	7.04	255.79	288.56	23.44	100.72	67.32	119.54	123.26	100.44	58.08	26.84	428.35
DPP74317	27/09/89	7.05	256.07	288.56	23.38	100.75	67.95	118.51	123.57	101.13	58.94	27.10	429.21
DPP74318	27/09/89	7.04	255.86	288.49	23.26	100.14	68.50	116.60	123.57	101.71	59.72	27.15	428.63
DPP74319	27/09/89	7.04	255.86	288.42	23.21	102.05	68.48	122.60	125.88	102.98	59.85	27.67	438.44
DPP74320	27/09/89	7.04	256.00	288.49	23.13	100.11	67.62	118.22	122.88	100.55	59.02	26.81	427.77
DPP74320	27/09/89	7.04	256.14	288.56	23.11	102.78	68.48	125.14	126.95	103.82	60.50	27.80	444.50
DPP74321	27/09/89	7.04	256.07	288.49	23.08	99.78	69.18	117.99	123.84	102.28	60.65	27.00	431.81
DPP74322	27/09/89	7.05	256.14	288.56	23.05	101.49	69.73	119.78	125.72	103.67	61.38	27.46	439.02
DPP74323	27/09/89	7.05	256.00	288.49	23.14	101.98	70.41	118.39	126.49	104.56	62.11	27.75	439.60
DPP74324	27/09/89	7.05	256.00	288.62	23.05	101.74	71.11	114.81	126.80	105.59	63.17	28.01	439.02
DPP74325	27/09/89	7.05	256.14	288.69	23.21	101.58	71.78	113.48	127.15	106.02	63.98	28.22	439.60
DPP74326	27/09/89	7.05	256.07	288.56	23.14	101.16	72.44	112.39	127.68	106.56	64.65	28.24	440.18
DPP74327	27/09/89	7.04	255.93	288.56	23.16	101.25	73.07	115.16	128.57	106.83	65.38	28.40	443.93
DPP74328	27/09/89	7.05	256.00	288.56	23.14	100.62	73.69	111.93	127.26	106.67	66.06	28.48	440.75
DPP74329	27/09/89	7.05	256.14	288.56	23.16	100.58	74.36	111.18	127.61	107.36	66.84	28.74	441.91
DPP74330	27/09/89	7.04	256.14	288.56	23.16	101.22	74.92	112.33	128.99	108.52	67.67	29.02	446.81
DPP74331	27/09/89	7.05	256.06	288.56	23.27	101.63	75.61	111.46	130.01	109.18	68.51	29.37	449.17
DPP74331	27/09/89	7.04	256.07	288.56	23.26	100.10	75.59	109.44	128.45	108.10	68.37	29.41	443.35
DPP74332	27/09/89	7.04	256.14	288.56	23.22	101.39	76.33	112.39	130.88	109.98	69.48	29.67	452.30
DPP74333	27/09/89	7.05	255.79	288.56	23.21	101.47	76.91	110.60	129.61	109.83	69.74	29.72	450.56
DPP74334	27/09/89	7.04	255.79	288.56	23.24	100.79	77.66	104.25	124.18	109.60	69.17	31.52	438.45
DPP74335	27/09/89	7.05	256.07	288.69	23.25	101.23	78.14	105.75	123.84	110.37	70.08	32.03	438.73
DPP74336	27/09/89	7.04	256.00	288.56	23.30	102.81	78.83	106.27	124.84	112.17	72.05	33.44	447.97
DPP74337	27/09/89	7.05	256.07	288.56	23.30	101.33	79.45	105.58	115.64	111.14	71.12	31.00	448.83
DPP74338	27/09/89	7.04	256.00	288.56	23.38	100.91	80.06	109.50	117.14	111.83	71.04	31.07	443.93
DPB76300	27/09/89	7.05	258.05	259.15	24.09	133.29	0.00	38.69	38.69	38.69	38.69	38.69	193.48
DPB76301	27/09/89	7.05	257.91	266.66	24.09	133.39	5.02	39.10	39.08	38.85	38.78	38.77	195.21
DPB76302	27/09/89	7.05	257.98	273.82	24.08	134.58	10.10	40.09	39.88	39.74	39.47	39.29	198.39
DPB76303	27/09/89	7.05	257.98	280.75	24.18	134.87	15.02	40.60	40.31	40.08	39.69	39.50	200.12
DPB76304	27/09/89	7.05	257.98	287.07	24.14	137.34	19.90	42.34	42.15	41.74	41.35	41.01	208.77
DPB76305	27/09/89	7.04	258.05	288.08	24.21	133.81	25.14	65.88	40.65	40.38	39.78	39.38	226.38
DPB76306	27/09/89	7.04	257.91	288.15	24.22	136.86	30.04	90.40	55.61	42.03	41.58	41.03	271.10
DPB76307	27/09/89	7.05	257.85	288.15	24.21	134.41	35.27	112.17	78.40	43.65	40.10	39.60	314.10
DPB76308	27/09/89	7.05	257.91	288.28	24.13	136.36	39.98	132.08	96.10	52.81	41.24	41.01	363.16
DPB76309	27/09/89	7.05	257.71	288.22	24.15	133.93	44.88	144.49	111.88	65.32	40.28	39.60	400.96
DPB76309	27/09/89	7.04	257.98	288.15	24.29	133.50	44.96	144.49	112.26	65.89	40.08	39.34	401.24
DPB76309	27/09/89	7.05	257.85	288.28	24.25	133.08	50.29	155.67	129.34	79.39	42.03	39.15	444.23
DPB76310	27/09/89	7.05	257.57	288.42	24.21	132.44	50.31	156.32	129.42	79.36	42.13	39.22	445.10
DPB76311	27/09/89	7.03	258.05	288.15	24.37	134.07	54.94	166.30	144.43	91.86	45.99	39.66	486.36
DPB76312	27/09/89	7.05	258.05	288.56	24.27	135.25	60.04	175.48	157.74	104.53	51.56	40.06	527.05
DPB76313	27/09/89	7.05	257.91	288.49	24.41	135.34	65.04	181.77	168.40	116.25	58.42	40.20	562.84
DPB76314	27/09/89	7.05	258.05	288.56	24.45	134.97	70.08	183.67	175.48	126.14	65.91	40.24	588.53
DPB76314	27/09/89	7.05	258.05	288.56	24.37	134.77	70.04	183.33	175.43	126.07	66.04	40.20	588.23
DPB76315	27/09/89	7.05	258.05	288.56	24.41	134.78	75.04	185.11	182.13	135.30	73.91	40.69	613.91
DPC76315	27/09/89	7.05	258.05	288.56	24.43	135.79	79.73	185.52	187.35	142.04	81.16	41.76	634.97
DPP76314	27/09/89	7.04	258.12	288.56	24.58	136.53	78.52	189.90	189.13	142.04	79.84	42.06	640.17
DPP76315	27/09/89	7.05	258.53	288.56	25.03	136.18	79.24	189.21	189.09	142.30	80.66	42.17	640.76
DPP76316	27/09/89	7.04	258.46	288.56	25.07	135.91	79.82	188.68	189.56	143.49	82.07	42.41	642.78
DPP76317	27/09/89	7.04	258.33	288.56	25.20	135.98	80.43	187.42	189.37	143.99	82.79	42.25	642.48
DPP76318	27/09/89	7.04	258.46	288.62	25.38	135.48	81.21	187.42	189.63	144.15	83.79	42.28	643.92
DPP76319	27/09/89	7.05	258.39	288.62	25.48	135.48	81.74	186.39	189.59	143.85	84.51	42.38	643.34
DPP76320	27/09/89	7.04	258.46	288.62	25.59	136.66	82.32	190.65	192.79	146.61	85.88	43.01	656.04

DPP76321	27/09/89	7.04	258.39	288.69	25.75	136.95	83.22	189.39	193.56	147.15	86.93	43.27	657.20
DPP76322	27/09/89	7.04	258.46	288.56	25.92	136.56	83.67	188.92	193.60	148.04	88.18	43.50	659.21
DPP76323	27/09/89	7.06	258.53	288.69	26.12	137.06	84.34	187.65	194.14	147.85	88.66	43.72	658.65
DPP76324	27/09/89	7.05	258.46	288.56	26.25	135.61	85.02	178.77	191.90	147.85	90.07	43.22	649.70
DPP76325	27/09/89	7.05	258.46	288.62	26.42	135.64	85.80	176.92	191.90	148.35	91.02	43.40	647.96
DPP76326	27/09/89	7.05	258.53	288.56	26.55	135.63	86.41	175.77	192.37	149.04	92.18	43.65	650.28
DPP76327	27/09/89	7.04	258.46	288.56	26.75	135.65	87.17	175.24	192.98	150.08	93.54	43.81	652.59
DPP76328	27/09/89	7.04	258.53	288.56	27.07	135.89	87.75	174.38	192.82	150.58	94.49	43.86	653.45
DPP76329	27/09/89	7.03	258.53	288.56	27.27	135.85	88.32	172.93	192.82	151.39	95.71	44.20	653.73
DPP76330	27/09/89	7.05	258.53	288.69	27.35	135.76	89.10	172.18	192.48	151.92	96.57	44.33	654.32
DPP76331	27/09/89	7.05	258.53	288.76	27.38	136.88	89.75	174.14	194.67	153.23	97.46	44.77	660.66
DPP76332	27/09/89	7.04	258.60	288.76	27.44	136.68	90.47	172.58	193.75	153.85	98.90	45.01	661.23
DPP76333	27/09/89	7.06	258.53	288.90	27.62	135.62	91.09	166.76	189.43	152.51	99.26	44.38	648.83
DPP76334	27/09/89	7.06	258.53	288.83	27.64	135.59	91.74	166.93	189.56	153.20	100.15	44.77	651.42
DPP76335	27/09/89	7.04	258.53	288.62	27.82	135.18	92.40	166.52	189.29	153.96	101.40	44.90	652.88
DPP76336	27/09/89	7.05	258.53	288.76	27.93	135.11	92.97	165.38	187.67	154.05	102.10	45.06	651.71
DPP76337	27/09/89	7.04	258.53	288.76	27.97	134.60	93.59	165.20	186.75	154.58	103.15	45.19	652.01
DPP76338	27/09/89	7.05	258.53	288.90	27.98	135.27	94.34	164.51	185.67	154.65	104.04	45.34	651.42
DPP76339	27/09/89	7.05	258.53	288.83	27.98	135.01	94.92	163.64	184.56	155.15	105.21	45.74	651.71
DPP76340	27/09/89	7.04	258.60	288.69	28.05	134.44	95.53	164.57	182.93	155.70	106.32	45.84	652.59
DPP76341	27/09/89	7.05	258.67	288.96	28.14	134.91	96.25	166.18	179.09	155.42	107.10	46.10	651.14
DPP76342	27/09/89	7.04	258.53	288.76	28.14	134.55	96.91	167.80	176.24	155.89	108.24	46.31	652.01
DPP76343	27/09/89	7.06	258.60	288.76	28.15	135.34	97.52	169.42	173.90	155.92	109.21	46.51	653.15
DPP76344	27/09/89	7.05	258.74	289.03	28.19	135.79	98.20	170.98	175.54	156.27	110.40	47.01	654.90
DPP76345	27/09/89	7.04	258.87	288.69	28.22	136.01	98.85	172.54	173.70	156.58	111.54	47.29	656.63
DPB74100	27/09/89	7.04	281.30	282.18	29.85	81.05	0.00	17.69	17.69	17.69	17.69	17.69	88.46
DPB74101	27/09/89	7.04	281.03	288.01	29.84	94.24	4.86	29.92	25.35	22.69	22.52	22.44	122.22
DPB74102	27/09/89	7.05	282.18	288.22	29.99	95.94	10.21	53.01	46.82	37.74	28.88	25.14	190.61
DPB74103	27/09/89	7.05	283.13	288.22	30.04	95.05	15.04	65.53	61.44	48.43	38.08	26.05	238.80
DPB74104	27/09/89	7.05	280.96	288.08	30.18	93.56	19.94	80.08	74.75	57.94	43.12	28.26	282.67
DPB74105	27/09/89	7.04	283.74	288.15	30.32	93.46	25.02	89.37	85.71	71.44	54.05	34.44	333.45
DPB74106	27/09/89	7.05	284.22	288.15	30.50	92.67	30.04	95.25	91.68	79.44	60.83	38.93	364.91
DPB74107	27/09/89	7.04	285.03	288.28	30.48	96.83	35.00	104.55	100.37	89.18	69.79	44.44	407.04
DPB74108	27/09/89	7.05	284.76	288.28	30.57	96.25	40.04	107.14	103.41	92.95	74.25	46.46	422.91
DPB74109	27/09/89	7.05	285.10	288.35	30.64	94.49	45.10	109.34	108.95	97.72	80.02	49.89	444.84
DPB74109	27/09/89	7.04	285.10	288.35	30.66	95.09	45.12	107.89	107.68	96.91	79.11	49.34	440.51
DPC74110	27/09/89	7.04	285.10	288.42	30.66	94.60	50.25	106.34	110.84	100.07	83.47	52.02	452.34
DPP74108	27/09/89	7.04	285.03	288.42	30.69	94.27	49.02	108.70	110.72	99.34	82.93	51.79	452.63
DPP74109	27/09/89	7.05	282.38	288.18	30.64	91.48	49.77	120.74	120.67	106.65	84.75	50.09	483.16
DPP74110	27/09/89	7.05	285.10	288.35	30.71	96.44	50.37	118.40	117.96	104.80	87.71	54.72	483.80
DPP74111	27/09/89	7.04	283.06	288.22	30.68	96.60	51.62	121.17	120.92	106.49	87.14	52.23	487.55
DPP74112	27/09/89	7.06	281.91	288.49	30.81	96.45	53.01	122.50	122.50	107.69	86.72	50.49	489.86
DPP74113	27/09/89	7.04	282.86	288.42	30.76	96.61	54.24	121.52	123.07	108.99	89.50	53.24	496.20
DPP74114	27/09/89	7.04	283.00	288.35	30.76	94.81	55.14	118.46	121.27	107.99	89.53	53.45	491.30
DPP74115	27/09/89	7.05	282.93	288.49	30.81	95.11	55.90	118.69	121.69	108.53	89.91	53.58	493.32
DPP74116	27/09/89	7.04	282.86	288.35	30.96	94.33	56.52	119.21	122.11	109.11	90.62	53.97	495.63
DPP74117	27/09/89	7.04	282.72	288.49	30.83	94.97	57.13	119.61	123.19	110.26	91.42	54.31	499.67
DPP74118	27/09/89	7.04	282.72	288.35	30.90	95.14	58.03	119.32	123.23	110.76	92.38	54.88	501.98
DPP74119	27/09/89	7.05	283.27	288.56	30.91	94.83	59.04	118.23	123.19	111.34	93.47	55.97	503.71
DPP74120	27/09/89	7.05	282.52	288.49	30.84	94.62	59.88	117.88	123.77	112.07	93.55	55.50	504.28
DPP74121	27/09/89	7.05	283.00	288.56	30.85	95.02	61.06	113.26	124.27	113.65	95.84	57.50	506.59
DPP74122	27/09/89	7.04	282.86	288.49	30.73	95.82	62.15	113.67	126.00	115.42	97.52	58.10	512.36
DPP74123	27/09/89	7.05	283.06	288.56	30.80	96.10	63.03	111.76	125.42	116.15	98.54	59.14	513.23
DPP74124	27/09/89	7.04	282.93	288.56	30.68	96.09	64.08	109.40	124.46	116.73	99.06	59.40	510.92
DPP74125	27/09/89	7.05	282.72	288.56	30.66	95.54	65.02	108.59	124.27	117.54	99.84	59.65	512.65
DPP74126	27/09/89	7.04	282.79	288.49	30.59	95.95	66.17	108.18	124.42	118.77	101.16	60.54	515.54
DPP74127	27/09/89	7.04	283.06	288.56	30.62	96.12	66.93	107.26	123.57	119.77	102.59	61.86	517.85
DPP74128	27/09/89	7.05	282.66	288.49	30.72	96.51	68.07	107.20	121.53	120.38	102.67	61.81	516.11
DPP74129	27/09/89	7.05	282.66	288.49	30.88	96.36	68.97	109.34	118.07	120.77	103.34	62.62	516.98

DPP74130	27/09/89	7.05	282.79	288.56	30.96	96.07	70.00	110.61	115.69	121.11	103.76	62.98	517.56
DPP74131	27/09/89	7.04	282.79	288.56	30.97	96.03	70.96	112.74	114.19	121.92	104.90	64.19	521.31
DPP74132	27/09/89	7.05	282.86	288.56	30.76	96.02	72.01	114.01	111.61	122.11	104.54	64.54	520.15
DPP74133	27/09/89	7.05	282.18	288.56	30.69	95.33	72.99	115.86	111.61	122.65	104.46	64.25	521.88
DPP74134	27/09/89	7.04	283.00	288.56	30.47	95.33	73.97	117.82	108.61	122.04	104.56	65.73	522.46
DPP74135	27/09/89	7.05	282.72	288.56	30.50	95.93	75.10	120.53	109.76	123.27	105.21	66.12	528.23
DPP74136	27/09/89	7.04	282.79	288.56	30.44	95.70	76.00	123.02	109.15	123.54	105.89	67.08	532.56
DPP74137	27/09/89	7.04	282.66	288.35	30.43	95.39	77.05	124.86	108.30	122.73	105.99	67.37	533.14
DPP74138	27/09/89	7.04	282.38	288.49	30.50	94.99	77.72	126.31	107.45	122.31	105.99	67.42	534.01
DPP74139	27/09/89	7.05	282.79	288.56	30.43	94.83	78.83	128.90	107.30	121.61	106.51	68.15	537.47
DPP74140	27/09/89	7.04	282.72	288.49	30.36	95.18	80.08	131.79	107.41	121.27	107.70	68.93	541.51
DPP74140	27/09/89	7.04	282.79	288.42	30.37	95.12	79.16	130.23	108.22	122.31	107.45	68.82	540.93
DPB77500	28/09/89	7.03	224.22	225.32	30.78	159.40	0.00	50.95	50.95	50.95	50.95	50.95	254.77
DPB77501	28/09/89	7.04	224.01	232.02	30.71	162.38	5.00	53.38	53.22	53.06	52.92	52.84	264.87
DPB77502	28/09/89	7.04	224.22	238.84	30.73	162.28	10.35	53.62	53.35	53.02	52.88	52.77	264.54
DPB77503	28/09/89	7.04	224.15	244.68	30.83	161.90	15.16	54.01	53.88	53.42	53.24	53.00	266.02
DPB77503	28/09/89	7.05	224.29	251.27	30.78	162.19	20.20	54.47	53.95	53.52	53.20	52.95	267.18
DPB77505	28/09/89	7.04	224.29	257.09	30.66	162.48	25.04	54.70	54.22	53.56	53.15	52.74	267.18
DPB77506	28/09/89	7.05	224.22	263.25	30.73	161.69	29.94	54.99	54.62	53.56	53.15	52.64	268.33
DPB77507	28/09/89	7.04	224.29	269.25	30.74	161.84	35.25	55.63	55.12	53.83	53.28	52.72	269.48
DPB77508	28/09/89	7.03	224.29	275.11	30.79	161.12	40.16	55.81	55.19	53.88	53.15	52.53	269.48
DPB77509	28/09/89	7.04	224.29	280.62	30.83	161.43	45.00	55.81	55.53	53.99	53.24	52.48	270.06
DPB77510	28/09/89	7.06	224.29	286.66	30.86	159.92	50.02	58.17	55.15	53.49	52.53	51.75	270.35
DPB77510	28/09/89	7.03	224.36	286.66	30.89	159.18	50.02	58.92	55.35	53.52	52.51	51.73	270.93
DPB77511	28/09/89	7.03	224.29	288.01	30.93	159.44	55.08	79.01	55.72	53.99	52.92	51.96	292.86
DPB77512	28/09/89	7.03	224.22	287.95	30.90	160.59	60.04	107.29	57.47	54.38	53.36	52.30	324.02
DPB77512	28/09/89	7.05	224.29	288.08	30.93	160.14	60.10	106.43	57.65	54.29	53.36	52.33	323.45
DPB77513	28/09/89	7.03	224.01	288.01	30.85	161.26	64.94	134.18	64.38	54.68	54.01	52.79	359.23
DPB77514	28/09/89	7.04	224.29	288.08	31.00	163.53	70.00	160.26	78.13	56.18	55.54	54.25	403.96
DPB77515	28/09/89	7.03	224.84	288.08	31.00	160.80	75.04	186.01	102.82	55.65	53.63	52.58	448.68
DPB77517	28/09/89	7.03	224.15	288.08	31.08	162.90	84.98	221.45	139.03	61.42	54.90	53.83	527.46
DPB77518	28/09/89	7.04	224.15	288.08	31.22	159.42	90.10	230.10	157.18	68.07	53.36	52.30	556.61
DPB77519	28/09/89	7.03	224.01	288.08	31.09	163.38	94.88	241.93	170.46	75.65	55.59	54.40	593.54
DPB77520	28/09/89	7.04	224.29	288.42	31.03	162.03	100.14	242.45	182.28	88.50	55.54	53.96	617.79
DPB77521	28/09/89	7.03	224.29	288.35	30.47	163.96	104.94	243.84	190.51	100.35	57.08	54.84	641.73
DPC77521	28/09/89	7.04	224.36	288.56	30.52	162.60	108.55	235.99	191.59	111.17	57.47	54.12	645.48
DPP77520	28/09/89	7.03	224.36	288.56	30.66	162.76	107.15	239.04	191.51	107.35	57.20	54.01	643.76
DPP77521	28/09/89	7.03	224.36	288.56	30.73	162.98	108.53	236.15	191.51	111.39	57.59	54.07	644.63
DPP77522	28/09/89	7.03	224.36	288.56	30.53	162.53	108.97	236.86	192.43	112.67	57.58	54.07	648.08
DPP77523	28/09/89	7.04	224.36	288.56	30.55	162.35	109.51	236.96	192.98	113.82	57.58	53.96	649.53
DPP77524	28/09/89	7.03	224.36	288.56	30.75	162.38	110.08	236.92	193.82	115.75	57.65	53.68	651.83
DPP77525	28/09/89	7.03	224.36	288.56	30.71	162.86	110.61	235.24	194.32	116.89	57.83	53.75	652.70
DPP77526	28/09/89	7.03	224.43	288.56	30.77	163.37	111.27	228.37	195.51	118.67	58.33	54.27	649.53
DPB77100	29/09/89	7.04	283.81	285.50	31.92	162.70	0.00	57.56	57.56	57.56	57.56	57.56	287.80
DPB77101	29/09/89	7.04	283.74	288.01	31.97	160.65	5.02	78.17	60.10	56.94	56.86	56.65	309.15
DPB77102	29/09/89	7.04	283.94	287.88	31.85	159.85	10.08	103.68	89.45	70.60	56.63	56.28	377.26
DPB77103	29/09/89	7.04	282.45	288.01	31.69	161.00	14.88	125.26	104.38	81.99	58.42	57.24	428.33
DPB77104	29/09/89	7.04	282.86	288.01	31.69	159.50	20.10	150.48	124.39	98.65	66.73	56.18	498.16
DPB77105	29/09/89	7.03	283.20	287.95	31.65	162.39	25.00	177.72	146.86	115.35	79.25	58.31	578.96
DPB77106	29/09/89	7.03	283.27	288.01	31.71	159.44	30.08	191.46	161.09	126.35	89.25	56.85	627.15
DPB77107	29/09/89	7.04	282.93	288.08	31.67	161.07	35.18	209.52	178.79	140.70	99.30	59.11	689.77
DPB77108	29/09/89	7.03	283.27	288.08	31.72	160.41	39.90	219.91	191.87	153.05	108.91	61.53	738.54
DPB77110	29/09/89	7.03	283.27	288.28	31.47	158.88	50.25	234.28	214.23	176.60	126.41	68.46	823.09
DPB77111	29/09/89	7.04	283.27	288.35	31.24	159.21	55.00	238.21	223.19	187.10	134.51	72.36	858.87
DPB77112	29/09/89	7.04	283.27	288.42	31.45	160.32	60.04	241.84	231.73	198.11	143.53	76.75	895.52
DPB77113	29/09/89	7.04	283.27	288.56	31.22	159.85	65.20	243.05	235.89	206.42	151.16	80.85	920.62
DPB77114	29/09/89	7.05	283.33	288.56	31.24	159.46	70.10	244.44	237.47	212.65	157.94	84.98	941.69
DPB77115	29/09/89	7.03	283.67	288.56	31.28	159.04	75.06	246.11	236.70	217.31	164.80	90.41	959.58
DPC77115	29/09/89	7.04	283.33	288.56	31.14	158.08	78.50	246.81	236.66	219.54	167.63	92.43	967.66

DPP77114	29/09/89	7.03	283.33	288.56	31.19	158.46	77.11	247.09	236.97	218.85	166.36	91.50	964.48
DPP77115	29/09/89	7.04	283.54	288.56	31.08	158.09	78.46	246.92	236.39	219.62	167.99	93.06	967.66
DPP77116	29/09/89	7.03	283.33	288.56	31.10	157.88	79.34	247.09	236.74	220.16	168.85	93.58	970.54
DPP77117	29/09/89	7.03	283.33	288.62	31.30	157.98	80.39	246.34	236.70	220.66	169.34	94.10	971.12
DPP77118	29/09/89	7.04	283.27	288.62	31.28	158.23	81.48	244.61	237.31	221.69	170.28	94.82	971.99
DPP77119	29/09/89	7.04	283.33	288.69	31.16	158.05	82.60	242.48	237.93	222.62	171.96	96.51	975.74
DPP77120	29/09/89	7.03	283.20	288.62	31.11	158.52	83.53	240.40	239.04	223.85	172.46	96.74	976.60
DPP77121	29/09/89	7.04	283.33	288.76	31.05	159.01	84.49	236.42	239.28	224.81	173.89	98.28	976.89
DPP77122	29/09/89	7.03	283.33	288.56	31.03	158.55	85.59	233.65	239.85	225.70	175.37	99.91	978.62
DPP77123	29/09/89	7.04	283.27	288.76	30.66	158.52	86.50	232.38	240.51	226.39	175.37	99.97	978.91
DPP77124	29/09/89	7.04	283.74	288.90	30.55	159.05	87.38	229.72	240.28	226.96	176.87	102.04	980.06
DPP77125	29/09/89	7.04	283.27	288.96	30.57	159.37	88.59	229.43	241.24	227.77	176.59	101.99	980.93
DPP77126	29/09/89	7.04	283.60	288.76	30.55	158.82	89.45	228.86	239.81	228.04	177.52	104.17	982.95
DPP77127	29/09/89	7.03	283.27	288.69	30.55	159.39	90.53	229.14	240.78	228.85	177.08	104.20	983.24
DPP77128	29/09/89	7.03	283.54	288.83	30.53	159.66	91.60	228.74	239.54	228.43	177.86	106.17	985.26
DPP77129	29/09/89	7.04	283.33	288.83	30.46	159.83	92.54	228.68	239.20	229.24	177.55	106.51	985.55
DPP77130	29/09/89	7.03	283.60	288.83	30.39	159.73	93.53	228.05	237.97	229.31	178.04	108.22	985.84
DPP77131	29/09/89	7.04	283.33	288.96	30.37	160.16	94.47	229.32	237.39	229.24	177.16	107.84	985.26
DPP77132	29/09/89	7.04	283.33	288.90	30.46	159.83	95.47	232.32	233.43	228.58	177.44	109.63	985.26
DPP77133	29/09/89	7.03	283.40	288.76	30.48	160.52	96.50	235.55	229.89	228.66	177.83	111.32	987.28
DPP77134	29/09/89	7.03	283.40	288.83	30.52	160.44	97.48	238.44	227.00	227.73	177.03	112.09	985.55
DPP77135	29/09/89	7.04	283.33	288.96	30.54	161.16	98.46	241.38	225.62	226.85	176.56	112.59	987.86
DPP77136	29/09/89	7.04	283.33	288.96	30.64	161.32	99.59	245.42	222.58	225.70	176.30	114.04	988.72
DPP77137	29/09/89	7.04	283.27	289.03	30.73	162.01	100.49	248.02	221.23	224.23	175.73	114.28	989.01
DPP77138	29/09/89	7.04	283.54	288.96	30.80	161.32	101.45	251.59	217.81	222.23	175.78	116.09	988.15
DPP77139	29/09/89	7.03	283.33	288.96	30.83	161.70	102.54	255.98	216.58	221.08	175.45	117.11	989.88
DPP77140	29/09/89	7.03	283.33	288.90	30.94	162.43	103.42	259.16	214.04	218.77	174.61	118.02	989.59
DPP77141	29/09/89	7.04	283.33	289.03	30.95	161.95	104.47	262.62	212.84	216.88	173.71	118.51	989.30
DPP77142	29/09/89	7.03	283.33	288.90	31.05	162.24	105.55	267.41	211.07	214.04	172.59	120.01	989.59
DPP77143	29/09/89	7.04	283.33	289.03	31.01	163.21	106.50	271.85	209.19	212.15	171.63	121.31	991.61
DPP77144	29/09/89	7.04	283.33	289.03	31.01	163.58	107.46	276.07	205.22	210.73	170.51	122.22	990.74
DPP77145	29/09/89	7.04	283.13	289.03	31.51	164.51	107.99	279.47	203.15	209.84	170.28	122.72	990.74
DPP77136	29/09/89	7.04	283.33	288.96	31.98	160.54	98.97	242.01	226.12	226.39	175.52	112.12	987.28
DPB74500	02/11/89	7.03	223.39	224.22	29.86	101.12	0.00	23.64	23.64	23.64	23.64	23.64	118.19
DPB74501	02/11/89	7.04	222.91	234.50	30.94	100.65	5.04	23.52	23.60	23.53	23.51	23.46	118.47
DPB74502	02/11/89	7.04	222.84	244.61	31.18	100.53	10.21	23.69	23.71	23.64	23.56	23.54	119.05
DPB74504	02/11/89	7.04	222.35	263.45	29.82	101.73	20.22	24.50	24.48	24.26	24.08	23.98	121.94
DPB74506	02/11/89	7.04	222.42	281.57	29.17	101.50	30.08	25.14	24.83	24.60	24.31	24.13	123.38
DPB74508	02/11/89	7.04	222.42	288.35	28.95	100.80	40.19	50.59	26.18	24.45	24.16	23.87	151.08
DPB74512	02/11/89	7.03	222.22	288.15	28.68	101.37	60.23	110.78	76.46	35.99	24.52	24.29	276.32
DPB74514	02/11/89	7.04	221.94	288.49	28.51	99.80	70.10	123.54	97.66	53.85	25.07	23.67	329.70
DPC74515	02/11/89	7.04	221.94	288.56	28.52	102.14	79.49	130.75	113.98	70.89	29.09	24.50	375.59
DPP74514	02/11/89	7.03	222.22	288.56	28.54	102.25	79.16	131.04	113.71	70.51	28.91	24.47	375.59
DPP74515	02/11/89	7.04	222.35	288.56	28.50	100.69	80.96	127.92	115.86	73.97	29.82	23.95	378.47
DPP74516	02/11/89	7.03	222.42	288.56	28.56	101.03	82.44	125.56	118.59	76.89	31.02	23.87	383.09
DPP74517	02/11/89	7.04	222.42	288.56	28.44	101.07	84.06	124.17	120.94	79.28	31.98	24.03	387.42
DPB76500	03/11/89	7.00	225.32	226.29	28.73	141.05	0.00	41.17	41.17	41.17	41.17	41.17	205.85
DPB76501	03/11/89	7.00	224.70	233.53	29.03	138.47	4.90	40.42	40.40	40.33	40.28	40.26	202.67
DPB76502	03/11/89	7.00	224.70	240.63	28.93	142.33	10.10	42.61	42.48	42.33	42.28	42.13	212.78
DPB76504	03/11/89	7.00	224.77	254.22	28.84	142.05	19.84	42.96	42.63	42.40	42.21	41.95	213.06
DPB76506	03/11/89	7.00	224.70	268.09	28.84	141.16	29.94	43.59	43.01	42.63	42.18	41.87	215.08
DPB76508	03/11/89	7.00	224.50	281.03	28.65	141.61	40.00	44.80	44.05	43.40	42.93	42.34	218.84
DPB76510	03/11/89	7.00	224.22	288.01	28.77	137.55	49.94	73.43	42.98	42.13	41.27	40.60	242.21
DPB76512	03/11/89	7.00	224.56	287.88	28.73	141.30	59.75	121.85	59.40	43.44	43.06	42.11	313.48
DPB76514	03/11/89	7.00	224.36	288.08	29.63	137.67	70.16	162.94	96.03	45.52	41.32	40.65	391.97
DPB76515	03/11/89	7.00	224.29	288.08	29.86	138.03	75.04	177.72	112.08	50.60	41.66	40.94	429.49
DPB76516	03/11/89	7.00	224.36	288.01	29.77	139.43	80.14	190.07	126.93	58.91	42.28	41.49	466.71
DPB76517	03/11/89	7.00	224.36	288.08	29.86	138.47	85.24	195.84	138.24	70.22	42.18	41.10	494.99
DPB76518	03/11/89	7.00	224.36	288.08	30.01	137.20	90.06	197.45	147.90	82.07	42.54	40.73	518.94

DPB76519	03/11/89	7.00	224.84	288.15	30.28	139.23	95.10	202.94	158.40	92.80	44.85	41.90	549.53
DPB76520	03/11/89	7.00	224.77	288.08	29.88	141.18	100.04	204.73	166.56	104.58	46.98	42.81	574.35
DPC76520	03/11/89	7.00	224.77	288.15	30.11	139.89	99.92	199.70	165.40	105.39	46.39	41.82	567.42
DPP76519	03/11/89	7.00	224.77	288.08	30.00	139.56	99.08	200.80	164.44	103.31	45.87	41.56	563.96
DPP76520	03/11/89	7.00	224.77	288.15	29.87	138.42	100.76	194.40	165.63	108.00	46.05	40.94	563.96
DPP76521	03/11/89	7.00	224.84	288.22	29.90	139.75	102.13	192.78	167.40	110.73	47.24	41.59	568.86
DPB76100	03/11/89	6.97	282.52	283.67	29.90	135.56	0.00	41.38	41.38	41.38	41.38	41.38	206.91
DPB76101	03/11/89	7.00	280.89	287.67	29.89	139.51	4.92	47.32	44.61	44.65	44.52	44.42	224.80
DPB76102	03/11/89	7.00	282.18	287.81	29.88	137.25	10.39	80.97	68.81	53.80	43.72	43.59	292.03
DPB76104	03/11/89	7.00	282.52	287.88	29.90	136.07	20.10	121.20	102.02	81.97	58.13	43.26	410.05
DPB76106	03/11/89	6.99	282.45	287.81	29.88	136.84	29.98	147.97	131.18	107.40	77.72	45.93	515.96
DPB76108	03/11/89	6.99	282.79	287.88	29.99	137.55	40.18	169.33	151.96	130.52	94.67	53.38	607.43
DPB76110	03/11/89	7.00	280.28	288.15	29.83	137.60	50.04	183.99	167.46	145.57	103.43	55.31	664.28
DPB76112	03/11/89	7.00	280.28	288.22	29.91	136.94	60.02	189.53	179.51	161.19	117.71	62.24	719.40
DPB76114	03/11/89	7.00	280.48	288.28	29.87	137.19	70.00	195.64	187.01	174.31	132.38	71.36	771.34
DPC76114	03/11/89	7.01	281.16	288.35	29.79	138.53	71.80	198.24	190.28	178.46	136.90	74.97	788.65
DPP76113	03/11/89	7.00	280.96	288.22	29.83	139.09	71.23	199.45	190.17	177.96	136.23	74.34	788.65
DPP76114	03/11/89	7.00	281.03	288.28	29.97	138.38	72.73	198.36	190.78	179.54	138.12	75.77	792.98
DPP76115	03/11/89	7.00	280.96	288.28	29.85	138.69	74.51	196.45	191.17	180.62	139.68	77.17	796.15
DPP76116	03/11/89	7.00	280.96	288.35	29.97	138.35	75.88	192.41	192.01	182.04	140.98	78.03	796.15
DPP76117	03/11/89	7.00	280.96	288.42	29.90	138.48	77.79	186.58	192.17	183.54	143.00	80.11	795.58
DPP76118	03/11/89	7.00	281.16	288.56	29.86	138.25	79.36	181.79	191.82	183.89	144.28	81.67	793.27
DPP76119	03/11/89	7.00	280.96	288.42	29.96	137.15	81.07	177.75	189.20	183.20	144.17	82.73	786.92
DPP76120	03/11/89	7.00	281.03	288.56	29.87	138.24	82.70	179.31	190.67	185.50	145.26	84.24	795.00
DPP76121	03/11/89	7.00	280.75	288.42	29.92	137.36	84.43	177.58	188.66	185.58	144.75	84.84	792.11
DPP76122	03/11/89	7.00	280.96	288.62	29.84	139.63	86.00	180.64	190.86	188.81	147.37	87.48	805.39
DPP76123	03/11/89	7.00	281.16	288.62	29.95	139.23	87.72	183.47	184.12	188.58	148.12	89.28	803.94
DPP76124	03/11/89	7.00	281.09	288.62	29.86	139.37	89.26	186.81	178.70	187.85	148.04	90.42	802.21
DPP76125	03/11/89	7.00	281.09	288.62	29.99	139.25	91.05	191.55	175.28	187.31	148.41	91.80	804.81
DPP76126	03/11/89	7.00	281.30	288.76	30.13	139.05	92.70	196.51	172.54	186.66	149.47	93.56	808.85
DPP76127	03/11/89	6.99	281.37	288.62	30.04	139.24	94.47	201.07	168.70	184.70	149.65	94.86	809.43
DPP76128	03/11/89	7.00	280.96	288.69	30.11	139.51	96.11	205.34	166.08	182.54	149.58	95.74	810.58
DPP76129	03/11/89	7.00	281.23	288.62	30.05	139.94	97.60	211.05	164.42	180.46	150.20	97.53	813.47
DPB56200	03/11/89	5.03	242.07	243.03	29.95	142.95	0.00	42.84	42.84	42.84	42.84	42.84	214.20
DPB56201	03/11/89	5.03	243.99	252.44	30.09	142.37	5.19	42.43	42.42	42.45	42.27	42.22	211.32
DPB56202	03/11/89	5.02	244.41	259.49	30.03	141.01	9.96	42.43	42.30	42.26	42.01	41.88	210.45
DPB56204	03/11/89	5.03	244.61	266.73	29.49	141.15	20.10	80.46	43.92	42.22	41.83	41.54	249.99
DPB56206	03/11/89	5.02	244.48	266.59	29.28	141.42	30.02	148.16	97.17	48.72	42.61	42.50	382.72
DPB56208	03/11/89	5.03	244.61	266.73	29.28	142.86	40.06	198.95	147.30	82.58	43.31	42.94	521.24
DPB56210	03/11/89	5.03	245.37	266.80	29.05	141.61	49.49	228.55	186.78	120.79	54.06	42.19	640.70
DPB56212	03/11/89	5.03	245.09	266.87	28.95	142.08	60.12	262.84	218.14	154.49	71.90	42.45	759.01
DPB56214	03/11/89	5.03	245.30	267.21	28.98	142.85	69.71	286.04	241.87	182.89	89.90	43.57	854.81
DPB56215	03/11/89	5.03	245.16	267.34	29.02	140.49	80.12	291.58	261.54	206.40	110.63	45.15	926.96
DPC56217	03/11/89	5.03	245.09	267.48	28.99	140.48	84.80	291.81	270.12	216.05	119.59	46.55	956.68
DPP56216	03/11/89	5.03	245.09	267.27	28.96	140.44	84.36	292.16	269.08	214.67	118.42	46.29	953.50
DPP56217	03/11/89	5.03	245.16	267.62	29.01	141.06	85.98	294.75	273.69	219.32	121.87	47.23	969.95
DPP56218	03/11/89	5.03	245.30	267.55	29.20	142.34	87.64	297.70	277.66	223.06	124.68	48.09	984.67
DPP56219	03/11/89	5.03	245.09	267.62	29.03	140.91	89.28	294.00	277.96	224.90	127.32	48.42	985.53
DPP56220	03/11/89	5.02	245.16	267.62	28.88	141.12	91.05	285.52	280.81	228.67	131.53	49.23	987.84
DPP56221	03/11/89	5.03	245.09	267.62	28.64	140.72	92.83	279.57	281.89	231.21	134.26	49.85	989.86
DPP56222	03/11/89	5.03	245.09	267.62	28.61	140.53	94.45	276.57	283.81	234.06	137.27	50.68	995.35
DPP56223	03/11/89	5.02	245.09	267.62	28.59	140.84	95.98	273.69	284.58	237.18	140.57	51.75	1000.54
DPP56224	03/11/89	5.03	245.09	267.68	28.60	140.42	97.73	271.03	284.93	238.98	142.91	52.50	1003.71
DPP56225	03/11/89	5.03	245.16	267.62	28.52	142.89	99.38	278.82	292.32	244.60	146.49	53.70	1029.11
DPP56226	03/11/89	5.03	245.09	267.82	28.46	142.42	101.03	275.88	289.85	246.41	149.24	54.55	1027.95
DPP56227	03/11/89	5.03	245.16	267.82	28.47	141.20	102.79	272.99	287.20	247.06	152.10	55.59	1029.11
DPP56228	03/11/89	5.03	245.09	267.68	28.47	141.22	104.28	272.71	287.04	249.30	155.06	56.50	1034.30
DPP56229	03/11/89	5.03	245.09	267.62	28.46	140.35	106.07	273.34	283.43	250.72	157.81	57.49	1035.74
DPP56230	03/11/89	5.03	245.09	267.68	28.40	140.02	107.64	278.48	277.27	252.14	160.72	58.68	1040.36

DPB54200	03/11/89	5.02	242.69	243.65	28.62	103.91	0.00	25.05	25.05	25.05	25.05	25.05	125.24
DPB54201	03/11/89	5.03	242.76	253.87	28.43	103.73	5.22	25.11	25.01	24.98	24.92	24.92	125.24
DPB54202	03/11/89	5.03	243.03	263.38	28.51	103.52	10.21	25.34	25.24	25.13	25.05	24.97	125.82
DPB54204	03/11/89	5.03	242.69	266.73	28.56	102.83	20.08	67.36	41.82	25.40	24.98	24.84	185.84
DPB54206	03/11/89	5.02	242.76	266.59	28.71	104.11	30.16	112.14	84.65	50.33	26.14	25.46	302.13
DPB54208	03/11/89	5.02	242.69	266.59	28.57	104.93	39.88	142.27	117.93	78.27	37.49	25.62	407.46
DPB54210	03/11/89	5.03	242.96	266.66	28.57	103.28	50.08	165.30	141.90	105.58	53.73	25.62	499.22
DPB54212	03/11/89	5.03	242.89	267.07	28.59	104.38	59.94	187.98	163.56	128.59	69.98	28.37	586.94
DPB54214	03/11/89	5.02	242.69	267.14	28.73	102.73	69.53	189.53	181.14	146.64	86.68	32.14	644.95
DPC54214	03/11/89	5.03	242.89	267.14	28.66	103.04	70.06	188.26	182.49	147.21	87.59	32.42	646.97
DPP54213	03/11/89	5.03	242.76	267.14	28.71	102.77	69.59	189.13	182.18	146.48	86.68	32.29	646.39
DPP54213	03/11/89	5.03	242.76	267.14	28.73	102.49	69.59	188.61	181.72	146.41	86.79	32.19	645.23
DPP54214	03/11/89	5.03	242.82	267.14	28.70	102.33	71.09	188.09	184.26	149.06	88.97	32.92	653.03
DPP54215	03/11/89	5.03	242.96	267.14	28.69	102.89	72.73	189.19	186.99	152.14	91.64	33.93	664.28
DPP54216	03/11/89	5.03	242.69	267.14	28.77	102.73	74.51	188.67	189.30	155.49	93.88	34.68	672.07
DPP54217	03/11/89	5.03	242.69	267.34	28.99	102.91	75.86	182.78	191.42	158.03	96.55	35.64	674.09
DPP54218	03/11/89	5.03	242.76	267.34	29.03	103.33	77.83	180.24	194.19	161.87	99.23	36.81	681.59
DPP54219	03/11/89	5.03	242.82	267.14	28.95	102.82	79.43	177.30	194.88	164.83	101.77	37.98	686.79
DPP54220	03/11/89	5.03	242.69	267.48	28.96	102.31	81.05	174.18	193.84	166.91	103.20	38.76	686.50
DPP54221	03/11/89	5.02	242.69	267.21	28.97	103.41	82.72	175.63	196.76	171.41	106.29	40.03	699.77
DPP54222	03/11/89	5.02	242.82	267.41	28.94	102.93	84.43	174.18	194.92	173.91	108.16	41.12	702.95
DPP54223	03/11/89	5.03	242.69	267.55	28.73	102.60	86.13	173.32	192.76	175.88	109.75	41.93	704.39
DPB98200	26/10/89	9.57	295.19	295.19	31.40	185.12	0.00	74.59	74.59	74.59	74.59	74.59	372.96
DPB99200	26/10/89	9.57	296.27	296.27	31.59	207.80	0.00	92.76	92.76	92.76	92.76	92.76	463.82

V. PREVIOUS PUBLICATIONS BY THIS AUTHOR ON TWO-PHASE FLOW, BOILING HEAT TRANSFER AND PRESSURE DROP

PUBLICATIONS

Salcudean, M.E., Leung, L.K.H. and Groeneveld, D.C., Pressure Drop Through Obstructions in Horizontal Annular Flow, Proceedings of the 9th Canadian Congress of Applied Mechanics, May 30-June 3, Saskatchewan, Canada, pp. 515-516, 1981.

Salcudean, M.E., Groeneveld, D.C. and Leung, L.K.H., Effect of Flow Obstruction Geometry on Pressure Drops in Horizontal Air-Water Flow, Int. J. Multiphase Flow, Vol. 9, No. 1, pp. 73-85, 1983.

Leung, L.K.H., Salcudean, M.E,, Snoek, C.W. and Groeneveld, D.C., Effect of Streamlining on Bundle Pressure Drop, Proceedings of the 3rd Multi-Phase Flow and Heat Transfer Symposium-Workshop, April 18-20, Florida, USA, pp. 405-420, 1983.

Salcudean, M.E. and Leung, L.K.H., Effect of Flow Obstruction on Two-Phase Pressure Drops in both Horizontal and Vertical Annular Flows, Proceedings of the 2nd International Conference on Multiphase Flow, June 19-21, London, U.K. pp. 215-228, 1985.

Salcudean, M.E. and Leung, L.K.H., Pressure Losses through Obstruction in both Horizontal and Vertical Bubbly Flows, Proceedings of the International Symposium on Fundamental Aspects of Gas-Liquid Flows, ASME Winter Annual Meeting, Nov. 17-21, Florida, USA, 1985.

Groeneveld, D.C., Leung, L.K.H., Kiameh, B.P. and Cheng, S.C., A Universal Method for Predicting Critical Heat Flux for Aqueous and Non-Aqueous Fluids in Forced Convective Boiling, HTFS Research Symposium Proceedings, Sept., Edinburgh, U.K., 1986.

Snoek, C.W. and Leung, L.K.H., An Accurate Model for Pressure Drop Prediction in Multi-Element CANDU Fuel Channels, Proceedings of the 4th International Symposium on Multi-Phase Transport and Particulate Phenomena, Miami Beach, USA, 1986.

Groeneveld, D.C., Leung, L.K.H. and Cheng, S.C., A Generalized Heat Transfer Prediction Package for Single- and Two-Phase Flow, Proceedings of the 37th Canadian Chemical Engineering Conference, May 18-21, Montreal, Canada, 1987.

Leung, L.K.H., Cheng, S.C. and Groeneveld, D.C., A Heat Transfer Correlation Package for Aqueous and Non-Aqueous Fluids Suitable for Micro-computer Applications, Proceedings of the 11th Canadian Congress of Applied Mechanics, May 31-June 4, Edmonton, Canada, 1987.

Groeneveld, D.C., Leung, L.K.H., Snoek, C.W., Cheng, S.C. and Wong, S., Recent Developments in Thermalhydraulic Prediction Methods, Proceedings of the 3rd Symposium on Nuclear Science and Engineering, Sept. 30-Oct. 1, Hamilton, Canada, p. 32, 1987.

Leung, L.K.H., Groeneveld, D.C., Cheng, S.C. and Truong, Q.S., Microcomputer-Based Heat Transfer Prediction Package, Proceedings of the 3rd Symposium on Nuclear Science and Engineering, Sept. 30-Oct. 1, Hamilton, Canada, p. 34, 1987.

Salcudean, M.E. and Leung, L.K.H., Pressure Drop due to Flow Obstruction, Nuclear Engineering & Design, Vol. 105, pp. 349-362, 1988.

Groeneveld, D.C. and Leung, L.K.H., Quantification of Uncertainties of Thermal-hydraulics Correlations Used in BE Codes Impacting PCT in LOCA, Proceedings of the EPRI Workshop on Best-Estimate Methods, Boston, Mass., Aug. 11-12, 1988.

Snoek, C.W. and Leung, L.K.H., A Model for Predicting Diabatic Pressure Drops in Multi-Element Fuel Channels, Nuclear Engineering & Design, Vol. 110, pp. 299-312, 1989.

Groeneveld, D.C., Cheng, S.C., Leung, L.K.H. and Nguyen, C., Computation of Single- and Two-Phase Heat Transfer Rates Suitable for Water-Cooled Heat Transfer Equipment, Nuclear Engineering and Design, Vol. 114, pp. 61-77, 1989.

Groeneveld, D.C. and Leung, L.K.H., Tabular Approach for Predicting Critical Heat Flux and Post-Dryout Heat Transfer, Proceedings of the 4th International Topical Meeting on Nuclear Reactor Thermal-Hydraulics, Oct. 10-13, Karlsruhe, F.R.G., pp. 109-114, 1989.

Sutradhar, S.C., Groeneveld, D.C. and Leung, L.K.H., Transient Effects on Critical Heat Flux and Quenching in Directly Heated Tubes, Proceedings of the CNA/CNS Annual Conference, June 3-6, Toronto, Canada, 1990.

Groeneveld, D.C. and Leung, L.K.H., Tabular Approach for Predicting Critical Heat Flux, Proceedings of the CNA/CNS Annual Conference, June 3-6, Toronto, Canada, 1990.

Leung, L.K.H. and Groeneveld, D.C., An Efficient Heat Transfer Prediction Package Suitable for Steady-State and Accident Analysis, Proceedings of the CNA/CNS Annual Conference, June 3-6, Toronto, Canada, 1990.

Leung, L.K.H. and Groeneveld, D.C., Two-Phase Pressure Drop and Wall Temperature Measurements at Steady-State in High-Pressure Film-Boiling Regime, Proceedings of the CNA/CNS Annual Conference, June 3-6, Toronto, Canada, 1990.

Leung, L.K.H. and Groeneveld, D.C., Frictional Pressure Gradient in the Pre- and Post-CHF Heat-Transfer Regions, Proceedings of the International Conference on Multiphase Flow, Tsukuba, Japan, Vol. 2, pp. 493-496, 1991.

Groeneveld, D.C., Doerffer, S., Leung, L.K.H., Rudzinski, K.F. and Yin, S.T., CHF Separate-Effects Studies at Chalk River Laboratories, Proceedings of the 17th Annual CNS Simulation Symposium on Nuclear Engineering, Kingston, Canada, Aug. 16-18, 1992.

Groeneveld, D.C., Joober, K., Doerffer, S., Wong, W., Leung, L.K.H. and Cheng, S.C., The Effect of Fuel Subchannel Geometry on CHF, Proceedings of the 5th International Topical

Meeting on Reactor Thermal Hydraulics-NURETH-5, Salt Lake City, UT, USA, September 21-24, Vol. III, pp. 683-690, 1992.

Groeneveld, D.C., Leung, L.K.H., Kirillov, P.L., Bobkov, V.P., Erbacher, F.J. and Zeggel, W., An Improved Table Look-Up Method for Predicting CHF, Proceedings of the International Workshop on CHF Fundamentals, Braunschweig, Germany, March 2-4, 1993.

Groeneveld, D.C., Leung, L.K.H., Kirillov, P.L., Bobkov, V.P., Erbacher, F.J. and Zeggel, W., The CHF Look-Up Table for Predicting Critical Heat Flux in Water-Cooled Channels, Proceedings of the Technical Committee Meeting on Thermohydraulic of Cooling Systems in Advanced Water-Cooled Reactors, Villigen, Switzerland, May 25-28, 1993.

Leung, L.K.H. and Groeneveld, D.C., An Assessment of Prediction Methods of CHF in Tubes with A Large Experimental Data Bank, Proceedings of the 4th CNS International Conference on Simulation Methods in Nuclear Engineering, Montreal, June 2-4, 1993.

Groeneveld, D.C., Leung, L.K.H., Kirillov, P.J., Bobkov, V.P., Erbacher, F.J. and Zeggel, W., An Improved Table Look-Up Method for Predicting Critical Heat Flux, Proceedings of the 6th International Topical Meeting on Nuclear Reactor Thermalhydraulics, Grenoble, France, Oct. 4-8, Vol. 1, pp. 223-230, 1993.

Leung, L.K.H., Groeneveld, D.C., Aube, F. and Tapucu, A. New Studies of the Effect of Surface Heating on Frictional Pressure Drop in Single- and Two-Phase Flow, Proceedings of the 6th International Topical Meeting on Nuclear Reactor Thermalhydraulics, Grenoble, France, Oct. 4-8, Vol. 2, pp. 867-874, 1993.

THESIS

Leung, L.K.H., Effect of Flow Obstruction on Pressure Loss, Master of Applied Science Thesis, University of Ottawa, Ottawa, Ontario, Canada, 1983.

Leung, L.K.H., A Model for Predicting the Pressure Gradient Along a Heated Channel During Flow Boiling, Ph.D. Thesis, University of Ottawa, Ottawa, Ontario, Canada, 1994.

REPORTS

Salcudean, M.E. and Leung, L.K.H., Effect of Streamlining on Bundle Pressure Loss, Report submitted to Chalk River Nuclear Laboratories, University of Ottawa, Ottawa, Ontario, 1983.

Salcudean, M.E. and Leung, L.K.H., Effect of Flow Obstruction on Pressure Loss in Vertical Flow, Report submitted to Chalk River Nuclear Laboratories, University of Ottawa, Ottawa, Ontario, 1983.

Leung, L.K.H. and Groeneveld, D.C., Tabulation of Experimental Post-Dryout Tube Data for Water, APRP-TD-17, 1985.

Leung, L.K.H. and Groeneveld, D.C., Post-Dryout Correlation Development, APRP-TD-18, 1985.

Cheng, S.C., Groeneveld, D.C., Leung, L.K.H., Wong, S.Y.L. and Nguyen, C., Progress Report submitted to the Atomic Energy Control Board, 1986.

Schneider, G.R., Laperriere, A., Shaw, B.P., Groeneveld, D.C. and Leung, L.K.H., Post-Dryout Analysis of the U-1 Segmented Cosine Bundle Data, CRNL-2728, 1987.

Groeneveld, D.C. and Leung, L.K.H., Compendium of Thermalhydraulic Correlations and Fluid Properties, Editors and Authors, CRNL-4062 (also CANDEV-86-75), 1987.

Cheng, S.C., Groeneveld, D.C., Leung, L.K.H., Wong, S.Y.L. and Nguyen, C., Microcomputer Based Program for Predicting Heat Transfer Under Reactor Accident Conditions, Final Report submitted to the Atomic Energy Control Board, 1987.

Groeneveld, D.C., Leung, L.K.H. and Chang, S.H., Proposed Strategy for the Completion of EPRI Contract RP2639-3, ARD-TD-79, 1987.

Leung, L.K.H. and Groeneveld, D.C., EPRI Thermalhydraulic Correlations Assessment Program-Progress Report 2, ARD-TD-89, 1987.

Leung, L.K.H. and Snoek, C.W., Assessment of a Two-Phase Pressure Drop Model with 37- and 41-Element Geometries Cooled by Water and Refrigerant-12, ARD-TD-76, 1988.

Leung, L.K.H. and Groeneveld, D.C., Assessment of Wahba Correlation for Predicting CHF in 37-element CANDU Fuel Bundles, Report prepared for Ontario Hydro, Aug. 1988.

Leung, L.K.H. and Groeneveld, D.C., Development of Post-Dryout Look-up Tables for Loss-of-Regulation Accident Conditions, RC-34 (also CANDEV-88-68), 1988.

Leung, L.K.H. and Groeneveld, D.C., Updated of Compendium of Thermalhydraulic Correlations and Fluid Properties, CRNL-4062 (Rev. 1) also CANDEV-86-75 (Rev. 1), 1988.

Leung, L.K.H. and Groeneveld, D.C., Assessment of Thermalhydraulic Prediction Methods Used in ECC System Codes, ARD-TD-112, 1988.

Leung, L.K.H., Survey of Experimental Results for CHF Obtained with a String of 37-Element Fully-Segmented CANDU-Type Bundles, ARD-TD-146, 1988.

Groeneveld, D.C. and Leung, L.K.H., Prediction of CHF in 37-Element Bundles at High Flows, ARD-TD-154, 1989.

Leung, L.K.H., Tabular Approach for Evaluating Critical-Channel-Power in a Channel Containing 37-element CANDU Fuel Bundles, ARD-TD-163, 1989.

Groeneveld, D.C. and Leung, L.K.H., The 1988 Updated Sections for the Compendium on Thermalhydraulic Correlations and Fluid Properties, ARD-TD-173 (also COG-89-88), 1989.

Groeneveld, D.C., Leung, L.K.H. and Yin, S.T., EPDC Task 13.3 Part 2: A Method of predicting the Effect of Radial Flux Distribution on Critical Heat Flux in 37-element Bundles, ARD-TD-158, 1989.

Leung, L.K.H. and Groeneveld, D.C., Assessment of Thermalhydraulic Prediction Methods Used in ECC System Codes, Final report submitted to the EPRI, ARD-TD-200 (also RC-M-1), 1989.

Leung, L.K.H. and Snoek, C.W., Assessment of Chexal-Lellouche Model for Predicting Void Fraction, Final report submitted to the EPRI, ARD-TD-212, 1989.

Leung, L.K.H. and Groeneveld, D.C., Look-Up Table of Critical Heat Flux (CHF) for a String of Horizontal, 37-Element Bundles, COG-89-221 (also ARD-TD-163), 1989.

Leung, L.K.H. and Groeneveld, D.C., Prediction of the Effect of Axial Flux Distribution on CHF, COG-90-15 (also ARD-TD-216), 1990.

Leung, L.K.H., Yin, S.T. and Martin, J., Measurements of Critical Heat Flux, Post-Dryout Pressure Drops and Wall Temperature in Tubes, COG-90-32 (also ARD-TD-227), 1990.

Leung, L.K.H. and Groeneveld, D.C., Revision of the AECL-UO, Look-Up Table for Critical Heat Flux (CHF) in Tubes, COG-90-69 (also ARD-TD-236), 1990.

Leung, L.K.H., Estimation of Dryout Power and Pressure Drop in a String of 37-Element Bundles for the Water-CHF Test, COG-90-134 (also ARD-TD-259), 1990.

Groeneveld, D.C. and Leung, L.K.H., Compendium of Thermalhydraulic Correlations and Fluid Properties (Version 1991, Revision 0), Editors and Authors, COG-90-86 (also ARD-TD-243), 1991.

Leung, L.K.H. and Groeneveld, D.C., A Method for Predicting Critical Heat Flux of a String of CANFLEX Bundles, ARD-TD-304, 1991.

Leung, L.K.H. and Groeneveld, D.C., Response To Comments from AECB Staff Regarding CANDU-3 CHF Predictions at High Flows, ARD-TD-313, 1991.

Leung, L.K.H. and Groeneveld, D.C., Prediction of Critical Heat Flux for Zero-Void Reactivity Bundles, ARD-TD-310, 1992.

Groeneveld, D.C., Sutradhar, S.C. and Leung, L.K.H., The Effect of Radial-Flux Distribution on Critical Heat Flux or Dryout Power in 37-Element Bundles, ARD-TD-317 (also COG-91-202), 1992.

Groeneveld, D.C. and Leung, L.K.H., Strategy for Developing CHF and Post-CHF Prediction Methods for CANDU-6 Fuel Bundles, ARD-TD-360, 1992.

Groeneveld, D.C., Joober, K., Leung, L.K.H., Doerffer, S., Rudzinski, K.F. and Wong, W., Effect of Flow Geometry on Critical Heat Flux: Phase I - Observed Effects and Preliminary Prediction Method for Subchannels, ARD-TD-338 (also COG-91-286), 1992.

Leung, L.K.H. and Groeneveld, D.C., 1993 Update of the Critical Heat-Flux Table for Upward Flow of Steam-Water Mixtures in Uniformly Heated Tubes (Version LW-T-1993), ARD-TD-397 (also COG-92-395 and RC-888), 1993.

Dowlati, R., Groeneveld, D.C., Nguyen, T.Q. and Leung, L.K.H., Analysis of the Full-Scale 37-Element Bundle Obtained at Stern Laboratories - Interim report 1, 1993.